Biosynthese und Funktion von Naturstoffen aus *Mortierella alpina*

Dissertation
zur Erlangung des akademischen Grades
„doctor rerum naturalium“ (Dr. rer. nat.)

vorgelegt dem Rat der Fakultät für Biowissenschaften
der Friedrich-Schiller-Universität Jena

von Dipl.-Pharm. Jacob Martin Wurlitzer

geboren am 02.03.1995 **in** Erlabrunn

Die praktischen Arbeiten für diese Dissertation wurden von Januar 2019 bis April 2022 am Lehrstuhl für Pharmazeutische Mikrobiologie der Friedrich-Schiller-Universität durchgeführt.

Gutachter 1:	Prof. Dr. Dirk Hoffmeister Friedrich-Schiller-Universität Jena
Gutachter 2:	Dr. Hajo Kries Leibniz-Institut für Naturstoff-Forschung und Infektionsbiologie Jena
Externer Gutachter:	Prof. Dr Markus Nett Technische Universität Dortmund

Tag der Verteidigung: 18.09.2023

Es gibt mehr Leute, die kapitulieren, als solche, die scheitern.

Henry Ford

Inhaltsverzeichnis

Abkürzungsverzeichnis

4'-PP	4'-Phosphopantetheinyl
AA	Arachidonsäure
ACV-Synthetasen	L-δ-(α-Aminoadipoyl)-L-cysteinyl-D-Valin-Synthetasen
ADA-Domäne	Adenylierungs-Aktivierungs-Domäne
A-Domäne	Adenylierungsdomäne
AMP	Adenosin-5'-monophosphat
AS	Aminosäure
ATP	Adenosin-5'-triphosphat
BGC	Biosynthetischer Gencluster
BRE	*Burkholderia*-verwandte Endosymbionten (*Burkholderia*-related endosymbionts)
C-Domäne	Kondensationsdomäne
C_S-Domäne	Starter-Kondensationsdomäne
DHA	Docosahexaensäure
DHB	Dehydrobutyrin
duale E/C-Domäne	duale Epimerisierungs- und Kondensationsdomäne
E-Domäne	Epimerisierungsdomäne
EDF	Früh-entwickelte Pilze (early-diverging fungi)
EGT	Endosymbiontischer Gentransfer
HGT	Horizontaler Gentransfer
M-Domäne	Methylierungsdomäne
MRE	*Mycoplasma*-verwandte Endosymbionten (*Mycoplamsma*-related endosymbionts)
NMR	Kernspinresonanz (Nuclear Magnetic Resonance)
NRPS	Nichtribosomale Peptidsynthetase
PDB	Vorläufer-dirigierte Biosynthese (precursor directed biosynthesis)
PKS	Polyketidsynthase
PPTase	4'-Phosphopantetheinyl-Transferase
PUFAs	Mehrfach-ungesättigte Fettsäuren (Polyunsaturrated fatty acids)
RIPP	Ribosomal produzierte und posttranslational modifizierte Peptide
T-Domäne	Thiolierungsdomäne
TE-Domäne	Thioesterasedomäne
TF	Transkriptionsfaktor

Abbildungsverzeichnis

Tabellenverzeichnis

1 Einleitung

1.1 Die Biologie basaler Pilze

1.1.1 Der Mensch und basale Pilze

Über 155.000 Pilzarten sind aktuell bei der *Global Biodiversity Information Facility* hinterlegt [1]. So groß diese Zahl scheint, so klein wirkt sie im Gegensatz zu Schätzungen verschiedener Wissenschaftler:innen, die von 2.2 bis 5.1 Millionen Pilzarten insgesamt ausgehen [2, 3]. Um in dieser Menge den Überblick nicht zu verlieren, ist eine zuverlässige Ordnung, eine eindeutige Phylogenie, notwendig.

Bis Ende des 20. Jahrhunderts basierte die Einteilung von Pilzen auf morphologischen Eigenschaften. Die *Eumycota*, die echten Pilze, wurden in vier Abteilungen eingeteilt: die Ständerpilze (*Basidiomycota*), Schlauchpilze (*Ascomycota*), Tröpfchenpilze (*Chytridiomycota*) und die Jochpilze (*Zygomycota*) [4]. Letztere erhielten ihre Bezeichnung durch jochartige Strukturen die sich während der Sporenreifung bilden [5]. Fortschritte in der Molekularbiologie, besonders im Bereich der Sequenziertechnik und Bioinformatik, sowie der Eintritt in das „genomische Zeitalter“ führten dazu, dass Stammbäume nicht mehr nur auf Grundlage von morphologischen Merkmalen erstellt wurden. Heutzutage geschieht dies anhand von Sequenzvergleichen konservierter Gene und Sequenzen, z.B. der ribosomalen DNA [6]. Final führte dies dazu, dass die Zygomyceten nicht mehr als eigenständige Abteilung angesehen werden, da es sich bei diesen um eine paraphyletische Gruppe handelt [7, 8]. Seitdem wurden viele ehemalige Zygomyceten den Abteilungen der *Mucoromycota* und *Zoopagomycota* zugeordnet. Diese werden, zusammen mit allen Nicht-Dikarya Pilzen, als basale Pilze oder früh-entwickelte Pilze (early-diverging fungi, EDF) bezeichnet [9]. Die *Mucoromycota*, welche die Kerngruppe der ehemaligen *Zygomycota* enthält, lassen sich noch in drei Unterabteilungen einteilen: die *Mucoromycotina*, die *Mortierellomycotina* und die *Glomeromycotina* [10].

Wir kennen basale Pilze wie *Rhizopus stolonifer* größtenteils nur als Schimmelpilze auf Brot, Erdbeeren oder Tomaten [11]. Im starken Kontrast dazu stehen Asco- und Basidiomyceten: Diese Pilze und ihre Stoffwechselprodukte finden u.a. Anwendung in Bäckereien, Brauereien und auf Weingütern zur Produktion von Lebensmitteln, sowie in der (agro)chemischen und pharmazeutischen Industrie. Besonders prominent sind Basidiomyceten, da viele Arten im Herbst als Ständerpilze im

Wald zu finden sind und die populäre Vorstellung von Pilzen dominieren.

Höhere Pilze werden pharmazeutisch zur biotechnologischen Gewinnung von Wirk- und Hilfstoffen angewendet. Antibiotika wie das Benzylpenicillin (**1**) oder das Griseofulvin (**2**), Immunsuppressiva wie das Ciclosporin A (**3**) und andere Arzneistoffe wie Ergotamin (**4**) und Lovastatin (**5**) stellen pilzliche Naturstoffe dar (Abbildung 1) [12]. Derartige pharmazeutisch bedeutsame Beispiele sucht

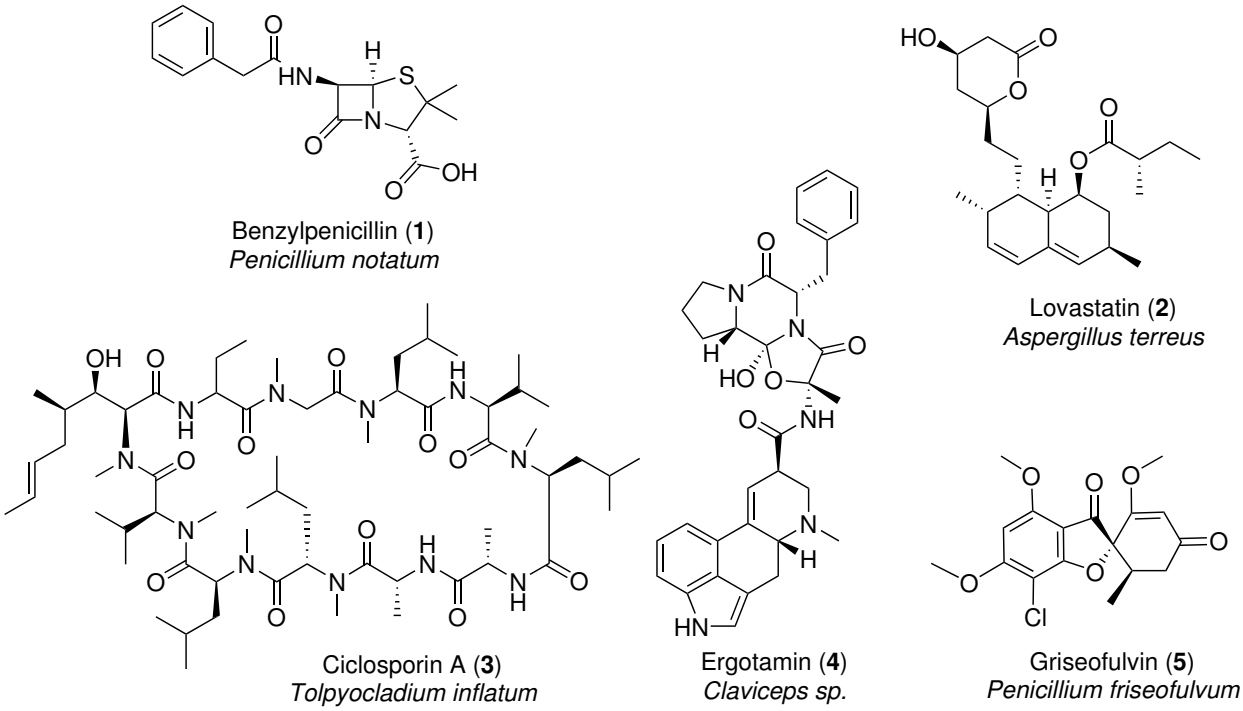

Abbildung 1: Arzneistoffe und Leitstrukturen aus Pilzen

man bei den basalen Pilzen vergeblich. In der Naturstoffforschung hält sich das Dogma, dass diese nicht zu einer eigenständigen, umfangreichen Naturstoffproduktion befähigt sind [13, 14]. Die Herkunft und Beweggründe für diese These lassen sich nicht mehr nachvollziehen. Es ist unklar, ob basale Pilze als Reservoirs übersehen wurden oder ob Ansätze zur Isolation von Naturstoffen scheiterten. Das zugrundeliegende Dogma herauszufordern stellt den Grundgedanken dieser Arbeit dar.

Neben ihrer ökologischen und pharmazeutischen Bedeutung können Pilze als Humanpathogene auftreten. Neben *Candida albicans* (Candidose), *Trichophyton rubrum* (Fußpilz), *Cryptococcus neoformans* und *Aspergillus fumigatus* (beide Atemwegsinfektionen), die ubiquitär verbreitete (fakultative) Pathogene darstellen, existieren einige humanpathogene basale Pilze. So können Stämme der

Gattung *Mucor* schwere Gewebsinfektionen auslösen [15]. Im Zuge der weltweiten Corona-Pandemie 2020 kam es v.a. in Indien zu einer Häufung von Fällen, in denen *Mucor*-Arten Auslöser von Superinfektionen war [16].

1.1.2 Biotechnologische Anwendung basaler Pilze

Im asiatischen Raum werden Arten der Gattungen *Rhizopus, Mucor, Actinomucor* und *Amylomyces* schon seit Jahrtausenden zur Lebensmittelproduktion eingesetzt [17, 18]. Das indonesische 'Tempeh', wird dabei aus Sojabohnen durch Mischfermentationen mithilfe von Pilzen wie *Rhizopus oryzae* und nützlichen Bakterien hergestellt [19]. Es zeichnet sich durch einen hohen Protein- und Vitamin B_{12}-Gehalt, aber auch seinen ungewöhnlichen Geschmack aus [20]. Ähnliche Produkte werden in China 'Sufu' genannt. Dabei handelt es sich um fermentierten Tofu, der mithilfe verschiedenen *Mucor*-, *Rhizopus*- oder *Actinomucor*-Stämmen hergestellt werden kann. In Indien und dem Himalaya werden aus verschiedenen stärkehaltigen Substraten 'jnards', süß-saure alkoholische Getränke, durch Fermentation mit *Mucor* und *Rhizopus* hergestellt [21, 22]. Gleichsam finden niedere Pilze in geringerem Umfang Anwendung in der Biotechnologie und Biotransformation. Organische Säuren wie Milchsäure oder Fumarsäure [23–25], β-Carotin [26, 27] oder Enzyme, wie Amylasen [28], Cellulasen [29] oder Hydroxylasen [30], werden von diesen produziert und finden industriell Verwendung.

Das wohl bekannteste biotechnologische Anwendungsfeld ist die Produktion von mehrfach-ungesättigten Fettsäuren (polyunsaturated fatty acids, PUFAs) durch den ölhaltigen Pilz *Mortierella alpina* und andere *Mortierella*-Stämme [31, 32]. Zwar konnte für viele *Mortierellaceae* gezeigt werden, dass diese PUFAs produzieren, doch sind die Titer in *M. alpina* am höchsten [33–35]. Da Arachidonsäure (AA) bis zu 78% der Gesamtfettsäuren und bis zu 25% der trockenen Biomasse ausmacht, erlaubt dies eine einfache Isolation und Aufreinigung [31]. Anwendung findet Öl aus *M. alpina* vor allem in Säuglingsanfangs- und Folgenahrung [32, 36]. Vorteile gegenüber herkömmlichen AA- und Docosahexaensäure (DHA)-reichen Fisch-Ölen sind dabei die Reduktion der Überfischung und die erhöhte Verbrauchersicherheit durch die Abwesenheit von z.B. Dioxin oder Schwermetallen [37].

1.1.3 Die Gattung *Mortierella*

Innerhalb des Subphylums der *Mucoromycota* ist die Ordnung *Mortierellales* mit rund 125 Arten zu finden [6, 38]. Namensgebend war hierbei die Gattung *Mortierella* (Phylum *Mucoromycota*, Subphylum *Mortierellomycotina*, Ordnung *Mortierellales*, Familie *Mortierellaceae*), welche 1863 erstmals durch E. Coemans beschrieben wurde und nach M. Du Mortier benannt worden ist [39]. Als saprotrophe Bodenpilze sind *Mortierellaceae* ubiquitär in allen Klimazonen anzutreffen [40–43]. *Mortierellaceae* sind schnell wachsende Pilze, die als Erstbesiedler mit verschiedensten Stickstoffquellen und einem breiten Temperaturfenster zurechtkommen. Ihre biologische Nische teilen sie sich mit Bakterien, anderen Bodenpilzen, Pflanzen und Insekten (siehe Abbildung 2).
Basale Pilze der engverwandten Unterabteilungen *Glomeromycotina* und *Mucoromycotina* können als Mykorrhizapilze mit Pflanzen auftreten [44]. Aus der Abteilung der *Mortierellomycotina* sind nur einige Endophyten bekannt, während die meisten Vertreter nicht zu den mykorrhizabildenden Pilzen gehören [45]. So konnten auf Wurzeln von Fichten und Erlen *Mortierella*-Arten am häu-

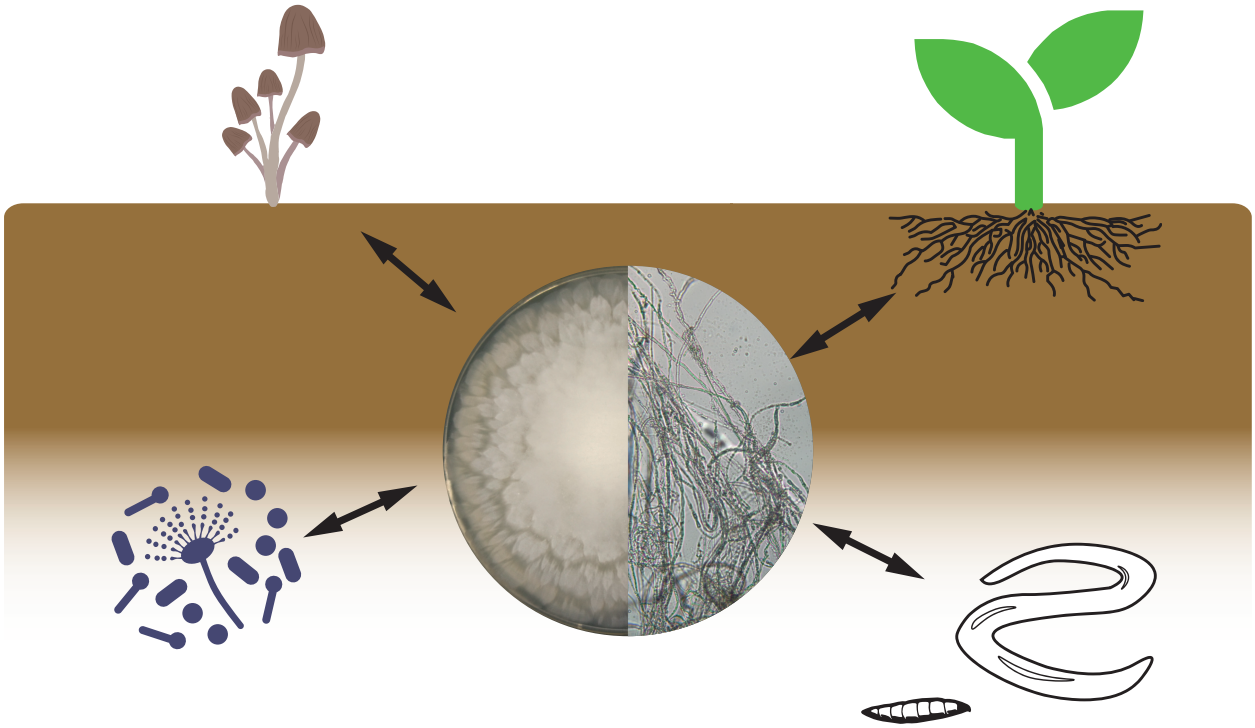

Abbildung 2: Interaktionspartner von *Mortierella alpina* im Boden; zusammen mit Pflanzen, Insekten, Tieren und anderen Mikroorganismen teilt sich *M. alpina* eine biologische Nische; *M. alpina* als Plattenaufsicht (links) und mikroskopische Aufnahme des Pilzmyzels mit granulären Pilztröpfchen (rechts)

figsten nachgewiesen werden [46]. Für einige *Mortierellomycotina* konnte gezeigt werden, dass sich deren Anwesenheit positiv auf die umgebende Flora auswirkt. So fördert *M. hyalina* das Wachstum der Acker-Schmalwand (*Arabidopsis thaliana*) um bis zu 50% [47]. Neben *M. hyalina* konnten auch für *M. alpina, M. elongata* und *M. capitata* derartige Effekte nachgewiesen werden [48–50]. Ursächlich hierfür kann sein, dass *Mortierella* die Bioverfügbarkeit von Phosphor und Eisen im Boden erhöht [50]. Ein weiterer Teil des positiven Effekts auf die Flora lässt sich auf die Lipid-Produktion zurückführen. Ausgebracht auf 100 m^2 Ackerfläche, wirken schon wenige Milligramm eines Arachidonsäure-haltigen Extrakts aus *Mortierella hygrophila* positiv auf die Resistenz von Kartoffelpflanzen gegenüber Krankheiten [51]. Ob dies auf eine antifungale Wirkung der Fettsäuren-Mischung auf fruchtschädigende Pilze, oder einer Steigerung der Resilienz der Pflanzen zurückzuführen ist, wurde nicht abschließend geklärt.
Die räumliche Nähe der *Mortierellaceae* mit Bodenbakterien ist vermutlich ursächlich für die Entwicklung von symbiotischen und endosymbiotischen Partnerschaften. So wurden sowohl *Mycoplasma*-verwandte Endosymbionten (*Mycoplasma*-related endosymbionts, MRE) als auch *Burkholderia*-verwandte Endosymbionten (*Burkholderia*-related endosymbionts, BRE) in *Mortierellaceae* nachgewiesen [52–55]. Endosymbionten-beherbergende Pilze (Wirte bzw. engl. „hosts“) sind dabei über alle *Mortierellomycotina*-Untergruppen verteilt [53]. In verschiedenen Untersuchungen konnten in 3-13% der Stämme Endosymbionten nachgewiesen werden [52, 53]. Der Einfluss von Endosymbionten auf *M. alpina* und andere basale Pilze, besonders im Bezug auf die Produktion von Naturstoffen, wird nachfolgend noch thematisiert (siehe Kapitel 1.4).

1.2 Pilzliche Naturstoffe und deren Synthese

1.2.1 Allgemeine Prinzipien der Naturstoffsynthese

Weit gefasste Definitionen verstehen unter Naturstoffen niedermolekulare Moleküle die aus biologischen Quellen stammen [56]. Genauer ist die Unterscheidung von Primär- und Sekundärmetaboliten, wobei der Übergang zwischen diesen fließend ist. Während Primärmetabolite für Wachstum, Fortpflanzung und andere überlebenswichtige Prozesse biologischen Lebens benötigt werden, stellen Sekundärmetabolite einen Weg für Mikroorganismen dar, um mit ihrer Umwelt zu interagieren. So dienen diese zur Abwehr von Fraßfeinden [57], der Aufnahme von Mineralstoffen [58], als Virulenzfaktoren [59], zur Sporenbildung [60], zur Kommunikation wie dem Quorum-Sensing [61] oder

zur Verteidigung gegen andere Mikroorganismen, die Konkurrenten um wichtige Nährstoffe oder weitere Ressourcen darstellen [62].

Neben Polyketiden und Terpenen/Terpenoiden zählen peptidische Naturstoffe zu den am weitesten verbreiteten Metaboliten [63, 64]. Oft missachtet, stellen volatile organische Verbindungen eine inoffizielle vierte Gruppe dar, deren Vertreter zwar eine gemeinsame physikochemische Eigenschaft aufweisen, aber aus verschiedenen Biosynthesewegen stammen [65]. Neben Alkoholen, Ketonen und einfachen aromatischen Verbindungen können auch bestimmte Terpene und Polyene zu den Volatilen gezählt werden [66].

Naturstoffe werden von einem oder mehreren Enzymen produziert. Sind mehrere Eznyme an der Biosynthese beteiligt, so können deren Gene zusammen „geclustert“ in einem Locus vorliegen [67]. Ein für eine Terpencyclase, Polyketidsynthase oder nichtribosomale Peptidsynthetase (NRPS) codierendes Gen stellt dabei meist das zentrale Biosynthesegen dar [68]. Betrachtet man die Verteilung der Metabolite und Enzyme innerhalb der Asco- ,Basidio- und Zygomyceten, so lassen sich Unterschiede erkennen. Während Ascomyceten zu multimodularen Polyketidsynthase (PKS)-, nichtribosomale Peptidsynthetase (NRPS)-Genen und Hybriden aus diesen tendieren, sind in Basidiomyceten vorrangig für Terpencyclasen, PKS-NRPS-Hybride oder für NRPS-ähnlichen-Synthetasen codierende Gene finden [68, 69]. In Zygomyceten lassen sich nach aktuellem Stand fast ausschließlich NRPS- und Terpencyclasen-codierende Gene finden [70, 71].

Terpene und Terpenoide werden dabei aus den Isomeren Isopentenyl-Pyrophosphat (IPP) und Dimethylallyl-Pyrophosphat (DMAPP) synthetisiert. Beide Metabolite stammen aus dem Primärmetabolismus, wobei diese je nach Organismus aus Acetyl-CoA oder Pyruvat und Glycerinaldehyd-3-Phosphat aufgebaut werden [72]. Zwischen DMAPP und einem oder mehreren IPP-Molekülen kommt es durch Kondensation zur Ausbildung von C-C Bindungen und dadurch zur Bildung der multimeren Zwischenverbindungen [73]. Anschließend werden diese durch weitere Enzyme zusätzlich modifiziert

Polyketide werden hauptsächlich aus Acetyl-CoA und Malonyl-CoA aufgebaut, die biosynthetisch aus dem Primärstoffwechsel stammen [74]. Auf ein biochemisch aktiviertes Startermolekül werden die Monomere schrittweise durch decarboxylierende Claisen-Kondensation übertragen. Strukturelle Organisation und katalysierte Reaktionen ähneln dabei der Biosynthese von Fettsäuren [75].

Aminosäure-abgeleitete Naturstoffe können in Pilzen durch verschiedene Enzyme hergestellt werden. Dabei wird zwischen ribosomal produzierten und posttranslational modifizierten Peptiden

(RIPPs) und Ribosom-unabhängig produzierten Peptiden unterschieden. RIPPs traten dabei erst kürzlich in den Fokus der Naturstoffforschung und stellen ein immer noch wachsendes Feld dar [76]. Für Organismen ist dies ein metabolisch günstiger Weg der Naturstoffproduktion, da die benötigte enzymatische Maschinerie, das Ribosom, bereits vorhanden ist. Während die RIPP-Synthese auf 20 proteinogene Aminosäuren (AS) beschränkt ist, trifft dies für die anderen peptidischen Naturstoffklassen nicht zu. NRPSs stellen unabhängig vom Ribosom und von mRNA Peptide her. Dabei können neben proteinogenen AS auch nicht-proteinogene AS wie β-Aminosäuren, α-Hydroxysäuren, halogenierte AS oder viele weitere in das synthetisierte Peptid eingebaut werden [77]. Häufig übersehen, stellen monomere Naturstoffe aus AS eine interessante Naturstoffklasse dar. Ohne den Bedarf riesiger Multienzymkomplexe können aus Aminosäuren Isoxazole wie das Muscimol [78] oder Indolamine wie das Psilocybin [79] synthetisiert werden. Im folgenden wird auf die ribosomal-unabhängige Naturstoffsynthese genauer eingegangen.

1.2.2 Nichtribosomale Peptidbiosynthese

Nichtribosomale Peptidsynthetasen (NRPSs), im klassischen Sinn, sind multimodulare Megaenzymkomplexe [80]. Die Basis eines Moduls, der kleinsten Ordnungseinheit eines solchen Komplexes, besteht dabei aus einer Adenylierungsdomäne (A-Domäne), einer Thiolierungsdomäne (T-Domäne), welche auch Peptid-Binde-Domäne (peptide carrier protein, PCP) genannt wird und der Kondensationsdomäne (C-Domäne) [77, 81, 82]. Die inaktive apo-Form der NRPSs wird zuerst in die aktive holo-Form überführt, indem der 4'-Phosphopantetheinyl (4'-PP)-Arm posttranslational auf einen konservierten Serin-Rest der T-Domäne durch eine 4'-Phosphopantetheinyl-Transferase (PPTase) übertragen wird [83]. Die A-Domäne aktiviert bzw. adenyliert eine AS mittels Adenosin-5'-triphosphat (ATP) und lädt diese anschließend auf den 4'-PP-Arm der katalytisch inaktiven T-Domäne (Abbildung 3, Schritt 1) [84]. Mithilfe dieser werden die gebundenen Aminosäuren und Peptide zwischen den Domänen und Modulen transportiert [85]. Anschließend kann die gebundene AS in das aktive Zentrum der C-Domäne transloziert werden, wo sie auf die aktivierte und T-Domänen-gebundene Aminosäure des nächsten Moduls übertragen wird (Abbildung 3, Schritt 2). Die wachsende Peptidkette wird so von einer T-Domäne auf die Nächste übertragen. Die Termination der NRPS-Synthese und die Abspaltung des Peptids erfolgt final durch Thioesterasedomänen (TE-Domänen) oder spezialisierte terminale C-Domänen (C_T) (Abbildung 3,

Schritt 3) [86, 87]. In Pilzen und selten auch in Bakterien kann die NRP-Biosynthese durch Reduktasedomänen terminiert werden [69, 88]. Neben den zuvorgenannten existieren weitere spezialisierte Domänen wie Methylierungs-, Formylierungs-, Oxidations-, Heterocyclisierungs-, Reduktions- oder Epimerisierungsdomänen, die verschiedenste Reaktionen katalysieren können [77, 89].

In Analogie zu PKS wurde kürzlich ein Klassifizierungssystem für ribosomal-unabhängige Peptid-

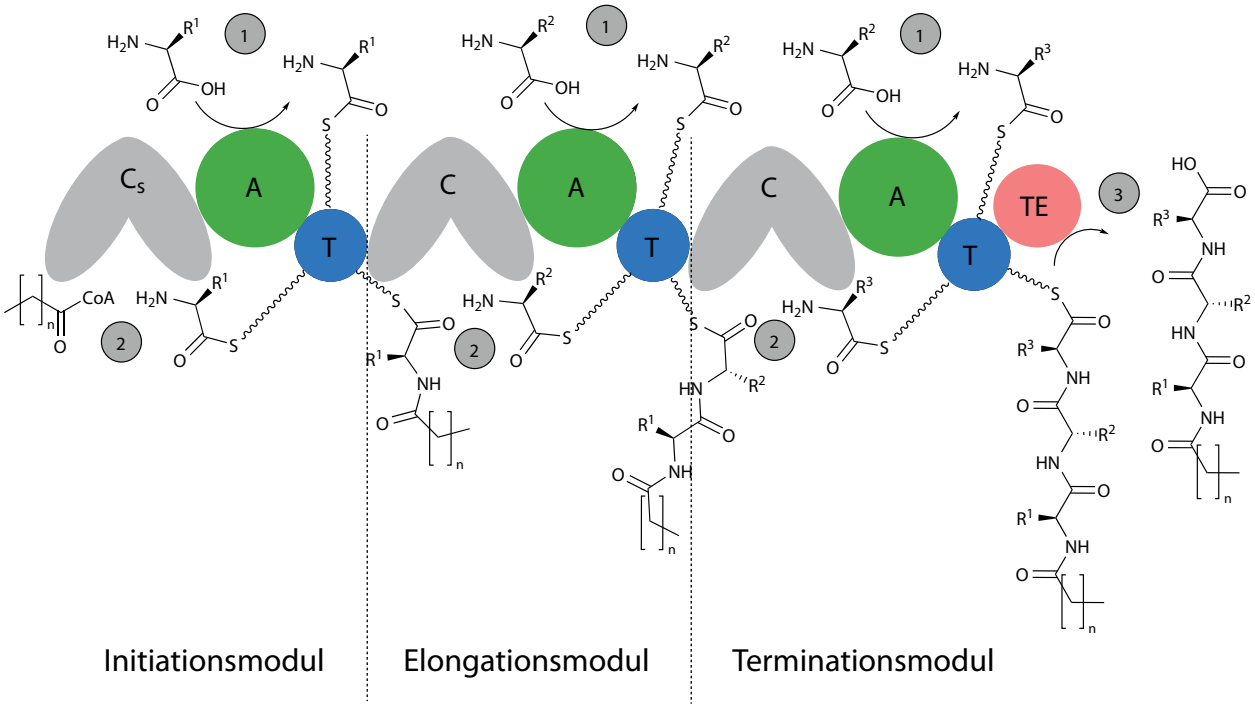

Abbildung 3: Bildung eines nicht-ribosomalen Peptids durch eine multimodulare NRPS; die dargestellte Starter-Kondensationsdomäne (C_S-Domäne) ist dabei nicht in allen NRPSs vorhanden.

synthesemaschinerien vorgeschlagen [80]. Unterscheidungsmerkmale sind dabei die Abhängigkeit von Transportdomänen, welcher Proteinfamilie die Enzyme angehören, welche die Amidbindung katalysieren und ob die Synthetasen einen modularen Aufbau besitzen. „Klassische“ kanonische NRPSs entsprechen dabei Typ I oder Typ II, je nachdem, ob die Domänen als lineare Megaenzyme auftreten. Für diese Megaenzyme entwickelte sich kurz nach deren Entdeckung die Hypothese der Kollinearität zwischen Peptidlänge und Modulzahl. So entspricht die Anzahl der Module der Anzahl der Aminosäuren im fertigen Peptid [90]. Obwohl dies für viele NRPSs gilt, können NRPSs auch iterativ arbeiten, wobei die einzelnen Module mehrmals durchlaufen werden [91]. In Typ III ribosomal-unabhängigen Peptidsynthetasen werden aktivierte Aminosäuren an den 4'-PP Arm einer T-Domäne gebunden, doch wird die Kondensation nicht durch eine C-Domäne, sondern z.B.

eine Transglutaminase, katalysiert. Bei Enzymen der Klassen IV und V ist die Bildung der Amidbindung unabhängig von Transportproteinen, wobei die Aminosäuren tRNA-gebunden vorliegen können.

Adenylierungsdomänen sind Teil der ANL Enzymfamilie. Diese enthält Acyl-CoA Synthetasen, NRPS A-Domänen und Luziferase-Enzyme [92]. A-Domänen katalysieren dabei zwei Teilschritte. Im ersten Teilschritt werden eine Aminosäure und ATP als Substrate in ein Aminoacyl-Adenosin-5'-monophosphat (AMP)-Intermediat überführt. Im zweiten Schritt wird der Acyl-Rest auf eine Thiolgruppe unter Thioesterbildung übertragen [92].

Strukturell sind A-Domänen 60 kDa schwere Enzyme und bestehen aus zwei Subdomänen, A_{core} und A_{sub}. Innerhalb der schwereren A_{core} Subdomäne (50 kDa) werden Substrat und ATP gebunden, während beide Subdomänen zusammen das Substrat koordinieren. Für die Aktivierung und Übertragung der Aminosäure nimmt die kleinere (ca. 10 kDa) und flexible A_{sub} verschiedene Positionen ein, um hydrolyseanfällige Zwischenprodukte vor Wasser zu schützen und eine Translokation der T-Domäne zu ermöglichen. Verteilt über A_{core} und A_{sub} sind zehn konservierte Motive zu finden (A1-A10), die sowohl strukturgebende, als auch katalytische Aufgaben besitzen [90]. In den Motiven A4 und A10 sind die zwei hochkonservierten AS Asparaginsäure (D235) in A_{core} und Lysin (L517) in A_{sub} zu finden. Für die Seitenketten dieser zwei AS konnte durch Kokristallisation von Substrat und Domäne gezeigt werden, dass diese die Amino- und Carboxylgruppe des akzeptierten Substrats stabilisieren [84]. α-Hydroxy-Säuren-akzeptierende A-Domänen können dabei Serin oder Valin anstatt Asparaginsäure in ersterer Position besitzen [93–95]. Die Seitenketten von bis zu acht weiteren AS bilden zusammen mit D235 und L517 eine Bindetasche für das Substrat [96]. Entscheidend für die Selektivität einer A-Domäne sind Polarität, Sterik, Größe und Aromatizität der Seitenketten dieser zehn AS. Zusammen werden diese als nichtribosomaler Code bezeichnet. In Anlehnung an dessen Entdecker in den späten 1990ern wird dieser auch Stachelhaus-Code genannt [96]. Bioinformatische Algorithmen können heute, basierend auf bereits charakterisierten Domänen, Substratspezifitäten uncharakterisierter Domänen vorhersagen. Eine Übertragbarkeit des Codes von bakteriellen Domänen, wo dieser ausgezeichnet etabliert ist, auf pilzliche Domänen ist nur in Einzelfällen möglich [97]. Zu diesen Ausnahmen zählen L-δ-(α-Aminoadipoyl)-L-cysteinyl-D-Valin-Synthetasen (ACV-Synthetasen) bei denen bakterielle Domänen auf Pilze durch horizontalen Gentransfer übergegangen sind [98]. Selbst zwischen pilzlichen A-Domänen lässt sich der nichtribosomale Code oft nicht zuverlässig vergleichen [97, 99]. Innerhalb von Adenylierungsdomänen können

Methylierungsdomänen (M-Domänen) und andere Domänen codiert sein. So sind drei A-Domänen der Enzyme TioS und TioN, verantwortlich für die Synthese der Thiocoraline, unterbrochen von M-Domänen [100]. Die A-Domänen sind dabei zwischen A3 und A4 sowie zwischen A8 und A9 unterbrochen. Für die Biosyntheseenzyme der Kutzneride [101], der Microcystine [102] und weiterer Enzyme sind ähnliche Beispiele bekannt [103]. Der Grund für die Platzierung von Auxiliardomänen innerhalb der A-Domänen ist zum jetzigen Stand unbekannt.

Kondensationsdomänen. Anders als bei A-Domänen ist der Reaktionsmechanismus von Kondensationsdomänen nicht abschließend geklärt. Als V-förmige, 50 kDa große Pseudodimere bestehen C-Domänen aus einer N-terminalen Domäne (C_{NTD}) und einer C-terminalen Domäne (C_{CTD}) [104]. Durch ihren nahezu symmetrischen Aufbau besitzen C-Domänen zwei Bindetaschen; auf der Akzeptorseite und der Donorseite [105]. In deren Mitte befindet sich das aktive Zentrum mit einem hoch konservierten HHxxxDG Motiv [90]. Mehrere postulierte Reaktionsmechanismen gehen davon aus, dass das zweite Histidin des konservierten Motivs Teil des aktiven Zentrums ist [87]. Beide Bindetaschen zeigen Selektivität gegenüber der Chiralität und Sterik der Seitenkette der akzeptierten Aminosäuren. Dabei weist die Donorseite eine höhere Substratpromiskuität auf [106]. Diese akzeptieren oft nur die AS, welche von der benachbarter A-Domäne aktiviert worden ist [107].
Neben $^{L}C_{L}$-Domänen und $^{D}C_{L}$-Domänen, die Amidbindungen zwischen Aminosäuren der indizierten Konfigurationen katalysieren, existieren weitere Subtypen von C-Domänen [108]. Duale Epimerisierungs- und Kondensationsdomänen (duale E/C Domänen) katalysieren sowohl die Kondensationsreaktion, als auch die Epimerisierung der C-terminalen Aminosäure. C_S-Domänen sind vor der ersten A-Domäne codiert, katalysieren die Acylierung der ersten Aminosäure und sind meist an der Biosynthese von Lipopeptiden beteiligt [108, 109]. In seltenen Fällen, wie z.B. bei der Ciclosporin A (**3**) -Biosynthese, sind diese C_S-Domänen inaktiv und tragen vermutlich lediglich zur Stabilität des ersten Moduls bei [110]. Duale E/C-Domänen und C_S-Domänen verfügen ebenfalls über das oben genannte Doppel-Histidinmotiv, wobei duale E/C-Domänen ein zweites ähnliches Motiv besitzen [108]. Zusätzlich sind C-Domänen dazu befähigt, eine Vielzahl verschiedener Reaktionen zu katalysieren: neben Kondensationen können Epimerisierungen, Heterocyclisierungen, Makrocyclisierungen, terminale Abspaltung und β-Lactam-Bildung stattfinden [87]. Daneben können Pictet-Spengler-Reaktionen katalysiert und Oxidasen rekrutiert werden.

1.2.3 Naturstoffforschung im genomischen Zeitalter

Frühe Naturstoffforscher:innen mussten sich auf organoleptische Methoden zur Identifizierung von Naturstoffquellen verlassen. So handelt es sich bei den zuerst untersuchten pilzlichen Naturstoffen um Farbstoffe wie Atromentin [111] oder Xylindein [112]. Pflanzen und Pilze, die traditionell in der Medizin verwendet wurden, waren die wichtigsten Reservoirs für neue Substanzen [113].
Mit Fortschreiten der analytischen Chemie, der Entwicklung von HPLC, IR, Kernspinresonanz (Nuclear Magnetic Resonance, NMR) und weiterer spektroskopischer Methoden, eröffneten sich viele Möglichkeiten der Naturstoffisolation und -charakterisierung. Sobald erste Genomsequenzen zur Verfügung standen wurde jedoch offensichtlich, dass durch chemisch-analytische Methoden nur ein Teil des Naturstoffreservoirs von Pilzen und Bakterien aufgeklärt wurde. Allein in verschiedenen *Streptomyceten* fanden Forscher:innen fünfmal mehr Gencluster als beschriebene Naturstoffe [114, 115]. „Stille“ Gencluster, die unter natürlichen Bedingungen nicht exprimiert sind, wurden in der folgenden Zeit zum Forschungsobjekt vieler Naturstoffforscher:innen. Mit verschiedenen Kultivierungsbedingungen, Supplementierung von Substraten, Kokultierung mit anderen Organismen oder durch Zugabe von Chemikalien wurde so nach dem OSMAC-Prinzip (**O**ne **S**train-**MA**ny **C**ompounds) versucht, stille biosynthetische Gencluster (BGCs) zu aktivieren [116–118]. „genome mining“, also die gezielte Suche nach Genclustern, basierend auf Methoden der Genomanalytik, ist seitdem Grundlage vieler Forschungsansätze [119].
Die Detektion dieser Gencluster beruht dabei auf automatisierten Sequenzvergleichen mit Genen und Proteinen bereits bekannter Naturstoffbiosynthesewege. So können NRPS-Domänen und deren akzeptierte Substrate über konservierte Motive und den nichtribosomalen Code vorhergesagt werden [90, 96]. Durch Programme wie ANTIsmash [120, 121], die verschiedene Algorithmen der Gen- und Proteinvorhersage zusammenfassen, wurden solche Vorhersagen einer breiten Masse an Wissenschaftler:innen zugänglich. Diese vergleichenden Ansätze sind auf umfassende Datenbanken angewiesen, wie am Beispiel der RIPP zu sehen. Durch die steigende Anzahl beschriebener RIPP BGCs konnte ANTIsmash, das anfänglich in Version 3.0 nur Lanthipeptide vorhersagen konnte, kontinuierlich verbessert werden, sodass in Version 6.0 auch bereits modifizierende Enzyme der RIPP-Synthese sicher vorhergesagt identifiziert werden können [121].
Um die Qualität bioinformatischer Vorhersagen zu verbessern und um neue Biosynthesewege aufzuklären, wurden Projekte wie das „1000 fungal genomes project“ gestartet. Ab 2014 sollten innerhalb

von fünf Jahren je mindestens zwei Referenzgenome aus 500 pilzlichen Familien sequenziert werden [122–124]. Bis heute wurden über 2250 pilzliche Genome sequenziert und frei zugänglich gemacht. Diese Menge an verfügbaren Daten ermöglicht mittlerweile weitaus umfassendere Untersuchungen, wie z.B. über die Verteilung von BGCs [69]. Zusammen mit Transkriptomdaten lässt sich so ein umfänglicher Einblick in die biosynthetische Kapazität der Pilze erlangen. Während genome mining und die Vorhersage vermuteter Strukturen computerisierbar und automatisierbar ist, beruht der anschließende (bio)chemische Nachweis immer noch größtenteils auf händischer Laborarbeit.

1.3 Naturstoffsynthese in basalen Pilzen

Trotz des weit verbreiteten Dogmas, Zygomyceten wären nicht zur Produktion von Naturstoffen befähigt, finden sich einige aus Zygomyceten stammende Metabolite [13]. Das C18-Terpenoid Trisporsäure (**6**) wird sowohl von *Mucor circinelloides*, *Blakeslea trispora*, als auch durch *Phycomyces blakesleanus* produziert und initiiert dort die Bildung von Zygosporen [125]. Ausgehend von β-Carotin werden Vorstufen von **6** wechselseitig von beiden Kreuzungstypen (engl. mating types) produziert und anschließend sezerniert, bis das Endprodukt für beide vorliegt [126, 127].
Auch Arten des Genus *Mortierella* scheinen Ausnahmen des oben genannten Dogmas darzustellen. So wurden in *M. elongata* (syn. *Podila elongata*) die beiden PKS-Produkte CJ-12950 (**7a**) und CJ-13357 (**7b**) nachgewiesen [128]. Aus *M. alpina* konnten mehrere peptidische Naturstoffe isoliert werden. Der Thrombininhibitor Ro-09-1679 (**8**) [129] fällt dabei durch sein C-terminales Arginal (Abbildung 4) auf, das wahrscheinlich durch Reduktion bei der Abspaltung von der NRPS entsteht. Die antimycobakterielle Verbindung Calpinactam (**9**) [130, 131], sowie die Arginin-enthaltenden Peptide MBJ-0173 (**10a**) und MBJ-0174 (**11**) [132] wurden ebenfalls in verschiedenen *M. alpina*-Stämmen entdeckt. In den letzten Jahren kamen zu diesem Portfolio noch Malpinin A-D (**10a**–**d**) und Malpibaldin A-B (**12a**,**b**) hinzu. Die einzelnen Metabolite dieser Naturstoffklassen weisen dabei eine gemeinsame Grundstruktur auf, unterscheiden sich aber in einzelnen Aminosäuren [133]. Die Mortiamide A-D (**13a**–**d**) konnten weiterhin aus *M. antarctica* isoliert werden [134]. Daneben wurden die antibakteriellen und antifungalen Trimethylbenzoesäure-Derivate Mortivinacin A und Mortivinacin B (**14a**,**b**) aus *M. vinacae* isoliert [135].
Aus dem basalen Pilz *Rhizopus chinensis* (Syn. *R. microsporus*), dem Auslöser der Reiskeimlingsfäule, konnte das Makrolid Rhizoxin (**15**) isoliert werden [136]. **15** wirkt dabei sowohl antifungal, als

auch zytostatisch in verschiedenen humanen und murinen Krebszelllinien [136, 137]. Beide Wirkungen sind auf die Bindung an β-Tubulin zurückzuführen, wodurch dessen Polymerisierung behindert und Zellteilung unterbunden wird [138]. Zwei Jahrzehnte nach der Entdeckung des Rhizoxins (**15**) konnten Endosymbionten in *Rhizopus* nachgewiesen werden [139]. Dabei wurde entdeckt, dass der Endosymbiont *Mycetohabitans rhizoxinica* (ehemals *Burkholderia rhizoxinica*) und nicht der Pilz Produzent des Naturstoffs ist [140, 141]. Dies prägte das Dogma der biosynthetisch inaktiven Zygomyceten weiter.

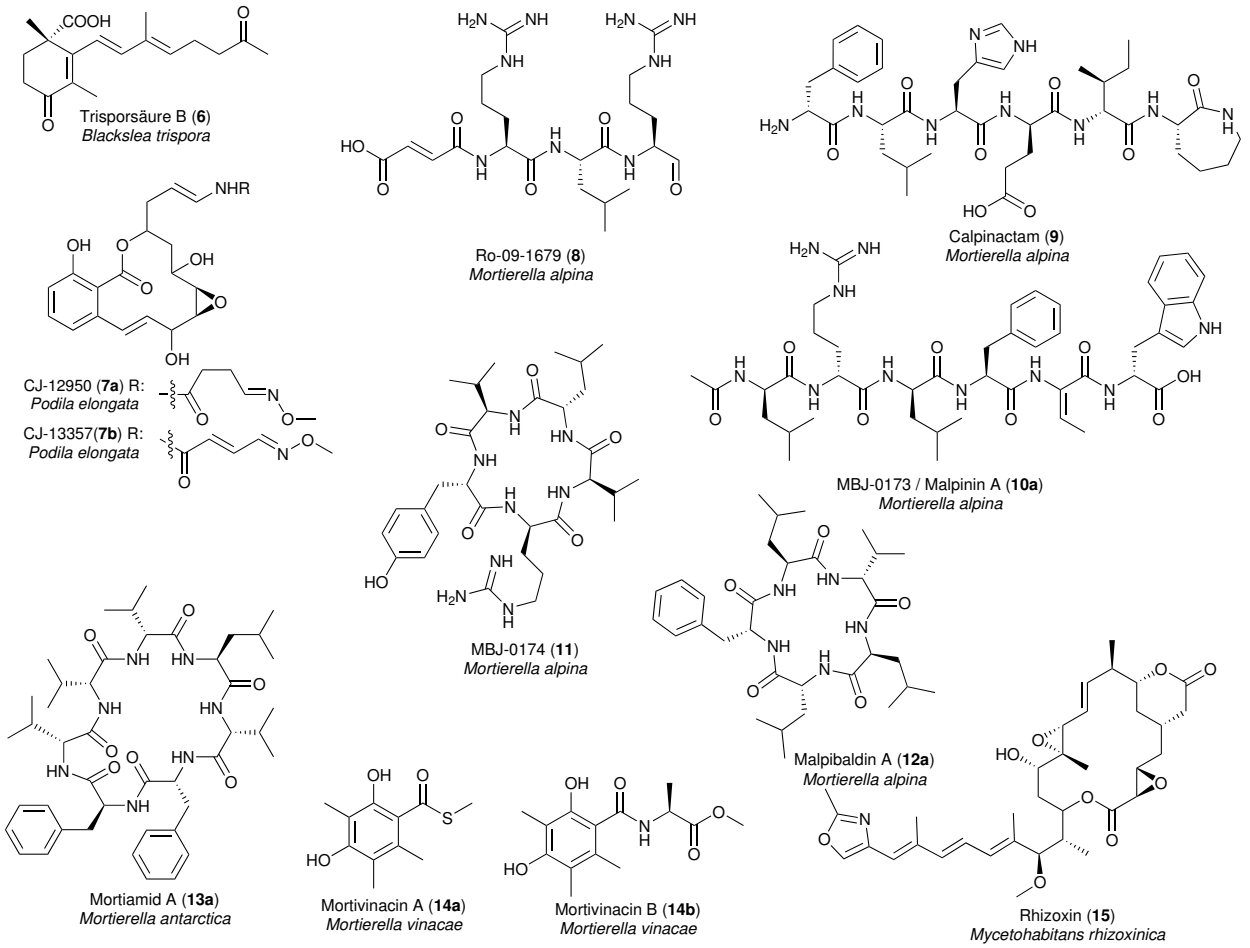

Abbildung 4: Aus basalen Pilzen isolierte Metabolite; für Metabolitklassen ist jeweils nur ein Vertreter dargestellt

1.4 Endosymbionten und deren Bedeutung

Interaktionen von Pilzen und Bakterien haben umfassende Auswirkungen auf alle Aspekte der Umwelt [142]. Dabei können Pilze und Bakterien in Konkurrenz stehen, kommensal koexistieren oder Symbiosen eingehen. Endosymbiose ist dabei eine Symbioseform, in der ein Partner als Endosymbiont innerhalb eines anderen Partners, des Wirts, lebt. Bisher sind solche Pilz-Bakterium-Endosymbiose-Partnerschaften fast ausschließlich in basalen Pilzen nachgewiesen worden. Zu den am besten untersuchten Symbiosepartnerschaften zählen: *Geosiphon pyriformis* (*Glomeromycota*) mit *Nostoc punctiforme* [143], *Rhizopus microsporus* (*Mucoromycota*) mit *Mycetohabitans rhizoxinica* [141], der arbuskuläre Mykorrhizapilz *Gigaspora margarita* (*Glomeromycota*) mit *Candidatus Glomeribacter gigasporarum* [144] oder *Mortierella elongata* (*Mucoromycota*) mit *Mycoavidus cysteinexigens* [145, 146]. Die Endobakterien sind dabei entweder den gramnegativen β-Proteobakterien und Cyanobakterien oder den *Mollicutes* zuzuordnen. Endocyten bilden eigene phylogenetische Klassen und stehen getrennt von frei lebenden Bakterien [53, 55].

Für den Gast ist der Vorteil dieser Beziehung klar, da dieser Nährstoffe und Metabolite des Wirts nutzen kann. So ist der Endosymbiont *M. cysteinexigens* auf die L-Cystein-Biosynthese seines Wirts angewiesen [146], während *M. rhizoxinica* Glycerin aus dem Primärstoffwechsels des Wirts als Kohlenstoffquelle verwendet [147]. Gleichzeitig sind Endosymbioten in ihren Wirten vor Einflüssen der belebten und unbelebten Umwelt geschützt. Für die Wirte kann die Beherbergung von Endosymbionten hingegen einen Nachteil darstellen. Für *Mortierella elongata* konnte gezeigt werden, dass dessen Endosymbionten sowohl das Wachstum, als auch die Bildung von Luftmyzel beeinträchtigt [53]. Ein Weg, wie die Endobakterien ihren Wirten nützen, scheinen Naturstoffe zu sein: Am Beispiel von *R. microsporus* und verschiedenen BRE konnte dies zuerst gezeigt werden. Die produzierten Naturstoffe Rhizoxin (**15**) [139], Rhizonin A-B (**16a**,**b**) [148], Holrhizin (**17**) [149] und Heptarhizin (**18**) [150] tragen zur Pathogenität des Komplexes aus Wirt und Endosymbiont bei. Necroxim A-B (**19a**,**b**) [151] sind hingegen für den Schutz des Wirts vor Nematoden verantwortlich. Gleichzeitig kontrolliert *M. rhizoxinica* über die Produktion von Naturstoffen die Sporulation seines Wirts, wobei der Mechanismus dieser Regulation unbekannt ist [152].

In *Mortierella verticillata* konnten die beiden PKS-Produkte CJ-12950 (**7a**) und CJ-13357 (**7b**), die strukturell mit den Necroximen verwandt sind, auf den BRE *Mycoavidus necroximicus* zurückgeführt werden [55]. Strukturell unterscheiden sich diese lediglich durch ein verestertes Lysin,

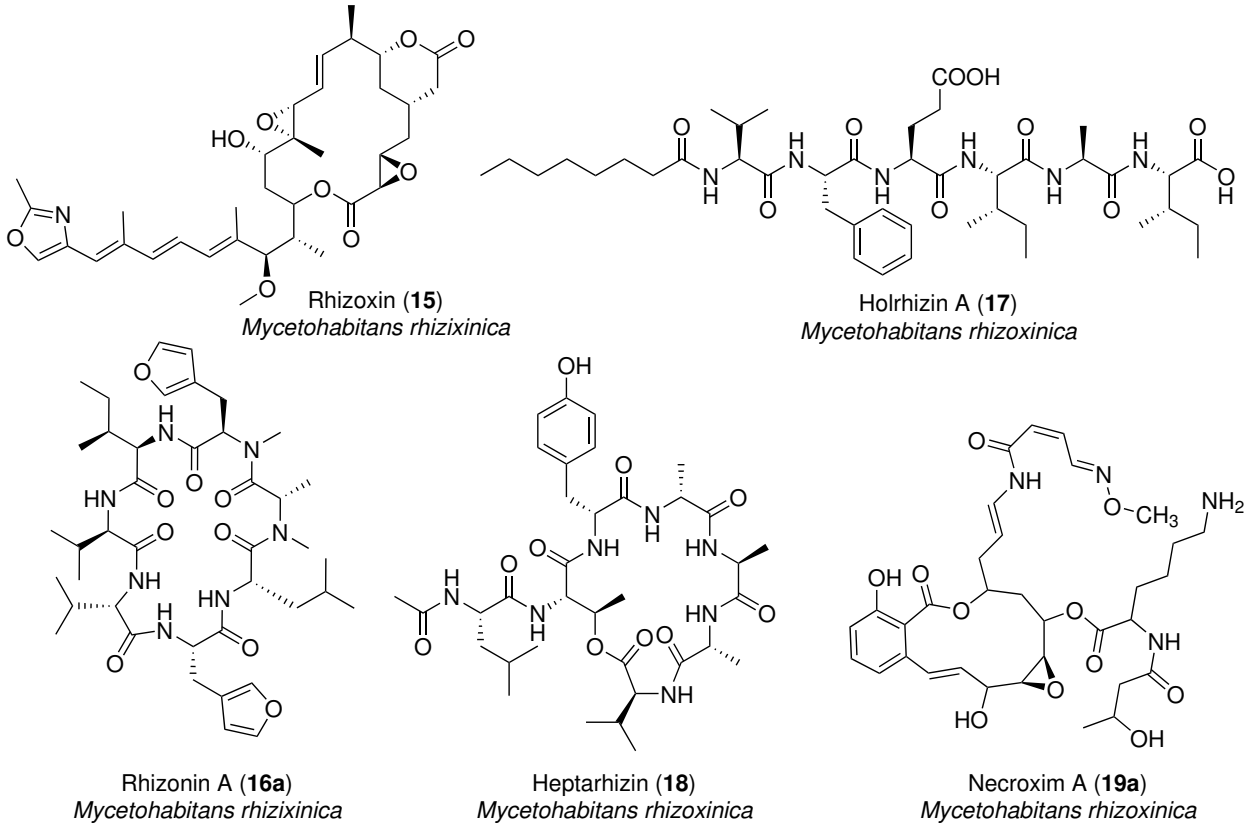

Abbildung 5: An Endosymbiont-Pilz-Interaktionen beteiligte Naturstoffe

welches bei den Necroximen (**19**) am Hauptring gebunden ist, während das komplexe bicyclische PKS-Grundgerüst mit dehydrierten Seitenketten identisch aufgebaut ist (Vgl. Abbildung 4 und 5). Wie bei den Necroximen, stellt die Produktion von **7a**,**b** durch den Endosymbionten einen Verteidigungsmechanismus für den Wirt gegen Fraßfeinde dar [55].

2 Zielsetzung

Im Gegensatz zu höheren Pilzen sind basale Pilze nicht dafür bekannt, in einem nennenswerten Umfang eigenständig Naturstoffe zu synthetisieren. Dies führt dazu, dass auch Pilze wie *Mortierella alpina*, in denen bereits Naturstoffe identifiziert worden sind, nicht im Fokus der Forschung stehen. Um basale Pilze als Reservoirs von bioaktiven Naturstoffen zu etablieren, sollten folgende Fragestellungen bearbeitet werden:

I Können in *Mortierellaceae* neue Naturstoffe identifiziert werden?
Mit bis zu 22 codierten NRPS-Genen zeigt *M. alpina* ein hohes Potential für neue Naturstoffe. Durch die Wahl verschiedener Kultivierungsbedingungen soll die Produktion neuer unbekannter Metabolite induziert werden. Deren Strukturaufklärung soll zum Verständnis der chemischen Diversität der Naturstoffe in *Mortierellaceae* beitragen.

II Lassen sich Naturstoffe mit konkreten pilzlichen Biosynthesegenen verknüpfen?
Da in der Vergangenheit vermeintlich pilzliche Naturstoffe als bakteriell identifiziert worden sind, soll der biosynthetische und evolutionäre Ursprung der Biosynthesegene untersucht werden. Naturstoffe wie Malpibaldine, Malpinine, Calpinactam oder Ro-09-1679 enthalten ungewöhnliche AS-abgeleitete Strukturen wie Dehydrobutyrin, Caprolactam oder Arginal, deren Biosynthese auch in höheren Pilzen und Bakterien nicht abschließend geklärt ist. Erkenntnisse aus der Aufklärung der Synthese in *M. alpina* könnten anschließend auf höhere Pilze übertragen werden.

III Übernehmen Naturstoffe in *M. alpina* ökologische Funktionen?
Für Naturstoffe wie das Calpinactam und die Malpinine konnten bereits biologische Aktivitäten nachgewiesen werden, doch fehlt eine ökologische Betrachtung aller sekundären Metabolite.

IV Können Naturstoffe oder deren Biosyntheseenzyme Anwendung für den Menschen z.B. in der Pharmazie finden?
Der Bedarf neuer Wirkstoffe und Leitstrukturen, nicht nur bei den Antiinfektiva, stellt den Antrieb vieler Naturstoffforschungsansätze dar. Daneben soll untersucht werden, ob Enzyme oder Domänen aus Biosynthesegenen Anwendung in der synthetischen Mikrobiologie finden können.

3 Publikationsübersicht

Bestandteil der vorliegenden Arbeit sind drei publizierte Originalarbeiten sowie ein Manuskript in Vorbereitung.

Manuskript 1
Kapitel 4.1

Bacterial-Like Nonribosomal Peptide Synthetases Produce Cyclopeptides in the Zycomycetous Fungus *Mortierella alpina*

Wurlitzer, Jacob M.; Stanišić, Aleksa; Wasmuth, Ina; Jungmann, Sandra; Fischer, Dagmar; Kries, Hajo; Gressler, Markus

Applied and Environmental Microbiology **2021**, 87 (3) e02051-20

Neben der Identifikation und Strukturaufklärung der Malpicycline wird erstmals in einem Zygomyceten die Biosynthese von zwei pilzlichen Naturstoffen nachgewiesen. Die Gene *mpcA* und *mpbA* aus *Mortierella alpina* enthalten dabei bakterielle Gensequenzen, was auf einen horizontalen Gentransfer dieser Gene hindeutet.

Manuskript 2
Kapitel 4.2

Macrophage-targeting Oligopeptides from *Mortierella alpina*

Wurlitzer, Jacob M.; Stanišić, Aleksa; Ziethe, Sebastian; Jordan, Paul M.; Günther, Kerstin; Werz, Oliver; Kries, Hajo; Gressler, Markus

Chemical Science **2022**, 13, 9091-9101

Durch die biochemische Charakterisierung heterolog produzierter NRPS-Module wurde die NRPS MalA mit der Malpinin-Biosynthese verknüpft. Die dabei beobachtete hohe Substratflexibilität der Adenylierungsdomänen wurde biotechnologisch ausgenutzt, um chemisch-modifizierbare Malpinin-Derivate zu generieren. Mit diesen Derivaten konnte eine gezielte Aufnahme der Malpinine in humane Immunzellen nachgewiesen werden.

Manuskript 3 **A Genetic Tool to Express Long Fungal Biosynthetic Genes**

Kapitel 4.3

Kirchgässner, Leo; Wurlitzer, Jacob M.; Seibold, Paula S.; Rakhmanov, Malik; Gressler, Markus

Fungal Biology and Biotechnology **2023**, 10, 4

Diese Publikation befasst sich mit der Etablierung eines heterologen Expressionssystems, mit welchem, basierend auf homologer Rekombination, auch Gene > 20 kb in *Aspergillus niger* exprimiert werden können. Auf diese Weise, konnte durch die Expressions des Gens *calA* aus *Mortierella alpina*, das antimykobakterielle Calpinactam biotechnologisch hergestellt und dessen Biosynthese geklärt werden.

Manuskript 4 **Insecticidal Cyclodepsitetrapeptides from *Mortierella alpina***

Kapitel 4.4

Rassbach, Johannes; Merseburger, Peter; Wurlitzer, Jacob M.; Binnemann, Nico; Voigt, Kerstin; Rohlfs, Marko; Gressler, Markuss

Manuskript zur Begutachtung eingereicht bei: *Journal of Natural Products*

In dieser Studie wurden die zyklischen verzweigtkettigen Depsipeptide Cycloacetamid A-F identifiziert und deren Struktur aufgeklärt. Durch mannigfaltige biologische Tests konnten sowohl für die Cycloacetamide, als auch die Malpicycline antilarvale Eigenschaften nachgewiesen werden. Basierend darauf wird der Beitrag dieser Verbindungen zur chemischen Ökologie von *M. alpina* diskutiert.

4 Manuskripte

4.1 Manuskript 1

Bacterial-Like Nonribosomal Peptide Synthetases Produce Cyclopeptides in the Zygomycetous Fungus *Mortierella alpina*

Wurlitzer, Jacob M.; Stanišić, Aleksa; Wasmuth, Ina; Jungmann, Sandra; Fischer, Dagmar; Kries, Hajo; Gressler, Markus

veröffentlich unter: *Applied and Environmental Microbiology* **2021**, 87 (3) e02051-20;

DOI: 10.1128/AEM.02051-20

Zusammenfassung:

Während Asco- und Basidiomyceten seit Jahrzehnten als ausgezeichnete Synthetiker von Naturstoffen gelten, wurden Zygomyceten oft vernachlässigt. Erstmals konnte mit dieser Publikation ein Naturstoff eines basalen Pilzes mit einem Biosynthesegen in Verbindung gebracht werden. So codieren die Gene *mpbA* und *mpcA* für NRPSs, welche für die Bildung der bekannten Malpibaldine und der neu beschriebenen Malpicycline in *Mortierella alpina* verantwortlich sind. Bakterielle duale Epimerisierungs- und Kondensationsdomänen und der bakterielle Ursprung der Adenylierungsdomänen in den jeweiligen Enzymen weist auf einen horizontalen Gentransfer der codierenden Naturstoffgene hin. Solche Übertragungen genetischer Information zwischen verschiedenen Spezies stellt bei Naturstoffgenen ein selten beobachtetes Phänomen dar.

Der Kandidat ist:

☒ Erstautor ☐ Co-Erstautor ☐ Korresp. Autor ☐ Coautor

Eigenanteil

Autor/-in	Konzeptionell	Datenanalyse	Experimentell	Verfassen des Manuskriptes
Wurlitzer, JM	50%	80%	75%	20%
Gressler, M	50%	-	-	65%
5 weitere Autoren	-	20%	25%	15%
Summe	100%	100%	100%	100%

AMERICAN SOCIETY FOR MICROBIOLOGY | Applied and Environmental Microbiology®

PHYSIOLOGY

Bacterial-Like Nonribosomal Peptide Synthetases Produce Cyclopeptides in the Zygomycetous Fungus *Mortierella alpina*

Jacob M. Wurlitzer,[a] Aleksa Stanišić,[b] Ina Wasmuth,[a] Sandra Jungmann,[c] Dagmar Fischer,[c] Hajo Kries,[b] Markus Gressler[a]

[a]Department of Pharmaceutical Microbiology, Leibniz Institute for Natural Product Research and Infection Biology (Hans Knöll Institute) and Friedrich Schiller University, Jena, Germany

[b]Junior Research Group Biosynthetic Design of Natural Products, Leibniz Institute for Natural Product Research and Infection Biology (Hans Knöll Institute), Jena, Germany

[c]Pharmaceutical Technology and Biopharmacy, Friedrich Schiller University Jena, Jena, Germany

ABSTRACT Fungi are traditionally considered a reservoir of biologically active natural products. However, an active secondary metabolism has long not been attributed to early-diverging fungi such as *Mortierella*. Here, we report on the biosynthesis of two series of cyclic pentapeptides, the malpicyclins and malpibaldins, as products of *Mortierella alpina* ATCC 32222. The molecular structures of malpicyclins were elucidated by high-resolution tandem mass spectrometry (HR-MS/MS), Marfey's method, and one-dimensional (1D) and 2D nuclear magnetic resonance (NMR) spectroscopy. In addition, malpibaldin biosynthesis was confirmed by HR-MS. Genome mining and comparative quantitative real-time PCR (qRT-PCR) expression analysis pointed at two pentamodular nonribosomal peptide synthetases (NRPSs), malpicyclin synthetase MpcA and malpibaldin synthetase MpbA, as candidate biosynthetic enzymes. Heterologous production of the respective adenylation domains and substrate specificity assays confirmed the existence of promiscuous substrate selection and also confirmed their respective biosynthetic roles. In stark contrast to known fungal NRPSs, MpbA and MpcA contain bacterial-like dual epimerase/condensation domains allowing the racemization of enzyme-tethered L-amino acids and the subsequent incorporation of D-amino acids into the metabolites. Phylogenetic analyses of both NRPS genes indicated a bacterial origin and a horizontal gene transfer into the fungal genome. We report on the as-yet-unexplored nonribosomal peptide biosynthesis in basal fungi which highlights this paraphylum as a novel and underrated resource of natural products.

IMPORTANCE Fungal natural compounds are industrially produced, with applications in antibiotic treatment, cancer medications, and crop plant protection. Traditionally, higher fungi have been intensively investigated for their metabolic potential, but reidentification of already known compounds is frequently observed. Hence, alternative strategies to acquire novel bioactive molecules are required. We present the genus *Mortierella* as representative of the early-diverging fungi as an underestimated resource of natural products. *Mortierella alpina* produces two families of cyclopeptides, designated malpicyclins and malpibaldins, via two pentamodular nonribosomal peptide synthetases (NRPSs). These enzymes are much more closely related to bacterial than to other fungal NRPSs, suggesting a bacterial origin of these NRPS genes in *Mortierella*. Both enzymes were biochemically characterized and are involved in as-yet-unknown biosynthetic pathways of natural products in basal fungi. Hence, this report establishes early-diverging fungi as prolific natural compound producers and sheds light on the origin of their biosynthetic capacity.

KEYWORDS Mortierellales, NRPS, adenylation domain, cyclopeptide, horizontal gene transfer, zygomycetes

Citation Wurlitzer JM, Stanišić A, Wasmuth I, Jungmann S, Fischer D, Kries H, Gressler M. 2021. Bacterial-like nonribosomal peptide synthetases produce cyclopeptides in the zygomycetous fungus *Mortierella alpina*. Appl Environ Microbiol 87:e02051-20. https://doi.org/10.1128/AEM.02051-20.

Editor Ning-Yi Zhou, Shanghai Jiao Tong University

Address correspondence to Markus Gressler, markus.gressler@leibniz-hki.de.

Received 21 August 2020
Accepted 30 October 2020
Accepted manuscript posted online 6 November 2020
Published 15 January 2021

The increasing number of human-pathogenic microbes resistant against well-established antibiotics requires an unbiased search of novel producers of bioactive natural products. Bacteria (e.g., *Actinomyces* and *Streptomyces* spp.) and filamentous higher fungi (e.g., *Aspergillus*, *Penicillium*, and *Fusarium*) are well-investigated resources of natural products such as nonribosomal peptides (NRP), polyketides, and terpenoids (1–4). In contrast, early-diverging fungi—formerly combined in the paraphylum zygomycetes (5, 6)—have long been thought to lack secondary metabolites (7). Still, apart from the C_{18} terpenoid trisporic acid isolated from *Blakeslea trispora* and *Mucor mucedo* as a signaling compound during mating (8–10), secondary metabolites are rarely observed in zygomycetes. *Mortierella alpina*, a species of the subdivision Mucoromycotina, is a strain that is generally regarded as safe (GRAS) and serves as an industrial producer of polyunsaturated fatty acids such as arachidonic acid and linoleic acid (11–13).

Although lipid extracts of *M. alpina* are useful as immunomodulating leukotriene precursor molecules in pharmaceutical applications or as nutritional supplements in baby food (14), the secondary metabolome of the fungus has never been investigated in detail. Case reports on *M. alpina* species indicate the capacity to produce some oligopeptides, such as calpinactam (15) and Ro 09-1679 (16), harboring antimycobacterial and thrombin-inhibiting bioactivities, respectively (Fig. 1A). The metabolic potential of *M. alpina* was expanded by the recent discovery of a family of linear, acetylated hexapeptides, malpinins A to D, that have surface tension-lowering properties (Fig. 1A) (17, 18). Furthermore, the fungus produces the highly hydrophobic cyclopentapeptides known as malpibaldins (compounds 1 to 3) (17). Cyclopentapeptides have been isolated from various biological sources (ascomycetes, algae, and bacteria) and harbor diverse pharmaceutically relevant antiviral, antibiotic, apoptotic, and antiangiogenic properties (Fig. 1B) (19–25). Of interest, malpibaldins from *M. alpina* are structurally similar to luminmide B, a D-amino acid-containing cyclic pentapeptide from the insect-pathogenic gammaproteobacterium *Photorhabdus luminescens* (24). Biosynthetically, luminmide B is produced by a pentamodular NRP synthetase (NRPS), Plu3263, by sequential condensation of five aliphatic L-amino acids activated by specific adenylation (A) domains, and D-amino acids are introduced by the activity of dual epimerization/condensation (E/C) domains (24).

The biosynthetic origin of all above-mentioned peptides from *M. alpina* has never been illuminated. The publicly available 38.38-Mb genome of *M. alpina* (26) harbors 22 genes encoding polymodular NRPS or monomodular NRPS-like proteins, indicating its high biosynthetic potential (7). However, the frequent occurrence of D-amino acids in peptides of Mortierellales is biosynthetically surprising, since mainly bacteria (27), but rarely fungi (28–30), use D-amino acids as building blocks for NRP synthesis. Investigations on the mucoromycete *Rhizopus microsporus* revealed that its D-amino acid-containing peptides rhizonin and heptarhizin are produced not by the fungus but by its in-host endosymbiotic proteobacterium *Paraburkholderia* (syn. *Mycetohabitans*) *rhizoxinica* (31, 32). Similarly, *Burkholderia*-related endosymbionts (BRE) such as *Mycoavidus cysteinexigens* are frequently observed in *Mortierellales* (33, 34). In addition, non-culturable *Mycoplasma*-related obligate endosymbionts (MRE) have been identified by 16S ribosomal DNA (rDNA) sequencing in Mortierellomycotina (35). Therefore, we considered a possible involvement of endosymbionts in the secondary metabolism of *M. alpina*.

Here, we report the biosynthesis of malpibaldins and a novel set of cyclopentapeptides, called malpicyclins A to F (compounds 4 to 9), in *M. alpina*. The latter compounds are composed of D/L-Leu, D/L-Val, D-Phe, D-Trp, D-Tyr, and D-Arg and show moderate activity against Gram-positive bacteria. The production of both peptide families does not rely on fungus-associated bacteria. Instead, two fungal genes encoding pentamodular NRPSs are expressed during metabolite production and their amino acid sequence similarity to bacterial NRPSs suggests a genetic transfer across kingdoms. By combination of differential expression analysis, metabolite profiling, and *in silico* bioinformatic substrate binding studies, the NRPS genes *mpbA* and *mpcA* were specifically

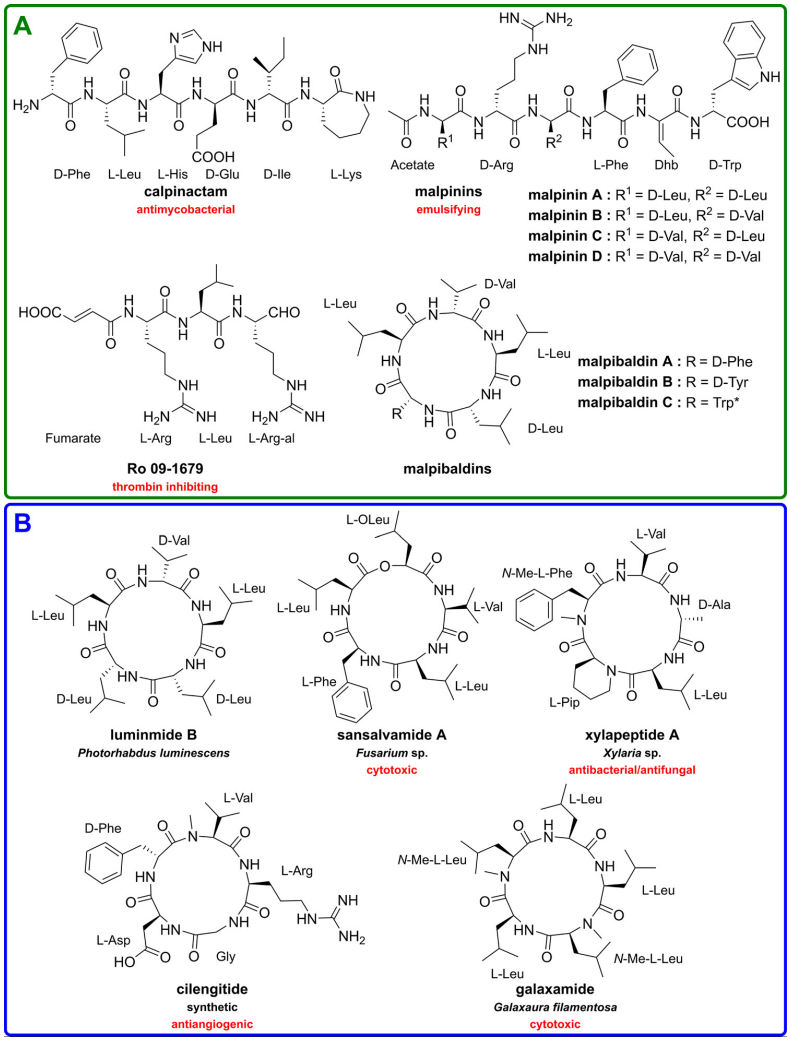

FIG 1 Linear and cyclic oligopeptides from *M. alpina* and other resources. (A) Oligopeptides isolated from *Mortierella alpina* (15–18). (B) Malpibaldin-related cyclopentapeptides from other sources (19, 21–24). *, configuration of the Trp moiety was not determined (17). L-Arg-al, L-arginal; Dhb, dehydrobutyrine; L-Pip, L-pipecolinic acid.

linked to the biosynthesis of malpibaldins and malpicyclins, respectively. Heterologous production of MpbA and MpcA modules in *Escherichia coli* and subsequent substrate turnover assays confirmed their activity.

RESULTS

Metabolic profiling of *M. alpina* revealed the malpicyclin family. The high abundance of the previously reported small peptides (17) prompted us to screen alternative cultivation conditions to induce oligopeptide production in *M. alpina*. Cultivation in potato dextrose broth (PDB) resulted solely in the production of malpinins (17) in the mycelium according to ultrahigh-performance liquid chromatography-mass spectrometry (UHPLC-MS) measurements (Fig. 2A). In contrast, when cultivated in

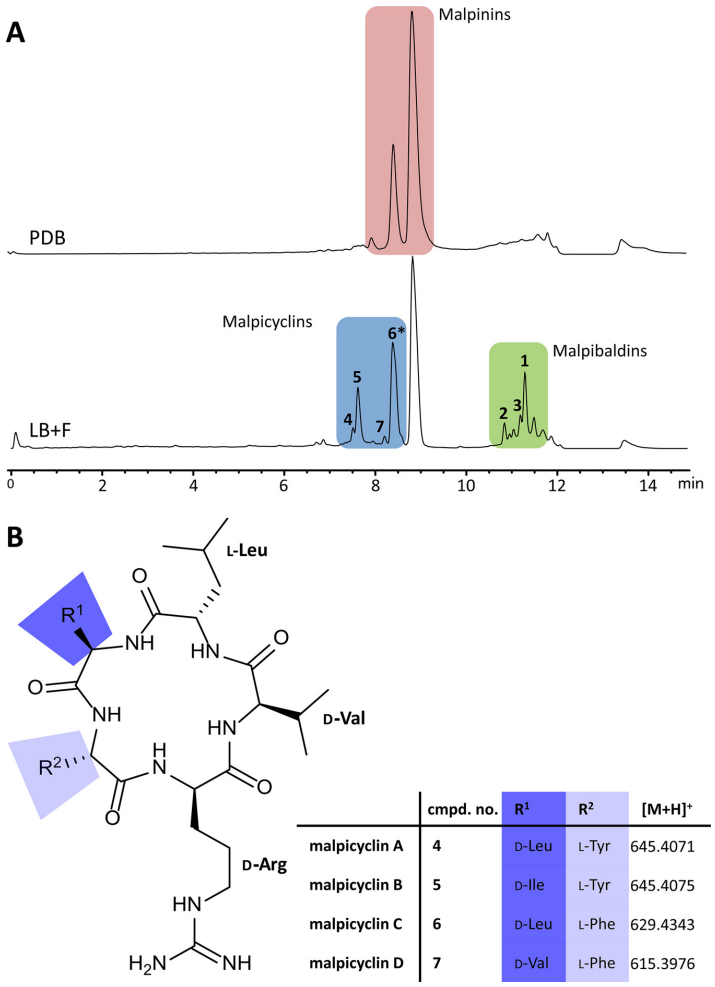

	cmpd. no.	R^1	R^2	$[M+H]^+$
malpicyclin A	4	D-Leu	L-Tyr	645.4071
malpicyclin B	5	D-Ile	L-Tyr	645.4075
malpicyclin C	6	D-Leu	L-Phe	629.4343
malpicyclin D	7	D-Val	L-Phe	615.3976

FIG 2 Identification of malpicyclins from *M. alpina* extracts. (A) UHPLC-MS profile of mycelial crude extracts from *M. alpina* after cultivation in potato dextrose broth (PDB) or modified lysogeny broth (LB+F, LB medium supplemented with 2% fructose) for 7 days (total ion chromatogram [TIC]). (B) Scheme of the chemical structure of malpicyclins A to D (compounds 4 to 7). *, signal overlap; malpicyclin C (compound 6) coelutes with malpinin B.

lysogeny broth supplemented with 2% fructose (LB+F), the previously reported malpibaldins A to C (compounds 1 to 3) (17) and an additional series of four masses $[M+H]^+$ of unknown nature (compounds 4 to 7) were detected (Fig. 2A). Upscaling of the culture to 4 liters and subsequent isolation of the metabolites by semipreparative HPLC enabled the identification of the four cyclopentapeptides malpicyclins A, B, C, and D (*m/z* 645.4074 $[M+H]^+$, *m/z* 645.4065 $[M+H]^+$, *m/z* 629.4343 $[M+H]^+$, and *m/z* 615.3976 $[M+H]^+$, compounds 4 to 7) by one-dimensional (1D) and 2D nuclear magnetic resonance (NMR) analysis (Fig. 2B, Table 1, Tables S1 to S4, and Fig. S1 to S27). ^{13}C NMR experiments and the calculated molecular formulae revealed by high-resolution mass spectrometry (HR-MS) suggested five carbonyl atoms and eight nitrogen atoms in compounds 4 to 7 and indicate pentapeptides that include a guanidinium group from arginine. MS/MS experiments and $^1H,^1H$ correlation spectroscopy (COSY)

TABLE 1 HR-ESI-MS data of isolated cyclopentapeptides from *M. alpina* ATCC 32222

Compound no.	Name	*m/z* [M + H]$^+$	Planar structure	Reference(s)
1	Malpibaldin A	586.3963	Cyclo(-L-Leu-D-Leu-D-Phe-L-Leu-D-Val-)	17
2	Malpibaldin B	625.4062	Cyclo(-L-Leu-D-Leu-D-Trp-L-Leu-D-Val-)	17
3	Malpibaldin C*	602.3912	Cyclo(-Leu-Leu-Trp-Leu-Val-)	17
4	Malpicyclin A (plactin B)	645.4074	Cyclo(-D-Leu-L-Tyr-D-Arg-D-Val-L-Leu-)	38, 39, 75
5	Malpicyclin B	645.4065	Cyclo(-D-Ile-L-Tyr-D-Arg-D-Val-L-Leu-)	This study
6	Malpicyclin C (plactin D)	629.4343	Cyclo(-D-Leu-L-Phe-D-Arg-D-Val-L-Leu-)	38, 39, 75
7	Malpicyclin D	615.3976	Cyclo(-D-Val-L-Phe-D-Arg-D-Val-L-Leu-)	This study
8	Malpicyclin E[a]	668.4228	Cyclo(-Leu-Trp-Arg-Val-Leu-)	This study
9	Malpicyclin F (MBJ-0174)	631.3959	Cyclo(-D-Val-L-Tyr-D-Arg-D-Val-L-Leu-)	18

[a]Absolute configuration of amino acids was not determined.

analysis suggested a cyclic ring structure which was confirmed by heteronuclear multiple-bond correlation (HMBC) and heteronuclear single quantum coherence (HSQC) 2D analysis experiments. Both COSY and HMBC data allowed the assignment of the amino acid side chains and revealed the planar structure: cyclo-(-Leu/Ile/Val-Tyr/Phe-Arg-Val-Leu-) (Fig. S6). The absolute configuration of the side chains was elucidated by the advanced Marfey's method (36, 37) (Table S5). D-Amino acids are solely incorporated at positions 1, 3, and 4 in compounds 4 to 7. Of note, besides D-Arg at position 3, L-Arg was confirmed as second building unit as evident by dual signals in Marfey's analysis (Table S5) and the presence of two symmetric scalar couplings (δ_H 1.63 and δ_H 1.45 in malpicyclin C) in HSQC spectra (Fig. S21). In addition to compounds 4 to 7, two by-products (compounds 8 and 9) were detected by HR-MS (Table 1 and Tables S1 and S2) but were produced in insufficient amounts for NMR analysis. The MS/MS fragmentation of compound 8 (malpicyclin E, *m/z* 668.4228 $[M+H]^+$) showed a pattern similar to that of compound 4 (Fig. S5) and suggested a tryptophan as the aromatic amino acid at the 3rd position (Table 1). According to HR-MS data, compound 9 (malpicyclin F, *m/z* 631.3959 $[M+H]^+$) is probably identical to the arginine-containing cyclopeptide MBJ-0174, previously isolated from *Mortierella alpina* strain f28740 (18).

Antimicrobial testing of compounds 4 to 7 revealed a moderate antibacterial activity against Gram-positive bacteria, with MIC values ranging from 97.3 to 357.8 μM, while Gram-negative representatives or fungi were not affected (Table 2 and Fig. S28 and S29). Interestingly, compounds 4 and 6 are structurally identical to the cyclopeptides plactin B and plactin D, which have formerly been isolated from an unspecified fungal strain, F165 (38). Plactin D showed blood plasma-dependent fibrinolytic activity by enhancing the prothrombin protease activity (39). Since amphiphilic malpinins have been described as surface-active metabolites, we also checked for tenside properties of malpicyclins by the ring tear-off method (17). Indeed, malpicyclins demonstrated a biphasic profile with a fast decrease of the surface tension up to a concentration of 62.5 μg/ml, followed by a slower decrease (Fig. S30). However, the calculated critical micelle concentration (CMC) of 93.9 μg/ml (147 μM) is 10-fold higher than that of malpinins (17), suggesting only a moderate contribution to *Mortierella*'s biosurfactant activities.

Malpicyclins and malpibaldins are fungal products. In 1984, the macrolactone antibiotic rhizoxin was isolated from the zygomycete *Rhizopus microsporus* and was

TABLE 2 MIC_{50}s of malpicyclins A to D tested against *Bacillus subtilis* and *Escherichia coli*

	MIC_{50} (μM)	
Compound no. or name	*B. subtilis*	*E. coli*
4	181.1 ± 89.6	>1,000
5	97.3 ± 16.5	>1,000
6	357.8 ± 124.4	>1,000
7	255.9 ± 15.2	>1,000
Ciprofloxacin[a]	0.022 ± 0.002	0.101 ± 0.003

[a]Ciprofloxacin served as a positive control.

seemingly of fungal origin (40). However, 23 years later, Hertweck's group demonstrated in pioneering work that the fungus harbors the endosymbiotic betaproteobacterium *P. rhizoxinica*, which that produces this macrocyclic polyketide (41). Analogously, *Mortierella elongata* can be infected by the endobacterium *Mycoavidus cysteinexigens*, whose genome encodes at least three NRPSs, while the host genome does not (34). Indeed, an approach screening 30 different *Mortierella* isolates revealed that 13% were infected by *Mycoavidus*-related endosymbionts (MRE) (34). To investigate whether cyclopentapeptides in *M. alpina* ATCC 32222 are of fungal or bacterial origin, the strain was repeatedly treated with an antibiotic cocktail known to cure potential infected hyphae (41). However, metabolite production—represented by quantifying the major compound of each metabolite class (malpicyclin C [compound 6] and malpibaldin A [compound 1])—was not affected by the antibiotic treatment, suggesting that the metabolite is produced by the fungus (Fig. S31). Moreover, a subsequent PCR amplification of bacterial 16S rDNA from treated and untreated fungal mycelium of *M. alpina* failed and pointed to the absence of endobacteria (Fig. S32). Both experiments indicate that (i) *M. alpina* isolate ATCC 32222 does not harbor endobacteria and (ii) the isolated metabolites are fungal rather than bacterial products.

Genome mining of *M. alpina* revealed the identification of cyclopeptide synthetases. A whole-genome survey of *M. alpina* (26) using antiSMASH (42) revealed 22 genes encoding NRPS and NRPS-like proteins in *M. alpina*. According to the molecular structure and D-amino acid distribution in malpicyclins and malpibaldins, two five-module NRPS with at least three epimerization domains (E) or dual epimerase/condensation domains (E/C) are required. Indeed, two candidate NRPS genes (*mpcA* and *mpbA*) were identified in the genome (Fig. 3). The potential NRPS gene product MpcA (5,532 amino acids [aa]) comprises a pentamodular NRPS with a scaffold C_s-A-T-E/C-A-T-C-A-T-E/C-A-T-E/C-A-T-TE, which includes an expected pattern of bacterial-like dual E/C domains (in modules 2, 4, and 5) as required for malpicyclin biosynthesis. The high similarity to bacterial domains facilitated the prediction of the *M. alpina* A domain specificities, which can be a difficult task for fungal domains. Analysis of putative substrate preference of the A domains by alignment with the GrsA A domain from *Aneurinibacillus migulanus* (43) suggested acceptance of hydrophobic amino acid substrates in all A domains of MpcA, with exception of domain A3 (Table 3 and Table S6). Here, hydrophilic residues (Ser and Thr) are found at positions 278 and 330 (GrsA numbering) of the NRPS code and, moreover, an Asp at position 331 might ion-pair with cationic amino acids such as Arg (44, 45), which is abundant in all malpicyclins (compounds 4 to 7). Hence, we hypothesized that a positively charged amino acid would be accepted by the MpcA A3 domain.

The second candidate gene encodes an NRPS (MpbA) with an identical domain pattern and a size (5,541 aa) similar to that of MpcA (73.6% aa sequence identity). However, *in silico* substrate specificity analysis revealed exclusively hydrophobic binding pockets in all five A domains, as expected for the malpibaldin building blocks (Table 3). MpbA A3 and MpbA A2 share similar NRPS codes, suggesting that both domains accept the same—probably aromatic—substrates. MpbA is structurally related to the bacterial luminmide B synthetase Plu3263 from *P. luminescens* (50.2% identity; 65.9% similarity), and both NRPSs may produce highly similar cyclopentapeptides NRP (Fig. 1 and 2). However, the specificity codes of the A domains are not identical (Table 3), suggesting that zygomycetous NRPSs use a dissimilar code.

In contrast to Plu3263, both MpcA and MpbA contain a starter condensation (C_S) domain-like N terminus (252 and 247 aa, respectively) known to transfer β-hydroxycarboxylic acid residues from acyl coenzyme A (acyl-CoA) donors to the N termini of bacterial lipopeptides (46). However, the domains are N-terminally truncated and the tandem histidine motifs (HH) responsible for the deprotonation of the substrate prior to the condensation step (47) is missing in the active sites of both domains. Taken together, the proposed domain structure and distribution of dual E/C domains fulfilled the requirement for incorporation of D-amino acids at the expected positions in

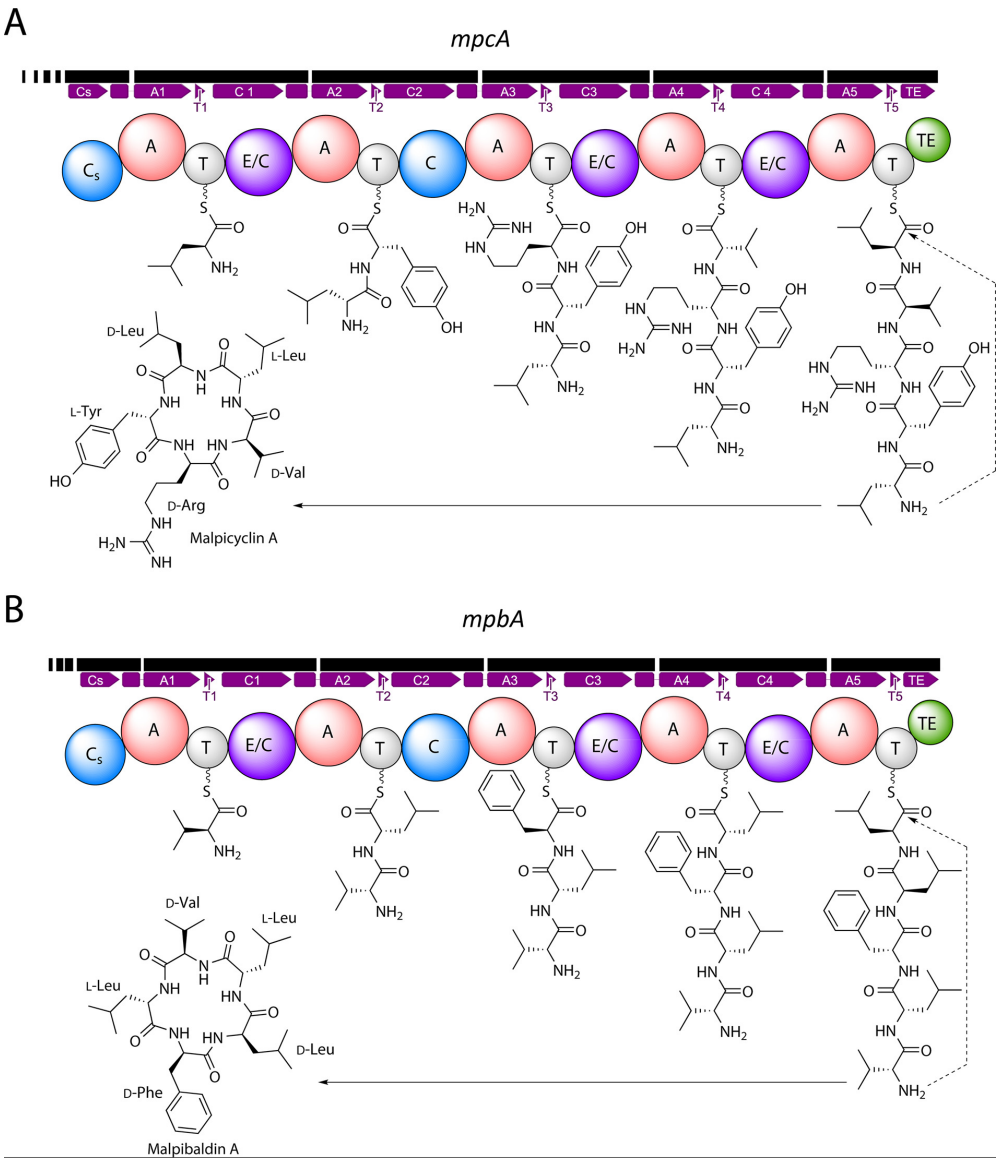

FIG 3 Proposed biosynthesis of malpicyclin A and malpibaldin A. (A) Gene structure of *mpcA* and domain structure of its encoded malpicyclin synthetase, MpcA. (B) Gene structure of *mpbA* and domain structure of its encoded malpibaldin synthetase, MpbA. A, adenylating domain; C condensation domain of the canonical $^{L}C_{L}$ type; E/C, dual epimerization/condensation domain; C_{s}, truncated starter condensation domain; T, thiolation domain; TE, thioesterase domain. Either gene (bold black lines) is interrupted by nine introns. Vertical white lines represent introns, black rectangles exons.

malpicyclins and malpibaldins and prompted us to study the malpicyclin synthetase gene (*mpcA*) and malpibaldin synthetase gene (*mpbA*) in detail.

Fungal NRPS genes *mpcA* and *mpbA* are coexpressed in the presence of fructose. To confirm active transcription of the NRPS genes, quantitative real-time PCR (qRT-PCR) expression experiments were performed. The fungus was cultivated in media

TABLE 3 NRPS codes for adenylating domains of the *Mortierella* NRPS (MpcA and MpbA) and related biochemically investigated bacterial and fungal NRPS modules[a]

Protein domain	Organism*	substrate	Residue position according to GrsA Phe numbering									
			235	236	239	278	299	301	322	330	331	527
MpcA_A2	*M. alpina*	Tyr/Phe	D	P	F	T	M	G	A	V	V	K
MpbA_A3	*M. alpina*	Trp/Tyr/Phe	D	P	F	V	M	G	G	T	V	K
Plu3263_A3	*P. luminescens*	Phe	D	A	W	C	I	A	A	V	C	K
BacC_A2	*B. subtilis*	Phe	D	A	F	T	V	A	A	V	C	K
CepA_A1	*A. orientalis*	Tyr	D	A	S	T	V	A	A	V	C	K
GliP_A1	*A. fumigatus*	Phe	D	G	S	I	L	G	A	C	A	K
MpbA_A1/ MpcA_A4	*M. alpina*	Val	D	A	F	W	L	G	G	T	F	K
MpcA_A1	*M. alpina*	Leu/Ile/Val	D	A	F	F	I	G	A	M	L	K
MpbA_A2	*M. alpina*	Leu	D	A	F	F	I	G	A	M	V	K
MpbA_A4/A5	*M. alpina*	Leu	D	A	I	F	L	G	A	T	I	K
MpcA_A5	*M. alpina*	Leu	D	A	M	F	I	G	G	T	I	K
Plu3263_A2/ A4/A5	*P. luminescens*	Leu	D	A	W	C	I	G	A	V	C	K
GrsB_A1	*A. migulanus*	Val	D	A	F	W	I	G	G	T	F	K
CssA_A9	*T. inflatum*	Val	D	A	W	M	F	A	A	V	L	K
MpcA_A3	*M. alpina*	Arg	D	A	A	S	V	G	A	T	D	K
SyrE_A5	*P. syringae*	Arg	D	V	A	D	V	C	A	I	D	K
McyC_A1	*M. aeruginosa*	Arg	D	V	W	T	I	G	A	V	D	K
PpzA-1_A2	*E. festucae*	Arg	D	V	S	D	T	G	A	P	T	K

[a]The proposed activated substrates are listed in column 3. The residues are mapped relative to *Aneurinibacillus migulanus* (former *Brevibacillus brevis*) GrsA-A numbering (81). NRPS codes were partially extracted from Bian et al. (82). Amino acid residues in the NRPS code are colored according to their physicochemical properties: acidic (red), small/hydrophobic (gray), aromatic/hydrophobic (amber), hydrophilic (green), and basic (blue). *, organisms are colored according to their phylogenetic origin: basal fungi (blue), higher fungi (brown), and bacteria (green). A detailed alignment is provided as Table S6.

to induce (LB+F) or repress (PDB) cyclopeptide production (Fig. 2A and 4A). Gene expression was determined after 48 h and 4 days of cultivation, and data were normalized against expression profiles derived from freshly germinated *M. alpina* mycelia, which do not produce secondary metabolites (data not shown). Neither NRPS gene *mpcA* nor *mpbA* was expressed in PDB medium, but expression was induced 5.4- or 8.2-fold, respectively, after 48 h of cultivation in LB medium compared to PDB medium. These results matched the observed enrichment of malpibaldin A (compound 7) and malpicyclin C (compound 3) in mycelial metabolite extracts obtained from cultivation in LB medium (Fig. 4B). In contrast, negligible amounts of both metabolites were found in mycelium after cultivation in noninducing PDB medium.

Adenylation domains of MpcA and MpbA activate L-amino acids. Unlike Aspergilli, Mortierellaceae are hardly genetically tractable, and targeted gene deletion occurs with very low frequency and genomic stability (48, 49). Hence, we verified the substrate specificity of the most characteristic modules (C-A-T) in both NRPSs, i.e., module 3 of MpcA (MpcA-m3, 122.45 kDa) and module 3 of MpbA (MpbA-m3, 122.40 kDa), by heterologous production in *E. coli* (Fig. S33). The purified double-His_6-tagged fusion proteins (50) were subjected to specificity testing by the recently established multiplexed hydroxamate-based adenylation domain assay (HAMA) (51), which detects the formation of stable amino acid hydroxamates after enzymatic adenylation by A domains. All proteinogenic L-amino acids and two of its enantiomer counterparts (D-Val and D-Phe) were tested in parallel.

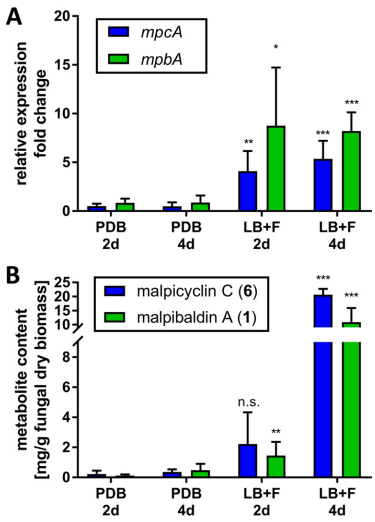

FIG 4 Gene expression of malpicyclin and malpibaldin synthetase genes, *mpcA* and *mpbA*, and metabolite production. *M. alpina* was cultivated under noninducing (PDB) and inducing (LB+F) conditions for up to 4 days. Expression analysis and metabolite quantification by UHPLC-MS were carried out 2 days and 4 days postinoculation (p.i.) (A) Expression analysis of *mpcA* and *mpbA*. Gene expression was normalized against the housekeeping genes *actA*, encoding α-actin, and *gpdA*, encoding the glyceraldehyde-3-phosphate dehydrogenase. cDNA from freshly germinated mitospores (in PDB) served as a reference (set to 1). (B) Metabolite quantification of the malpicyclin C (compound 6) and malpibaldin A (compound 1). Representative of each series, the amount of the most abundant metabolites (malpicyclin C and malpibaldin A) was determined by UHPLC-MS mass chromatograms (EIC) from *M. alpina* mycelium. Statistical significance compared to noninduced control (PDB, 2 days) is indicated as follows: n.s., not significant; *, $P \leq 0.05$; **, $P \leq 0.01$; and ***, $P \leq 0.001$ (paired Student's *t* test). Metabolite production and gene expression correlated with Pearson correlation coefficients of 0.84 ($P = 0.004$) for malpicyclin C/*mpcA* and 0.72 ($P = 0.02$) for malpibaldin A/*mpbA* at day 4.

For MpcA-m3, solely the corresponding L-Arg product formation was observed, confirming the findings of the NMR analysis and *in silico* substrate prediction (Fig. 5A). However, due to a lack of an authentic hydroxamate standard, incorporation of D-Arg could not be excluded. Hence, in a complementary experiment, substrate specificity was confirmed by an ATP-[$^{32}PP_i$] exchange assay (52) (Fig. S34 and Table S7). First, pools

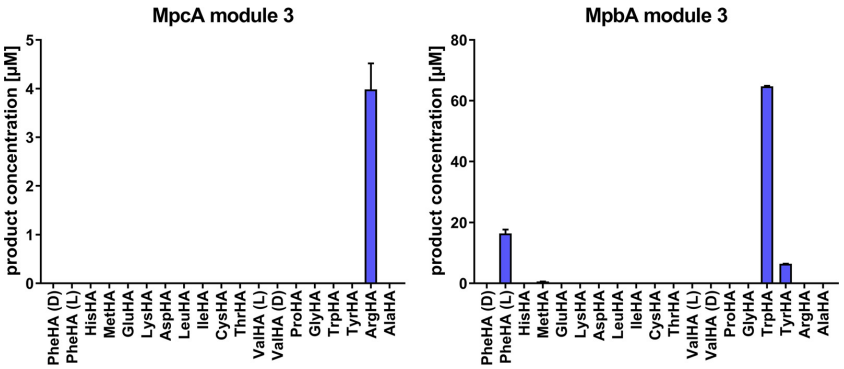

FIG 5 Substrate specificity testing of NRPS modules by the multiplexed hydroxamate assay (HAMA). Modules 3 (C-A-T) of MpcA (A) and of MpbA (B) were separately tested. Substrates were all proteinogenic amino acids (except L-Asn, L-Gln, and L-Ser), D-Phe, and D-Val. Amino acyl hydroxamates were quantified using HAMA ($n = 3$).

of physiochemically similar L-amino acids were tested, followed by a subsequent determination of single amino acids in the active pools. Again, MpcA-m3 showed the highest turnover with L-Arg (2.2×10^5 dpm). However, 11% of ATP-$^{32}PP_i$ conversion was also observed for D-Arg (2×10^4 dpm), suggesting that the A domain is not entirely enantioselective. Poor discrimination against D-amino acids is not surprising when the D-enantiomers are not present as competing substrates. For instance, strong side activities for D-Phe and D-homoserine (D-Hse) have been reported for usually L-amino acid-activating A domains in tyrocidine and ralsolamycin biosynthesis, respectively (52, 53).

The HAMA of MpbA-m3 revealed a promiscuous acceptance of aromatic amino acids, with preference L-Trp > L-Phe > L-Tyr (Fig. 5B). These side chain identities perfectly match residues found in malpibaldins C, A, and B, respectively, but are not in line with the preference for product formation. In *M. alpina*, malpibaldin A (L-Phe derivative) is the major compound (17). Such discrepancies between adenylation preference and relative product formation rate may be caused by side chain specificity of downstream reaction steps or differences in intracellular amino acid availability (51). Promiscuous adenylation leading to the parallel production of multiple products from one NRPS assembly line has been well studied in cyanobacterial enzymes and may be an important springboard for evolutionary diversification (45, 54).

From this knowledge, we predicted the biosynthesis of malpicyclins and malpibaldins by successive activation and, if required, racemization of L-amino acids, which are subsequently condensed to give a nascent, linear pentapeptide tethered to the T domains of the enzymes (Fig. 3). The final cyclization is probably catalyzed in *cis* by the C-terminal type I thioesterase (TE) domain, which has been demonstrated for several cyclopeptides from bacteria (52, 55, 56).

NRPS genes of *M. alpina* are of (endo)bacterial origin. Since no zygomycetous NRPS has been identified before, we were interested in the evolutionary origin of the genes and enzymes. A phylogenetic analysis of the extracted A domains both from *M. alpina* NRPS proteins and from verified fungal and bacterial NRPS, NRPS-like, and PKS-NRPS hybrid proteins was performed. Surprisingly, the zygomycetous A domains clustered in a monophylum with bacterial—but not with fungal—A domains independent of substrate specificity (Fig. 6 and Table S8). Moreover, the A domains share high similarity to A domains from NRPSs of endobacteria such as *Paraburkholderia* or *Mycoavidus*, known to infect zygomycetes, but are more distantly related to other Gram-negative (*Pseudomonas* or *Ralstonia*) or Gram-positive representatives (*Streptomycetes*). Hence, both *Mortierella* NRPSs are most likely of (endo)bacterial but not fungal origin and may have been evolved independently of the fungal counterparts.

A phylogenetic analysis based on the more conserved condensation (C) domains showed a similar outcome (Fig. S35 and S36 and Tables S9 and S10). Most interestingly, C domains from *M. alpina* NRPSs fall into three groups: $^{L}C_L$, common C domains condensing L-amino acids; C_s, N-terminal starter condensation domains; and dual E/C domains, epimerizing enzyme-tethered L-amino acids to their D-enantiomers prior to condensation. The canonical $^{L}C_L$ domains from *Mortierella* cluster with both bacterial and fungal $^{L}C_L$ domains (Fig. S35 and S36). In addition, the truncated C_s domains have most likely evolved from *Mortierella* $^{L}C_L$ domains and show no similarity to acyltransferring C_s domains found in bacterial lipopeptide NRPSs (Fig. S35). In contrast, the six dual E/C domains from MpcA and MpbA cluster with those of endobacteria such as *Paraburkholderia* (Fig. S35), but they have no close counterpart among fungal C domains (Fig. S36). To date, dual E/C domains have been found solely in bacteria and not in fungi. Indeed, the zygomycetous E/C domains occupy a unique, separate C domain clade among the fungal kingdom. In addition, BLASTP analyses using MpcA and MpbA as queries identified putative NPRS candidates from both bacteria (*Photorhabdus*) and early-diverging fungi (*Basidiobolus meristosporus* and *Mortierella verticillata*) (Tables S11 to S14).

FIG 6 Phylogenetic analysis of A domains from *M. alpina* and other fungal or bacterial representatives. The A domains were extracted from NRPSs, NRPS-like proteins, and PKS/NRPS hybrids from *M. alpina* (blue), (endo)bacteria (green), and higher fungi (taupe/amber) (refer to Table S8). The A domain of the cytoplasmatic tryptophanyl-tRNA synthetase Wrs1 from *Saccharomyces cerevisiae* served as the outgroup (red). Note that the zygomycetous A domains from *M. alpina* cluster together with bacterial A domains. The percentual bootstrap support is labeled next to the branches. AAA red, α-2-aminoadipate reductase; AA Red, aryl acid reductase; NRPS, nonribosomal peptide synthetase; PKS-NRPS, polyketide synthase-nonribosomal peptide synthetase hybrid; Ser Red, serine reductase; Tyr Red, tyrosine reductase.

Taking all these findings together, we postulate a probable horizontal gene transfer (HGT) from an unknown bacterial endosymbiont to the *Mortierella* host. However, the GC contents of *mpcA* (55.0%) and *mpbA* (54.6%) are similar to that of the *M. alpina* genome (51.8%), and the codon usage of their coding sequences is nearly identical to that of the housekeeping genes from *M. alpina*. Both findings suggest an early HGT event in *Mortierella*.

DISCUSSION

Zygomycetes of the order Mortierellales are an established resource for enzymes in industrial detergent manufacturing or for polyunsaturated fatty acids in the food industry. Recent publications revealed highly bioactive compounds such as the antiplasmodial cycloheptapeptide mortiamide A (57) or the surface-active hexapeptide malpinin A (17). Hence, this fungal order seems to be a prolific resource of pharmaceutically relevant natural products, too. However, the biosynthetic basis of the peptide compounds from zygomycetes has never been investigated. We provide here evidence that secondary metabolite genes are actively transcribed in zygomycetes and encode functional enzymes, called zygomycetous NRPSs.

The zygomycetous NRPSs MpcA and MpbA combine properties of both bacterial and fungal NRPSs. A bacterial origin of the NRPS genes is likely since they encode A and C domains, which exclusively cluster with bacterial representatives. Most of the known NRP from *Mortierella* species use D-amino acids as building blocks. To incorporate D-amino acids into the NRP backbone, fungi require a separate, pre-NRPS-acting amino acid racemase as shown for the biosynthesis routes of cyclosporine in *Tolypocladium niveum* or HC toxin in *Cochliobolus carbonum* (28, 58). Alternatively, fungal NRPSs possess a dedicated epimerase domain N-terminally located to a $^{D}C_{L}$ domain (E-C didomain) that solely accepts D-amino acids as the substrate, i.e., in the fusaoctaxin A synthetase NRPS 5 from *Fusarium graminearum* (29). Recently, Tang's group demonstrated that an E-C didomain in the single-module NRPS IvoA catalyzes the ATP-dependent stereoinversion of L- to D-tryptophan, the precursor for the conidiophore pigment in *Aspergillus nidulans* (59). Instead of E-C didomains, zygomycetous NRPSs use bacterial-like dual E/C domains combining both catalytic activities, i.e., epimerization and condensation, in one single domain. Bacterial dual E/C domains are characterized by two consecutive histidine repeats (HH) in condensation domain motifs C1 (HH[I/L]XXXXGD) and C3 (HHXXXGDH) which are required for epimerization and condensation, respectively (60). Similar catalytic HH motifs are present in the *Mortierella* dual E/C domains (C1 ,HH[M/L][M/L]A[T/A]EGD, and C3, HH[I/L][IV][G/I]DH), suggesting a functional racemization.

Another distinctive feature of the zygomycetous NRPSs is the N-terminally truncated starter C-domain (C_s) in both MpcA and MpbA. *Mortierella* C_s domains do not cluster with β-hydroxy acyl-transferring C_s domains from lipopeptide-producing NRPSs from bacteria (46). Instead, our phylogenetic analysis indicated that these domains have evolved from the *Mortierella* canonical $^{L}C_{L}$ domains. Truncated C_s domains with unknown function were also found in fungal NRPSs such as the cyclosporine synthetase SimA from *Tolypocladium inflatum* (61), the tryptoquialanine synthetase TquA from *Penicillium aethiopicum* (62), and the pyrrolopyrazine synthetase PpzA-1 from *Epicholoë festucae* (63) and are thought to be an evolutionary relic required to maintain A domain stability (64). In bacterial macrocyclic-producing NRPSs, the final peptide is cyclized by a terminal *cis*-acting type I TE domain, which is often replaced by a specialized cyclase-like C domain (C_T) in fungi (30). Both domains preferably catalyze a head-to-tail macrolactamization of peptides with D- and L-configured residues at the N and C termini, respectively (65). Hence, the presence of C-terminal TE domains in MpcA and MpbA and the presence of a dual E/C domain at their N termini point at a bacterial-like cyclization mechanism in zygomycetous NRPSs.

Surprisingly, based on the amino acid sequence, MpbA is highly related to bacterial NRPSs, such as the luminmide B synthetase Plu3263 from *P. luminescens*. Both NRPSs produce highly similar NRP with identical amino acid configurations (24). The A domains of Plu3263 are extraordinary flexible and accept a variety of (non)proteinogenic amino acid substrates resulting in the production of novel luminmide variants (luminmides C to I) by simple substrate feeding (66). Similarly, in *M. alpina* quantity and quality of malpibaldins and malpinins are dependent on the amino acids supplied in the medium (17), which was confirmed by the promiscuity of the MpbA A3 domain accepting at least three aromatic substrates. Interestingly, the NRPS code of the

zygomycetous A domains shows higher similarity to bacterial than to fungal A domains. For example, the arginine-activating A3 domain of MpcA comprises a guanidinium-stabilizing aspartate residue which is also present in the arginine-adenylating A domains of the bacterial NRPSs from *Pseudomonas syringae* pv. syringae (67) and *Microcystis aeruginosa* (54) but is absent in fungal NRPSs such as from the ascomycete *E. festucae* (63).

Taking all these finding together and considering the fact that *Mortierella* strains are frequently infected with NRPS-encoding proteobacteria from the genus *Mycoavidus* (35), a horizontal gene transfer from an (endo)bacterial symbiont into the fungal host is highly plausible. A similar phenomenon is postulated for the L-δ-(α-aminoadipoyl)-L-cysteinyl-D-valine synthetase (ACVS) genes responsible for β-lactam antibiotic biosynthesis: the ACVS-like NRPS genes from *A. nidulans* and *Penicillium chrysogenum* have most likely arisen from *Lysobacter*-like or *Streptomyces*-like bacterial ancestors (68–70). In phylogenetic analyses, A domains of fungal ACVS-NRPS clustered with bacterial representatives into one unique monophyletic group (71), similarly to MpcA and MpbA with endobacterial NRPSs in this study. However, neither codon usage nor GC content of the *Mortierella* NRPS genes matches that of the endosymbiotic *Mycoavidus* genes but are highly similar to that of *Mortierella* housekeeping genes. As expected for fungal genes, both *mpcA* and *mpbA* contain introns of an average size of 102 bp, indicating a comparably early gene transfer during evolution of *M. alpina* and a subsequent adaptation of the genes to the requirements of the eukaryotic mRNA processing (72). Recently, HGT events have been postulated as the main driver of secondary metabolism diversity in the zygomycetous genus *Basidiobolus*, as supported by the phylogenetic reconstructions of NRPS gene clusters with bacterial homologs (73). *Basidiobolus* species are common inhabitants of the amphibian gut and, similar to *Mortierella* species, live in close association with proteobacteria (74).

The ecological function of zygomycetous NRPs is still to be deciphered. However, from a pharmaceutical angle, malpicyclins A and C are structurally identical to the cyclopentapeptide plactins B and D, respectively, which were previously isolated from an uncharacterized fungus (38, 75) and exhibit fibrinolytic activities by elevating the activity of cellular urokinase-type plasminogen activator (39). The anticoagulating effects of plactins and derived cyclopentapeptides such as malformin A_1 are under investigation in treatment of thrombic disorders (76). Hence, *M. alpina* is not only of nutritional benefit by production of polyunsaturated fatty acids but also of pharmaceutical interest as a producer of bioactive natural products. Moreover, the abundance of natural products in *M. alpina* under certain growth conditions raises safety concerns regarding the biotechnological use of this strain.

In sum, this report disproves a long-standing dogma of a marginal secondary metabolism in zygomycetes and, instead, establishes Mortierellales as a promising, previously overlooked reservoir for bioactive metabolites.

Conclusion. Zygomycetes have long been industrially used as producers of long-chain unsaturated fatty acids, but their use as a resource for natural products has not been investigated yet. Here, we report on early-diverging fungi as a novel resource of bioactive compounds and demonstrated that their genomes encode functional secondary metabolite genes. The two cyclopentapeptide synthetases, MpcA and MpbA, from *M. alpina* are responsible for malpicyclin and malpibaldin biosynthesis, respectively. The surprising structural and mechanistic similarity to bacterial nonribosomal peptide synthetases (NRPSs) points to an endobacterial origin of *Mortierella* NRPS genes that differ from their asco- and basidiomycete counterparts and may have evolved independently.

MATERIALS AND METHODS

Organisms and culture maintenance. The fungal strain *Mortierella alpina* ATCC 32222 was purchased from the American Type Culture Collection (ATCC). Cultures were maintained on MEP agar plates (30 g/liter of malt extract, 3 g/liter of soy peptone, 18 g/liter of agar) for 7 days at 25°C. For antibiotic treatment of *M. alpina* and subsequent analyses (16S rDNA detection, metabolite quantification), refer to the supplemental experimental procedures. *Bacillus subtilis* subsp. *subtilis* 168 (DSM 23778) and *Esche-*

TABLE 4 Oligonucleotides used in this study

Name	Sequence (5′–3′)	Target	Purpose/restriction site	Primer efficiency (R^2)	Amplicon length cDNA/gDNA
oITS1	TCCGTAGGTGAACCTGCGG	ITS region	Strain identification		
oITS4	TCCTCCGCTTATTGATATGC	ITS region	Strain identification		
oJMW01	CATCGATCTGGCCTACATGG	*gpdA*	qPCR	1.94 (0.999)	80/229
oJMW02	CCACCTTGCCCTTGTAGC	*gpdA*	qPCR	1.94 (0.999)	80/229
oJMW03	GTATGTGCAAGGCCGGTTTCG	*actB*	qPCR	2.10 (0.998)	100/224
oJMW04	CCCATACCGACCATCACACC	*actB*	qPCR	2.10 (0.998)	100/224
oJMW30	GCCACTGCATTGGACTTGC	*mpbA/nps15*	qPCR	1.90 (0.991)	80/140
oJMW31	CCTCTTTGCTTTGCAGTTCGG	*mpbA/nps15*	qPCR	1.90 (0.991)	80/140
oJMW55	GCATAAATTGGTCCACGCTG	*mpcA/nps16*	qPCR	1.92 (0.999)	173/173
oJMW56	CGCTGTCCTCGACGATGAAC	*mpcA/nps16*	qPCR	1.92 (0.999)	173/173
oJMW63	CACGATGATCAAACCCTATCAATCATTC	*mpcA* module 3	Amplification		
oJMW64	CTGTTGAAGGTCGATGAGTGGC	*mpcA* module 3	Amplification		
oJMW67	TATATATATAGGCTAGCATGCACGATGATCAAACCCTATC	*mpcA* module 3	pET28 vector cloning (NheI)		
oJMW68	TATATATACTATGCGGCCGCCTGTTGAAGGTCGATGAGTG	*mpcA* module 3	pET28 vector cloning (NotI)		
oIW009	CAGGATGATCAGTCGCACAAC	*mpbA* module 3	Amplification		
oIW010	CAGGTGTCTCTGGCACTTCAC	*mpbA* module 3	Amplification		
oIW011	TATATAGCTAGCCAGGATGATCAGTCGCACAAC	*mpbA* module 3	pET28 vector cloning (NheI)		
oJMW12	ATATATGCGGCCGCAGGTGTCTCTGGCACTTC	*mpbA* module 3	pET28 vector cloning (NotI)		
oMG342	AGAGTTTGATCCTGGCTCAG	16S-rDNA	Endobacterial rDNA		
oMG343	CGGTTACCTTGTTACGACTT	16S-rDNA	Endobacterial rDNA		

richia coli DSM 498 were maintained on LB agar plates at 37°C. *E. coli* XL1-Blue (Agilent) and *E. coli* KRX (Promega) were used for plasmid propagation and for protein production, respectively, and were maintained in LB medium (5 g/liter of yeast extract, 10 g/liter of tryptone, 10 g/liter of sodium chloride) supplemented with 50 μg/ml of carbenicillin or 100 μg/ml of kanamycin (both Sigma-Aldrich), if applicable.

Chemical analysis and metabolite structure elucidation. (i) General. All chromatographic methods are summarized in Table S15. UHPLC-MS measurements of compounds 1 to 9 were carried out on an Agilent 1290 infinity II UHPLC coupled with an Agilent 6130 single quadrupole mass spectrometer (positive ionization mode) using methods A and B (Table S15) for routine metabolite detection and for metabolite quantification. High-resolution mass spectra and MS/MS fragmentation patterns of compounds 1 to 8 were recorded using a Q Exactive Plus mass spectrometer (Thermo Scientific). Chromatography for determination of amino acyl hydroxamate was performed on a Waters Acquity H-class UPLC system coupled to a Xevo TQ-S micro (Waters) tandem quadrupole instrument with electrospray ionization (ESI) source in positive ion mode (desolvation gas, N_2; collision gas, Ar; capillary voltage, 1.5 kV; cone voltage, 65 V; desolvation temperature, 500°C; desolvation gas flow, 1,000 liters/h). NMR spectra were recorded on a Bruker Avance III 600-MHz spectrometer at 300 K using dimethyl sulfoxide (DMSO) as the solvent and internal standard. Peaks were adjusted to δ_H 2.49 ppm and δ_C 39.5 ppm.

(ii) Metabolite isolation, structure elucidation, and antibiotic testing. Eight flasks with 500 ml of LB medium amended with 2% (wt/vol) fructose were inoculated with six agar blocks (2 by 2 mm) of *M. alpina* grown on MEP agar. After 7 days of cultivation at 160 rpm and 25°C, mycelium was harvested, resuspended in 1 liter of methanol/butanol/DMSO (12:12:1), and homogenized using a blender (Ultra-Turrax; IKA). The extract was filtered, and extraction of the fungal biomass was repeated. Both extracts were pooled and evaporated to dryness. The residue was resuspended in 25 ml of methanol/DMSO (10:1) and subjected to an Agilent Infinity 1260 preparative HPLC equipped with a Luna C_{18} column (250 by 21.2 mm, 10 μm; Phenomenex). The metabolites were separated according to method C (Table S15) (t_R = 8 to 10 min). Subsequently, the compounds were purified using method D (Table S15) on an Agilent 1200 HPLC system. Purified compounds were dissolved in DMSO-d_6 for NMR analyses. Absolute configurations of amino acids in the peptides 4 to 7 were determined using Marfey's method (see supplemental experimental procedures and method E in Table S15). Antimicrobial activities were determined by agar diffusion plates according to a published procedure (17), and MIC analysis was carried out as described in the supplemental experimental procedures.

NRPS identification and expression analysis. The genome of *M. alpina* ATCC 32222 was accessed from NCBI (National Center for Biotechnology Information) under Assembly accession number GCA_000240685.2. Putative NRPS genes were annotated using the fungal antiSMASH 5.0 software (42), and if required, putative intron-exon junctions were curated manually by alignment to fungal/bacterial NRPSs (Tables S8 to S10). Expression primers for *mpcA* and *mpbA* as well as housekeeping genes encoding β-actin (*actB*) and the glyceraldehyde-3-phosphate dehydrogenase (*gpdA*) were designed (cutoff PCR efficiency of at least 0.95) (Table 4). *M. alpina* was grown in LB medium amended with 2% of fructose (LB+F medium) or in potato dextrose broth (PDB; Sigma-Aldrich) at 160 rpm and 25°C for up to 4 days. RNA was extracted using the SV total RNA isolation system (Promega), and residual genomic DNA (gDNA) was digested with Baseline-Zero DNase (Biozym). cDNA was synthesized with RevertAid reverse transcriptase (Thermo Fisher) using oligo$(dT)_{18}$ primers. For quantitative real-time PCR (qRT-PCR), the qPCR Mix EvaGreen (BioSell) was used in a qPCR Cycler qTower³ (Analytik Jena) following the manufacturer's instructions and qPCR protocol: initiation at 95°C for 15 min, followed by 40 amplification

TABLE 5 Plasmids used in this study

Plasmid	Vector backbone	Purpose	Gene product	Source or reference
pJET1.2		Amplification of DNA		Thermo Fisher
pET28a (+)		Expression vector		Agilent
pJMW007	pET28a (+)	Expression of *mpcA*-M3	MpcA module 3	This study
pJMW023	pET28a (+)	expression of *mpbA*-M3	MpcA module 3	This study

cycles (95°C, 15 s; 60°C, 20 s; and 72°C, 20 s) and final recording of a melting curve (60 to 95°C). Expression data were calculated according to the threshold cycle ($\Delta\Delta C_T$) method by Pfaffl (77) using the housekeeping genes as internal, nonregulated reference controls.

Heterologous protein production and determination of enzymatic activity of A domains. For detailed cloning procedures and protein production protocols, refer to the supplemental experimental procedures and Tables 4 and 5. In brief, intron-free coding sequences of MpcA module 3 (*mpcA*-M3) and MpbA module 3 (*mpbA*-M3) were amplified from cDNA and ligated into the blunt pJET1.2 vector system (Thermo) prior to final subcloning into pET28a(+) expression vectors. NRPS modules were produced in *E. coli* KRX (Promega) at 16°C using 0.1% L-rhamnose as the inducer. Proteins were purified from cell-free lysate by metal ion affinity chromatography with Protino nickel-nitrilotriacetic acid (Ni-NTA) agarose (Macherey-Nagel) as the matrix, followed by ultrafiltration (Amicon Ultra-15 centrifugal filter units; Merck).

ATP-[^{32}P]PP$_i$ exchange assay. The assay was carried out as previously described (52, 64) using 5 nM MpcA-m3 in a 100-μl reaction mixture. Initially, pools of L-amino acids were used as substrates (Table S7), followed by testing of single substrates.

Multiplexed hydroxamate based adenylation domain assay (HAMA). The hydroxamate formation assay was conducted as previously described (51). In brief, the assay was carried out at room temperature in a 100-μl volume containing 50 mM Tris (pH 7.6), 5 mM $MgCl_2$, 150 mM hydroxylamine (pH 7.5 to 8, adjusted with NaOH), 5 mM ATP (A2383; Sigma), 1 mM tris(2-carboxyethyl)phosphine (TCEP), and 1 μM enzyme. Reactions were started by adding a mixture of 5 mM amino acids in 100 mM Tris (pH 8) to a final concentration of 1 mM or only buffer as a control. L-Phe, L-Val, and L-Leu were distinguished from D-Phe, D-Val, and L-Ile, respectively, by using enantiopure, deuterium-labeled standards. Reactions were quenched by 10-fold dilution in acetonitrile containing 0.1% formic acid and subjected to UPLC-MS analysis (method F in Table S15). Compounds were detected via specific mass transitions recorded in multiple reaction monitoring (MRM) mode. Data acquisition and quantitation were conducted using the MassLynx and TargetLynx software (version 4.1). Quantitation was done by external calibration with standard solutions of hydroxamates ranging from 0.0032 to 10 μM.

Phylogenetic analysis. The genomes of the zygomycete *M. alpina* ATCC 32222 and the endofungal bacteria *Mycoavidus cysteinexigens* AG77 and *Paraburkholderia* (syn. *Mycetohabitans*) *rhizoxinica* HKI 0454^T were obtained from the JGI fungal genomics resource database or NCBI genome database and were subjected to a screening analysis for fungal and bacterial secondary metabolite gene clusters by the antiSMASH 5.0 software (42). The A and C domains were extracted from putative enzymes and, additionally, from experimentally proven endobacterial, bacterial, and fungal NRPS and NRPS-like enzymes (Tables S8 to S10). For A domain phylogeny, a total set of 108 amino acid sequences (Table S8) were aligned using the ClustalW algorithm implemented in the Geneious 10.2.4 software. For phylogenetic analysis of C domains, altogether 225 bacterial and 90 fungal sequences of C domains of verified NRPS and NRPS-like proteins (Tables S9 and S10) were aligned by MAFFT version 7 using the E-INS-i algorithm and BLOSUM62 scoring matrix (78). The evolutionary history was inferred using the Neighbor-Joining method (79). The evolutionary distances were computed using the Jukes Cantor genetic distance model implemented in the MEGA X software (80). A bootstrap support of $\geq$50% is given for 1,000 replicates each.

Data availability. The sequence of full-length transcripts of *mpcA* and *mpbA* were deposited in GenBank (accession numbers MT800760 and MT800759).

SUPPLEMENTAL MATERIAL

Supplemental material is available online only.

SUPPLEMENTAL FILE 1, PDF file, 7.4 MB.

ACKNOWLEDGMENTS

We are grateful to Heike Heinecke and Andrea Perner (both from Hans Knöll Institute [HKI], Jena, Germany) for their technical assistance in recording NMR and HR-MS/MS spectra, respectively. We thank Kerstin Voigt (Jena Microbial Resource Collection, Jena, Germany) for initial antimicrobial testing and Sarah Niehs (HKI) for donation of genomic DNA from *R. microsporus* and *P. rhizoxinica*.

Hajo Kries gratefully acknowledges a fellowship from the Daimler und Benz Foundation and financial support from the DFG (grant number 441781663) and the Fonds der Chemischen Industrie (FCI).

REFERENCES

1. Smith DJ, Burnham MK, Edwards J, Earl AJ, Turner G. 1990. Cloning and heterologous expression of the penicillin biosynthetic gene cluster from *Penicillium chrysogenum*. Biotechnology (NY) 8:39–41. https://doi.org/10.1038/nbt0190-39.
2. Campbell CD, Vederas JC. 2010. Biosynthesis of lovastatin and related metabolites formed by fungal iterative PKS enzymes. Biopolymers 93:755–763. https://doi.org/10.1002/bip.21428.
3. Gajdacs M. 2019. The continuing threat of methicillin-resistant *Staphylococcus aureus*. Antibiotics (Basel) 8:e52.
4. Weber JM, Wierman CK, Hutchinson CR. 1985. Genetic analysis of erythromycin production in *Streptomyces erythreus*. J Bacteriol 164:425–433. https://doi.org/10.1128/JB.164.1.425-433.1985.
5. Hibbett DS, Binder M, Bischoff JF, Blackwell M, Cannon PF, Eriksson OE, Huhndorf S, James T, Kirk PM, Lucking R, Thorsten Lumbsch H, Lutzoni F, Matheny PB, McLaughlin DJ, Powell MJ, Redhead S, Schoch CL, Spatafora JW, Stalpers JA, Vilgalys R, Aime MC, Aptroot A, Bauer R, Begerow D, Benny GL, Castlebury LA, Crous PW, Dai YC, Gams W, Geiser DM, Griffith GW, Gueidan C, Hawksworth DL, Hestmark G, Hosaka K, Humber RA, Hyde KD, Ironside JE, Koljalg U, Kurtzman CP, Larsson KH, Lichtwardt R, Longcore J, Miadlikowska J, Miller A, Moncalvo JM, Mozley-Standridge S, Oberwinkler F, Parmasto E, Reeb V, et al. 2007. A higher-level phylogenetic classification of the Fungi. Mycol Res 111:509–547. https://doi.org/10.1016/j.mycres.2007.03.004.
6. Spatafora JW, Chang Y, Benny GL, Lazarus K, Smith ME, Berbee ML, Bonito G, Corradi N, Grigoriev I, Gryganskyi A, James TY, O'Donnell K, Roberson RW, Taylor TN, Uehling J, Vilgalys R, White MM, Stajich JE. 2016. A phylum-level phylogenetic classification of zygomycete fungi based on genome-scale data. Mycologia 108:1028–1046. https://doi.org/10.3852/16-042.
7. Voigt K, Wolf T, Ochsenreiter K, Nagy G, Kaerger K, Shelest E, Papp T. 2016. Genetic and metabolic aspects of primary and secondary metabolism of the Zygomycetes, p 361–385. *In* Hoffmeister D (ed), The Mycota, vol III. Biochemistry and molecular biology, 3rd ed. Springer International Publishing, Cham, Switzerland. https://doi.org/10.1007/978-3-319-27790-5_15.
8. Sutter RP. 1970. Trisporic acid synthesis in *Blakeslea trispora*. Science 168:1590–1592. https://doi.org/10.1126/science.168.3939.1590.
9. Sutter RP, Capage DA, Harrison TL, Keen WA. 1973. Trisporic acid biosynthesis in separate plus and minus cultures of *Blakeslea trispora*. J Bacteriol 114:1074–1082. https://doi.org/10.1128/JB.114.3.1074-1082.1973.
10. Sahadevan Y, Richter-Fecken M, Kaerger K, Voigt K, Boland W. 2013. Early and late trisporoids differentially regulate beta-carotene production and gene transcript levels in the mucoralean fungi *Blakeslea trispora* and *Mucor mucedo*. Appl Environ Microbiol 79:7466–7475. https://doi.org/10.1128/AEM.02096-13.
11. Bajpai PK, Bajpai P, Ward OP. 1991. Production of arachidonic acid by *Mortierella alpina* ATCC 32222. J Ind Microbiol 8:179–185. https://doi.org/10.1007/BF01575851.
12. Bajpai PK, Bajpai P, Ward OP. 1991. Arachidonic acid production by fungi. Appl Environ Microbiol 57:1255–1258. https://doi.org/10.1128/AEM.57.4.1255-1258.1991.
13. Kawashima H, Akimoto K, Higashiyama K, Fujikawa S, Shimizu S. 2000. Industrial production of dihomo-gamma-linolenic acid by a Delta-5-desaturase-defective mutant of *Mortierella alpina* 1S-4 fungus. J Am Oil Chem Soc 77:1135–1138. https://doi.org/10.1007/s11746-000-0178-2.
14. Tallima H, El Ridi R. 2018. Arachidonic acid: physiological roles and potential health benefits—a review. J Adv Res 11:33–41. https://doi.org/10.1016/j.jare.2017.11.004.
15. Koyama N, Kojima S, Nonaka K, Masuma R, Matsumoto M, Omura S, Tomoda H. 2010. Calpinactam, a new anti-mycobacterial agent, produced by *Mortierella alpina* FKI-4905. J Antibiot (Tokyo) 63:183–186. https://doi.org/10.1038/ja.2010.14.
16. Kamiyama T, Umino T, Nakayama N, Itezono Y, Satoh T, Yamashita Y, Yamaguchi A, Yokose K. 1992. Ro 09-1679, a novel thrombin inhibitor. J Antibiot (Tokyo) 45:424–427. https://doi.org/10.7164/antibiotics.45.424.
17. Baldeweg F, Warncke P, Fischer D, Gressler M. 2019. Fungal biosurfactants from *Mortierella alpina*. Org Lett 21:1444–1448. https://doi.org/10.1021/acs.orglett.9b00193.
18. Kawahara T, Itoh M, Izumikawa M, Sakata N, Tsuchida T, Shin-Ya K. 2017. Novel arginine-containing peptides MBJ-0173 and MBJ-0174 from *Mortierella alpina* f28740. J Antibiot (Tokyo) 70:226–229. https://doi.org/10.1038/ja.2016.116.
19. Burke PA, DeNardo SJ, Miers LA, Lamborn KR, Matzku S, DeNardo GL. 2002. Cilengitide targeting of alpha(v)beta(3) integrin receptor synergizes with radioimmunotherapy to increase efficacy and apoptosis in breast cancer xenografts. Cancer Res 62:4263–4272.
20. Hwang Y, Rowley D, Rhodes D, Gertsch J, Fenical W, Bushman F. 1999. Mechanism of inhibition of a poxvirus topoisomerase by the marine natural product sansalvamide A. Mol Pharmacol 55:1049–1053. https://doi.org/10.1124/mol.55.6.1049.
21. Xu WJ, Liao XJ, Xu SH, Diao JZ, Du B, Zhou XL, Pan SS. 2008. Isolation, structure determination, and synthesis of galaxamide, a rare cytotoxic cyclic pentapeptide from a marine algae *Galaxaura filamentosa*. Org Lett 10:4569–4572. https://doi.org/10.1021/ol801799d.
22. Xu WF, Hou XM, Yao FH, Zheng N, Li J, Wang CY, Yang RY, Shao CL. 2017. Xylapeptide A, an antibacterial cyclopentapeptide with an uncommon L-pipecolinic acid moiety from the associated fungus *Xylaria* sp. (GDG-102). Sci Rep 7:e6937. https://doi.org/10.1038/s41598-017-07331-4.
23. Belofsky GN, Jensen PR, Fenical W. 1999. Sansalvamide: a new cytotoxic cyclic depsipeptide produced by a marine fungus of the genus *Fusarium*. Tetrahedron Lett 40:2919–2926.
24. Fu J, Bian X, Hu S, Wang H, Huang F, Seibert PM, Plaza A, Xia L, Muller R, Stewart AF, Zhang Y. 2012. Full-length RecE enhances linear-linear homologous recombination and facilitates direct cloning for bioprospecting. Nat Biotechnol 30:440–446. https://doi.org/10.1038/nbt.2183.
25. Kaweewan I, Hemmi H, Komaki H, Kodani S. 2020. Isolation and structure determination of a new antibacterial peptide pentaminomycin C from *Streptomyces cacaoi* subsp. *cacaoi*. J Antibiot (Tokyo) 73:224–229. https://doi.org/10.1038/s41429-019-0272-y.
26. Wang L, Chen W, Feng Y, Ren Y, Gu Z, Chen H, Wang H, Thomas MJ, Zhang B, Berquin IM, Li Y, Wu J, Zhang H, Song Y, Liu X, Norris JS, Wang S, Du P, Shen J, Wang N, Yang Y, Wang W, Feng L, Ratledge C, Zhang H, Chen YQ. 2011. Genome characterization of the oleaginous fungus *Mortierella alpina*. PLoS One 6:e28319. https://doi.org/10.1371/journal.pone.0028319.
27. Walsh CT, O'Brien RV, Khosla C. 2013. Nonproteinogenic amino acid building blocks for nonribosomal peptide and hybrid polyketide scaffolds. Angew Chem Int Ed Engl 52:7098–7124. https://doi.org/10.1002/anie.201208344.
28. Hoffmann K, Schneider-Scherzer E, Kleinkauf H, Zocher R. 1994. Purification and characterization of eucaryotic alanine racemase acting as key enzyme in cyclosporin biosynthesis. J Biol Chem 269:12710–12714.
29. Jia LJ, Tang HY, Wang WQ, Yuan TL, Wei WQ, Pang B, Gong XM, Wang SF, Li YJ, Zhang D, Liu W, Tang WH. 2019. A linear nonribosomal octapeptide from *Fusarium graminearum* facilitates cell-to-cell invasion of wheat. Nat Commun 10:e922. https://doi.org/10.1038/s41467-019-08726-9.
30. Gao X, Haynes SW, Ames BD, Wang P, Vien LP, Walsh CT, Tang Y. 2012. Cyclization of fungal nonribosomal peptides by a terminal condensation-like domain. Nat Chem Biol 8:823–830. https://doi.org/10.1038/nchembio.1047.
31. Partida-Martinez LP, de Looss CF, Ishida K, Ishida M, Roth M, Buder K, Hertweck C. 2007. Rhizonin, the first mycotoxin isolated from the zygomycota, is not a fungal metabolite but is produced by bacterial endosymbionts. Appl Environ Microbiol 73:793–797. https://doi.org/10.1128/AEM.01784-06.
32. Niehs SP, Dose B, Scherlach K, Roth M, Hertweck C. 2018. Genomics-driven discovery of a symbiont-specific cyclopeptide from bacteria residing in the rice seedling blight fungus. Chembiochem 19:2167–2172. https://doi.org/10.1002/cbic.201800400.
33. Ohshima S, Sato Y, Fujimura R, Takashima Y, Hamada M, Nishizawa T, Narisawa K, Ohta H. 2016. *Mycoavidus cysteinexigens* gen. nov., sp. nov., an endohyphal bacterium isolated from a soil isolate of the fungus *Mortierella elongata*. Int J Syst Evol Microbiol 66:2052–2057. https://doi.org/10.1099/ijsem.0.000990.
34. Uehling J, Gryganskyi A, Hameed K, Tschaplinski T, Misztal PK, Wu S, Desiro A, Vande Pol N, Du Z, Zienkiewicz A, Zienkiewicz K, Morin E, Tisserant E, Splivallo R, Hainaut M, Henrissat B, Ohm R, Kuo A, Yan J, Lipzen A, Nolan M, LaButti K, Barry K, Goldstein AH, Labbe J, Schadt C, Tuskan G, Grigoriev I, Martin F, Vilgalys R, Bonito G. 2017. Comparative

genomics of *Mortierella elongata* and its bacterial endosymbiont *Mycoavidus cysteinexigens*. Environ Microbiol 19:2964–2983. https://doi.org/10.1111/1462-2920.13669.
35. Desiro A, Hao Z, Liber JA, Benucci GMN, Lowry D, Roberson R, Bonito G. 2018. *Mycoplasma*-related endobacteria within *Mortierellomycotina* fungi: diversity, distribution and functional insights into their lifestyle. ISME J 12:1743–1757. https://doi.org/10.1038/s41396-018-0053-9.
36. Marfey P. 1984. Determination of D-amino acids. 2. Use of a bifunctional reagent, 1,5-difluoro-2,4-dinitrobenzene. Carlsberg Res Commun 49:591–596. https://doi.org/10.1007/BF02908688.
37. Harada K, Fujii K, Mayumi T, Hibino Y, Suzuki M, Ikai Y, Oka H. 1995. A method using LC/MS for determination of absolute configuration of constituent amino acids in peptide—advanced Marfey's method. Tetrahedron Lett 36:1515–1518. https://doi.org/10.1016/0040-4039(95)00078-Q.
38. Inoue T, Hasumi K, Kuniyasu T, Endo A. 1996. Isolation of plactins A, B, C and D, novel cyclic pentapeptides that stimulate cellular fibrinolytic activity. J Antibiot (Tokyo) 49:45–49. https://doi.org/10.7164/antibiotics.49.45.
39. Harada T, Tsuruta T, Yamagata K, Inoue T, Hasumi K. 2009. Dual modulation of prothrombin activation by the cyclopentapeptide plactin. FEBS J 276:2516–2528. https://doi.org/10.1111/j.1742-4658.2009.06976.x.
40. Iwasaki S, Kobayashi H, Furukawa J, Namikoshi M, Okuda S, Sato Z, Matsuda I, Noda T. 1984. Studies on macrocyclic lactone antibiotics. VII. Structure of a phytotoxin "rhizoxin" produced by *Rhizopus chinensis*. J Antibiot (Tokyo) 37:354–362. https://doi.org/10.7164/antibiotics.37.354.
41. Partida-Martinez LP, Hertweck C. 2005. Pathogenic fungus harbours endosymbiotic bacteria for toxin production. Nature 437:884–888. https://doi.org/10.1038/nature03997.
42. Blin K, Shaw S, Steinke K, Villebro R, Ziemert N, Lee SY, Medema MH, Weber T. 2019. antiSMASH 5.0: updates to the secondary metabolite genome mining pipeline. Nucleic Acids Res 47:W81–W87. https://doi.org/10.1093/nar/gkz310.
43. Stachelhaus T, Mootz HD, Marahiel MA. 1999. The specificity-conferring code of adenylation domains in nonribosomal peptide synthetases. Chem Biol 6:493–505. https://doi.org/10.1016/S1074-5521(99)80082-9.
44. Sohn YS, Nam DH, Ryu DD. 2001. Biosynthetic pathway of cephabacins in *Lysobacter lactamgenus*: molecular and biochemical characterization of the upstream region of the gene clusters for engineering of novel antibiotics. Metab Eng 3:380–392. https://doi.org/10.1006/mben.2001.0200.
45. Kaljunen H, Schiefelbein SH, Stummer D, Kozak S, Meijers R, Christiansen G, Rentmeister A. 2015. Structural elucidation of the bispecificity of A domains as a basis for activating non-natural amino acids. Angew Chem Int Ed Engl 54:8833–8836. https://doi.org/10.1002/anie.201503275.
46. Kraas FI, Helmetag V, Wittmann M, Strieker M, Marahiel MA. 2010. Functional dissection of surfactin synthetase initiation module reveals insights into the mechanism of lipoinitiation. Chem Biol 17:872–880. https://doi.org/10.1016/j.chembiol.2010.06.015.
47. Bergendahl V, Linne U, Marahiel MA. 2002. Mutational analysis of the C-domain in nonribosomal peptide synthesis. Eur J Biochem 269:620–629. https://doi.org/10.1046/j.0014-2956.2001.02691.x.
48. Kikukawa H, Sakuradani E, Ando A, Shimizu S, Ogawa J. 2018. Arachidonic acid production by the oleaginous fungus *Mortierella alpina* 1S-4: a review. J Adv Res 11:15–22. https://doi.org/10.1016/j.jare.2018.02.003.
49. Kikukawa H, Sakuradani E, Ando A, Okuda T, Ochiai M, Shimizu S, Ogawa J. 2015. Disruption of lig4 improves gene targeting efficiency in the oleaginous fungus *Mortierella alpina* 1S-4. J Biotechnol 208:63–69. https://doi.org/10.1016/j.jbiotec.2015.05.020.
50. Khan F, He M, Taussig MJ. 2006. Double-hexahistidine tag with high-affinity binding for protein immobilization, purification, and detection on ni-nitrilotriacetic acid surfaces. Anal Chem 78:3072–3079. https://doi.org/10.1021/ac060184l.
51. Stanišić A, Hüsken A, Kries H. 2019. HAMA: a multiplexed LC-MS/MS assay for specificity profiling of adenylate-forming enzymes. Chem Sci 10:10395–10399. https://doi.org/10.1039/c9sc04222a.
52. Baldeweg F, Kage H, Schieferdecker S, Allen C, Hoffmeister D, Nett M. 2017. Structure of ralsolamycin, the interkingdom morphogen from the crop plant pathogen *Ralstonia solanacearum*. Org Lett 19:4868–4871. https://doi.org/10.1021/acs.orglett.7b02329.
53. Villiers BR, Hollfelder F. 2009. Mapping the limits of substrate specificity of the adenylation domain of TycA. Chembiochem 10:671–682. https://doi.org/10.1002/cbic.200800553.
54. Meyer S, Kehr JC, Mainz A, Dehm D, Petras D, Süssmuth RD, Dittmann E. 2016. Biochemical dissection of the natural diversification of microcystin provides lessons for synthetic biology of NRPS. Cell Chem Biol 23:462–471. https://doi.org/10.1016/j.chembiol.2016.03.011.
55. Romans-Fuertes P, Sondergaard TE, Sandmann MI, Wollenberg RD, Nielsen KF, Hansen FT, Giese H, Brodersen DE, Sorensen JL. 2016. Identification of the non-ribosomal peptide synthetase responsible for biosynthesis of the potential anti-cancer drug sansalvamide in *Fusarium solani*. Curr Genet 62:799–807. https://doi.org/10.1007/s00294-016-0584-4.
56. Bruner SD, Weber T, Kohli RM, Schwarzer D, Marahiel MA, Walsh CT, Stubbs MT. 2002. Structural basis for the cyclization of the lipopeptide antibiotic surfactin by the thioesterase domain SrfTE. Structure 10:301–310. https://doi.org/10.1016/s0969-2126(02)00716-5.
57. Grunwald AL, Berrue F, Robertson AW, Overy DP, Kerr RG. 2017. Mortiamides A–D, cyclic heptapeptides from a novel *Mortierella* sp. obtained from Frobisher Bay. J Nat Prod 80:2677–2683. https://doi.org/10.1021/acs.jnatprod.7b00383.
58. Walton JD. 2006. HC-toxin. Phytochemistry 67:1406–1413. https://doi.org/10.1016/j.phytochem.2006.05.033.
59. Hai Y, Jenner M, Tang Y. 2019. Complete stereoinversion of L-tryptophan by a fungal single-module nonribosomal peptide synthetase. J Am Chem Soc 141:16222–16226. https://doi.org/10.1021/jacs.9b08898.
60. Rausch C, Hoof I, Weber T, Wohlleben W, Huson DH. 2007. Phylogenetic analysis of condensation domains in NRPS sheds light on their functional evolution. BMC Evol Biol 7:78. https://doi.org/10.1186/1471-2148-7-78.
61. Yang X, Feng P, Yin Y, Bushley K, Spatafora JW, Wang C. 2018. Cyclosporine biosynthesis in *Tolypocladium inflatum* benefits fungal adaptation to the environment. mBio 9:e01211-18. https://doi.org/10.1128/mBio.01211-18.
62. Gao X, Chooi YH, Ames BD, Wang P, Walsh CT, Tang Y. 2011. Fungal indole alkaloid biosynthesis: genetic and biochemical investigation of the tryptoquialanine pathway in *Penicillium aethiopicum*. J Am Chem Soc 133:2729–2741. https://doi.org/10.1021/ja1101085.
63. Berry D, Mace W, Grage K, Wesche F, Gore S, Schardl CL, Young CA, Dijkwel PP, Leuchtmann A, Bode HB, Scott B. 2019. Efficient nonenzymatic cyclization and domain shuffling drive pyrrolopyrazine diversity from truncated variants of a fungal NRPS. Proc Natl Acad Sci U S A 116:25614–25623. https://doi.org/10.1073/pnas.1913080116.
64. Kalb D, Lackner G, Hoffmeister D. 2014. Functional and phylogenetic divergence of fungal adenylate-forming reductases. Appl Environ Microbiol 80:6175–6183. https://doi.org/10.1128/AEM.01767-14.
65. Matsuda K, Zhai R, Mori T, Kobayashi M, Sano A, Abe I, Wakimoto T. 2020. Heterochiral coupling in non-ribosomal peptide macrolactamization. Nat Catal 3:507–515. https://doi.org/10.1038/s41929-020-0456-7.
66. Weyler C, Heinzle E. 2017. Synthesis of natural variants and synthetic derivatives of the cyclic nonribosomal peptide luminmide in permeabilized *E. coli* Nissle and product formation kinetics. Appl Microbiol Biotechnol 101:131–138. https://doi.org/10.1007/s00253-016-7770-7.
67. Guenzi E, Galli G, Grgurina I, Gross DC, Grandi G. 1998. Characterization of the syringomycin synthetase gene cluster. A link between prokaryotic and eukaryotic peptide synthetases. J Biol Chem 273:32857–32863. https://doi.org/10.1074/jbc.273.49.32857.
68. Landan G, Cohen G, Aharonowitz Y, Shuali Y, Graur D, Shiffman D. 1990. Evolution of isopenicillin N synthase genes may have involved horizontal gene transfer. Mol Biol Evol 7:399–406. https://doi.org/10.1093/oxfordjournals.molbev.a040615.
69. Liras P, Martin JF. 2006. Gene clusters for beta-lactam antibiotics and control of their expression: why have clusters evolved, and from where did they originate? Int Microbiol 9:9–19.
70. Bushley KE, Turgeon BG. 2010. Phylogenomics reveals subfamilies of fungal nonribosomal peptide synthetases and their evolutionary relationships. BMC Evol Biol 10:e26. https://doi.org/10.1186/1471-2148-10-26.
71. Lawrence DP, Kroken S, Pryor BM, Arnold AE. 2011. Interkingdom gene transfer of a hybrid NPS/PKS from bacteria to filamentous Ascomycota. PLoS One 6:e28231. https://doi.org/10.1371/journal.pone.0028231.
72. Da Lage JL, Binder M, Hua-Van A, Janecek S, Casane D. 2013. Gene make-up: rapid and massive intron gains after horizontal transfer of a bacterial alpha-amylase gene to Basidiomycetes. BMC Evol Biol 13:e40. https://doi.org/10.1186/1471-2148-13-40.
73. Tabima JF, Trautman IA, Chang Y, Wang Y, Mondo S, Kuo A, Salamov A, Grigoriev IV, Stajich JE, Spatafora JW. 2020. Phylogenomic analyses of non-Dikarya fungi supports horizontal gene transfer driving diversification of secondary metabolism in the amphibian gastrointestinal symbiont, *Basidiobolus*. G3 (Bethesda) 10:3417–3433. https://doi.org/10.1534/g3.120.401516.

74. Henk DA, Fisher MC. 2012. The gut fungus *Basidiobolus ranarum* has a large genome and different copy numbers of putatively functionally redundant elongation factor genes. PLoS One 7:e31268. https://doi.org/10.1371/journal.pone.0031268.
75. Inoue T, Hasumi K, Sugimoto M, Endo A. 1998. Enhancement of fibrinolysis by plactins: structure-activity relationship and effects in human U937 cells and in mice. Thromb Haemost 79:591–596. https://doi.org/10.1055/s-0037-1614951.
76. Koizumi Y, Nagai K, Gao L, Koyota S, Yamaguchi T, Natsui M, Imai Y, Hasumi K, Sugiyama T, Kuba K. 2018. Involvement of RSK1 activation in malformin-enhanced cellular fibrinolytic activity. Sci Rep 8:e5472. https://doi.org/10.1038/s41598-018-23745-0.
77. Pfaffl MW. 2001. A new mathematical model for relative quantification in real-time RT-PCR. Nucleic Acids Res 29:e45. https://doi.org/10.1093/nar/29.9.e45.
78. Katoh K, Standley DM. 2013. MAFFT multiple sequence alignment software version 7: improvements in performance and usability. Mol Biol Evol 30:772–780. https://doi.org/10.1093/molbev/mst010.
79. Saitou N, Nei M. 1987. The neighbor-joining method: a new method for reconstructing phylogenetic trees. Mol Biol Evol 4:406–425. https://doi.org/10.1093/oxfordjournals.molbev.a040454.
80. Kumar S, Stecher G, Li M, Knyaz C, Tamura K. 2018. MEGA X: molecular evolutionary genetics analysis across computing platforms. Mol Biol Evol 35:1547–1549. https://doi.org/10.1093/molbev/msy096.
81. Conti E, Stachelhaus T, Marahiel MA, Brick P. 1997. Structural basis for the activation of phenylalanine in the non-ribosomal biosynthesis of gramicidin S. EMBO J 16:4174–4183. https://doi.org/10.1093/emboj/16.14.4174.
82. Bian X, Plaza A, Yan F, Zhang Y, Müller R. 2015. Rational and efficient site-directed mutagenesis of adenylation domain alters relative yields of luminmide derivatives *in vivo*. Biotechnol Bioeng 112:1343–1353. https://doi.org/10.1002/bit.25560.

Supplemental Material

Bacterial-like nonribosomal peptide synthetases produce cyclopeptides in the zygomycetous fungus *Mortierella alpina*

Jacob Martin Wurlitzer,[a] Aleksa Stanišić,[b] Ina Wasmuth,[a] Sandra Jungmann,[c] Dagmar Fischer,[c] Hajo Kries,[b] Markus Gressler[a]

[a] Pharmaceutical Microbiology, Leibniz Institute for Natural Product Research and Infection Biology – Hans Knöll-Institute, Friedrich-Schiller-University Jena, Winzerlaer Strasse 2, 07745 Jena, Germany

[b] Junior Research Group "Biosynthetic Design of Natural Products", Leibniz Institute for Natural Product Research and Infection Biology, Hans Knöll-Institute, Beutenbergstrasse 11a, 07745 Jena, Germany

[c] Pharmaceutical Technology and Biopharmacy, Friedrich-Schiller-University Jena, Lessingstrasse 8, 07743 Jena, Germany

Table of contents

Experimental procedures

Metabolite quantification and 16S-rDNA detection in antibiotic treated *M. alpina*.

Antibiotic treatment. To cure *M. alpina* from potential bacterial endosymbionts, the fungus was cultivated on MEP agar plates amended with 200 µg mL^{-1} ciprofloxacin and 200 µg mL^{-1} spectinomycin (both Sigma Aldrich) for seven days at 25°C. The mycelium was transferred to a new plate and cultivation was repeated six times. Plates without antibiotics served as controls.

Metabolite quantification. To check for altered product formation, flasks containing 50 mL LB medium supplemented with 200 µg mL^{-1} ciprofloxacin and 200 µg mL^{-1} spectinomycin were inoculated with agar blocks from plates of each generation. After 7 days of cultivation at 160 rpm at 25 °C, mycelium was harvested, lyophilized and ground using mortar and pistil. Lysed mycelium was extracted using 5 mL methanol/butanol/DMSO (12:12:1), centrifuged and diluted 1:10 using methanol. Metabolites were quantified on an UHPLC-MS system (method A, Table S15) using serial dilutions of authentic standards. Metabolite abundance was adjusted to the dried biomass.

16S-rDNA detection. To determine the presence of endobacteria, genomic DNA (gDNA) from *M. alpina* was isolated from the treated and untreated fungal cell lines grown in LB medium (48 h, 160 rpm, 25 °C) with the DNeasy Plant Mini Kit (Qiagen) according to manufacturer's instructions. The fungal internal transcribed spacer (ITS) spanning region and the bacterial 16S-rDNA sequences were amplified with Phusion DNA polymerase (Thermo) according to manufacturer´s instructions using oligonucleotides oITS1 and oITS4 or oMG342 and oMG343, respectively (Table 4). After gel purification, the DNA fragments were sequenced and compared to microbial sequences using NCBI BLASTn. DNA extracted from the soil bacterium *B. subtilis 168*, the fungus *Rhizopus microsporus* and its bacterial endosymbiont *Paraburkholderia (syn. Mycetohabitans) rhizoxinica* HKI 0454^T were used as positive control for 16S-rDNA amplification. In absence of a 16S-rDNA signal, the amplification of the fungal ITS region served as internal verification of template DNA (loading control).

Chemical analysis

Advanced Marfey's method. Absolute configuration of amino acids in the peptides **4-7** was determined using Marfey´s method (1) with slight modifications. In brief, 100 – 200 µg purified compounds were hydrolyzed with 6 N HCl overnight at 100°C. After neutralization with 6 N KOH, water was evaporated and the residual was dissolved in 100 µL H_2O. 25 µL hydrolysate were mixed with 10 µL 1 M $NaHCO_3$ and 50 µL 1% L-FDLA (*N*-α-[5-fluoro-2,4-dinitrophenyl]-L-leucinyl-amide) (2) in acetone and incubated at 40 °C for 60 min. The reaction was stopped by addition of 10 µL 1 N HCl. Samples

were diluted in methanol (1:10) and products were analyzed by UHPLC-MS using method E (Table S15). L-FDLA derivatives of L- and D-configured amino acid served as reference standards. Coupled amino acids were detected by mass according (m/z $[M+H]^+ = M_{aa} + M_{FDLA} - M_{Fluorine}$).

Determination of bioactivities and physicochemical properties of 4-7.

Determination of antimicrobial activities. Initially, purified metabolites (**4-7**) were dissolved in methanol (1 mg mL $^{-1}$) and agar diffusion assays were performed (3) with the following test strains: *Bacillus subtilis* JMRC:STI:10880, *Enterococcus faecalis* (VRE) JMRC:ST:33700, *Escherichia coli* JMRC:ST:33699, *Pseudomonas aeruginosa* JRMC:ST33771, *Pseudomonas aeruginosa* JMRC:ST:33772, *Staphylococcus aureus* (MRSA) JMRC:ST:33793, *Mycobacterium vaccae* JMRC:STI:10670, *Candida albicans* JMRC:STI:50163, *Penicillium notatum* JMRC:STI:50164, *Sporobolomyces salmonicolor* JMRC:ST:35974. Ciprofloxacin (5 µg mL $^{-1}$), amphotericin B (10 µg ml $^{-1}$) and pure methanol served as controls.

Determination of MICs. For determination of the minimal inhibition concentration (MIC_{50}), compounds **4-7** - in gradual dilutions ranging from 0.98 µg mL^{-1} to 500 µg mL^{-1} - were added into sterile 96 well plates and kept at room temperature until residual solvent was evaporated. A total volume of 200 µl bacterial cell suspensions of *B. subtilis* 168 and *E. coli* DSM 498 (OD_{600} 0.1) were added and the plates were incubated in a microplate reader (ClarioStar BMG Labtech, agitation at 100 rpm for 10 s every 15 min) at 37 °C for a duration of 24 h. Growth was monitored at λ = 600 nm. The maximum slope in the exponential growth phase was determined and MIC_{50} values were calculated through sigmoidal 4PL interpolation (GraphPad Prism 7.04). Ciprofloxacin was used as control in concentrations ranging from 9.8 ng mL^{-1} to 5.0 µg mL^{-1} (against *E. coli*) and from 3.9 ng mL^{-1} to 2.0 µg mL^{-1} (against *B. subtilis*).

Surface tension measurements. The surface tension was measured using the De Noüy ring tensiometer (Krüss Processor Tensiometer K12, Krüss, Hamburg, Germany) with a standard platinum ring. After dissolution in DMSO (10 mg/mL), samples (a mixture of **4, 5, 6** and **7** in a ratio of 21:21:55:2) were diluted with deionized water to a concentration of 1 mg/mL (stock solution). Serial dilutions (1.95-1000 µg/mL) were performed using 10% (v/v) DMSO in water. The surface tension of each dilution was measured three times at 25 °C using the ring tear-off method. Sodium dodecyl sulfate (SDS, Carl Roth GmbH + Co. KG, Karlsruhe, Germany) was used as reference measured under the same conditions. Additionally, the surface tension of the 10% DMSO solution was measured as control. The critical micelle concentration (CMC) of the sample was calculated by means of surface tension concentration plots and determination of the intersection point.

Protein production and enzymatic activity assays.

Heterologous protein production. The coding regions of MpcA module 3 (*mpcA*-M3) and MpbA module 3 (*mpbA*-M3) spanning the C-A-T tri-domain coding regions were amplified from cDNA by PCR using the oligonucleotides oJMW063 and oJMW064 or oIW011 and oJMW112, respectively (Table 4). After blunt-end ligation into pJET1.2, fragments were excised using *Nhe*I and *Not*I restriction sites flanking the fragment upstream and downstream, respectively. Both fragments were ligated into an analogously digested expression vector pET28a(+) using the T4-DNA-Ligase (Thermo) to gain plasmids pJMW007 (*mpcA*-M3 expressing) and pJMW023 (*mpbA*-M3 expressing) (Table 5). The plasmids were propagated in *E. coli* XL-1 blue (Agilent) and subsequently used for transformation of *E. coli* expression strain KRX (Promega). Transformants were cultivated in 500 mL LB medium supplemented with 100 µg mL^{-1} kanamycin at 37°C until an OD_{600} of 0.6 was reached. Temperature was shifted to 16°C and gene expression was induced by addition of 0.1% L-rhamnose. After continued cultivation for additional 20 h, cells were centrifuged (3,200 × g, 40 min, 4 °C). The cell pellet was suspended in lysis buffer (20 mM imidazole, 50 mM sodium phosphate, 300 mM sodium chloride, pH 8.0) and lysed by a Sonoplus ultrasonic sonifier (Bandelin; impulse interval: 20 s, impulse duration: 5 s, impulse force 0.8 kJ, repetition cycles: 5). The soluble *N*-terminal His_6-tagged fusion proteins were purified by gravity flow metal ion affinity chromatography (Protino Ni-NTA Agarose, Macherey-Nagel). After rinsing with increasing imidazole concentrations (20 mM to 80 mM imidazole in lysis buffer), proteins were eluted with elution buffer (500 mM imidazole in lysis buffer). Proteins were concentrated and desalted by Amicon Ultra-15 centrifugal filter units with 100 kDa molecular weight cut-off (Merck) and re-buffered in phosphate reaction buffer (50 mM Tris pH 8.0, 200 mM NaCl, 10% glycerol). Protein concentration was quantified via Bradford assay (4) with the Protein Assay Kit (Bio-Rad) and enzymes were stored at -80°C.

Determination of the codon usage

Codon usage of the NRPS genes *mpcA* and *mpbA* from *M. alpina* and Plu3263 from *P. luminescens were* extracted from their specific CDS. For average codon usages in single strains from *Mortierella alpina, Photorhabdus luminescens* and *Mycoavidus cysteinexigens*, a total of 10,000 codons were extracted from approximately 100 housekeeping genes of each organism. Codon distribution is expressed as occurrence per corresponding amino acid (%). Codons for amino acids that are encoded by a single triplett (ATG for Met, UUG for Trp) were not considered in this analysis.

Table S1. Physicochemical properties of the identified metabolites **4**-**9**.

no.	compound	chemical formula	*m/z* $[M + H]^+$	λ_{max} (nm)	Yield (mg)	provided structural data
4	Malpicyclin A	$C_{32}H_{52}N_8O_6$	645.4071	224	8.5	HR-ESI-MS, ^1H and ^{13}C NMR
5	Malpicyclin B	$C_{32}H_{52}N_8O_6$	645.4075	224	7.0	HR-ESI-MS, ^1H and ^{13}C NMR
6	Malpicyclin C	$C_{32}H_{52}N_8O_5$	629.4343	224	6.5	HR-ESI-MS, ^1H and ^{13}C NMR
7	Malpicyclin D	$C_{31}H_{50}N_8O_5$	615.3976	224	1.5	HR-ESI-MS, ^1H and ^{13}C NMR
8	Malpicyclin E	$C_{34}H_{53}N_9O_5$	668.4228	n.d.	traces	HR-ESI-MS
9	Malpicyclin F	$C_{31}H_{50}N_8O_6$	631.3959	n.d.	traces	HR-ESI-MS

Table S2. HR-ESI-MS data of **4**-**9.**

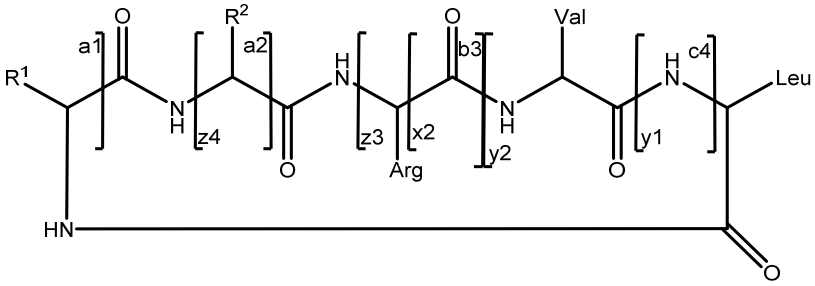

Cmpd.	Residue		*m/z* $[M+H]^+$ fragment										
	R^1	R^2	a1	a2	b3	c4	x2	y1	y2	z3	z4	-CO	arom. aa
4	Leu	Tyr	86.10	249.16	-	-	239.15	112.09	211.16	352.23	518.34	617.41	136.08
5	Ile	Tyr	86.10	249.16	-	546.34	239.15	112.09	211.16	353.23	518.34	617.41	136.08
6	Leu	Phe	86.10	233.16	417.26	530.34	239.15	112.09	211.16	352.23	499.30	601.42	120.08
7	Val	Phe	72.08	219.15	403.24	516.33	239.15	112.09	211.16	352.23	499.30	587.40	120.08
8	Leu	Trp	86.10	272.18	456.27	569.35	239.15	112.09	211.16	352.23	541.36	640.43	159.09
9	Val	Tyr	72.08	235.16	419.24	532.33	239.15	112.09	211.16	353.23	518.34	603.39	136.08

Table S3. NMR data of **4** and **5** in DMSO-d_6, * signals overlapping

malpicyclin A (**4**)				*malpicyclin B* (**5**)			
	*δ*C [ppm]	type	*δ*H [ppm], M (*J* [Hz])		*δ*C [ppm]	type	*δ*H [ppm], M (*J* [Hz])
	D-*leucine*				D-*isoleucine*		
1	171.0(1)	C=O	-	1	170.8	C=O	-
2	50.2	αC	4.33, m*	2	56.4	αC	4.10, t (8.6)
2-NH	-	NH	7.92, d (8.6)	2-NH	-	NH	7.70, d (8.9)
3	40.0	CH2	A: 1.32, m* B: 1.49, m*	3	36.3	CH	1.52, m*, 1.40, m*
4	24.1	CH	1.34, m*	4	14.6	CH3	0.72, m*
5	22.7	CH3	0.86, m*	5	25.4	CH2	A: 1.07, m, B: 0.87, m*
6	22.2	CH3	0.78, m*	6	11.1	CH3	0.75, m*
	L-*tyrosine*				L-*tyrosine*		
7	171.0 (2)	C=O	-	7	171.1	C=O	-
8	54.4	αC	4.34, m*	8	54.5	αC	4.38, m
8-NH	-	NH	8.18, d (7.5)	8-NH	-	NH	8.35, d (7.4)
9	36.5	CH2	2.7, d (7.4)	9	35.9	CH2	2.70, m
10	127.3	C (ar)	-	10	127.3	C (ar)	
11	130.0	CH (ar)	6.94, d (8.3)	11	130.0	CH (ar)	6.98, m
12	114.8	CH (ar)	6.63, d (8.4)	12	114.8	CH (ar)	6.62, d (6.6)
13	155.8	C (ar)	-	13	155.8	C (ar)	
13-OH	-	OH	9.16, s	13-OH	-	OH	9.15, s
14	114.8	CH (ar)	6.63, d (8.4)	14	114.8	CH (ar)	6.62, d (6.6)
15	130.0	CH (ar)	6.94, d (8.3)	15	130.0	CH (ar)	6.98, m
	D-*arginine*				D-*arginine*		
16	171.6	C=O	-	16	171.6	C=O	-
17	54.8	αC	3.87, m	17	54.6	αC	3.90, m
17-NH	-	NH	8.42, d (7.0)	17-NH	-	NH	8.54, d (6.9)
18	27.9	CH2	A: 1.67, m*, B: 1.51, m*	18	28.0	CH2	A: 1.70, m*, B: 1.54, m
19	25.4	CH2	1.33, m*	19	25.2	CH2	1.39, m
20	40.1	CH2	3.03, m	20	40.0	CH2	3.03, m
20-NH	-	NH	7.53, t (5.3)	20-NH	-	NH	7.49, m
21	156.7	C	-	21	156.1	C	-
	-	NH	-		-	NH	-
	-	NH2	-		-	NH2	-
	D-*valine*				D-*valine*		
22	170.8	C=O	-	22	170.6	C=O	-
23	57.5	αC	4.01, m	23	57.6	αC	4.03, t (8.1)
23-NH	-	NH	6.81, d (8.1)	23-NH	-	NH	6.84, d (7.9)
24	30.8	CH	1.84, m	24	30.7	CH	1.89, m
25	18.5	CH3	0.82, m*	25	18.6(1)	CH3	0.83, m*
26	18.7	CH3	0.75, m*	26	18.6(2)	CH3	0.76, m*
	L-*leucine*				L-*leucine*		
27	171.4	C=O	-	27	171.3	C=O	-
28	50.8	αC	4.18, t (8.2)	28	50.5	αC	4.25, m
28-NH	-	NH	8.65, d (7.4)	28-NH	-	NH	8.70, d (7.3)
29	37.3	CH2	A:1.51, m*, B: 1.38, m*	29	37.0	CH2	1.48, m*
30	24.0	CH	1.54, m*	30	24.0	CH	1.55, m*
31	22.6	CH3	0.87, m*	31	22.7	CH3	0.87, m*
32	21.5	CH3	0.80, m*	32	21.6	CH3	0.80, m*

Table S4. NMR data of **6** and **7** in DMSO-d_6, * signals overlapping.

malpicyclin C (**6**)				*malpicyclin D* (**7**)			
	δC [ppm]	type	δH [ppm], M (*J* [Hz])		δC [ppm]	type	δH [ppm], M (*J* [Hz])
	D-*leucine*				D-*valine*		
1	171.1	C=O	-	1	170.6	C=O	-
2	50.2	αC	4.34, m	2	57.8	αC	4.01, m*
2-NH	-	NH	7.95, d (8.7)	2-NH	-	NH	7.77, d (8.8)
3	40.03	CH2	1.39, m*	3	29.9	CH	1.74, m
4	24.1	CH	1.33, m*	4	18.4	CH3	0.76, m*
5	22.7	CH3	0.84, m*	5	19.0	CH3	0.64, m*
6	22.1	CH3	0.78, m*				
	L-*phenylalanine*				L-*phenylalanine*		
7	170.7	C=O	-	6	171.0	C=O	-
8	54.4	αC	4.42, m*	7	54.2	αC	4.48, m (7.5)
8-NH	-	NH	8.27, d (7.4)	7-NH	-	NH	8.39, d (7.5)
9	37.35	CH2	2.82, m	8	36.9	CH2	2.82, m
10	137.1	C (ar)	-	9	137.2	C (ar)	-
11	128.0	CH (ar)	7.23, d (7.4)	10		CH (ar)	7.23, d (7.5)
12	129.1	CH (ar)	7.15, d (7.7)	11	129.1	CH (ar)	7.20, m*
13	126.3	C (ar)	7.18, d (7.4)	12	126.3	C (ar)	7.19, m*
	-	-	-		-	-	-
14	129.1	CH (ar)	7.15, d (7.7)	13	129.1	CH (ar)	7.20, m*
15	128.0	CH (ar)	7.23, d (7.4)	14	128.1	CH (ar)	7.23, d (7.5)
	D-*arginine*				D-*arginine*		
16	171.6	C=O	-	15	171.6	C=O	-
17	54.8	αC	3.84, m	16	54.7	αC	3.87, m
17-NH	-	NH	8.41, d (7.2)	16-NH	-	NH	8.52, d (7.5)
18	27.8	CH2	A: 1.63, m*, B: 1.45, m	17	28.0	CH2	A: 1.66, m*, B: 1.51, m*
19	25.1	CH2	1.21, m*	18	25.2	CH2	1.24, m*
20	40.01	CH2	2.97, m (6.2)	19	40.0	CH2	2.99, m
20-NH	-	NH	7.50, m*	19-NH	-	NH	7.45, t (9.8)
21	156.6	C	-	20	156.6	C	-
	-	NH	-		-	NH	-
	-	NH2	-		-	NH2	-
	D-*valine*				D-*valine*		
22	170.8	C=O	-	21	170.7	C=O	-
23	57.5	αC	4.02, m	22	57.6	αC	4.03, m*
23-NH	-	NH	6.81, d (8.0)	22-NH	-	NH	6.81, d (8.2)
24	30.9	CH	1.82, m	23	30.8	CH	1.89, m
25	18.5	CH3	0.82, m*	24	18.6	CH3	0.79, m*
26	18.7	CH3	0.75, m*	25	18.5	CH3	0.79, m*
	L-*leucine*				L-*leucine*		
27	171.4	C=O	-	26	171.2	C=O	-
28	50.8	αC	4.21, m*	27	50.5	αC	4.25, m
28-NH	-	NH	8.66, d (7.3)	27-NH	-	NH	8.71 , d (7.5)
29	37.37	CH2	A: 1.53, m*, B: 1.39, m*	28	37.0	CH2	1.50, m*
30	24.0	CH	1.56, m*	29	24.0	CH	1.56, m*
31	22.6	CH3	0.87, m*	30	21.6	CH3	0.81, m*
32	21.5	CH3	0.79, m*	31	22.7	CH3	0.88, m*

Table S5. Results of Marfey´s analysis for **4-7**. Retention times (in min) of the respective FDLA-amino amids are given. L- and D standards are highlighted in red and blue respectively.

sample	Leu	Ile	Val	Arg	Phe	Tyr
$M_{AS\text{-}FDLA}$ [g/mol]	426	426	412	469	460	476
L-standard	7.84	7.80	7.25	5.48	8.08	7.02
D-standard	9.21	9.16	8.52	5.32	9.09	7.58
4	7.84 + 9.21 (1:1)	-	8.52	5.31	-	7.03
5	7.85	9.16	8.52	5.33	-	7.03
6	7.84 + 9.21 (1:1)	-	8.53	5.31	8.09	-
7	7.84	-	8.52	5.33	8.09	-

Table S6. NRPS codes for adenylating domains of NRPS from *Mortierella* and related species. The proposed activated substrates are listed in column 3. The residues are mapped relative to *Aneurinibacillus migulanus* (former *Brevibacillus brevis)* GrsA-A numbering (5). NRPS codes were partially extracted from Bian *et al.* (6). Amino acid residues in the NRPS code are highlighted according to their physicochemical properties: acidic (red), small/hydrophobic (grey), aromatic/hydrophobic (ocher), hydrophilic (green), and basic (blue). *Organisms are highlighted according to their phylogenetic origin: basal fungi (blue), higher fungi (brown), and bacteria (green). Aaa= α-2-amino adipic acid.

Protein	**Organism***	**substrate**	**Residue position according to GrsA Phe numbering**									
domain			**235**	**236**	**239**	**278**	**299**	**301**	**322**	**330**	**331**	**527**
MpcA_A2	*M. alpina*	Tyr/Phe	D	P	F	T	M	G	A	V	V	K
MpbA_A3	*M. alpina*	Trp/Tyr/Phe	D	P	F	V	M	G	G	T	V	K
Plu3263_A3	*P. luminescens*	Phe	D	A	W	C	I	A	A	V	C	K
BacC_A2	*B. subtilis*	Phe	D	A	F	T	V	A	A	V	C	K
GrsA_A1	*A. migulanus*	Phe	D	A	W	T	I	A	A	I	C	K
TycA_A1	*A. migulanus*	Phe	D	A	W	T	I	A	A	I	C	K
CepA_A1	*A. orientalis*	Tyr	D	A	S	T	V	A	A	V	C	K
TycC_A1	*A. migulanus*	Tyr	D	A	L	T	T	G	E	V	V	K
GliP_A1	*A. fumigatus*	Phe	D	G	S	I	L	G	A	C	A	K
BEAS_A2	*B. bassiana*	Phe	D	G	Y	I	M	A	A	V	M	K
MpbA_A1/ MpcA_A4	*M. alpina*	Val	D	A	F	W	L	G	G	T	F	K
MpcA_A1	*M. alpina*	Leu/Ile/Val	D	A	F	F	I	G	A	M	L	K
MpbA_A2	*M. alpina*	Leu	D	A	F	F	I	G	A	M	V	K
MpbA_A4/A5	*M. alpina*	Leu	D	A	I	F	L	G	A	T	I	K
MpcA_A5	*M. alpina*	Leu	D	A	M	F	I	G	G	T	I	K
Plu3263_A2/ A4/A5	*P. luminescens*	Leu	D	A	W	C	I	G	A	V	C	K
GrsAmut_A1	*A. migulanus*	Leu	D	A	W	M	I	G	A	I	C	K
SrfAA_A2	*B. subtilis*	Leu	D	A	F	M	M	G	M	V	F	K
GrsB_A1	*A. migulanus*	Val	D	A	F	W	I	G	G	T	F	K
EasA_A3	*A. nidulans*	Leu	D	I	H	F	V	G	A	I	A	K
BSLS_A2	*B. bassiana*	Leu	D	G	Y	I	I	G	G	V	F	K
CssA_A9	*T. inflatum*	Val	D	A	W	M	F	A	A	V	L	K
MpcA_A3	*M. alpina*	Arg	D	A	A	S	V	G	A	T	D	K
SyrE_A5	*P. syringae*	Arg	D	V	A	D	V	C	A	I	D	K
McyC_A1	*M. aeruginosa*	Arg	D	V	W	T	I	G	A	V	D	K
McyB_A1	*M. aeruginosa*	Arg	D	V	W	T	I	G	A	V	E	K
PpzA-1_A2	*E. festucae*	Arg	D	V	S	D	T	G	A	P	T	K
Lys2_A1	*S. cerevisiae*	Aaa	D	P	R	H	F	V	M	R	A	K

Table S7. Amino acid pools used for ATP-[^{32}P]PP$_i$ exchange assay**.**

pool no.	biochemical properties	composition (1 mM each)
#1	small, aliphatic	Gly, L-Ala, L-Val, L-Leu, L-Ile
#2	S-/O containing	L-Cys, L-Met, L-Ser, L-Thr, L-Pro
#3	large, aromatic	L-His, L-Phe, L-Tyr, L-Trp
#4	acids and amides	L-Asp, L-Asn, L-Glu, L-Gln
#5	basic	L-Lys, L-Arg, L-Orn

Table S8. Protein sequences used for phylogenetic analysis of A domains. Protein sequences were obtained from the databases NCBI, KEGG or JGI. # "PKS-NRPS" indicates NRPS, that use a polyketide derived from a PKS as substrate. "PKS/NRPS" indicate hybrid proteins with both enzymatic activities on the same protein. *Experimentally verified function.

kingdom	organism	enzyme class #	protein abbreviation	protein ID or locus	metabolite/ verified function*	Reference
(soil) bacteria	*Pseudomonas aeruginosa*	NRPS	PvdD	AAX16295.1	Pyoverdine	(7)
		NRPS	PvdI	AAX16297.1	Pyoverdine	(7)
		NRPS	PvdJ	NP_251090.2	Pyoverdine	(7)
		NRPS	PvdI	NP_251114.1	Pyoverdine	(7)
	Ralstonia solanacearum	NRPS	RmyA	WP_011003939.1	Ralsolamycin A	(8)
		NRPS	RmyB	WP_011003940.1	Ralsolamycin A	(8)
	Photorhabdus luminescens	NRPS	plu3263	CAE15637.1	Luminmide A and B	(9, 10)
	Streptomyces anulatus (syn. *chrysomallus)*	NRPS	AcmA	WP_057667193.1	Actinomycin	(11)
		NRPS	AcmB	WP_057667184.1	Actinomycin	(11)
		NRPS	AcmC	WP_057667177.1	Actinomycin	(11)
(endo)bacteria	*Mycoavidus cysteinexigens*	NRPS	Nps1	ctg1_626: SMCOG1127	unknown	(12)
		NRPS	Nps3	ctg1_2014: SMCOG1127	unknown	(12)
	Paraburkholderia (syn. Mycetohabitans) rhizoxinica	NRPS	RBRH_01504	CBW76463.1	Heptarhizin and Rhizomide A-C	(13-15)
		NRPS	RBRH_01792	CBW76913.1	Holrhizin	(15, 16)
fungi	*Agaricus bisporus var. bisporus*	NRPS-like (aryl acid reductase)	XP_006462975	XP_006462975.1	unknown	(17)
	Aspergillus clavatus	NRPS-like	XP_001275157.1	XP_001275157.1	unknown	(17)

		(L-serine reductase)				
		PKS/NRPS	CcsA	A1CLY8.1	Cytochalasin	(18)
	Aspergillus nidulans	NRPS-like (aryl acid reductase)	XP_664048	XP_664048.1	unknown	(17)
		PKS-NRPS	EasA	C8VPS9.1	Emercillamide	(19)
		PKS/NRPS	ApdA	XP_681681.1	Aspyridone A	(20)
	Aspergillus flavus	NRPS-like (L-Tyr reductase)	LnaA	XP_002384042.1	L-tyrosine reduction	(17)
		NRPS-like (L-Tyr reductase)	LnbA	XP_002384859.1	L-tyrosine reduction	(17)
		PKS/NRPS	CpaS	BAI43678.1	α-cyclopiazonic acid	(21)
	Aspergillus fumigatus	NRPS	GliP	AAW03307.1	Gliotoxin	(22)
		PKS/NRPS	PsoA	XP_747151.2	Pseurotin A	(23)
		NRPS-like (L-serine reductase)	XP_001481395.1	XP_001481395.1	unknown	(17)
	Aspergillus terreus	NRPS-like (aryl acid reductase)	ATEG_03630	XP_001212808.1	unknown	(17)
		PKS/NRPS	FlaA	XP_001210411.1	Isoflavipucine	(24)
	Candida albicans	NRPS-like (α-amino adipate reductase)	Lys2	AOW25963	α-amino adipate reduction (α-AA-δ-semialdehyde)	(25)
	Dichomitus squalens	NRPS-like (α-amino adipate reductase)	Lys2	EJF63849.1	unknown	(17)
		NRPS-like (L-serine reductase)	Nps1	EJF63449.1	unknown	(17)

	Fusarium graminearum	NRPS	NRPS5	ATA65242.1	Fusaoctaxin	(26)
	Fusarium heterosporum	PKS/NRPS	EquS	AAV66110.2	Equisetin	(27)
	Fusarium oxysporum f. sp. vasinfectum	NRPS-like (L-serine reductase)	EXM16769.1	EXM16769.1	unknown	(17)
	Gelatoporia (Ceriporiopsis) subvermispora B	NRPS-like (α-amino adipate reductase)	Nps3	EMD34789.1	α-amino adipate reduction (α-AA-δ-semialdehyde)	(17)
		NRPS-like (L-serine reductase)	Nps1	EMD40260.1	L-serine reduction	(17)
	Gloeophyllum trabeum	NRPS-like (aryl acid reductase)	EPQ54396	EPQ54396.1	unknown	(17)
	Heterobasidion irregulare	NRPS-like (α-amino adipate reductase)	Lys2	ETW75842.1	unknown	(17)
	Moniliophthora roreri	NRPS-like (aryl acid reductase)	ESK96610	ESK96610.1	unknown	(17)
	Mortierella alpina	NRPS	NRPS15 (MpbA)	ADAG01001033 ctg645_orf22+23	Malpibaldin A-C	This study
		NRPS	NRPS16 (MpcA)	ADAG01001033 ctg645_orf36	Malpicyclin A-E	This study
	Punctularia strigosozonata	NRPS-like (α-amino adipate reductase)	Nps2	EIN08908.1	unknown	(17)
	Rigidoporus microspora	NRPS-like (α-amino adipate reductase)	Lys2	924741 fgenesh1_pm.14_#_30	unknown	(15)
	Saccharomyces cerevisiae	NRPS-like (α-amino adipate reductase)	Lys2	NP_009673.1	α-amino adipate reduction	(28)

13

					(α-AA-δ-semialdehyde)	
		L-Trp-tRNA ligase	Wrs1	A6ZNB3_YEAS7	[served as outgroup]	(29)
	Serpula lacrymans	NRPS-like (aryl acid reductase)	Nps11	ANX99775.1	unknown	(17)
	Stereum hirsutum	NRPS-like (L-serine reductase)	Nps3	EIM85977.1	unknown	(17)
		NRPS-like (α-amino adipate reductase)	Lys1	EIM82061.1	unknown	(17)
	Tolypocladium inflatum	NRPS	SimA	CAA82227.1	Cyclosporin	(30),(31)
	Trametes versicolor	NRPS-like (L-serine reductase)	Nps7	EIW59229.1	unknown	(17)
		NRPS-like (α-amino adipate reductase)	Nps4	EIW55513.1	unknown	(17)
	Trichoderma reesei	NRPS-like (aryl acid reductase)	XP_006964071	XP_006964071.1	unknown	(17)
	Trichoderma virens	NRPS-like (aryl acid reductase)	EHK23193	EHK23193.1	unknown	(17)
		NRPS-like (L-serine reductase)	EHK20896.1	EHK20896.1	unknown	(17)
	Xylaria sp.	PKS/NRPS	XylA	AAS46233.1	Xyrrolin	(32)

Table S9. Protein sequences used for phylogenetic analysis of C domains from bacterial NRPS and *Mortierella* NRPS. Protein sequences were obtained from the databases NCBI, KEGG or JGI. # "PKS-NRPS" indicates NRPS, that use a polyketide (derived from a separate PKS) as starter substrate. "PKS/NRPS" indicate hybrid proteins with both enzymatic activities on the same protein. *Experimentally verified function.

kingdom	organism	enzyme class#	protein abbreviation	protein ID or locus	metabolite/ verified function*	Reference
bacteria	*Aneurinibacillus migulanus*	NRPS	GrsA	P0C062.1	Gramicidin S	(33)
	(former *Brevibacillus brevis*)	NRPS	GrsB	CAA43838.1	Gramicidin S	(33)
		NRPS	TyrA	P09095.2	Tyrocidine	(34)
		NRPS	TyrB	O30408.1	Tyrocidine	(34)
		NRPS	TyrC	O30409.1	Tyrocidine	(34)
	Bacillus licheniformis	NRPS	BacA	AAC06346.1	Bacitracin	(35)
		NRPS	BacB	AAC06347.1	Bacitracin	(35)
		NRPS	BacC	AAC06348.1	Bacitracin	(35)
		NRPS	LicA	AAD04757.1	Lichenysin	(36)
		NRPS	LicB	AAD04758.1	Lichenysin	(36)
		NRPS	LicC	AAD04759.1	Lichenysin	(36)
	Bacillus subitilis	NRPS	DhbF	AAD56240.1	Bacillibactin	(37)
		NRPS	PpsA	NP_389716.1	Plipastatin	(38)
		NRPS	PpsB	NP_389715.1	Plipastatin	(38)
		NRPS	PpsC	NP_389714.1	Plipastatin	(38)
		NRPS	PpsD	NP_389713.1	Plipastatin	(38)
		NRPS	SrfA-A	BAA08982.1	Surfactin	(39)
		NRPS	SrfA-B	NP_388231.1	Surfactin	(39)
		NRPS	SrfA-C	BAA08985.1	Surfactin	(39)

		NRPS	FenA	AAB80955.2	Fengycin	(40)
		NRPS	FenB	AAB00093.1	Fengycin	(40)
		NRPS	FenC	AAC36721.1	Fengycin	(40)
		NRPS	FenD	CAA09819.1	Fengycin	(40)
		NRPS	FenE	AAB80956.1	Fengycin	(40)
		NRPS	ItuA	AMM04304.1	Iturin	(41)
		NRPS	ItuB	AMM04305.1	Iturin	(41)
		NRPS	ItuC	AMM04306.1	Itruin	(41)
		NRPS	MyoA	Q9R9J1.1	Myosubtilin	(42)
		NRPS	MyoB	Q9R9J0.1	Myosubtilin	(42)
		NRPS	MyoC	Q9R9I9.1	Myosubtilin	(42)
	Bradyrhizobium diazoefficiens	PKS-NRPS	-	WP_011084903.1	unknown	-
	Burkholderia mallei	NRPS	-	WP_011204623.1	unknown	-
		NRPS	-	WP_011204624.1	unknown	-
	Burkholderia pseudomallei	NRPS	-	WP_011205655.1	unknown	-
	Chromobacterium violaceum	NRPS	NPS1	WP_011136349.1	unknown	-
	Escherichia coli	NRPS	EntB	AAA92015.1	Enterobactin	(43)
	Microcystis aeruginosa	PKS-NRPS	McyB	BAA83993.1	Microcystin-LR	(44)
		PKS-NRPS	McyC	BAA83994.1	Microcystin-LR	(44)
		PKS-NRPS	McyE	BAA83996.1	Microcystin-LR	(44)
	Micromonospora sp.	NRPS	TioR	CAJ34374.1	Thiocoraline	(45)
		NRPS	TioS	CAJ34375.1	Thiocoraline	(45)
	Nostoc spec.	PKS/NRPS	NosA	Q9RAH4	Nostopeptolide A	(46)
		PKS/NRPS	NosC	Q9RAH2	Nostopeptolide A	(46)
		PKS/NRPS	NosD	Q9RAH1	Nostopeptolide A	(46)

	Pectobacterium atrosepticum	NRPS	-	WP_011093070.1	unknown	-
		NRPS	-	WP_011093071.1	unknown	-
	Photorhabdus luminescens	NRPS	Plu3263	CAE15637.1	Luminmide A and B	(9, 10)
		NRPS	Plu2670	NP_929905.1	Compound 1-3	(47)
	Pseudomonas aeruginosa	NRPS	PA3327	NP_252017.1	unknown	(48)
		NRPS	PchE	WP_057391644.1	Pyochelin	(49)
		NRPS	PchF	AAD55801	Pyochelin	(49)
	Pseudomonas protegens	NRPS	OfaA	WP_011060446.1	Orfamide A	(50)
	Pseudomonas sp.	NRPS	ArfA	Q84BQ4	Arthrofactin	(51)
		NRPS	ArfC	Q84BQ6	Arthrofactin	(51)
	Pseudomonas syringae	NRPS	SyrE	AAC80285.1	Syringomycin	(52)
		NRPS	SyfA	NP_792633.1	Syringafactin	(53)
		NRPS	SyfB	NP_792634.1	Syringafactin	(53)
	Ralstonia solanacearum	PKS-NRPS	RmyA	WP_011003939.1	Ralsolamycin	(8)
		PKS-NRPS	RmyB	WP_011003940.1	Ralsolamycin	(8)
	Salinispora arenoicola	NRPS	CymA		Cyclomarin A	(54)
	Streptomyces anulatus (syn. *chrysomallus)*	NRPS	AcmB	WP_057667184.1	Actinomycin	(11)
		NRPS	AcmC	WP_057667177.1	Actinomycin	(11)
	Streptomyces coelicolor	NRPS	CdaPS1	NP_627443.1	Calcium-Dependent Antibiotic	(55)
		NRPS	CdaPS2	NP_627444.1	Calcium-Dependent Antibiotic	(55)
		NRPS	CdaPS3	NP_733597.1	Calcium-Dependent Antibiotic	(55)
	Streptomyces lavendulae	NRPS	ComB	AAK81825.1	Complestatin	(56)

17

		NRPS	ComC	AAK81826.1	Complestatin	(56)
		NRPS	ComD	AAK81827.1	Complestatin	(56)
	Streptomyces pristinaespiralis	NRPS	SnbC	CAA67248.1	Pristinamycin	(57)
		NRPS	SnbDE	CAA67249.1	Pristinamycin	(57)
	Streptomyces verticillus	NRPS	BlmIV	AA02364.1	Bleomycin	(58)
		NRPS	BlmVI	AA02359.1	Bleomycin	(58)
		NRPS	BlmX	AA02355.1	Bleomycin	(58)
	Yersinia pestis	PKS/NRPS	Irp1	WP_141450873.1	Yerseniabactin	(59)
		NRPS	Irp2	WP_012229554.1	Yerseniabactin	(59)
(endo) bacteria	*Mycoavidus cysteinexigens*	NRPS	Nps1	ctg1_626: SMCOG1127	-	(12)
		NRPS	Nps3	ctg1_2014: SMCOG1127	-	(12)
	Paraburkholderia (syn. Mycetohabitans) rhizoxinica	NRPS	RBRH_01504	CBW76463.1	Heptarhizin and Rhizomide A-C	(13-15)
fungi	*Mortierella alpina*	NRPS	NRPS15 (MpbA)	ADAG01001033 ctg645_orf22+23	Malpibaldin A-C	This study
		NRPS	NRPS16 (MpcA)	ADAG01001033 ctg645_orf36	Malpicyclin A-E	This study

Table S10. Protein sequences used for phylogenetic analysis of C domains from fungal NRPS and NRPS-like proteins. Protein sequences were obtained from the databases NCBI, KEGG or JGI. # "PKS-NRPS" indicates NRPS, that use a polyketide (derived from a separate PKS) as starter substrate. "PKS/NRPS" indicate hybrid proteins with both enzymatic activities on the same protein. *Experimentally verified function.

kingdom	organism	enzyme class#	protein abbreviation	protein ID or locus	metabolite/ verified function*	Reference
fungi	*Aspergillus clavatus*	PKS/NRPS	CcsA	A1CLY8.1	Cytochalasin	(18)
	Aspergillus flavus	NRPS	AgiA	XP_002385303	Aspergillicin A-F	(60)
		PKS/NRPS	CpaS	BAI43678.1	α-cyclopiazonic acid	(21)
	Aspergillus nidulans	PKS-NRPS	EasA	C8VPS9.1	Emercillamide	(19)
		PKS/NRPS	ApdA	XP_681681.1	Aspyridone A	(20)
	Aspergillus fumigatus	PKS/NRPS	PsoA	XP_747151.2	Pseurotin A	(23)
	Aspergillus terreus	PKS/NRPS	FlaA	XP_001210411.1	Isoflavipucine	(24)
	Aureobasidium pullans	NRPS	Aba1	ACJ04424.1	Aureobasidin A1	(61)
	Beauveria bassiana	NRPS	BEAS	ACI30655	Beauvericin	(62)
		NRPS	BSLS	AFP96785	Bassianolide	(63)
		PKS/NRPS	TenS	CAL69597.1	Tenellin	(64)
	Cochliobolus carbonum	NRPS	HTS1	Q01886	HC-Toxin	(65)
	Dichomitus squalens	NRPS-like (α-amino adipate reductase)	Lys2	EJF63849.1	-	(17)
	Fomitopsis pinicola	NRPS-like (α-amino adipate reductase)	Lys2	EPS97414.1	-	(17)
	Fusarium graminearum	NRPS	NRPS5	ATA65242.1	Fusaoctaxin	(26)
		NRPS	NRPS9	XP_011325380.1	Fusaoctaxin	(26)
		PKS/NRPS	FUSS	XP_011327617.1	Fusarin C	(66)
	Fusarium heterosporum	PKS/NRPS	EqiS	AAV66110.2	Equisetin	(27)

	Fusarium incarnatum	PKS	Aps1	ACZ66258.1	Apicidin	(67)
	Fusarium solani	NRPS	NRPS30	XP_003049233.1	Sansalvamide	(68)
	Gelatoporia (Ceriporiopsis) subvermispora B	NRPS-like (α-amino adipate reductase)	Nps3	EMD34789.1	α-amino adipate reduction (α-AA-δ-semialdehyde)	(17)
	Heterobasidion irregulare	NRPS-like (α-amino adipate reductase)	Lys2	ETW75842.1	-	(17)
	Mortierella alpina	NRPS-like (α-amino adipate reductase)	Lys2	ADAG01001006 ctg618_orf28	-	(69)
		NRPS	NRPS15 (MpbA)	ADAG01001033 ctg645_orf22+23	Malpibaldin A-C	This study
		NRPS	NRPS16 (MpcA)	ADAG01001033 ctg645_orf36	Malpicyclin A-E	This study
	Neosartorya fischeri	NRPS	AnaPS	A1DN09.1	Acetylaszonalenin	(70)
	Penicillium aethiopicum	NRPS	TquA	ADY16697.1	Tryptoquialanine	(71)
	Penicillium chrysogenum	NRPS	Acv1	ABR12615.1	(Iso-)Penicillins	(72)
	Penicillium expansum	PKS/NRPS	CheA	CAO91861.1	Cytochalasan	(73)
	Punctularia strigosozonata	NRPS-like (α-amino adipate reductase)	Nps2	EIN08908.1	-	(17)
	Rigidoporus microspora	NRPS-like (α-amino adipate reductase)	Lys2	924741 fgenesh1_pm.14_#_30	-	(15)
	Stereum hirsutum	NRPS-like (α-amino adipate reductase)	Lys1	EIM82061.1	-	(17)
	Tolypocladium inflatum	NRPS	SimA	CAA82227.1	Cyclosporin	(30),(31)

20

	Trametes versicolor	NRPS-like (α-amino adipate reductase)	Nps4	EIW55513.1	-	(17)
	Xylaria sp.	PKS/NRPS	XylA	AAS46233.1	Xyrrolin	(32)

21

Table S11. BlastP analysis against proven endobacterial symbionts using MpbA as query**.** The 5 best hits are shown.

Description	Max Score	Total Score	Query cover	E value	Per. Ident.	Accession
***Paraburkholderia rhizoxinica* (syn. *Mycetorhabitans endofungorum*)**						
amino acid adenylation domain-containing protein, partial [*Mycetohabitans endofungorum*]	3425	13690	93%	0.0	44.13%	WP_146064104.1
non-ribosomal peptide synthetase [*Mycetohabitans endofungorum*]	3174	8732	97%	0.0	46.28%	WP_104078507.1
amino acid adenylation domain-containing protein, partial [*Mycetohabitans endofungorum*]	2218	8460	93%	0.0	42.08%	WP_146064109.1
non-ribosomal peptide synthetase, partial [*Mycetohabitans endofungorum*]	1716	5990	97%	0.0	52.67%	WP_146064101.1
amino acid adenylation domain-containing protein, partial [*Mycetohabitans endofungorum*]	1578	6178	93%	0.0	45.08%	WP_146064113.1
Mycoavidus cysteinexigens						
hypothetical protein [*Mycoavidus cysteinexigens*]	225	454	7%	2e-67	56.74%	WP_081953460.1
non-ribosomal peptide synthetase module [*Mycoavidus cysteinexigens*]	189	189	2%	3e-55	54.19%	BBE09234.1
acyl--CoA ligase [*Mycoavidus cysteinexigens*]	120	509	43%	1e-28	26.05%	WP_081953598.1
long-chain-fatty-acid-CoA ligase [*Mycoavidus cysteinexigens*]	107	212	18%	4e-24	23.82%	WP_045364454.1

Table S12. BlastP analysis against proven endobacterial symbionts using MpcA as query**.** The 5 best hits are shown.

Description	Max Score	Total Score	Query cover	E value	Per. Ident.	Accession
***Paraburkholderia rhizoxinica* (syn. *Mycetorhabitans endofungorum*)**						
non-ribosomal peptide synthetase [*Mycetohabitans rhizoxinica*]	4230	18088	97%	0.0	47.69%	WP_013428324.1
non-ribosomal peptide synthetase [*Mycetohabitans rhizoxinica*]	4095	7602	97%	0.0	44.14%	WP_013428370.1
amino acid adenylation domain-containing protein [*Mycetohabitans rhizoxinica*]	3846	10703	97%	0.0	51.50%	WP_157864516.1
Non-ribosomal peptide synthetase modules (EC 6.3.2.-) [*Mycetohabitans rhizoxinica* HKI 454]	3846	10703	97%	0.0	51.50%	CBW76566.1
endopyrrole NRPS A [Mycetohabitans rhizoxinica]	3821	11795	93%	0.0	44.36%	QIH29228.1
Mycoavidus cysteinexigens						
hypothetical protein [*Mycoavidus cysteinexigens*]	225	454	7%	2e-67	56.74%	WP_081953460.1
non-ribosomal peptide synthetase module [*Mycoavidus cysteinexigens*]	189	189	2%	3e-55	54.19%	BBE09234.1
acyl--CoA ligase [*Mycoavidus cysteinexigens*]	120	509	43%	1e-28	26.05%	WP_081953598.1
long-chain-fatty-acid-CoA ligase [*Mycoavidus cysteinexigens*]	107	212	18%	4e-24	23.82%	WP_045364454.1

Table S13. BlastP analysis against bacterial genomes using MpcA and MpbA as queries. The 10 best hits are shown.

Description	Max Score	Total Score	Query cover	E value	Per. Ident.	Accession
MpcA						
Tyrocidine synthase 3 [*Photorhabdus namnaonensis*]	5256	21493	93%	0.0	52.61%	OCA53451.1
non-ribosomal peptide synthase/polyketide synthase [*Photorhabdus luminescens*]	5249	44902	95%	0.0	52.67%	WP_181148642.1
non-ribosomal peptide synthase/polyketide synthase [*Photorhabdus luminescens*]	5249	35932	93%	0.0	52.69%	WP_146111043.1
non-ribosomal peptide synthetase [*Photorhabdus luminescens*]	5237	40485	95%	0.0	52.58%	WP_036775943.1
amino acid adenylation domain-containing protein [*Photorhabdus luminescens*]	5225	36261	96%	0.0	52.22%	SCZ57159.1
non-ribosomal peptide synthase/polyketide synthase [*Photorhabdus luminescens*]	5223	26071	93%	0.0	52.25%	WP_132343500.1
non-ribosomal peptide synthase/polyketide synthase [*Photorhabdus luminescens*]	5222	36236	96%	0.0	52.22%	WP_139180488.1
non-ribosomal peptide synthetase [*Photorhabdus laumondii*]	5221	42443	96%	0.0	52.35%	WP_011146892.1
non-ribosomal peptide synthase/polyketide synthase [*Photorhabdus laumondii*]	5220	42445	96%	0.0	52.35%	WP_109791633.1
non-ribosomal peptide synthetase [*Photorhabdus luminescens*]	5220	36641	96%	0.0	52.24%	WP_088374444.1
MpbA						
Tyrocidine synthase 3 [*Photorhabdus namnaonensis*]	5204	19158	93%	0.0	52.01%	OCA53451.1
non-ribosomal peptide synthase/polyketide synthase [*Photorhabdus luminescens*]	5199	33449	93%	0.0	51.94%	WP_146111043.1
non-ribosomal peptide synthase/polyketide synthase [*Photorhabdus luminescens*]	5181	40848	96%	0.0	51.91%	WP_181148642.1
non-ribosomal peptide synthetase [*Photorhabdus luminescens*]	5175	37713	96%	0.0	51.87%	WP_036775943.1
amino acid adenylation domain-containing protein [*Photorhabdus luminescens*]	5174	44869	96%	0.0	51.73%	SCZ57159.1
non-ribosomal peptide synthase/polyketide synthase [*Photorhabdus luminescens*]	5173	44852	96%	0.0	51.73%	WP_139180488.1
non-ribosomal peptide synthase/polyketide synthase [*Photorhabdus luminescens*]	5163	25136	93%	0.0	51.53%	WP_132343500.1
non-ribosomal peptide synthetase [*Photorhabdus* sp. S12-55]	5158	24779	93%	0.0	51.51%	RAW80350.1
non-ribosomal peptide synthase/polyketide synthase [*Photorhabdus* sp. S5P8-50]	5157	28360	93%	0.0	51.51%	WP_158537557.1
MULTISPECIES: non-ribosomal peptide synthase/polyketide synthase *[Photorhabdus*]	5156	24771	93%	0.0	51.51%	WP_158536437.1

Table S14. BlastP analysis against fungal genomes using MpbA and MpcA as queries. The 10 best hits are shown.

Description	Max Score	Total Score	Query Cover	E value	Per. ident	Accession
MpbA						
hypothetical protein MVEG_05915 [*Mortierella verticillata* NRRL 6337]	5129	7306	97%	0.0	49.97	KFH69114.1
amino acid adenylation enzyme/thioester reductase family protein [*Basidiobolus meristosporus* CBS 931.73]	4992	20587	92%	0.0	50.54	ORX93280.1
acetyl-CoA synthetase-like protein [*Basidiobolus meristosporus* CBS 931.73]	4055	12674	97%	0.0	43.91	ORX76564.1
acetyl-CoA synthetase-like protein [*Basidiobolus meristosporus* CBS 931.73]	3072	10020	93%	0.0	42.15	ORX82118.1
Non-ribosomal peptide synthetase module [*Basidiobolus meristosporus* CBS 931.73]	2565	4806	97%	0.0	46.24	ORX97912.1
hypothetical protein MVEG_11009 [*Mortierella verticillata* NRRL 6337]	2512	12020	97%	0.0	45.45	KFH62971.1
hypothetical protein MVEG_02802 [*Mortierella verticillata* NRRL 6337]	1971	6542	97%	0.0	52.68	KFH72512.1
amino acid adenylation [*Basidiobolus meristosporus* CBS 931.73]	1880	5182	93%	0.0	45.89	ORX94939.1
acetyl-CoA synthetase-like protein [*Neocallimastix californiae*]	1770	9054	92%	0.0	24.62	ORY33172.1
nonribosomal peptide synthetase DhbF [*Mortierella verticillata* NRRL 6337]	1768	6379	93%	0.0	48.31	KFH72939.1
MpcA						
hypothetical protein MVEG_05915 [*Mortierella verticillata* NRRL 6337]	5127	7359	97%	0.0	49.72	KFH69114.1
amino acid adenylation enzyme/thioester reductase family protein [*Basidiobolus meristosporus* CBS 931.73]	5009	22416	93%	0.0.	50.57	ORX93280.1
acetyl-CoA synthetase-like protein [*Basidiobolus meristosporus* CBS 931.73]	4062	15035	97%	0.0	43.84	ORX76564.1
hypothetical protein MVEG_11009 [*Mortierella verticillata* NRRL 6337]	3785	7601	97%	0.0	40.97	KFH62971.1
acetyl-CoA synthetase-like protein [*Basidiobolus meristosporus* CBS 931.73]	3022	7820	93%	0.0	42.34	ORX82118.1
Non-ribosomal peptide synthetase module [*Basidiobolus meristosporus* CBS 931.73]	2565	4791	97%	0.0	46.18	ORX97912.1
hypothetical protein MVEG_02802 [*Mortierella verticillata* NRRL 6337]	1940	6529	97%	0.0	51.52	KFH72512.1
amino acid adenylation *[Basidiobolus meristosporus* CBS 931.73]	1895	5214	93%	0.0	46.05	ORX94939.1
acetyl-CoA synthetase-like protein [*Neocallimastix californiae*]	1854	8032	92%	0.0	25.54	ORY33172.1
nonribosomal peptide synthetase DhbF [*Mortierella verticillata* NRRL 6337]	1742	6838	96%	0.0	48.38	KFH72939.1

Table S15. HPLC methods used in this study

	method A	method B	method C	method D	method E	method F
system	Agilent 1290 infinity II UHPLC	Agilent 1290 infinity II UHPLC	Preparative HPLC Agilent 1260	Preparative HPLC Agilent 1200	Agilent 1290 infinity II UHPLC	Waters ACQUITY H-class UPLC system
solvent A	water + 0.1% FA	water + 0.1% FA	water + 0.1% TFA	water + 0.1% TFA	water + 0.1% FA	water + 0.1% FA
solvent B	acetonitril	acetonitril	acetonitril	acetonitril	acetonitril	acetonitril + 0.1% FA
gradient	0-4 min: 5-72% B 4-4.5min: 72-95% B 4.5-5 min: 95% B 5-5.5 min: 95-5% B 5.5-6 min: 5% B	0-10 min: 1-45% B 10-12 min: 45-95% B 12-13 min: 95% B 13-14 min: 95-1% B	0-20 min: 10-100% B 20-27 min: 100% B 27-30 min: 100-10% B	0-0.5 min: 35% B 0.5-12.5 min: 35-65% B 12.5-13 min: 65-100% B 13-15 min: 100% B 15-15.5 min: 100-35% B 15.5-17 min: 35% B	0-10 min: 1-50% B 10-11min: 50-100% B 11-11.5 min: 100-1% B 11.5-12 min: 1% B	0-4 min: 10-50% A 5-9 min: 50-10% A
temperature	30°C	30°C	25°C	12°C	30°C	30°C
flow	1 mL min^{-1}	1 mL min^{-1}	20 mL min^{-1}	2.5 mL min^{-1}	1 mL min^{-1}	0.4 mL min^{-1}
column	Zorbax Eclipse Plus C18 RRHD (Agilent)	Zorbax Eclipse Plus C18 RRHD (Agilent)	Luna C18 (Phenomenex)	Zorbax Eclipse XDB-C18 (Agilent)	Luna Omega polar C18 column (Phenomenex)	ACQUITY UPLC BEH Amide column
column dimensions	50 mm x 2.1 mm, 1.8 µm	50 mm x 2.1 mm, 1.8 µm	250 mm x 21.2 mm, 10 µm	250 mm x 9.4 mm, 5 µm	50 mm x 2.1 mm, 1.6 µm	50 mm x 2.1 mm, 1.7 µm
detection	Agilent 6130 single quadrupole MS, ESI source	Agilent 6130 single quadrupole MS, ESI source	DAD, λ = 254 nm	DAD, λ = 254 nm	Agilent 6130 single quadrupole MS, ESI source	Xevo TQ-S micro tandem quadrupole instrument (waters)

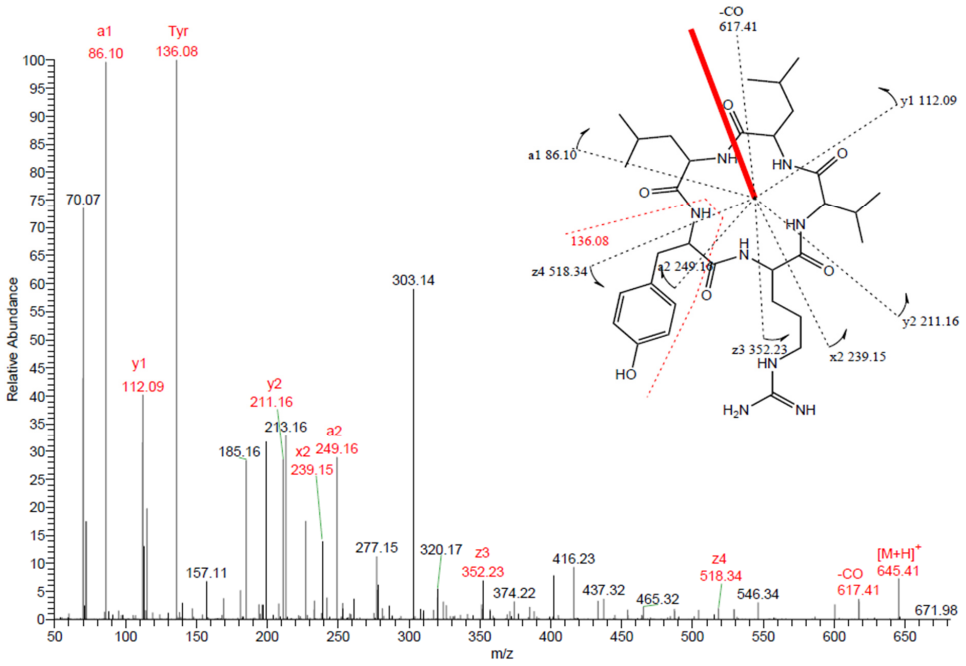

Figure S1. ESI-MS/MS spectrum of malpicyclin A (**4**).

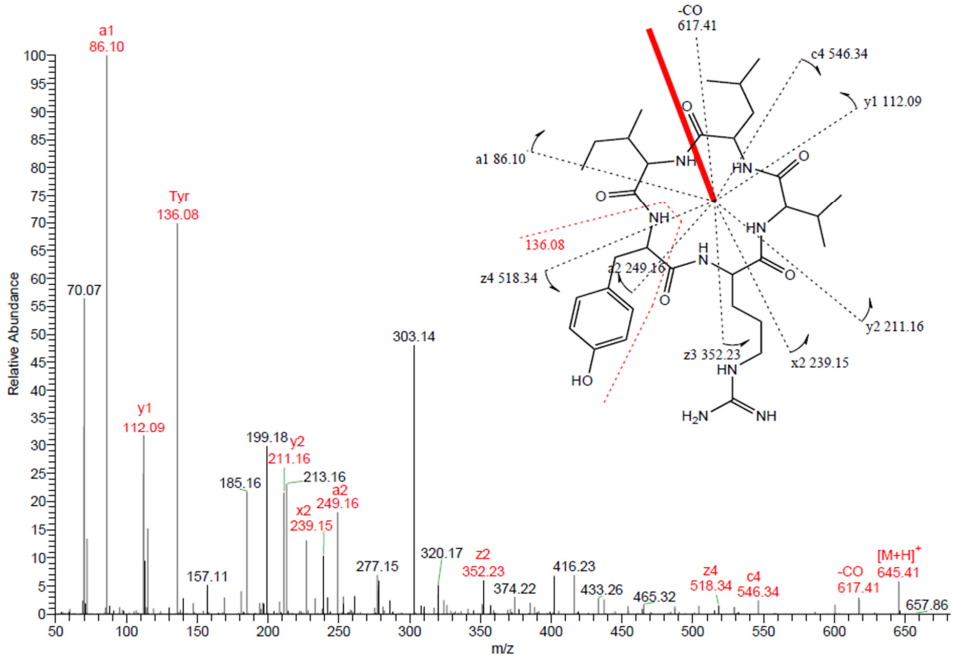

Figure S2. ESI-MS/MS spectrum of malpicyclin B (**5**).

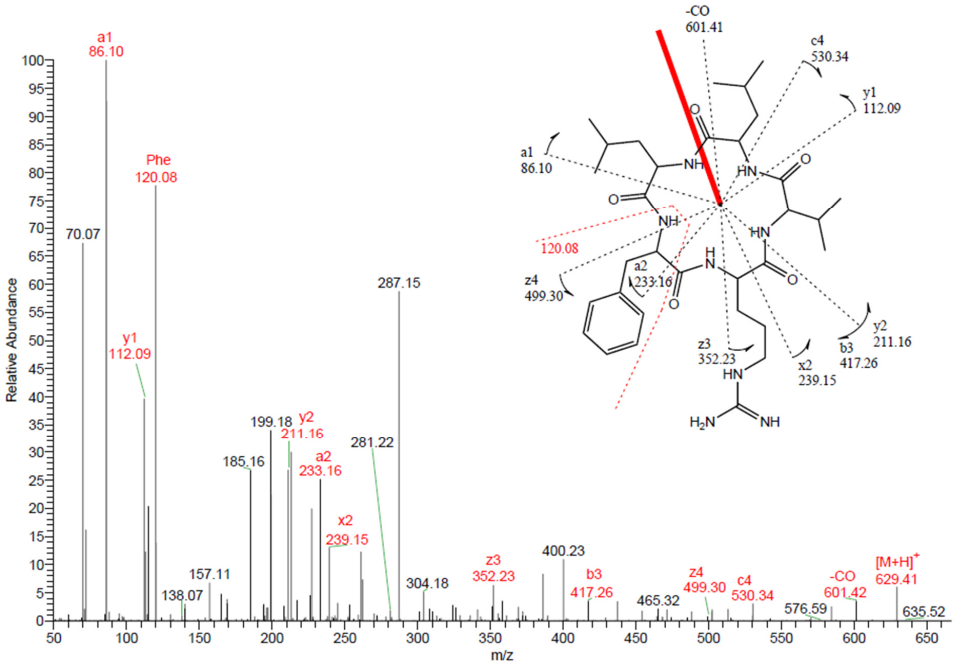

Figure S3. ESI-MS/MS spectrum of malpicyclin C (**6**).

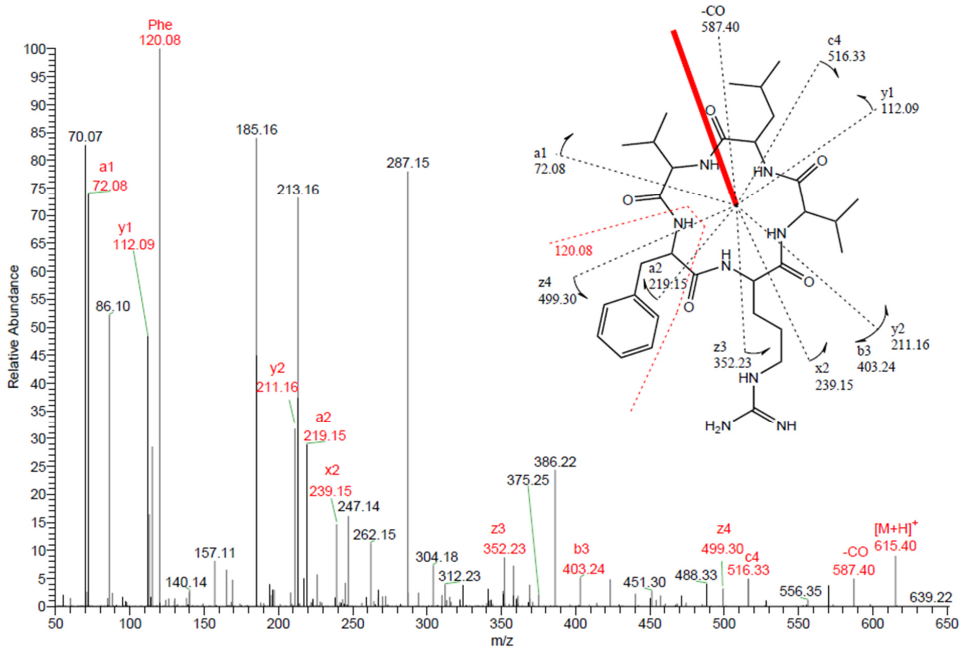

Figure S4. ESI-MS/MS spectrum of malpicyclin D (**7**).

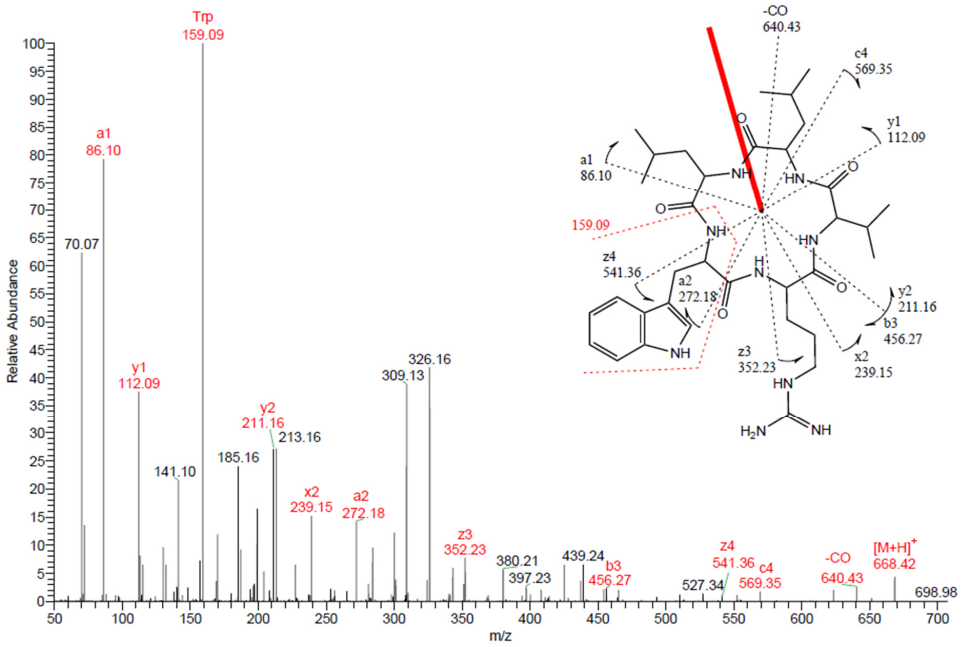

Figure S5. ESI-MS/MS spectrum of malpicyclin E (**8**).

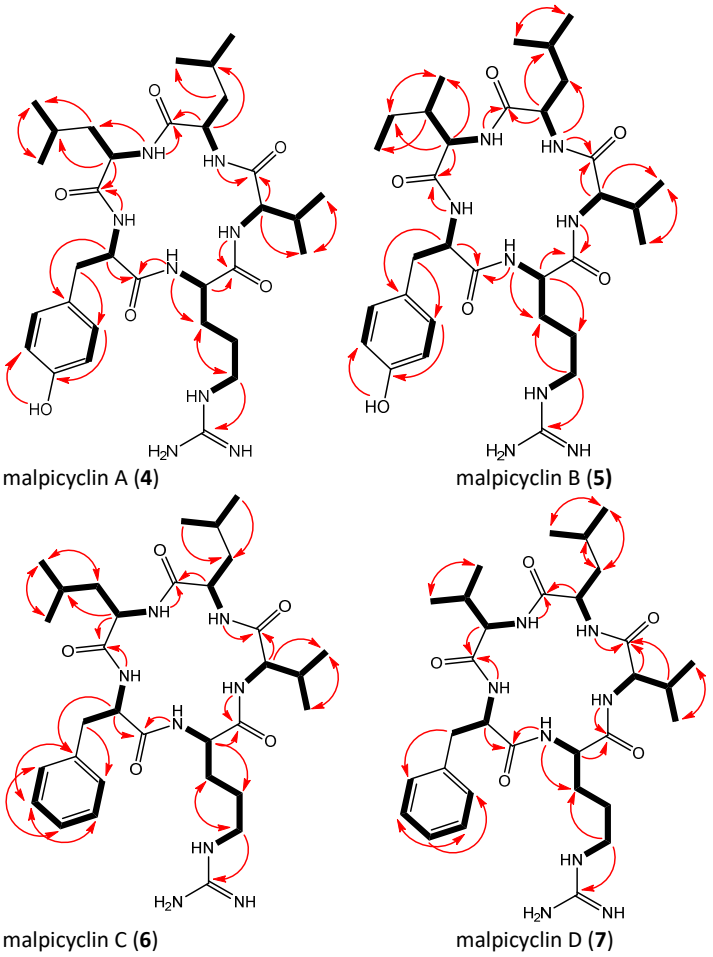

Figure S6. Key correlations of **4-7** in 2D NMR spectroscopy.

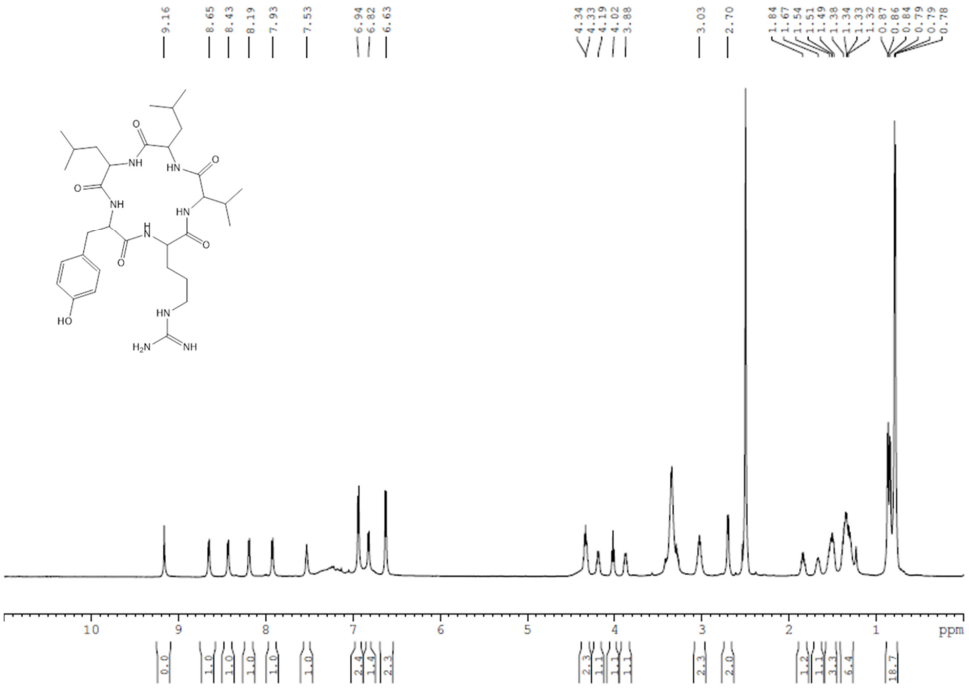

Figure S7. ^{1}H NMR spectrum of **4** in DMSO-d_6.

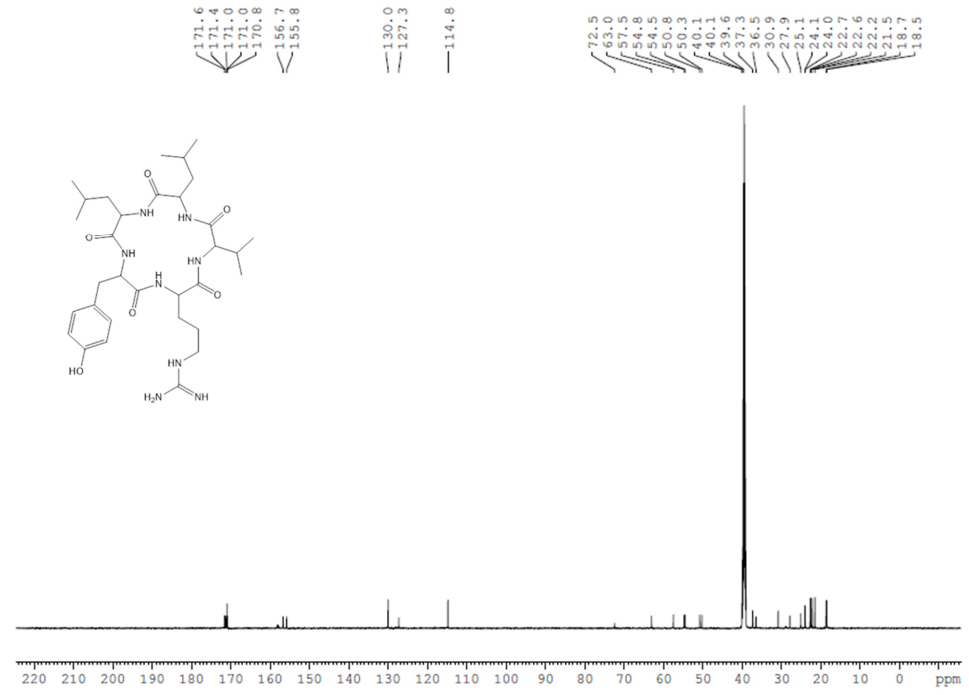

Figure S8. ^{13}C NMR spectrum of **4** in DMSO-d_6.

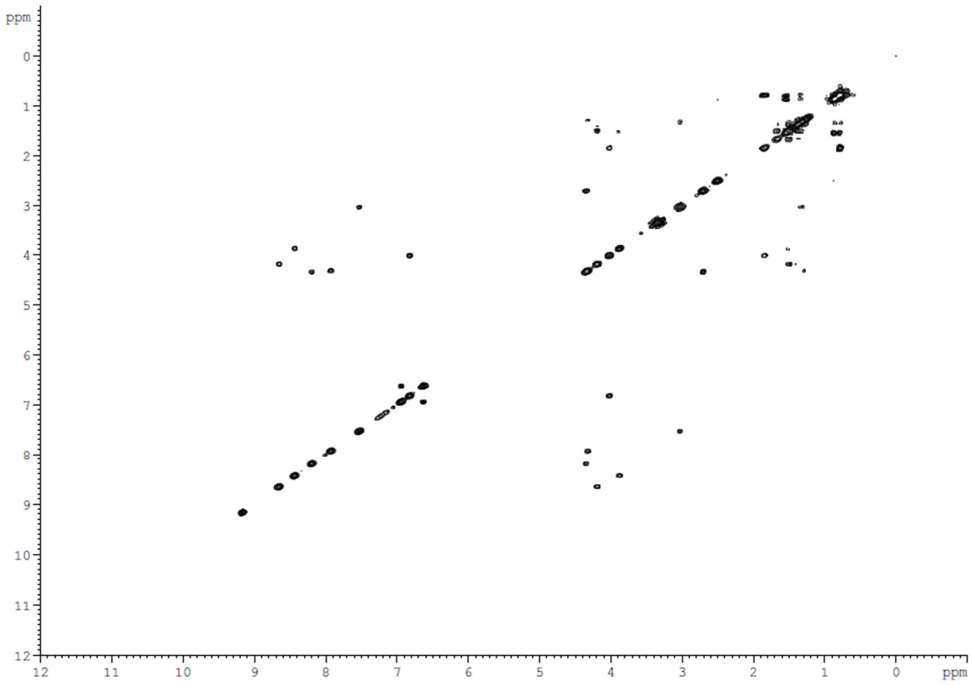

Figure S9. ^{1}H, ^{1}H COSY NMR spectrum of **4** in DMSO-d_6.

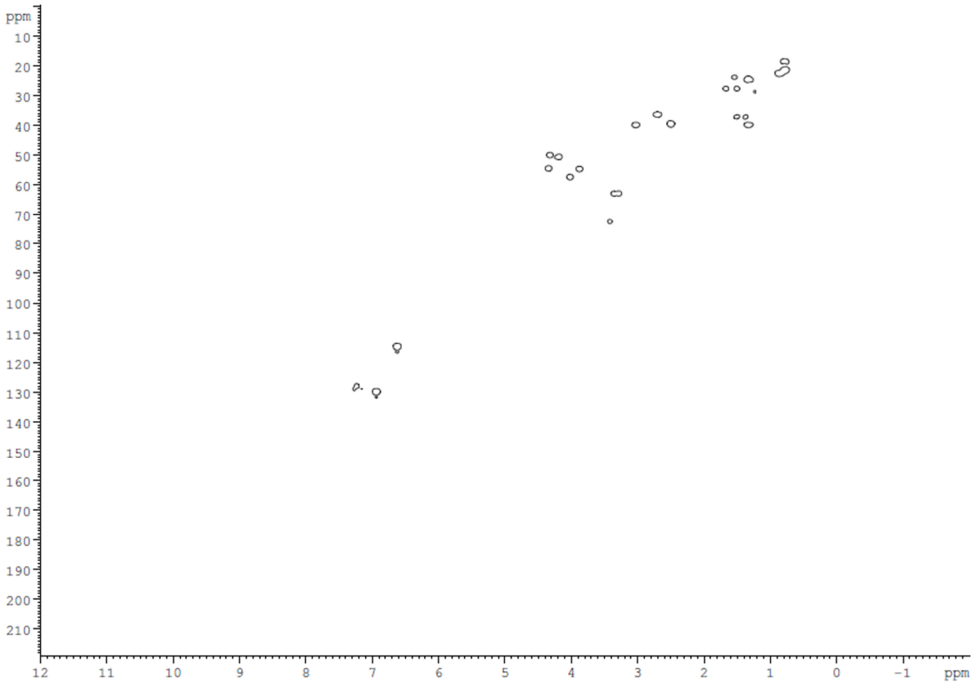

Figure S10. ^{1}H, ^{13}C HSQC NMR spectrum of **4** in DMSO-d_6.

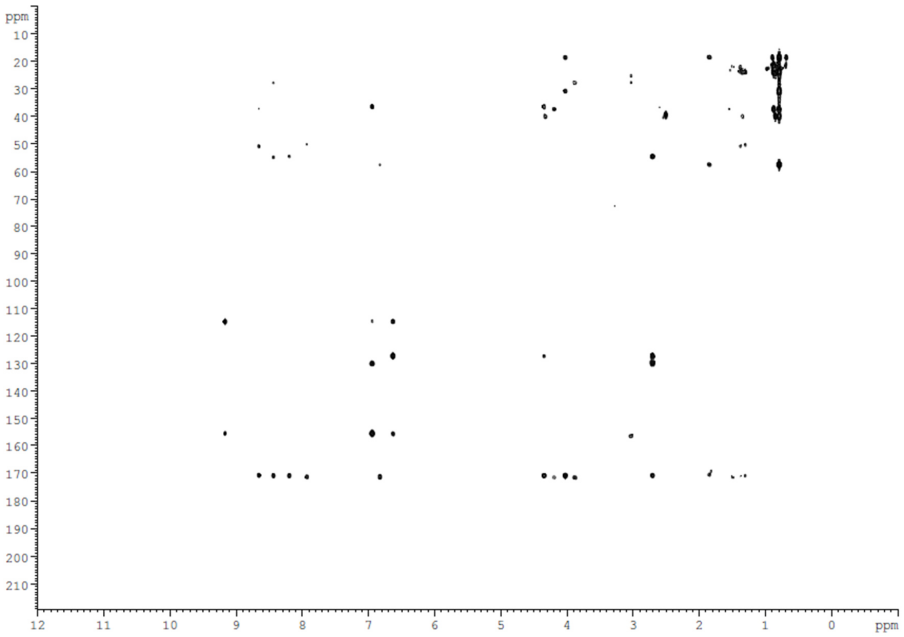

Figure S11. ^{1}H, ^{13}C HMBC NMR spectrum of **4** in DMSO-d_6.

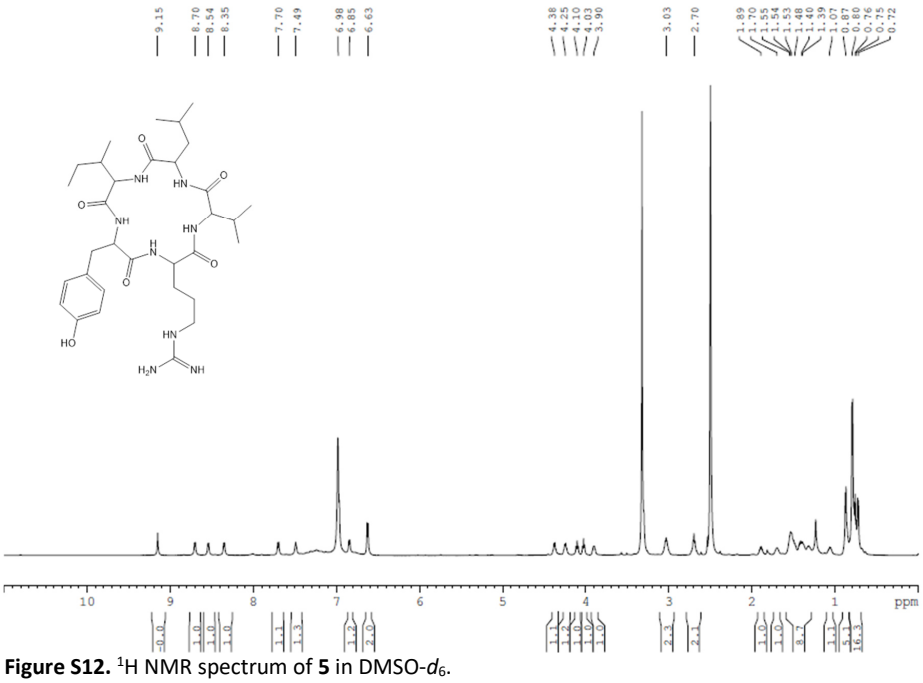

Figure S12. ^{1}H NMR spectrum of **5** in DMSO-d_6.

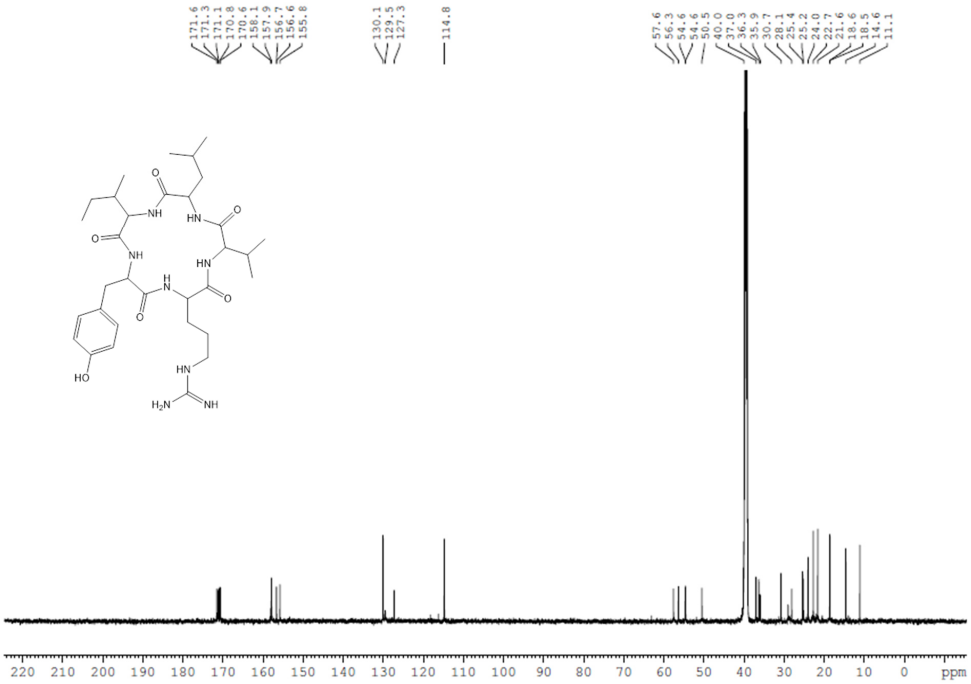

Figure S13. ^{13}C NMR spectrum of **5** in DMSO-d_6.

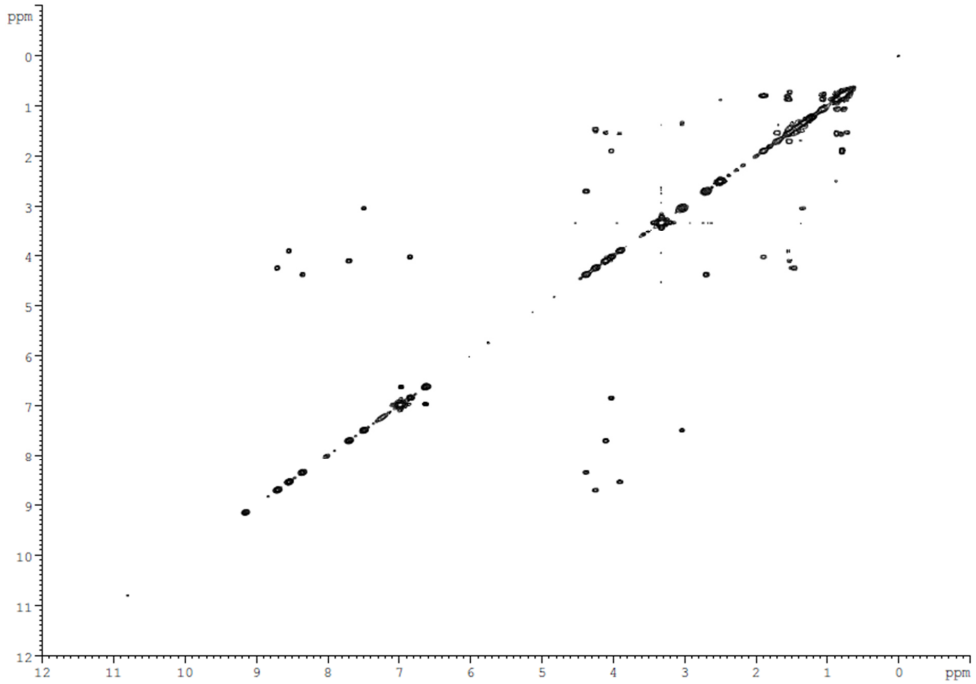

Figure S14. ^{1}H, ^{1}H COSY NMR spectrum of **5** in DMSO-d_6.

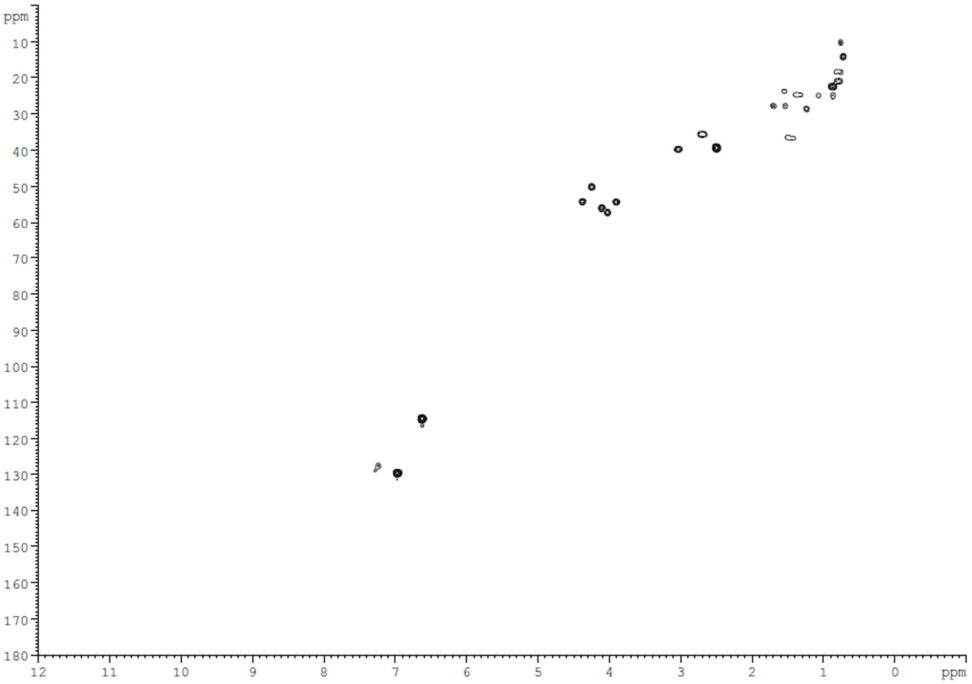

Figure S15. ^{1}H, ^{13}C HSQC NMR spectrum of **5** in DMSO-d_6.

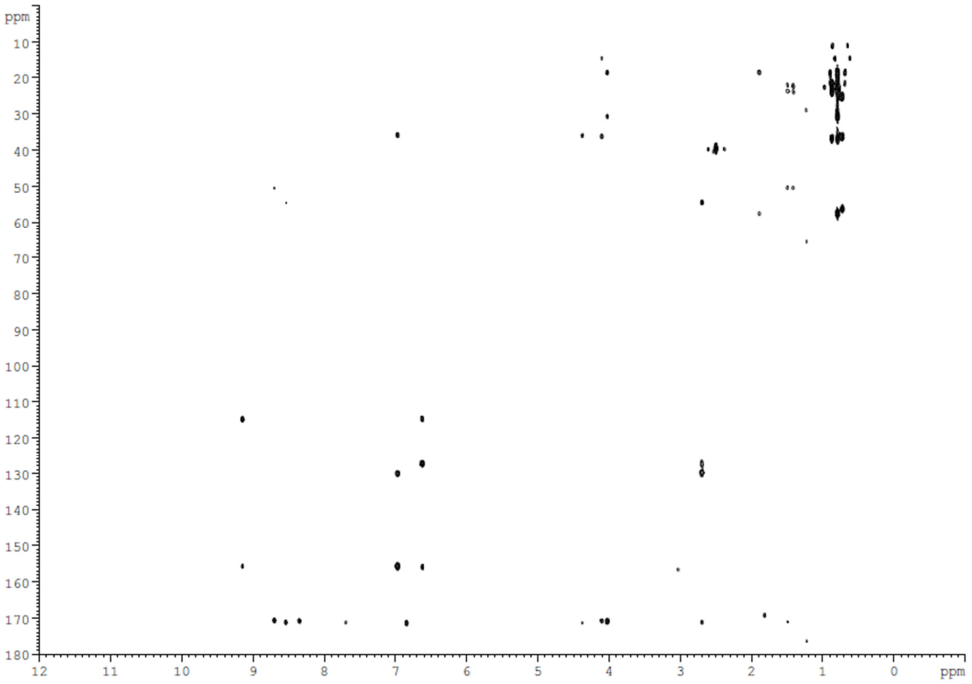

Figure S16. ^{1}H, ^{13}C HMBC NMR spectrum of **5** in DMSO-d_6.

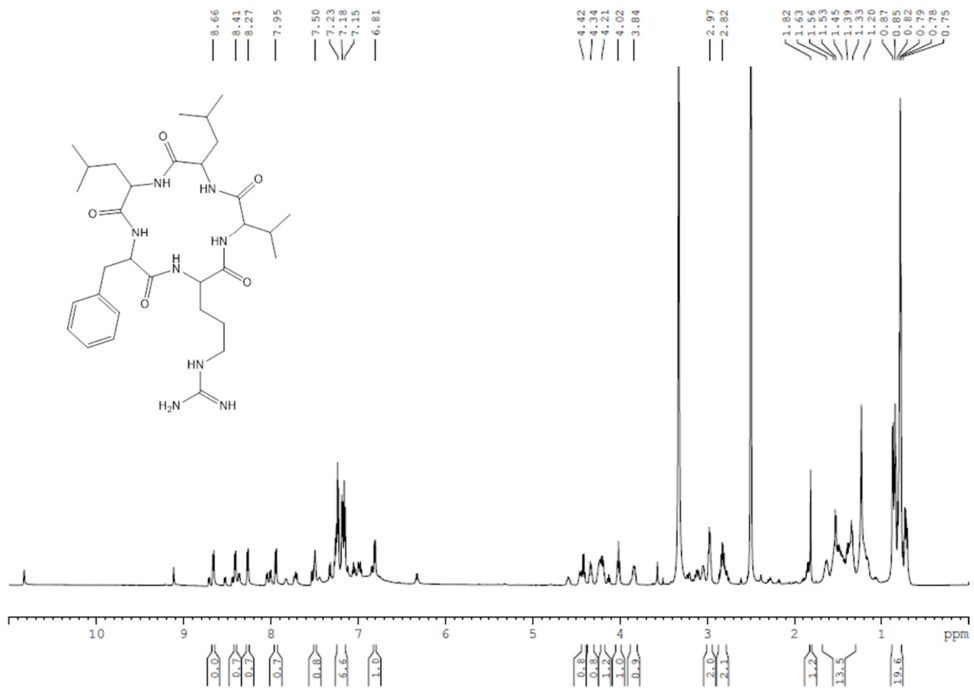

Figure S17. ^{1}H NMR spectrum of **6** in DMSO-d_6.

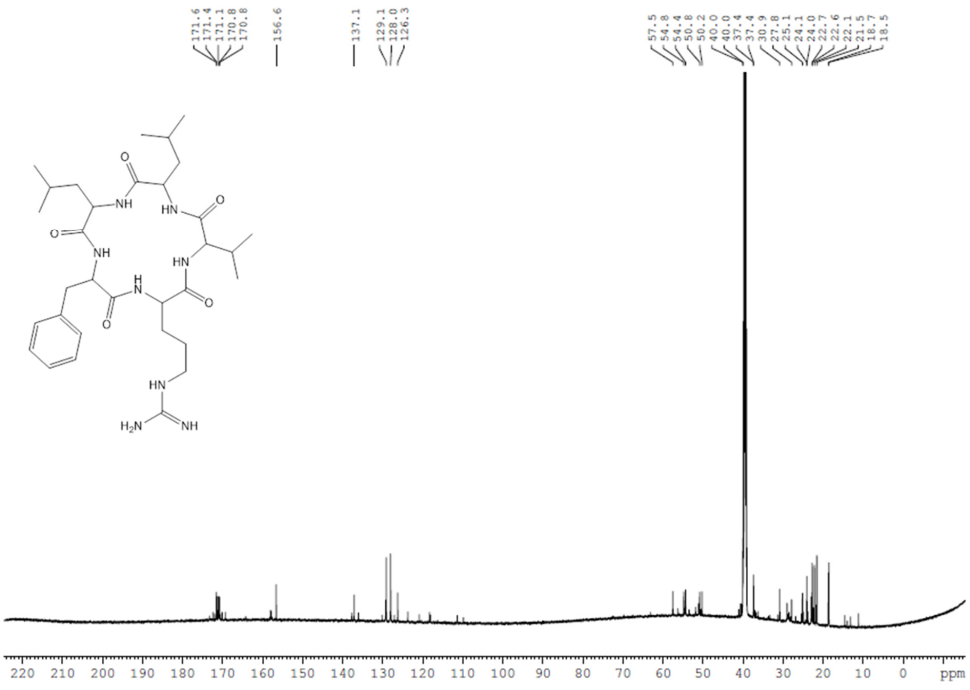

Figure S18. ^{13}C NMR spectrum of **6** in DMSO-d_6.

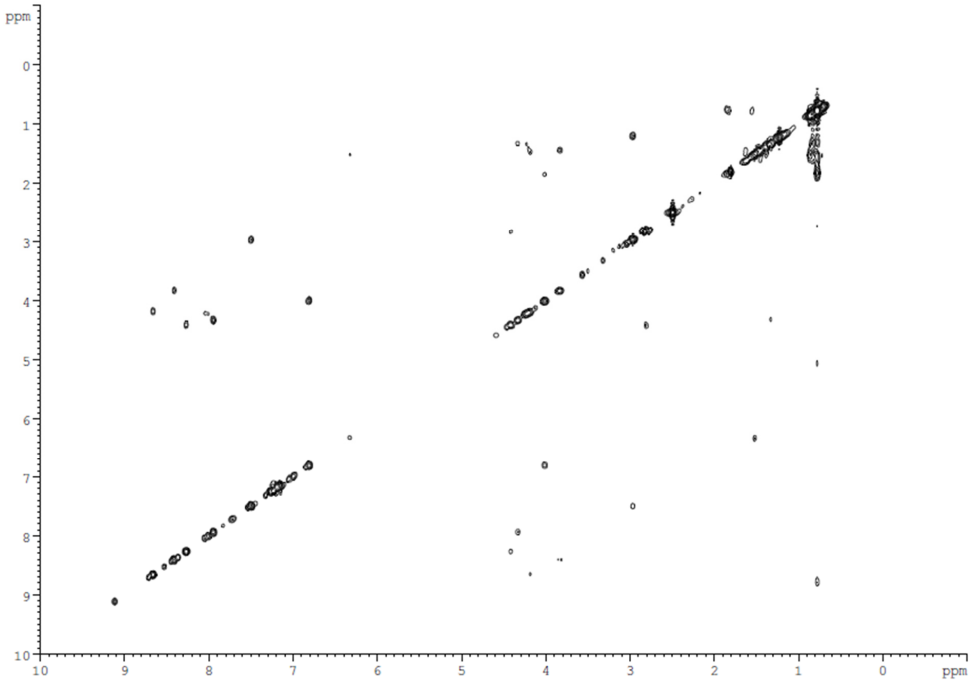

Figure S19. ^{1}H, ^{1}H COSY NMR spectrum of **6** in DMSO-d_6.

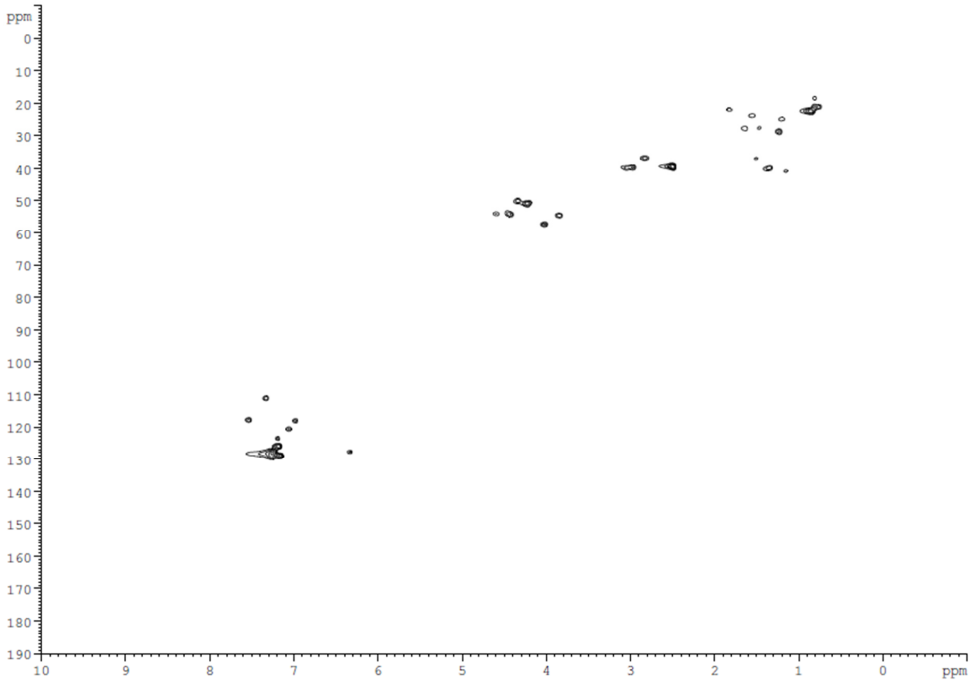

Figure S20. ^{1}H, ^{13}C HSQC NMR spectrum of **6** in DMSO-d_6.

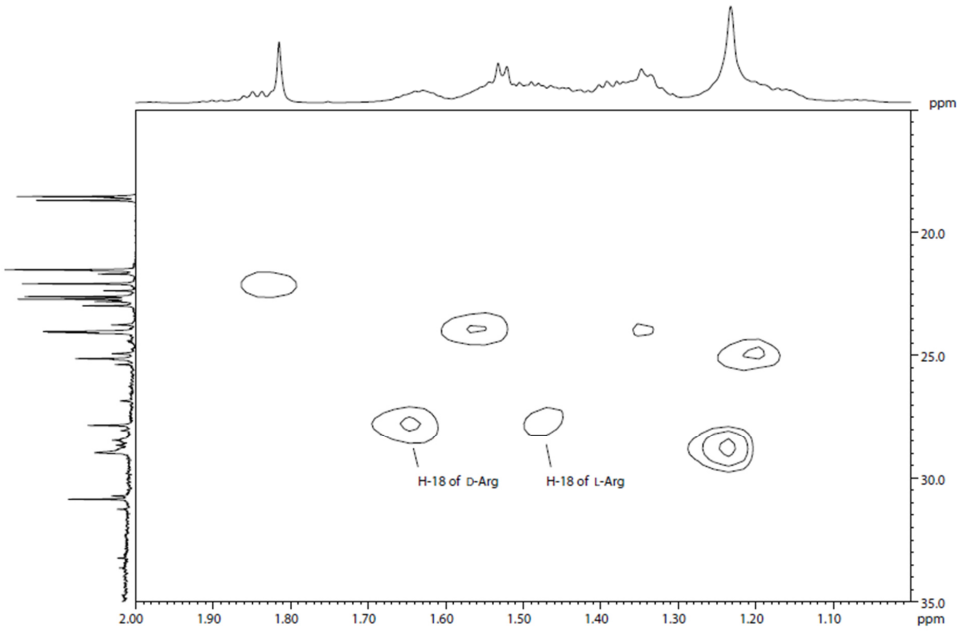

Figure S21. Detailed image section of the ^{1}H, ^{13}C HMBC NMR spectrum of **6** in DMSO-d_6. Note the coupling of C-18 (δ_c 27.8 ppm) with H-18 of D-Arg (δ_H 1.63 ppm,) as well as H-18 of L-Arg (1.45 ppm)

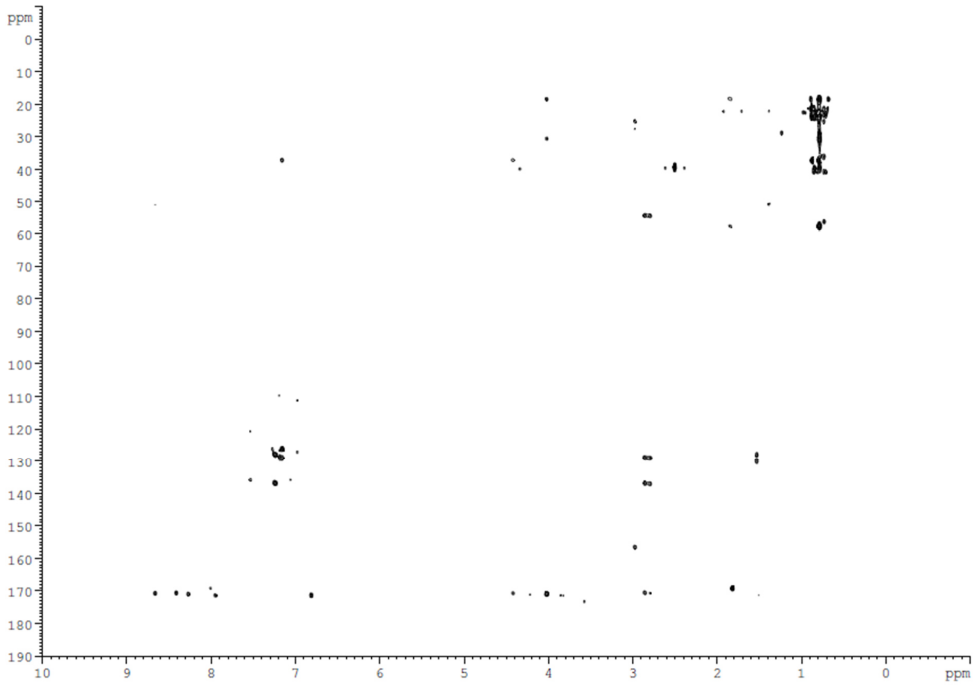

Figure S22. ^{1}H, ^{13}C HMBC NMR spectrum of **6** in DMSO-d_6.

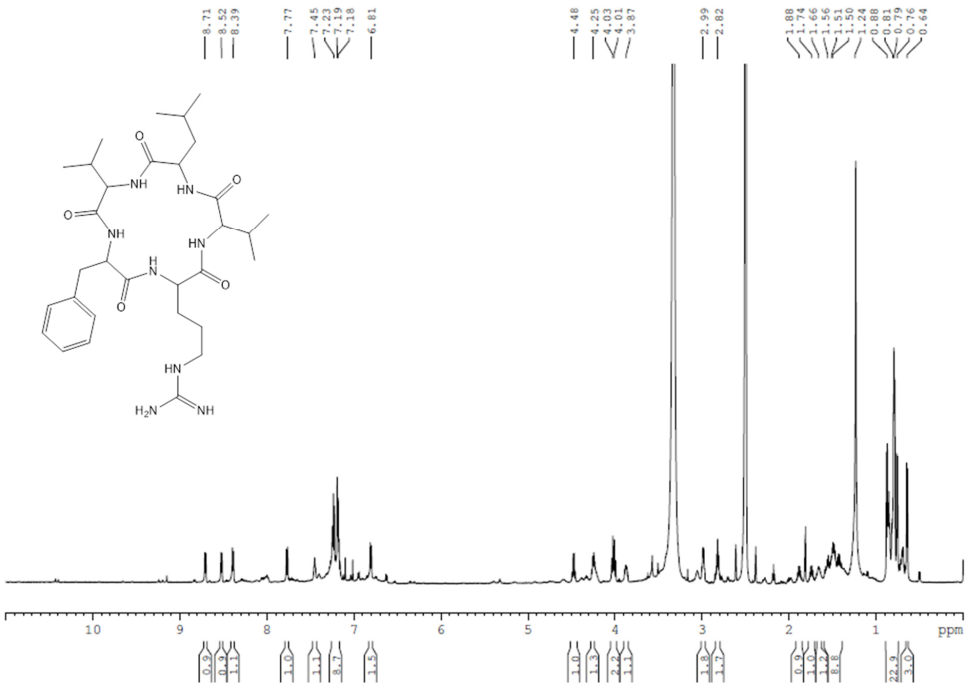

Figure S23. ^{1}H NMR spectrum of **7** in DMSO-d_6.

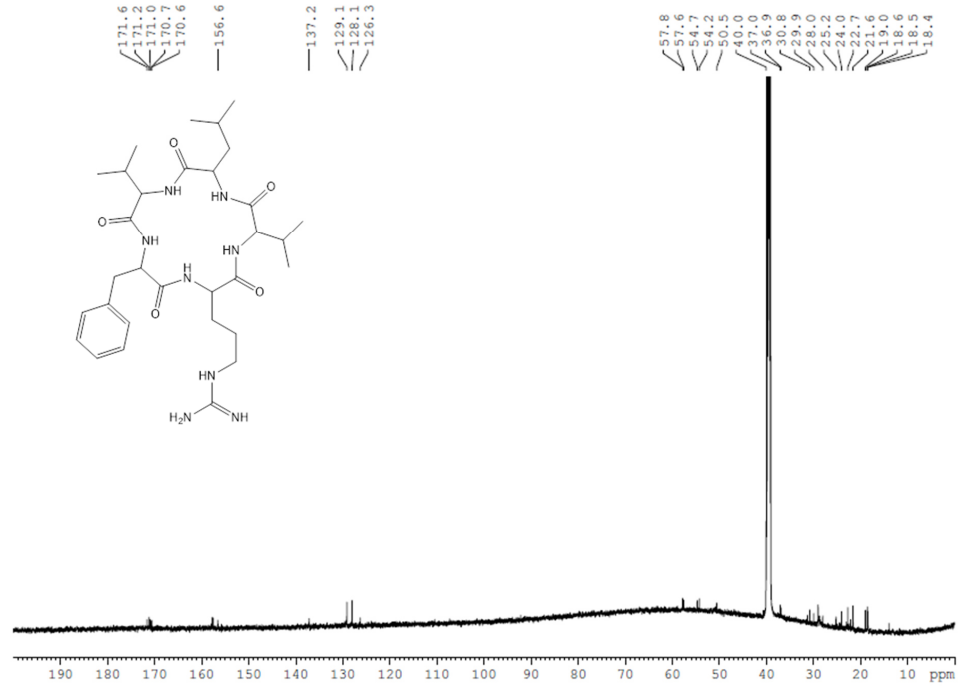

Figure S24. ^{13}C NMR spectrum of **7** in DMSO-d_6.

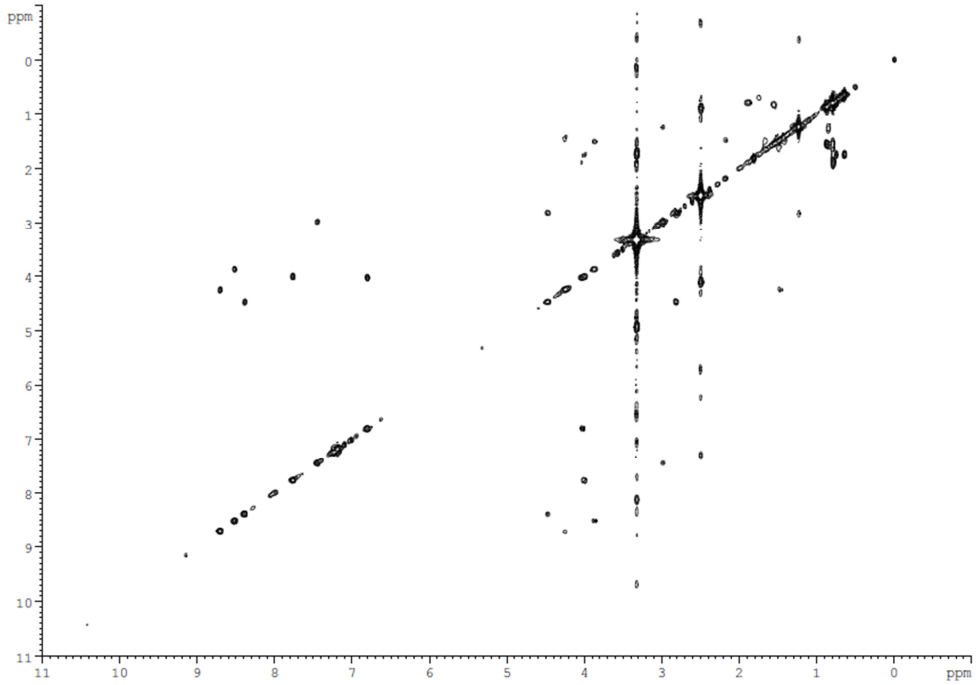

Figure S25. ^{1}H, ^{1}H COSY NMR spectrum of **7** in DMSO-d_6.

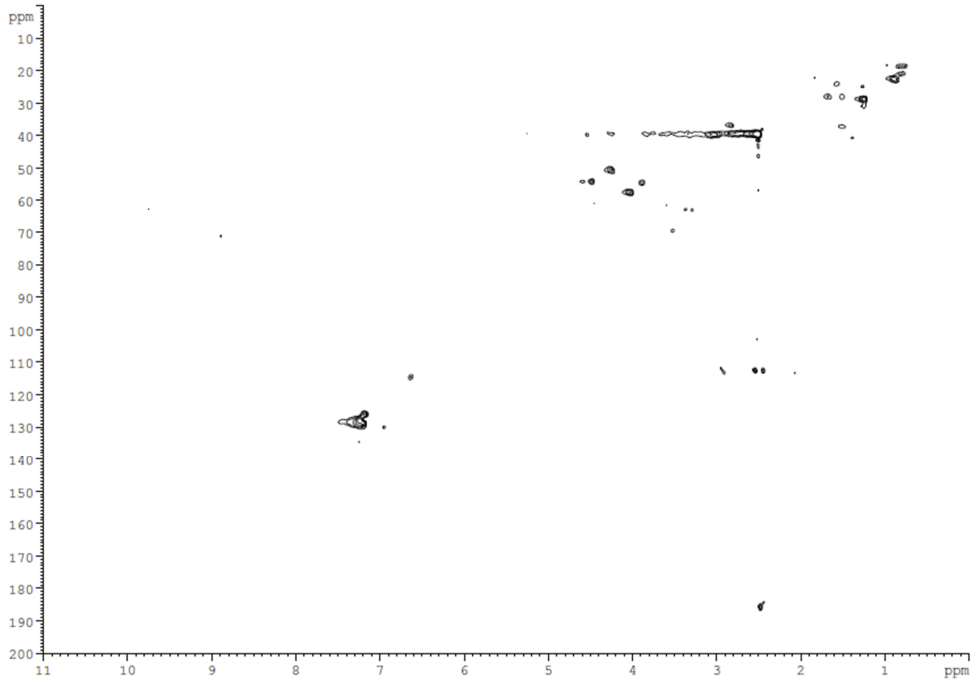

Figure S26. ^{1}H, ^{13}C HSQC NMR spectrum of **7** in DMSO-d_6.

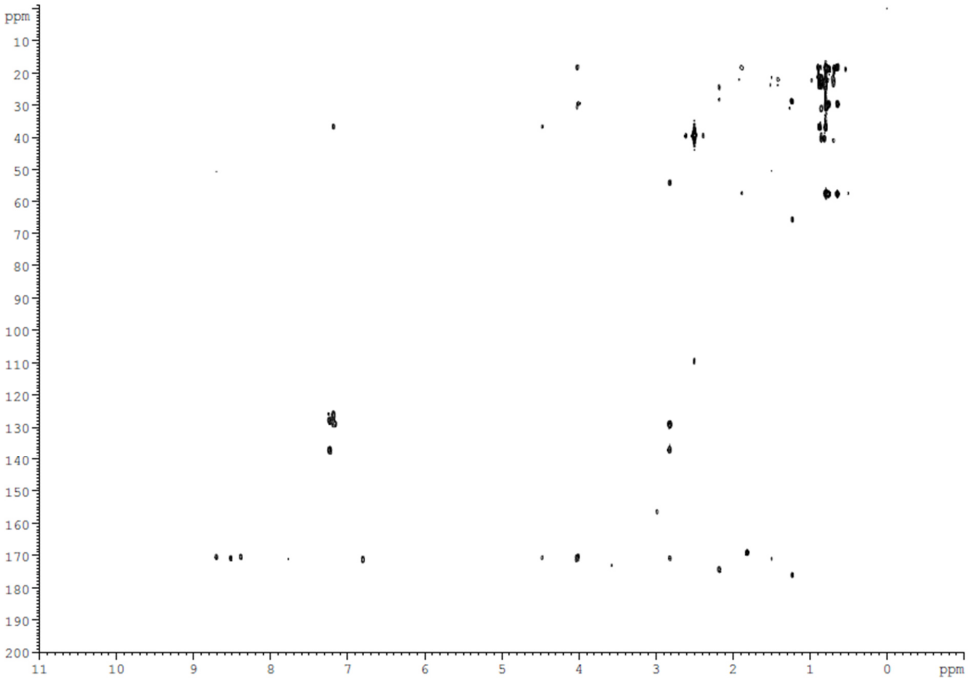

Figure S27. ^{1}H, ^{13}C HMBC NMR spectrum of **7** in DMSO-d_6.

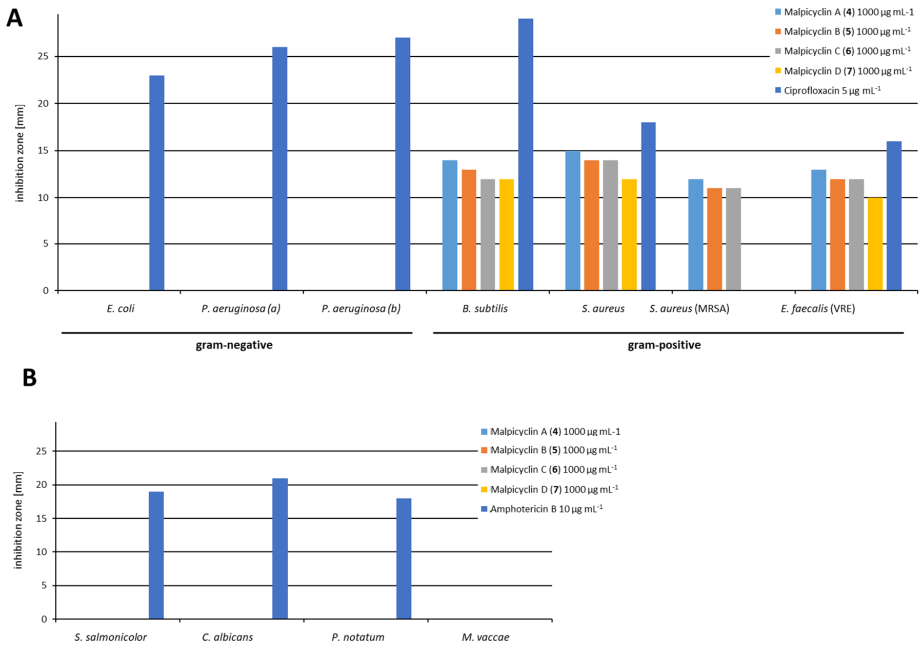

Figure S28. Antimicrobial activities of **4-7**. Compounds were tested at an initial concentration of 1000 µg/ml against bacteria (**A**) and fungi (**B**).

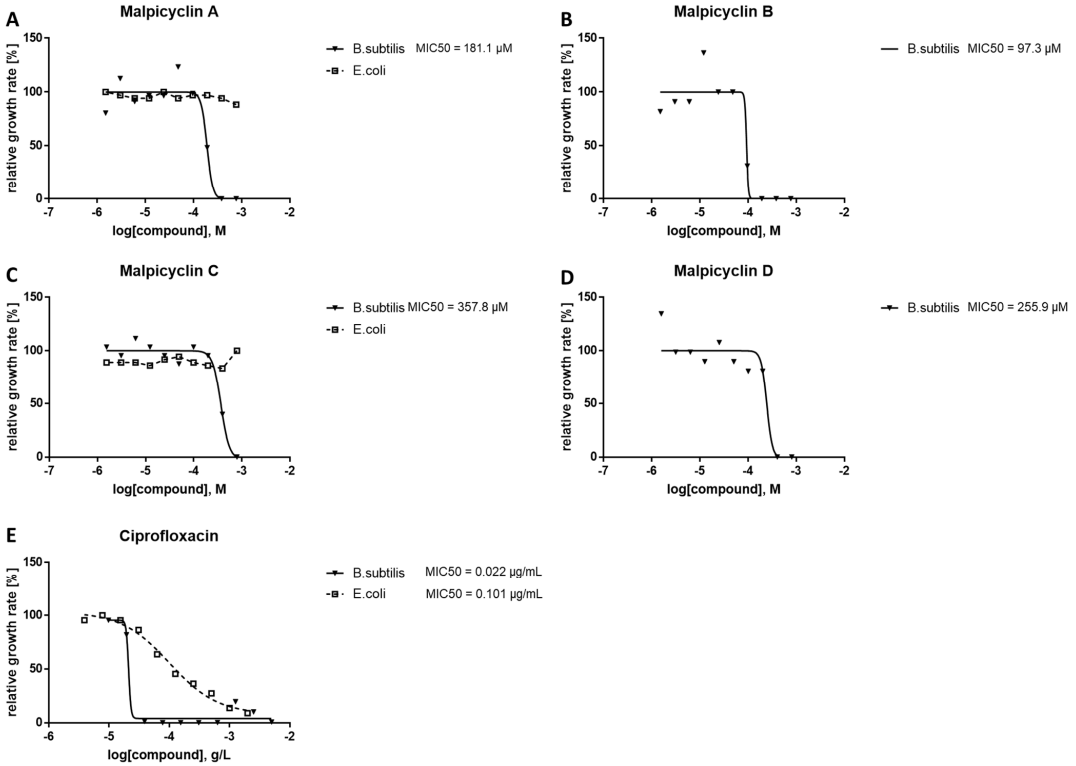

Figure S29. Minimal inhibitory concentration (MIC) for **4-7** against bacteria.
Ciprofloxacin served as external standard (**E**). **5** and **7** did not show activity against *E. coli* at >500 µM (Figure S28), and were hence excluded for detailed analysis.

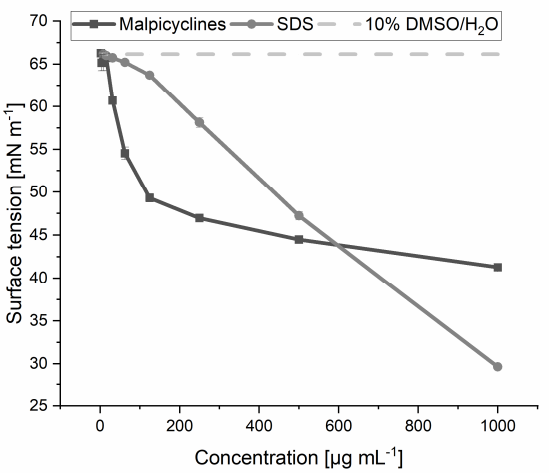

Figure S30. Detergent activities of **4-7**. Concentration dependent decrease of the surface tension of malpicyclins **4-7** compared to SDS reference and solvent (10% DMSO in water) measured by ring tear-off method (n=3).

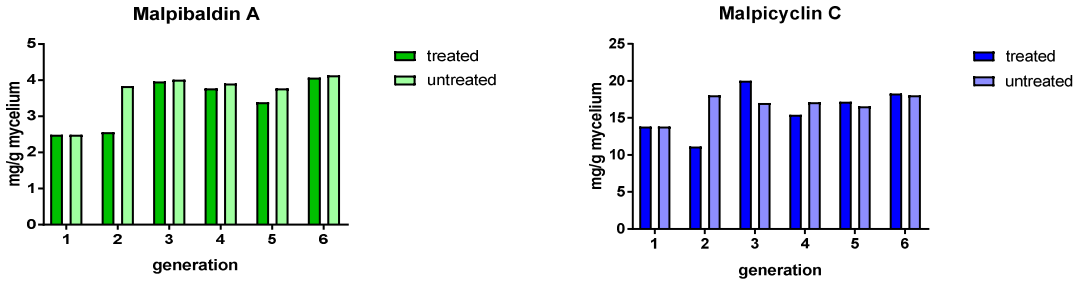

Figure S31. Cyclopentapeptide production in *M. alpina* after antibiotic treatment. *M. alpina* was cultivated on MEP plates amended with spectinomycin (200 µg mL^{-1}) and ciprofloxacin (200 µg mL^{-1}) in six generations. From each generation, the abundance of malpibaldin A (**1**) and malpicyclin C (**6**) was quantified (mg metabolite per g fungal dry biomass). A cultivation without antibiotics served as untreated control in each generation. All experiments were carried out in duplicate. Metabolite abundance is not altered by antibiotic treatment.

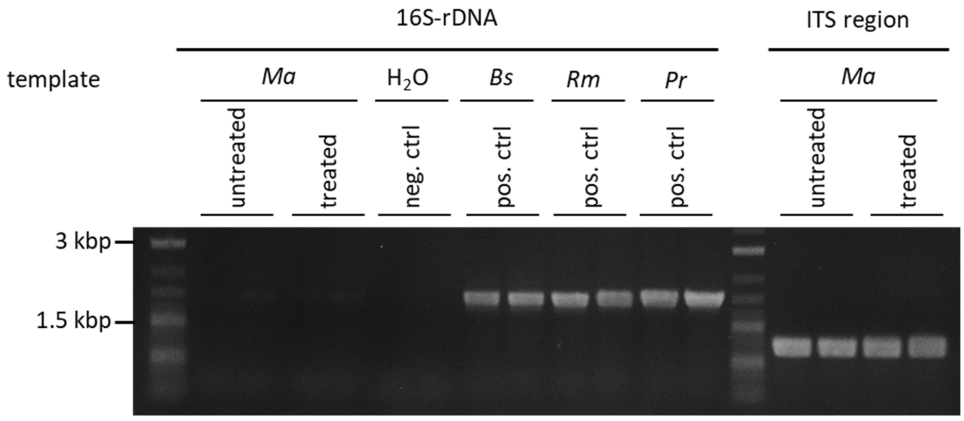

Figure S32. Amplification of 16S-rDNA from various species by PCR. Genomic DNA was isolated from *Bacillus subtilis* (*Bs*), *Rhizopus microsporus* (*Rm*) and its endosymbiont *Paraburkholderia rhizoxinica* (*Pr*). All these positive controls showed an amplification of 16SrDNA. However, 16S-rDNA amplification failed for *M. alpina* ATCC 32222 (*Ma*) with or without an antibiotic treatment (Figure S31) indicating the absence of endosymbiont sequences in this strain. Amplification of fungal ITS sequences of *M. alpina* served as internal DNA loading control. All experiments were done in duplicates.

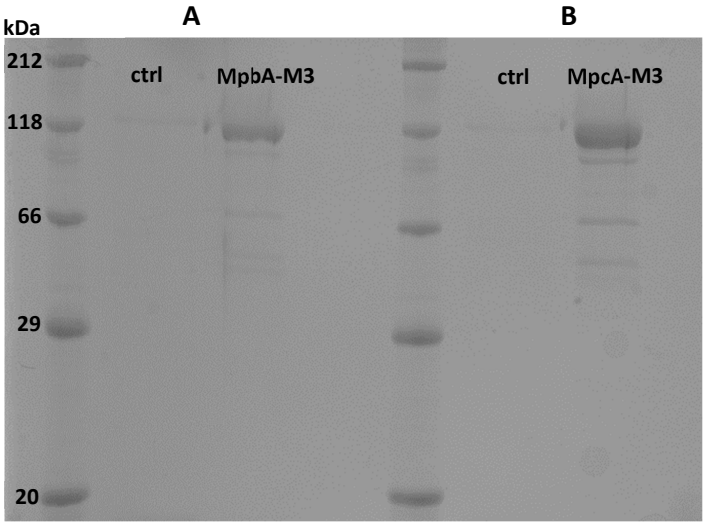

Figure S33. SDS polyacrylamide gel electrophoresis (SDS-PAGE) of purified His_6-tagged enzymes.
The purified enzymes MpbA-M3 (**A**) and MpcA-M3 (**B**) are shown. Purification from a mock-transformed *E. coli* KRX (empty vector) served as negative control (ctrl). The calculated protein mass for MpbA-M3 and MpcA-M3 are 122.40 kDa and 122.45 kDa, respectively. The dual *N*- and C-terminal His_6-tags add approximately 2 x 2.2 kDa.

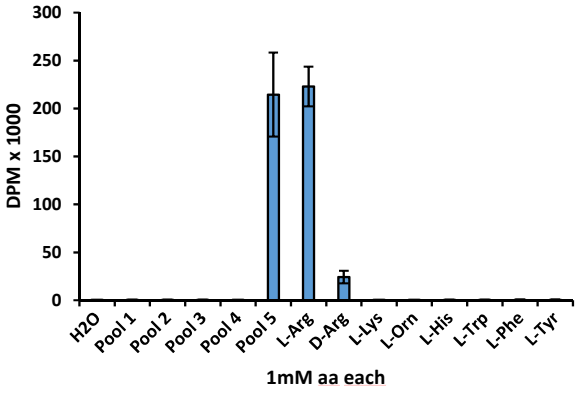

Figure S34. Substrate specificity assay with MpcA module 3 by the ATP-[^{32}PPi] exchange assay. Module 3 (C-A-T) of MpcA-M3 was tested against amino acid pools 1 to 5 (see Table S7) and subsequent single amino acids of pool 5 (L-Arg, D-Arg, L-Lys, L -Orn, L-His) and pool 2 (L-Trp, L-Phe, L-Tyr).

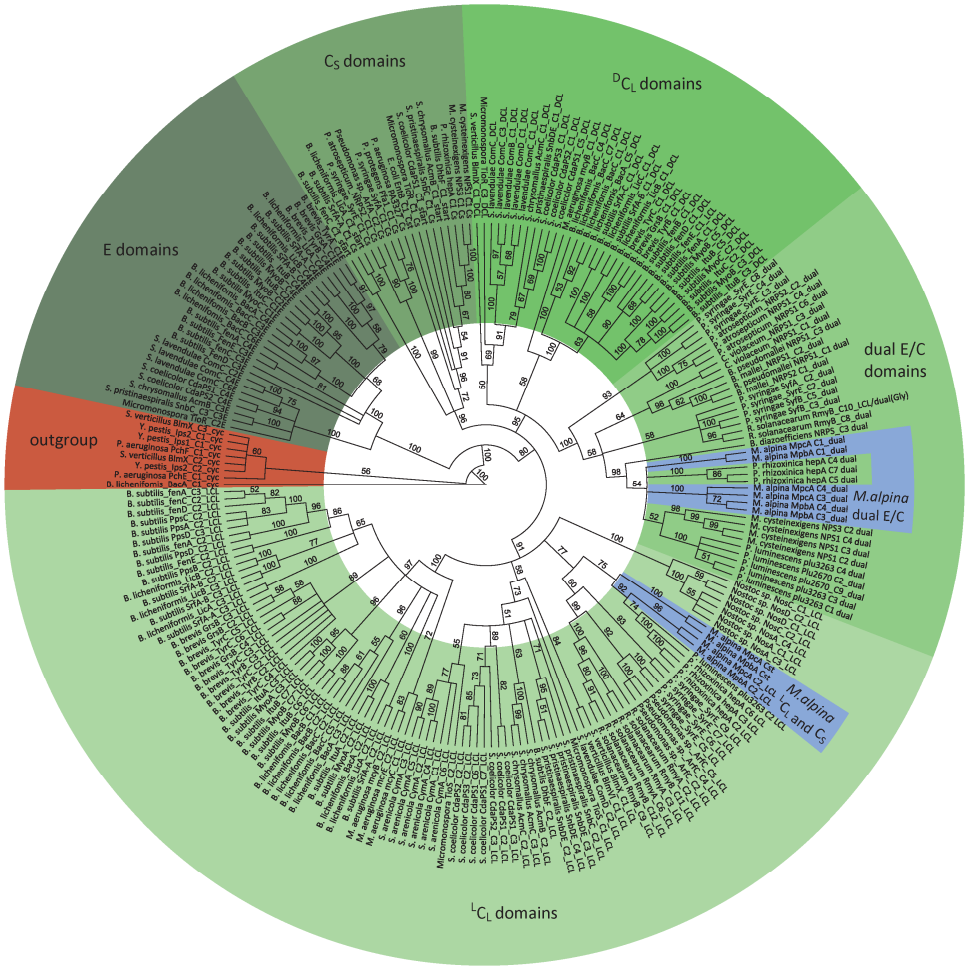

Figure S35. Phylogenetic analysis of MpcA and MpbA based on bacterial C-domain homology. Bacterial (green) and zygomycetous C-domains (blue) are highlighted. The cyclization domains (cyc) from NRPS served as outgroup (highlighted in red). $^{L}C_{L}$, canonical L-amino acid-transferring condensation domains; $^{D}C_{L}$, D-amino acid-transferring condensation domains; C_{s}, β-hydroxyacyl-transferring starter condensation domains; dual E/C, dual epimerization/condensation domains; E, epimerization domains.

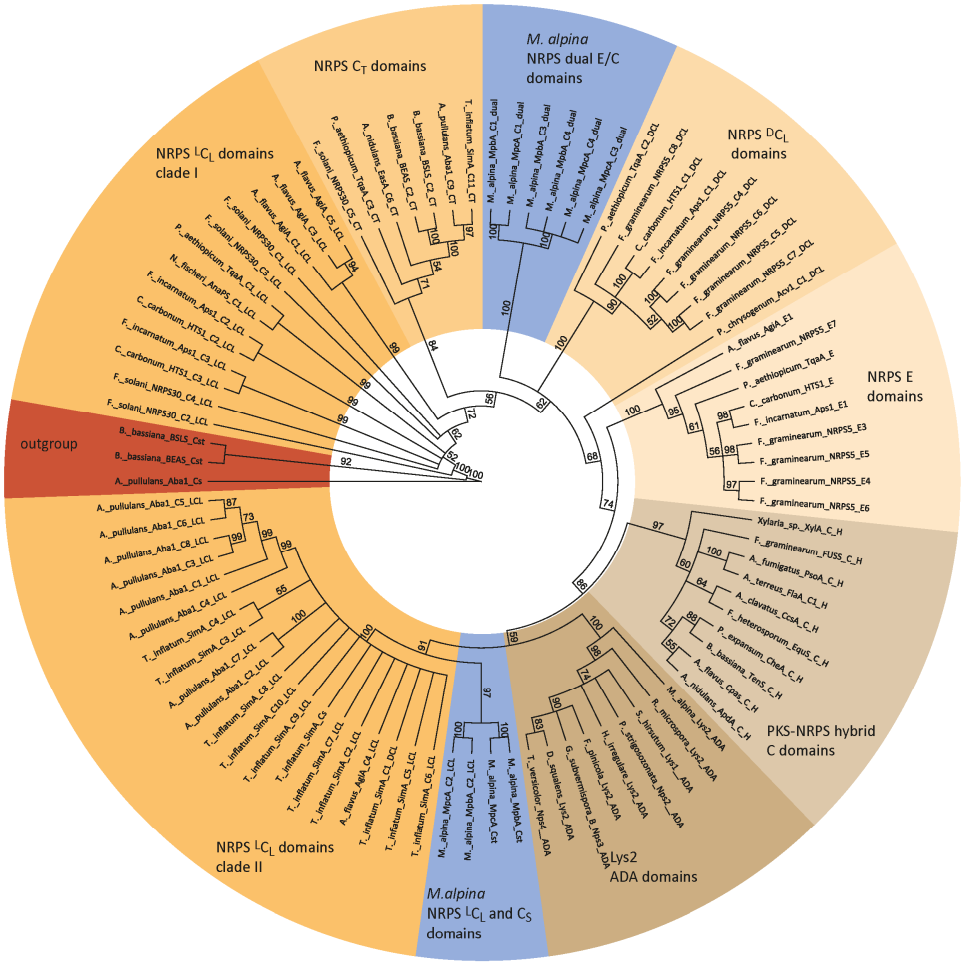

Figure S36. Phylogenetic analysis of MpcA and MpbA based on fungal C-domain homology. Zygomycetous (blue) and other fungal C-domains (brownish/ocher) are highlighted. Truncated starter C-domains (C_S) served as outgroup (red). ADA, condensation domain-like adenylation activating domain from NRPS-like Lys2 homologs (fungal L-lysine biosynthesis); $^{L}C_L$, canonical L-amino acid-transferring condensation domains; $^{D}C_L$, D-amino acid-transferring condensation domains; C_T, terminal peptide-releasing condensation domains; dual E/C, dual epimerization/condensation domains; E, epimerization domains; PKS-NRPS hybrid C, condensation domains from polyketide synthase/ nonribosomal peptide synthetase hybrid proteins.

References

1. **Marfey P.** 1984. Determination of D-Amino Acids .2. Use of a Bifunctional Reagent, 1,5-Difluoro-2,4-Dinitrobenzene. Carlsberg Res Commun **49:**591-596.
2. **Harada K, Matsui A, Shimizu Y, Ikemoto R, Fujii K.** 2001. Abnormal elution behavior of ornitine derivatized with 1-fluoro-2,4-dinitrophenyl-5-leucinamide in advanced Marfey's method. J Chromatogr A **921:**187-195.
3. **Baldeweg F, Warncke P, Fischer D, Gressler M.** 2019. Fungal Biosurfactants from *Mortierella alpina*. Org Lett **21:**1444-1448.
4. **Bradford MM.** 1976. A rapid and sensitive method for the quantitation of microgram quantities of protein utilizing the principle of protein-dye binding. Anal Biochem **72:**248-254.
5. **Conti E, Stachelhaus T, Marahiel MA, Brick P.** 1997. Structural basis for the activation of phenylalanine in the non-ribosomal biosynthesis of gramicidin S. EMBO J **16:**4174-4183.
6. **Bian X, Plaza A, Yan F, Zhang Y, Müller R.** 2015. Rational and efficient site-directed mutagenesis of adenylation domain alters relative yields of luminmide derivatives *in vivo*. Biotechnol Bioeng **112:**1343-1353.
7. **Georges C, Meyer JM.** 1995. High-molecular-mass, iron-repressed cytoplasmic proteins in fluorescent *Pseudomonas*: potential peptide-synthetases for pyoverdine biosynthesis. FEMS Microbiol Lett **132:**9-15.
8. **Baldeweg F, Kage H, Schieferdecker S, Allen C, Hoffmeister D, Nett M.** 2017. Structure of Ralsolamycin, the Interkingdom Morphogen from the Crop Plant Pathogen *Ralstonia solanacearum*. Org Lett **19:**4868-4871.
9. **Bian X, Plaza A, Yan F, Zhang Y, Müller R.** 2015. Rational and efficient site-directed mutagenesis of adenylation domain alters relative yields of luminmide derivatives in vivo. Biotechnol Bioeng **112:**1343-1353.
10. **Weyler C, Heinzle E.** 2017. Synthesis of natural variants and synthetic derivatives of the cyclic nonribosomal peptide luminmide in permeabilized *E. coli* Nissle and product formation kinetics. Appl Microbiol Biotechnol **101:**131-138.
11. **Schauwecker F, Pfennig F, Schröder W, Keller U.** 1998. Molecular cloning of the actinomycin synthetase gene cluster from *Streptomyces chrysomallus* and functional heterologous expression of the gene encoding actinomycin synthetase II. J Bacteriol **180:**2468-2474.
12. **Uehling J, Gryganskyi A, Hameed K, Tschaplinski T, Misztal PK, Wu S, Desiro A, Vande Pol N, Du Z, Zienkiewicz A, Zienkiewicz K, Morin E, Tisserant E, Splivallo R, Hainaut M, Henrissat B, Ohm R, Kuo A, Yan J, Lipzen A, Nolan M, LaButti K, Barry K, Goldstein AH, Labbe J, Schadt C, Tuskan G, Grigoriev I, Martin F, Vilgalys R, Bonito G.** 2017. Comparative genomics of *Mortierella elongata* and its bacterial endosymbiont *Mycoavidus cysteinexigens*. Environ Microbiol **19:**2964-2983.
13. **Niehs SP, Dose B, Scherlach K, Roth M, Hertweck C.** 2018. Genomics-Driven Discovery of a Symbiont-Specific Cyclopeptide from Bacteria Residing in the Rice Seedling Blight Fungus. ChemBioChem **19:**2167-2172.
14. **Wang X, Zhou H, Chen H, Jing X, Zheng W, Li R, Sun T, Liu J, Fu J, Huo L, Li YZ, Shen Y, Ding X, Muller R, Bian X, Zhang Y.** 2018. Discovery of recombinases enables genome mining of cryptic biosynthetic gene clusters in *Burkholderiales* species. Proc Natl Acad Sci U S A **115:**E4255-E4263.
15. **Lackner G, Moebius N, Partida-Martinez LP, Boland S, Hertweck C.** 2011. Evolution of an endofungal lifestyle: Deductions from the *Burkholderia rhizoxinica* genome. BMC Genomics **12:**210.
16. **Niehs SP, Scherlach K, Hertweck C.** 2018. Genomics-driven discovery of a linear lipopeptide promoting host colonization by endofungal bacteria. Org Biomol Chem **16:**8345-8352.
17. **Kalb D, Lackner G, Hoffmeister D.** 2014. Functional and phylogenetic divergence of fungal adenylate-forming reductases. Appl Environ Microbiol **80:**6175-6183.

18. **Qiao K, Chooi YH, Tang Y.** 2011. Identification and engineering of the cytochalasin gene cluster from *Aspergillus clavatus* NRRL 1. Metab Eng **13:**723-732.
19. **Chiang YM, Szewczyk E, Nayak T, Davidson AD, Sanchez JF, Lo HC, Ho WY, Simityan H, Kuo E, Praseuth A, Watanabe K, Oakley BR, Wang CC.** 2008. Molecular genetic mining of the Aspergillus secondary metabolome: discovery of the emericellamide biosynthetic pathway. Chem Biol **15:**527-532.
20. **Bergmann S, Schümann J, Scherlach K, Lange C, Brakhage AA, Hertweck C.** 2007. Genomics-driven discovery of PKS-NRPS hybrid metabolites from *Aspergillus nidulans*. Nat Chem Biol **3:**213-217.
21. **Seshime Y, Juvvadi PR, Tokuoka M, Koyama Y, Kitamoto K, Ebizuka Y, Fujii I.** 2009. Functional expression of the *Aspergillus flavus* PKS-NRPS hybrid CpaA involved in the biosynthesis of cyclopiazonic acid. Bioorg Med Chem Lett **19:**3288-3292.
22. **Balibar CJ, Walsh CT.** 2006. GliP, a multimodular nonribosomal peptide synthetase in *Aspergillus fumigatus*, makes the diketopiperazine scaffold of gliotoxin. Biochemistry **45:**15029-15038.
23. **Maiya S, Grundmann A, Li X, Li SM, Turner G.** 2007. Identification of a hybrid PKS/NRPS required for pseurotin A biosynthesis in the human pathogen *Aspergillus fumigatus*. ChemBioChem **8:**1736-1743.
24. **Gressler M, Zaehle C, Scherlach K, Hertweck C, Brock M.** 2011. Multifactorial induction of an orphan PKS-NRPS gene cluster in *Aspergillus terreus*. Chem Biol **18:**198-209.
25. **Bhattacherjee V, Bhattacharjee JK.** 1999. Characterization of a double gene disruption in the LYS2 locus of the pathogenic yeast, *Candida albicans*. Med Mycol **37:**411-417.
26. **Jia LJ, Tang HY, Wang WQ, Yuan TL, Wei WQ, Pang B, Gong XM, Wang SF, Li YJ, Zhang D, Liu W, Tang WH.** 2019. A linear nonribosomal octapeptide from *Fusarium graminearum* facilitates cell-to-cell invasion of wheat. Nat Commun **10:**922.
27. **Kakule TB, Sardar D, Lin Z, Schmidt EW.** 2013. Two related pyrrolidinedione synthetase loci in *Fusarium heterosporum* ATCC 74349 produce divergent metabolites. ACS Chem Biol **8:**1549-1557.
28. **Ehmann DE, Gehring AM, Walsh CT.** 1999. Lysine biosynthesis in *Saccharomyces cerevisiae*: mechanism of alpha-aminoadipate reductase (Lys2) involves posttranslational phosphopantetheinylation by Lys5. Biochemistry **38:**6171-6177.
29. **John TR, Ghosh M, Johnson JD.** 1997. Identification and expression of the *Saccharomyces cerevisiae* cytoplasmic tryptophanyl-tRNA synthetase gene. Yeast **13:**37-41.
30. **Hoffmann K, Schneider-Scherzer E, Kleinkauf H, Zocher R.** 1994. Purification and characterization of eucaryotic alanine racemase acting as key enzyme in cyclosporin biosynthesis. J Biol Chem **269:**12710-12714.
31. **Lawen A, Zocher R.** 1990. Cyclosporin synthetase. The most complex peptide synthesizing multienzyme polypeptide so far described. J Biol Chem **265:**11355-11360.
32. **Phonghanpot S, Punya J, Tachaleat A, Laoteng K, Bhavakul V, Tanticharoen M, Cheevadhanarak S.** 2012. Biosynthesis of xyrrolin, a new cytotoxic hybrid polyketide/non-ribosomal peptide pyrroline with anticancer potential, in *Xylaria* sp. BCC 1067. ChemBioChem **13:**895-903.
33. **Marahiel MA, Stachelhaus T, Mootz HD.** 1997. Modular Peptide Synthetases Involved in Nonribosomal Peptide Synthesis. Chem Rev **97:**2651-2674.
34. **Mootz HD, Marahiel MA.** 1997. The tyrocidine biosynthesis operon of *Bacillus brevis*: complete nucleotide sequence and biochemical characterization of functional internal adenylation domains. J Bacteriol **179:**6843-6850.
35. **Eppelmann K, Doekel S, Marahiel MA.** 2001. Engineered biosynthesis of the peptide antibiotic bacitracin in the surrogate host *Bacillus subtilis*. J Biol Chem **276:**34824-34831.
36. **Yakimov MM, Kroger A, Slepak TN, Giuliano L, Timmis KN, Golyshin PN.** 1998. A putative lichenysin A synthetase operon in *Bacillus licheniformis*: initial characterization. Biochim Biophys Acta **1399:**141-153.

37. **May JJ, Wendrich TM, Marahiel MA.** 2001. The dhb operon of *Bacillus subtilis* encodes the biosynthetic template for the catecholic siderophore 2,3-dihydroxybenzoate-glycine-threonine trimeric ester bacillibactin. J Biol Chem **276:**7209-7217.
38. **Tsuge K, Ano T, Hirai M, Nakamura Y, Shoda M.** 1999. The genes degQ, pps, and lpa-8 (sfp) are responsible for conversion of *Bacillus subtilis* 168 to plipastatin production. Antimicrob Agents Chemother **43:**2183-2192.
39. **Bruner SD, Weber T, Kohli RM, Schwarzer D, Marahiel MA, Walsh CT, Stubbs MT.** 2002. Structural basis for the cyclization of the lipopeptide antibiotic surfactin by the thioesterase domain SrfTE. Structure **10:**301-310.
40. **Lin TP, Chen CL, Chang LK, Tschen JS, Liu ST.** 1999. Functional and transcriptional analyses of a fengycin synthetase gene, *fenC*, from *Bacillus subtilis*. J Bacteriol **181:**5060-5067.
41. **Tsuge K, Akiyama T, Shoda M.** 2001. Cloning, sequencing, and characterization of the iturin A operon. J Bacteriol **183:**6265-6273.
42. **Duitman EH, Hamoen LW, Rembold M, Venema G, Seitz H, Saenger W, Bernhard F, Reinhardt R, Schmidt M, Ullrich C, Stein T, Leenders F, Vater J.** 1999. The mycosubtilin synthetase of *Bacillus subtilis* ATCC6633: a multifunctional hybrid between a peptide synthetase, an amino transferase, and a fatty acid synthase. Proc Natl Acad Sci U S A **96:**13294-13299.
43. **Woodrow GC, Young IG, Gibson F.** 1979. Biosynthesis of enterochelin in *Escherichia coli* K-12: separation of the polypeptides coded for by the *entD, E, F* and *G* genes. Biochim Biophys Acta **582:**145-153.
44. **Nishizawa T, Ueda A, Asayama M, Fujii K, Harada K, Ochi K, Shirai M.** 2000. Polyketide synthase gene coupled to the peptide synthetase module involved in the biosynthesis of the cyclic heptapeptide microcystin. J Biochem **127:**779-789.
45. **Lombo F, Velasco A, Castro A, de la Calle F, Brana AF, Sanchez-Puelles JM, Mendez C, Salas JA.** 2006. Deciphering the biosynthesis pathway of the antitumor thiocoraline from a marine actinomycete and its expression in two streptomyces species. ChemBioChem **7:**366-376.
46. **Hoffmann D, Hevel JM, Moore RE, Moore BS.** 2003. Sequence analysis and biochemical characterization of the nostopeptolide A biosynthetic gene cluster from *Nostoc* sp. GSV224. Gene **311:**171-180.
47. **Yin J, Zhu H, Xia L, Ding X, Hoffmann T, Hoffmann M, Bian X, Müller R, Fu J, Stewart AF, Zhang Y.** 2015. A new recombineering system for *Photorhabdus* and *Xenorhabdus*. Nucleic Acids Res **43:**e36.
48. **Gulick AM.** 2017. Nonribosomal peptide synthetase biosynthetic clusters of ESKAPE pathogens. Nat Prod Rep **34:**981-1009.
49. **Quadri LE, Keating TA, Patel HM, Walsh CT.** 1999. Assembly of the *Pseudomonas aeruginosa* nonribosomal peptide siderophore pyochelin: In vitro reconstitution of aryl-4, 2-bisthiazoline synthetase activity from PchD, PchE, and PchF. Biochemistry **38:**14941-14954.
50. **Ma Z, Geudens N, Kieu NP, Sinnaeve D, Ongena M, Martins JC, Hofte M.** 2016. Biosynthesis, Chemical Structure, and Structure-Activity Relationship of Orfamide Lipopeptides Produced by *Pseudomonas protegens* and Related Species. Front Microbiol **7:**e382.
51. **Morikawa M, Daido H, Takao T, Murata S, Shimonishi Y, Imanaka T.** 1993. A new lipopeptide biosurfactant produced by *Arthrobacter* sp. strain MIS38. J Bacteriol **175:**6459-6466.
52. **Gross H, Loper JE.** 2009. Genomics of secondary metabolite production by *Pseudomonas* spp. Nat Prod Rep **26:**1408-1446.
53. **Berti AD, Greve NJ, Christensen QH, Thomas MG.** 2007. Identification of a biosynthetic gene cluster and the six associated lipopeptides involved in swarming motility of *Pseudomonas syringae* pv. tomato DC3000. J Bacteriol **189:**6312-6323.
54. **Schultz AW, Oh DC, Carney JR, Williamson RT, Udwary DW, Jensen PR, Gould SJ, Fenical W, Moore BS.** 2008. Biosynthesis and structures of cyclomarins and cyclomarazines, prenylated cyclic peptides of marine actinobacterial origin. J Am Chem Soc **130:**4507-4516.

55. **Hojati Z, Milne C, Harvey B, Gordon L, Borg M, Flett F, Wilkinson B, Sidebottom PJ, Rudd BA, Hayes MA, Smith CP, Micklefield J.** 2002. Structure, biosynthetic origin, and engineered biosynthesis of calcium-dependent antibiotics from *Streptomyces coelicolor*. Chem Biol **9:**1175-1187.
56. **Chiu HT, Hubbard BK, Shah AN, Eide J, Fredenburg RA, Walsh CT, Khosla C.** 2001. Molecular cloning and sequence analysis of the complestatin biosynthetic gene cluster. Proc Natl Acad Sci U S A **98:**8548-8553.
57. **Mast Y, Weber T, Golz M, Ort-Winklbauer R, Gondran A, Wohlleben W, Schinko E.** 2011. Characterization of the 'pristinamycin supercluster' of *Streptomyces pristinaespiralis*. Microb Biotechnol **4:**192-206.
58. **Du L, Sanchez C, Chen M, Edwards DJ, Shen B.** 2000. The biosynthetic gene cluster for the antitumor drug bleomycin from *Streptomyces verticillus* ATCC15003 supporting functional interactions between nonribosomal peptide synthetases and a polyketide synthase. Chem Biol **7:**623-642.
59. **Gehring AM, DeMoll E, Fetherston JD, Mori I, Mayhew GF, Blattner FR, Walsh CT, Perry RD.** 1998. Iron acquisition in plague: modular logic in enzymatic biogenesis of yersiniabactin by *Yersinia pestis*. Chem Biol **5:**573-586.
60. **Greco C, Pfannenstiel BT, Liu JC, Keller NP.** 2019. Depsipeptide Aspergillicins Revealed by Chromatin Reader Protein Deletion. ACS Chem Biol **14:**1121-1128.
61. **Slightom JL, Metzger BP, Luu HT, Elhammer AP.** 2009. Cloning and molecular characterization of the gene encoding the Aureobasidin A biosynthesis complex in *Aureobasidium pullulans* BP-1938. Gene **431:**67-79.
62. **Xu Y, Orozco R, Wijeratne EM, Gunatilaka AA, Stock SP, Molnar I.** 2008. Biosynthesis of the cyclooligomer depsipeptide beauvericin, a virulence factor of the entomopathogenic fungus *Beauveria bassiana*. Chem Biol **15:**898-907.
63. **Xu Y, Orozco R, Kithsiri Wijeratne EM, Espinosa-Artiles P, Leslie Gunatilaka AA, Patricia Stock S, Molnar I.** 2009. Biosynthesis of the cyclooligomer depsipeptide bassianolide, an insecticidal virulence factor of *Beauveria bassiana*. Fungal Genet Biol **46:**353-364.
64. **Eley KL, Halo LM, Song Z, Powles H, Cox RJ, Bailey AM, Lazarus CM, Simpson TJ.** 2007. Biosynthesis of the 2-pyridone tenellin in the insect pathogenic fungus *Beauveria bassiana*. ChemBioChem **8:**289-297.
65. **Panaccione DG, Scott-Craig JS, Pocard JA, Walton JD.** 1992. A cyclic peptide synthetase gene required for pathogenicity of the fungus *Cochliobolus carbonum* on maize. Proc Natl Acad Sci U S A **89:**6590-6594.
66. **Song Z, Cox RJ, Lazarus CM, Simpson TT.** 2004. Fusarin C biosynthesis in *Fusarium moniliforme* and *Fusarium venenatum*. ChemBioChem **5:**1196-1203.
67. **Villani A, Proctor RH, Kim HS, Brown DW, Logrieco AF, Amatulli MT, Moretti A, Susca A.** 2019. Variation in secondary metabolite production potential in the *Fusarium incarnatum*-equiseti species complex revealed by comparative analysis of 13 genomes. BMC Genomics **20:**e314.
68. **Romans-Fuertes P, Sondergaard TE, Sandmann MI, Wollenberg RD, Nielsen KF, Hansen FT, Giese H, Brodersen DE, Sorensen JL.** 2016. Identification of the non-ribosomal peptide synthetase responsible for biosynthesis of the potential anti-cancer drug sansalvamide in *Fusarium solani*. Curr Genet **62:**799-807.
69. **Wang L, Chen W, Feng Y, Ren Y, Gu Z, Chen H, Wang H, Thomas MJ, Zhang B, Berquin IM, Li Y, Wu J, Zhang H, Song Y, Liu X, Norris JS, Wang S, Du P, Shen J, Wang N, Yang Y, Wang W, Feng L, Ratledge C, Zhang H, Chen YQ.** 2011. Genome characterization of the oleaginous fungus Mortierella alpina. PLoS One **6:**e28319.
70. **Yin WB, Grundmann A, Cheng J, Li SM.** 2009. Acetylaszonalenin biosynthesis in *Neosartorya fischeri*. Identification of the biosynthetic gene cluster by genomic mining and functional proof of the genes by biochemical investigation. J Biol Chem **284:**100-109.

71. **Gao X, Chooi YH, Ames BD, Wang P, Walsh CT, Tang Y.** 2011. Fungal indole alkaloid biosynthesis: genetic and biochemical investigation of the tryptoquialanine pathway in *Penicillium aethiopicum*. J Am Chem Soc **133:**2729-2741.
72. **Burzlaff NI, Rutledge PJ, Clifton IJ, Hensgens CM, Pickford M, Adlington RM, Roach PL, Baldwin JE.** 1999. The reaction cycle of isopenicillin N synthase observed by X-ray diffraction. Nature **401:**721-724.
73. **Schümann J, Hertweck C.** 2007. Molecular basis of cytochalasan biosynthesis in fungi: gene cluster analysis and evidence for the involvement of a PKS-NRPS hybrid synthase by RNA silencing. J Am Chem Soc **129:**9564-9565.

4.2 Manuskript 2

Macrophage-targeting Oligopeptides from *Mortierella alpina*

Wurlitzer, Jacob M.; Stanišić, Aleksa; Ziethe, Sebastian; Jordan, Paul M.; Günther, Kerstin; Werz, Oliver; Kries, Hajo; Gressler, Markus

veröffentlich unter: *Chemical Science* **2022**, 13, 9091-9101; DOI: 10.1039/D2SC00860B

Zusammenfassung:

Die oberflächenaktiven Malpinine werden von *Mortierella alpina* in großen Mengen gebildet. In dieser Arbeit konnte das NRPS-Gen *malA* als Biosynthesegen der Malpinine identifiziert werden. Dies wurde durch *de-novo* Sequenzierung, RT-qPCR-Analyse sowie heterologe Expression und biochemische Charakterisierung aller NRPS-Module erreicht. Für die heptamodulare NRPS MalA konnte so gezeigt werden, dass die terminale A-Domäne inaktiv ist und bei der Malpinin-Biosynthese übersprungen wird. Bei der *in vitro* Charakterisierung konnte eine breite Substratspezifität der A-Domänen beobachtet werden, welche anschließend in Fütterungsversuchen mit Vorläuferverbindungen ausgenutzt wurde. Auf diese Weise wurden 20 neue Malpinine identifiziert, darunter solche mit chemisch-modifizierbaren Seitengruppen. Exemplarisch wurden diese mit einem Fluoreszenzfarbstoff kovalent gebunden, um Malpinine als mögliche Vehikel für gezielten Wirkstofftransport zu untersuchen.

Der Kandidat ist:

☒ Erstautor ☐ Co-Erstautor ☐ Korresp. Autor ☐ Coautor

Eigenanteil

Autor/-in	Konzeptionell	Datenanalyse	Experimentell	Verfassen des Manuskriptes
Wurlitzer, JM	50%	75%	70%	25%
Stanišić, A	-	20%	20%	5%
Gressler, M	50%	-	-	65%
6 weitere Autoren	-	5%	10%	5%
Summe	100%	100%	100%	100%

Chemical Science

ROYAL SOCIETY OF CHEMISTRY

EDGE ARTICLE

View Article Online
View Journal | View Issue

Check for updates

Cite this: *Chem. Sci.*, 2022, **13**, 9091

All publication charges for this article have been paid for by the Royal Society of Chemistry

Received 10th February 2022
Accepted 15th July 2022

DOI: 10.1039/d2sc00860b

rsc.li/chemical-science

Macrophage-targeting oligopeptides from *Mortierella alpina*†

Jacob M. Wurlitzer,[a] Aleksa Stanišić,[b] Sebastian Ziethe,[a] Paul M. Jordan,[c] Kerstin Günther,[c] Oliver Werz,[c] Hajo Kries[b] and Markus Gressler[*a]

The realm of natural products of early diverging fungi such as *Mortierella* species is largely unexplored. Herein, the nonribosomal peptide synthetase (NRPS) MalA catalysing the biosynthesis of the surface-active biosurfactants, malpinins, has been identified and biochemically characterised. The investigation of the substrate specificity of respective adenylation (A) domains indicated a substrate-tolerant enzyme with an unusual, inactive C-terminal NRPS module. Specificity-based precursor-directed biosynthesis yielded 20 new congeners produced by a single enzyme. Moreover, MalA incorporates artificial, click-functionalised amino acids which allowed postbiosynthetic coupling to a fluorophore. The fluorescent malpinin conjugate penetrates mammalian cell membranes *via* an phagocytosis-mediated mechanism, suggesting *Mortierella* oligopeptides as carrier peptides for directed cell targeting. The current study demonstrates substrate-specificity testing as a powerful tool to identify flexible NRPS modules and highlights basal fungi as reservoir for chemically tractable compounds in pharmaceutical applications.

Introduction

Among natural products, non-ribosomal peptides (NRP) are of medicinal importance and include antibiotic, anticancer or immunomodulating drugs. Attempts have been made to produce novel NRPs *via* classical solid-phase peptide synthesis[1] or by enzyme engineering within the emerging field of synthetic biology.[2] However, most clinically relevant compounds are still isolated from their microbial producers, *i.e.* bacteria and higher fungi. In contrast, basal fungi such as *Mortierella* sp. have traditionally been used as a resource for polyunsaturated fatty acids in the food industry,[3] but have not been considered as NRP producers. However, recent investigations of the secondary metabolism of *Mortierella alpina* revealed an unexpected potential for the production of small oligopeptides of pharmaceutical interest including the surface-active malpinins A–E (**1**–**5**) (Fig. 1).[4] Additionally, cyclic pentapeptides such as malpibaldins and the antibacterial malpicyclins are produced.[5] The biosynthesis of the latter compounds has recently been

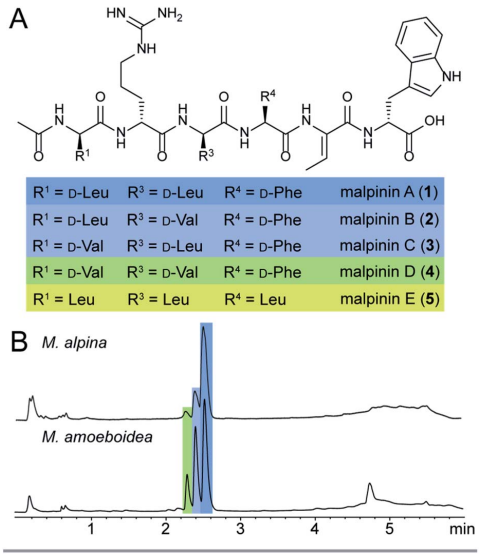

Fig. 1 Native malpinins. A. Chemical structures of malpinin A–E (**1**–**5**). The stereoconfiguration of 5 has not been determined. B. UV chromatograms ($\lambda = 280$ nm) of crude extracts of mycelia from *M. alpina* ATCC32222 and *M. amoeboidea* CBS 889.72 grown on YPD. Compound **1** is the predominant metabolite, whereas compound **5** is detectable only in traces (not depicted).

[a]*Department Pharmaceutical Microbiology at the Leibniz Institute for Natural Product Research and Infection Biology (Hans-Knöll-Institute), Friedrich-Schiller-University, Winzerlaer Strasse 2, Jena 07745, Germany. E-mail: markus.gressler@leibniz-hki.de*
[b]*Junior Group Biosynthetic Design of Natural Products at the Leibniz Institute for Natural Product Research and Infection Biology (Hans-Knöll-Institute), Beutenbergstrasse 11a, Jena 07745, Germany*
[c]*Department Pharmaceutical/Medicinal Chemistry at the Friedrich-Schiller-University, Philosophenweg 14, Jena 07743, Germany*

† Electronic supplementary information (ESI) available: Additional experimental procedures, Figu. S1–S62 and Tables S1–S16. See https://doi.org/10.1039/d2sc00860b

View Article Online
Chemical Science Edge Article

assigned to two bacterial-like nonribosomal peptide synthetases (NRPSs), malpibaldin synthetase MpbA and malpicyclin synthetase MpcA, respectively.[5] Both enzymes are composed of five consecutive modules (C-A-T) each harbouring a condensation (C) domain, an ATP-dependent adenylation (A) domain and a thiolation (T) domain, which act in concert to provide a linear pentapeptide that is subsequently cyclised by a C-terminal thioesterase domain (TE). Whilst L-amino acids are incorporated by the action of canonical C domains, D-amino acid building blocks are introduced by bacterial-like dual epimerization/condensation (E/C) domains.

In contrast to *Mortierella* cyclopentapeptides, the biosynthetic origin of the biosurfactant **1–5** is still enigmatic. Malpinins have a surface tension-lowering activity with a critical micelle concentration (CMC) of 14 μM that is 580-fold lower than that of the commonly used anionic detergent sodium dodecyl sulfate (SDS).[4] Their low cytotoxicity makes these biosurfactants valuable candidates for pharmaceutical or medicinal applications. However, information on the malpinin uptake into mammalian cells has been lacking. Malpinins are acetylated hexapeptides (Ac-D-Leu/Val-D-Arg-D-Leu/Val-L-Phe/Leu-Dhb-D-Trp) with two striking structural features (Fig. 1): (i) a non-canonical amino acid, (*Z*)-dehydrobutyrine (Dhb), at position 5, and (ii) a C-terminal D-amino acid, D-tryptophan, that can be oxidised to kynurenine.[4] Moreover, incorporated D-amino acids in positions 1, 3 and 4 were variable resulting in the **1**-congeners **2–5**. Consequently, a hexamodular NRPS with flexible modules 1, 3 and 4 is expected for the malpinin biosynthesis matching the above-mentioned catalytic features.

Substrate promiscuity is a key feature of many enzymes which enables both natural enzyme evolution[6] and enzyme engineering[7] in synthetic biology.[8] In NRPSs, substrate promiscuity has been occasionally encountered in A domains[9] and harnessed for producing non-natural products[7] but has not been systematically investigated. Several adenylation assays have been established to measure the activity of A domains.[10,11] Recently, the hydroxamate specificity assay (HAMA) was developed which unravels specificity profiles of A domains under competition conditions in a straightforward fashion. HAMA is based on the quenching of aminoacyl adenylates by hydroxylamine and LC-MS/MS detection of respective hydroxamate products allowing parallel testing of multiple competing substrates.[12] Hence, we choose HAMA to investigate putatively substrate tolerant A domains[5] in the malpinin synthetase.

In this report, we use a combination of state-of-the-art genome sequencing techniques and UHPLC-MS/MS-based metabolite screening to identify the malpinin synthase MalA. A thorough substrate specificity analysis of the complete set of its NRPS modules led to the identification of 20 novel malpinin congeners, among them unusual methionine-containing compounds. Using substrate profiling by HAMA, the enzyme's relaxed substrate tolerance was determined and exploited to incorporate non-natural, "clickable" amino acid substrates. The bioorthogonally labelled fluorescent *Mortierella* oligopeptide permeates membranes of mammalian cells in a phagocytose-dependent process. Hence, malpinins represent potential carrier peptides for drugs in macrophage-associated diseases.

Results and discussion

Identification of the malpinin synthetase MalA

The published genome of *M. alpina*[13] does not provide appropriate NRPS candidate genes for malpinin biosynthesis. Therefore, a comparative genome analysis of *M. alpina* ATCC32222 and its close relative *Mortierella amoeboidea* CBS889.72 (ref. 14) was used to identify the malpinin synthetase gene. Both species produce **1–5** as determined by UHPLC-MS and ESI-MS/MS (Fig. 1, and ESI, S1†) and were subjected to genome sequencing (Table S1†). Subsequent analysis of both genomes using the antiSMASH[15] platform lead to the identification of at least 16 potential NRPS and NRPS-like genes in both species (Table S2†). Consistent with the metabolite screening (Fig. S1†), either genome encodes the two cyclopentapeptide NRPSs MpbA (85% amino acid identity between both species) and MpcA (90%), which catalyse the production of malpibaldins and malpicyclins, respectively. In addition, both species share three large genes encoding one hexamodular (Nps5, 89% identity), one heptamodular (Nps3 [MalA], 90% identity) and one octamodular NRPS (Nps2, 73% identity), which are plausible candidates for malpinin biosynthesis (Tables 1, S2 and Fig. S2†). An expression analysis by qRT-PCR revealed that the *nps*2 gene is hardly expressed under laboratory conditions, whilst transcripts of both *nps*3 (*malA*) and *nps*5 are highly abundant (Fig. S3†). However, solely *malA* expression levels correlated with titers of **1**, *i.e.* the major metabolite in *Mortierella* metabolite extracts, according to LC-MS-based metabolite quantification (Fig. S3†). Moreover, the candidate enzyme MalA shows the required distribution of C and E/C domains (Table 1), although the 7th module seems to be obsolete for the production of a hexapeptide.

MalA modules 1, 3 and 4 are highly promiscuous

The full-length 24.5 kb transcript of *malA* has been verified by Sanger sequencing and encodes a heptamodular NRPS MalA spanning over 7760 aa (853 kDa). As described for NRPSs of other basal fungi,[5,16] the A domains of MalA cluster phylogenetically with bacterial counterparts (Fig. S4†). Since knock-out strategies are hardly applicable for early diverging fungi,[17] we used *in vitro* specificity profiling to assign all A domains of MalA to a particular adenylation step in the malpinin biosynthesis. Heterologous production of all seven C-A-T modules (M1-7) as bi-terminal His_6-tagged fusion proteins was accomplished in *Escherichia coli* (Fig. S2, S5 and Table S3†). The formation of aminoacyl adenylate during the adenylation reactions was tracked by conversion to stable aminoacyl hydroxamates that were quantified using multiplexed LC-MS/MS measurements (HAMA, Fig. 2 and Table S4†).[12] HAMA revealed that both M1 and M3 have relaxed specificity towards aliphatic amino acids (L-Leu > L-Met > L/D-Val > L-Cys), explaining Val at position 1 and 3 in **1**-congeners **2–4** (Fig. 1). The incorporation of L-Leu, but not *N*-acetyl-L-Leu by module 1 was also confirmed (Fig. S6†) suggesting the *N*-terminal acetylation occurs at a later stage of biosynthesis. Similar to M1 and M3, M4 has a broad substrate spectrum showing the highest activity with L-Phe followed by

View Article Online
Edge Article Chemical Science

Table 1 Multi-module NRPSs in *M. alpina*. For domain abbreviations refer to Fig. 3

Gene	Length incl. introns (bp)	Protein size (aa)	Domain architecture of the enzyme
nps2	26 963	8125	A-T-E/C-A-T-C-A-T-E/C-A-T-C-A-T-C-A-T-C-A-T-C-A-T-TE
nps3 (*malA*)	24 471	7760	C_S-A-T-E/C-A-T-E/C-A-T-E/C-A-T-C-A-T-C*-A-T-E/C-A-T-TE
nps5	20 143	6489	C_S-A-T-E/C-A-T-C-A-T-E/C-A-T-E/C-A-T-C-A-T-TE

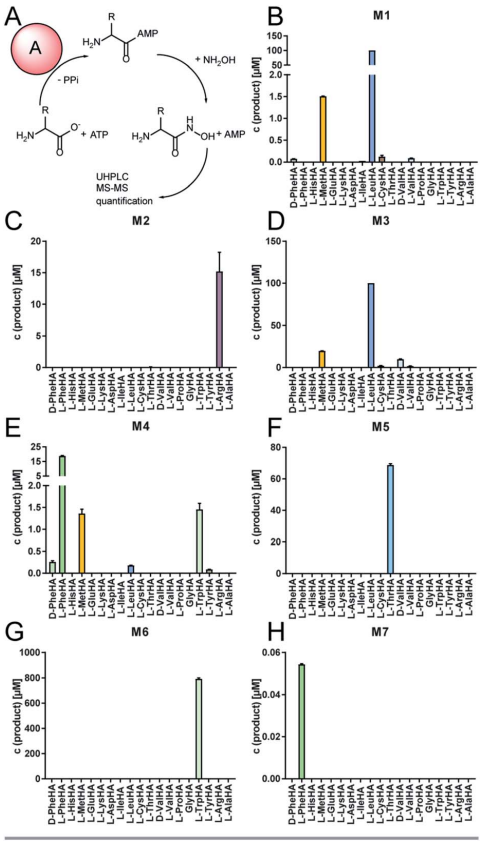

Fig. 2 Specificity profiles of the NRPS modules of MalA. (A) Adenylation reaction and hydroxamate formation during HAMA. Modules and substrates were mixed at a final concentration of 1 µM and 1 mM, respectively, and were incubated for 60 min at 37 °C. The resulting aminoacyl hydroxamates (HA) were subsequently analysed by UHPLC-MS. (B–H) Specificity profiles of the complete set of NRPS modules 1–7 (M1–M7) of MalA determined by the HAMA assay. Note that M7 shows lowest activity.

other hydrophobic amino acids (L-Phe > L-Met = L-Trp). In contrast, M2, M5 and M6 are highly specific for L-Arg, L-Thr, and L-Trp, respectively (Fig. 2). Solely, M7 converted its preferred substrate (L-Phe) with a 15 000-fold reduced turnover rate compared to the most active module M6, indicating that its A domain cannot contribute to the malpinin biosynthesis due to low activity. The residual activity for L-Phe may indicate that a 7th residue was present in an evolutionary precursor to the malpinin family. An inactive terminal module has been shown for the indanomycin synthase in *Streptomyces antibioticus*.[18] Since the last T domain in MalA is apparently not loaded with an amino acid, either the TE domain must offload the oligopeptide from the preceding T domain or the dual E/C domain of M7 must transfer the final peptide chain to the free acceptor T domain of M7 prior to release. In any case, this E/C domain is required for the stereo inversion of the C-terminal L-Trp to D-Trp in **1–5**. A similar mechanism is proposed for the epimerase (E) domain of the ß-(L-α-aminoadipyl)-L-Cys-D-Val (LLD-ACV) synthetase from ß-lactam producing fungi.[19–21] Building on our expression analysis and HAMA-based *in vitro* activity assays, a biosynthetic pathway for malpinins by MalA is proposed, which includes (i) a canonical successive peptide biosynthesis, (ii) epimerizations of L-amino acids by dual E/C domains, if required, and (iii) an early peptide offloading at module 7 after five condensation steps (Fig. 3).

In bacteria, *N*-terminal acylation of peptides is catalysed by C-starter (C_S) domains that transfer various acyl chains from acyl-CoA, a standalone acyl carrier protein (ACP) or an acylated C-A-T module selectively to the *N*-terminus of the nascent NRP.[22–24] Recently, a fungal C_S domain has been described to *N*-terminally acetylate the NRP aspergillicin A from *Aspergillus flavus*.[25] However, the C_S domain of MalA is truncated and lacks the essential C1–C4 core motifs at its *N*-terminal region including the highly conserved tandem His–His motif in the active site of C3 (Fig. S7 and S8†). An acetylation of L- or D-leucyl-SNAC, that mimics the thiotemplated leucyl moiety,[24] could not be determined for MalA-C_S (Fig. S9†) suggesting an inactive C_S domain. The presence of such truncated, non-functional, but structurally required C_S domains have been demonstrated for fungal NRPSs, *e.g.* in cyclosporine and penicillin biosynthesis.[26,27] However, *N*-acetylation of leucyl-SNAC thioesters was detectable in *M. alpina* protein crude extracts when incubated with acetyl-CoA (Fig. S9†). These findings and the observation that no acetyl transferase gene is co-expressed in the malpinin A gene cluster (Fig. S10†), point to a co- or post-synthetic acetylation *in trans* by an acetyltransferase encoded elsewhere in the genome – a phenomenon that has recently been described for the erinacine biosynthesis in the mushroom *Hericium erinaceus*.[28] Indeed, the precursor deacetyl-**1** (*m*/*z* 817.4716 $[M + H]^+$) is detectable in *M. alpina* with moderate abundance (Fig. S11 and S12†).

Remarkably, malpinins contain (*Z*)-Dhb as non-proteinogenic amino acid. Dhb is present in a variety of

View Article Online
Chemical Science Edge Article

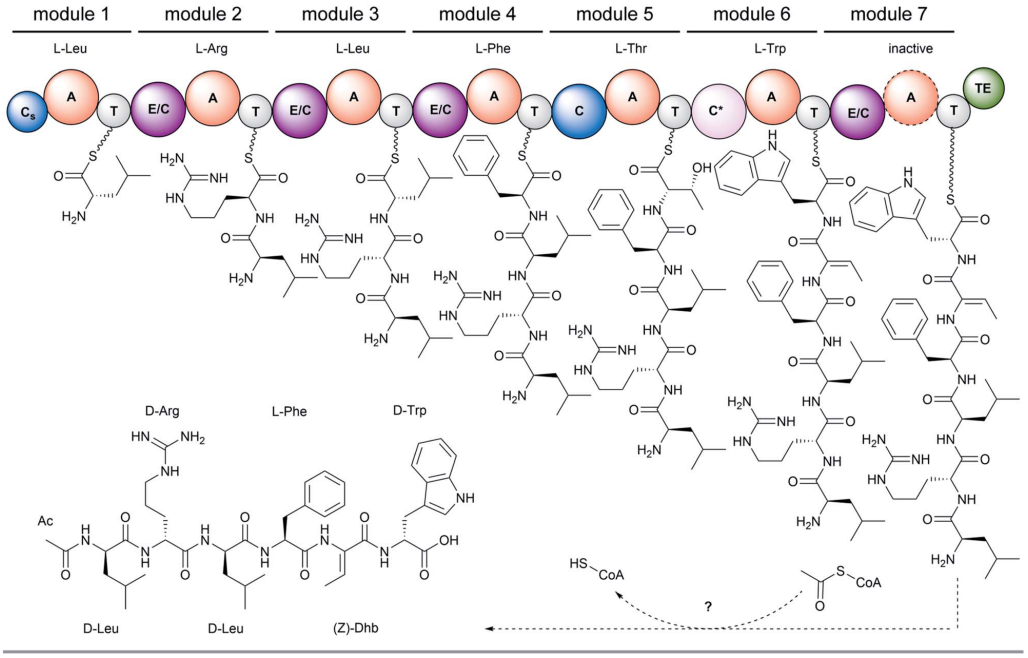

Fig. 3 Biosynthesis of malpinins by MalA shown for **1**. Involved domains are: A, adenylation domain; C, canonical condensation domain; C_s, starter condensation domain (inactive); C*, dual dehydration/condensation domain; E/C, dual epimerization/condensation domain; T, thiolation domain; TE, thioesterase domain. Note, that the final adenylation domain (in M7) is inactive and offloading occurs either by the final dual E/C domain or the C-terminal T or TE domain.

cyanobacterial NRP.[29–32] To incorporate Dhb in ribosomally and post-translationally modified peptides (RiPPs) such as the lantibiotic precursor prenisin or the lacticin-481 propeptide, Thr residues are post-translationally dehydrated by a downstream processing dehydratase (NisB)[33] or by a bifunctional dehydratase/cyclase (LctM),[34] respectively. However, no homologous genes are encoded in the genomes of *M. alpina* and *M. amoeboidea.* During malpinin biosynthesis, Thr is most likely incorporated by M5 (Fig. 2) and is then dehydrated by the subsequent dual E/C domain of M6 to give the α,β-unsaturated amino acid (*Z*)-Dhb (Fig. 3). In dual E/C domains, the α-C atom is first deprotonated resulting in an enolate intermediate and the epimerisation is achieved through addition of a proton from the opposite side.[35] However, the latter step is apparently avoided by M6 and a hydroxyl group is eliminated instead. Recently, the origin of such α,β-unsaturated amino acyl moieties in the NRP albopeptide from *Streptomyces albofaciens* has been assigned to a novel class of dual β-elimination/condensation domains (C*) in the NRPS AlbB.[36] Consistently, the amino acid sequence of the dual E/C domain of M6 shows the same conserved motifs as the C* domains of AlbB, *i.e.* the catalytic ^{136}HHXXXD^{141} condensation motif and a E^{367} residue, which is discussed to be involved in the dehydration reaction.[36] Hence, our findings imply a similar mechanism of incorporation of (*Z*)-Dhb in malpinins. This assumption is further supported by the fact that Thr- and Dhb-specific A domains from bacteria and *Mortierella* share the same residues in the specificity determining binding pocket (Table S5†).

Enzymatic promiscuity facilitates the production of diverse malpinin congeners

The substrate specificity data confirmed MalA as malpinin synthetase and disclosed substrate tolerance of its modules M1, M3, and M4. In-depth analysis of kinetic parameters of the A domain for M3 by MesG activity assays[11] revealed highest specificity for L-Leu ($k_{cat}/K_M = 61$ mM^{-1} min^{-1}) followed by L-Val ($k_{cat}/K_M = 4.8$ mM^{-1} min^{-1}) and L-Met ($k_{cat}/K_M = 0.47$ mM^{-1} min^{-1}) which matches the probability of occurrence of Leu over Val at position 3 in native malpinins **1–5** (Fig. 1 and S13†). However, Met-containing malpinins have never been detected. Surprisingly, the turnover number for the three tested substrates is similarly high ($k_{cat} \sim 2.2$ min^{-1}) and seems sufficient to support a typical rate of peptide formation (approx. 1 min^{-1}) with all of them.[37] In other words, the adenylation kinetics suggest that the amino acid composition of malpinins can be simply altered by providing elevated concentrations of alternative substrates such as L-Met and L-Cys (for M1, M3, and M4) or L-Trp (for M4). To test this hypothesis, fungal cultures were supplemented with six different canonical amino acids (L-

Leu, L-Val, L-Met, L-Trp, L-Cys, L-Phe) in a precursor-directed biosynthesis approach. While L-Leu feeding resulted in production of **1** and **5** as main metabolites, L-Val feeding enlarged the metabolite variety mainly to **2–5**, which is consistent with a previous report.[4] In accordance to the predictions made by the HAMA assay, L-Met supplementation strongly increased the metabolic diversity by at least 12 additional compounds (malpinins F-Q, **6–17**), according to EIC-based quantification by two independent UHPLC-MS methods (Fig. 4A and Tables S6–S8, Fig. S14†). Subsequent ESI-MS/MS-fragmentation confirmed their **1**-derived lead structures and suggested a replacement of Leu and/or Phe by one, two or three Met moieties at the expected flexible positions 1, 3, and/or 4 (Fig. S15–S23†).

Two metabolites (malpinin F and G, **6** and **7**) show nearly the same molecular weight (*m*/*z* 877.4368 and 877.4374 $[M + H]^+$) and are most likely constitutional isomers (Fig. 4B). They were purified from upscaled fungal cultures by preparative HPLC subjected to extensive 1D and 2D NMR analyses (Table S9 and Fig. S24–S34†). ^{13}C NMR spectra of **6** and **7** revealed seven signals above 160 ppm, accounting for seven carbonyl moieties. Fifteen signals in the aromatic range of the spectrum were identified. Five signals ranging from δ_C 50 to 55 ppm hinted to five α-carbon atoms, that could be confirmed by HSQC spectra,

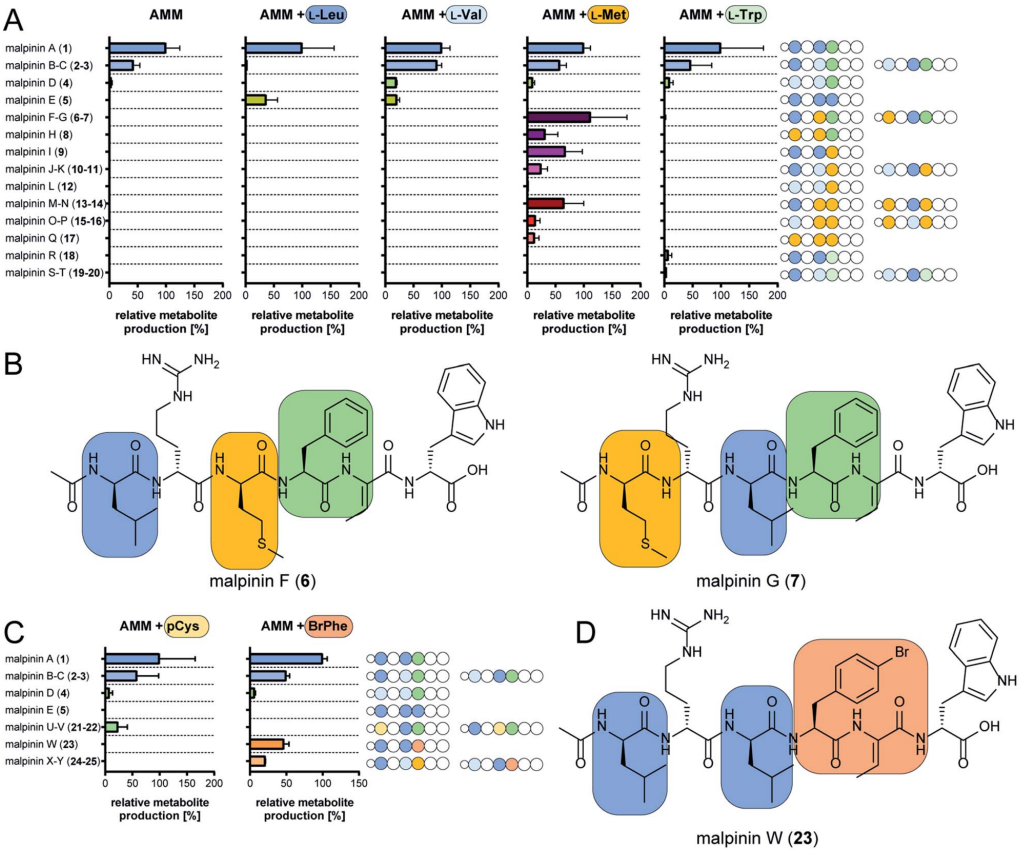

Fig. 4 Precursor-directed biosynthesis of novel malpinins. (A) Distribution of native (**1–5**) and novel malpinins (**6–20**) by feeding canonical amino acids predicted by HAMA. For detailed HR-ESI-MS/MS analysis see Table S6 (properties of metabolites) and Fig. S14–S23 and S37–S39.† Experiments were carried out in *Aspergillus* minimal medium without supplementation (AMM) or amended with 5 mM L-Leu, L-Val, L-Met, or L-Trp. Amino acid sequences of **1–20** are shown schematically as stings of beads with variable amino acids highlighted in colour (indigo, Leu; light blue, Val; green, Phe; brown, Met; dark green, Trp). (B) NMR-verified novel malpinins F (**6**) and G (**7**). For structure elucidation refer to Tables S7, S9, S10 and Fig. S24–S34.† (C) Distribution of native (**1–5**) and novel malpinins with non-natural amino acids (**21–25**) after feeding *S*-propargyl-L-Cys (pCys) or 4-bromo-L-Phe (BrPhe). Amino acid sequence of **1–5** and **21–25** are shown schematically as a string of beads with variable amino acids highlighted in colour (indigo, Leu; light blue, Val; green, Phe; gold, pCys; ochre, Br-Phe). For detailed HR-ESI-MS/MS analysis see ESI (Table S7 and Fig. S41–S45†). (D) NMR-verified, clickable malpinin W (**23**). For structure elucidation refer to Tables S10, S11 and Fig. S46–S51.†

View Article Online
Chemical Science Edge Article

linking them to their respective α-C protons (δ_H 4.20–4.70 ppm). As expected, the eight amide protons (δ_H 7.54–9.18 ppm) did not show any scalar couplings in HSQC spectra. The final peptide backbone was constructed using COSY couplings between amide and α-C protons as well as HMBC correlations between α-C protons and the following carbonyl C atoms (Fig. S34†). Starting from the α-C proton signals, the amino acid side chains were elucidated by COSY, HSQC and HMBC. In **6** and **7**, the ^{13}C signal of the terminal methylene group in the aliphatic side chains of Met (δ_C 29.0 ppm and δ_C 29.5 ppm, respectively) correlated with a highly abundant ^{1}H singlet signal derived from the lone-standing methyl group (δ_H 1.92 ppm and 2.00 ppm). With a chemical shift of δ_C 156.6 ppm as part of the guanidinium group of Arg, δ_C 128.0 as double signal of Dhb, and 3 and 4 double bond signals each for Phe and Trp, respectively, a total number of eight C=X double bonds and eight C=C double bonds were identified. The stereo configuration of **6** and **7** was finally determined by advanced Marfey's analysis[38] (Table S10†) and revealed incorporation of D-configured Met in both metabolites.

In sum, the NMR analysis confirmed the incorporation of D-Met in position 1 and 3 in **6** and **7**, respectively, as suggested by the previous ESI-MS/MS experiments. Among the proteogenic amino acids, Met is underrepresented as building block in NRPs.[39] Met-containing peptides have been extracted from cyanobacteria[40] or marine sponges[41–43] and harbour diverse biological activities including anti-cancer and phosphatase–inhibitory properties. However, **6** and **7** do not show any antimicrobial activity (Fig. S35†), but have a similar critical micelle concentration (CMC) as **1** (Fig. S36†).

Aside from the Met-containing metabolites **6–17**, but to a lower extent, three Trp-containing **1**-congeners (malpinin R-T, **18–20**) were produced by L-Trp feeding (Fig. 4A and S37–S39†). In all cases, Trp was incorporated at position 4 in agreement with the relaxed specificity observed in the HAMA profile of M4 (Fig. 2). However, no altered metabolite profiles were obtained by feeding L-Cys or L-Phe (Fig. S40†).

The first A domain of the hexamodular anabaenopeptin synthetase accepts the chemically divergent amino acids Arg and Tyr.[7,44] Similarly, substrate flexibility led to the biosynthesis of up to 16 structural variants of microcystins in the cyanobacterium *Phormidium*.[45] Here, promiscuity of A domains 2 and 4 has been assigned to altered residues in positions 236, 239 and 278 in the substrate binding pockets. Similar to cyanobacteria, relaxed substrate specificity is the major driver of metabolic diversity in *Mortierellaceae* resulting in 20 natural malpinins (**1–20**). Modules M1, M3, and M4 of MalA incorporate hydrophobic amino acids such as L-Met or L-Trp – in addition to their native substrates L-Leu, L-Val or L-Phe *in vitro* and *in vivo*. This raised the question, if non-natural clickable amino acids would be accepted as well.

Clickable amino acids enable synthesis of malpinin conjugates

Malpinins possess surface-active properties, but marginal cytotoxicity, and are hence promising for medicine and material science. Despite the Dhb moiety, the bottleneck in chemical tractability is the availability and accessibility of coupling moieties for "click" chemistry within the molecules. To investigate a potential incorporation of non-proteinogenic, but click-functionalised amino acids, fungal cultures were fed with the Met-congener *S*-propargyl-L-cysteine (pCys) or the Phe-homolog 4-bromo-L-phenylalanine (BrPhe) and malpinin derivative production was quantified by UHPLC-MS (Fig. 4C).

Feeding with pCys led to poor growth of the fungus and moderate incorporation (24%) into malpinins: the Leu moieties in positions 1 and 3 were replaced by pCys in malpinin U (**21**), *m*/*z* 887.4224 $[M + H]^+$ and malpinin V (**22**), *m*/*z* 887.4224 $[M + H]^+$, respectively (Fig. S41, S42 and Tables S6, S7†). In contrast, BrPhe was incorporated in suitable amounts (47%) in place of Phe in position 4: the **1**-congener malpinin W (**23**, *m*/*z* 937.3920 $[M + H]^+$), and the two minor **2**- and **3**-congeners malpinin X (**24**, *m*/*z* 923.3766 $[M + H]^+$) and malpinin Y (**25**, *m*/*z* 923.3767 $[M + H]^+$) were detected (Fig. 4D, S43–S45 and Tables S6, S7†). This relaxed substrate specificity is a remarkable feature of MalA, since acceptance of non-natural amino acids by A domains of other enzymes required time-consuming, systematic mutagenesis of residues in the substrate binding pocket.[7] Preferred incorporation of halogenated and other Phe analogs has been previously accomplished by a Trp-to-Ser point mutation in module 1 of the gramicidin S synthetase GrsA and module 4 of the tyrocidine synthetase TycA.[46,47] However, MalA M4 contains the respective Trp (W^{3852}) and the intrinsic substrate flexibility must be due to other reasons (Table S5†).

We isolated 12.8 mg of **23** from a 3 L culture and confirmed its structure by NMR (Table S11 and Fig. S46–S51†) and Marfey's analysis (Table S10†). The inspection of the ^{1}H-NMR spectrum revealed the absence of the δ_H 7.17 signal corresponding to the replacement of the C4 proton by a bromine atom in the Phe moiety at position 4 when compared to the ^{1}H-NMR spectrum of **1** (Fig. S46 and Table S11†). The high field chemical shift of C4 from δ_C 126.3 ppm (in **1**) to δ_C 119.5 ppm (in **23**) in the ^{13}C-NMR spectrum confirmed the successful 4-bromo-L-Phe integration (Fig. S47†).

To test the suitability of malpinins as cell-permeating compounds, **23** was coupled to the fluorescent dye 5-carboxyfluorescein (5-FAM). To this end, the aryl-halide (**23**) was substituted by an aryl-azide (**26**, *m*/*z* 900.4836 $[M + H]^+$, Fig. S52†) *via* an Ullmann-type copper catalysed nucleophilic aromatic substitution[48] (Fig. 5A). The clickable **26** was successfully coupled to the 5′-FAM-alkyne by a Cu(I)-catalysed azide-alkyne click reaction (CuAAC) to finally yield 24 mg of **27** (*m*/*z* 1313.5734 $[M + H]^+$, Fig. S53†). The structure of the product was confirmed by 1D- and 2D-NMR (Fig. S54–S59 and Table S12†).

Consistently with ^{13}C-NMR data from 1,2,3-triazole ring systems,[49] the chemical shifts of C1′ and C2′ (δ_C 73.1 ppm and δ_C 80.9 ppm in the alkyne) were altered towards δ_C 120.9 ppm and δ_C 145.9 ppm in **27**. The bond between malpinin and 5-FAM was established by inspection of the HMBC spectra through a weak coupling between C1′ (δ_C 120.9 ppm) of 5-FAM and the C21 proton (δ_H 7.81) of Phe in malpinin. Similarly to 5-FAM, the malpinin-conjugate **27** showed fluorescent properties, *i.e.* an emission maximum at $\lambda = 526$ nm (Fig. S60†).

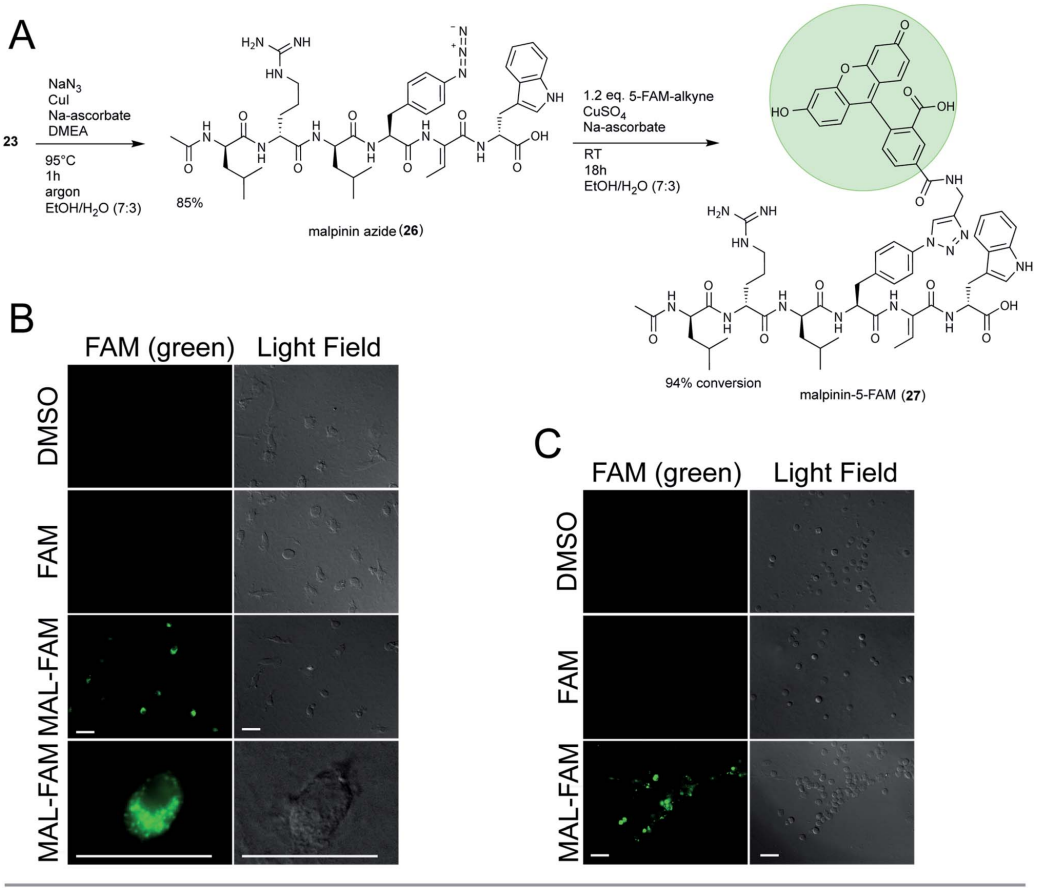

Fig. 5 Phagocytosis-triggered uptake of the fluorescent malpinin-conjugate **27**. (A) Synthesis of the triazole-linked 5-FAM conjugate **27**. (B and C) Microscopy of human macrophages (B) or neutrophils (C) after fluorophore treatment. Cells were incubated with 30 μM 5-FAM, **27** (MAL-FAM) or pure DMSO (negative control) for 3 h (macrophages) or 1 h (neutrophils) prior to microscopy. Pictures were taken using the green fluorescent channel (λ_{ex} = 492 nm, λ_{em} = 518 nm, left panels) or light field (right panels). Scale bar = 10 μm.

Malpinin-conjugates penetrate phagocytic cells

Malpinins show surface-active properties concomitant with low cytotoxicity. To test their potential pharmaceutical application, malpinin trafficking into human cells was studied. 5-FAM and **27** were incubated with human monocyte-derived macrophages and fluorophore localization was determined by fluorescence microscopy. Whilst pure 5-FAM was not able to penetrate the cell membrane, the fluorescent **27** was taken up by the cells (Fig. 5B). In contrast to our expectations, **27** did not attach to the cell membrane, but persisted in the cytoplasm. Hence, we concluded that malpinins enable the uptake of coupled compounds of interest, for which FAM serves as a proof of principle. To study the mechanism of uptake more profoundly, also human neutrophils and embryonic kidney cells (HEK293) were tested. Phagocytic neutrophils share a similar intracellular fluorescence pattern when incubated with **27** (Fig. 5C). In contrast, nonphagocytic HEK293 cells[50] hardly showed fluorescence signals, when **27** was applied (Fig. S61†). Hence, uptake of malpinin conjugates appears specific for phagocytotic cells. The use of macrophage-targeting agents is a promising prospect in cancer immunotherapy by modulation of the recruitment and survival of macrophages or by inhibition of their tumor-promoting function.[51] Moreover, macrophages are used as "trojan horses" to carry drug-loaded nanoparticles to a source of infection or into a tumor environment.[52] Hence, malpinin-conjugates may provide a small-molecular alternative with low cytotoxicity. Future studies will reveal the effectiveness of this approach. In this respect, the high production titers of malpinins up to 10% of the fungal dry biomass[53] provide an environmentally sustainable alternative to solid-phase peptide biosynthesis.

View Article Online
Chemical Science Edge Article

Conclusions

The current study demonstrates the potential of substrate profiling of A domains for biosynthetic diversification of NRPs. Feeding alternative substrates to a flexible NRPS of a basal fungus strongly shifted product profiles and enabled the production of click-functionalised compounds. The final bioorthogonal-labelling of malpinins uncovered its new pharmaceutical application as peptide carriers for phagocyte-specific drugs.

In the current study, a complete determination of substrate specificities of an NRPS system was carried out, which in turn led to the identification of a wealth of new metabolites (Fig. S62†). Promiscuity-based broadening of product diversity is a common strategy in nature to switch the biosynthesis from one compound to another with a higher selective advantage (screening hypothesis).[54] The synthetic biology can benefit from this evolutionary-driven approach: In the past ten years, tremendous progress has been made to reconstitute and engineer trajectorial NRP biosynthesis *in vitro* by combining several NRPS modules by either an inter-domain peptide linker or docking domains[55–58] or, alternatively, a DNA template as binding platform.[59] The substrate tolerant A domains of NRPSs from basal fungi bear excellent prospects for combinatorial enzyme engineering[60] in the future.

Besides their use in food industry, basal fungi are a promising resource of antibiotic and anticoagulating peptide compounds.[61,62] With this report, we add a new, third level of application: The malpinins can be used as carrier peptides triggering the uptake of compounds into human macrophages. Macrophages are common drug targets for several disease treatments, because they are involved in cancer and inflammation processes.[51] Mesoporous silica nanoparticles are currently being investigated as drug carrier, but their metabolism is still a problem that hinders successful clinical translation.[63] In this respect, malpinins represent a natural, small molecular weight alternative.

Experimental section

Organisms and culture maintenance

The fungal strains *Mortierella alpina* ATCC 32222 and *Mortierella* (syn. *Linnemannia*) *amoeboidea* CBS 889.72 were purchased from the American Type Culture Collection (ATCC) and the Westerdijk Fungal Biodiversity Institute (CBS), respectively (Table S13†). Cultures were maintained on malt extract peptone (MEP) agar plates (30 g L^{-1} malt extract, 3 g L^{-1} soy peptone, 18 g L^{-1} agar) for 7 days at 25 °C.

Liquid cultures (100 mL) for metabolite quantification and expression analyses were inoculated with five agar blocks (2 × 2 mm) and incubated at 25 °C and 140 rpm for 3, 7 or 14 days (depending on the experiment). Media were MEP, potato dextrose broth (PDB, Sigma Aldrich), yeast extract peptone dextrose medium (YPD; 20 g L^{-1} peptone, 10 g L^{-1} yeast extract, 20 g L^{-1} glucose), lysogeny broth (LB; 10 g L^{-1} tryptone, 5 g L^{-1} yeast extract, 10 g L^{-1} sodium chloride), or hay medium (HM, 25 g L^{-1} hay, extracted with hot water, 100 mM phosphate buffer, pH 5.6). For the precursor-directed biosynthesis, 100 mL *Aspergillus* minimal medium[64] supplemented with 100 mM D-glucose and 20 mM ammonium nitrate was amended with 5 to 10 mM of the respective amino acid.

Escherichia coli strains (Table S13†) used for plasmid propagation or heterologous protein production were maintained in LB medium amended with carbenicillin (50 μg L^{-1}) or kanamycin (100 μg L^{-1}), if required.

Molecular biological techniques and microscopy

Details on isolation of nucleic acids, genome sequencing, genome annotation, cloning of DNA in expression vectors, gene expression analysis and fluorescence microscopy are provided in the ESI.† Constructed plasmids and oligonucleotides are listed in Tables S14 and S15.†

Protein purification

Heterologous protein production in *Escherichia coli* and purification by affinity chromatography were carried out as previously described.[5] For details on the purification procedure, protein yields and SDS polyacrylamide gels, see ESI (Fig. S3 and Table S3†).

Adenylation enzyme activity assays

Multiplexed hydroxamate assay (HAMA). The HAMA was carried out as previously described.[12] The hydroxamate samples were quantified on a Waters ACQUITY H-class UPLC system coupled to a Xevo TQ-S micro (Waters) tandem quadrupole instrument with ESI ionisation source in positive mode (method A, Table S16†), by external calibration using a serial dilution of synthetic hydroxamate standards.

MesG assay. The determination of kinetic parameters for MalA module 3 was conducted as previously described[12] using a continuous kinetic adenylation assay using the enzyme-coupled conversion of the chromogenic substrate 7-methyl-6-thioguanosine (MesG) in the presence of hydroxylamine.[11] The enzymatic reaction was started by addition of 4 μM enzyme to a final reaction volume of 100 μL. Absorbance of released 7-methyl-6-thioguanin was monitored at λ_{max} = 355 nm on a Synergy H1 (BioTek) microplate reader at 30 °C.

Acetylation assay. The determination of the acetylation activity of the C_s domain of MalA-M1 and *M. alpina* protein crude extracts was carried out using a previously published protocol[65] and is described in detail in the ESI.†

Chemical analysis of metabolites

General. Metabolite samples were routinely measured on an Agilent 1290 Infinity II UHPLC coupled with an Agilent 6130 single quadrupole mass spectrometer (positive ionisation mode) using method B (Table S16†). Metabolite preparation was conducted on an Agilent 1260 and 1200 HPLC chromatographs. HR-MS/MS spectra of identified compounds were recorded on a Q Exactive Plus mass spectrometer (Thermo Scientific). NMR spectra were recorded on a Bruker Avance III 600 MHz spectrometer at 300 K using d_6-DMSO as solvent and

View Article Online
Edge Article Chemical Science

internal standard (δ_C 39.5 ppm). Residual non-deuterated solvent was used as standard for ^{1}H NMR spectra (δ_H 2.50 ppm).

Precursor-directed biosynthesis and metabolite quantification. After 7 days of cultivation in 100 mL AMM with 5 mM of the respective amino acid, mycelia were harvested and the culture broth was extracted three times with an equal volume of ethyl acetate. After solvent evaporation to dryness, the residue was dissolved in 5 mL methanol, and 10 μL were subjected to UHPLC-MS analysis (method B for **1–5** and **18–27**, method C for **1–4** and **6–17**, Table S16†). Metabolites were quantified by integration of the area under the curve (AUC) of the extracted ion chromatograms (EIC) (Fig. S14, S37, S42 and S45†). A calibration curve of an authentic standard of **1** ranging from 0.005 to 5 mg mL^{-1} served as reference. Calculated metabolite amounts were were correlated to the fungal dry biomass and were finally expressed as ratios relative to **1** in each sample.

Advanced Marfey's analysis. Compound hydrolysis and amino acid derivatization were carried out as described.[5,66] In brief, 0.1 mg of **6** or **7** were hydrolysed in 6 M HCl at 100 °C overnight. The hydrolysate was neutralised (6 M KOH), evaporated to dryness and dissolved in 100 μL H_2O. In a total reaction volume of 100 μL, 25 μL of the hydrolysate (approx. 1 μM) were derivatised with 15 mM 1-fluoro-2,4-dinitrophenyl-5-L-leucine-amid (L-FDLA). For authentic standards, 10 μL of L- or D-configured amino acids (100 mM) were used. Finally, the reaction was stopped by addition of 25 μL methanol and measured by UHPLC-MS with method D (Table S16†). Retention times of respective coupling products were determined from extracted ion chromatograms (EIC).

Metabolite extraction and isolation

Extraction and isolation of 6 and 7. Ten flasks, each containing 1 L AMM medium amended with 100 mM D-glucose, 20 mM ammonium nitrate and 8 mM L-Met, were inoculated with *M. alpina* and cultivated for 7 days. Freeze-dried, ground mycelium was extracted three times using a mixture of methanol, butanol and DMSO (12 : 12 : 1, 400 mL). The culture broth was extracted three times using the same amount of ethyl acetate. Extracts were pooled, dried under vacuum and dissolved in 50 mL methanol. For initial separation, crude extracts were submitted to preparative HPLC using method E (Table S16†). Fractions containing **6** and **7** were then transferred to a semipreparative HPLC and a separation from **1** as main contaminant was achieved by method F (Table S16†). Method G (Table S16†) was applied to purify **6** and **7** from **2** and **3** using a methanol gradient. Final separation of the isomers **6** (9 mg) and **7** (16 mg) was accomplished on a C_{18} reverse phase column using an acetonitrile gradient (method H, Table S16†).

Extraction and isolation of 23. **23** was produced in 15 flasks, each containing 200 mL AMM medium and 5 mM 4-bromophenylalanine, inoculated with *M. alpina* as described above. The cultures were harvested and extracted as described for **6** and **7**. After the first preparative separation step by HPLC (method E, Table S16†), fractions containing **23** were submitted to further purification using method F (Table S16†) yielding 12.8 mg pure **23**.

Chemical synthesis

Synthesis and purification of 26. A total of 360 mg crude extract containing **23** were dissolved in 1 mL reaction solvent (EtOH : water = 7 : 3). 2 eq. NaN_3, 0.1 eq. CuI (catalyst), 0.1 eq. *N*,*N*′-dimethylethylenediamine (DMEA, ligand) and 0.2 eq. sodium ascorbate were added to a final reaction volume of 5 mL as described elsewhere.[48] After incubation at 95 °C for 1 h under argon atmosphere, the reaction was evaporated *in vacuo*, dissolved in methanol and **26** was purified using method E (Table S16†), yielding 38 mg (85%). The structure of **26** was verified by HR-MS/MS (Tables S6, S7 and Fig. S52†).

Synthesis of malpinin-coupled 5-FAM dye (27). The synthesis was accomplished by mixing 20 μmol (18.3 mg) **26** and 16.9 μmol (7 mg) 5-FAM-alkyne (Jena Bioscience) in 13 mL reaction solvent (EtOH : water = 7 : 3). 50 μL of 0.5 M $CuSO_4$ and 150 μL of 0.5 M sodium ascorbate (both Jena Bioscience) were added immediately and after a reaction time of 24 h.[49] After 42 h at RT under gentle agitation (100 rpm) the reaction mixture was dried by lyophilisation and dissolved in methanol. Separation was performed by HPLC using method E (Table S16†). 24 mg of 27 were recovered and submitted to NMR and HR-MS/MS structure verification (Tables S6, S7, S12 and Fig. S53–S59†).

Physicochemical and antimicrobial properties of 6 and 7

Determination of surface tension and critical micelle concentration (CMC) was conducted by the ring tear off method using a De Noüy ring tensiometer (Krüss Processor Tensiometer K12, Krüss, Hamburg, Germany) in a concentration range from 1000 to 1.95 μg mL^{-1} as described previously.[4] Antimicrobial activity testing was carried out by agar diffusion tests.[4] Ciprofloxacin dissolved in water (5 μg mL^{-1}) and amphotericin B in DMSO/methanol (1 : 1) (10 μg mL^{-1}) served as controls.

Statistical analysis

Statistical analysis was carried out using GraphPad Prism 7 software. Pearson correlation was calculated assuming Gaussian distribution with a confidence interval of 95% and a significance level of 5%.

Data availability

The draft genomes of *M. alpina* ATCC32222 and *M. amoeboidea* CBS 889.72 are accessible under Genbank accession numbers JALIRG010000000 and JALIGY010000000, respectively. The sequences of the *malA* genes from *M. alpina* and *M. amoeboidea* are deposited under Genbank accession numbers MW984675 and MW984676, respectively.

Author contributions

The manuscript was written by OW, HK and MG. JMW and AS performed the experimental work, with guidance and supervision from HK and MG. SZ performed cloning and the full-length gene sequencing of *malA*. PJ and KG performed the microscopical imaging. MG designed and managed the project.

View Article Online
Chemical Science Edge Article

Conflicts of interest

There are no conflicts to declare.

Acknowledgements

We are grateful to Heike Heinecke, Andrea Perner and Veit Hänsch (all from the Hans Knöll Institute [HKI], Jena, Germany) for their technical assistance in recording NMR and HR-MS/MS spectra, respectively. We thank Kerstin Voigt (Jena Microbial Resource Collection, Jena, Germany) and Sandra Jungmann (FSU, Jena) for antimicrobial testings and biphasic measurements, respectively. We also thank Christian Kretzer for initial fluorescence-imaging experiments. Hajo Kries gratefully acknowledges a fellowship from the Daimler und Benz Foundation and financial support from the DFG (grant number 441781663) and the Fonds der Chemischen Industrie (FCI).

Notes and references

1 A. Isidro-Llobet, M. N. Kenworthy, S. Mukherjee, M. E. Kopach, K. Wegner, F. Gallou, A. G. Smith and F. Roschangar, *J. Org. Chem.*, 2019, **84**, 4615–4628.
2 K. A. J. Bozhüyük, F. Fleischhacker, A. Linck, F. Wesche, A. Tietze, C. P. Niesert and H. B. Bode, *Nat. Chem.*, 2018, **10**, 275–281.
3 H. Kikukawa, E. Sakuradani, A. Ando, S. Shimizu and J. Ogawa, *J. Adv. Res.*, 2018, **11**, 15–22.
4 F. Baldeweg, P. Warncke, D. Fischer and M. Gressler, *Org. Lett.*, 2019, **21**, 1444–1448.
5 J. M. Wurlitzer, A. Stanišic, I. Wasmuth, S. Jungmann, D. Fischer, H. Kries and M. Gressler, *Appl. Environ. Microbiol.*, 2020, **87**, e02051–02020.
6 S. D. Copley, *Curr. Opin. Struct. Biol.*, 2017, **47**, 167–175.
7 H. Kaljunen, S. H. Schiefelbein, D. Stummer, S. Kozak, R. Meijers, G. Christiansen and A. Rentmeister, *Angew. Chem.*, 2015, **54**, 8833–8836.
8 A. Stanišić and H. Kries, *ChemBioChem*, 2019, **20**, 1347–1356.
9 S. Meyer, J. C. Kehr, A. Mainz, D. Dehm, D. Petras, R. D. Süssmuth and E. Dittmann, *Cell Chem. Biol.*, 2016, **23**, 462–471.
10 L. G. Otten, M. L. Schaffer, B. R. Villiers, T. Stachelhaus and F. Hollfelder, *Biotechnol. J.*, 2007, **2**, 232–240.
11 D. J. Wilson and C. C. Aldrich, *Anal. Biochem.*, 2010, **404**, 56–63.
12 A. Stanišić, A. Hüsken and H. Kries, *Chem. Sci.*, 2019, **10**, 10395–10399.
13 L. Wang, W. Chen, Y. Feng, Y. Ren, Z. Gu, H. Chen, H. Wang, M. J. Thomas, B. Zhang, I. M. Berquin, Y. Li, J. Wu, H. Zhang, Y. Song, X. Liu, J. S. Norris, S. Wang, P. Du, J. Shen, N. Wang, Y. Yang, W. Wang, L. Feng, C. Ratledge, H. Zhang and Y. Q. Chen, *PLoS One*, 2011, **6**, e28319.
14 L. Wagner, B. Stielow, K. Hoffmann, T. Petkovits, T. Papp, C. Vagvolgyi, G. S. de Hoog, G. Verkley and K. Voigt, *Persoonia*, 2013, **30**, 77–93.
15 K. Blin, S. Shaw, K. Steinke, R. Villebro, N. Ziemert, S. Y. Lee, M. H. Medema and T. Weber, *Nucleic Acids Res.*, 2019, **47**, W81–W87.
16 J. F. Tabima, I. A. Trautman, Y. Chang, Y. Wang, S. Mondo, A. Kuo, A. Salamov, I. V. Grigoriev, J. E. Stajich and J. W. Spatafora, *G3: Genes, Genomes, Genet.*, 2020, **10**, 3417–3433.
17 H. Kikukawa, E. Sakuradani, A. Ando, T. Okuda, M. Ochiai, S. Shimizu and J. Ogawa, *J. Biotechnol.*, 2015, **208**, 63–69.
18 C. Li, K. E. Roege and W. L. Kelly, *ChemBioChem*, 2009, **10**, 1064–1072.
19 B. Diez, S. Gutierrez, J. L. Barredo, P. van Solingen, L. H. van der Voort and J. F. Martin, *J. Biol. Chem.*, 1990, **265**, 16358–16365.
20 W. Kallow, J. Kennedy, B. Arezi, G. Turner and H. von Döhren, *J. Mol. Biol.*, 2000, **297**, 395–408.
21 J. F. Martin, *J. Antibiot.*, 2000, **53**, 1008–1021.
22 M. Wittmann, U. Linne, V. Pohlmann and M. A. Marahiel, *FEBS J.*, 2008, **275**, 5343–5354.
23 H. J. Imker, D. Krahn, J. Clerc, M. Kaiser and C. T. Walsh, *Chem. Biol.*, 2010, **17**, 1077–1083.
24 L. Zhong, X. Diao, N. Zhang, F. Li, H. Zhou, H. Chen, X. Bai, X. Ren, Y. Zhang, D. Wu and X. Bian, *Nat. Commun.*, 2021, **12**, 296.
25 C. Greco, B. T. Pfannenstiel, J. C. Liu and N. P. Keller, *ACS Chem. Biol.*, 2019, **14**, 1121–1128.
26 X. Yang, P. Feng, Y. Yin, K. Bushley, J. W. Spatafora and C. Wang, *mBio*, 2018, **9**, e01211–e01218.
27 R. Iacovelli, L. Mozsik, R. A. L. Bovenberg and A. J. M. Driessen, *Microbiologyopen*, 2021, **10**, e1145.
28 C. Liu, A. Minami, T. Ozaki, J. Wu, H. Kawagishi, J. I. Maruyama and H. Oikawa, *J. Am. Chem. Soc.*, 2019, **141**, 15519–15523.
29 C. Mehner, D. Müller, A. Krick, S. Kehraus, R. Löser, M. Gütschow, A. Maier, H. F. Fiebig, R. Brun and G. M. König, *Eur. J. Org. Chem.*, 2008, **10**, 1732–1739.
30 I. Pergament and S. Carmeli, *Tetrahedron Lett.*, 1994, **35**, 8473–8476.
31 P. N. Leao, A. R. Pereira, W. T. Liu, J. Ng, P. A. Pevzner, P. C. Dorrestein, G. M. König, V. M. Vasconcelos and W. H. Gerwick, *Proc. Natl. Acad. Sci. U. S. A.*, 2010, **107**, 11183–11188.
32 E. N. Zainuddin, R. Jansen, M. Nimtz, V. Wray, M. Preisitsch, M. Lalk and S. Mundt, *J. Nat. Prod.*, 2009, **72**, 1373–1378.
33 A. Mavaro, A. Abts, P. J. Bakkes, G. N. Moll, A. J. Driessen, S. H. Smits and L. Schmitt, *J. Biol. Chem.*, 2011, **286**, 30552–30560.
34 M. R. Levengood, C. C. Kerwood, C. Chatterjee and W. A. van der Donk, *ChemBioChem*, 2009, **10**, 911–919.
35 W. H. Chen, K. Li, N. S. Guntaka and S. D. Bruner, *ACS Chem. Biol.*, 2016, **11**, 2293–2303.
36 S. Wang, Q. Fang, Z. Lu, Y. Gao, L. Trembleau, R. Ebel, J. H. Andersen, C. Philips, S. Law and H. Deng, *Angew. Chem.*, 2021, **60**, 3229–3237.
37 S. Doekel and M. A. Marahiel, *Chem. Biol.*, 2000, **7**, 373–384.
38 P. Marfey, *Carlsberg Res. Commun.*, 1984, **49**, 591–596.

39 S. Caboche, V. Leclère, M. Pupin, G. Kucherov and P. Jacques, *J. Bacteriol.*, 2010, **192**, 5143–5150.
40 T. Sano, T. Usui, K. Ueda, H. Osada and K. Kaya, *J. Nat. Prod.*, 2001, **64**, 1052–1055.
41 M. A. Rashid, K. R. Gustafson, J. L. Boswell and M. R. Boyd, *J. Nat. Prod.*, 2000, **63**, 956–959.
42 J. Kobayashi, T. Nakamura and M. Tsuda, *Tetrahedron*, 1996, **52**, 6355–6360.
43 G. R. Pettit, B. E. Toki, J. P. Xu and D. C. Brune, *J. Nat. Prod.*, 2000, **63**, 22–28.
44 G. Christiansen, B. Philmus, T. Hemscheidt and R. Kurmayer, *J. Bacteriol.*, 2011, **193**, 3822–3831.
45 T. K. Shishido, J. Jokela, A. Humisto, S. Suurnakki, M. Wahlsten, D. O. Alvarenga, K. Sivonen and D. P. Fewer, *Mar. Drugs*, 2019, **17**(5), 271.
46 D. L. Niquille, I. B. Folger, S. Basler and D. Hilvert, *J. Am. Chem. Soc.*, 2021, **143**, 2736–2740.
47 H. Kries, R. Wachtel, A. Pabst, B. Wanner, D. Niquille and D. Hilvert, *Angew. Chem.*, 2014, **53**, 10105–10108.
48 J. Andersen, U. Madsen, F. Björkling and X. F. Liang, *Synlett*, 2005, **1**, 2209–2213.
49 M. Dörfer, D. Heine, S. König, S. Gore, O. Werz, C. Hertweck, M. Gressler and D. Hoffmeister, *Org. Biomol. Chem.*, 2019, **17**, 4906–4916.
50 I. Licona-Limon, C. A. Garay-Canales, O. Munoz-Paleta and E. Ortega, *J. Leukocyte Biol.*, 2015, **98**, 85–98.
51 Z. Duan and Y. Luo, *Signal Transduction Targeted Ther.*, 2021, **6**, 127.
52 Y. Qi, X. Yan, T. Xia and S. J. Liu, *Mater. Des.*, 2021, **198**, 109388.
53 R. Sonnabend, L. Seiler and M. Gressler, *J. Fungi*, 2022, **8**, e196.
54 R. D. Firn and C. G. Jones, *Nat. Prod. Rep.*, 2003, **20**, 382–391.
55 M. Kaniusaite, R. J. A. Goode, J. Tailhades, R. B. Schittenhelm and M. J. Cryle, *Chem. Sci.*, 2020, **11**, 9443–9458.
56 K. A. J. Bozhüyük, J. Watzel, N. Abbood and H. B. Bode, *Angew. Chem., Int. Ed.*, 2021, **60**, 17531–17538.
57 A. S. Brown, M. J. Calcott, J. G. Owen and D. F. Ackerley, *Nat. Prod. Rep.*, 2018, **35**, 1210–1228.
58 C. Kegler and H. B. Bode, *Angew. Chem.*, 2020, **59**, 13463–13467.
59 H. M. Huang, P. Stephan and H. Kries, *Cell Chem. Biol.*, 2021, **28**, 221–227.
60 S. Galanie, D. Entwistle and J. Lalonde, *Nat. Prod. Rep.*, 2020, **37**, 1122–1143.
61 N. Koyama, S. Kojima, T. Fukuda, T. Nagamitsu, T. Yasuhara, S. Omura and H. Tomoda, *Org. Lett.*, 2010, **12**, 432–435.
62 N. Koyama, S. Kojima, K. Nonaka, R. Masuma, M. Matsumoto, S. Omura and H. Tomoda, *J. Antibiot.*, 2010, **63**, 183–186.
63 D. Kwon, B. G. Cha, Y. Cho, J. Min, E. B. Park, S. J. Kang and J. Kim, *Nano Lett.*, 2017, **17**, 2747–2756.
64 R. W. Barratt, G. B. Johnson and W. N. Ogata, *Genetics*, 1965, **52**, 233–246.
65 F. I. Kraas, V. Helmetag, M. Wittmann, M. Strieker and M. A. Marahiel, *Chem. Biol.*, 2010, **17**, 872–880.
66 E. H. Hashimoto, H. Kato, Y. Kawasaki, Y. Nozawa, K. Tsuji, E. Y. Hirooka and K. Harada, *Chem. Res. Toxicol.*, 2009, **22**, 391–398.

Electronic Supplementary Material

Macrophage-targeting oligopeptides from *Mortierella alpina*

Jacob M. Wurlitzer,[a] Aleksa Stanišić,[b] Sebastian Ziethe,[a] Paul M. Jordan,[c] Kerstin Günther,[c] Oliver Werz,[c] Hajo Kries,[b] Markus Gressler[a,*]

[a] *Department Pharmaceutical Microbiology at the Leibniz Institute for Natural Product Research and Infection Biology (Hans-Knöll-Institute), Friedrich-Schiller-University, Winzerlaer Strasse 2, 07745 Jena (Germany)*
[b] *Junior Group Biosynthetic Design of Natural Products at the Leibniz Institute for Natural Product Research and Infection Biology (Hans-Knöll-Institute), Beutenbergstrasse 11a, 07745 Jena (Germany)*
[c] *Department Pharmaceutical/Medicinal Chemistry at the Friedrich-Schiller-University, Philosophenweg 14, 07743 Jena (Germany)*
* corresponding author: markus.gressler@leibniz-hki.de

Table of content

Experimental procedures

Isolation of genomic DNA

Young mycelia (4 d, MEP medium) from *M. alpina* ATCC32222 and *M. amoeboidea* CBS889.72 were ground under liquid nitrogen. DNA was isolated from 50 mg ground material using the DNeasy Plant mini kit (Qiagen) according to manufacturer's instructions except for the following adjustments: Tissue lysis at 65°C was extended up to 2 h, and 20 µg proteinase K (Merck) was added after 1 h of incubation. Eluted DNA from different 3 aliquots were pooled and DNA was extracted three times with a mixture of phenol, chloroform and isoamyl alcohol (25:24:1, Carl Roth). DNA was precipitated with a double volume of ice-cold isopropanol at -20°C for 30 min. After centrifugation (14,000 g, 30 min), the pellet was washed 12 times with 70% ethanol, dried under airflow, and dissolved over night at 4°C in 10 mM TRIS buffer (pH 8.0). DNA quality was examined using a Scandrop photometer (Analytik Jena), for detection of impurities of protein or RNA, and a Tapestation 4150 (Agilent) for size distribution and integrity. Samples showing absorption values of $1.75 < A_{260/280} < 1.9$ and $A_{260/230} > 2.0$ and a mean fragment size above 20 kbp were chosen for genome sequence-library preparation and ITS sequencing.

Strain identification

Strains were identified by sequencing the internal transcribed spacer (ITS) regions. The two ITS regions of ribosomal DNA were amplified from genomic DNA using the oligonucleotides oITS1/oITS4 (Table S14) and Phusion DNA polymerase (Thermo) according to the manufacturer's instructions. PCR products were sequenced.

Genome sequencing and annotation

Libraries were generated from 400 ng DNA using the SQK-RAD004 kit (Oxford Nanopore Technologies, ONT) following the manufacturer's instructions except for the use of nuclease free water instead of "loading beads". Sequencing was carried out on a MinION using a FLO-MIN106D (ONT) (R9 chemistry). After 24 h, a nuclease-digest was performed utilizing the EXP-WSH003 (ONT) flow cell wash kit and sequencing was continued with a new generated library. Raw reads were basecalled with GUPPY v.3.2.6 GPU version. Genomes were assembled using CANU[1, 2] v.1.9. assuming a genome size of 40 Mbp based on genomes related *Mortierella* isolates accessed through JGI Mycosom[3] and an available *M. alpina* genome.[4]

To improve assemblies, signal level reads were indexed to the draft genomes by Nanopolish[5] and after sorting and mapping using minimap[6] and SAMtools[7], an improved consensus sequence was calculated using Nanopolish[8]. Genes were annotated using the AUGUSTUS Web server.[9] The *Rhizopus oryzae* genome was chosen as reference and genes were identified on both strands. Genome completeness was check by BUSCO[10] using the option "auto-lineage_euk" resulting in the automated selection of the "mucorales_odb10" dataset.

Identification of genes and expression analysis

The assembled genomes of *M. alpina* and *M. amoeboidea* were screened for NRPS genes using the antiSMASH 5.0 website.[11] NRPS domain borders were manually adjusted using Pfam[12] and clustal W2

alignment tools[13] using fungal and bacterial NRPS as templates. Intron/exon borders were identified with the AUGUSTUS annotation tool.[9]

RNA from mycelium was isolated using SV Total RNA Isolation System (Promega) and gDNA was digested with Baseline-Zero DNAse (Biozym). cDNA synthesis was carried out with RevertAid Reverse Transcriptase (Thermo Fisher), RiboLock RNase inhibitor (Thermo Fisher) and anchored oligo(dT)$_{18}$ primers. Oligonucleotides for candidate NRPS genes (*nps2*, *nps3* (*malA*) and *nps5*) as well as the two housekeeping genes *actB* (encoding β-actin) and *gpdA* (encoding glycerinaldehyde-3-phosphate dehydrogenase) were designed, and PCR efficiency was checked to be at least 95% (Table S14). For analysis of the malpinin biosynthetic gene cluster, additional primer pairs for five genes adjacent to *malA* were included (*orf27, orf29, orf32, orf34, orf35*). qRT-PCR (quantitative real-time PCR) was performed on the qPCR cycler qTower^3 (Analytik Jena) using the qPCR Mix EvaGreen (BioSELL) following the manufacturer's instructions. The following qPCR protocol was run: 15 min initial denaturation 95°C, 40 cycles of amplification (95°C, 15 s; 60°C, 20 s; 72°C, 20 s) and a final monitoring of a melting curve from 60 to 95°C in 1°C increments.

Cloning procedure

A first set of oligonucleotides was used to amplify the coding sequences (CDS) of the modules 2-7 (C-A-T tri-domains) of *malA* from *M. alpina* cDNA (Table S14) by PCR. Using these fragments as templates, the respective restriction sites at the 5' and 3' flank were introduced by a second PCR run with an additional set of oligonucleotides (Tables S14). Phusion high fidelity DNA polymerase (NEB) was used according to manufacturer's protocol and the following gradient was applied: initial denaturation 98°C, 2 min; 40 cycles of amplification (98°C, 20 s; 60°C, 20 s; 72°C, 180 s); final extension 72°C, 5 min. After blunt end ligation into pJET1.2 cloning vector (Thermo Fisher), fragments were excised from purified plasmids using the restriction enzymes listed in Table S14 and were ligated with an accordingly digested pET28a (+) vector using the T4-DNA-Ligase (NEB).

The CDS of module 1 of *malA* was amplified using oligonucleotides oMG270 and oMG285 (Table S11) and its pET28a vector backbone was amplified using oligonucleotides oMG283 and oMG284. Both fragments were ligated using the In-Fusion® HD Cloning Plus kit (TaKaRa).

The ligation mixtures were used to transform *Escherichia coli* XL1 blue to propagate the plasmids (Table S15) and *E. coli* expression strains (Table S3).

Heterologous protein production and purification

E. coli expression strains were cultivated in 500 mL LB medium containing 100 µg mL^{-1} kanamycin (CarlRoth) at 37°C until an OD_{600} of 0.4-0.6 was reached. Subsequently, the incubation temperature was set to 16°C and gene expression was induced by addition of 0.1% L-rhamnose (Carl Roth) for *E. coli* KRX and 1 mM isopropyl-β-D-1-thiogalactopyranoside for *E. coli* strains BL21 and SoluBL21. After cultivation overnight, cells were harvested by centrifugation (3,200 × g, 40 min, 4°C) and the cell pellet was resuspended in lysis buffer (20 mM imidazole, 50 mM sodium phosphate, 300 mM sodium chloride, pH 8.0). Lysis was accomplished by sonification with a Sonoplus ultrasonic sonifier (Bandelin) (5 cycles with 20 s impulse interval and 5 s impulse duration; 0.8 kJ total impulse energy). The N- and C-terminal His_6-tagged fusion proteins were purified by gravity flow metal ion affinity chromatography (Protino Ni-NTA agarose, Macherey-Nagel). The column was washed with lysis buffer and increasing concentrations of imidazole (40- and 80-mM). Tagged enzymes were eluted in lysis buffer with 250 mM imidazole. Proteins were desalted and concentrated by Amicon Ultra-15 centrifugal filter units 100 kDa

(Merck) and rebuffered in protein storage buffer (50 mM TRIS, 200 mM sodium chloride, 10% glycerol). Protein concentrations were determined according to Bradford with the Protein Assay Kit (BioRad).[14] Proteins were stored at -80°C.

Determination of the *N*-Acetylation

Synthesis of aminoacyl-*N*-acetylcysteamine (SNAC) thioesters

Aminoacyl SNACs were synthesised as described before.[15] In brief, 2 mmol of *N*-protected amino acids (*N*-Boc-L-leucine, *N*-Boc-D-leucine, *N*-acetyl-L-leucine, and *N*-acetyl-D-leucine), 2 mmol *N,N'*-dicyclohexylcarbodiimide (DCC), 2 mmol hydroxybenzotriazole (HOBt) and 2 mmol *N*-acetylcysteamine were solved in 30 mL THF and stirred at room temperature for 1h. After addition of 1 mmol K_2CO_3, the mixture was stirred for another 3h. The reaction was filtered and evaporated to dryness. The residue was dissolved in ethyl acetate and extracted twice with 10% aqueous $NaHCO_3$. The organic layer was dried over Na_2SO_4, evaporated and dissolved in dichloromethane (CH_2Cl_2). Purification was performed by flash chromatography (Büchi Pure C-810) using isocratic conditions (4% MeOH in CH_2Cl_2) and a 12g Silica column. Separation was monitored by UHPLC-MS (method B, Table S15) and fractions containing *N*-acetyl-leucyl-SNAC or *N*-Boc-leucyl-SNAC thioesters were pooled. Boc-protected products were deprotected by acidic treatment in 6 mL 50% TFA/CH_2Cl_2 for 1 h. TFA was removed by repeated addition and evaporation of CH_2Cl_2 *in vacuo*. Finally, the residues were dissolved in approx. 500 - 1000 µL of CH_2Cl_2 and precipitated with 9 mL diethyl ether. Precipitates was filtered, washed with diethyl ether and finally dried. All SNAC thioesters were dissolved in 1% aqueous TFA and stored at -80°C up to 3 days.

N*-Acetylation of leucyl-SNAC thioesters *in vitro

N-Acetylation of leucyl-SNAC thioesters was performed using a modified protocol according to Zhong et al.[16] In a total volume of 100 µL, heterologously produced MalA-M1 (10 µM) or *M. alpina* crude protein extract (400 µg mL^{-1}, determined by Bradford assay) were mixed with 500 µM acetyl-CoA and 2.5 mM L- or D-leucyl-SNAC in reaction buffer (50 mM Tris-HCl, 25 mM NaCl, 10 mM $MgCl_2$, pH 7.5). As controls, Ac-CoA was omitted from the reactions. After incubation for 30 min at 37°C, reactions were stopped by addition of 100 µL MeOH and centrifuged at 20.000 × g for 10 min. To prevent degradation of SNAC-thioesters, samples were measured instantly by UHPLC-MS using method B (Table S15). Separately synthesised *N*-acetyl-L-leucyl-SNAC and *N*-acetyl-D-leucyl-SNAC served as product standards.

To generated crude protein extract, mycelium of *M. alpina* was harvested from liquid cultures under malpinin-inducing conditions (LB medium, 160 rpm, 25 °C, 4 days) and ground under liquid nitrogen. The fungal powder was resuspended in reaction buffer and insoluble cell debris were removed by centrifugation (20.000 × g for 10 min). The protein concentration of the supernatant was determined by Bradford assay (ThermoFisher).

Microscopical imaging

Leukocyte concentrates were prepared from peripheral blood obtained from healthy human adult donors (Institute of Transfusion Medicine, University Hospital Jena, Germany). The approval for the protocol was given by the ethical committee of the University Hospital Jena and all methods were

performed in accordance with the relevant guidelines and regulations. The leukocyte concentrates were mixed with dextran (dextran from *Leuconostoc* spp. MW ~40,000) for sedimentation of erythrocytes; the supernatant was centrifuged on lymphocyte separation medium (Histopaque®-1077). Contaminating erythrocytes in the pelleted neutrophils were removed by hypotonic lysis using water. Neutrophils were then washed twice in ice-cold phosphate-buffered saline (PBS) and finally resuspended in PBS. The peripheral blood mononuclear cell (PBMC) fraction on top of the lymphocyte separation medium was washed with ice-cold PBS and seeded in cell culture flasks (Greiner Bio-one, Nuertingen, Germany) for 1.5 h (37 °C, 5% CO_2) in PBS with Ca^{2+}/Mg^{2+} to isolate monocytes by adherence. For the differentiation of monocytes towards macrophages, we followed published procedures.[17] Thus, adherent monocytes were treated with 20 ng mL^{-1} granulocyte macrophage-colony stimulating factor (GM-CSF) (Peprotech, Hamburg, Germany) for 6 days in RPMI 1640 supplemented with 10% fetal calf serum (FCS), 2 mM L-glutamine, penicillin (100 U mL^{-1}) and streptomycin (100 µg mL^{-1}) to get monocyte-derived macrophages. The purity of these macrophages was routinely checked by flow cytometry (LSRFortessa™ cell analyzer, BD Biosciences, Heidelberg, Germany) as reported[18] using the following antibodies: FITC anti-human CD14 (clone M5E2, BD Biosciences), APC-H7 anti-human CD80 (clone L307.4, BD Biosciences), PE-Cy7 anti-human CD54 (clone HA58, Biolegend, Koblenz, Germany), PE anti-human CD163 (clone GHI/61, BD Biosciences), and APC anti-human CD206 (clone 19.2, BD Biosciences).

HEK293 cells (ATCC, Manassas, US) were cultured in monolayers (37 °C, 5% CO_2) in DMEM containing FCS (10%), penicillin (100 U mL^{-1}) and streptomycin (100 µg mL^{-1}).

Microscopy and treatment with FAM and 27

Macrophages (1 × 10^6 cells), neutrophils (2 × 10^6 cells) and HEK cells (0.5 × 10^6 cells) were seeded onto polylysine-coated glass coverslips in 12-well plates and cultured at 37°C for 1 h for neutrophils and 24 h for macrophages and HEK cells. FAM, FAM-coupled malpinin (**27**) or vehicle (DMSO) were added and macrophages were incubated for 3 h and neutrophils and HEK cells for 1 h at 37 °C. Cells were then fixed using 4% paraformaldehyde solution. Cells were stained with ProLong Diamond Antifade Mountant with DAPI (Thermo Fisher Scientific, Waltham, MA, United States). Samples were analyzed by a Zeiss Axiovert 200M microscope with a Plan Neofluar × 40/1.30 Oil (DIC III) objective (Carl Zeiss, Jena, Germany) and the 38HE-green fluorescent reflector to measure FAM intensity. An AxioCam MR camera (Carl Zeiss) was used for image acquisition.

Phylogenetic analysis

Phylogenetic analysis of fungal and bacterial A domains was performed as described by Wurlitzer *et al*.[19] A set of 123 A domains were extracted from NRPSs, NRPS-like proteins (including the α-2-aminoadipate reductases, aryl acid reductases, tyrosine reductases, and serine reductases), and PKS/NRPS hybrids from *M. alpina* (MalA, MpcA and MpbA), (endo)bacteria, and higher fungi. The A domain of the tryptophanyl-tRNA synthetase Wrs1 from *Saccharomyces cerevisiae* served as the outgroup. The percentual bootstrap support was calculated for 1000 replicates.

Structural modelling of the starter condensation domain MalA-C_s

The N-terminal domain of MalA has been structurally modelled with AlphaFold v2.1.0[20] using a publicly available script on Google Colab (AlphaFold.ipynb). The model has been superimposed with a crystal structure of the C_s domain from CDA biosynthesis (PDB 4JN3, grey cartoon) in Pymol v2.2.2 using the "super" command.

Table S1. Comparison of *M. alpina* and *M. amoeboidea* genomes. [#] According to BUSCO analysis.[10]

	M. alpina ATCC32222	*M. alpina* ATCC32222	*M. amoeboidea* CBS889.72
Genbank accession	GCA_000240685.2	JALIRG010000000	JALIGY010000000
BioSample	SAMN02981246	SAMN27177060	SAMN27177162
BioProject	PRJNA41211	PRJNA817090	PRJNA817100
sequencing method	pyrosequencing and Sanger sequencing	nanopore sequencing	nanopore sequencing
total sequence length	38,042,092	39,295,276	38,155,153
number of contigs	1,099	43	24
completeness[#]		90.4%	94.8%
coverage	31.8x	39.7x	144.0x
contig N50	171,448	2,196,674	2,511,580
contig L50	70	7	6
contig N90	44,192	811,690	1,667,963
contig L90	235	16	14
reference	[4]	This study.	This study.

Table S2. Identified NRPS genes in *M. alpina* and *M. amoeboidea.* The protein domain architecture is presented. A, adenylation domain; C canonical condensation domain; Cs, starter condensation domain; E/C, dual epimerisation/condensation domain; T, thiolation domain; TE, thioesterase domain; TD, terminal reductase domain. Highly homologous NRPS genes in both species (>70% identity) are highlighted in green.

	***M. alpina* ATCC32222**	modules	encoding contig	gene
Nps1	Cs-A-T-C-A-T-E/C-A-T-E/C-A-T-C-A-T-C-A-T-E/C-A-T-C-A-T-E/C-A-T-TE	9	tig00000075	
Nps2	A-T-E/C-A-T-C-A-T-E/C-A-T-C-A-T-C-A-T-C-A-T-C-A-T-TE	8	tig00000075	
Nps3	Cs-A-T-E/C-A-T-E/C-A-T-E/C-A-T-C-A-T-E/C-A-T-E/C-A-T-TE	7	tig00000075	*malA*
Nps4	Cs-A-T-C-A-T-C-A-T-E/C-A-T-E/C-A-T-E/C-A-T-C-A-T-TE	7	tig00002287	
Nps5	Cs-A-T-E/C-A-T-C-A-E/C-A-T-E/C-A-T-C-A-T-TE	6	tig00080470	
Nps6	Cs-A-T-C-A-T-C-A-T-C-A-T-C-A-T-E/C-A-T-TE	6	tig00080470	
Nps7	Cs-A-T-E/C-A-T-C-A-T-C-A-T-C-A-T-C-A-T-TE	6	tig00000137	
Nps8	Cs-A-T-E/C-A-T-C-A-T-E/C-A-T-E/C-A-T-TE	5	tig00002279	*mpcA*
Nps9	Cs-A-T-E/C-A-T-C-A-T-E/C-A-T-E/C-A-T-TE	5	tig00002279	*mpbA*
Nps10	Cs-A-T-E/C-A-T-C-A-T-C-A-T-TD	4	tig00000022	
Nps11	Cs-A-T-C-A-T-E/C-A-T-E/C-A-T-TE	4	tig00002287	
Nps12	Cs-A-T-C-A-T-C-A-T-C-A-T-TE	4	tig00080466	
Nps13	Cs-A-T-C-A-T-TE	2	tig00002287	
Nps14	A-T-C-T-C-A-TD	?	tig00000022	
Nps15	Cs-A-T-TE	1	tig00002287	
Nps16	A-T-TD	1	tig00000005	*lys2*

	***M. amoeboidea* CBS 889.72**	modules	encoding contig	homologs in *M.alpina* genome		Protein identity
Nps1	Cs-A-T-C-A-T-C-A-T-E/C-A-T-C-A-T-C-A-T-C-A-T-C-A-T-E/C-A-T-TE	9	tig00000044	*nps1*		43.59%
Nps2	A-T-E/C-A-T-C-A-T-E/C-A-T-C-A-T-C-A-T-C-A-T-C-A-T-TE	8	tig00000028	*nps2*		72.81%
Nps3	Cs-A-T-E/C-A-T-E/C-A-T-E/C-A-T-C-A-T-E/C-A-T-E/C-A-T-TE	7	tig00000028	*nps3*	*malA*	90.20%
Nps4	Cs-A-T-C-A-T-C-A-T-C-A-T-C-A-T-C-A-T-C-A-T-TE	7	tig00000038	*nps4*		63%
Nps5	Cs-A-T-E/C-A-T-C-A-T-C-A-T-E/C-A-T-E/C-A-T-TE	6	tig00000033	*nps5*		89.16%
Nps6	Cs-A-T-E/C-A-T-C-A-T-E/C-A-T-E/C-A-T-TE	5	tig00000040	*nps8*	*mpcA*	90.04%
Nps7	Cs-A-T-E/C-A-T-C-A-T-E/C-A-T-E/C-A-T-TE	5	tig00000040	*nps9*	*mpbA*	84.88%
Nps8	A-T-E/C-A-T-E/C-A-T-E/C-A-T-E/C-A-T-TE	5	tig00000030	-		
Nps9	A-T-E/C-A-T-C-A-T-C-A-T-TD	4	tig00000002	*nps10*		84.44%
Nps10	A-T-C-A-T-C-A-T-C-A-T-TE	4	tig00000111	*nps12*		78.76%
Nps11	T-C-A-T-C-A-T-C-A-T-C-A-T-TD	4	tig00000028	-		
Nps12	Cs-A-T-E/C-A-T-C-A-T-TE	3	tig00000044	-		
Nps13	A-T-C-A-T-TE	2	tig00000028	*nps13*		42.97%
Nps14	C-A-T-TD	1	tig00000028	-		
Nps15	A-T-TD	1	tig00000002	-		
Nps16	A-T-?	1	tig00000040	-		
Nps17	A-T-TD	1	tig00013576	*nps16*	*lys2*	94.09%

Table S3. Heterologously produced proteins after Ni^{2+}-NTA-affinity chromatography. Yields refer to a 500 ml bacterial culture.

MalA-module	plasmid	*E. coli* expression strain	His_6-tag	protein MW	yield [mg]
M1	pMG027	*E. coli* KRX	N+C-terminal	110.9 kDa	0.070
M2	pJMW31	*E. coli* SoluBL21	N+C-terminal	120.1 kDa	0.226
M3	pJMW33	*E. coli* SoluBL21	N+C-terminal	119.6 kDa	0.180
M4	pJMW10	*E. coli* KRX	N+C-terminal	123.8 kDa	0.420
M5	pJMW24	*E. coli* KRX	N+C-terminal	123.1 kDa	0.062
M6	pJMW27	*E. coli* BL21	N+C-terminal	125.5 kDa	0.180
M7	pJMW26	*E. coli* SoluBL21	N+C-terminal	120.2 kDa	0.044

Table S4. Quantification of aminoacyl hydroxamates in adenylation domain assays. Values are expressed in µM.

	M1		M2		M3		M4		M5		M6		M7	
	mean	SD	mean	SD	mean	SD	mean	SD	mean	SD	mean	SD	mean	SD
D-PheHA	0.076	0.003	0	0	0.541	0.020	0.258	0.019	0	0	0.038	0.001	0	0
L-PheHA	0	0	0	0	0.157	0.003	18.797	0.246	0.040	0.001	0.781	0.029	0.054	0.000
L-HisHA	0	0	0	0	0	0	0	0	0	0	0	0	0	0
L-MetHA	1.508	0.004	0	0	19.638	0.128	1.358	0.072	0	0	0	0	0	0
L-GluHA	0	0	0	0	0	0	0	0	0	0	0	0	0	0
L-LysHA	0	0	0	0	0	0	0	0	0	0	0	0	0	0
L-AspHA	0	0	0	0	0	0	0	0	0	0	0	0	0	0
L-IlleHA	0.028	0.000	0	0	0	0	0	0	0	0	0	0	0	0
L-LeuHA	100.000	0.000	0	0	100.000	0.000	0.178	0.005	0	0	0.071	0.002	0	0
L-CysHA	0.127	0.019	0	0	2.083	0.194	0	0	0	0	0	0	0	0
L-ThrHA	0	0	0.073	0.011	0	0	0	0	68.825	0.594	0	0	0	0
D-ValHA	0	0	0	0	9.866	0.269	0	0	0.252	0.004	0	0	0	0
L-ValHA	0.091	0.004	0	0	1.700	0.211	0	0	0	0	0	0	0	0
L-ProHA	0	0	0	0	0	0	0	0	0	0	0	0	0	0
GlyHA	0	0	0	0	0	0	0	0	0	0	0	0	0	0
L-TrpHA	0	0	0	0	0	0	1.453	0.101	0	0	792.672	5.572	0	0
L-TyrHA	0	0	0	0	0	0	0	0	0	0	0	0	0	0
L-ArgHA	0	0	15.201	2.153	0	0	0	0	0	0	0	0	0	0
L-AlaHA	0	0	0	0	0	0	0	0	0	0	0	0	0	0

Table S5. Substrate specificity code for MalA adenylation domains and related domains.
The proposed activated substrates are listed in column 3. The residues are mapped based on positions according to *Aneurinibacillus migulanus* (former *Brevibacillus brevis)* GrsA-A numbering [21]. NRPS codes were extracted from various sources.[22-24] Amino acid residues in the NRPS code are highlighted according to their physicochemical properties: acidic (red), small/hydrophobic (grey), aromatic/hydrophobic (ocher), hydrophilic (green), and basic (blue).

Protein domain	Organism*	substrate	Residue position according to GrsA Phe numbering									
			235	236	239	278	299	301	322	330	331	527
MalA_A1	*M. alpina*	Leu/Val/Met	D	F	W	N	F	G	L	I	Y	K
MalA_A1	*M. amoeboidea*	Leu/Val	D	F	W	N	F	G	L	I	Y	K
MalA_A3	*M. alpina*	Leu/Val/Met	D	F	W	A	A	G	L	I	A	K
MalA_A3	*M. amoeboidea*	Leu/Val	D	F	W	A	S	G	I	I	A	K
MpbA_A1	*M. alpina*	Val	D	A	F	W	L	G	G	T	F	K
MpcA_A1	*M. alpina*	Leu/Ile/Val	D	A	F	F	I	G	A	M	L	K
MpbA_A2	*M. alpina*	Leu	D	A	F	F	I	G	A	M	V	K
MpbA_A4	*M. alpina*	Leu	D	A	I	F	L	G	A	T	I	K
MpcA_A5	*M. alpina*	Leu	D	A	M	F	I	G	G	T	I	K
Plu3263_A2	*P. luminescens*	Leu	D	A	W	C	I	G	A	V	C	K
SrfAA_A2	*B. subtilis*	Leu	D	A	F	M	M	G	M	V	F	K
GrsB_A1	*A. migulanus*	Val	D	A	F	W	I	G	G	T	F	K
EasA_A3	*A. nidulans*	Leu	D	I	H	F	V	G	A	I	A	K
BSLS_A2	*B. bassiana*	Leu	D	G	Y	I	I	G	G	V	F	K
CssA_A9	*T. inflatum*	Val	D	A	W	M	F	A	A	V	L	K
MalA_A2	*M. alpina*	Arg	D	F	W	T	T	G	D	I	S	K
MalA_A2	*M. amoeboidea*	Arg	D	F	W	T	T	G	D	I	S	K
MpcA_A3	*M. alpina*	Arg	D	A	A	S	V	G	A	T	D	K
SyrE_A5	*P. syringae*	Arg	D	V	A	D	V	C	A	I	D	K
McyC_A1	*M. aeruginosa*	Arg	D	V	W	T	I	G	A	V	D	K
McyB_A1	*M. aeruginosa*	Arg	D	V	W	T	I	G	A	V	E	K
PpzA-1_A2	*E. festucae*	Arg	D	V	S	D	T	G	A	P	T	K
MalA_A4	*M. alpina*	Phe	D	P	W	I	L	G	E	I	A	K
MalA_A4	*M. amoeboidea*	Phe	D	P	W	I	L	G	E	I	A	K
MpcA_A2	*M. alpina*	Tyr/Phe	D	P	F	T	M	G	A	V	V	K
MpbA_A3	*M. alpina*	Tyr/Phe/Trp	D	P	F	V	M	G	G	T	V	K
Plu3263_A3	*P. luminescens*	Phe	D	A	W	C	I	A	A	V	C	K
BacC_A2	*B. subtilis*	Phe	D	A	F	T	V	A	A	V	C	K
GrsA_A1	*A. migulanus*	Phe	D	A	W	T	I	A	A	I	C	K
TycA_A1	*A. migulanus*	Phe	D	A	W	T	I	A	A	I	C	K
CepA_A1	*A. orientalis*	Tyr	D	A	S	T	V	A	A	V	C	K
TycC_A1	*A. migulanus*	Tyr	D	A	L	T	T	G	E	V	V	K
GliP_A1	*A. fumigatus*	Phe	D	G	S	I	L	G	A	C	A	K
BEAS_A2	*B. bassiana*	Phe	D	G	Y	I	M	A	A	V	M	K
MalA_A5	*M. alpina*	Thr/Dhb	D	F	W	N	V	G	M	V	H	K
MalA_A5	*M. amoeboidea*	Thr/Dhb	D	F	W	N	V	G	M	V	H	K
HgdA_A1	*B. gladioli*	Dhb	D	F	W	N	V	G	M	V	H	K
HgdA_A2	*B. gladioli*	Dhb	D	F	W	N	V	G	M	V	H	K
AcmB_A1	*S. chrysomallus*	Thr	D	F	W	N	V	G	M	V	H	K
SnbC_A1	*S. pristinaespiralis*	Thr	D	F	W	N	V	G	M	V	H	K
SyrB_A1	*P. syringae*	Thr	D	F	W	S	V	G	M	V	H	K
PvdD_A1	*P. aeruginosa*	Thr	D	F	W	N	I	G	M	V	H	K
BgdA_A1	*B. gladioli*	Dhb	D	F	W	N	I	G	M	V	H	K
AgiA_A1	*A. flavus*	Thr	D	A	G	A	M	G	T	V	D	K
MalA_A6	*M. alpina*	Trp	D	A	L	A	I	G	E	V	A	K
MalA_A6	*M. amoeboidea*	Trp	D	A	L	A	I	G	E	V	A	K
DaptA_A1	*S. roseosporus*	Trp	D	V	S	S	I	G	A	V	E	K
TqaA_A2	*P. aethiopicum*	Trp	D	G	M	H	V	V	G	V	S	K
IvoA_A1	*A. nidulans*	Trp	D	V	D	L	Q	G	V	V	A	K
MalA_A7	*M. alpina*	inactive	D	P	L	I	L	G	E	I	A	K
MalA_A7	*M. amoeboidea*	inactive	D	P	L	I	L	G	E	I	A	K

*Organisms are highlighted according to their phylogenetic origin: basal fungi (blue), higher fungi (brown), and bacteria (green).

Table S6. Properties of metabolites determined in this study. DOI, degrees of unsaturation; Dhb, dehydrobutyrine; pCys, *S*-propargyl-L-cysteine; BrPhe, 4-bromo-L-phenylalanine; FAM, 5-carboxyflourescein; N_3Phe, 4-azido-L-phenylalanine; t_R, retention time according to UHPLC-MS analysis (method B and method C, Table S16). Met-containing metabolites (**6-17**) other malpinins (**1-5** and **18-27**) were quantified by method B and method C, respectively. Asterisks (*) indicates metabolite structure elucidation by ESI-MS/MS, absolute configuration was not determined. For respective MS/MS spectra see Figures S12, S15-S23, S38-S39, S41, S43, S44, S52 and S53. n.d., not determined.

cmpd.	name	$[M+H]^+$	formula	DOI	composition	t_R (min) meth. B	t_R (min) meth. C
1	Malpinin A	859.4827	$C_{44}H_{62}N_{10}O_8$	19	Ac-D-Leu-D-Arg-D-Leu-L-Phe-Dhb-D-Trp	2.65	9.91
2	Malpinin B	845.4665	$C_{43}H_{60}N_{10}O_8$	19	Ac-D-Leu-D-Arg-D-Val-L-Phe-Dhb-D-Trp	2.50	9.26
3	Malpinin C	845.4674	$C_{43}H_{60}N_{10}O_8$	19	Ac-D-Val-D-Arg-D-Leu-L-Phe-Dhb-D-Trp	2.50	9.26
4	Malpinin D	831.4515	$C_{42}H_{58}N_{10}O_8$	19	Ac-D-Val-D-Arg-D-Val-L-Phe-Dhb-D-Trp	2.37	8.69
5	Malpinin E*	825.4971	$C_{41}H_{65}N_{10}O_8$	15	Ac-Leu-Arg-Leu-Leu-Dhb-Trp	2.54	n.d.
6	Malpinin F	877.4368	$C_{43}H_{60}N_{10}O_8S$	19	Ac-D-Leu-D-Arg-D-Met-L-Phe-Dhb-D-Trp	n.d.	9.38
7	Malpinin G	877.4374	$C_{43}H_{60}N_{10}O_8S$	19	Ac-D-Met-D-Arg-D-Leu-L-Phe-Dhb-D-Trp	n.d.	9.38
8	Malpinin H*	895.3948	$C_{42}H_{58}N_{10}O_8S_2$	19	Ac-Met-Arg-Met-Phe-Dhb-Trp	n.d.	8.74
9	Malpinin I*	843.4547	$C_{40}H_{62}N_{10}O_8S$	15	Ac-Leu-Arg-Leu-Met-Dhb-Trp	n.d.	8.96
10	Malpinin J*	829.4379	$C_{39}H_{60}N_{10}O_8S$	15	Ac-Leu-Arg-Val-Met-Dhb-Trp	n.d.	8.33
11	Malpinin K*	829.4379	$C_{39}H_{60}N_{10}O_8S$	15	Ac-Val-Arg-Leu-Met-Dhb-Trp	n.d.	8.33
12	Malpinin L*	815.4222	$C_{38}H_{58}N_{10}O_8S$	15	Ac-Val-Arg-Val-Met-Dhb-Trp	n.d.	7.75
13	Malpinin M*	861.4098	$C_{39}H_{60}N_{10}O_8S_2$	15	Ac-Leu-Arg-Met-Met-Dhb-Trp	n.d.	8.43
14	Malpinin N*	861.4098	$C_{39}H_{60}N_{10}O_8S_2$	15	Ac-Met-Arg-Leu-Met-Dhb-Trp	n.d.	8.43
15	Malpinin O*	847.3946	$C_{38}H_{58}N_{10}O_8S_2$	15	Ac-Met-Arg-Val-Met-Dhb-Trp	n.d.	7.84
16	Malpinin P*	847.3946	$C_{38}H_{58}N_{10}O_8S_2$	15	Ac-Val-Arg-Met-Met-Dhb-Trp	n.d.	7.84
17	Malpinin Q*	879.3653	$C_{38}H_{58}N_{10}O_8S_3$	15	Ac-Met-Arg-Met-Met-Dhb-Trp	n.d.	7.87
18	Malpinin R*	898.4911	$C_{46}H_{63}N_{11}O_8$	21	Ac-Leu-Arg-Leu-Trp-Dhb-Trp	2.59	n.d.
19	Malpinin S*	884.4770	$C_{45}H_{61}N_{11}O_8$	21	Ac-Leu-Arg-Val-Trp-Dhb-Trp	2.45	n.d.
20	Malpinin T*	884.4770	$C_{45}H_{61}N_{11}O_8$	21	Ac-Val-Arg-Leu-Trp-Dhb-Trp	2.45	n.d.
21	Malpinin U*	887.42244	$C_{44}H_{58}N_{10}O_8S$	21	Ac-pCys-Arg-Leu-Phe-Dhb-Trp	2.54	n.d.
22	Malpinin V*	887.42244	$C_{44}H_{58}N_{10}O_8S$	21	Ac-Leu-Arg-pCys-Phe-Dhb-Trp	2.54	n.d.
23	Malpinin W	937.39196	$C_{44}H_{61}N_{10}O_8Br$	19	Ac-Leu-Arg-Leu-BrPhe-Dhb-Trp	2.79	n.d.
24	Malpinin X*	923.37666	$C_{43}H_{59}N_{10}O_8Br$	19	Ac-Leu-Arg-Val-BrPhe-Dhb-Trp	2.67	n.d.
25	Malpinin Y*	923.37666	$C_{43}H_{59}N_{10}O_8Br$	19	Ac-Val-Arg-Leu-BrPhe-Dhb-Trp	2.67	n.d.
26	-	900.48357	$C_{44}H_{61}N_{13}O_8$	21	Ac-Val-Arg-Leu-N_3Phe-Dhb-Trp	2.66	n.d.
27	Malpinin-coupled 5-FAM	1313.5734	$C_{68}H_{76}N_{14}O_{14}$	38	Ac-Leu-Arg-Leu-(Phe-triazole-5-FAM)-Dhb-Trp	2.51	n.d.
Deacetyl-**1**	Deacetyl-Malpinin A*	817.4716	$C_{42}H_{60}N_{10}O_7$	18	Leu-Arg-Leu-Phe-Dhb-Trp	2.25	n.d.

Table S7. HR-ESI-MS/MS data of compounds 1 and 6-27. The N-terminal charged fragment ions are indicated as a and b. The subscript n denotes the number of amino acid residues. Compound fragmentation for **1** served as reference.[25] * Fragments of low abundance.

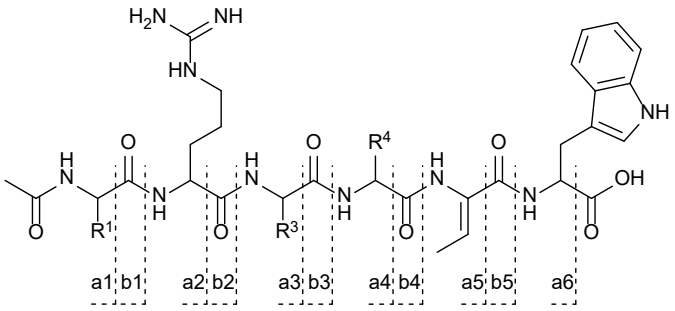

	R¹	R³	R⁴	a_1	b_1	a_2	b_2	a_3	b_3	a_4	b_4	a_5 +2H	b_5	a_6
Malpinin A (**1**)	Leu	Leu	Phe	128.11	-	284.21	-	397.29	-	544.36	-	629.41	-	813.47
Malpinin F (**6**)	Leu	Met	Phe	128.11	156.10	284.21	312.20	415.25	443.24	562.32	590.31	647.37	673.35	831.43
Malpinin G (**7**)	Met	Leu	Phe	146.06	174.06	302.16	330.16	415.25	443.24	562.32	590.31	647.37	673.35	831.44
Malpinin H (**8**)	Met	Met	Phe	146.06	174.06	302.16	330.16	433.21	461.2	580.27	608.27	665.33	691.3	849.39
Malpinin I (**9**)	Leu	Leu	Met	128.11	156.1	284.21	312.2	397.29	425.28	528.33	556.33	613.39	639.36	797.45
Malpinin J (**10**)	Leu	Val	Met	128.11	156.1	284.21	312.2	383.28	411.27	514.32	542.31	599.37	625.35	783.43
Malpinin K (**11**)	Val	Leu	Met	114.09	142.09	270.18	298.19	383.28	411.27	514.32	542.31	599.37	625.35	783.43
Malpinin L (**12**)	Val	Val	Met	114.09	142.09	270.19	298.19	369.29	397.26	500.3	528.3	585.35	611.33	769.42
Malpinin M (**13**)	Leu	Met	Met	128.11	156.1	284.21	312.2	415.25	443.24	546.29	574.28	631.34	657.32	815.41
Malpinin N (**14**)	Met	Leu	Met	146.06	174.06	302.16	330.16	415.25	443.24	546.29	574.28	631.34	657.32	815.41
Malpinin O (**15**)	Met	Val	Met	146.06	174.06	302.16	330.16	401.23	429.23	532.27	560.27	617.33	643.31	801.39
Malpinin P (**16**)	Val	Met	Met	114.09	142.09	270.19	298.19	401.23	429.23	532.27	560.27	617.33	643.31	801.39
Malpinin Q (**17**)	Met	Met	Met	146.06	174.06	302.16	330.16	433.21	461.2	564.25	592.24	649.3	675.28	833.36
Malpinin R (**18**)	Leu	Leu	Trp	128.11	156.1	284.21	312.2	397.29	425.29	583.37	611.37	668.42	694.4	852.49
Malpinin S (**19**)	Leu	Val	Trp	128.11	156.1	284.21	312.2	383.28	411.27	569.36	597.35	654.41	680.39	838.47
Malpinin T (**20**)	Val	Leu	Trp	114.09	142.09	270.18	298.19	383.28	411.27	569.36	597.35	654.41	680.39	838.47
Malpinin U (**21**)	pCys	Leu	Phe	156.05 *	184.04	312.15*	340.14	425.23	453.23	572.3	600.3	657.35	683.33	841.42
Malpinin V (**22**)	Leu	pCys	Phe	128.11	156.1	284.21	312.2	425.23	453.23	572.3	600.3	657.35	683.33	841.42
Malpinin W (**23**)	Leu	Leu	BrPhe	128.11	156.1	284.21	312.2	397.29	425.29	622.27	650.27	707.32	733.3	891.39
Malpinin X (**24**)	Leu	Val	BrPhe	128.11	156.1	284.21	312.2	383.28	411.27	608.26	636.25	693.29	719.29	877.37
Malpinin Y (**25**)	Val	Leu	BrPhe	114.09	142.09	270.18	298.19	383.28	411.27	608.26	636.25	693.29	719.29	877.37
Malpinin azide (**26**)	Leu	Leu	N_3Phe	128.11	156.1	284.21	312.2	397.29	-	545.36 ($-N_3$)	571.34 ($-N_3$)	-	654.37 ($-N_3$)	827.47 ($-N_2$)
Malpinin-coupled 5-FAM (**27**)	Leu	Leu	Phe-5-FAM	128.11	156.1	284.21	312.2	397.29	425.29	998.44	1026.45	1081.48 (a5)	1109.48	1267.56
Deacetyl-**1**	Leu	Leu	Phe	86.10	114.09*	242.20*	270.19	355.28	383.28	502.35	530.35	-	613.38	-

Table S8. Malpinins in cultures supplemented with single amino acids. *M. alpina* was cultivated in Aspergillus Minimal Medium with supplementation of 10 mM proteinogenic amino acids **(A)** Leu, Val, Ile, Phe and Cys, **(B)** Met and Trp or **(C)** non-proteinogenic amino acids pCys and BrPhe. Yields are expressed as signal intensity per fungal dry biomass [AUC /g mycelium]. BrPhe, 4-bromo-L-phenylalanine, pCys, S-propargyl-L-cysteine; SD, standard deviation (n=3). See also: Figures 4 and S40.

A

		ctrl		Leu		Val		Ile	
cmpd.	**name**	**yield**	**SD**	**yield**	**SD**	**yield**	**SD**	**yield**	**SD**
1	malpinin A	2.89E+08	7.08E+07	2.33E+07	1.31E+07	2.01E+08	2.85E+07	1.33E+08	1.88E+07
2-3	malpinin B-C	1.24E+08	3.21E+07	7.14E+05	9.52E+04	1.84E+08	1.59E+07	9.20E+07	1.82E+07
4	malpinin D	1.07E+07	3.43E+06	0.00E+00	0.00E+00	4.01E+07	1.67E+06	4.74E+06	1.32E+06
5	malpinin E	2.17E+06	7.14E+05	8.54E+06	4.57E+06	4.22E+07	8.67E+06	1.45E+06	4.14E+05
6-7	malpinin F-G	-	-	-	-	-	-	-	-
8	malpinin H	-	-	-	-	-	-	-	-
9	malpinin I	-	-	-	-	6.66E+05	1.30E+05	-	-
10-11	malpinin J-K	-	-	-	-	-	-	-	-
12	malpinin L	-	-	-	-	-	-	-	-
13-14	malpinin M-N	-	-	-	-	-	-	-	-
15-16	malpinin O-P	-	-	-	-	-	-	-	-
17	malpinin Q	-	-	-	-	-	-	-	-
18	malpinin R	-	-	-	-	-	-	-	-
19-20	malpinin S-T	-	-	-	-	-	-	-	-
deacetyl-1	deacetyl-malpinin A	1.71E+06	9.88E+05	7.22E+05	8.91E+05	1.78E+06	2.74E+05	1.65E+06	4.73E+05

		Phe		Cys		LB-Medium	
cmpd.	**name**	**yield**	**SD**	**yield**	**SD**	**yield**	**SD**
1	malpinin A	7.63E+06	1.27E+06	3.58E+06	4.47E+05	5.19E+06	4.99E+04
2-3	malpinin B-C	5.18E+06	1.17E+06	2.09E+06	3.01E+05	1.68E+06	6.88E+03
4	malpinin D	6.79E+05	1.49E+05	2.09E+05	3.35E+04	3.45E+05	2.38E+04
5	malpinin E	-	-	-	-	1.64E+05	8.21E+03
6-7	malpinin F-G	-	-	-	-	1.11E+05	5.65E+03
8	malpinin H	-	-	-	-	-	-
9	malpinin I	-	-	-	-	2.07E+04	6.16E+03
10-11	malpinin J-K	-	-	-	-	-	-
12	malpinin L	-	-	-	-	-	-
13-14	malpinin M-N	-	-	-	-	-	-
15-16	malpinin O-P	-	-	-	-	-	-
17	malpinin Q	-	-	-	-	-	-
18	malpinin R	-	-	-	-	-	-
19-20	malpinin S-T	-	-	-	-	-	-
deacetyl-1	deacetyl-malpinin A	-	-	-	-	8.37E+04	5.01E+03

B

		Met		Trp	
cmpd.	**name**	**yield**	**SD**	**yield**	**SD**
1	malpinin A	2.05E+08	2.39E+07	2.19E+08	1.64E+08
2-3	malpinin B-C	1.18E+08	2.31E+07	1.03E+08	8.10E+07
4	malpinin D	2.04E+07	6.59E+06	2.11E+07	1.28E+07
5	malpinin E	-	-	1.17E+06	3.95E+05
6-7	malpinin F-G	2.29E+08	1.31E+08	3.17E+06	2.14E+06
8	malpinin H	6.56E+07	4.47E+07	-	-
9	malpinin I	1.38E+08	6.06E+07	-	-
10-11	malpinin J-K	5.05E+07	2.25E+07	-	-
12	malpinin L	4.34E+06	1.94E+06	-	-
13-14	malpinin M-N	1.34E+08	7.04E+07	-	-
15-16	malpinin O-P	3.02E+07	1.61E+07	-	-
17	malpinin Q	2.67E+07	1.58E+07	-	-
18	malpinin R	-	-	1.62E+07	1.25E+07
19-20	malpinin S-T	-	-	8.96E+06	6.08E+06

C

		ctrl		pCys		BrPhe	
cmpd.	**name**	**yield**	**SD**	**yield**	**SD**	**yield**	**SD**
1	malpinin A	1.70E+09	8.83E+08	1.99E+08	1.29E+08	714235078	44809821.2
2-3	malpinin B-C	7.98E+08	4.26E+08	1.16E+08	7.87E+07	357457616	32725988.5
4	malpinin D	1.06E+08	5.40E+07	1.59E+07	1.12E+07	46902840.8	7042333.95
5	malpinin E	1.01E+07	3.83E+06	-	-	-	-
21-22	malpinin U-V	-	-	4.75E+07	3.33E+07	-	-
23	malpinin W	-	-	-	-	335822906	47885510.7
24-25	malpinin X-Y	-	-	-	-	151904122	26360990.4

Table S9. NMR data of 6 and 7 in DMSO-d_6. For detailed atom numbering see Figure S34. * Signals overlap.

malpinin F (6)			**malpinin G (7)**		
pos.	δ_C [ppm]	δ_H [ppm], M (*J* [Hz])	pos.	δ_C [ppm]	δ_H [ppm], M (*J* [Hz])
tryptophan (Trp)			tryptophan (Trp)		
1	173.3		1	173.3	
2	53.4	4.47, q (7.9, 13.5)	2	53.4	4.47, q (7.9, 13.1)
2 NH	-	7.85, d (7.5)	2 NH	-	7.84, d (7.4)
3	26.8	a: 3.12, m *	3	26.8	a: 3.21, d (4.6)
		b: 3.20, d (4.8)			b: 3.13, m *
4	109.8	-	4	109.8	-
5	123.7	7.18, d (2.1)	5	123.7	7.18, m (8.0)
5 NH	-	10.84, d (1.8)	5 NH	-	10.85, s
6	127.1	-	6	127.1	-
7	118.0	7.53, d (7.8)	7	118.0	7.53, d (8.0)
8	118.3	6.98, t (7.4)	8	118.3	6.98, t (7.4)
9	120.9	7.05, t (7.5)	9	120.9	7.06, t (7.4)
10	111.4	7.33, d (8.0)	10	111.4	7.33, d (8.0)
11	136.1	-	11	136.1	-
dehydrobutyrine (Dhb)			dehydrobutyrine (Dhb)		
12	164.3	-	12	164.2	-
13	130.2	-	13	130.1	-
13 NH	-	9.18, s	13 NH	-	9.12, s
14	128.0	6.32, q (7.1, 14.1)	14	128.1	6.33, q (6.8, 13.8)
15	13.1	1.53, d (7.0)	15	13.1	1.53, d (6.9)
phenylalanine (Phe)			phenylalanine (Phe)		
16	170.0	-	16	170.2	
17	54.1	4.65, m	17	54.3	4.59, m
17 NH		8.34, d (8.0)	17 NH	-	8.36, d (7.7)
18	37.4	2.77, dd (11.0, 13.4)	18	37.3	2.78, dd (10.8, 13.4)
19	137.6	-	19	137.7	-
20	129.2	7.26, m *	20	129.3	7.27, d (7.3)
21	128.0	7.24, m *	21	128.0	7.24, t (7.1)
22	126.3	7.17, m *	22	126.2	7.18, m *
23	128.0	7.24, m *	23	128.0	7.24, t (7.1)
24	129.2	7.26, m *	24	129.3	7.27, d (7.3)
methionine (Met)			leucine (Leu)		
25	170.8	-	25	172.1	-
26	51.8	4.30, q (7.7, 12.6)	26	51.0	4.26, m *
26 NH	-	7.79, d (7.6)	26 NH	-	7.80, d (7.6)
27	32.0	a: 1.68, m *	27	41.0	1.16, q (7.3, 13.2)
		b: 1.52, m *	28	23.8	1.23, m *
28	29.0	2.09, t (15.8)	29	21.7	0.71, d (6.4)
29	14.4	1.92, s	30	22.8	0.74, d (6.4)
arginine (Arg)			arginine (Arg)		
30	171.1	-	31	171.0	
31	52.0	4.20, m *	32	52.02	4.23, m *
31 NH	-	8.07, d (7.7)	32 NH	-	8.06, d (7.5)
32	28.4	a: 1.65, m *	33	28.6	a: 1.61
		b: 1.48, m *			b: 1.47
33	25.0	a: 1.39, m *	34	25.0	1.38, m *
		b: 1.47, m *			1.45 m *
34	40.0	3.05, m *	35	40.4	3.05, m
34 NH	-	7.54, m *	35 NH	-	7.56, m *
35	156.6	-	36	156.7	-
leucine (Leu)			methionine (Met)		
36	172.5	-	37	171.5	-
37	51.1	4.22, m *	38	51.98	4.29, m *
37 NH	-	8.02, d (7.6)	38 NH	-	8.10, d (7.4)
38	40.4	1.39, m *	39	31.8	1.75, m (5.3)
39	24.1	1.58, m*	40	29.5	2.42, m (6.6)
40	23.0	0.86, d (6.9)	41	14.5	2.00, s
41	21.5	0.81, d (6.5)			
acetic acid (Ac)			acetic acid (Ac)		
42	169.4	-	42	169.5	-
43	22.4	1.82, s	43	22.4	1.83, s

Table S10. Determination of the absolute configuration of 6, 7 and 23 by advanced Marfey´s method. Retention times [min] of respective FDLA products are highlighted in red (L-stereoisomer) and blue (D-isomer). An authentic standard for (*Z*)-Dhb is not available due to instability (reactivity of α,β-unsaturated carbonyl moiety).

amino acid	$M_{AA\text{-}FDLA}$ [g/mol]	L-standard	D-standard	malpinin F (6)	malpinin G (7)	malpinin W (23)
leucine	426	7.70	9.08	9.10	9.10	9.10
arginine	469	5.44	5.30	5.32	5.35	5.30
methionine	444	7.05	8.14	8.16	8.16	-
phenylalanine	460	7.86	8.87	7.87	7.86	-
threonine	414	5.62	6.66	-	-	-
tryptophan	499	7.81	8.62	8.64	8.65	8.64
4-Br-phenylalanine	538	8.66	9.65	-	-	8.65

Table S11. NMR data of 23. For atom numbering see Figure S51. * signals overlapping

malpinin W (23)

pos.	δ_C [ppm]	δ_H [ppm], M (J [Hz])
tryptophan		
1	173.3	-
2	-	7.85, d (7.43)
2 NH	53.4	4.47, m*
3	26.8	B: 3.22, m*
		A: 3.13, m*
4	109.9	-
5	123.8	7.19, d (1.6)
5 NH	-	10.84, m
6	127.1	-
7	118.1	7.52, d (7.80)
8	118.3	6.98, m*
9	120.9	7.04, m*
10	111.4	7.33, d (8.07)
11	136.1	-
dehydrobutyrine		
12	164.3	-
13	130.2	-
13 NH		9.13
14	127.9	6.32, q (6.9)
15	13.1	1.55, d (7.0)
4-bromo-phenylalanine		
16	169.9	-
17	53.9	4.62, m (11.5)
17 NH	-	8.37, d (8.3)
18	36.7	A: 2.72, dd (11.1, 13.6)
		B: 3.10, m*
19	137.2	-
20, 24	131.6	7.27, d (8.3)
21, 23	130.9	7.43, d (8.1)
22	119.5	-

pos.	δ_C [ppm]	δ_H [ppm], M (J [Hz])
leucine		
25	172.0	-
26	51.06	4.21, m*
26 NH	-	7.72, d (7.5)
27	41.1	1.11, m*
28	23.8	1.15, m*
29	22.8	0.73, d (6.1)
30	21.7	0.71, d (6.3)
arginine		
31	170.9	
32	51.9	4.22, m*
32 NH		8.04, d (8.0)
33	28.5	A: 1.48, m*
		B: 1.63, m*
34	25.0	A: 1.45, m *
		B: 1.39, m *
35	40.4	3.05, m*
35 NH	-	7.52, m*
36	156.7	
leucine		
37	172.5	-
38	51.14	4.24, m*
38 NH		8.02, d (7.6)
39	40.6	1.38, m*
40	24.1	1.58, m *
41	23.0	0.85, d (6.4)
42	21.6	0.81, d (6.5)
acetic acid		
43	169.4	-
44	22.4	1.82, s

Table S12. NMR data of 27. For atom numbering see Figure S59. * signals overlapping

malpinin-5-FAM (27)

pos.	δ_C [ppm]	δ_H [ppm], M (J [Hz])
tryptophan		
1	173.3	-
2	53.4	4.49, m*
2 NH	-	7.84, m*
3	26.8	3.21, m*
4	109.8	-
5	123.7	7.19, m*
5 NH	-	10.83, s
6	127.1	-
7	118.0	7.53, d (7.9)
8	118.3	6.98, t (7.4)
9	120.9 (1)	7.06, t (7.6)
10	111.3	7.33, d (8.2)
11	136.1	-
dehydrobutyrine		
12	164.3	-
13	130.2	-
13 NH	-	9.14, s
14	127.9	6.33, q (6.9)
15	13.4	1.55, d (6.9)
phenylalanine		
16	169.9	-
17	54.0	4.68, m*
17 NH	-	8.42, dd (8.0, 7.2)
18	36.8	2.83, dd (13.2, 11.1)
19	138.4	-
20, 24	130.6	7.46, d (8.3)
21, 23	119.4	7.81, d (8.2)
22	135.1	-
16	169.9	-
leucine		
25	172.0	-
26	51.04	4.22, m*
26 NH	-	7.71, m*
27	41.0	1.15
28	23.7	1.30, m*
29	22.7	0.66, m*
30	21.7	0.68, m*

pos.	δ_C [ppm]	δ_H [ppm], M (J [Hz])
arginine		
31	170.9	-
32	51.8	4.23, m*
32 NH	-	8.02, m*
33	28.5	1.25, m*
34	24.9	A: 1.47
		B: 1.40
35	40.4	3.04, m*
35 NH		7.44, m*
36	156.6	-
leucine		
37	172.4	-
38	51.14	4.21, m*
38 NH	-	7.99, m*
39	40.6	1.38, m*
40	40	24.1
41	21.5	0.80, m
42	22.9	0.84, m
acetic acid		
43	169.4	-
44	22.4	1.81, s
5-FAM		
1'	120.9 (2)	8.66, m*
2'	145.9	-
3'	35.0	4.66, d (5.0)
3' NH	-	9.44, m
4'	164.7	-
5'	126.4	-
6'	134.8	8.29, d (8.2)
7'	124.2	7.39, d (8.0)
8'	154.8	-
9'	168.1	-
10'	123.5	8.52, s
11'	135.9	-
11' OH	-	-
12'	83.2	-
13', 24'	109.0	
14', 23'	129.0	6.56, m*
15', 22'	102.3	6.69, t (2.2)
16', 21'	159.6	-
17', 20'	112.6	6.55, m*
18', 19'	151.8	-

Table S13. Organisms used in this study.

species	strain numbers	origin	reference
Escherichia coli	XL1 blue	Agilent	
	KRX	Promega	
	SoluBL21	Genlantis	
	BL21	NEB	
Mortierella alpina	ATCC32222	ATCC (American Type Culture Collection)	[26]
Mortierella amoeboidea	CBS889.72	JMRC (Jena Microbial Resource Collection)	[27]

Table S14. Oligonucleotides used in this study. Restriction sites are underlined. Primer efficiency with its correlation coefficient (R^2) is indicated for qPCR primers using gDNA of *M. alpina* as template.

name	sequence 5'-3'	target	purpose/restriction site	qPCR efficiency /R^2	qPCR length (bp) cDNA/gDNA
oJMW001	CATCGATCTGGCCTACATGG	*gpdA*	qPCR housekeeping gene	0.98/0.999	80/229
oJMW002	CCACCTTGCCCTTGTAGC	*gpdA*	qPCR housekeeping gene	0.98/0.999	80/229
oJMW003	GTATGTGCAAGGCCGGTTTCG	*actB*	qPCR housekeeping gene	1.00/0.999	100/224
oJMW004	CCCATACCGACCATCACACC	*actB*	qPCR housekeeping gene	1.00/0.999	100/224
oJMW157	GGGTGCAGAAGCCAACAAAC	*nps2*	qPCR GOI (NRPS gene)	1.02/0.999	160/263
oJMW158	CTGGGACCATGTAGTCAGGC	*nps2*	qPCR GOI (NRPS gene)	1.02/0.999	160/263
oJMW175	TACGAGGAGCCAAGAGGTG	*nps3 (malA)*	qPCR GOI (NRPS gene)	0.98/0.999	99/99
oJMW176	GACAAAGAAGCCGTCGTTCC	*nps3 (malA)*	qPCR GOI (NRPS gene)	0.98/0.999	99/99
oJMW161	CTCCGACAGTGGTGCCAAG	*nps5*	qPCR GOI (NRPS gene)	0.95/0.998	170/291
oJMW162	CATATGCCGTGTCAAGACTGG	*nps5*	qPCR GOI (NRPS gene)	0.95/0.998	170/291
oJMW163	GTTAGTTTCGGGTCAGGCAAC	*orf35*	qPCR (transcription factor)	1.02/0.995	80/229
oJMW164	GGTAAACCTGGTCCCACTGC	*orf35*	qPCR (transcription factor)	1.02/0.995	80/229
oJMW285	CGCAGTTTGGTTCACGTC	*orf34*	qPCR (glucosaminyl transferase)	1.00/0.999	201/326
oJMW286	GGCACTTTAGCACATGGAGC	*orf34*	qPCR (glucosaminyl transferase)	1.00/0.999	201/326
oJMW165	CTCAAGCGCATCAAGAAACTCC	*orf32*	qPCR (dehydratase)	0.97/0.998	167/167
oJMW166	GTTTGCGTCCTGATTCACCC	*orf32*	qPCR (dehydratase)	0.97/0.998	167/167
oJMW173	GATTGCTAGACGCCTCTGCAG	*orf29*	qPCR (amidase)	0.99/0.998	154/154
oJMW174	GCAGAGCTGTCTCCGGAAAC	*orf29*	qPCR (amidase)	0.99/0.998	154/154
oJMW169	CGGATACATACACATCTGGCGG	*orf27*	qPCR (protein kinase)	1.00/0.999	122/251
oJMW170	CCGATACCATCTCCAGTGCATC	*orf27*	qPCR (protein kinase)	1.00/0.999	122/251
oITS1	TCCGTAGGTGAACCTGCGG	ITS	strain identification		
oITS4	TCCTCCGCTTATTGATATGC	ITS	strain identification		
oMG270	GTGGTGGTGCTCGAGGATGGCACGGTGCTGTCCGAT	*malA* module 1	amplification		
oMG285	AGGAGATATACCATGATGAACAACATTGACCATC	*malA* module 1	amplification		
oMG283	CATGGTATATCTCCTTCTTAAAG	pET28a vector	vector amplification		
oMG284	CTCGAGCACCACCACCACCACC	pET28a vector	vector amplification		
oJMW079	GATCACATTGTCGAGCAAGTGC	*malA* module 2	amplification		
oJMW080	GACATTCGGTGGCACCACAATG	*malA* module 2	amplification		
oJMW081	ATATATGCTAGCGATCACATTGTCGAGCAAGTGC	*malA* module 2	vector cloning (*Nhe*I)		
oJMW153	ATATATGCGGCCGCGACATTCGGTGGCACCACAATG	*malA* module 2	vector cloning (*Not*I)		
oJMW149	GTCGACCAAATCCCAGGAGG	*malA* module 3	amplification		
oJMW150	CGTGATGACGTTCGATGGCAC	*malA* module 3	amplification		
oJMW151	ATATATGCTAGCGTCGACCAAATCCCAGGAGG	*malA* module 3	vector cloning (*Nhe*I)		
oJMW152	ATATATAAGCTTCGTGATGACGTTCGATGGCAC	*malA* module 3	vector cloning (*Hind*III)		
oIW021	GCTCTCGCTCAGTCCATCG	*malA* module 4	amplification		
oIW022	CTCTTCCTGTGCCAACTGTTC	*malA* module 4	amplification		
oIW023	TATATAGGCTAGCGCTCTCGCTCAGTCCATCG	*malA* module 4	vector cloning (*Nhe*I)		
oIW024	ATATATGCGGCCGCTACTCTTCCTGTGCCAACTGTT	*malA* module 4	vector cloning (*Not*I)		
oJMW141	ATGGCCATTACACCCGTCTC	*malA* module 5	amplification		
oJMW142	AGGTATGACAATGGCTTGATGGT	*malA* module 5	amplification		
oBWma01	ATATATGCTAGCATGGCCATTACACCCGTCTCGA	*malA* module 5	vector cloning (*Nhe*I)		
oBWma02	ATATATAAGCTTAGGTATGACAATGGCTTGATGGTGTC	*malA* module 5	vector cloning (*Hind*III)		
oJMW145	GCCGCATCTATCGGACACC	*malA* module 6	amplification		
oJMW146	CGGAGTGATGTAGTTCGGAGG	*malA* module 6	amplification		
oJMW147	ATATATGCTAGCGCCGCATCTATCGGACACC	*malA* module 6	vector cloning (*Nhe*I)		
oJMW148	CTCTCTAAGCTTCGGAGTGATGTAGTTCGGAGG	*malA* module 6	vector cloning (*Hind*III)		
oJMW143	GTTCCTGGCGGAGTTGCC	*malA* module 7	Amplification		
oJMW144	ATCGTAGGACTCGTCCTGTGTC	*malA* module 7	Amplification		
oBWma03	ATATATCATATGGTTCCTGGCGGAGTTGCCAAC	*malA* module 7	vector cloning (*Nde*I)		
oBWma04	ATATATAAGCTTATCGTAGGACTCGTCCTGTGTCA	*malA* module 7	vector cloning (*Hind*III)		

Table S15. Plasmids used in this study.

plasmid	vector backbone	purpose	gene product	source/reference
pJET1.2	-	Amplification of DNA	-	ThermoFisher
pET28a (+)	-	expression vector	-	Agilent
pMG027	pET28a (+)	expression of *malA*-M1	MalA module 1	This study.
pJMW31	pET28a (+)	expression of *malA*-M2	MalA module 2	This study.
pJMW33	pET28a (+)	expression of *malA*-M3	MalA module 3	This study.
pJMW10	pET28a (+)	expression of *malA*-M4	MalA module 4	This study.
pJMW24	pET28a (+)	expression of *malA*-M5	MalA module 5	This study.
pJMW27	pET28a (+)	expression of *malA*-M6	MalA module 6	This study.
pJMW26	pET28a (+)	expression of *malA*-M7	MalA module 7	This study.

Table S16. HPLC methods used in this study.

	method A	method B	method C	method D
instrument	Waters ACQUITY H-class UPLC	Agilent 1290 infinity II UHPLC	Agilent 1290 infinity II UHPLC	Agilent 1290 infinity II UHPLC
solvent A	water + 0.1% FA	water + 0.1% FA	water + 0.1% FA	water + 0.1% FA
solvent B	acetonitrile	acetonitrile	acetonitrile	acetonitrile
gradient	0-4 min: 10-50% A, 5-9 min: 50-10% A	0-4 min: 5-72% B, 4-4.5 min: 72-95% B, 4.5-5 min: 95% B	0-10 min: 1-40% B, 10-12 min: 40-95% B, 12-13 min: 95% B, 13-14 min 95-1% B	0-10 min: 1-50% B, 10-11 min: 50-100% B
temperature	30°C	30°C	30°C	30°C
flow	0.4 mL min^{-1}	1 mL min^{-1}	1 mL min-1	1 mL min-1
column	ACQUITY UPLC BEH Amide column	Zorbax Eclipse Plus C18 RRHD (Agilent)	Zorbax Eclipse Plus C18 RRHD (Agilent)	Luna Omega polar C18 column (Phenomenex)
column dimension	50 mm × 2.1 mm, 1.7 µm	50 mm × 2.1 mm, 1.8 µm	50 mm × 2.1 mm, 1.8 µm	50 mm × 2.1 mm, 1.6 µm
detection	Waters Xevo TQ-S micro tandem quadrupole instrument	Agilent 6130 single quadrupole MS, ESI ionization source	Agilent 6130 single quadrupole MS, ESI ionization source	Agilent 6130 single quadrupole MS, ESI ionization source

	method E	method F	method G	method H
instrument	Preparative HPLC Agilent 1260	Preparative HPLC Agilent 1200	Preparative HPLC Agilent 1200	Preparative HPLC Agilent 1200
solvent A	water + 0.1% TFA	water + 0.1% TFA	water + 0.1% TFA	water + 0.1% TFA
solvent B	acetonitrile	acetonitrile	methanol	acetonitrile
gradient	0-20 min: 10-100% B, 20-27 min: 100% B	0-0.5 min: 35% B, 0.5-12.5 min: 35-65% B, 12.5-13 min: 65-100% B, 13-14 min: 100% B	0-0.5 min: 70% B, 0.5-15 min: 70-100% B, 15-16 min: 100% B	0-9.5 min: 45% B, 9-9.5 min: 45-100% B, 9.5-10 min 100% B
temperature	25°C	12°C	12°C	40°C
flow	20 mL min-1	2.5 mL min^{-1}	2 mL min^{-1}	2 mL min^{-1}
column	Luna C18 (Phenomenex)	Zorbax Eclipse XDB-C18 (Agilent)	SynergiHydro-RP 80 Å (Phenomenex)	Zorbax Rx-C18 (Agilent)
column dimension	250 mm × 21.2 mm, 10 µm	250 mm × 9.4 mm, 5 µm	250 × 10 mm, 4 µm	250 x 9.4 mm, 5 µm
detection	DAD, λ = 254 nm	DAD, λ = 254 nm	DAD, λ = 254 nm	DAD, λ = 225 nm

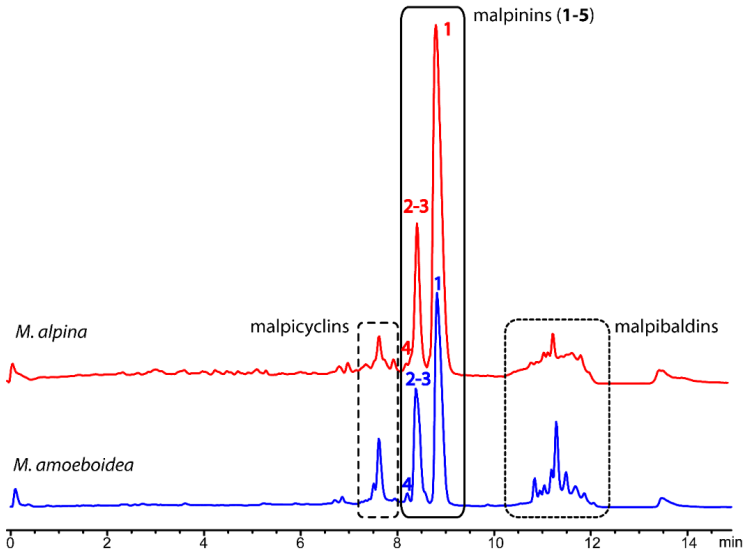

Figure S1. Total ion chromatograms of crude metabolite extracts from *M. alpina* and *M. amoeboidea*. The three major series of peptides, malpinins (**1-5**, box with continuous line), malpibaldins (dotted line) and malpicyclins (dashed line), are produced in both strains in varying amounts. Total ion counts were monitored from *m/z* 100 to 1600 (positive mode). Compound **5** is produced in traces (not shown).

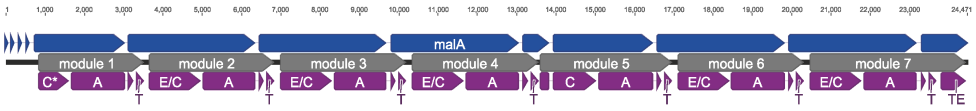

Figure S2. Schematic representation of the *malA* (*nps3*) gene. The intron/exon pattern is indicated by blue arrows (first row). Exons are boxed. Note, that all exons encoding A domains contain one intron each at near identical positions. The individual modules are highlighted in grey (second row). The required enzyme domains are indicated in purple (lowest row). Note, that the first C starter domain is truncated and inactive (asterisk). A, adenylation domain; C, condensation domain; E/C, dual epimerization/condensation domain; T, thiolation domain; TE, thioesterase.

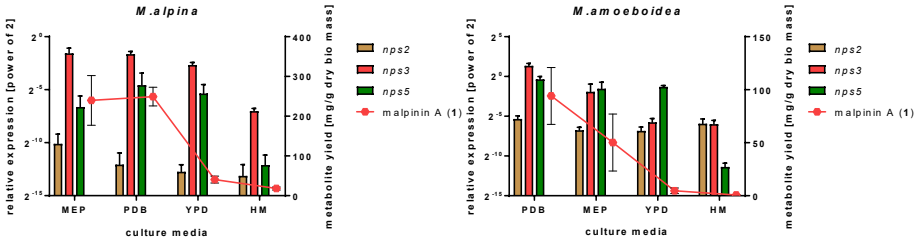

strain	candidate NRPS	Pearson R	P value
M. alpina	*nps2*	0.657	0.343
	nps3 (malA)	**0.943**	**0.057**
	nps5	0.499	0.501
M. amoeboidea	*nps2*	0.649	0.351
	nps3 (malA)	**0.904**	**0.096**
	nps5	0.838	0.162

Figure S3. Expression analysis of candidate *nps* genes in *M. alpina* and *M. amoeboidea.* qRT-PCR analysis was carried out using the actin gene (*actA*) and glyceraldehyde-3-phosphate dehydrogenase (*gpdA*) as internal reference gene.[19] Fold expression of candidate genes *nps2*, *nps3* (*malA*) and *nps5* (left ordinate) and malpinin A yields per fungal biomass (right ordinate) are presented for *M. alpina* (left panel) and *M. amoeboidea* (right panel). A strong linear correlation between gene expression and malpinin production was determined for *malA* in both strains (Pearson´s Correlation Coefficient R > 0.90). MEP, malt extract - peptone; PDB, potato dextrose broth; YPD, yeast extract - peptone - dextrose; HM, hay medium.

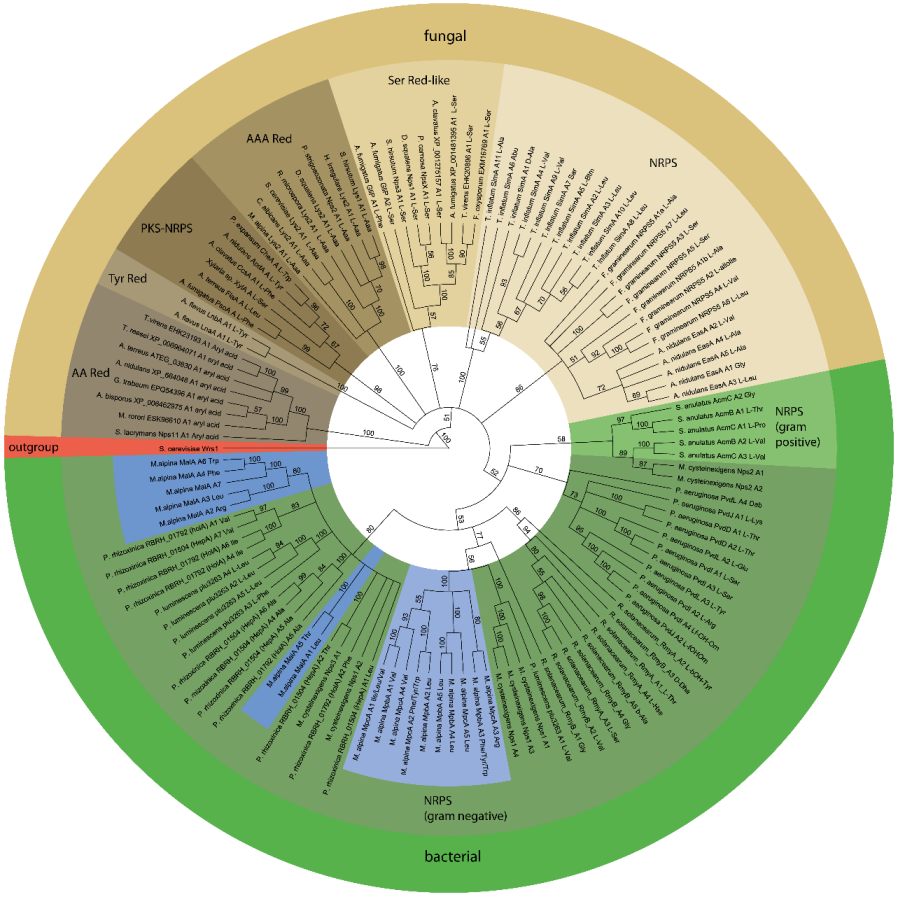

Figure S4. Phylogenetic analysis of A domains from *M. alpina* and other fungal or bacterial representatives. A set of 123 A domains were extracted from NRPSs, NRPS-like proteins, and PKS/NRPS hybrids from *M. alpina* (blue), (endo)bacteria (green), and higher fungi (taupe/amber) as described previously.[19] The A domain of the cytoplasmatic tryptophanyl-tRNA synthetase Wrs1 from *Saccharomyces cerevisiae* served as the outgroup (red). The A domains from *M. alpina* - including A domains from MalA - cluster together with bacterial counterparts. The percentual bootstrap support is indicated. AAA red, α-2-aminoadipate reductase; AA Red, aryl acid reductase; NRPS, nonribosomal peptide synthetase; PKS-NRPS, polyketide synthase-nonribosomal peptide synthetase hybrid; Ser Red, serine reductase; Tyr Red, tyrosine reductase.

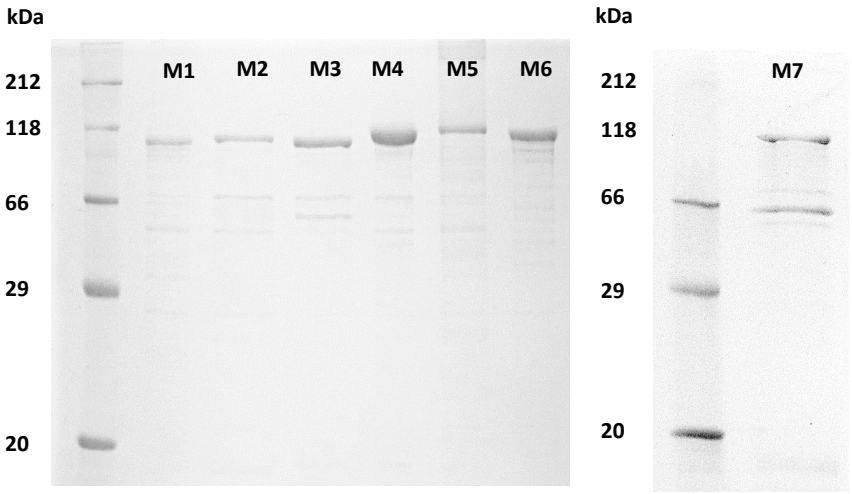

Figure S5. SDS polyacrylamide gel electrophoresis of MalA modules 1-7. A total of 1-3 µg biHis$_6$-tagged enzyme are loaded per lane. The expected molecular weights are: M1, 110.9 kDa; M2, 120.1 kDa; M3, 119.6 kDa; M4, 123.8 kDa; M5, 123.1 kDa; M6, 125.5 kDa; and M7, 120.2 kDa.

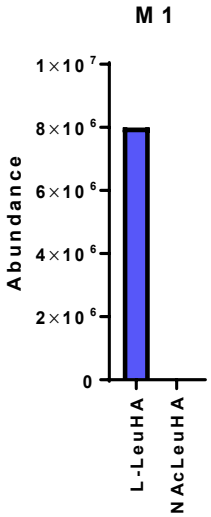

Figure S6. HAMA analysis of MalA-M1 with L-leucine and *N*-acetyl-L-leucine as substrates. L-leucine was successfully converted to L-leucine-hydroxamate (L-LeuHA) by MalA-M1. In contrast, the corresponding *N*-acetyl-L-leucine-hydroxamate (NAcLeuHA) was not determined when *N*-acetyl-L-leucine was applied.

Figure S7. Sequence alignment of the MalA starter C (C_s) domain and other experimentally characterised starter C domains. Sequence alignment of N-terminal C starter domains (C_s) are shown for: AMYAL_RS0130210,[28] ErcD,[29] Hep,[30] ArfA,[31] SyfA (Accession: EPF66764)[32], JesA,[33] and MalA (this study). The canonical condensation domain C3 of the gramicidin S synthetase GrsB[34] served as reference to identify the seven core motifs (C1- C7).[35] With the exception of MalA C_s and ACV2 C_s, a conserved double histidine motif is evident (C3 motif). C domains were obtained from proteins from bacteria (*Brevibacillus brevis* (syn. *Aneurinibacillus migulanus*), *Amycolatopsis alba, Saccharopolyspora erythraea, Mycetohabitans rhizoxinica, Pseudomonas syringae* and two additional *Pseudomonas* spec.) and fungi (*Aspergillus flavus*, *Tolypocladium inflatum*, *Mortierella alpina* and *Penicillium rubens*).

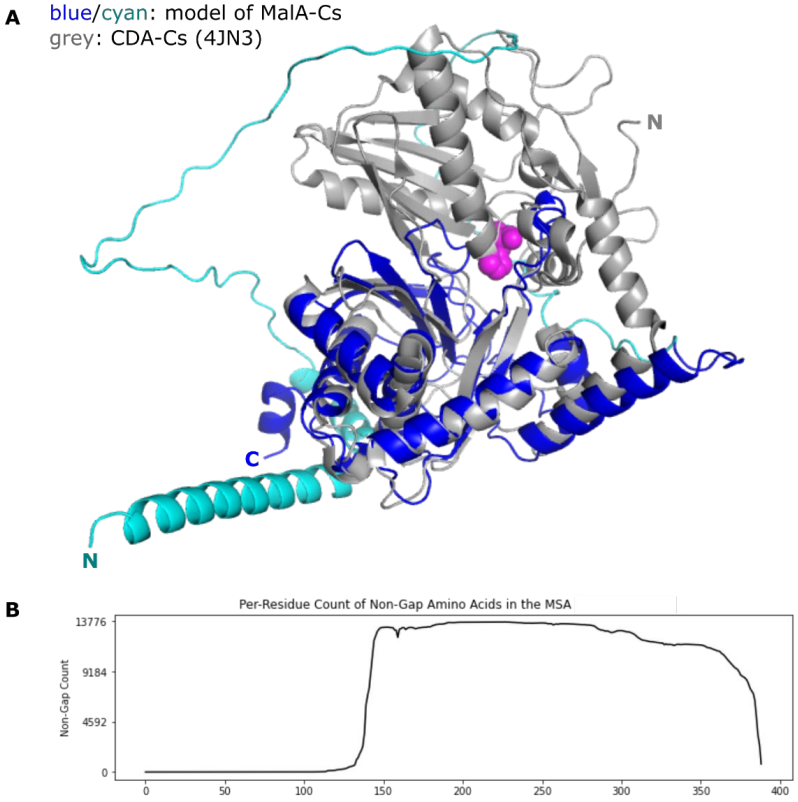

Figure S8. **A**. Structural model of MalA-C_s. The N-terminal domain of MalA, which shows partial homology to Cs domains, has been structurally modelled with AlphaFold v2.1.0[20] using a publicly available script on Google Colab (AlphaFold.ipynb). The model has been superimposed with a crystal structure of the C_s domain from CDA biosynthesis (PDB 4JN3, grey cartoon) in Pymol v2.2.2 using the "super" command. Only the C-terminal part of the model (blue cartoon) shows sequence homology and aligns with the C_s domain structure (RMSD = 1.632 Å for residues 129-389). The N-terminal lobe of the C_s-domain carrying the important catalytic His residue (His157, spheres in magenta) cannot be modelled in the N-terminal MalA domain (cartoon in cyan) because a multiple sequence alignment (**B**) for this part of the protein could not be obtained. Therefore, the N-terminal domain of MalA is highly unlikely to be a catalytically active acyl transferase.

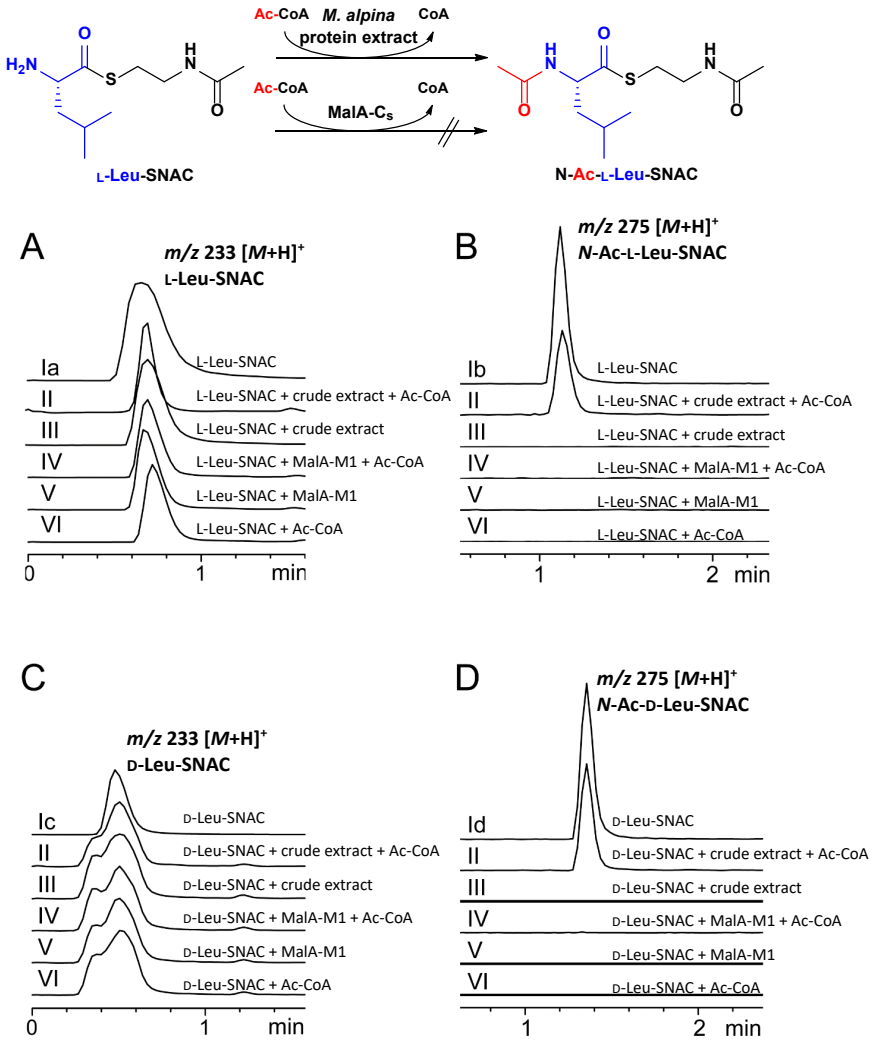

Figure S9. Chromatographic analysis of *N*-acetylation of leucyl-SNAC thioesters. *M. alpina* protein crude extracts or purified MalA-M1 was incubated with L-Leu-SNAC (**A, B**) or D-Leu-SNAC (**C, D**) in presence and absence of Ac-CoA. Extracted ion chromatograms (EIC) were recorded for L- and D-leucyl-SNAC at *m/z* 233 (**A** and **C**) and for their respective acetyl amides, L- and D-*N*-acetyl-leucyl-SNAC at *m/z* 275 (**B** and **D**). The traces are: I) respective synthetic standard (Ia L-Leu-SNAC; Ib N-acetyl-L-Leu-SNAC, Ic D-Leu-SNAC, Id N-acetyl-D-Leu-SNAC), II) *M. alpina* crude protein extract with substrate and Ac-CoA, III) *M. alpina* crude protein extract with substrate, but without Ac-CoA, IV) purified MalA-M1 with substrate and Ac-CoA; V) purified MalA-M1 with substrate, but without Ac-CoA, VI) substrates with Ac-CoA without enzyme. Note, that acetylation of both L- and D-Leu-SNAC is detectable with *M. alpina* protein crude extract, but not with MalA-C_s.

A

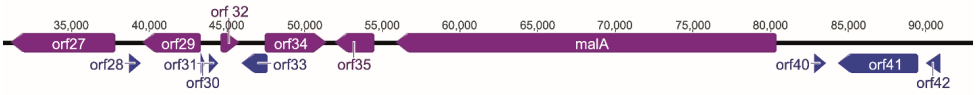

			Pearson´s correlation coefficient R (*p* value)						
	location on contig tig00000075	function	orf27	orf29	orf32	orf34	orf35	malA	malpinin A (**1**)
orf27	37833 -> 31089	protein kinase	-	0.906 (0.094)	0.265 (0.735)	0.155 (0.845)	0.161 (0.839)	-0.448 (0.552)	-0.714 (0.286)
orf29	40822 -> 39567	amidase		-	0.605 (0.395)	0.546 (0.454)	-0.227 (0.773)	-0.197 (0.803)	-0.509 (0.491)
orf32	44581 -> 45830	epimerase/dehydratase			-	0.764 (0.236)	-0.522 (0.478)	0.629 (0.371)	0.359 (0.641)
orf34	47439 -> 51400	N-Ac-glucosaminyl transferase				-	-0.925 (0.075)	0.226 (0.774)	0.052 (0.948)
orf35	54490 -> 51959	transcription factor					-	-0.174 (0.826)	-0.124 (0.876)
malA	80366 -> 55894	NRPS						-	**0.943 (0.057)**

B

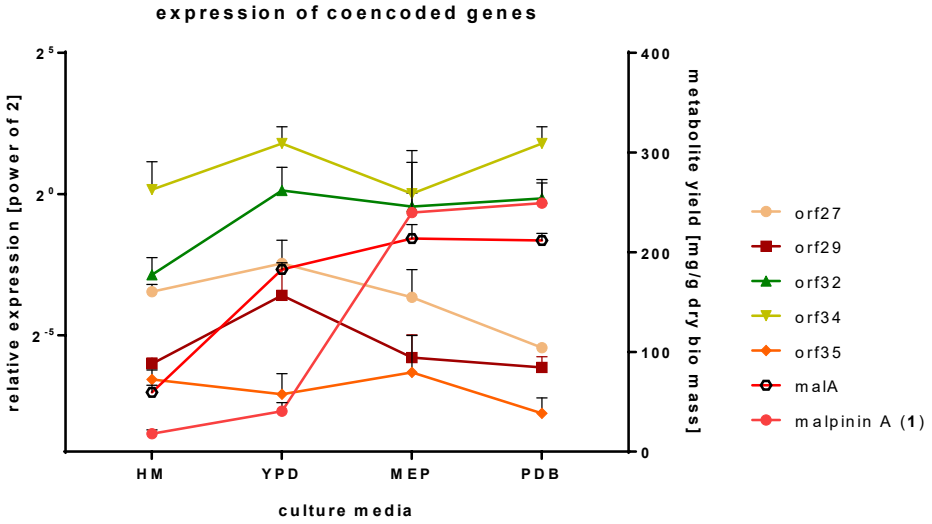

Figure S10. Bioinformatic and expression analysis of genes encoded adjacent to *malA*. A. Potential malpinin biosynthesis gene cluster**.** Open reading frames were predicted using Augustus[36] plugin for Geneious 10.2.4. The genome of *Rhizopus oryzae* served as reference. Genes with distinct predicted function (purple) are listed in the table. Open reading frames with unknown function are highlighted in blue. **B.** Expression analysis of genes adjacent to *malA*. Expression values of the genes (left y-axis), and metabolite production rate (right y-axis) are indicated. qRT-PCR analysis was carried out using the actin gene (*actA*) and glyceraldehyde-3-phosphate dehydrogenase (*gpdA*) as internal reference gene. A strong linear correlation (R > 0.94) between gene expression and malpinin A production was evident for *malA,* but for none of the remaining genes. Pearson´s Correlation Coefficient R and according *p* values are given in the table. MEP, malt extract – peptone medium; PDB, potato dextrose broth; YPD, yeast extract - peptone – dextrose medium; HM, hay medium.

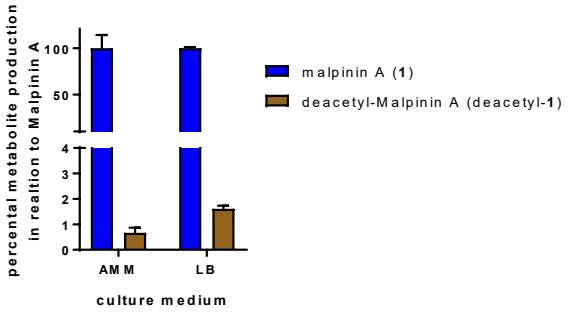

Figure S11. Production of deacetyl-1 in AMM and LB medium. Yields are given as ratios in relation to **1.**

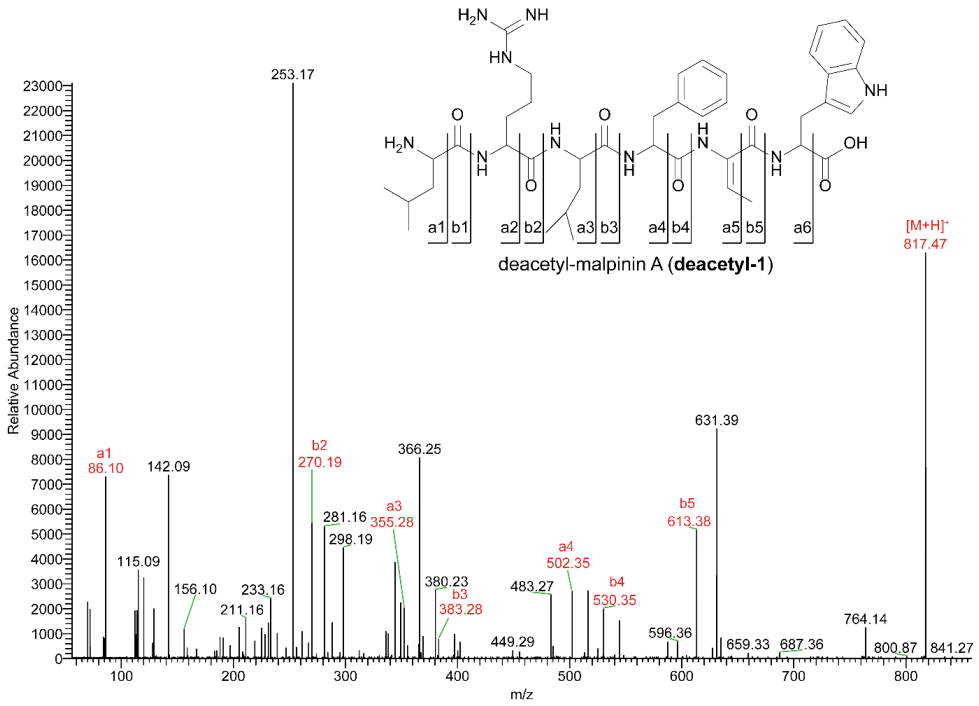

Figure S12. HR-ESI-MS/MS spectra of deacetyl-1. Spectra were obtained using 30% collision energy.

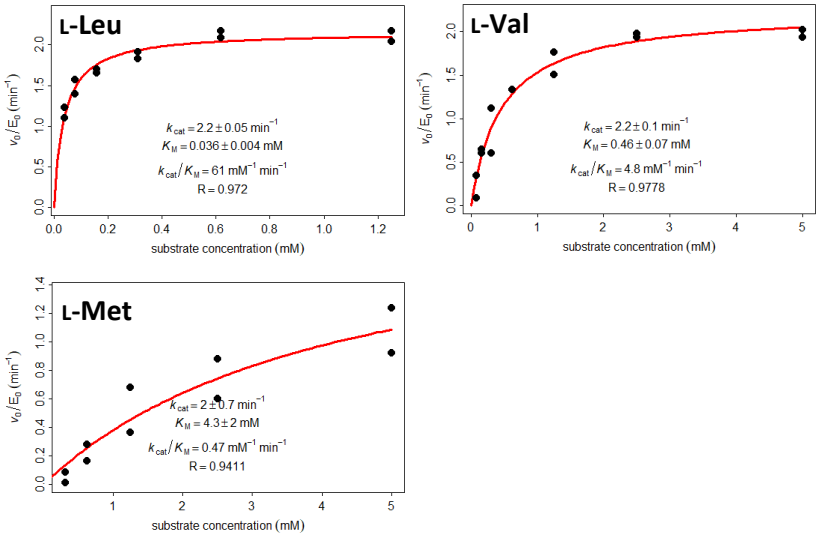

Figure S13. Michaelis-Menten kinetics of MalA-M3 for different substrates. MalA-M3 was incubated with various concentrations (0.1 – 5 mM) of substrate amino acids (L-leucine, L-valine and L-methionine) and turnover was determined by the MesG assay.

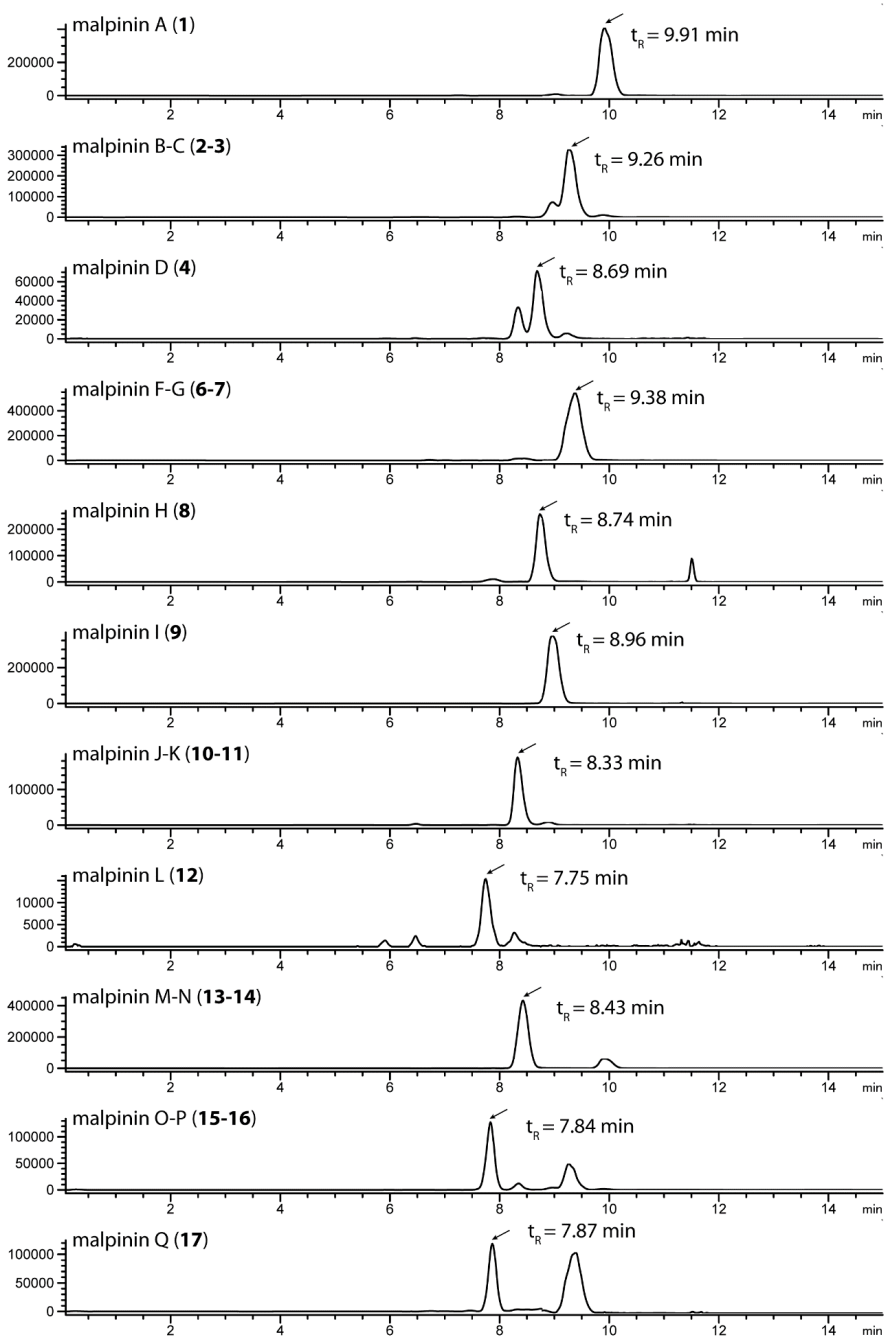

Figure S14. Extracted ion chromatograms (EICs) of metabolite extracts from cultures supplemented with L-methionine, recorded by UHPLC method C (Table S16) for better resolution and to inhibit coelution of metabolites.

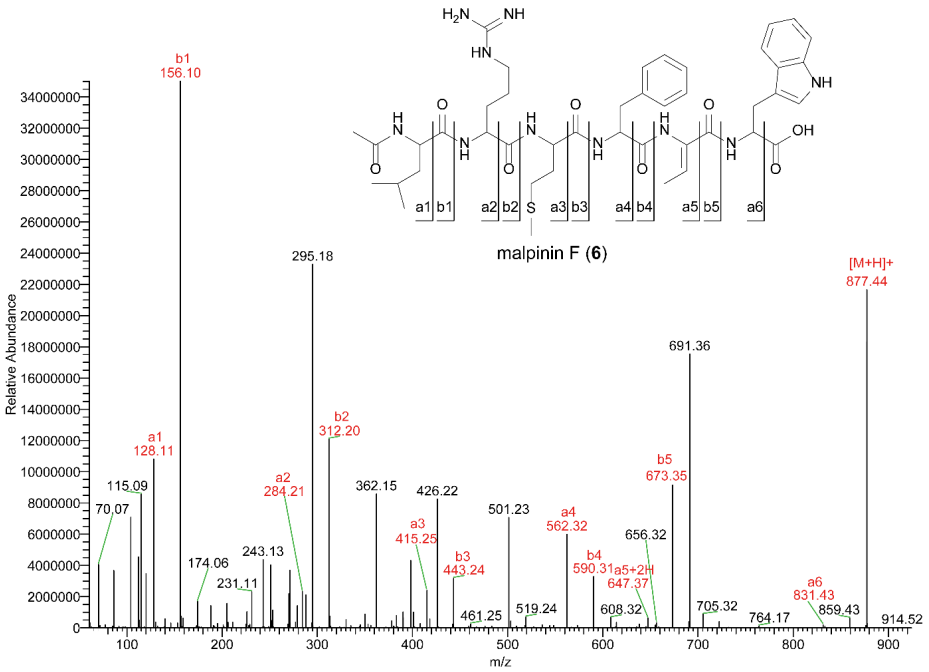

Figure S15. HR-ESI-MS/MS spectrum of 6.

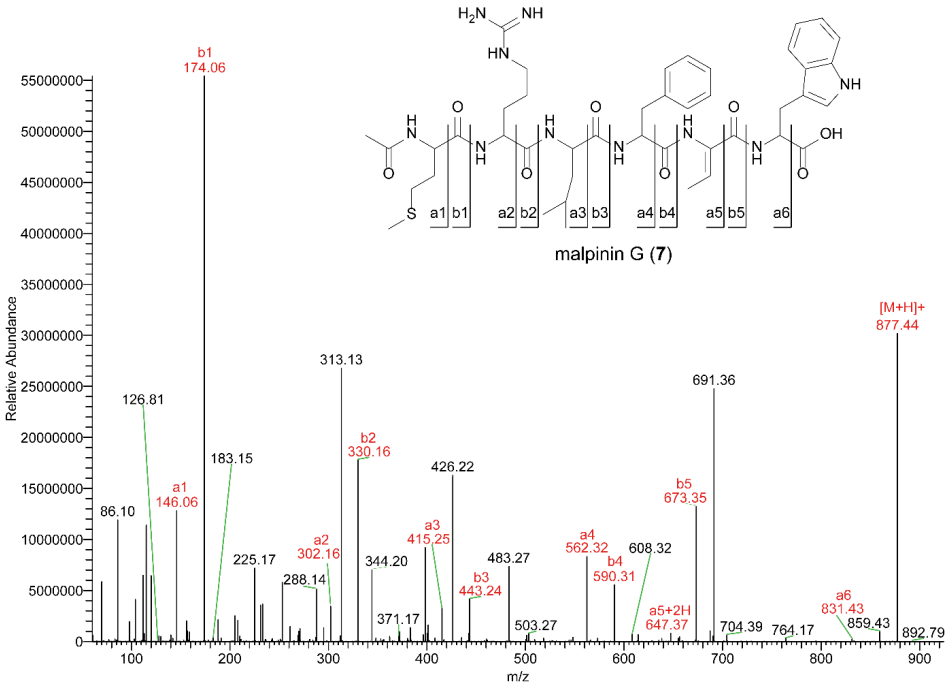

Figure S16. HR-ESI-MS/MS spectrum of 7.

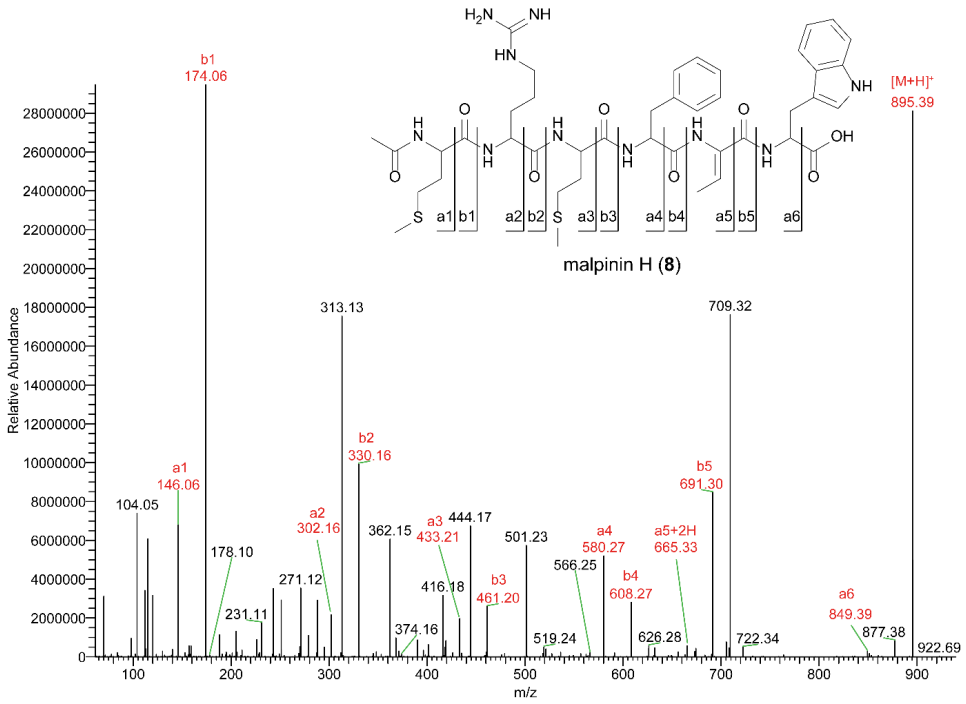

Figure S17. HR-ESI-MS/MS spectrum of 8.

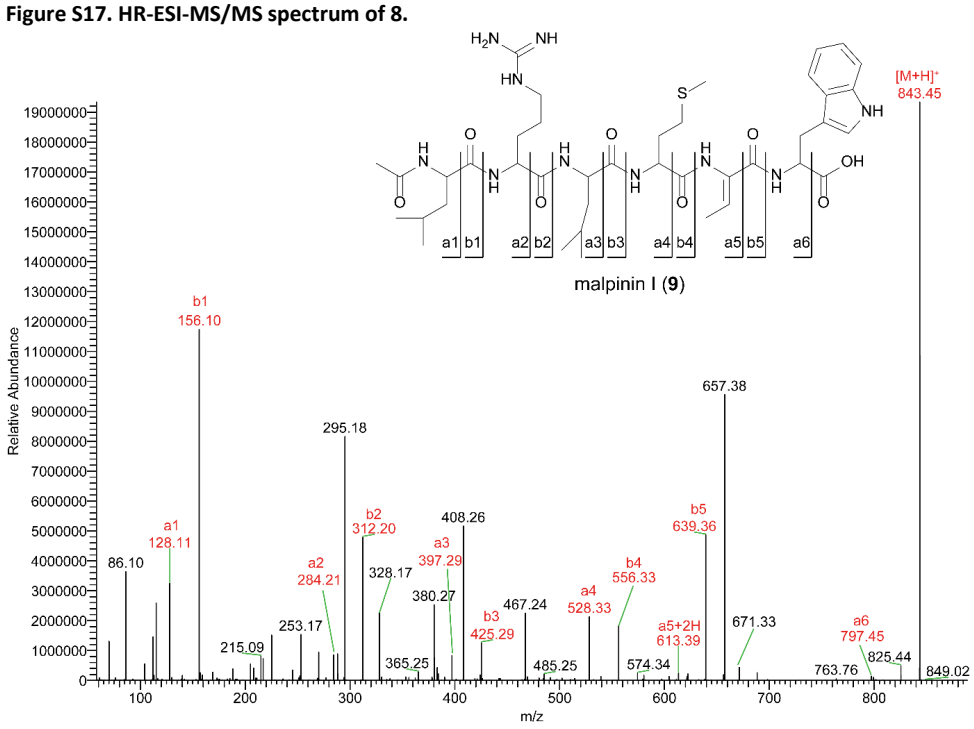

Figure S18. HR-ESI-MS/MS spectrum of 9.

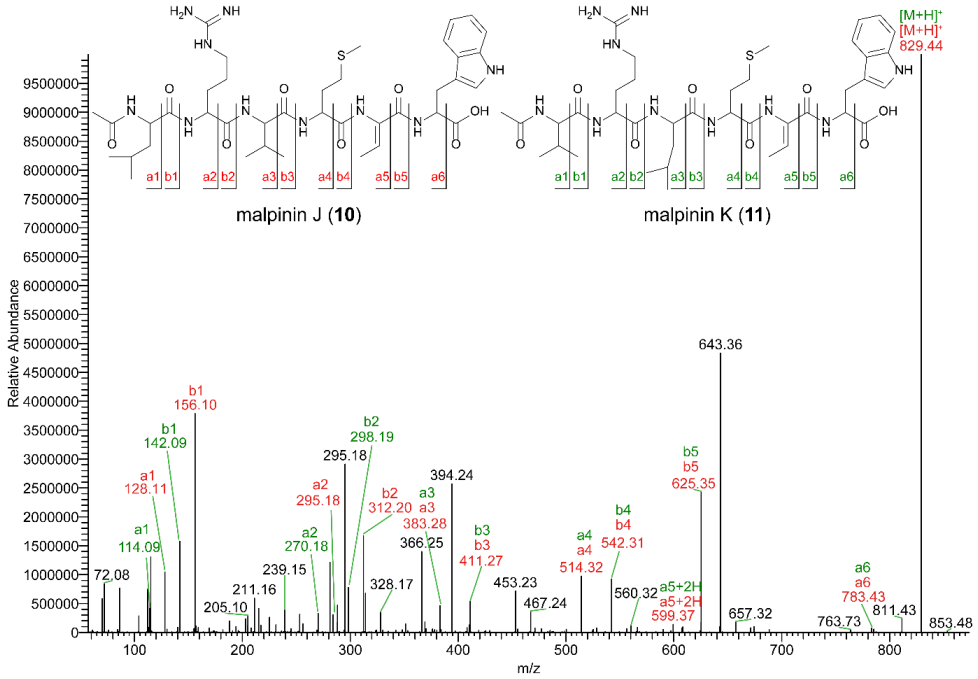

Figure S19. HR-ESI-MS/MS spectrum of the two coeluting isomers 10 and 11.

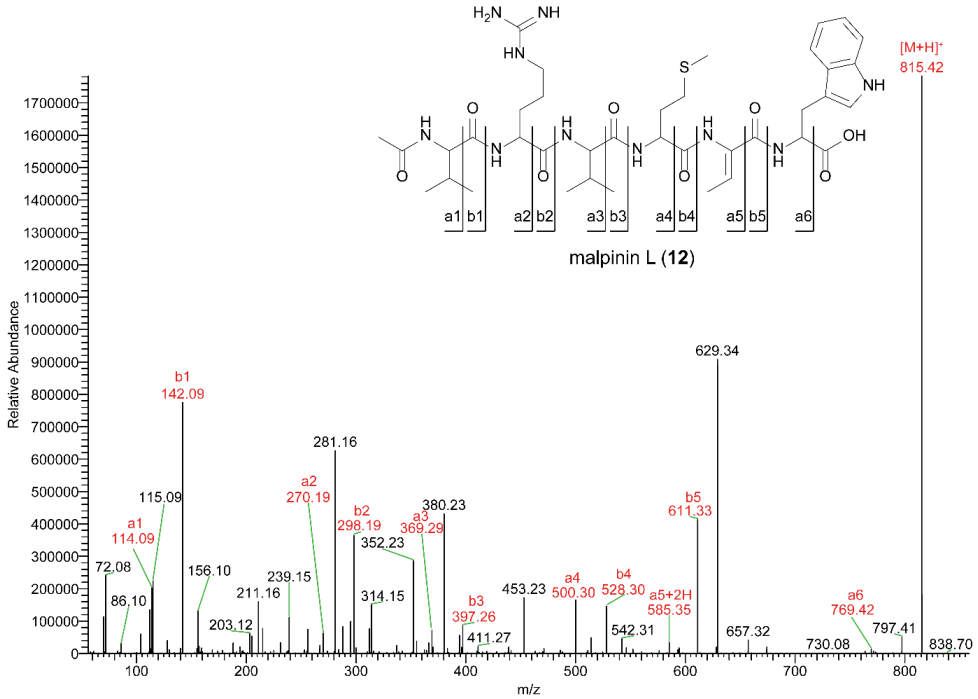

Figure S20. HR-ESI-MS/MS spectrum of 12.

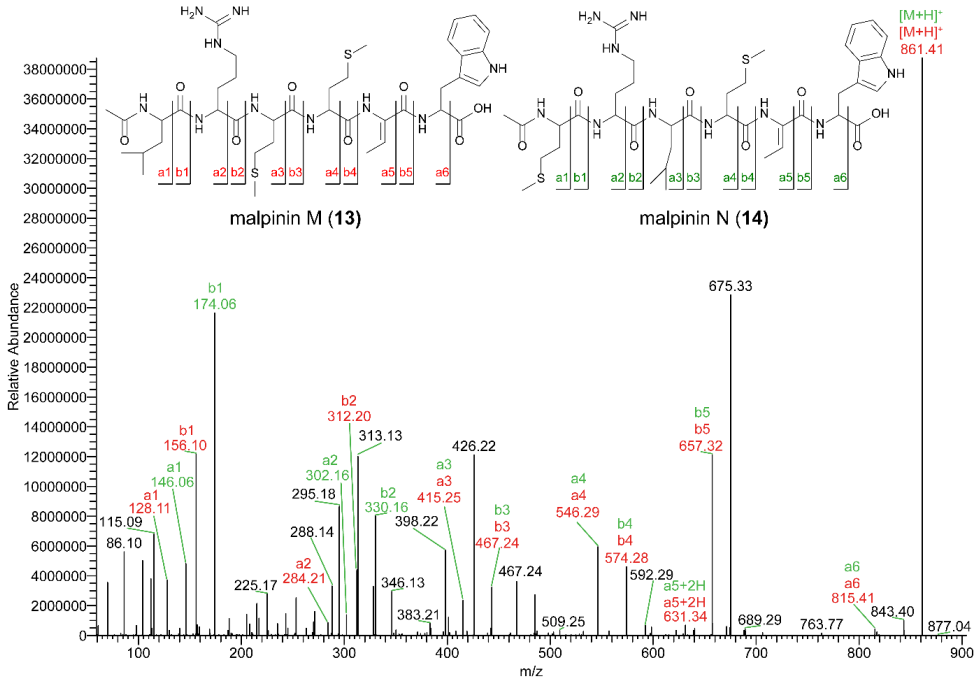

Figure S21. HR-ESI-MS/MS spectrum of the two coeluting isomers 13 and 14.

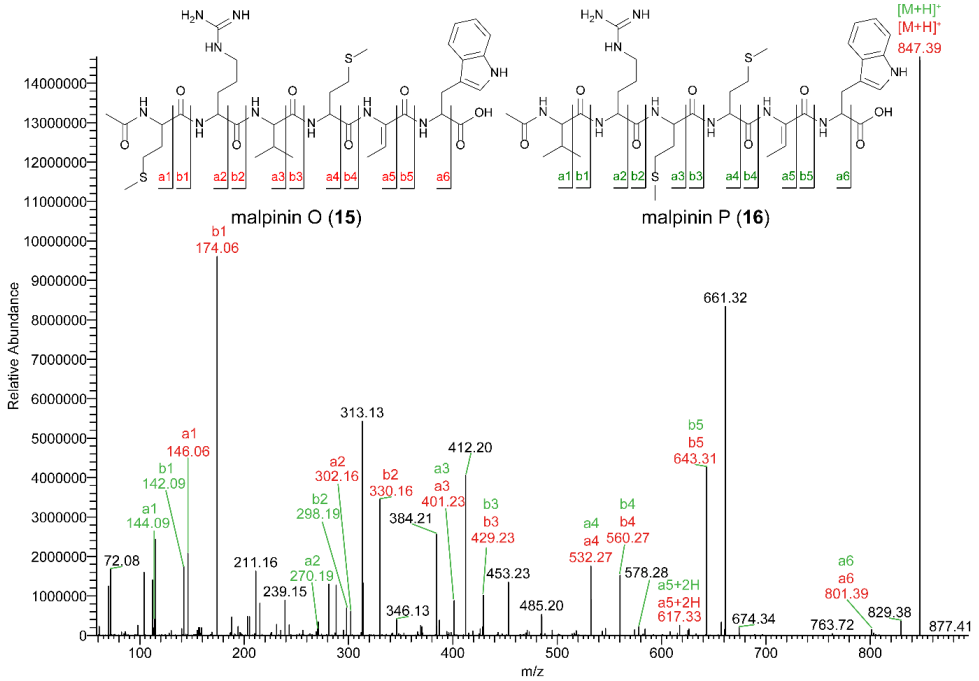

Figure S22. HR-ESI-MS/MS spectra of the two coeluting isomers 15 and 16.

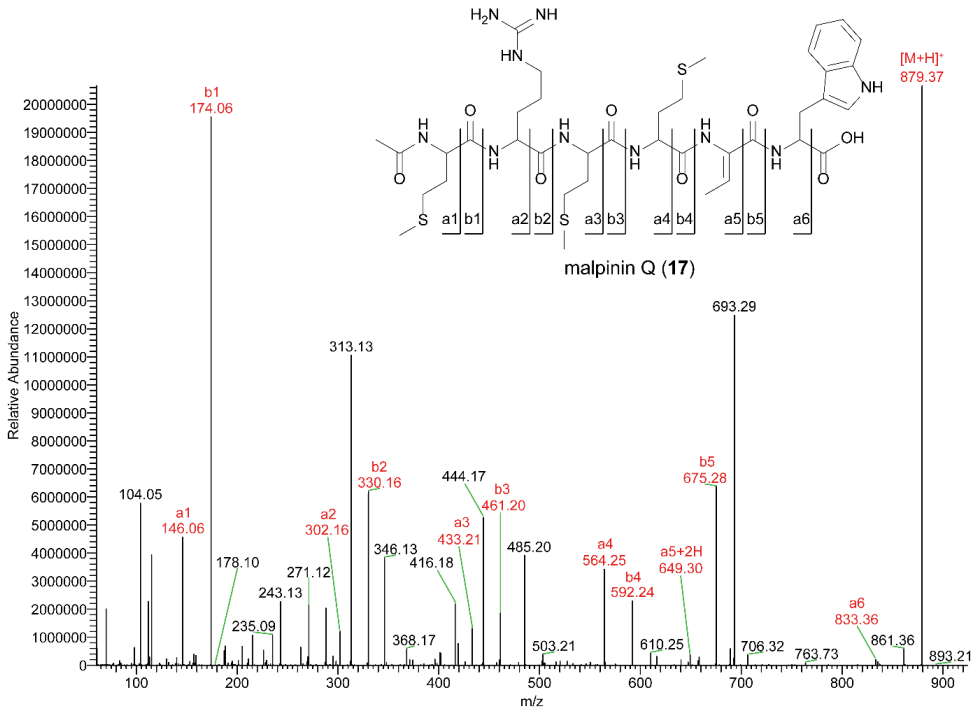

Figure S23. HR-ESI-MS/MS spectrum of 17.

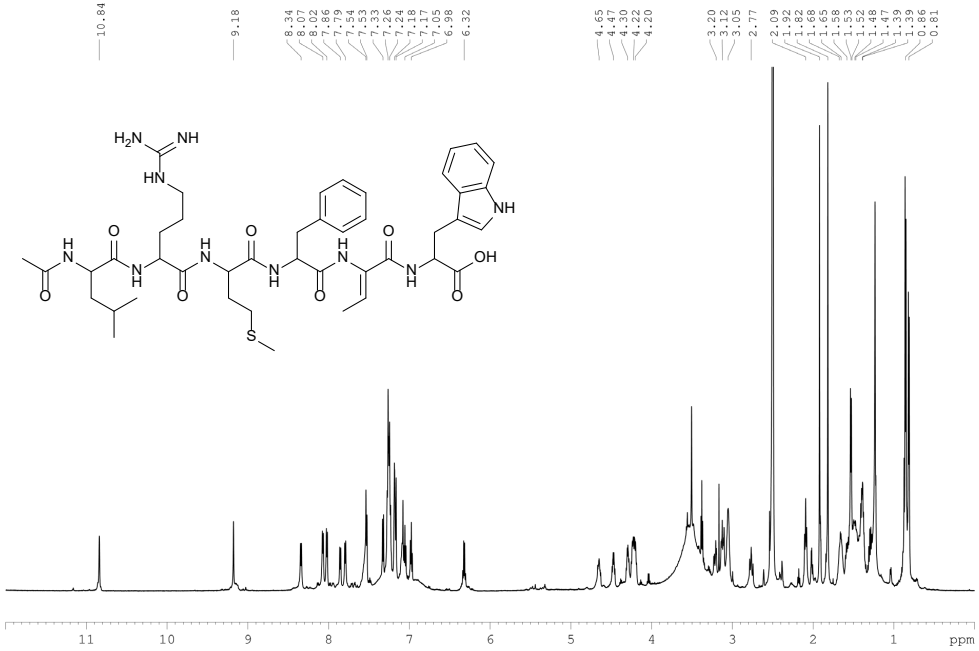

Figure S24. ^{1}H NMR spectrum of 6 in DMSO-d_6.

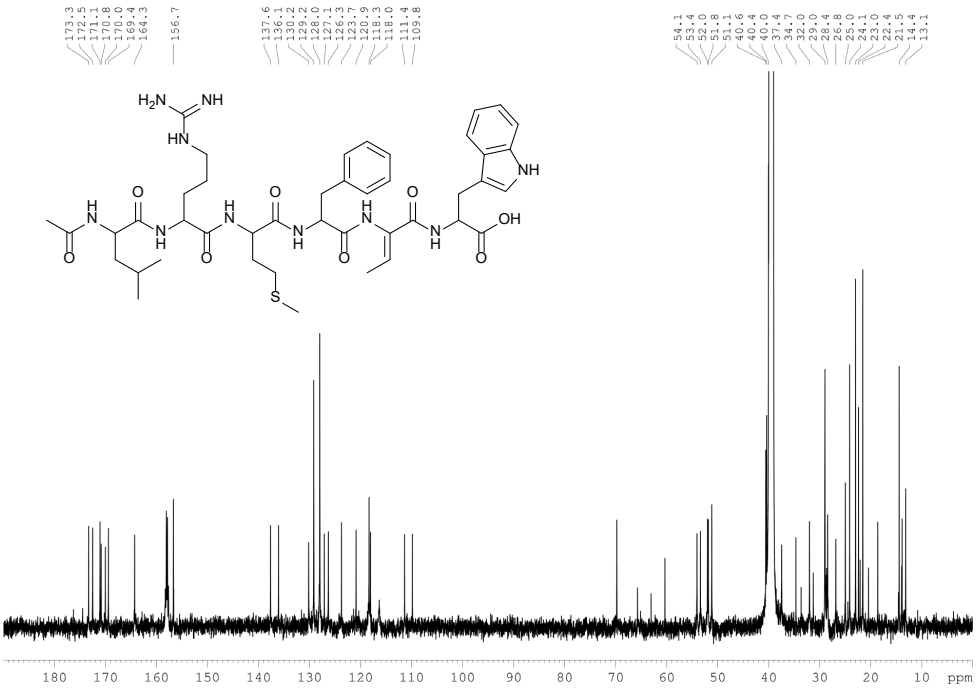

Figure S25. ^{13}C NMR spectrum of 6 in DMSO-d_6.

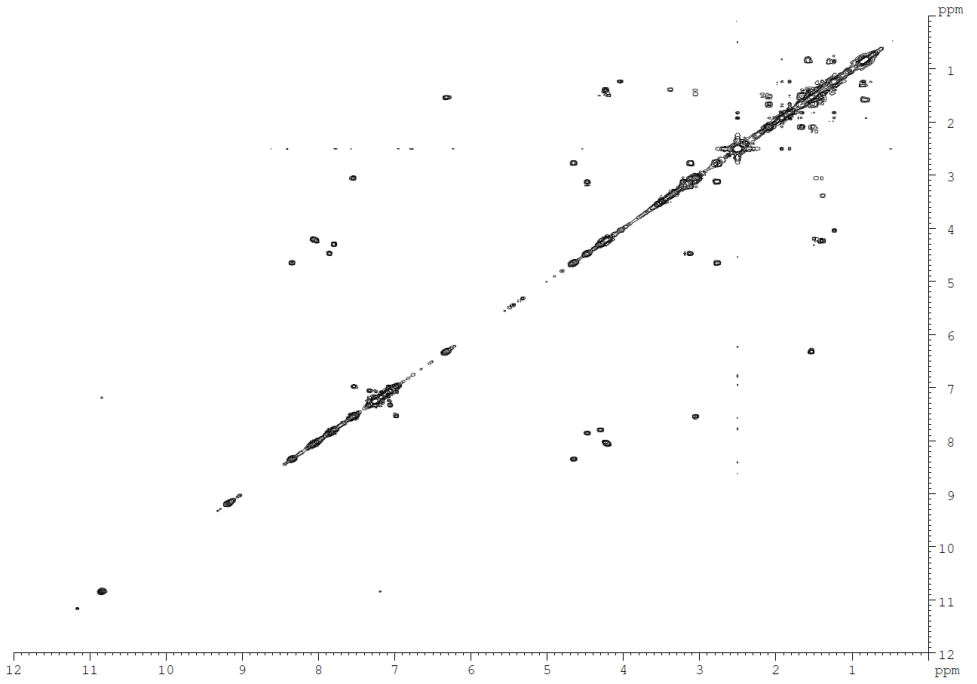

Figure S26. ^{1}H,^{1}H COSY NMR spectrum of 6 in DMSO-d_6.

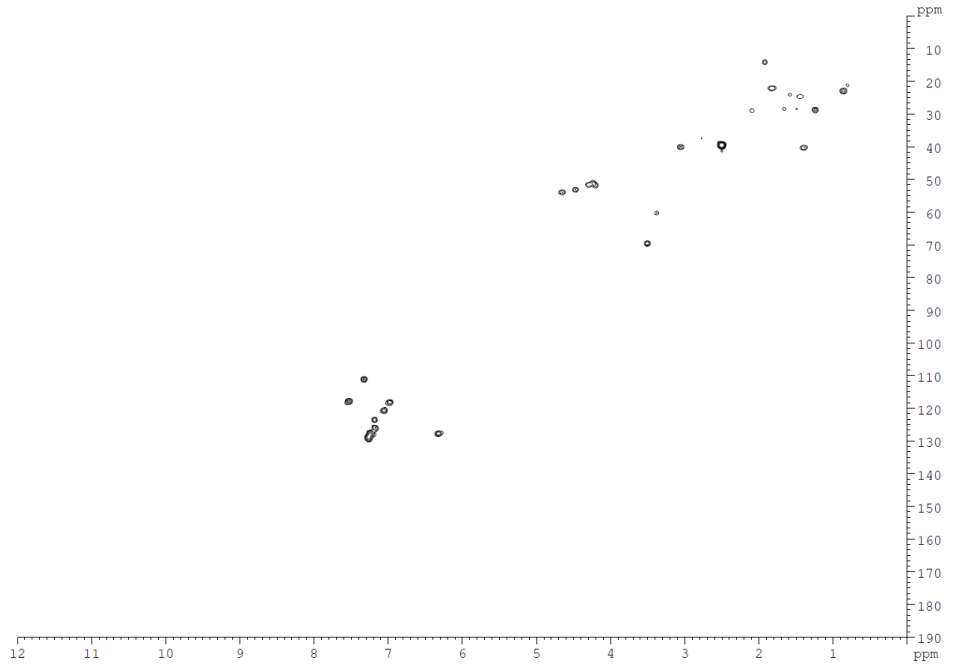

Figure S27. $^{1}H,^{13}C$ HSQC NMR spectrum of 6 in DMSO-d_6.

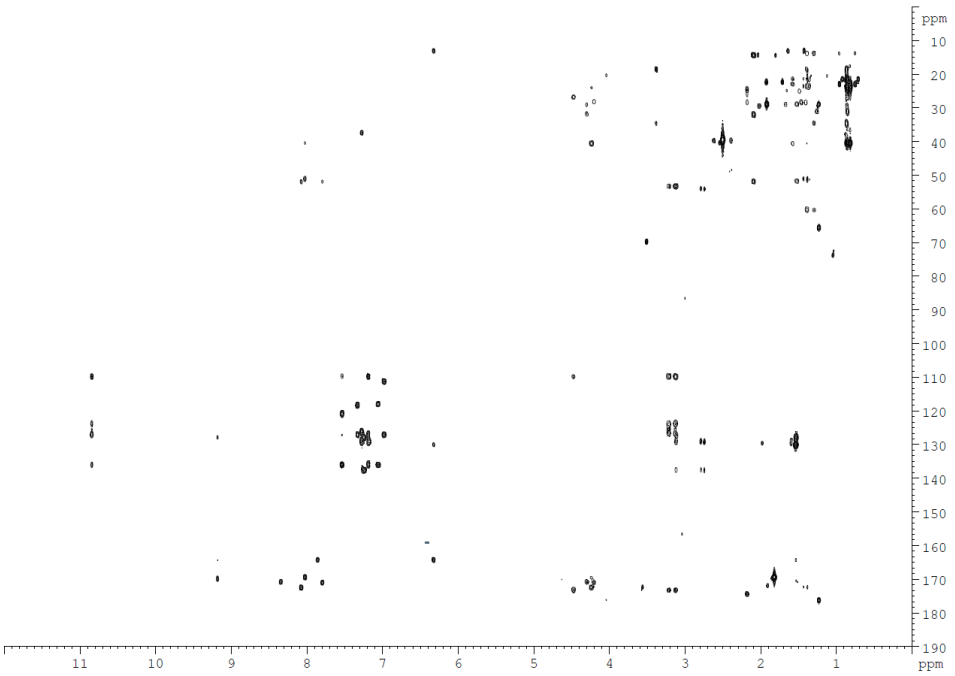

Figure S28. $^{1}H,^{13}C$ HMBC NMR spectrum of 6 in DMSO-d_6.

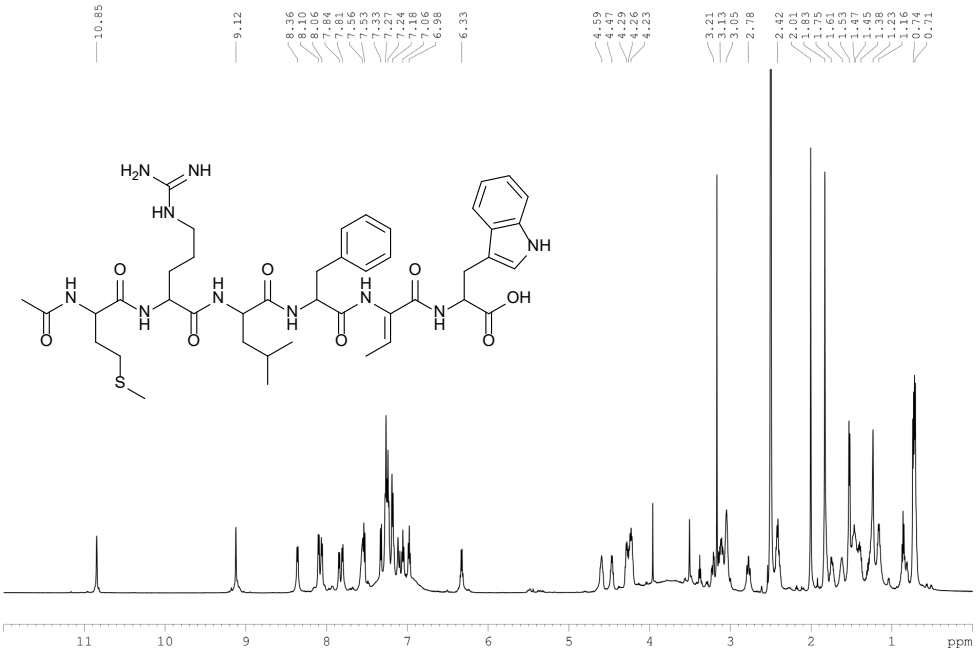

Figure S29. ^{1}H NMR spectrum of 7 in DMSO-d_6.

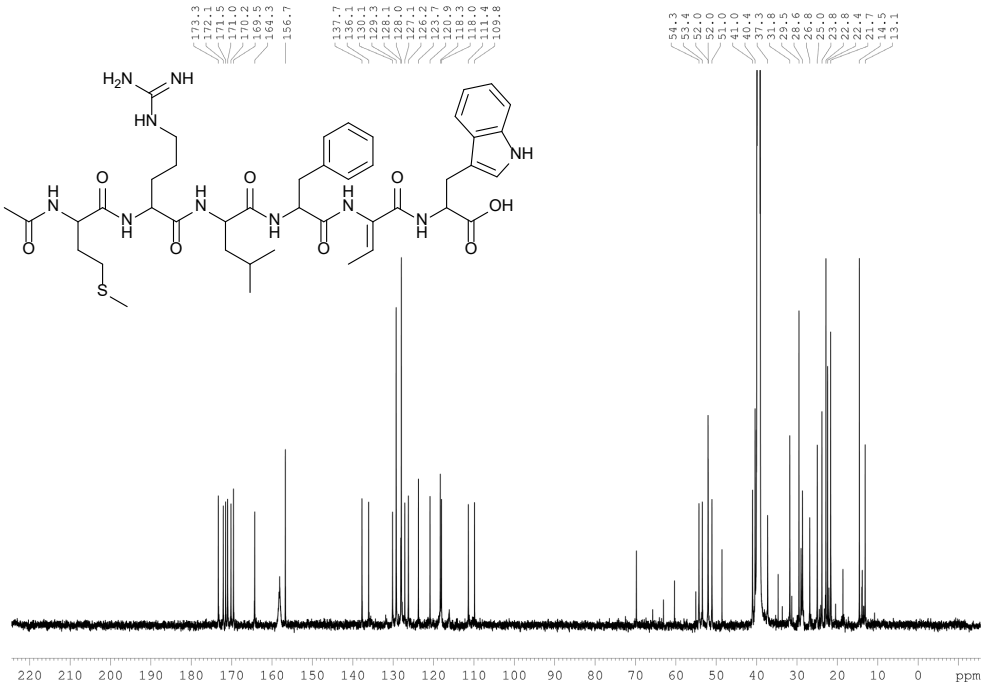

Figure S30. ^{13}C NMR spectrum of 7 in DMSO-d_6.

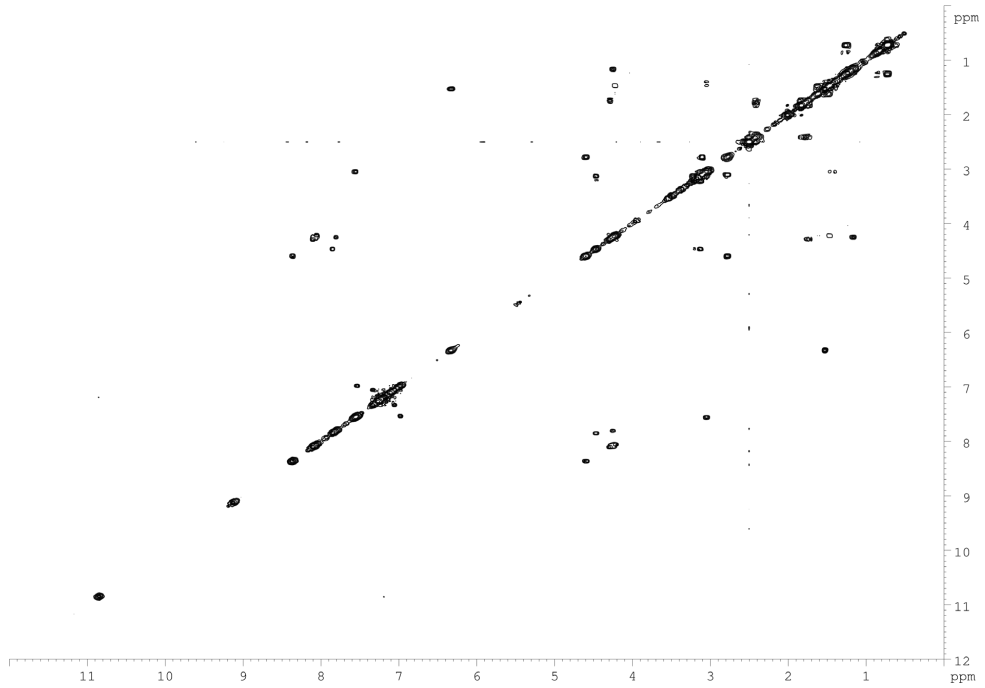

Figure S31. ^{1}H,^{1}H COSY NMR spectrum of 7 in DMSO-d_6.

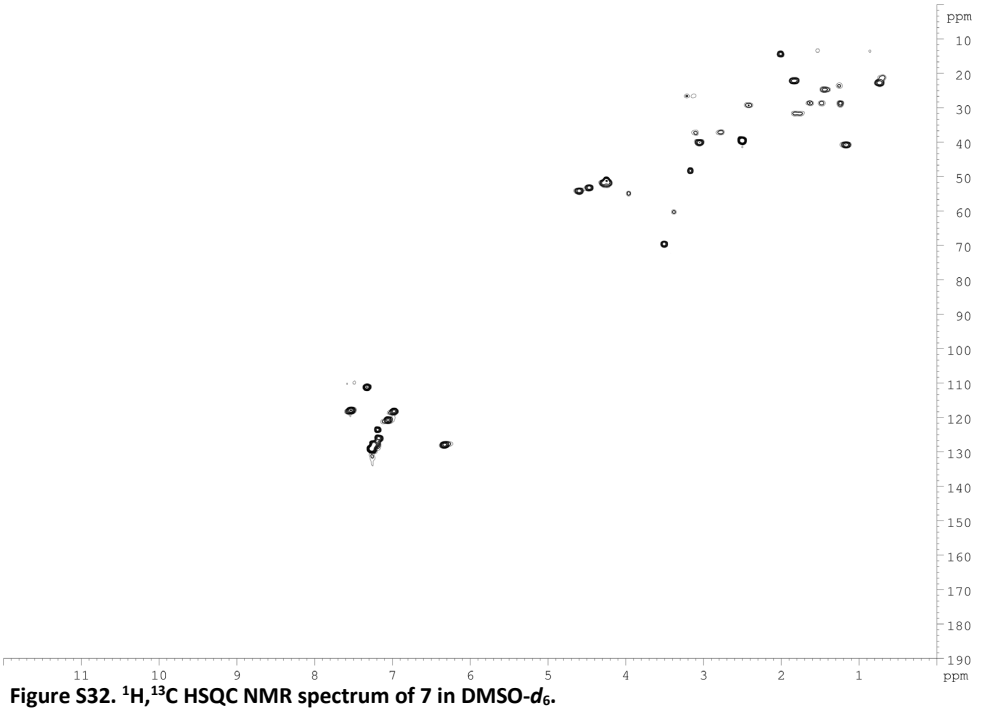

Figure S32. ^{1}H,^{13}C HSQC NMR spectrum of 7 in DMSO-d_6.

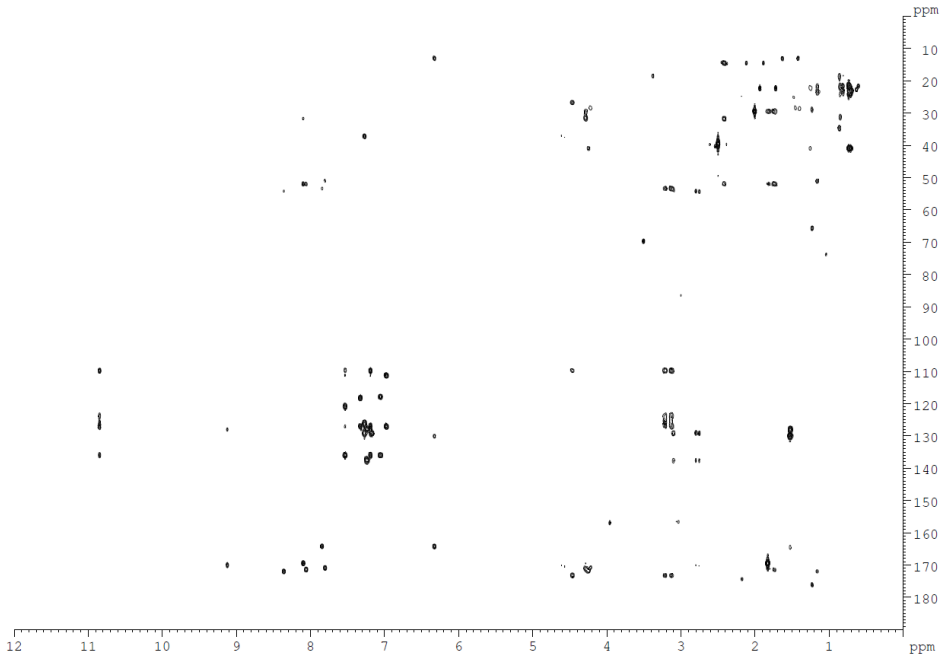

Figure S33. $^{1}H,^{13}C$ HMBC NMR spectrum of 7 in DMSO-d_6.

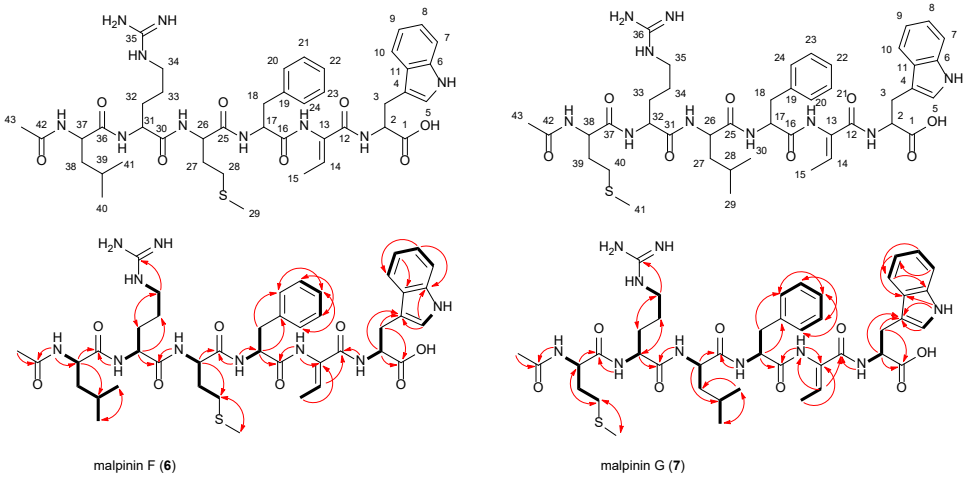

Figure S34. Carbon numbering, COSY and HMBC correlation of 6 and 7. COSY key correlations and HMBC key correlations are indicated as bold lines and red arrows, respectively.

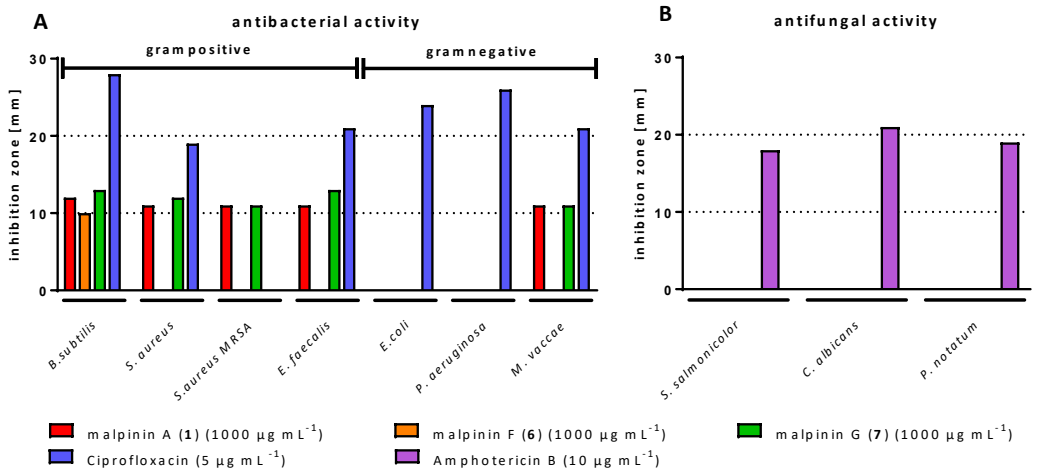

Figure S35. Antimicrobial activities of 1, 6 and 7. Metabolites were tested against bacteria (**A**) and fungi (**B**) using ciprofloxacin or amphotericin B as positive controls.

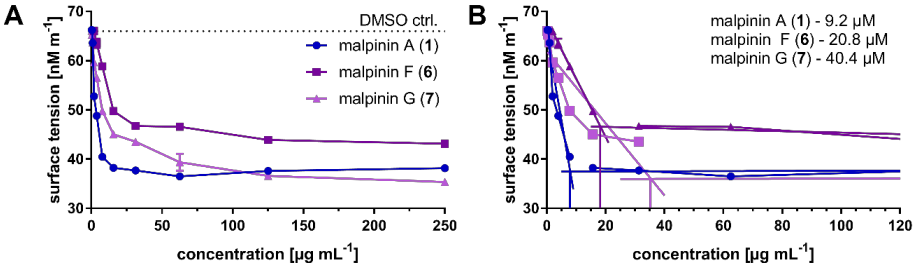

Figure S36. Surface tension lowering activity of 1, 6 and 7. Surface tension reducing activity of pure **1, 6** and **7** in comparison to 10% DMSO which was used as solvent. Error bars represents the standard error of the mean (SEM). **B**. Determination of the critical micelle concentration (CMC) by point of intersection of linear regression of plateau and lowering range.

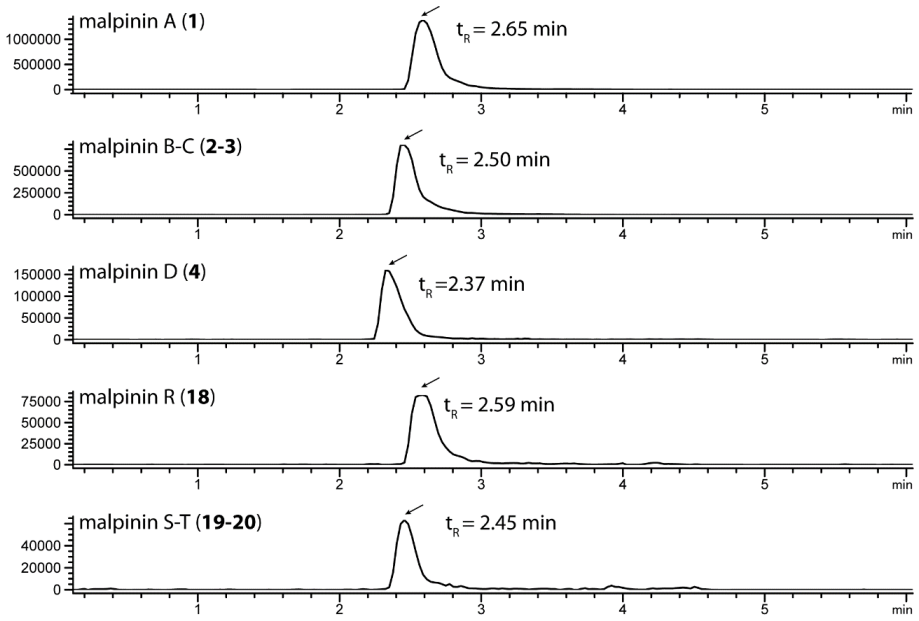

Figure S37. Extracted ion chromatograms (EICs) of metabolite extracts from cultures supplemented with L-tryptophan, recorded by UHPLC method B (Table S16).

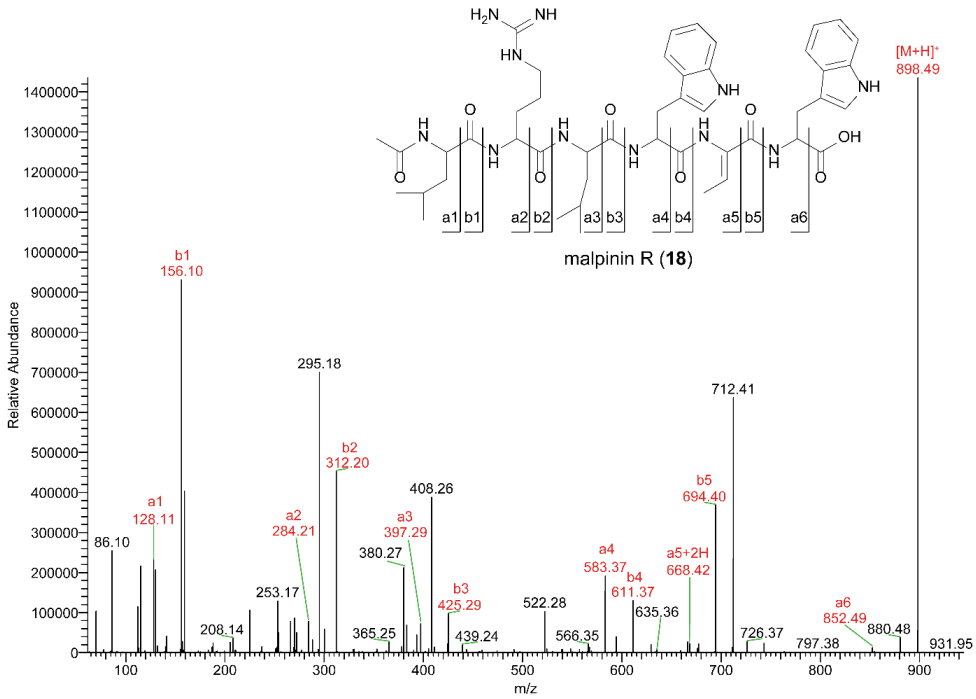

Figure S38. HR-ESI-MS/MS spectrum of 18.

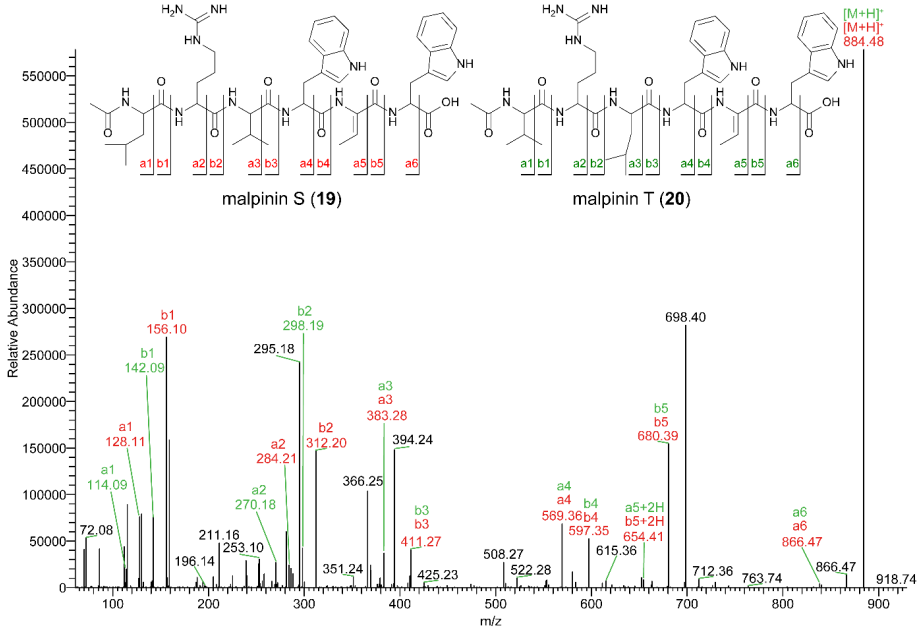

Figure S39. HR-ESI-MS/MS spectrum of the two coeluting isomers 19 and 20.

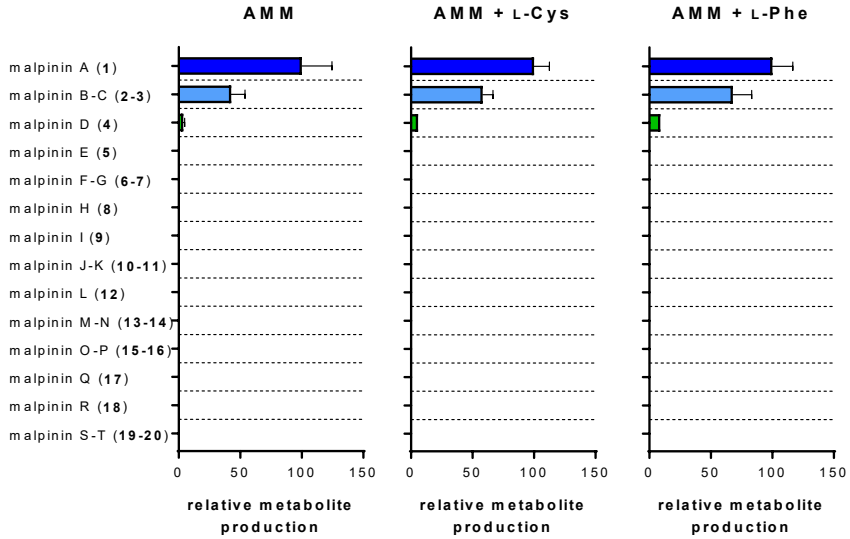

Figure S40. Quantification of malpinins in *M. alpina* cultures by UHPLC-MS. AMM medium was supplemented with 5 mM amino acids. Note that the metabolic profile did not change regardless of the supplementation.

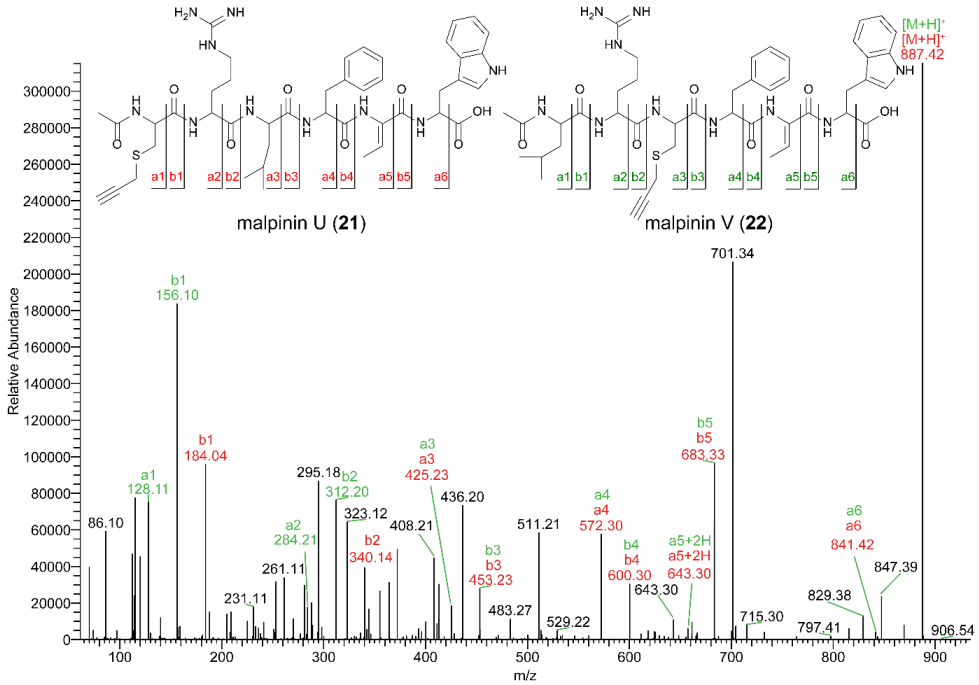

Figure S41. HR-ESI-MS/MS spectrum of the two coeluting isomers 21 and 22.

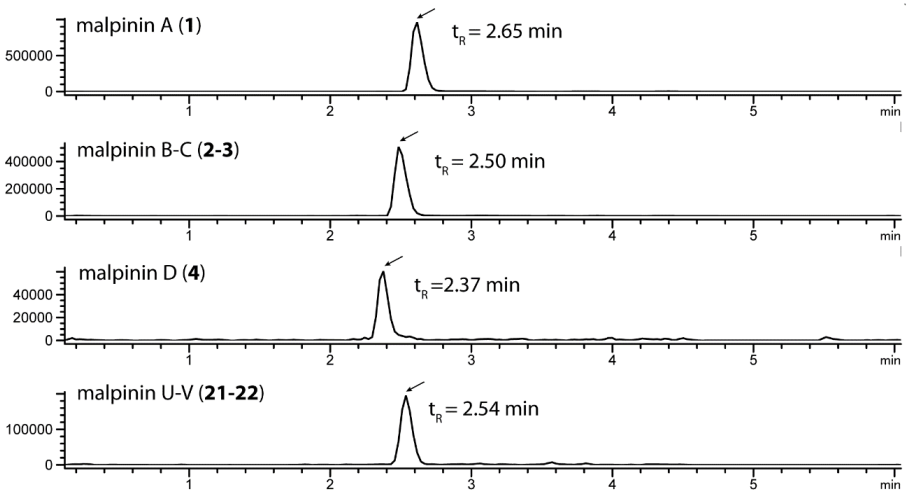

Figure S42. Extracted ion chromatograms (EICs) of metabolite extracts from cultures supplemented with S-propargyl-L-cysteine, recorded by UHPLC method B (Table S16).

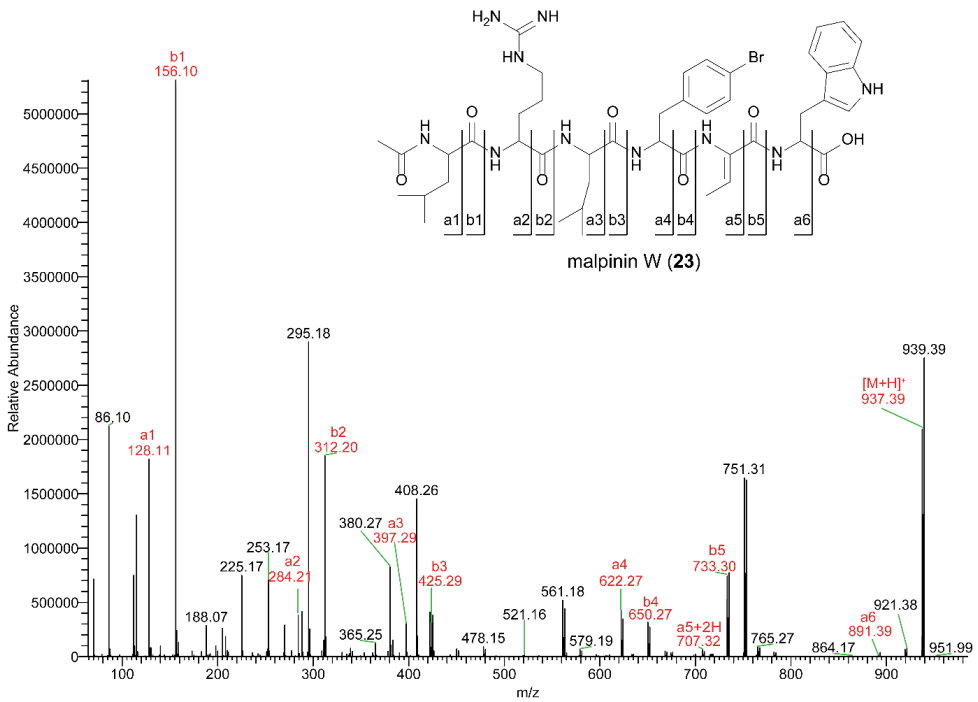

Figure S43. HR-ESI-MS/MS spectrum of 23.

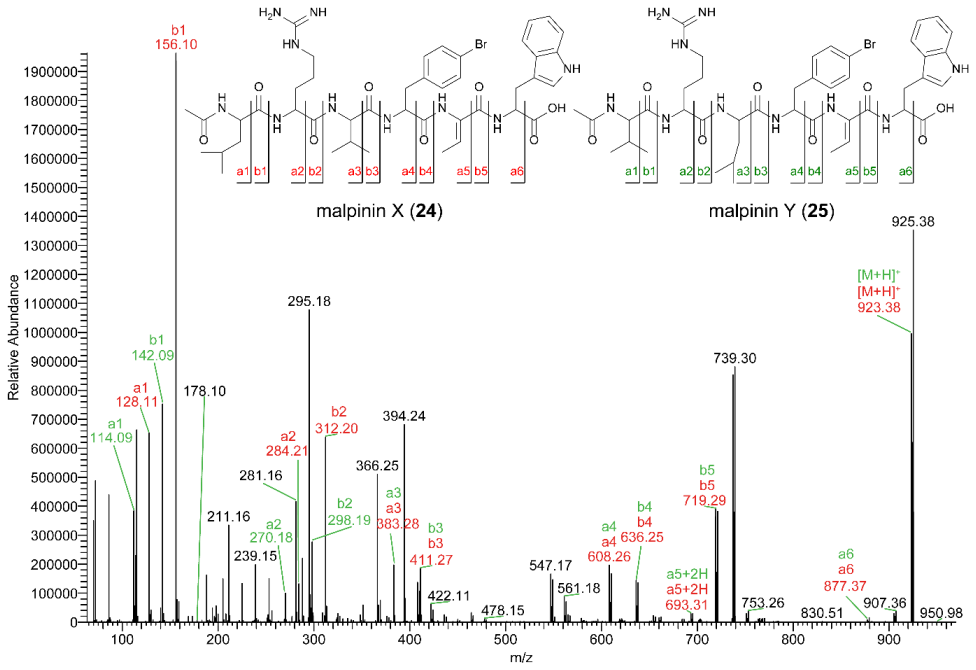

Figure S44. HR-ESI-MS/MS spectrum of the two coeluting isomers 24 and 25.

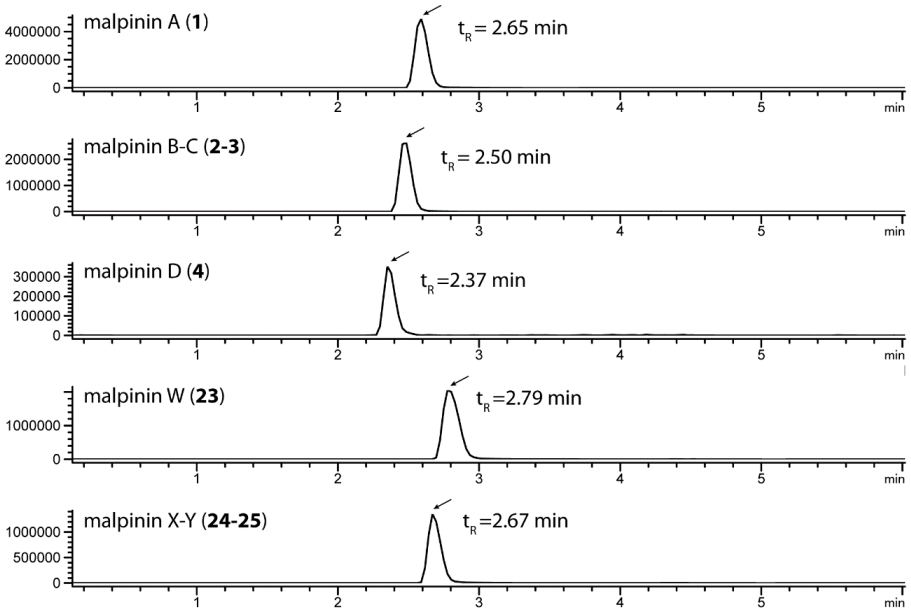

Figure S45. Extracted ion chromatograms (EICs) of metabolite extracts from cultures supplemented with 4-bromo-L-phenylalanine, recorded by UHPLC method B (Table S16).

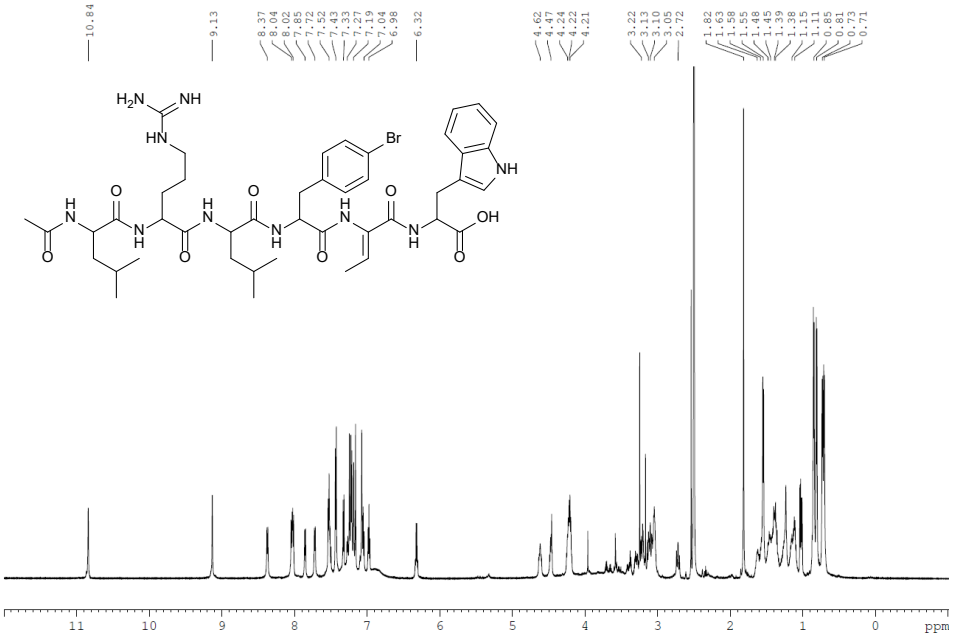

Figure S46. ^{1}H NMR spectrum of 23 in DMSO-d_6.

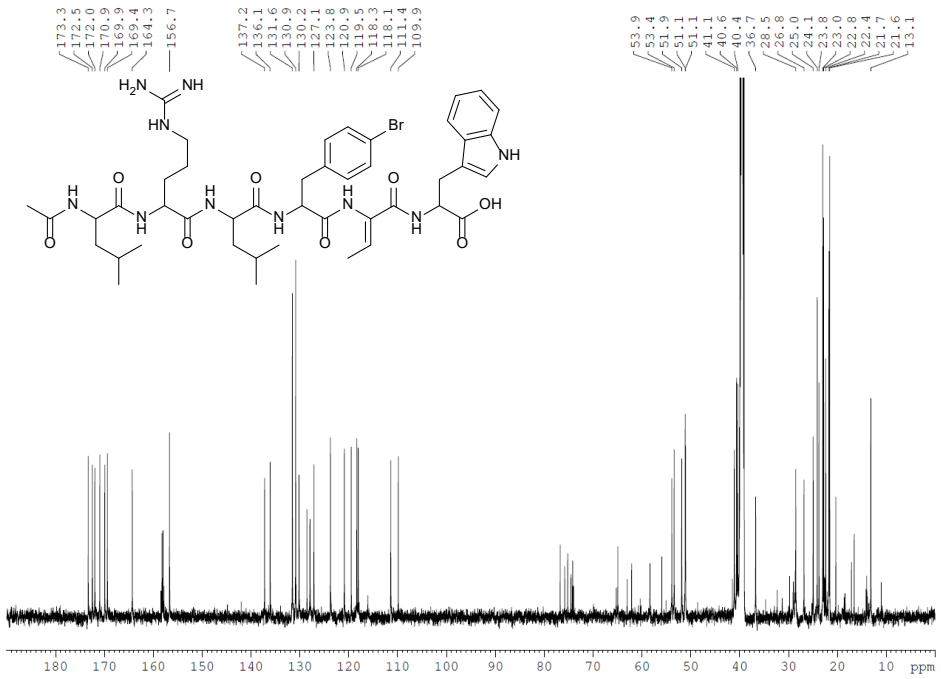

Figure S47. ^{13}C NMR spectrum of 23 in DMSO-d_6.

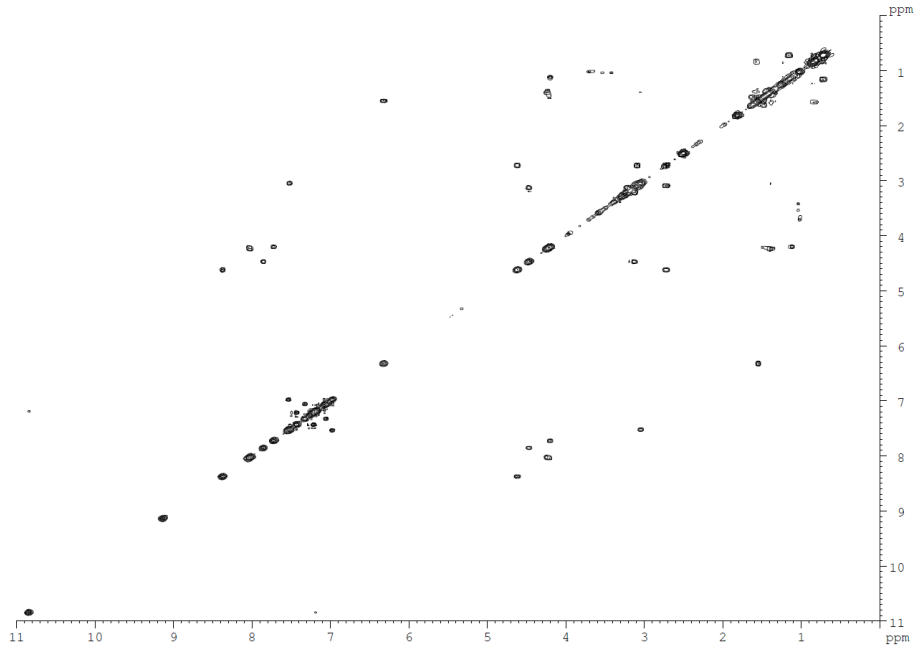

Figure S48. ^{1}H,^{1}H COSY NMR spectrum of 23 in DMSO-d_6.

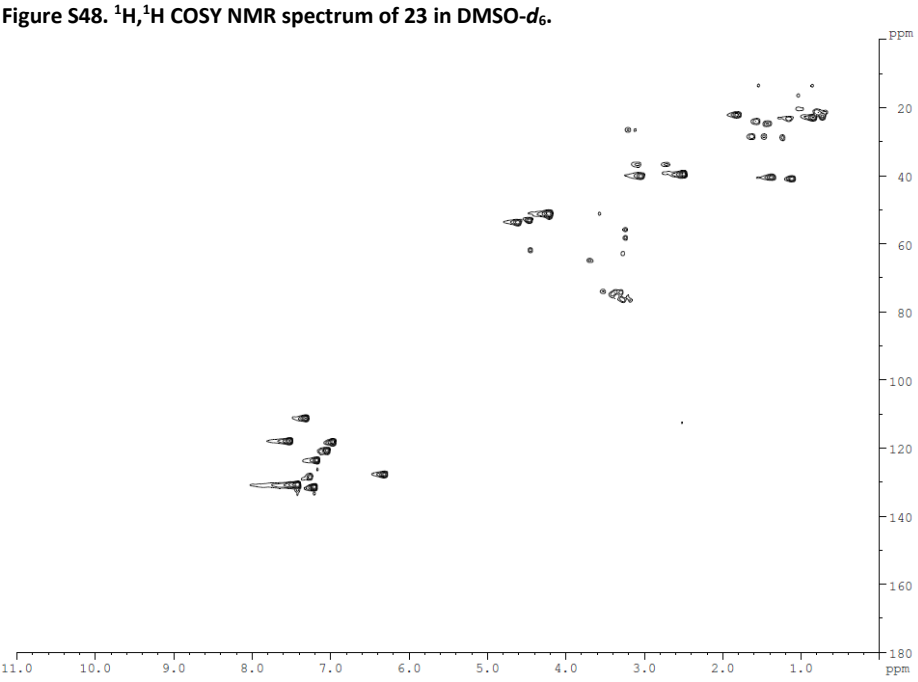

Figure S49. ^{1}H,^{13}C HSQC NMR spectrum of 23 in DMSO-d_6.

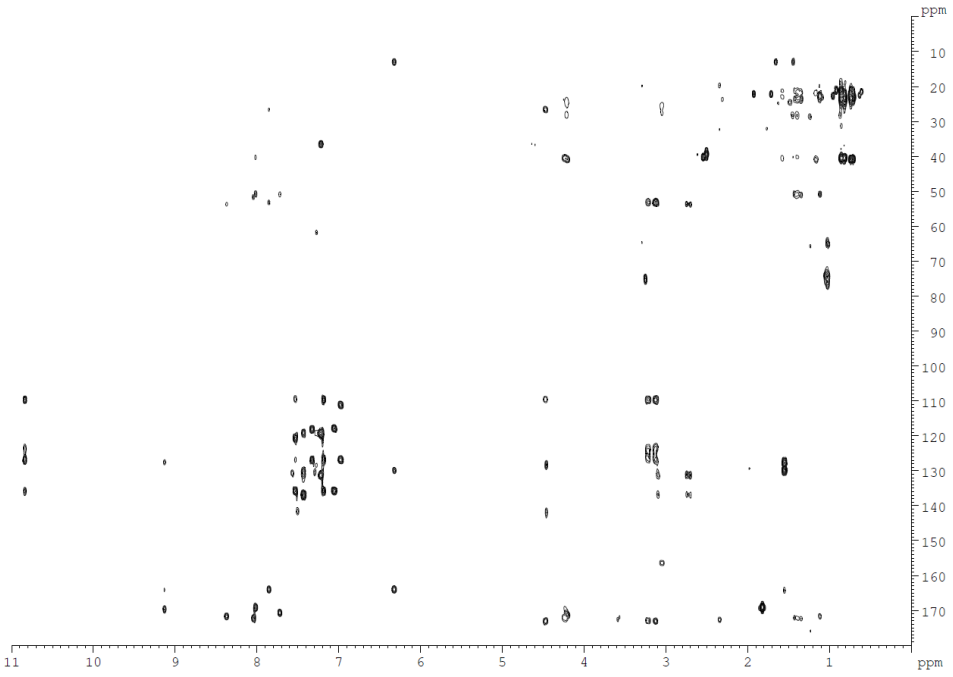

Figure S50. $^{1}H,^{13}C$ HMBC NMR spectrum of 23 in DMSO-d_6.

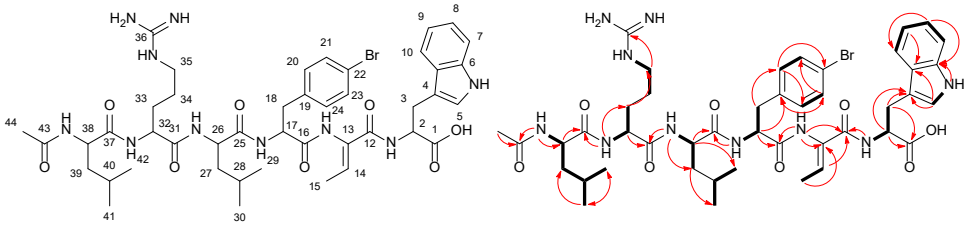

Figure S51. Carbon numbering, COSY and HMBC correlation of malpinin W (23). COSY key correlations and HMBC key correlations are indicated as bold lines and red arrows, respectively.

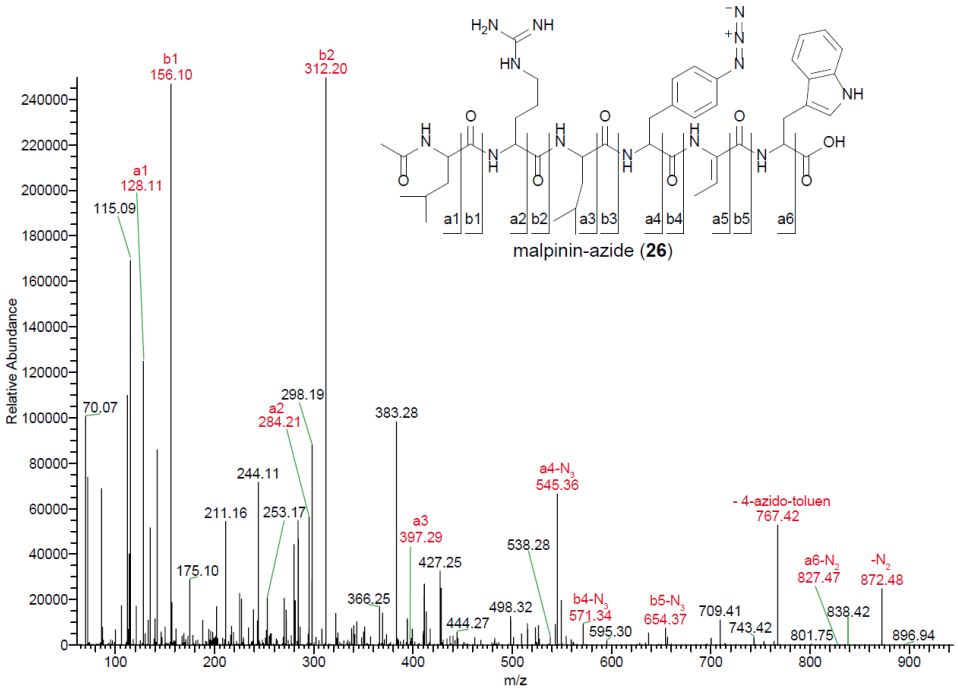

Figure S52. HR-ESI-MS/MS spectrum of 26.

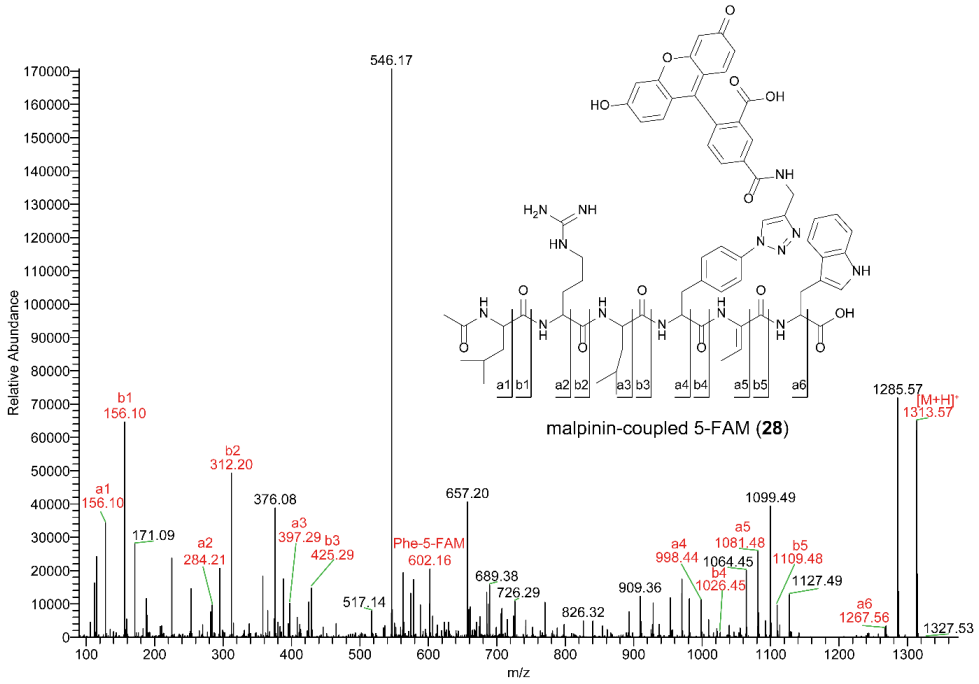

Figure S53. HR-ESI-MS/MS spectrum of 27.

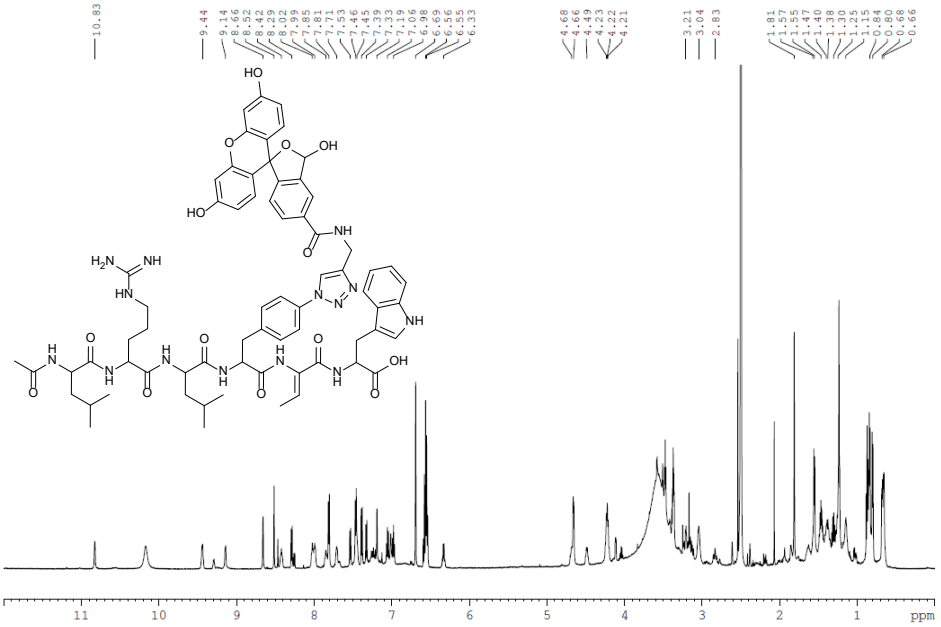

Figure S54. ^{1}H NMR spectrum of 27 in DMSO-d_6.

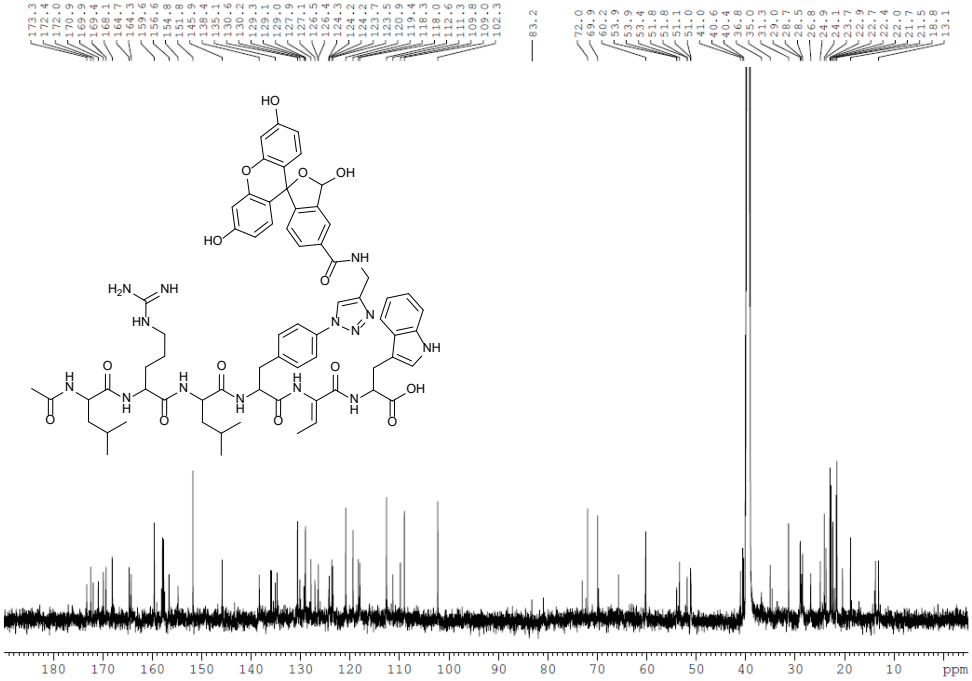

Figure S55. 13C NMR spectrum of 27 in DMSO-d_6.

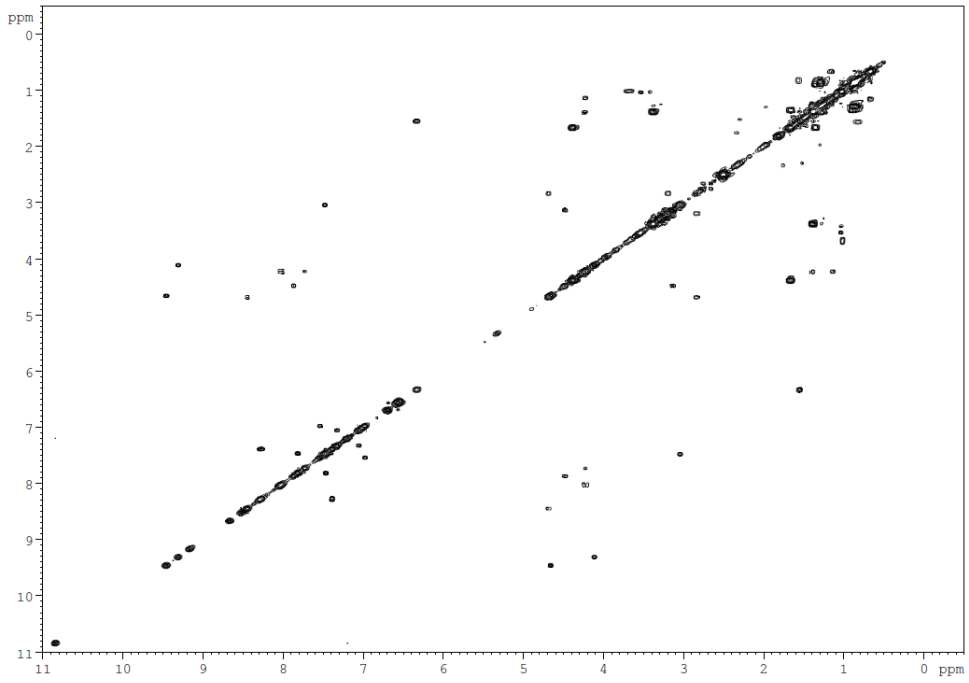

Figure S56. ^{1}H,^{1}H COSY NMR spectrum of 27 in DMSO-d_6.

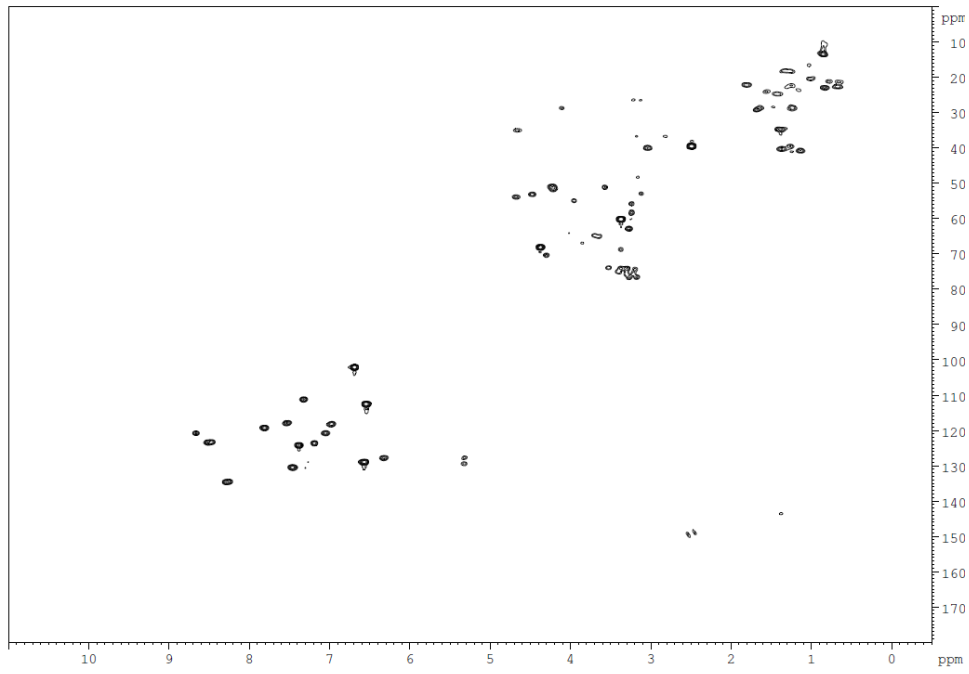

Figure S57. ^{1}H,^{13}C HSQC NMR spectrum of 27 in DMSO-d_6.

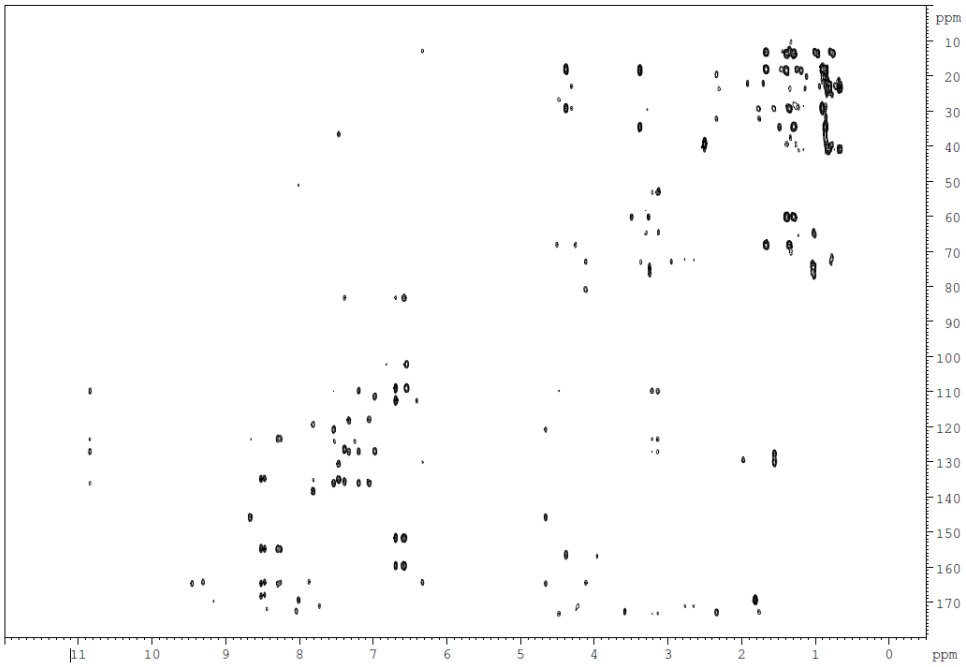

Figure S58. $^{1}H,^{13}C$ HMBC NMR spectrum of 27 in DMSO-d_6.

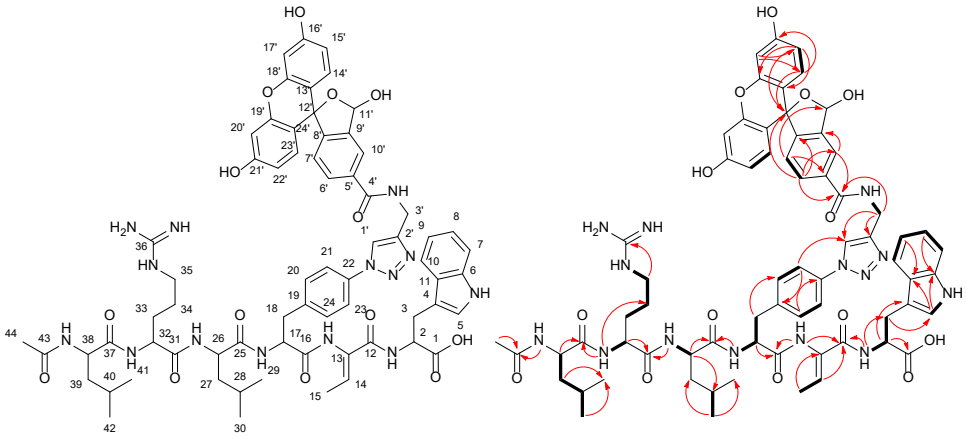

Figure S59. Carbon numbering, COSY and HMBC correlation of malpinin-5-FAM (27). COSY key correlations and HMBC key correlations are indicated as bold lines and red arrows, respectively.

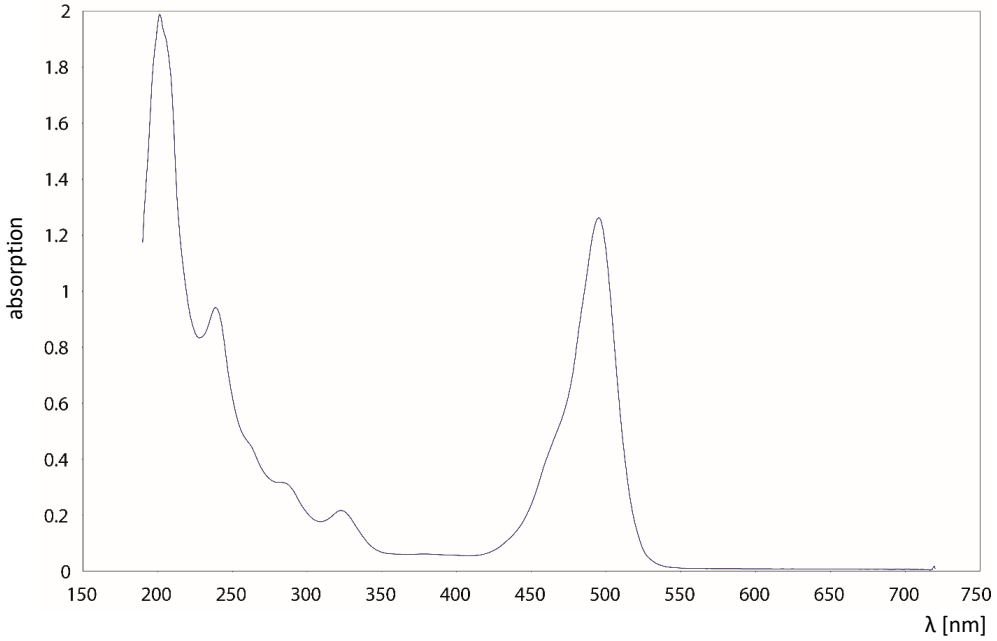

Figure S60. UV/Vis spectrum of 27 in H_2O.

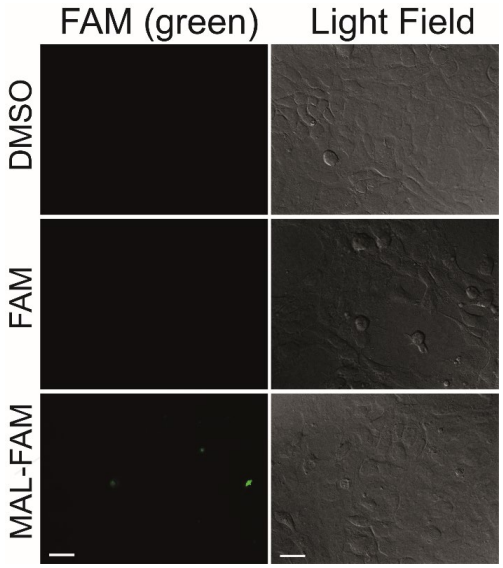

Figure S61. Fluorescence microscopy of HEK-cells. HEK-293-cells (1 x 10^6) were incubated with 30 µM fluorescein (FAM), malpinin-coupled FAM (MAL-FAM, **27**) or DMSO (0.1%) as vehicle for 1 h at 37 °C. Pictures are representative images from n = 3. Scale bar is 10 µm.

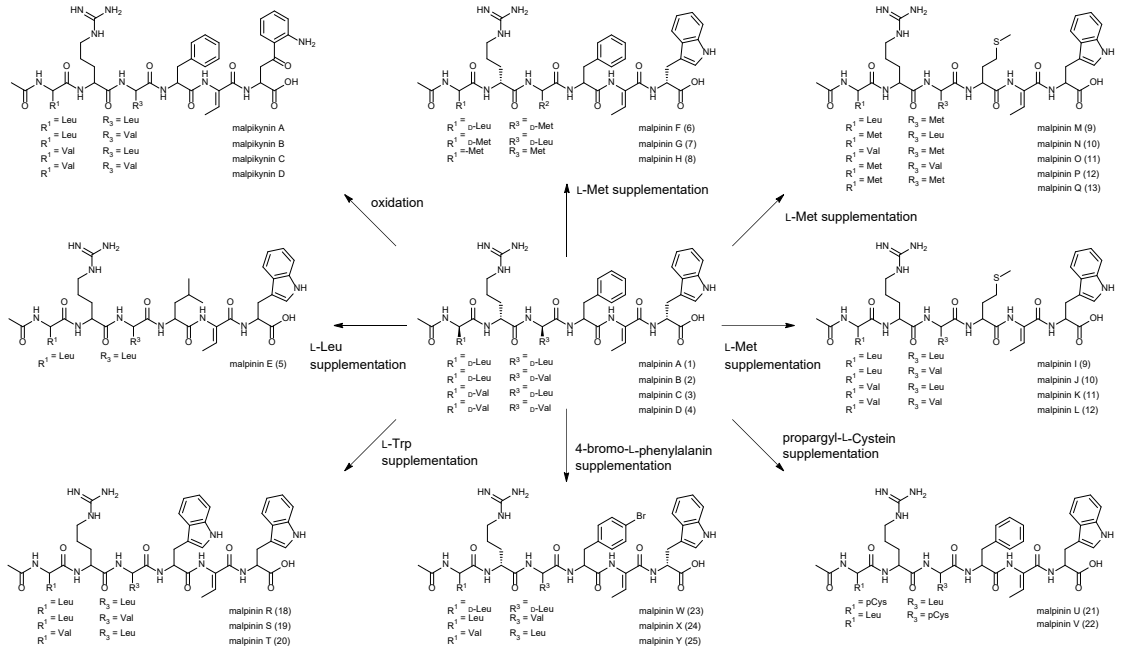

Figure S62. Malpinin A-related metabolites synthesised by MalA.

References

1. S. Koren, B. P. Walenz, K. Berlin, J. R. Miller, N. H. Bergman and A. M. Phillippy, *Genome Res.*, 2017, **27**, 722-736.
2. S. Koren, A. Rhie, B. P. Walenz, A. T. Dilthey, D. M. Bickhart, S. B. Kingan, S. Hiendleder, J. L. Williams, T. P. L. Smith and A. M. Phillippy, *Nat. Biotechnol.*, 2018, **36**, 1174-1182.
3. I. V. Grigoriev, R. Nikitin, S. Haridas, A. Kuo, R. Ohm, R. Otillar, R. Riley, A. Salamov, X. Zhao, F. Korzeniewski, T. Smirnova, H. Nordberg, I. Dubchak and I. Shabalov, *Nucleic Acids Res.*, 2014, **42**, 699-704.
4. L. Wang, W. Chen, Y. Feng, Y. Ren, Z. Gu, H. Chen, H. Wang, M. J. Thomas, B. Zhang, I. M. Berquin, Y. Li, J. Wu, H. Zhang, Y. Song, X. Liu, J. S. Norris, S. Wang, P. Du, J. Shen, N. Wang, Y. Yang, W. Wang, L. Feng, C. Ratledge, H. Zhang and Y. Q. Chen, *PLoS One*, 2011, **6**, e28319.
5. R. R. Wick, L. M. Judd and K. E. Holt, *Genome Biol.*, 2019, **20**, e129.
6. H. Li, *Bioinformatics*, 2018, **34**, 3094-3100.
7. H. Li, B. Handsaker, A. Wysoker, T. Fennell, J. Ruan, N. Homer, G. Marth, G. Abecasis, R. Durbin and S. Genome Project Data Processing, *Bioinformatics*, 2009, **25**, 2078-2079.
8. N. J. Loman, J. Quick and J. T. Simpson, *Nat. Methods*, 2015, **12**, 733-735.
9. M. Stanke and B. Morgenstern, *Nucleic Acids Res.*, 2005, **33**, 465-467.
10. M. Manni, M. R. Berkeley, M. Seppey, F. A. Simao and E. M. Zdobnov, *Mol. Biol. Evol.*, 2021, **38**, 4647-4654.
11. K. Blin, S. Shaw, K. Steinke, R. Villebro, N. Ziemert, S. Y. Lee, M. H. Medema and T. Weber, *Nucleic Acids Res.*, 2019, **47**, 81-87.
12. S. El-Gebali, J. Mistry, A. Bateman, S. R. Eddy, A. Luciani, S. C. Potter, M. Qureshi, L. J. Richardson, G. A. Salazar, A. Smart, E. L. L. Sonnhammer, L. Hirsh, L. Paladin, D. Piovesan, S. C. E. Tosatto and R. D. Finn, *Nucleic Acids Res.*, 2019, **47**, 427-432.
13. M. A. Larkin, G. Blackshields, N. P. Brown, R. Chenna, P. A. McGettigan, H. McWilliam, F. Valentin, I. M. Wallace, A. Wilm, R. Lopez, J. D. Thompson, T. J. Gibson and D. G. Higgins, *Bioinformatics*, 2007, **23**, 2947-2948.
14. M. M. Bradford, *Anal. Biochem.*, 1976, **72**, 248-254.
15. D. E. Ehmann, J. W. Trauger, T. Stachelhaus and C. T. Walsh, *Chem. Biol.*, 2000, **7**, 765-772.
16. L. Zhong, X. Diao, N. Zhang, F. Li, H. Zhou, H. Chen, X. Bai, X. Ren, Y. Zhang, D. Wu and X. Bian, *Nat Commun*, 2021, **12**, 296.
17. O. Werz, J. Gerstmeier, S. Libreros, X. De la Rosa, M. Werner, P. C. Norris, N. Chiang and C. N. Serhan, *Nat Commun*, 2018, **9**, 1-12.
18. M. Werner, P. M. Jordan, E. Romp, A. Czapka, Z. Rao, C. Kretzer, A. Koeberle, U. Garscha, S. Pace, H. E. Claesson, C. N. Serhan, O. Werz and J. Gerstmeier, *FASEB J.*, 2019, **33**, 6140-6153.
19. J. M. Wurlitzer, A. Stanišić, I. Wasmuth, S. Jungmann, D. Fischer, H. Kries and M. Gressler, *Appl. Environ. Microbiol.*, 2021, **87**.
20. J. Jumper, R. Evans, A. Pritzel, T. Green, M. Figurnov, O. Ronneberger, K. Tunyasuvunakool, R. Bates, A. Zidek, A. Potapenko, A. Bridgland, C. Meyer, S. A. A. Kohl, A. J. Ballard, A. Cowie, B. Romera-Paredes, S. Nikolov, R. Jain, J. Adler, T. Back, S. Petersen, D. Reiman, E. Clancy, M. Zielinski, M. Steinegger, M. Pacholska, T. Berghammer, S. Bodenstein, D. Silver, O. Vinyals, A. W. Senior, K. Kavukcuoglu, P. Kohli and D. Hassabis, *Nature*, 2021, **596**, 583-589.
21. E. Conti, T. Stachelhaus, M. A. Marahiel and P. Brick, *EMBO J.*, 1997, **16**, 4174-4183.
22. X. Bian, A. Plaza, F. Yan, Y. Zhang and R. Müller, *Biotechnol. Bioeng.*, 2015, **112**, 1343-1353.
23. D. F. Ackerley, T. T. Caradoc-Davies and I. L. Lamont, *J. Bacteriol.*, 2003, **185**, 2848-2855.
24. T. Thongkongkaew, W. Ding, E. Bratovanov, E. Oueis, A. A. M. A. Garci, N. Zaburannyi, K. Harmrolfs, Y. Zhang, K. Scherlach, R. Müller and C. Hertweck, *ACS Chem Biol.*, 2018, **13**, 1370-1379.
25. F. Baldeweg, P. Warncke, D. Fischer and M. Gressler, *Org. Lett.*, 2019, **21**, 1444-1448.
26. E. G. Kuhlman, *Mycologia*, 1975, **67**, 678-681.
27. L. Wagner, B. Stielow, K. Hoffmann, T. Petkovits, T. Papp, C. Vagvolgyi, G. S. de Hoog, G. Verkley and K. Voigt, *Persoonia*, 2013, **30**, 77-93.

28. S. Kodani, H. Komaki, M. Suzuki, H. Hemmi and M. Ohnishi-Kameyama, *Biometals*, 2015, **28**, 381-389.
29. O. Lazos, M. Tosin, A. L. Slusarczyk, S. Boakes, J. Cortes, P. J. Sidebottom and P. F. Leadlay, *Chem. Biol.*, 2010, **17**, 160-173.
30. S. P. Niehs, B. Dose, K. Scherlach, M. Roth and C. Hertweck, *ChemBioChem*, 2018, **19**, 2167-2172.
31. S. Götze and P. Stallforth, *Nat. Prod. Rep.*, 2020, **37**, 29-54.
32. A. D. Berti, N. J. Greve, Q. H. Christensen and M. G. Thomas, *J. Bacteriol.*, 2007, **189**, 6312-6323.
33. J. Arp, S. Götze, R. Mukherji, D. J. Mattern, M. Garcia-Altares, M. Klapper, D. A. Brock, A. A. Brakhage, J. E. Strassmann, D. C. Queller, B. Bardl, K. Willing, G. Peschel and P. Stallforth, *Proc. Natl. Acad. Sci. U S A*, 2018, **115**, 3758-3763.
34. J. Krätzschmar, M. Krause and M. A. Marahiel, *J. Bacteriol.*, 1989, **171**, 5422-5429.
35. M. A. Marahiel, T. Stachelhaus and H. D. Mootz, *Chem. Rev.*, 1997, **97**, 2651-2674.
36. M. Stanke and B. Morgenstern, *Nucleic Acids Res.*, 2005, **33**, 465-467.

4.3 Manuskript 3

A Genetic Tool to Express Long Fungal Biosynthetic Genes

Kirchgässner, Leo; **Wurlitzer, Jacob M.**; Seibold, Paula S.; Rakhmanov, Malik; Gressler, Markus veröffentlich unter: *Fungal biology and biotechnology* **2023**, 10, 4; DOI: 10.1186/s40694-023-00152-3

Zusammenfassung:

Die Forschung an Naturstoffgenen beruht oft auf der genetischen Modifizierbarkeit des zu untersuchenden Organismus oder auf cDNA-basierten Ansätzen. Sollen stille Gene in gentechnisch nicht zugänglichen Organismen wie *Mortierella alpina* untersuchen werden, so stößt man bei Genen $>$ 10 kb an die Grenzen gängiger Methoden. Hier wurde ein Ansatz etabliert, in welchem ungespleißte Gene $>$ 20 kb in bis zu fünf DNA-Fragmenten in *Aspergillus niger* korrekt rekombiniert und ins Genom integriert wurden. Die Gene *lpaA* aus *Laetiporus sulphureus* und *calA* aus *M. alpina* konnten auf diese Weise kloniert und anschließend exprimiert werden. Für die Klonierung der *calA* stellte dies gleichzeitig den Nachweis des biosynthetischen Ursprungs des antimycobakteriellen Calpinactams dar. Dieser heterologe Ansatz eröffnet sowohl Möglichkeiten zur Untersuchung von Naturstoffgenen aus basalen Pilzen, als auch zur großtechnischen Produktion von pharmazeutisch interessanten Naturstoffen.

Der Kandidat ist:

☐ Erstautor ☒ Co-Erstautor ☐ Korresp. Autor ☐ Coautor

Eigenanteil:

Autor/-in	Konzeptionell	Datenanalyse	Experimentell	Verfassen des Manuskriptes
Kirchgässner, L	10%	20%	30%	10%
Wurlitzer, JM	10%	20%	30%	10%
Seibold, P	10%	15%	15%	20%
Rakhmanov, M	-	-	5%	-
Gressler, M	70%	45%	20%	60%
Summe	100%	100%	100%	100%

Kirchgaessner *et al.*
Fungal Biology and Biotechnology (2023) 10:4
https://doi.org/10.1186/s40694-023-00152-3

Fungal Biology and Biotechnology

RESEARCH Open Access

A genetic tool to express long fungal biosynthetic genes

Leo Kirchgaessner[1,2,3], Jacob M. Wurlitzer[1,2], Paula S. Seibold[1,2], Malik Rakhmanov[1,2] and Markus Gressler[1,2*]

Abstract

Background Secondary metabolites (SMs) from mushroom-forming fungi (*Basidiomycota*) and early diverging fungi (EDF) such as *Mucoromycota* are scarcely investigated. In many cases, production of SMs is induced by unknown stress factors or is accompanied by seasonable developmental changes on fungal morphology. Moreover, many of these fungi are considered as non-culturable under laboratory conditions which impedes investigation into SM. In the post-genomic era, numerous novel SM genes have been identified especially from EDF. As most of them encode multi-module enzymes, these genes are usually long which limits cloning and heterologous expression in traditional hosts.

Results An expression system in *Aspergillus niger* is presented that is suitable for the production of SMs from both Basidiomycota and EDF. The *akuB* gene was deleted in the expression host *A. niger* ATNTΔ*pyrG*, resulting in a deficient nonhomologous end-joining repair mechanism which in turn facilitates the targeted gene deletion via homologous recombination. The Δ*akuB* mutant tLK01 served as a platform to integrate overlapping DNA fragments of long SM genes into the *fwnA* locus required for the black pigmentation of conidia. This enables an easy discrimination of correct transformants by screening the transformation plates for fawn-colored colonies. Expression of the gene of interest (GOI) is induced dose-dependently by addition of doxycycline and is enhanced by the dual TetON/terrein synthase promoter system (ATNT) from *Aspergillus terreus*. We show that the 8 kb polyketide synthase gene *lpaA* from the basidiomycete *Laetiporus sulphureus* is correctly assembled from five overlapping DNA fragments and laetiporic acids are produced. In a second approach, we expressed the yet uncharacterized > 20 kb nonribosomal peptide synthetase gene *calA* from the EDF *Mortierella alpina*. Gene expression and subsequent LC–MS/MS analysis of mycelial extracts revealed the production of the antimycobacterial compound calpinactam. This is the first report on the heterologous production of a full-length SM multidomain enzyme from EDF.

Conclusions The system allows the assembly, targeted integration and expression of genes of > 20 kb size in *A. niger* in one single step. The system is suitable for evolutionary distantly related SM genes from both Basidiomycota and EDF. This uncovers new SM resources including genetically intractable or non-culturable fungi.

Keywords Early diverging fungi, Nonribosomal peptide synthetase, Polyketide synthase, Laetiporic acid, Calpinactam

*Correspondence:
Markus Gressler
markus.gressler@leibniz-hki.de
[1] Institute of Pharmacy, Department Pharmaceutical Microbiology, Friedrich Schiller University Jena, Winzerlaer Strasse 2, 07745 Jena, Germany
[2] Department Pharmaceutical Microbiology, Leibniz Institute for Natural Product Research and Infection Biology - Hans Knöll Institute, Winzerlaer Strasse 2, 07745 Jena, Germany
[3] Faculty Medical Technology and Biotechnology, Ernst Abbe University of Applied Sciences Jena, Carl-Zeiss-Promenade 2, 07745 Jena, Germany

Introduction

Ascomycetes such as *Aspergilli* have become a powerful platform to heterologously biosynthesize secondary metabolites (SM) from various fungi [1]. Several classes of SM enzymes including polyketide synthases (PKSs), non-ribosomal peptide synthetases (NRPSs), PKS-NRPS hybrids, and terpene cyclases (TC) were successfully produced [2, 3]. However, fungal natural product research mainly focused on SM genes of manageable and

cloneable size [4–7]. In contrast, longer genes (> 12 kb) have been preferably studied by either knock-out or promoter replacement strategies (or combination of both) [8], but have hardly been investigated by production in heterologous hosts. Both strategies require cultivability and transformability of the investigated fungi. These requirement are frequently met by Ascomycota, but are scarcely applicable to EDF such as *Mucoromycota* or higher fungi, i.e. *Basidiomycota* [9]. Hence, current knowledge on fungal secondary metabolite genes and their natural products is mostly based on work on ascomycetes and is thus biased. This is also founded on the elevated number of SM biosynthetic genes that have been identified in ascomycetes (10–30 NRPS and NRPS-like, 10–30 PKS, and > 4 TC genes per genome) *versus* basidiomycetes (1–6 NRPS and NRPS-like, 1–6 PKS, and 6–34 TC genes per genome) or EDF (0–15 NRPS and NRPS-likes, 0–15 PKS, 0–10 TC genes per genome) [9–12].

Several tools for the production of SM genes have been developed in ascomycetes. The heterologous expression of genes of interest (GOI) in *Aspergilli* require either a strong and constitutive promoter, such as the glycerinaldehyde-3-phosphate dehydrogenase promoter (P*gpdA*) [13] and the α-amylase promoter (P*amyB*) [14], or an inducible promoter system, such as the alcohol-inducible P*alcA*/*alcR* system [15], the tetracycline-dependent TetON system [16], or the ATNT system, i.e. a combination of the TetON system with the regulatory terrein biosynthetic promoter P*terA* [17, 18]. To date, both the P*alcA*/*alcR* system in *Aspergillus nidulans* and the ATNT system in *Aspergillus niger* are frequently used fungal expression platforms for genes encoding SM biosynthetic enzymes including PKSs [19, 20], NRPSs [21], and NRPS-like enzymes [22, 23]. However, alternative fungal systems have been developed, among them (i) the HEx platform using an engineered *Saccharomyces cerevisiae* strain producing additional SM auxiliary enzymes [24], (ii) the multiauxotrophic *Aspergillus oryzae* strains M2-3 and NSAR1 [25, 26], and various systems developed for *A. nidulans* including (iii) polyauxotrophic strains sensitive to various antibiotics [27], (iv) strains with strongly reduced intrinsic metabolic background [28, 29], (v) the nitrate-inducible *aflR/S* CoIN system [30], and (vi) an AfoA-inducible platform [31]. Traditionally, single SM biosynthetic genes were expressed in phylogenetically distantly related hosts such as *Escherichia coli* and *S. cerevisiae* [4, 32]. However, the latter two platforms require adaptations and adjustments such as (i) the co-production of SM specific phosphopantetheinyl transferases to produce holoenzymes [33], or (ii) the expression of additional tRNAs to ensure active enzymes of sufficient yield [34] and, moreover, may fail due to limitations of intron splicing [24]. In any case and prior to transformation of the heterologous host, the GOI must be amplified from DNA and cloned in plasmids that are usually assembled and propagated in *E. coli* or *S. cerevisiae* [35, 36].

Fungal genes encoding highly reducing PKSs (8–9 kb), PKS-NRPS hybrids (12 kb) and multimodule NRPSs (10–26 kb) are of extraordinary size and can be even longer if interspaced by introns. Hence, a full-length amplification by PCR using genomic DNA as template is not recommendable. An amplification from cDNA is the gold standard, but is impaired as: (i) reverse transcriptases possess low processivities at long templates [37], and (ii) most fungal SM genes remain silent under standard laboratory conditions—a fact, which reduces the availability of a full-length RNA template [38]. Hence, an amplification and cloning in small fragments is a conceivable way to manage long GOI. Since 1990 artificial chromosomes (FACs, YACs and BACs) has been frequently used [39, 40], and are suitable to express entire gene clusters of 50–150 kb size. [40] However, identification and metabolic screening of correct clones is laborious and time-consuming. Moreover, FACs and BACs rely on an intrinsic activation of the transgenic promoters in the expression host which is hardly achieved for genes from distantly related species.

Here, an alternative strategy to clone and express long GOI is presented, which is based on the well-established ATNT expression system in *A. niger* and does not require cloning of the full-length gene. Instead, the GOI is amplified in up to five fragments and is assembled with high fidelity by homologous recombination within the host in one single step. On-site integration into the *fwnA* locus responsible for conidial pigmentation allowed a simple visual screening for the correct transformants. The system's versatility was proven by the integration of two GOI from phylogenetically divergent fungi: First, the *lpaA* gene (8.2 kb) from the basidiomycete *Laetiporus sulphureus*, known to encode a PKS responsible for the chromophoric laetiporic acids [41], was precisely integrated in five DNA fragments. Furthermore, an unknown NRPS gene (*calA*, 20.0 kb) from the EDF *Mortierella alpina* was successfully expressed and assigned as a synthetase for calpinactam, an anti-mycobacterial peptide. Hence, the system sets the basis to study long biosynthetic genes from various biological sources including EDF.

Results

Deletion of the *akuB* gene in ATNT favors homologous recombination

Aspergilli randomly integrate transgenes into their genomes and multiple integration events are frequently observed [42]. It has been demonstrated, that *Aspergillus* or *Neurospora* deletion mutants defective in the

non-homologous end-joining (NHEJ) repair mechanism such as Δ*akuA*^{KU70},Δ*akuB*^{KU80}, or Δ*ligA*, facilitate the targeted gene deletion by homologous recombination [43–45]. Moreover, these mutants can integrate transgenes in two overlapping fragments [29]. This "split-marker" recombination is broadly used for efficient targeted gene deletion in fungi [46]. To investigate the applicability of a deletion of the NHEJ system for a targeted multi-fragment gene integration, the *akuB* gene from the *A. niger* expression strain ATNTΔ*pyrG* was replaced by the hygromycin B resistance cassette and the *akuB* deletion in the obtained mutant *A. niger* ATNTΔ*akuB* (tLK01) was confirmed by Southern Blot (Additional file 5: Fig. S1). To test the frequency of transgene integration, the *fwnA*$^{albA/pksP}$ gene encoding the polyketide synthase responsible for conidial pigmentation [47] was deleted in both *A. niger* ATNT and mutant tLK01 (Fig. 1A). To this end, the overexpression plasmid pPS01 [41] containing the inducible promoter P*terA*, the terminator T*trpC,* and an URA blaster was expanded by the upstream and downstream flanks of *fwnA* (5′ *fwnA*up and 3′ *fwnA*dn) resulting in expression plasmid pLK04 (Additional file 6: Fig. S2). When both ATNT and tLK01 were transformed with the overlapping fragments of the

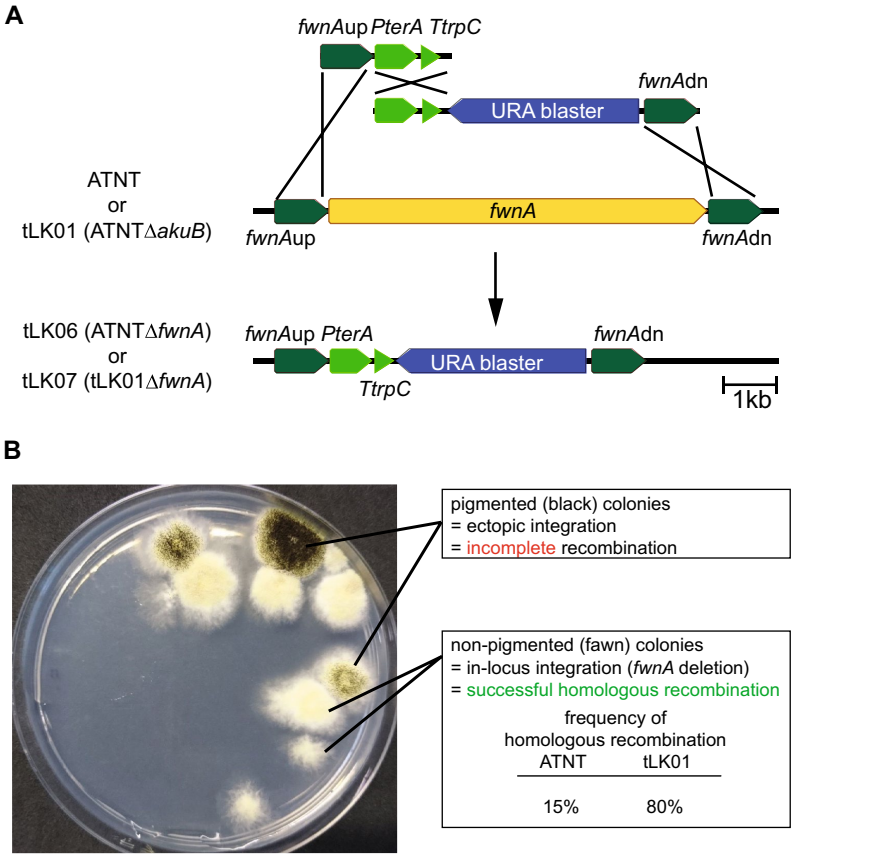

Fig. 1 Principle of the recombination and Δ*fwnA* selection system. **A** Construction of the *fwnA* deletion mutants in the parental strains *A. niger* ATNT and tLK01 (ATNTΔ*akuB*). Homologous recombination of the two PCR amplicons into the *fwnA* locus in the parental strains led to the deletion of the *fwnA* gene resulting in *A. niger* strains tLK06 (ATNTΔ*fwnA*) and tLK07 (tLK01Δ*fwnA*). **B** Representative agar plate of a transformation of the *A. niger* tLK01 parental strain with the split-marker *fwnA* deletion constructs. Non-pigmented, fawn colonies are resulting from the *fwnA* deletion suggesting a successful recombination event whilst pigmented, black colonies indicate false-positive transformants. The frequency of homologous recombination is significantly increased in the *A. niger* Δ*akuB* deletion strain tLK01

construct, the frequency of targeted recombination was significantly higher for tLK01, i.e. the relative number of non-pigmented transformants was increased from 15 to 80% when compared to the parental strain (Fig. 1B, Additional file 2: Table S1, Additional file 7: Fig. S3). A successful genomic integration was additionally confirmed by PCR (Additional file 8: Fig. S4). One of these *A. niger* tLK01Δ*fwnA* transformants (tLK07) served as null mutant (empty vector control) in subsequent metabolite analyses.

Aspergillus niger tLK01 is competent to integrate five-fragment expression constructs

As a proof of concept to integrate long SM genes in the *fwnA* locus of *A. niger* tLK01 by application of multiple DNA fragments, we used the 8196 bp PKS gene *lpaA* from the "chicken of the woods" mushroom *L. sulphureus* [41]. Recently, this gene has been successfully expressed in *Aspergilli* and was assigned to the biosynthesis of polyenes of various chain lengths (C_{26}–C_{32}), i.e. laetiporic acids A_1-D_1 (LA A_1–D_1) and their 7-*trans*-isomers A_2 -D_2 (LA A_2–D_2) [41], which both are currently discussed to be natural alternative colorants in cosmetics and for textiles [48]. Due to their absorption maxima between 450 and 470 nm, the mycelium of producing cultures exhibit an orange hue allowing an easy read-out of positive transformants. We fused a 1 kb fragment of either end of *lpaA* and ligated the fusion fragment into pLK04. Five fragments with a 1 kb overlap were amplified by PCR (Fig. 2A), mixed equimolarly and used to transform *A. niger* tLK01 using uridine prototrophy as selection marker. Five non-pigmented transformants were randomly picked and checked by PCR for the full-length integration of the expression construct (Fig. 2B) and by Southern Blot for homologous integration into the *fwnA* locus (Additional file 9: Fig. S5). Indeed, four out of five fawn tLK04 transformants (4/5, 80%) successfully assembled and integrated the *lpaA* expression construct into the *fwnA* locus. Finally, the transformant tLK04 and the respective empty vector control strain

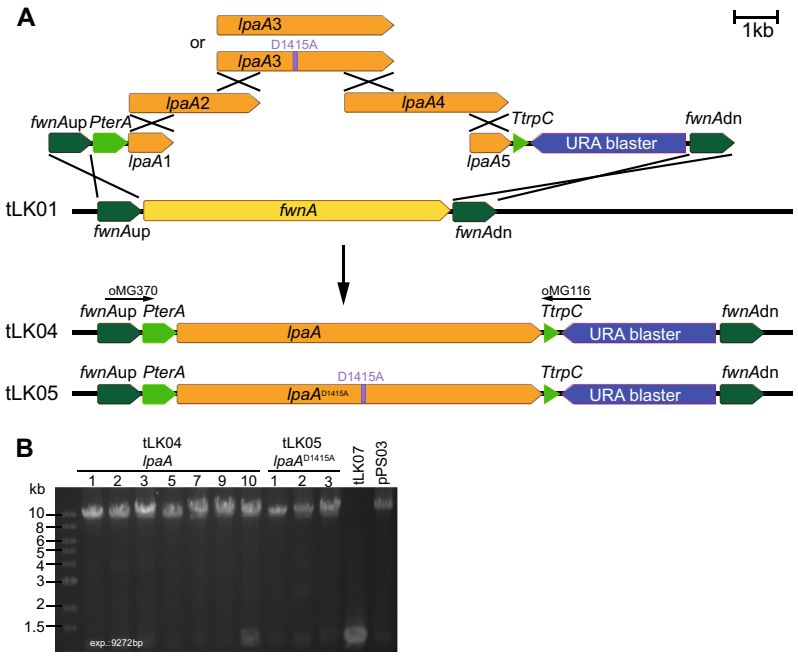

Fig. 2 Determination of the full-length integration of the P*terA*:*lpaA*:T*trpC* construct into the *fwnA* genomic locus of the *A. niger* recipient strain tLK01. **A** Schematic representation of the integration event of the five *lpaA* fragments into the genomic *fwnA* locus of *A. niger* tLK01. To mutate the SAM binding site in the C-methyltransferase domain of LpaA, the triplet GAC (pos. 4245–4247) encoding Asp^{1415} (probably binding the ribose moiety of SAM) was site-mutated into the triplet GCC encoding Ala^{1415}. **B** An agarose gel of a PCR targeting the P*terA* promoter and the T*trpC* terminator has been performed (oligonucleotides oMG370/oMG116). The expected amplicon size is indicated. Full length integration was evident for seven tLK04 (producing native LpaA) and three tLK05 transformants (producing $LpaA^{D1415A}$). The genomic DNA of tLK07 (transformed with an empty vector) and the *lpaA*-encoding plasmid pPS03 [41] served as negative and positive controls, respectively

tLK07 were fermented under non-inducing and inducing conditions (by addition of doxycycline). Metabolites were extracted and analyzed by UHPLC-MS (Fig. 3A) and by high resolution MS fragmentation (Additional file 10: Fig. S6). During cultivation the color of the fungal mycelium turned orange and the expected polyene products LA A_1–D_2 were primarily detectable from mycelium of the doxycycline-induced cultures of tLK04 suggesting that the five DNA fragments have been accurately assembled. Overall, seven out of seven PCR-positive transformants (Fig. 2B) produced the expected compounds (7/7, 100%). Minor signals of LAs with 100-fold less abundances were detectable from non-induced cultures, suggesting that the promoter is not entirely silent (not shown). In addition, no laetiporic acids were obtained from the empty vector control tLK07 under inducing conditions (Fig. 3A).

The expression system is suitable for point mutation analysis

Next, the suitability of system to study point mutations of long GOI was investigated. Structurally, linear polyenes including the antifungal laetiporic acids from *L. sulphureus* [41], piptoporic acid from curry punk fungus *Piptoporus australiensis* [49], and the two antilarval polyenes from the undescribed stereaceous basidiomycete BY1 [50, 51], feature a 1-methyl-2-oxo-propylidene head as plausible pharmacophore (Fig. 3B). We speculated on the intrinsic activity of the C-methyl transferase (C-MT) domain in LpaA to catalyze this *S*-adenosyl-methionine (SAM) dependent C-transfer after two cycles of acyl condensation. Hence, we aimed at the inactivation of the C-MT domain. In a previous study, an aspartate (D^{2019}) in the active site of citrinin polyketide synthase PksCT was shown to be essential for the methylation of the polyketide citrinin by coordination of 2′-OH and 3′-OH of the ribose moiety of the cofactor SAM [52]. Hence, to inactive the C-MT activity of LpaA, the GAC triplett encoding the homolog aspartate (D^{1415}) was mutated into GCC (A^{1415}). To this end, five DNA fragments were used to transform *A. niger* tLK01, of which fragment 3 contained the mutated sequence encoding the potential dysfunctional MT^{D1415A} (Fig. 2A). Full-length integration of $lpaA^{D1415A}$ was confirmed by PCR (Fig. 2B) and the point mutation was additionally confirmed by Sanger sequencing. Surprisingly, whilst cultures of the *lpaA*-expressing strain tLK04 turned orange after induction, the induced transformants expressing the $lpaA^{D1415A}$ gene (tLK05)

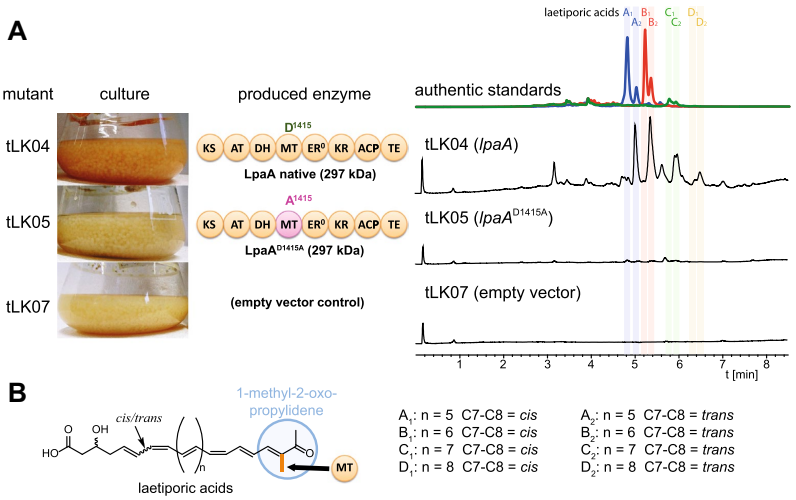

Fig. 3 Laetiporic acid production in the *A. niger* Δ*fwnA* mutants tLK04, tLK05 and tLK07. **A** Cultures photographs, representative domain structure of LpaA mutant proteins and HPLC profiles of metabolite extracts. Photographs depict 3-days cultures at 30 °C, 150 rpm. HPLC chromatograms of extracts of mycelia from tLK04, tLK05 and tLK07 were monitored at a wavelength of λ = 450 nm. Note, that tLK04 expressing the native *lpaA* gene produces laetiporic acids A_1–D_2, whereas no metabolites are detectable in tLK05 (expressing the mutant $lpaA^{D1415A}$ gene) or in tLK07 (empty vector control). Authentic standards of laetiporic acids (LA-$A_{1/2}$, LA-$B_{1/2}$ and LA-$C_{1/2}$) served as controls. An authentic standard for LA-$D_{1/2}$ was not available. For MS and MS/MS spectra please refer to Additional file 10: Fig. S6. The pearls on a string represent the domain structure of the PKS LpaA and include: KS, β-ketoacyl synthase; AT, acyl transferase; DH, dehydratase; MT, C-methyltransferase; ER^0, (inactive) enoyl reductase; KR, keto reductase; ACP, acyl carrier protein; TE, thioesterase. **B** Chemical structure of laetiporic acids A_1–D_2. Note the common 1-methyl-2-oxo-propylidene group, which requires the action of the intrinsic C-MT domain

neither changed mycelial color nor produced any additional compound when compared to the empty vector control (tLK07) (Fig. 3A). This observation is not based on an altered transcription because *lpaA* in tLK04 and *lpaA*^{D1415A} in tLK05 showed identical expression levels (Additional file 11: Fig. S7). Hence, the C-MT seemed to be essential for polyketide production. This finding in turn, implies that the 1-methyl-2-oxo-propylidene head in laetiporic acids is required for a successful chain elongation. In sum, the strain tLK01 is convenient to assemble DNA constructs from up to five fragments and directly express the GOI in one step. Moreover, the system is suitable to induce point mutations in long GOIs to study modified enzymes.

The NRPS gene *calA* encodes the calpinactam synthetase in *Mortierella alpina*

In contrast to Dikarya, early diverging fungi (EDF) are a comparably new resource of natural products. Although the genomes of *Mortierella* sp. (Phylum *Mucoromycota*) and *Basidiobolus* sp. (Phylum *Zoopagomycota*) encode numerous of long NRPS genes (up to 26 kb), only a few have been assigned to specific products [10]. Calpinactam, produced by *M. alpina* FKI-4905, is a hexapeptide with an unusual C-terminal ε-caprolactam moiety (Fig. 4A) [53]. Calpinactam—but not its chemically closely related derivatives [54, 55]—is a proven anti-mycobacterial agent with MICs of 0.78 µg mL^{-1} and 12.5 µg mL^{-1} against *Mycobacterium smegmatis* or *Mycobacterium tuberculosis,* respectively [53]. Although of high pharmaceutical interest, the corresponding gene for calpinactam biosynthesis has never been identified. We examined the metabolome and genome of the *M. alpina* sequencing reference strain ATCC32222 [56]. The strain produces and secretes calpinactam into the supernatant as confirmed by UHPLC-MS and comparative MS–MS fragmentation patterns versus a commercially available authentic standard (Fig. 4C and D). Three hexamodular candidate NRPS genes (*nps5*, *nps6* and *nps7*) were identified in the *M. alpina* genome [57]. Since *Mortierella* NRPS genes are likely of bacterial origin [58], we predicted the substrate specificity codes of the candidate enzymes versus the bacterial gramicidin S synthetase GrsA from *Aneurinibacillus migulanus* as reference (Table 1). While at least three of the adenylation (A) domains encoded by *nps6* or *nps7* are expected to use identical amino acids, the six A domains encoded by *nps5* (*calA*) accept six dissimilar substrates as required for calpinactam (Fig. 4A, Table 1). Moreover, the arrangement of condensation (C) and dual epimerization/condensation (E/C) domains in CalA directly reflects the sequence of L- and D-amino acids in the final peptide chain of calpinactam according to the NRPS collinearity principle [59] (Table 2). Hence, the postulated domain structure and the predicted A domain substrate specificities of CalA perfectly matched an NRPS assembly line for calpinactam.

Full-length *calA* gene expression in *A. niger* enables a heterologous calpinactam production

Given its length of 20,015 bp, we decided to heterologously express *calA* from *M. alpina* in *A. niger* tLK01 in a similar fashion as *lpaA* using collectively five *calA* DNA fragments of up to 7000 bp (Fig. 4B). 30 transformants were obtained of which three randomly picked transformants (tJMW06.3, tJMW06.13, tJMW06.26) showed a full-length integration of *calA* into the genome of *A. niger* as confirmed by multiple PCRs (Additional file 12: Fig. S8) and by Southern Blot (Additional file 13: Fig. S9). Profiling the metabolome of the tJMW06 transformants, an additional metabolite was detected under inducing conditions, whose ion mass (*m/z* 768.4411 $[M+H]^+$) and retention time (2.1 min) was identical to that of the commercial calpinactam standard (MW 768.4330 Da) (Fig. 4C). The identical MS/MS-fragmentation pattern confirmed the heterologous production of calpinactam (Fig. 4D). In contrast, calpinactam was not detectable in the empty vector control strain tLK07 (Fig. 4C). Hence, we established *calA* as the calpinactam biosynthetic gene.

The production of calpinactam in *A. niger* tJMW06 was highest (20 µg g^{-1} fungal dry weight), when the transgenic fungus was cultivated at 25 °C (Additional file 14: Fig. S10), i.e. the temperature optimum for *M. alpina* enzymes [60]. However, titers of calpinactam remained low compared to the original producer strain *M. alpina* (1438 µg g^{-1}). The > 20 kb *calA* gene includes six potential introns of 90 to 112 bp length (Fig. 5A). Hence, we checked for the correct splicing pattern of the *calA* transcript by comparative PCR on the *M. alpina* and *A. niger* tJMW06 cDNA (Fig. 5B). The complete set of introns were spliced in its original producer strain *M. alpina* as predicted, although introns 3 and 4 showed only partial splicing. Similarly, the splicing of introns 1, 2, 3, 5 and 6 appeared at the correct sites in the transgenic *A. niger* tJMW06. However, only marginal pre-mRNA maturation was detectable for intron 4, as genomic DNA and cDNA show the same PCR fragment sizes (Fig. 5B). The unspliced intron 4 would result in a premature termination at a UAG stop codon at position 11,148. Hence, this incomplete splicing event results in a loss-of-function version of CalA and may explain the low calpinactam titers in *A. niger* tJMW06 (Fig. 5C). To bypass this limitation, we removed the intron 4 by amplification and PCR-fusion of the adjacent exons of fragment 3 and transformed the recipient strain *A. niger* tLK01 with the altered version of *calA* fragments. However, this

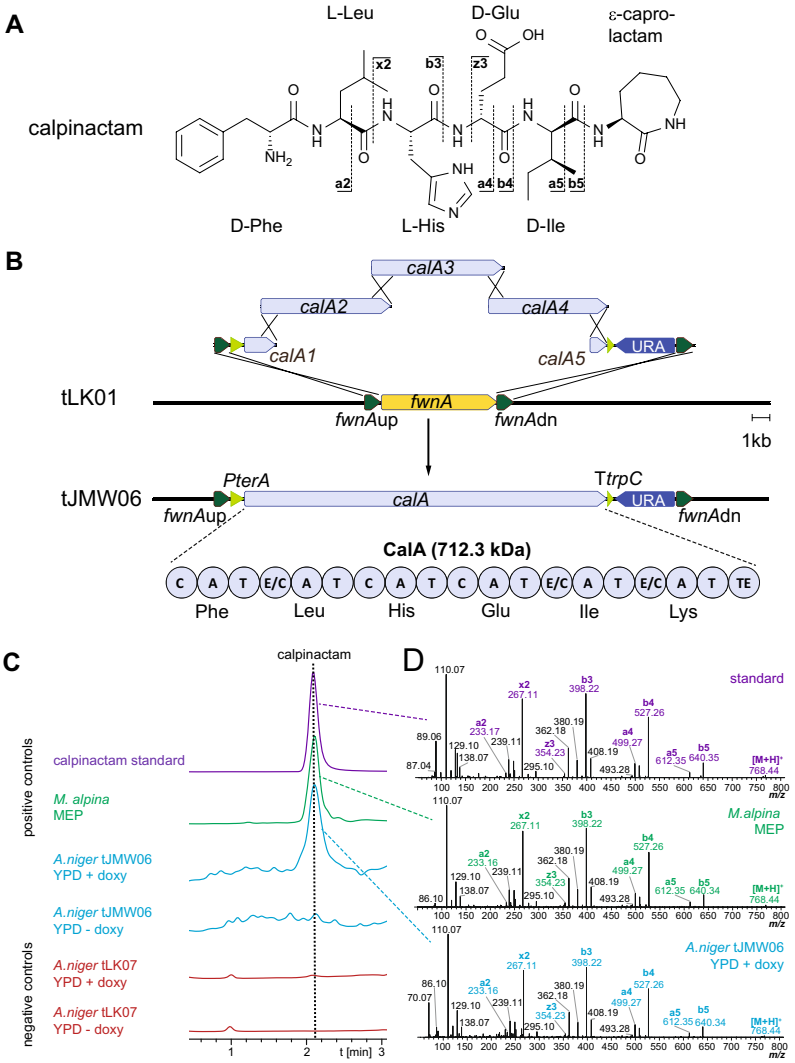

Fig. 4 Calpinactam production in *M. alpina* and transgenic *A. niger* Δ*fwnA* mutants tJMW06 and tLK07. **A** Chemical structure and calculated MS/MS fragments of calpinactam. **B** Schematic representation of the integration event of the five *calA* fragments into the genomic *fwnA* locus of *A. niger* tLK01. The pearls on a string represent the domain structure of the 6-module NRPS CalA and include: C, condensation domain; A, adenylation domain; T, thiolation domain; E/C dual epimerization/condensation domain; TE, thioesterase. Note that the 1st (starter) C domain is truncated and inactive. **C** Extracted ion chromatograms of the synthesized calpinactam standard and metabolic extracts from various fungal mycelia. *M. alpina* ATCC32222 was cultivated on MEP, whilst transgenic *A. niger* tJMW06 (*calA* expressing) and tLK07 (empty vector control) was cultivated in *Aspergillus* Minimal Medium (AMM) under inducing (+ doxycycline) or non-inducing (− doxycycline) conditions. MS data was monitored in positive ionization mode at *m/z* 768.6844 $[M+H]^+$. **D** MS/MS spectra highlighting the specific daughter ion fragments of calpinactam of the authentic standard and the metabolic extracts from *M. alpina* ATCC32222 and transgenic *A. niger* tJMW06

Table 1 Substrate specificity code for adenylation domains of hexamodular NRPSs of *Mortierella alpina*

protein	domain	substrate	residue position according to GrsA Phe numbering									
			235	236	239	278	299	301	322	330	331	527
CalA	A1	Phe	D	P	F	I	I	G	V	V	I	K
	A2	Leu	D	A	F	L	V	G	A	V	I	K
	A3	His	D	P	F	H	T	A	R	V	D	K
	A4	Glu	D	P	F	Y	F	G	R	V	N	K
	A5	Ile	D	A	F	F	L	G	C	T	F	K
	A6	Lys	D	A	A	E	V	G	T	V	I	K
Nps6	A1	-	D	H	S	S	V	M	E	V	A	K
	A2	-	D	V	W	N	I	A	M	V	H	K
	A3	-	D	H	S	S	V	M	E	V	A	K
	A4	-	D	H	S	S	V	M	E	V	A	K
	A5	-	D	V	W	N	I	A	M	V	H	K
	A6	-	D	V	W	N	I	A	M	V	Y	K
Nps7	A1	-	D	T	H	H	N	N	G	I	G	K
	A2	-	D	V	Q	M	L	G	Q	V	A	K
	A3	-	D	A	S	V	T	T	Q	I	P	K
	A4	-	D	V	Q	M	L	G	Q	V	A	K
	A5	-	D	V	Q	M	L	G	Q	V	A	K
	A6	-	D	V	Q	M	L	G	Q	V	A	K

The residues are mapped based on positions according to *Aneurinibacillus migulanus* (former *Brevibacillus brevis*) GrsA-A numbering [101]. Amino acid residues in the NRPS code are highlighted according to their physicochemical properties: acidic (red), small/hydrophobic (grey), aromatic/hydrophobic (ocher), hydrophilic (green), and basic (blue)

manipulation did not change the titers (data not shown), suggesting that additional adjustments such as codon-optimization and balanced supply of precursors might be required for increased calpinactam titers. In summary, in this pilot study we established for the first time a successful five-fragment assembly and heterologous expression of a > 20 kb natural product biosynthetic gene from an early diverging fungus.

Discussion

Over the past four decades, 60% of all new antibiotic lead structures were based on natural products [61]. Although new antibiotics are urgently needed especially to treat nosocomial infections, natural product research slowed down as mainly bacteria and ascomycetes were investigated concerning their metabolic potential and rediscovery of known compounds is

Table 2 Domain architecture of predicted hexamodular NRPSs in *M.alpina*

protein	domain architecture	modules	size (aa)	encoding contig
Nps5 (CalA)	Cs-A-T-E/C-A-T-C-A-T-C-A-T-E/C-A-T-E/C-A-T-TE	6	6,473	tig00080470
Nps6	Cs-A-T-C-A-T-C-A-T-E/C-A-T-C-A-T-C-A-T-TE	6	6,159	tig00080470
Nps7	Cs-A-T-E/C-A-T-C-A-T-C-A-T-C-A-T-E/C-A-T-TE	6	6,011	tig00000137

For clarity, individual modules are highlighted in alternating red and blue color. A, adenylation domain; C, condensation domain; Cs (inactive) starter condensation domain; E/C, dual epimerization/condensation domain; TE, thioesterase domain

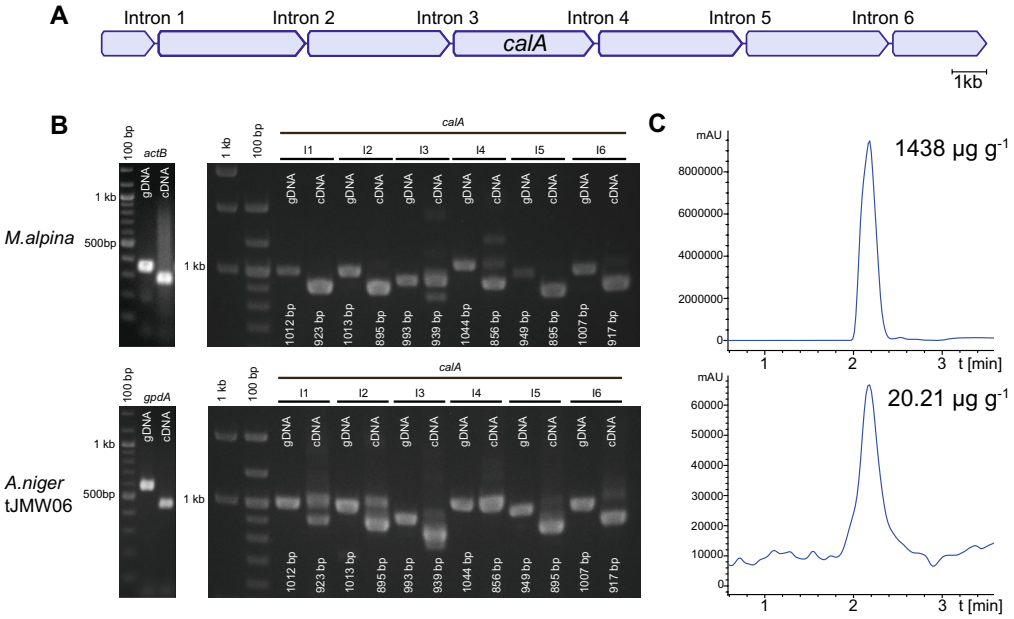

Fig. 5 Splicing events in the *calA* gene in *M. alpina* and transgenic *A. niger* tJMW06. **A** Structure of the full-length 20 kb *calA* gene. The gene is disrupted by six introns. **B** Splicing pattern of natively expressed *calA* in *M. alpina* and heterologously expressed *calA* in *A. niger* tJMW06. Both strains were cultivated under inducing conditions (*M. alpina* in MEP medium, *A. niger* tJMW06 in AMM with doxycycline). Genomic (gDNA) and cDNA served as templates for diagnostic PCRs spanning the intron in a housekeeping gene (*actB* or *gpdA*, respectively) or individually spanning the six introns of *calA*. Expected fragment sizes are indicated. **C** MS profile at *m/z* 768.44 $[M+H]^+$ of the induced cultures from *M. alpina* (upper lane) and *A. niger* tJMW06 (lower lane). The indicated titer of calpinactam is normalized to the fungal dry weight (calculated from three replicates)

frequently observed [62]. In contrast basidiomycetes and especially EDF are an attractive resource of bioactive agents but are rather genetically uninvestigated which is due to their challenging cultivability and the lack of genetic accessibility [9, 63]. Here, we present a molecular tool to express entire long SM genes to unravel the metabolic treasure chest of these fungi.

Multiple gene expression tools have been developed for ascomycetes (genera *Aspergillus*, *Fusarium*, *Penicillium*, *Pichia* and *Saccharomyces*) and partially for

basidiomycetes (genera *Ustilago, Coprinus*). No system for EDF has been established yet. Although anectodical evidence for their transformability exists using the more complex molecular tools such as CRISPR/Cas9 or TALEN/exonuclease [64–66], no common strategy for a targeted gene deletion exists since the *ku70/80* homologs are generally not expressed in these fungi [64]. Hence, unrevealing the function of the SM biosynthetic genes from Basidiomycota and EDF still rely on heterologous expression. However, main issue is the size of the SM genes and its interruption with introns which impedes an expression in traditional bacterial hosts [9]. Several molecular tools to clone and express entire bacterial gene clusters of > 40 kb were developed in *Streptomyces* species [67]. However, the current fungal expression systems mainly vary in their type of promoter activation, but most of them require are a pre-cloning of the GOI into a specific vector, which limits their applicability to long SM biosynthetic genes. Effort was done with the yeast/*E.coli* shuttle vectors in yeast, allowing a multi-gene assembly and co-expression of smaller biosynthetic genes in yeast and *Aspergillus* [68–70]. Alternatively, reiterative recombination systems assemble multigene constructs in *S. cerevisiae*, but this endonuclease-induced recombination requires multiple rounds of transformation to recycle selectable markers and is hence a robust, but more laborious technique [71]. Moreover, the genes of *S. cerevisiae* rarely possess introns (0.04 introns per gene) in comparison to *Aspergillus* species (0.96) making yeast to a less suitable host for multiple spliced transgenes [72].

The herein described system combines current knowledge of fungal biotechnology including the higher recombination frequency by deletion of the *akuB* gene [73], the easy transformability of *Aspergilli* [27], the discrimination of positive transformants by altered pigmentation [29] and the possibility to express > 20 kb genes in *Aspergilli* [16, 18]. The method is advantageous since (i) genomic DNA can be used as template, (ii) cloning steps are set to a minimum, (iii) assembly and expression of long genes is accomplished in a single step, and (iv) gene expression from different fungal divisions can be achieved. Similar in vivo recombination approaches have been conducted by heterologous expression of the entire aurofusarin and bikaverin biosynthetic gene clusters from *Fusarium* spec. in *A. nidulans* [74]. Moreover, along with our studies on *A. niger*, an AMA1-based vector was constructed for an in vivo recombination of various DNA fragments (encoding the *uidA* color enzyme or fluorescent proteins) into the conidial pigment gene *wA* of *A. nidulans, i.e.* homologous to the *fwnA* locus in *A. niger,* highlighting the general suitability of this biobricks approach [75]. A third example comprises the successful integration of the calbistrin cluster using six DNA fragments in an engineered *Penicillium rubens* platform strain resulting in the production of decumbenones A–C [76]. Although the calbistrin cluster is derived from the highly related species *Penicillium decumbens*, no production of calbistrins A–C was observed in the heterologous host, indicating that host specific effects can affect the metabolite production.

Indeed, inter-division gene expression is not a simple task because altered codon usage, intron recognition, protein folding or the lack of accessory proteins sometimes impedes successful heterologous protein production [9, 74]. Hence, it is the more astonishing as the NRPS gene *calA* from an EDF was successfully expressed in the ascomycete *A. niger*. However, the detected calpinactam titers are 71 times lower compared to the native producer, which may be caused by undesired splicing events or unstable transcripts in the host. The targeted recombination resulted in a single integration in the *fwnA* gene locus whilst multi-copy integrations may yield higher metabolite titers as shown in the biotechnological production of other natural compounds [17, 77]. To bypass this limitation, the introduced URA blaster might be excised by 5-fluoroorotic acid treatment of the expression strain to perform a second round of transformation into another locus [78].

The described system is suitable for expression of long genes of Basidiomycetes. We successfully assembled the 8 kb *lpaA* gene from five DNA fragments in *A. niger* and confirmed the functionality by the production of various methyl-branched polyenes of different chain length (C_{26}–C_{32}) and $\Delta^{7,8}$ *cis/trans* stereochemistry, which is in accordance with observations made by the heterologous expression of *lpaA* in *Aspergilli* in a previous report [41]. Increasing the metabolic diversity by premature chain truncation is a well-recognized phenomenon of fungal polyketide synthesis [20, 79, 80]. The C4-methyl group as part of the 1-methyl-2-oxo-propylidene head is a common feature of many fungal linear polyenes [49–51]. We showed that the inactivation of the C-MT of LpaA is critical for chain elongation and completely abolished laetiporic acid production. As demonstrated for the iterative type I PKS LovB in the lovastatin biosynthesis of *A. terreus*, the highly regioselective and comparably fast C-MT reactions are essential for the full extension of the lovastatin nonaketide chain [81, 82]. Deconstruction studies of single domains of the PKS PksCT producing the highly (C2,C4,C6)-trimethylated pentaketide citrinin showed that in absence of the C-MT domain, the minimal PKS solely produced an unmethylated triketide pyrone [52]. Similar to our results on the LpaA C-MT, single mutations in the catalytic dyad of the C-MT of the PKS *MtaltA* in the alternapyrone biosynthetic

pathway completely abolished product formation [83]. Since no intermediates are detectable in the *lpaA* C-MT mutant, C4-methylation occurs most likely at the thioester α-carbon following the first extension cycle and not on the fully elongated hexacosaketide.

In a second approach, we successfully integrated the 27.7 kb *calA* expression construct (including the *calA* gene and the required regulatory elements) into the genome of *A. niger*. The calpinactam synthetase CalA (712 kDa) is approximately one and a half the size of the largest heterologously NRPSs produced in *S. cerevisiae*, among them the α-L-aminoadipyl-L-cysteinyl-D-valine synthetase PcbAB (426 kDa), the fumiquinazoline F synthetase Afu6g12080 (438 kDa), the tryptoquialanine synthetase TqaA (450 kDa) and the aspyridone synthetase ApdA (498 kDa) [84–87]. Our work enables both an optimized calpinactam production by the original producer strain *M. alpina* and the biotechnologically tractable *A. niger* strain tJMW06. Although, further improvement is required to increase the yield of the compound, e.g. by codon-optimization [88], the described tool provides the first evidence for a functional heterologous expression of a natural product gene in full-length from an early diverging fungus. Calpinactam represents a promising alternative to conventional, often less effective antibiotics to treat tuberculosis [89]. The compound possesses an unusual C-terminal ε-caprolactam ring and resembles the structure of mycobactin, i.e. the hydroxamate siderophore of *M. tuberculosis*, and may interfere with the iron uptake system [53]. Inhibition of iron metabolism is a prospective and highly specific target for antimycobacterial drug development [90].

In our studies, no linear calpinactam peptides with hydrolyzed ε-caprolactam ring system were detected as side products—neither in the original nor in the transgenic producer. This suggests that the 7-membered azacycle is not spontaneously formed, but rely on the intrinsic activity of the releasing module of CalA. Caprolactam-containing metabolites—such as the nucleoside antibiotic capuramycins [91], bangamide A [92], the antifungal circinatin [93], the cytotoxin caprolactin A [94], terreazepine [39], the muscarinic acetylcholine receptor inhibitor nocardimicin [95] and the siderophore mycobactin [90]—are frequently isolated from microorganisms. The caprolactam structure in capuramycin originates from L-lysine and has been assigned to the action of the NRPS-like module CapU [91]. Future investigations on the 6th module of CalA might be of importance, as the current industrial production routes to ε-caprolactam, i.e. the monomeric precursor of the widely used synthetic fibers nylon-6 and PEBA2000 [96, 97], rely on expensive and energy-wasting classical chemical syntheses [98]. Alternative, sustainable production routes in mammalian cells [99], plants [98] or fungi are highly requested bio-based strategies.

Conclusions

The heterologous expression of genes encoding megasynth(et)ases for natural products has long time been a very challenging task. The presented expression system allows integration and expression of long genes of interest of > 20 kb in a single step. The tool is suitable for genes of various biological sources, including higher and early diverging fungi, and provide the basis to tap yet unexplored secondary metabolite producers such as non-cultivatable fungi.

Methods

Organisms and culture conditions

Aspergillus niger strains ATNT, tLK01 (ATNTΔ*akuB*), the *lpaA*-expressing strains tLK04 and tLK05, the *calA*-producing strain tJMW06 and the empty vector controls tLK06 and tLK07 were cultivated on *Aspergillus* Minimal Medium (AMM) agar plates supplemented with 2 mm L-glutamine [100]. To compensate uracil auxotrophy, 10 mm uridine (Carl Roth) was added for cultivation of the strains ATNT, tLK01 and tLK06. For tLK01 cultivation, 140 µg mL^{-1} hygromycin B (Carl Roth) was added. Plates were incubated at 30 °C for 4 d and conidia were harvested as previously described [41]. 100 mL AMM with 200 mm glucose and 20 mm L-glutamine or YPD (10 g L^{-1} yeast extract, 20 g L^{-1} soy peptone, 20 g L^{-1} D-glucose) were inoculated with a titer of 1×10^6 *A. niger* conidia mL^{-1} to produce laetiporic acids at 30 °C for 72 h or to produce calpinactam at 25 °C for 72 h, respectively. Transgenic *A. niger* cultures were induced with 30 µg mL^{-1} doxycycline (Merck). *Mortierella alpina* ATCC32222 was cultivated on MEP agar plates (20 g L^{-1} malt extract, 3 g L^{-1} soy peptone, 20 g L^{-1} agar, pH 5.6) at 25 °C for 7 d. To produce calpinactam, 100 mL MEP liquid medium was inoculated by addition of three agar blocks (3 × 3 mm) and cultivated at 25 °C for 4 d. *Escherichia coli* XL1 blue were used for plasmid propagation and were cultivated in LB medium (5 g L^{-1} yeast extract, 10 g L^{-1} tryptone, 10 g L^{-1} NaCl) supplemented with 100 µg mL^{-1} carbenicillin (Roth), if required. Authentic standards for laetiporic acids were obtained from fruiting bodies of *Laetiporus sulphureus* JMRC:SF:012,599 as described [41]. All strains used in this study are listed in Additional file 3: Table S2.

Strain construction

Details on the cloning procedures, strain transformation, used strains and oligonucleotides are given in the Additional file 1: Experimental procedures, Additional file 3: Table S2, Additional file 4: Table S3. In

brief, the *akuB* deletion mutant (tLK01) was generated by replacing the entire gene (2651 bp) with the hygromycin B resistance cassette (*hph*) [45] from plasmid pLK03. To replace the spore pigment polyketide synthase gene *fwnA* by overexpression constructs, the pSMX2-derived [18] expression vector pPS01 [41] was expanded by an 1 kb upstream and 1 kb downstream flank of *fwnA* to yield plasmid pLK04. The plasmid served either as vector to ligate DNA sequences or as template for subsequent fusion PCRs. For heterologous expression of *lpaA* (*A. niger* strains tLK04 and tLK05) and *calA* (*A. niger* strain tJMW06) in the recipient strain tLK01, the five gene fragments of the laetiporic acid synthase gene (from *L. sulphureus*) and the calpinactam synthetase gene (from *M. alpina*) were amplified from the plasmid pPS03 [41] or the genomic DNA of *M. alpina* strain ATCC32222, respectively. In either case, the orotidin-5′-phosphate-decarboxylase gene, *pyrG*, from *Aspergillus nidulans* was used as selectable marker. The generated transformants were checked by PCR (Fig. 2, Additional file 8: Fig. S4, Additional file 12: Fig. S8). Deletion of *akuB* in *A. niger* tLK01 and *fwnA* in *A. niger* tLK04 as well as the full-length integration of *calA* in tJMW06 were additionally confirmed by Southern blot analysis with digoxigenin-labeled probes as described (Figures S1, Additional file 9: Fig. S5, Additional file 13: Fig. S9) [45].

Expression and splicing analyses

To determine the expression of *lpaA* in *A. niger* (*lpaA*-expressing), tLK05 (*lpaA*^{D1415A}-expressing) and tLK07 (null mutant), fungi where cultivated in 200 mL AMM supplemented with 200 mm D-glucose and 20 mm L-glutamine at 30 °C for 48 h. To determine the expression of *calA* and its processed splicing products *M. alpina* ATCC32222 and *A. niger* tJMW06 was cultivated in 200 mL MEP for 72 h or in 200 mL YPD amended by 30 µg mL^{-1} doxycycline for 36 h, respectively. Mycelium was harvested, ground under liquid nitrogen, and RNA was isolated using the SV Total RNA Isolation System (Promega). Residual gDNA was digested using Baseline-Zero DNase (Biozym). cDNA was synthesized using the anchored oligo(dT)$_{20}$ primers and the RevertAid First Strand cDNA Synthesis Kit (Thermo Scientific). Semi-quantitative PCR was carried out with DreamTaq Green Polymerase (Thermo Scientific) and oligonucleotides listed in Additional file 4: Table S3 according to the manufacturer's instructions. As internal standard, the housekeeping genes encoding actin B (*actB*; for *M. alpina*) or the glycerinaldehyde-3-phosphate-dehydrogenase (*gpdA*; for *A. niger*) was used.

Extraction of laetiporic acids and calpinactam

Mycelia of *A. niger* tLK04 (*lpaA*-expressing), tLK05 (*lpaA*^{D1415A}-expressing), tLK07 (empty vector control) and *L. sulphureus* fruiting bodies were used to extract laetiporic acids. Accordingly, mycelia of *A. niger* tJMW06 (*calA* expressing), tLK07 (empty vector control) and *M. alpina* were used to produce calpinactam. Mycelia were harvested by filtration, rinsed with water and finally lyophilized to entire dryness. Mycelia were ground to a fine powder using a mortar and pestle and subsequently extracted with 20 mL acetone per gram dry weight (laetiporic acids) or with 20 mL methanol per gram dry weight (calpinactam) at 150 rpm for 2 h. The solvent phase was decanted, filtered and evaporated under reduced pressure in a rotary evaporator. The residue was dissolved in 1 mL methanol and 5 µL thereof was subjected to UHPLC-MS analyses.

Chemical standards

Authentic standards of laetiporic acids A_1, A_2, B_1, B_2, C_1, and C_2 were isolated from *L. sulphureus* fruiting bodies as described previously [41]. A commercial standard for calpinactam was obtained from Santa Cruz Biotechnology, Inc. (CAS 1205538-83-5).

UHPLC-MS measurement

Extracts and standards were measured on an Agilent Infinity II 1290 system connected to an Agilent 6130 single quadrupole mass spectrometer. To detect laetiporic acids the following gradient was applied on a Zorbax Eclipse Plus C18 RRHD column (Agilent; 50 mm × 2.1 mm, 1.8 µm) at a flow rate of 1 mL min^{-1} at 30 °C using water + 0.1% formic acid (solvent A) and acetonitrile (solvent B): 0–3 min: 5–50% B; 3–7 min: 50–75% B; 7–8 min: 75–100% B. Signals were recorded at wavelengths λ = 210–600 nm by a diode array detector and UV profiles were extracted at λ = 450 nm. Additionally, extracted ion chromatograms were recorded by ESI–MS in positive ionization mode (*m/z* 421, 447, 473, 499 $[M+H]^+$). Purified polyenes LA A_1–LA C_2 from *L. sulphureus* served as reference standard [41]. To detect calpinactam, the identical column and chromatograph were used and the following gradient were applied: 0–4 min: 5–72% B, 4–4.5 min: 72–95% B, 4.5–5 min: 95% B. Since calpinactam is hardly chromophore, mass signals were recorded in positive ionization mode and detection of calpinactam was based on selected ion monitoring (SIM) signals of *m/z* 768 $[M+H]^+$. For quantifications, a calibration curve was recorded with a commercial calpinactam standard (Santa Cruz Biotechnology, Inc.) in concentrations ranging from 0.488 to 125 µg mL^{-1}.

High resolution mass spectrometry

HR-MS and HR-MS/MS spectra of identified compounds and the respective standards were additionally recorded on a Q Exactive Plus mass spectrometer (Thermo Scientific) as described for polyenes [41] and peptides [57].

Supplementary Information

The online version contains supplementary material available at https://doi.org/10.1186/s40694-023-00152-3.

Additional file 1. Experimental procedures.

Additional file 2: Table S1. Calculation of the frequency of homologous recombination in *A. niger* ATNT and tLK01 transformed with the *fwnA* deletion construct. *T1-T3 indicate the number of transformants per 500 ng DNA from three independent transformations.

Additional file 3: Table S2. Organisms used in this study.

Additional file 4: Table S3. Oligonucleotides used in this study.

Additional file 5: Figure S1. Southern Blot analysis for determination of the *akuB* deletion strain tLK01. **A.** Schematic representation of the genomic *akuB* locus of the strain ATNT and tLK01 (ATNTΔ*akuB*) with its respective *EcoR*V (upper panel) and *Hind*III restriction sites (lower panel). **B.** Southern Blot analysis of the *A. niger* parental strain ATNT and the *akuB* deletion strain tLK01**.** Genomic DNA was digested with *EcoR*V or *Hind*III. A digoxigenin-labeled probe was generated with oMG482/oMG483 to hybridize with the *akuB* upstream sequence and signals were detected with CDPstar (Roche Diagnostics).

Additional file 6: Figure S2. Plasmid maps of the expression vectors. The plasmids pLK04 (**A**), pLK05 (**B**), pMG56 (**C**) and pMG58 (**D**) are based on the pSMX2-URA plasmid [1]. The gene fragments are: *bla*; β-lactamase (confers ampicillin resistance); *calA1/5*; 1 kb of the 5′or 3′ end of the *calA* gene; *fwnA*up and *fwnA*down, 1 kb up- and downstream the *A. niger fwnA* polyketide synthase gene; URA-blaster (dark blue, contains several genes; see below); P*terA*, promoter of the *terA* terrein polyketide synthase gene of *Aspergillus terreus*; Tag, encodes the hexahistidin tag (and includes an *SpeI* and *PacI* site for insertion of the GOI); T*trpC*, terminator of the *trpC* anthranilatsynthase component 2 gene of *A. terreus*; rep origin, origin of plasmid replication. The URA-blaster contains: P*pyrG*, promoter of the *pyrG* gene from *Aspergillus nidulans*; *pyrG*, orotidine 5′-phosphate decarboxylase gene from *A. nidulans* (confers uracil prototrophy); T*pyrG*, terminator of the *pyrG* gene from *A. nidulans*; and two *prpB* flanks that encode the methylcitrate synthase gene from *Escherichia coli* that facilitate a subsequent removal of the URA blaster cassette from the *A. niger* genome via a homologous recombination event (counter selection) by addition of 5-fluoroorotic acid [2].

Additional file 7: Figure S3. Photographs of *A. niger* ATNT and tLK01 transformed with the *fwnA* deletion construct. Both pigmented and non-pigmented transformants have been detected in both experiments, but frequency of the homologous recombination into the *fwnA* locus is significantly higher in tLK01. For calculation of frequency of recombination see Additional file 2: Table S1.

Additional file 8: Figure S4. Determination of the homologous integration of the P*terA*:T*trpC* construct into the *fwnA* locus of recipient strains ATNT and tLK01. **A.** Schematic representation of the genomic *fwnA* locus of the parental strain ATNT and tLK01 (ATNTΔ*akuB*) (upper lane) and the deletion mutants ATNTΔ*fwnA* (tLK06) and tLK07 (ATNTΔ*akuB*Δ*fwnA*). **B.** Agarose gel of two diagnostic PCRs targeting the *fwnA* gene (upper lane) and the P*terA* promoter (lower lane). In contrast to the parental strains ATNT and tLK01, the non-pigmented Δ*fwnA* mutants (tLK06 and tLK07) lack the signal of the *fwnA* gene (upper panel). In *lieu* thereof, the homologous integration of P*terA*:T*trpC* could be determined in the mutants (lower panel).

Additional file 9: Figure S5. Southern Blot analysis for determination of the *fwnA* deletion and *lpaA* overexpression in *A. niger* strains tLK04. **A.** Schematic representation of the genomic *fwnA* locus in the strain tLK01 (ATNTΔ*akuB*) and the Δ*fwnA*::*lpaA* overexpression strain tLK04 with its respective *Sac*II restriction sites. **B.** Southern Blot analysis of the *A. niger* parental strain tLK01 and five Δ*fwnA*::*lpaA* overexpression strains tLK04**.** Genomic DNA was digested with *Sac*II. A digoxigenin-labeled probe was generated with oMG504/oMG505 to hybridize with the *fwnA* downstream sequence and signals were detected with CDPstar (Roche Diagnostics). Strains used for subsequent metabolic analysis are highlighted in green.

Additional file 10: Figure S6. HR-MS and MS/MS spectra of laetiporic acids A_1-D_2 detectable in *A. niger* tLK04. High resolution MS/MS fragmentation of laetiporic acids A_1/A_2 (**A**), B_1/B_2 (**B**), C_1/C_2 (**C**) and D_1/D_2 (**D**) produced by *A. niger* tLK04. Indicated fragments are identical to the literature [1].

Additional file 11: Figure S7. Expression of *lpaA* in the transgenic *A. niger* tLK07 (null mutant), tLK04 (*lpaA* expressing) and tLK05 (*lpaA*^{D1415A} expressing). Expression was profiled by semi-quantitative PCR on the laetiporic acid synthase gene (*lpaA*) and referenced to the expression of the housekeeping gene encoding the glyceraldehyde-3-phosphate dehydrogenase (*gpdA*). RNA was isolated and cDNA was synthesized after cultivation for 36 h in inducing AMM (with doxycycline) at 30°C and 180 rpm. The genomic DNA (gDNA) of tLK07 or the *lpaA*-encoding plasmid pPS03 served as positive controls for *gpdA* and *lpaA* amplification, respectively.

Additional file 12: Figure S8. Integration of *calA* into the *fwnA* locus in *A.niger* tJMW06. **A.** Genomic locus of *fwnA* during recombination of the five *calA* DNA fragments in *A. niger* pJMW06. **B.** PCR amplification of four adjacent DNA fragment pairs was carried out using genomic DNA as templates. The *A. niger* parental strain tLK01 and the null mutant strain tLK07 (empty vector) served as negative controls. Three individual *calA*-expressing transformants tJMW06 #3, #13 and #26 showed the expected amplicon sizes of the recombined DNA fragments.

Additional file 13: Figure S9. Southern Blot analysis for determination of the full-length *calA* integration into the genome of *A. niger* strain tJMW06. **A**. Schematic representation of the genomic *fwnA* locus in the strain tLK01 (ATNTΔ*akuB*), theΔ*fwnA*::*calA* overexpression locus of strain tJMW06.3 and the native *calA* locus of the *calA* gene donor strain *M. alpina* ATCC32222. **B.** Southern Blot analysis of the *A. niger* parental strain tLK01, the Δ*fwnA*::*calA* overexpression strain tJMW06 and *M. alpina* ATCC32222**.** Genomic DNA was double-digested with *SmaI*/*DraI*. A digoxigenin-labeled probe was generated with oMG569/oMG548 to hybridize with the *fwnA* downstream sequence and signals were detected with CDPstar (Roche Diagnostics). Full-length *calA* integration was determined for *A. niger* tJMW06 and directly reflects the size of the *calA* gene fragment in the gene donor strain *M. alpina* ATCC32222.

Additional file 14: Figure S10. Temperature dependent production of calpinactam in *A. niger* tJMW06 and *M. alpina* ATCC32222. Calpinactam production (bars) and total fungal dry weight (boxes) are indicated for several cultivation conditions. The transformant *A. niger* tJMW06 was cultivated in YPD with 30 µg mL^{-1} doxycycline as inducer at 20, 25 and 30°C for 3 days. The *calA* gene donor strain *M. alpina* ATCC32222 was cultivated in MEP (25°C) for 4 days. Production rate in *A. niger* tJMW06 is optimal at 25 °C, which is the growth optimum for *M. alpina*. Experiments were carried in triplicate.

Acknowledgements

We are grateful to Andrea Perner (Leibniz Institute for Natural Product Research and Infection Biology (Hans-Knöll-Institute), Jena, Germany) for her technical assistance in recording HR-MS/MS spectra. We acknowledge Professor Matthias Brock (University of Nottingham, Nottingham, UK) for valuable discussions.

Author contributions

LK and JMW contributed equally to this work. LK, PSS and JMW performed the biological experiments and analyzed the genetic data. JMW and MG recorded chromatograms and analyzed mass spectra. MR extracted metabolites and manufactured the samples for HPLC analysis. PSS and JMW prepared the figures. MG designed the project, planned the experiments, interpreted the results and wrote the manuscript. All authors read and approved the manuscript.

Funding
Open Access funding enabled and organized by Projekt DEAL. This research received no specific grant from any funding agency in the public, commercial, or not-for-profit sectors.

Availability of data and materials
The sequence of the *calA* gene from *M. alpina* ATCC32222 is deposited under the GenBank accession number OP959498. The fungal strains are available upon request from the American Type Culture Collection (ATCC) or the Jena Microbial Resource Collection (JMRC) as listed in Additional file 3: Table S2.

Declarations

Ethics approval and consent to participate
Not applicable.

Consent for publication
Not applicable.

Competing interests
The authors declare no competing interests.

Received: 12 December 2022 Accepted: 22 January 2023
Published online: 01 February 2023

References

1. Meyer V, Basenko EY, Benz JP, Braus GH, Caddick MX, Csukai M, de Vries RP, Endy D, Frisvad JC, Gunde-Cimerman N, et al. Growing a circular economy with fungal biotechnology: a white paper. Fungal Biol Biotechnol. 2020;7:5.
2. Wang X, Jarmusch SA, Frisvad JC, Larsen TO. Current status of secondary metabolite pathways linked to their related biosynthetic gene clusters in *Aspergillus* section Nigri. Nat Prod Rep. 2022. https://doi.org/10.1039/D1NP00074H.
3. Chiang CY, Ohashi M, Tang Y. Deciphering chemical logic of fungal natural product biosynthesis through heterologous expression and genome mining. Nat Prod Rep. 2022. https://doi.org/10.1039/D2NP00050D.
4. Zhang JM, Wang HH, Liu X, Hu CH, Zou Y. Heterologous and engineered biosynthesis of nematocidal polyketide-nonribosomal peptide hybrid macrolactone from extreme thermophilic fungi. J Am Chem Soc. 2020;142(4):1957–65.
5. Ugai T, Minami A, Fujii R, Tanaka M, Oguri H, Gomi K, Oikawa H. Heterologous expression of highly reducing polyketide synthase involved in betaenone biosynthesis. Chem Commun (Camb). 2015;51(10):1878–81.
6. Wasil Z, Pahirulzaman KAK, Butts C, Simpson TJ, Lazarus CM, Cox RJ. One pathway, many compounds: heterologous expression of a fungal biosynthetic pathway reveals its intrinsic potential for diversity. Chem Sci. 2013;4(10):3845–56.
7. Matsuda Y, Wakimoto T, Mori T, Awakawa T, Abe I. Complete biosynthetic pathway of anditomin: nature's sophisticated synthetic route to a complex fungal meroterpenoid. J Am Chem Soc. 2014;136(43):15326–36.
8. Sato M, Dander JE, Sato C, Hung YS, Gao SS, Tang MC, Hang L, Winter JM, Garg NK, Watanabe K, et al. Collaborative biosynthesis of maleimide- and succinimide-containing natural products by fungal polyketide megasynthases. J Am Chem Soc. 2017;139(15):5317–20.
9. Gressler M, Löhr NA, Schäfer T, Lawrinowitz S, Seibold PS, Hoffmeister D. Mind the mushroom: natural product biosynthetic genes and enzymes of Basidiomycota. Nat Prod Rep. 2021;38(4):702–22.
10. Tabima JF, Trautman IA, Chang Y, Wang Y, Mondo S, Kuo A, Salamov A, Grigoriev IV, Stajich JE, Spatafora JW. Phylogenomic analyses of non-dikarya fungi supports horizontal gene transfer driving diversification of secondary metabolism in the amphibian gastrointestinal symbiont, *Basidiobolus*. G3. 2020;10(9):3417–33.
11. Koczyk G, Pawłowska J, Muszewska A. Terpenoid biosynthesis dominates among secondary metabolite clusters in Mucoromycotina genomes. J Fungi. 2021;7(4):285.
12. Rokas A, Wisecaver JH, Lind AL. The birth, evolution and death of metabolic gene clusters in fungi. Nat Rev Microbiol. 2018;16(12):731–44.
13. Punt PJ, Dingemanse MA, Kuyvenhoven A, Soede RD, Pouwels PH, van den Hondel CA. Functional elements in the promoter region of the *Aspergillus nidulans gpdA* gene encoding glyceraldehyde-3-phosphate dehydrogenase. Gene. 1990;93(1):101–9.
14. Tsuchiya K, Tada S, Gomi K, Kitamoto K, Kumagai C, Tamura G. Deletion analysis of the Taka-amylase A gene promoter using a homologous transformation system in *Aspergillus oryzae*. Biosci Biotechnol Biochem. 1992;56(11):1849–53.
15. Chiang YM, Szewczyk E, Davidson AD, Entwistle R, Keller NP, Wang CC, Oakley BR. Characterization of the *Aspergillus nidulans* monodictyphenone gene cluster. Appl Environ Microbiol. 2010;76(7):2067–74.
16. Meyer V, Wanka F, van Gent J, Arentshorst M, van den Hondel CA, Ram AF. Fungal gene expression on demand: an inducible, tunable, and metabolism-independent expression system for *Aspergillus niger*. Appl Environ Microbiol. 2011;77(9):2975–83.
17. Gressler M, Hortschansky P, Geib E, Brock M. A new high-performance heterologous fungal expression system based on regulatory elements from the *Aspergillus terreus* terrein gene cluster. Front Microbiol. 2015;6:e184.
18. Geib E, Brock M. ATNT: an enhanced system for expression of polycistronic secondary metabolite gene clusters in *Aspergillus niger*. Fungal Biol Biotechnol. 2017;4: e13.
19. Chiang YM, Szewczyk E, Davidson AD, Keller N, Oakley BR, Wang CC. A gene cluster containing two fungal polyketide synthases encodes the biosynthetic pathway for a polyketide, asperfuranone, in *Aspergillus nidulans*. J Am Chem Soc. 2009;131(8):2965–70.
20. Löhr NA, Eisen F, Thiele W, Platz L, Motter J, Hüttel W, Gressler M, Müller M, Hoffmeister D. Unprecedented mushroom polyketide synthases produce the universal Anthraquinone precursor. Angew Chem Int Ed Engl. 2022;61(24): e202116142.
21. Sung CT, Chang SL, Entwistle R, Ahn G, Lin TS, Petrova V, Yeh HH, Praseuth MB, Chiang YM, Oakley BR, et al. Overexpression of a three-gene conidial pigment biosynthetic pathway in *Aspergillus nidulans* reveals the first NRPS known to acetylate tryptophan. Fungal Genet Biol. 2017;101:1–6.
22. Yeh HH, Chiang YM, Entwistle R, Ahuja M, Lee KH, Bruno KS, Wu TK, Oakley BR, Wang CCC. Molecular genetic analysis reveals that a nonribosomal peptide synthetase-like (NRPS-like) gene in *Aspergillus nidulans* is responsible for microperfuranone biosynthesis. Appl Microbiol Biotechnol. 2012;96(3):739–48.
23. Geib E, Baldeweg F, Doerfer M, Nett M, Brock M. Cross-chemistry leads to product diversity from atromentin synthetases in *Aspergilli* from section *Nigri*. Cell Chem Biol. 2019;26(2):223–34.
24. Harvey CJB, Tang M, Schlecht U, Horecka J, Fischer CR, Lin HC, Li J, Naughton B, Cherry J, Miranda M, et al. HEx: a heterologous expression platform for the discovery of fungal natural products. Sci Adv. 2018;4(4):eaar5459.
25. Heneghan MN, Yakasai AA, Halo LM, Song Z, Bailey AM, Simpson TJ, Cox RJ, Lazarus CM. First heterologous reconstruction of a complete functional fungal biosynthetic multigene cluster. ChemBioChem. 2010;11(11):1508–12.
26. Jin FJ, Maruyama J, Juvvadi PR, Arioka M, Kitamoto K. Development of a novel quadruple auxotrophic host transformation system by *argB* gene disruption using *adeA* gene and exploiting adenine auxotrophy in *Aspergillus oryzae*. FEMS Microbiol Lett. 2004;239(1):79–85.
27. Nayak T, Szewczyk E, Oakley CE, Osmani A, Ukil L, Murray SL, Hynes MJ, Osmani SA, Oakley BR. A versatile and efficient gene-targeting system for *Aspergillus nidulans*. Genetics. 2006;172(3):1557–66.
28. Liu N, Hung YS, Gao SS, Hang L, Zou Y, Chooi YH, Tang Y. Identification and heterologous production of a benzoyl-primed tricarboxylic acid polyketide intermediate from the zaragozic acid a biosynthetic pathway. Org Lett. 2017;19(13):3560–3.
29. Chiang YM, Oakley CE, Ahuja M, Entwistle R, Schultz A, Chang SL, Sung CT, Wang CC, Oakley BR. An efficient system for heterologous expression of secondary metabolite genes in *Aspergillus nidulans*. J Am Chem Soc. 2013;135(20):7720–31.

30. Wiemann P, Soukup AA, Folz JS, Wang PM, Noack A, Keller NP. CoIN: co-inducible nitrate expression system for secondary metabolites in *Aspergillus nidulans*. Fungal Biol Biotechnol. 2018;5:6.
31. Chiang YM, Lin TS, Chang SL, Ahn G, Wang CCC. An *Aspergillus nidulans* platform for the complete cluster refactoring and total biosynthesis of fungal natural products. ACS Synth Biol. 2021;10(1):173–82.
32. Huhner E, Oqvist K, Li SM. Design of alpha-keto carboxylic acid dimers by domain recombination of nonribosomal peptide synthetase (NRPS)-like enzymes. Org Lett. 2019;21(2):498–502.
33. Lee KK, Da Silva NA, Kealey JT. Determination of the extent of phosphopantetheinylation of polyketide synthases expressed in *Escherichia coli* and *Saccharomyces cerevisiae*. Anal Biochem. 2009;394(1):75–80.
34. Ku J, Mirmira RG, Liu L, Santi DV. Expression of a functional non-ribosomal peptide synthetase module in *Escherichia coli* by coexpression with a phosphopantetheinyl transferase. Chem Biol. 1997;4(3):203–7.
35. Kuijpers NG, Solis-Escalante D, Bosman L, van den Broek M, Pronk JT, Daran JM, Daran-Lapujade P. A versatile, efficient strategy for assembly of multi-fragment expression vectors in *Saccharomyces cerevisiae* using 60 bp synthetic recombination sequences. Microb Cell Fact. 2013;12: e47.
36. Huang F, Spangler JR, Huang AY. In vivo cloning of up to 16 kb plasmids in *E. coli* is as simple as PCR. PLoS ONE. 2017;12(8): e0183974.
37. Bibillo A, Eickbush TH. High processivity of the reverse transcriptase from a non-long terminal repeat retrotransposon. J Biol Chem. 2002;277(38):34836–45.
38. Pillay LC, Nekati L, Makhwitine PJ, Ndlovu SI. Epigenetic activation of silent biosynthetic gene clusters in endophytic fungi using small molecular modifiers. Front Microbiol. 2022;13: e815008.
39. Caesar LK, Robey MT, Swyers M, Islam MN, Ye R, Vagadia PP, Schiltz GE, Thomas PM, Wu CC, Kelleher NL, et al. Heterologous expression of the unusual terreazepine biosynthetic gene cluster reveals a promising approach for identifying new chemical scaffolds. MBio. 2020;11(4):e01691-e11620.
40. Bok JW, Ye R, Clevenger KD, Mead D, Wagner M, Krerowicz A, Albright JC, Goering AW, Thomas PM, Kelleher NL, et al. Fungal artificial chromosomes for mining of the fungal secondary metabolome. BMC Genomics. 2015;16:343.
41. Seibold PS, Lenz C, Gressler M, Hoffmeister D. The *Laetiporus* polyketide synthase LpaA produces a series of antifungal polyenes. J Antibiot (Tokyo). 2020;73(10):711–20.
42. Oliveira JM, van der Veen D, de Graaff LH, Qin L. Efficient cloning system for construction of gene silencing vectors in *Aspergillus niger*. Appl Microbiol Biotechnol. 2008;80(5):917–24.
43. Mizutani O, Kudo Y, Saito A, Matsuura T, Inoue H, Abe K, Gomi K. A defect of LigD (human Lig4 homolog) for nonhomologous end joining significantly improves efficiency of gene-targeting in *Aspergillus oryzae*. Fungal Genet Biol. 2008;45(6):878–89.
44. Krappmann S, Sasse C, Braus GH. Gene targeting in *Aspergillus fumigatus* by homologous recombination is facilitated in a nonhomologous end- joining-deficient genetic background. Eukaryot Cell. 2006;5(1):212–5.
45. Gressler M, Zaehle C, Scherlach K, Hertweck C, Brock M. Multifactorial induction of an orphan PKS-NRPS gene cluster in *Aspergillus terreus*. Chem Biol. 2011;18(2):198–209.
46. Fairhead C, Llorente B, Denis F, Soler M, Dujon B. New vectors for combinatorial deletions in yeast chromosomes and for gap-repair cloning using 'split-marker' recombination. Yeast. 1996;12(14):1439–57.
47. Jørgensen TR, Nielsen KF, Arentshorst M, Park J, van den Hondel CA, Frisvad JC, Ram AF. Submerged conidiation and product formation by *Aspergillus niger* at low specific growth rates are affected in aerial developmental mutants. Appl Environ Microbiol. 2011;77(15):5270–7.
48. Bergmann P, Frank C, Reinhardt O, Takenberg M, Werner A, Berger RG, Ersoy F, Zschätzsch M. Pilot-scale production of the natural colorant laetiporic acid, its stability and potential applications. Fermentation. 2022;8:684.
49. Gill M. Polyolefinic 18-methyl-19-oxoicosenoic acid pigments from the fungus *Piptoporus australiensis* (Wakefield) Cunningham. J Chem Soc Perkin Trans. 1982. https://doi.org/10.1039/p19820001449.
50. Schwenk D, Nett M, Dahse HM, Horn U, Blanchette RA, Hoffmeister D. Injury-induced biosynthesis of methyl-branched polyene pigments in a white-rotting *Basidiomycete*. J Nat Prod. 2014;77(12):2658–63.
51. Brandt P, Garcia-Altares M, Nett M, Hertweck C, Hoffmeister D. Induced chemical defense of a mushroom by a double-bond-shifting polyene synthase. Angew Chem Int Ed Engl. 2017;56(21):5937–41.
52. Storm PA, Herbst DA, Maier T, Townsend CA. Functional and structural analysis of programmed C-methylation in the biosynthesis of the fungal polyketide citrinin. Cell Chem Biol. 2017;24(3):316–25.
53. Koyama N, Kojima S, Nonaka K, Masuma R, Matsumoto M, Omura S, Tomoda H. Calpinactam, a new anti-mycobacterial agent, produced by *Mortierella alpina* FKI-4905. J Antibiot (Tokyo). 2010;63(4):183–6.
54. Koyama N, Kojima S, Fukuda T, Nagamitsu T, Yasuhara T, Omura S, Tomoda H. Structure and total synthesis of fungal calpinactam, a new antimycobacterial agent. Org Lett. 2010;12(3):432–5.
55. Nagai K, Koyama N, Sato N, Yanagisawa C, Tomoda H. Synthesis and antimycobacterial activity of calpinactam derivatives. Bioorg Med Chem Lett. 2012;22(24):7739–41.
56. Wang L, Chen W, Feng Y, Ren Y, Gu Z, Chen H, Wang H, Thomas MJ, Zhang B, Berquin IM, et al. Genome characterization of the oleaginous fungus *Mortierella alpina*. PLoS ONE. 2011;6(12): e28319.
57. Wurlitzer JM, Stanišić A, Ziethe S, Jordan PM, Günther K, Werz O, Kries H, Gressler M. Macrophage-targeting oligopeptides from *Mortierella alpina*. Chem Sci. 2022;13(31):9091–101.
58. Wurlitzer JM, Stanišić A, Wasmuth I, Jungmann S, Fischer D, Kries H, Gressler M. Bacterial-like nonribosomal peptide synthetases produce cyclopeptides in the Zygomycetous fungus *Mortierella alpina*. Appl Environ Microbiol. 2021;87(3):e02051-e12020.
59. Bernhardt M, Berman S, Zechel D, Bechthold A. Role of two exceptional trans adenylation domains and MbtH-like proteins in the biosynthesis of the nonribosomal peptide WS9324A from *Streptomyces calvus* ATCC 13382. ChemBioChem. 2020;21(18):2659–66.
60. Sonnabend R, Seiler L, Gressler M. Regulation of the leucine metabolism in *Mortierella alpina*. J Fungi (Basel). 2022;8(2):196.
61. Miethke M, Pieroni M, Weber T, Bronstrup M, Hammann P, Halby L, Arimondo PB, Glaser P, Aigle B, Bode HB, et al. Towards the sustainable discovery and development of new antibiotics. Nat Rev Chem. 2021;5(10):726–49.
62. Tulp M, Bohlin L. Rediscovery of known natural compounds: nuisance or goldmine? Bioorg Med Chem. 2005;13(17):5274–82.
63. Voigt K, Wolf T, Ochsenreiter K, Nagy G, Kaerger K, Shelest E, Papp T. Genetic and metabolic aspects of primary and secondary metabolism of the Zygomycetes. In: Hoffmeister D, editor. The Mycota: biochemistry and molecular biology. 3rd ed. Cham: Springer International Publishing; 2016. p. 361–85.
64. Tsuboi Y, Sakuma T, Yamamoto T, Horiuchi H, Takahashi F, Igarashi K, Hagihara H, Takimura Y. Gene manipulation in the Mucorales fungus *Rhizopus oryzae* using TALENs with exonuclease overexpression. FEMS Microbiol Lett. 2022;369(1):fnac032.
65. Boontawon T, Nakazawa T, Inoue C, Osakabe K, Kawauchi M, Sakamoto M, Honda Y. Efficient genome editing with CRISPR/Cas9 in *Pleurotus ostreatus*. AMB Express. 2021;11(1):30.
66. Chen BX, Wei T, Ye ZW, Yun F, Kang LZ, Tang HB, Guo LQ, Lin JF. Efficient CRISPR-Cas9 gene disruption system in edible-medicinal mushroom *Cordyceps militaris*. Front Microbiol. 2018;9:1157.
67. Nah HJ, Pyeon HR, Kang SH, Choi SS, Kim ES. Cloning and heterologous expression of a large-sized natural product biosynthetic gene cluster in *Streptomyces* Species. Front Microbiol. 2017;8:394.
68. Yuan J, Mo Q, Fan C. New set of yeast vectors for shuttle expression in *Escherichia coli*. ACS Omega. 2021;6(10):7175–80.
69. Yamane M, Minami A, Liu C, Ozaki T, Takeuchi I, Tsukagoshi T, Tokiwano T, Gomi K, Oikawa H. Biosynthetic machinery of *Diterpene Pleuromutilin* isolated from basidiomycete fungi. ChemBioChem. 2017;18(23):2317–22.
70. Hoefgen S, Lin J, Fricke J, Stroe MC, Mattern DJ, Kufs JE, Hortschansky P, Brakhage AA, Hoffmeister D, Valiante V. Facile assembly and fluorescence-based screening method for heterologous expression of biosynthetic pathways in fungi. Metab Eng. 2018;48:44–51.
71. Wingler LM, Cornish VW. Reiterative recombination for the in vivo assembly of libraries of multigene pathways. Proc Natl Acad Sci USA. 2011;108(37):15135–40.
72. Kupfer DM, Drabenstot SD, Buchanan KL, Lai H, Zhu H, Dyer DW, Roe BA, Murphy JW. Introns and splicing elements of five diverse fungi. Eukaryot Cell. 2004;3(5):1088–100.

73. Ninomiya Y, Suzuki K, Ishii C, Inoue H. Highly efficient gene replacements in *Neurospora* strains deficient for nonhomologous end-joining. Proc Natl Acad Sci USA. 2004;101(33):12248–53.
74. de Reus E, Nielsen MR, Frandsen RJN. Metabolic and regulatory insights from the experimental horizontal gene transfer of the aurofusarin and bikaverin gene clusters to *Aspergillus nidulans*. Mol Microbiol. 2019;112(6):1684–700.
75. Jarczynska ZD, Vanegas KG, Deichmann M, Jensen CN, Scheeper MJ, Futyma ME, Strucko T, Contesini FJ, Jørgensen TS, Hoof JB, et al. A versatile in vivo DNA assembly toolbox for fungal strain engineering. ACS Synth Biol. 2022;11(10):3251–63.
76. Pohl C, Polli F, Schütze T, Viggiano A, Mózsik L, Jung S, de Vries M, Bovenberg RAL, Meyer V, Driessen AJM. A *Penicillium rubens* platform strain for secondary metabolite production. Sci Rep. 2020;10(1):7630.
77. Pikl S, Carrillo Rincon AF, Slemc L, Goranovic D, Avbelj M, Gjuracic K, Sucipto H, Stare K, Baebler S, Sala M, et al. Multiple copies of the oxytetracycline gene cluster in selected *Streptomyces rimosus* strains can provide significantly increased titers. Microb Cell Fact. 2021;20(1):47.
78. Hossain AH, Ter Beek A, Punt PJ. Itaconic acid degradation in *Aspergillus niger*: the role of unexpected bioconversion pathways. Fungal Biol Biotechnol. 2019;6:1.
79. Zaehle C, Gressler M, Shelest E, Geib E, Hertweck C, Brock M. Terrein biosynthesis in *Aspergillus terreus* and its impact on phytotoxicity. Chem Biol. 2014;21(6):719–31.
80. Watanabe A, Ebizuka Y. Unprecedented mechanism of chain length determination in fungal aromatic polyketide synthases. Chem Biol. 2004;11(8):1101–6.
81. Ma SM, Li JW, Choi JW, Zhou H, Lee KK, Moorthie VA, Xie X, Kealey JT, Da Silva NA, Vederas JC, et al. Complete reconstitution of a highly reducing iterative polyketide synthase. Science. 2009;326(5952):589–92.
82. Cacho RA, Thuss J, Xu W, Sanichar R, Gao Z, Nguyen A, Vederas JC, Tang Y. Understanding programming of fungal iterative polyketide synthases: the biochemical basis for regioselectivity by the methyltransferase domain in the lovastatin megasynthase. J Am Chem Soc. 2015;137(50):15688–91.
83. Phakeovilay J, Imaram W, Vuttipongchaikij S, Bunnak W, Lazarus CM, Wattana-Amorn P. C-Methylation controls the biosynthetic programming of alternapyrone. Org Biomol Chem. 2022;20(25):5050–4.
84. Awan AR, Blount BA, Bell DJ, Shaw WM, Ho JCH, McKiernan RM, Ellis T. Biosynthesis of the antibiotic nonribosomal peptide penicillin in baker's yeast. Nat Commun. 2017;8(4):15202.
85. Ishiuchi K, Nakazawa T, Ookuma T, Sugimoto S, Sato M, Tsunematsu Y, Ishikawa N, Noguchi H, Hotta K, Moriya H, et al. Establishing a new methodology for genome mining and biosynthesis of polyketides and peptides through yeast molecular genetics. ChemBioChem. 2012;13(6):846–54.
86. Xu W, Cai X, Jung ME, Tang Y. Analysis of intact and dissected fungal polyketide synthase-nonribosomal peptide synthetase in vitro and in *Saccharomyces cerevisiae*. J Am Chem Soc. 2010;132(39):13604–7.
87. Gao X, Haynes SW, Ames BD, Wang P, Vien LP, Walsh CT, Tang Y. Cyclization of fungal nonribosomal peptides by a terminal condensation-like domain. Nat Chem Biol. 2012;8(10):823–30.
88. Tokuoka M, Tanaka M, Ono K, Takagi S, Shintani T, Gomi K. Codon optimization increases steady-state mRNA levels in *Aspergillus oryzae* heterologous gene expression. Appl Environ Microbiol. 2008;74(21):6538–46.
89. Gygli SM, Borrell S, Trauner A, Gagneux S. Antimicrobial resistance in *Mycobacterium tuberculosis*: mechanistic and evolutionary perspectives. FEMS Microbiol Rev. 2017;41(3):354–73.
90. Shyam M, Shilkar D, Verma H, Dev A, Sinha BN, Brucoli F, Bhakta S, Jayaprakash V. The Mycobactin biosynthesis pathway: a prospective therapeutic target in the battle against tuberculosis. J Med Chem. 2021;64(1):71–100.
91. Liu X, Jin Y, Cui Z, Nonaka K, Baba S, Funabashi M, Yang Z, Van Lanen SG. The role of a nonribosomal peptide synthetase in L-lysine lactamization during capuramycin biosynthesis. ChemBioChem. 2016;17(9):804–10.
92. Adamczeski M, Quinoa E, Crews P. Novel sponge-derived amino acids. 5. Structures, stereochemistry, and synthesis of several new heterocycles. J Am Chem Soc. 1989;111(2):647–54.
93. Macko V, Stimmel MB, Wolpert TJ, Dunkle LD, Acklin W, Banteli R, Jaun B, Arigoni D. Structure of the host-specific toxins produced by the fungal pathogen *Periconia circinata*. Proc Natl Acad Sci USA. 1992;89(20):9574–8.
94. Davidson BS, Schumacher RW. Isolation and synthesis of caprolactin-a and caprolactin-B, new caprolactams from a marine bacterium. Tetrahedron. 1993;49(30):6569–74.
95. Ikeda Y, Nonaka H, Furumai T, Onaka H, Igarashi Y. Nocardimicins A, B, C, D, E, and F, siderophores with muscarinic M3 receptor inhibiting activity from *Nocardia* sp TP-A0674. J Nat Prod. 2005;68(7):1061–5.
96. Lasier WA, Rigby GW. Catalytic process for the production of caprolactam, amino-capronitrile and hexamethylene diamine. 1941. In., vol. U.S. Patent No. 2,234,566.
97. Chapman S, Potter ME, Raja R. The molecular design of active sites in nanoporous materials for sustainable catalysis. Molecules. 2017;22(12):2127.
98. Zong BN, Sun B, Cheng SB, Mu XH, Yang KY, Zhao JQ, Zhang XX, Wu W. Green production technology of the monomer of nylon-6: caprolactam. Engineering. 2017;3(3):379–84.
99. Krovi SA, Moreno Caffaro MM, Aravamudhan S, Mortensen NP, Johnson LM. Fabrication of Nylon-6 and Nylon-11 nanoplastics and evaluation in mammalian cells. Nanomaterials (Basel). 2022;12(15):2699.
100. Hill TW, Kafer E. Improved protocols for *Aspergillus* minimal medium: trace element and minimal medium salt stock solutions. Fungal Genet Rep. 2001;48(8):20–1.
101. Conti E, Stachelhaus T, Marahiel MA, Brick P. Structural basis for the activation of phenylalanine in the non-ribosomal biosynthesis of gramicidin S. EMBO J. 1997;16(14):4174–83.

Publisher's Note

A Genetic Tool to Express Long Fungal Biosynthetic Genes

Leo Kirchgaessner,[1,2,3] Jacob M. Wurlitzer,[1,2] Paula S. Seibold, [1,2] Malik Rakhmanov,[1,2] and Markus Gressler[1,2]

[1] Friedrich Schiller University Jena, Institute of Pharmacy, Department Pharmaceutical Microbiology, Winzerlaer Strasse 2, 07745 Jena, Germany

[2] Leibniz Institute for Natural Product Research and Infection Biology – Hans Knöll Institute, Department Pharmaceutical Microbiology, Winzerlaer Strasse 2, 07745 Jena, Germany

[3] Ernst Abbe University of Applied Sciences Jena, Faculty Medical Technology and Biotechnology, Carl-Zeiss-Promenade 2, 07745 Jena, Germany

Supporting information

Experimental procedures

A. Cloning and transformation procedures

General remarks. Polymerase chain reactions (PCRs) were carried out with the HotStart Phusion polymerase (NEB; for < 8 kb fragments), the Phire Hot Start II DNA Polymerase (Thermo Scientific; for > 8 kb fragments) or the DreamTaq Green DNA-Polymerase (Thermo Scientific; for diagnostic PCRs for <2 kb fragments) according to the manufacturer´s protocol. Oligonucleotides are listed in Table S3**.** Plasmid propagation was carried out in *Escherichia coli* XL1-blue. *A. niger* mutants were generated by PEG-mediated transformation of protoplasts by an established protocol [1]. Organisms used and generated in this study are listed in Table S2. Cultivation media were LB medium (5 g L^{-1} yeast extract, 10 g L^{-1} tryptone, 10 g L^{-1} NaCl), YPD medium (10 g L^{-1} yeast extract, 20 g L^{-1} soy peptone, 20 g L^{-1} D-glucose), MEP medium (20 g L^{-1} malt extract, 3 g L^{-1} soy peptone, pH 5.6), *Aspergillus* minimal medium (AMM, https://www.fgsc.net/methods/anidmed.html) and AMM supplemented with 200 mM D-glucose and 20 mM L-glutamine. If required, 140 µg mL^{-1} hygromycin B (Roth), 100 µg mL^{-1} carbenicillin (Roth), 30 µg mL^{-1} doxycycline (Merck) or 10 mM uridine (Roth) was used for antibiotic selection, *tetON* promoter induction or auxotrophic complementation.

Generation of the *akuB* deletion in *A. niger* ATNT. The 5´and 3´flanking regions (1 kb each) of the *akuB* gene were amplified by PCR using the Phusion Polymerase and the oligonucleotide couples oMG482/oMG483 (*akuB*up) and oMG484/oMG485 (*akuB*dn), respectively. Both amplicons were fused by PCR [1] and ligated into the plasmid pJET1.2. The fusion fragment was excised by *Kpn*I and ligated into an analogously digested pUC19 vector resulting in pLK02. The hygromycin B resistance (*hph*) cassette (2.9 kb) was obtained by *Not*I-digest of *hph*-pCRIV [1] and was inserted into the *Not*I-linearized pLK02 to give plasmid pLK03. The deletion cassette (*akuB*up-*hph*-*akuB*dn, 5 µg) was excised by *Kpn*I, gel-purified and used for PEG-mediated transformation protoplast of *A. niger* ATNT [2, 3]. Single transformants were selected on AMM plates with 140 µg/ml hygromycin B. Genomic DNA of the parental strain and the *akuB* deletion strain (tLK01) was digested separately with *Eco*RV and *Hind*III

and Southern Blot analysis was conducted using a digoxygenin-labelled probe amplified from pLK03 with oligonucleotides oMG482/oMG483 (Figure S1).

Generation of the expression plasmid pLK04. The upstream (*fwnA*up, 1007 bp) and the downstream fragment (*fwnA*dn, 1037 bp) of the *fwnA* gene were amplified using oligonucleotide pairs oMG501/oMG502 and oMG504/oMG505, respectively. An additional fragment (spanning the inducible *Aspergillus terreus terA* promoter, the *A. terreus trpC* terminator and the *Aspergillus fumigatus pyrG* gene) was amplified from plasmid pPS01 [4] using oMG370 and oMG109. The three fragments were fused with a *Pst*I-linearized pUC19 vector using the NEBuilder Assembly Tool (NEB). The final plasmid pLK04 is a bifunctional vector for deletion of the spore pigment PKS gene *fwnA* and simultaneous overexpression of genes of interest (GOI) in *Aspergillus niger* ATNT (Figure S2). The GOI can be integrated via *Pac*I or *Spe*I digest resulting in either N-terminal or C-terminal His_6-tagged proteins.

Generation of the null mutants *A. niger* tLK06 and tLK07 and determination of the frequency of recombination. To test the frequency of homologous recombination events in tLK01 in comparison to its parental strain ATNT, both strains were transformed with 500 ng of two empty vector fragments targeting the *fwnA* locus (primer pairs oMG501/oMG116 and oMG370/oMG505 priming pLK04; 2,054 bp and 5,827 bp, respectively). The experiment was carried out in triplicate. All black-colored and pigment-less colonies were counted for each transformation (tLK06 and tLK07) and frequency of homologous recombination was calculated as ratio of (fawn colonies) / (black + fawn colonies). Three white transformants from each transformation were checked for *fwnA* deletion by PCR using the oligonucleotides oMG539/oMG541 and oMG539 /oMG267.

Generation of the *lpaA* expression plasmid pLK05. The first 1027 bp of *lpaA* (*lpaA*1) and the terminal 1014 bp of *lpaA* (*lpaA*5) were amplified from pPS03 using oligonucleotides oMG527/oMG528 and oMG529/oMG530. Both fragments were fused by PCR as described [1] and ligated into the *Pac*I-digested expression vector pLK04. The obtained plasmid pLK05 served as template for various amplifications of *lpaA* fragments (see below).

Generation of the *lpaA*-expressing mutant *A. niger* tLK04 and the *lpaA*^{D1415A}-expressing mutant *A. niger* tLK05. The recipient strain tLK01 was transformed by PEG-mediated transformation using five DNA fragments. Fragment 1 (2,792 bp) spanned *fwnA*up:P*terA*:*lpaA*1 and was amplified from pLK05 using oMG501/oMG532. Fragments 2 (2,897 bp), 3 (3,966 bp), and 4 (3,669 bp) spanning overlapping regions of the *lpaA* gene were amplified from pPS03 using oCL46/oCL49, oCL34/oCL51, and oCL42/oMG530. For tLK05, fragment 3 was replaced by a fusion PCR construct amplified by PCR fusion of fragments 3a (2,437 bp) and 3b (1,581 bp), each amplified by oPS30/oPS45 and oPS46/oPS31. Finally, fragment 5 (5,971 bp) was generated from pLK05 using oMG531/oMG505 and spanned *lpaA*5:T*trpC:pyrG:fwnA*dn. All fragments (400-600 ng each) were mixed in an equimolar ratio in a final volume of 20 µl and were used for PEG-mediated transformation of the recipient strain tLK01. The resulting transformants (tLK04 and tLK05) were primarily screened by loss of conidial pigmentation and the genotype were subsequently determined by PCR (oMG370/oMG116) (Figure 2) and Southern Blot (Figure S5).

Generation of the *calA* expression plasmids pMG56 and pMG58. The first 846 bp of *calA* (*calA*1) and were amplified from genomic DNA from *M. alpina* ATCC32222 using oligonucleotides oMG569/oMG548. *cal*A1 was fused with the *Pac*I-digested expression vector pLK04 using the NEBuilder Assembly Tool (NEB) to obtain plasmid pMG56. The terminal 1026 bp of *calA* (*calA*5) was amplified using oligonucleotides oMG546/oMG547, subcloned into the pJET1.2 vector and finally ligated by *Mfe*I/ *Pac*I excision into a similar digested pLK04 to result in pMG58. Both vectors served as a template for various amplifications of *calA* fragments (see below).

Generation of the *calA*-expressing mutant *A. niger* tJMW06. The recipient strain tLK01 was transformed by PEG-mediated transformation using five DNA fragments. Fragment 1 spanned *fwnA*up:P*terA*:*calA*1 and was amplified from pMG56 using oMG501/oMG548. Fragments 2 (7,497 bp), 3 (7,607 bp), and 4 (6,875 bp) spanning overlapping regions of the *calA* gene were amplified from genomic DNA from *M. alpina* using oMG572/oMG507, oMG570/oMG509, and oMG510/oMG511. Finally, fragment 5 was amplified from pMG58 using oMG505/oMG547 and spanned

*calA*5:T*trpC:pyrG:fwnA*dn. All fragments (250 ng/ kb each) were mixed in an equimolar ratio in a final volume of 20 µl and were used for PEG-mediated protoplast transformation of the recipient strain tLK01. The genotype of the resulting transformants (tJMW06) was subsequently analyzed by PCR (Figure S8) and Southern Blot (Figure S9).

B. Genetic characterization of the *lpaA* and *calA* expressing *A. niger* mutants

Isolation of genomic DNA. *A. niger* strains or *M. alpina* were cultivated in 50 ml MEP for 36 h at 25°C. Mycelium was ground under liquid nitrogen and suspended in LETS buffer (100 mM lithium chloride, 20 mM EDTA, 10 mM TRIS, 0.5 % SDS, pH 8.0) and incubated with 25 µg ml^{-1} Monarch RNase A (NEB) at 65°C. After addition of 25 µg ml^{-1} Proteinase K (Merck) and a second incubation at 65°C, cell debris was removed by brief centrifugation at 20,000 × g. The cell-free supernatant was extracted three times with phenol/ chloroform/ isoamyl alcohol (25:24:1) (Carl Roth) and the organic phase was discarded every time. The DNA in the aqueous phase was precipitated by addition of the equal amount of ice-cold isopropanol. After centrifugation (4°C, 20,000 × g, 10 min), the DNA pellet was washed with 70% ethanol and dried at 37°C for 3 minutes. Finally, the gDNA was solved in 10 mM TRIS buffer (pH 8.0) and stored at 4°C.

Diagnostic PCR of the transformants. To estimate the integration of expression constructs, 200 ng genomic DNA of *A. niger* ATNT, tLK01, tLK04, tLK05, tLK06, tLK07 and tJMW06 and *M. alpin*a ATCC32222 served as template for PCR's using the Phire Hot Start II DNA Polymerase (for > 8kb fragments), HotStart Phusion polymerase (for 2-8 kb fragments), DreamTaq Green DNA Polymerase (for <2 kb fragments) according to the manufacturer´s protocols. The oligonucleotides used for each experiment are listed in Table S3 and are indicated in the figure legends of Figures 2, 5, S4, S7 and S8.

Southern Blot analysis. To verify the correct and full-length integration, Southern blot analysis were carried out. To determine the *akuB* deletion, genomic DNAs of ATNT and tLK01 were digested with *Hind*III or *Nco*I. To determine the *fwnA* deletion, the genomic DNA of tLK01 and tLK04 was digested

with *Sac*II. To determine the full-length integration of *calA* deletion, the genomic DNA of tLK01 and tLK04 was digested with *Sma*I/*Dra*I. Digested DNA fragments were electrophoreticly separated on a 0.7% agarose gel. Gels were treated with depurination solution (0.25 M HCl), denaturation solution (0.5 M NaOH, 1.5 M NaCl) and neutralization solution (1.5 M NaCl, 0.5 M TRIS, pH 7.5). Capillary blot onto an Amersham Hybond-N nylon membrane (VWR) was conducted in 20 x SSC buffer (0.3 M sodium citrate, 3 M NaCl) for 3 hours. Subsequently, DNA was cross-linked to the membrane by UV radiation. Hybridization, DNA labeling and detection was performed using the DIG-High Prime DNA Labeling and Detection Starter Kit II (Roche) and the Anti-Dig AP Fab fragment (Roche) according to manufacturer´s instructions. Probes were amplified from plasmid DNA (pLK03, pLK04 and pMG56) using DIG-11-UTP (Jena Bioscience) nucleotides and oligonucleotide pairs oMG482/483, oM504/505 and oMG569/548 for probes targeting *akuB*up, *fwnA*dn and *calA*, respectively.

References

1. Gressler M, Zaehle C, Scherlach K, Hertweck C, Brock M: **Multifactorial induction of an orphan PKS-NRPS gene cluster in *Aspergillus terreus***. *Chem Biol* 2011, **18**(2):198-209.
2. Geib E, Brock M: **ATNT: an enhanced system for expression of polycistronic secondary metabolite gene clusters in *Aspergillus niger***. *Fungal Biol Biotechnol* 2017, **4**(1):e13.
3. Geib E, Baldeweg F, Doerfer M, Nett M, Brock M: **Cross-Chemistry Leads to Product Diversity from Atromentin Synthetases in Aspergilli from Section Nigri**. *Cell Chem Biol* 2019, **26**(2):223-234 e226.
4. Seibold PS, Lenz C, Gressler M, Hoffmeister D: **The *Laetiporus* polyketide synthase LpaA produces a series of antifungal polyenes**. *J Antibiot (Tokyo)* 2020, **73**(10):711-720.

Table S1. Calculation of the frequency of homologous recombination in *A. niger* ATNT and tLK01 transformed with the *fwnA* deletion construct. *T1-T3 indicate the number of transformants per 500 ng DNA from three independent transformations.

parental strain	phenotype	T 1*	T 2*	T 3*	sum	frequency (HR)
ATNT	pigmented (ectopic)	8	9	10	27	
	non-pigmented (Δ*fwnA*)	2	1	2	5	**15%**
tLK01	pigmented (ectopic)	1	3	3	7	
	non-pigmented (Δ*fwnA*)	9	10	9	28	**80%**

Table S2. Organisms used in this study.

strain	genotype	remarks	reference
Aspergillus niger ATNTΔpyrG	TetOn:*terR_ble*; *pyrG*::*ptrA*	expression platform	[1]
Aspergillus niger tLK01	TetOn:*terR_ble*; *pyrG*::*ptrA; ΔakuB::hph*	expression platform for homologous integration	this study
Aspergillus niger tLK04	TetOn:*terR_ble*; *pyrG*::*ptrA; ΔakuB::hph; ΔfwnA::PterA:His6:lpaA_pyrG*	laetiporic acid production	this study
Aspergillus niger tLK05	TetOn:*terR_ble*; *pyrG*::*ptrA; ΔakuB::hph; ΔfwnA::PterA:His6:lpaA*^{D1415A}*_pyrG*	no laetiporic acid production	this study
Aspergillus niger tLK06	TetOn:*terR_ble*; *pyrG*::*ptrA; ΔfwnA::PterA:His6_pyrG*	-	this study
Aspergillus niger tLK07	TetOn:*terR_ble*; *pyrG*::*ptrA; ΔakuB::hph; ΔfwnA::PterA:His6_pyrG*	empty vector control	this study
Aspergillus niger tJMW06	TetOn:*terR_ble*; *pyrG*::*ptrA; ΔakuB::hph; ΔfwnA::PterA:His6:calA_pyrG*	calpinactam production	this study
Mortierella alpina ATCC32222	wildtype	native calpinactam producer	ATCC
Laetiporus sulphureus JMRC:SF:012599	wildtype	native laetiporic acids producer	JMRC [2]

References

1. Geib E, Brock M: **ATNT: an enhanced system for expression of polycistronic secondary metabolite gene clusters in *Aspergillus niger***. *Fungal Biol Biotechnol* 2017, **4**(1):e13
2. Seibold PS, Lenz C, Gressler M, Hoffmeister D: **The *Laetiporus* polyketide synthase LpaA produces a series of antifungal polyenes**. *J Antibiot (Tokyo)* 2020, **73**(10):711-720.

Table S3. Oligonucleotides used in this study.

name	sequence 5'-3'	target	purpose/restriction site
oMG482	GAATTCGAGCTCGGTACCTCTGACAGAGAATGCGGAGG	*A. niger akuB*	*akuB* deletion/ Southern Blot probe "*akuB*up"
oMG483	CGGTCTGCGCGGCCGCTTCCAGTATGAATGACTGAGATTATTGATG	*A. niger akuB*	*akuB* deletion/ Southern Blot probe "*akuB*up"
oMG484	CATACTGGAAGCGGCCGCGCAGACCGTTATTAATCCCTATTAG	*A. niger akuB*	*akuB* deletion
oMG485	GGATCCCCGGGTACCCGCAGCGACAGCATGAGAG	*A. niger akuB*	*akuB* deletion
oMG501	CCTCTAGAGTCGACCTGCAGGAGTTTCGGAAGTTGAATAAGC	*A. niger fwnA*	*fwnA* deletion
oMG502	ACAATATCAGAGAGAGGATCGTTTGCGGAAGATGTCTATTGATC	*A. niger fwnA*	*fwnA* deletion
oMG504	TGATGGTGCCAACAATCTGCATTGTTATGCATTACGCCTTCCTCC	*A. niger fwnA*	*fwnA* deletion / Southern Blot probe "*fwn*Adn"
oMG505	CCAAGCTTGCATGCCTGCAGCCTGTTCATACTACTCCCTGCC	*A. niger fwnA*	*fwnA* deletion / Southern Blot probe "*fwn*Adn"
oMG370	GATCCTCTCTCTGATATTGTCG	*A. terreus* P*terA*	amplification of P*terA*::T*trpC*::*pyrG* expression cassette / full-length integration of *lpaA* and *lpaA*^{D1415A}
oMG109	GAGCGGATAACAATTTCACACAGG	pUC19	amplification of P*terA*::T*trpC*::*pyrG* expression cassette
oMG527	ATCACCATCACCATTTAATTAACATGGCAGTGAGGCCGCCCAGC	*L. sulphureus lpaA*	amplification of *lpaA*/ construction of pLK05
oMG528	ACAGTCATGTATGAGCTGAGGTTGGCCTCGAGGGAGTCTC	*L. sulphureus lpaA*	amplification of *lpaA*/ construction of pLK05
oMG529	GAGACTCCCTCGAGGCCAACCTCAGCTCATACATGACTGTGG	*L. sulphureus lpaA*	amplification of *lpaA*/ construction of pLK05
oMG530	ATTGAAATCACTGCTGCTAGTTAATTAATCATGCCACAATGCCGTTCAATATC	*L. sulphureus lpaA*	amplification of *lpaA*/ construction of pLK05
oMG532	GTTGGCCTCGAGGGAGTCTC	*L. sulphureus lpaA*	amplification of *lpaA1*
oCL49	GGTAACGCCAGGGAACTCGAGGGCCATCTCG	*L. sulphureus lpaA*	amplification of *lpaA2*

oCL34	GGTATCAAGCCAAACGCTATGC	*L. sulphureus lpaA*	amplification of *lpaA3*
oCL51	GGTAGAGAAGATGGGCACGGCTGGGGAAGAGC	*L. sulphureus lpaA*	amplification of *lpaA3*
oCL42	GGATGGATTTCATCTTCGG	*L. sulphureus lpaA*	amplification of *lpaA4*
oMG531	CTCAGCTCATACATGACTGTGG	*L. sulphureus lpaA*	amplification of *lpaA5*
oCL46	ATGGCAGTGAGGCCGCCCAGCTAC	*L. sulphureus lpaA*	amplification of *lpaA* (full length) - intergar
oCL47	TCATGCCACAATGCCGTTCAATATCTC	*L. sulphureus lpaA*	amplification of *lpaA* (full length)
oPS30	GCTCTTCCCACCACAGAACA	*L. sulphureus lpaA*	amplification of *lpaA3*^{D1415A}
oPS45	TCGATATGGCCGTGCTGACATAATC	*L. sulphureus lpaA*	amplification of *lpaA3*^{D1415A}
oPS46	GATTATGTCAGCACGGCCATATCGA	*L. sulphureus lpaA*	amplification of *lpaA3*^{D1415A}
oPS31	CATCAGGGTTCAATGGCGTC	*L. sulphureus lpaA*	amplification of *lpaA3*^{D1415A}
oMG116	GAGATGTGGTAGACGATTGATCC	*A. terreus* T*trpC*	integration of *calA /* full-length integration of *lpaA* and *lpaA*^{D1415A}
oMG539	CAGCATGTTGGTTATATATTCGAGC	*A. niger fwnAup*	control homologous integration *fwnA* locus
oMG541	CTCCGAAATGCCTCTTTAGTTCG	*A. niger fwnAdown*	control homologous integration *fwnA* locus
oMG267	CATGGTGCTGTGATGAGAAG	pSMX2	control homologous integration *fwnA* locus
oMG569	CTTCTCATCACAGCACCATGACTAGTATGACCCGGCAGCCTTCAGAG	*M.alpina calA*	amplification of *calA1 /* Southern Blot probe *"calA"*
oMG548	CAACTGATGGATGCAGCGATC	*M.alpina calA*	amplification of *calA1 /* Southern Blot probe *"calA"*
oMG572	ATGACCCGGCAGCCTTCAG	*M.alpina calA*	amplification of *calA2*
oMG507	GCCTTCTCTACTTGATCCTCG	*M.alpina calA*	amplification of *calA2*
oMG570	GCTACGACCCCACTTGCTCC	*M.alpina calA*	amplification of *calA3*

oMG509	GAGTTCTCTTGGTCTGGTCTTCG	*M.alpina calA*	amplification of *calA3*
oMG510	GTGACCACTCTACGCTCGAGG	*M.alpina calA*	amplification of *calA4*
oMG511	CTACATCAGGTCCTCAATCCTTGC	*M.alpina calA*	amplification of *calA4*
oMG547	CCCGATAGCGCGTCTTTTGC	*M.alpina calA*	amplification of *calA5*
oMG546	TGAAATCACTGCTGCTAGTTAATTAACTACATCAGGTCCTCAATCCTTGC	*M.alpina calA*	amplification of *calA5*
oMG582	ATGTCTTCGAAGTCCCACCTC	*M.alpina calA*	verification of integration of *calA*
oMG25	GTATGTGCAAGGCCGGTTTCG	*M.alpina actB*	expression analysis (housekeeping gene)
oMG26	GTGACACCATCGCCAGAATCG	*M.alpina actB*	expression analysis (housekeeping gene)
oMG429	GCTGTCGGCAAGGTCATCC	*A. niger gpdA*	expression analysis (housekeeping gene)
oMG430	CTTGACGAAGTTGGAGTTAAGG	*A.niger gpdA*	expression analysis (housekeeping gene)
oMG659	AACAGAATCTGGATCCTGCG	*L. sulphureus lpaA*	expression analysis (*lpaA* expression)
oMG660	GCCATATGAGAAACAGAGCG	*L. sulphureus lpaA*	expression analysis (*lpaA* expression)
oMR35	CTCAGAACAAATTTGGACCGC	*A. niger fwnAup*	integration control of *calA*
oJMW251	GCTGCAGGACAAGGAGGATG	*M.alpina calA*	splicing of *calA* (intron 1)
oJMW252	GATGGTGGTCGAGAGCTTTC	*M.alpina calA*	splicing of *calA* (intron 1)/ integration of *calA*
oJMW253	GCTTCGCCCGATATGCCAG	*M.alpina calA*	splicing of *calA* (intron 2) / integration of *calA*
oJMW254	CTTGCTCGCCTCCACAGAC	*M.alpina calA*	splicing of *calA* (intron 2)
oJMW255	GACGACCGATGCGTTCACC	*M.alpina calA*	splicing of *calA* (intron 3)
oJMW256	CTCCGTATGACAGCACAGCC	*M.alpina calA*	splicing of *calA* (intron 3) / integration of *calA*
oJMW257	GATCGGTCTGTTGGTGAGGC	*M.alpina calA*	splicing of *calA* (intron 4) / integration of *calA*

oJMW258	CTCGAGCACGGCTGAGTAG	*M.alpina calA*	splicing of *calA* (intron 4)
oJMW259	GGAACAAGACCGAGGCTTCC	*M.alpina calA*	splicing of *calA* (intron 5)
oJMW260	TGGATCAGATGCTCGGGACC	*M.alpina calA*	splicing of *calA* (intron 5) / integration of *calA*
oJMW261	CCCGCTTCAGTCACTTTCAGTC	*M.alpina calA*	splicing of *calA* (intron 6) / integration of *calA*
oJMW262	CCGTGTAAGCCTCAATCAATCC	*M.alpina calA*	splicing of *calA* (intron 6)
oJMW263	CATCTCCGACAGTGGTGCC	*M.alpina calA*	amplification of *calA* probe
oJMW264	GGAAGTCCAGTCGATCCGG	*M.alpina calA*	amplification of *calA* probe

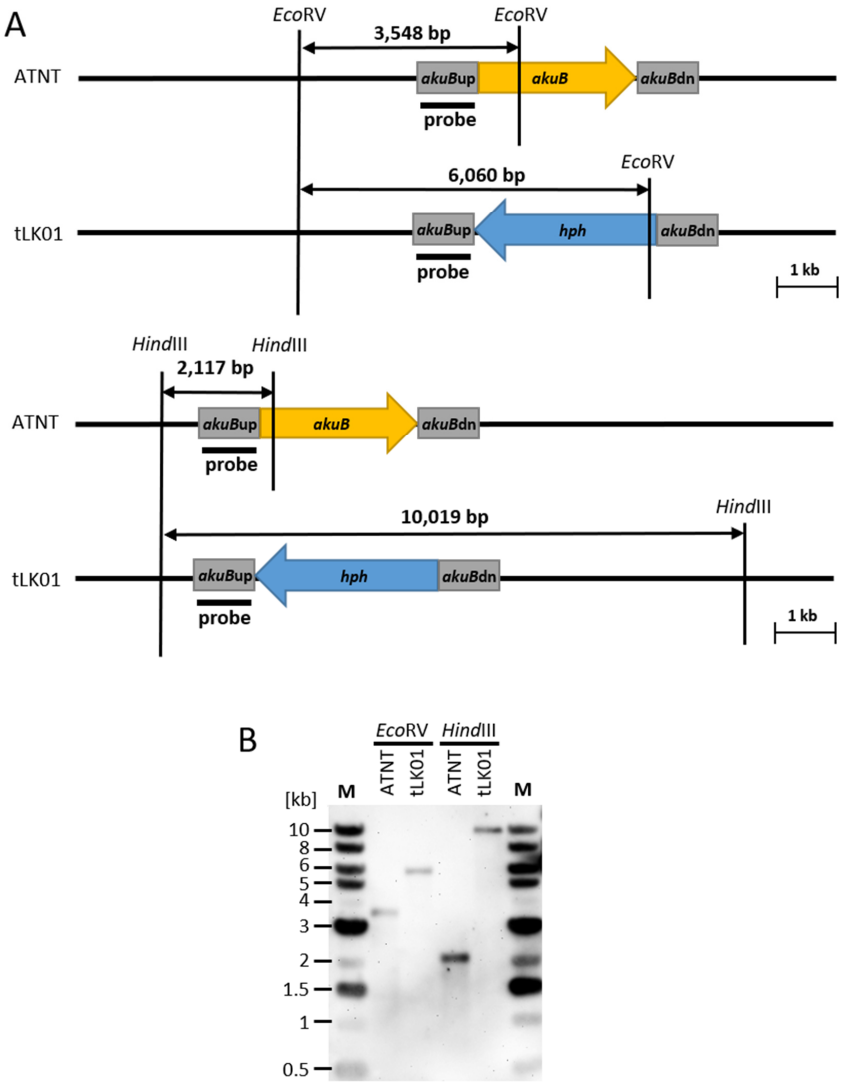

Figure S1. Southern Blot analysis for determination of the *akuB* deletion strain tLK01. A. Schematic representation of the genomic *akuB* locus of the strain ATNT and tLK01 (ATNTΔ*akuB*) with its respective *Eco*RV (upper panel) and *Hind*III restriction sites (lower panel). **B.** Southern Blot analysis of the *A. niger* parental strain ATNT and the *akuB* deletion strain tLK01**.** Genomic DNA was digested with *Eco*RV or *Hind*III. A digoxigenin-labeled probe was generated with oMG482/oMG483 to hybridize with *akuB* upstream sequence and signals were detected with CDPstar (Roche Diagnostics).

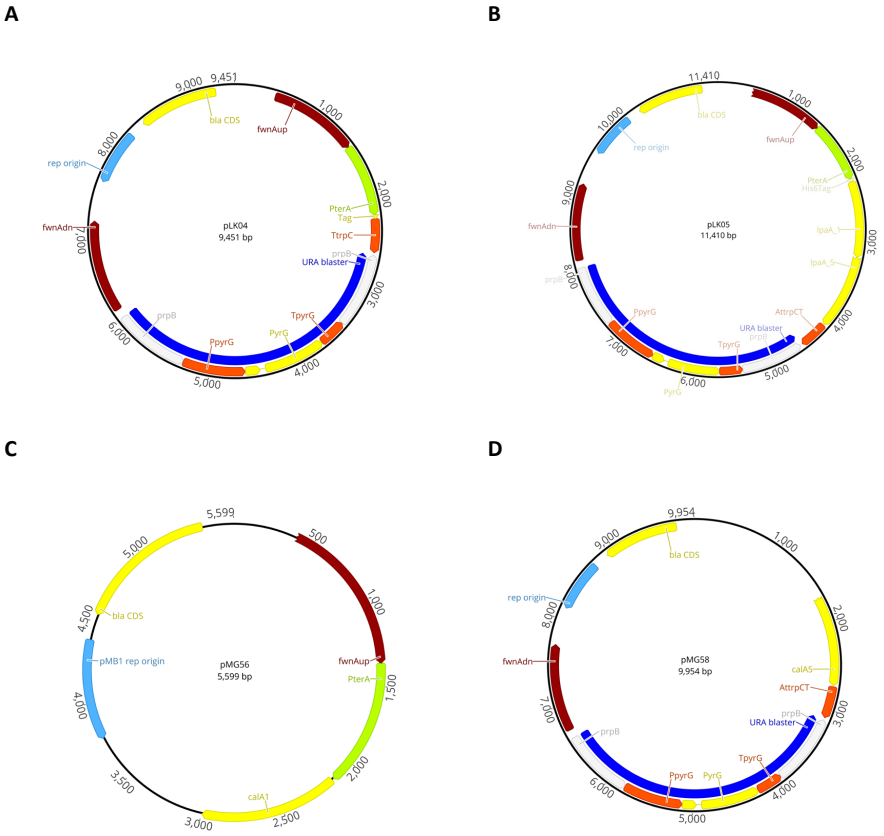

Figure S2. Plasmid maps of the expression vectors. The plasmids pLK04 (**A**), pLK05 (**B**), pMG56 (**C**) and pMG58 (**D**) are based on the pSMX2-URA plasmid [1]. The gene fragments are: *bla*; β-lactamase (confers ampicillin resistance); *calA1/5*; 1 kb of the 5´or 3´end of the *calA* gene; *fwnA*up and *fwnA*down, 1 kb up- and downstream the *A. niger fwnA* polyketide synthase gene; URA-blaster (dark blue, contains several genes; see below); P*terA*, promoter of the *terA* terrein polyketide synthase gene of *Aspergillus terreus*; Tag, encodes the hexahistidin tag (and includes an *SpeI* and *PacI* site for insertion of the GOI); T*trpC*, terminator of the *trpC* anthranilatsynthase component 2 gene of *A. terreus*; rep origin, origin of plasmid replication. The URA-blaster contains: P*pyrG*, promoter of the *pyrG* gene from *Aspergillus nidulans*; *pyrG*, orotidine 5´-phosphate decarboxylase gene from *A. nidulans* (confers uracil prototrophy); T*pyrG*, terminator of the *pyrG* gene from *A. nidulans*; and two *prpB* flanks that encode the methylcitrate synthase gene from *Escherichia coli* that facilitate a subsequent removal of the URA blaster cassette from the *A. niger* genome via a homologous recombination event (counter selection) by addition of 5-fluoroorotic acid [2].

Reference

1. Geib E, Brock M: **ATNT: an enhanced system for expression of polycistronic secondary metabolite gene clusters in *Aspergillus niger***. *Fungal Biol Biotechnol* 2017, **4**(1):e13.
2. Staab JF, Sundstrom P: **URA3 as a selectable marker for disruption and virulence assessment of *Candida albicans* genes**, *Trends in Microbiology*, 2003, **11**(2): 69-73.

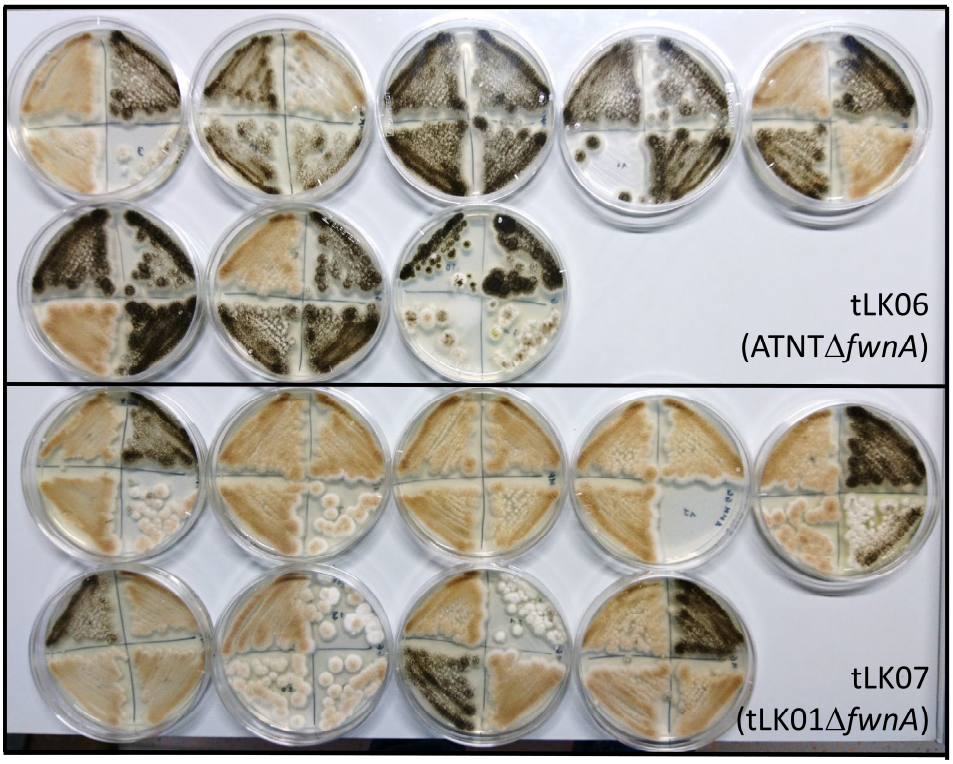

Figure S3. Photographs of *A. niger* ATNT and tLK01 transformed with the *fwnA* deletion construct. Both pigmented and non-pigmented transformants have been detected in both experiments, but frequency of the homologous recombination into the *fwnA* locus is significantly higher in tLK01. For calculation of frequency of recombination see Table S1.

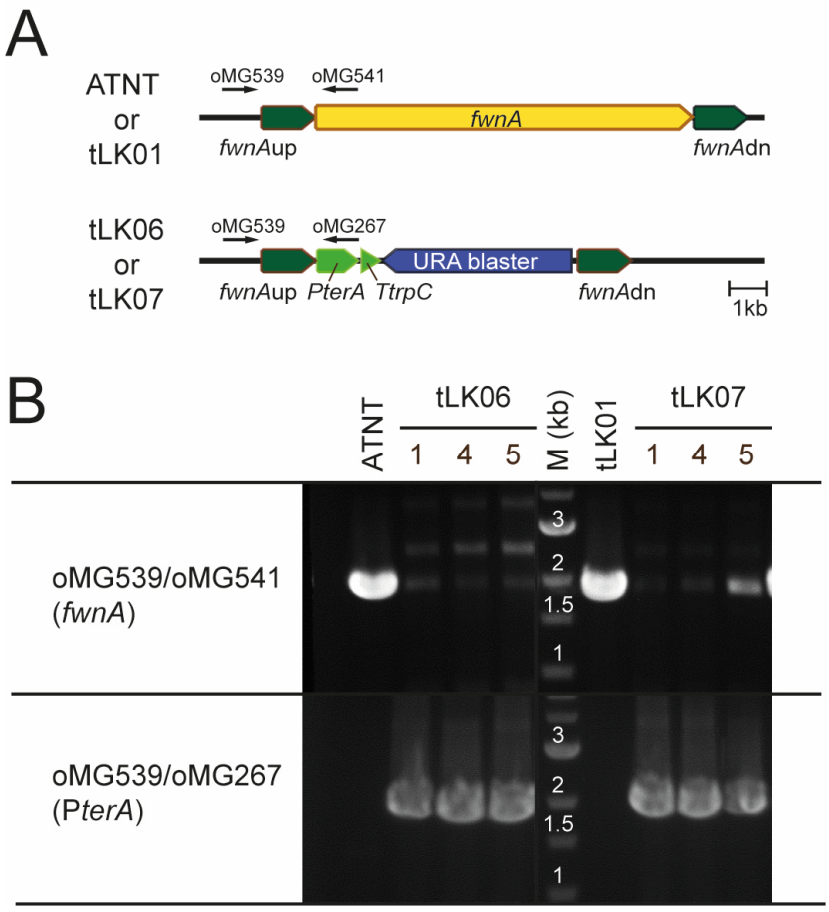

Figure S4. Determination of the homologous integration of the P*terA*:T*trpC* construct into the *fwnA* locus of recipient strains ATNT and tLK01. A. Schematic representation of the genomic *fwnA* locus of the parental strain ATNT and tLK01 (ATNTΔ*akuB*) (upper lane) and the deletion mutants ATNTΔ*fwnA* (tLK06) and tLK07 (ATNTΔ*akuB*Δ*fwnA*). **B.** Agarose gel of two diagnostic PCRs targeting the *fwnA* gene (upper lane) and the P*terA* promoter (lower lane). In contrast to the parental strains ATNT and tLK01, the non-pigmented Δ*fwnA* mutants (tLK06 and tLK07) lack the signal of the *fwnA* gene (upper panel). In *lieu* thereof, the homologous integration of P*terA*:T*trpC* could be determined in the mutants (lower panel).

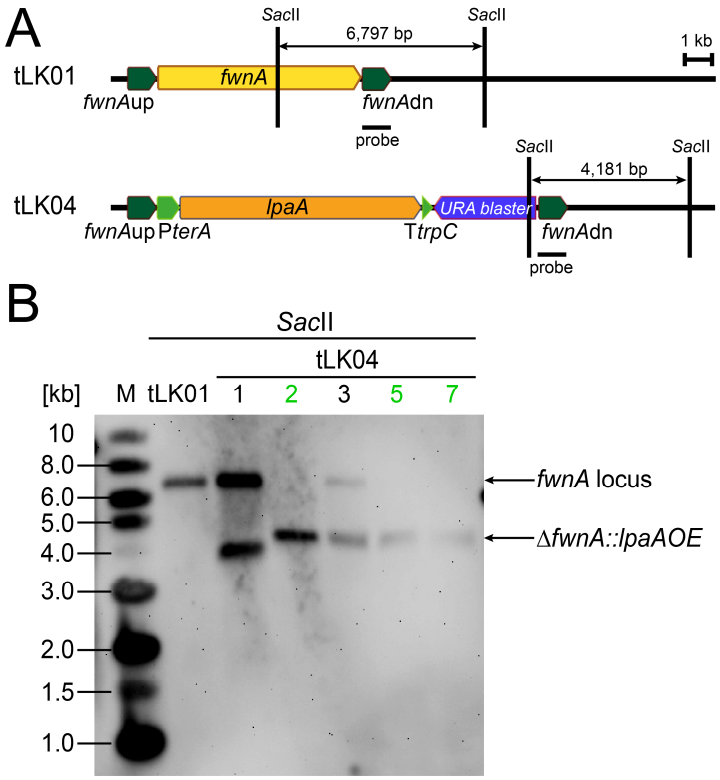

Figure S5. Southern Blot analysis for determination of the *fwnA* deletion and *lpaA* overexpression in *A. niger* strains tLK04. A. Schematic representation of the genomic *fwnA* locus in the strain tLK01 (ATNTΔ*akuB*) and the Δ*fwnA*::*lpaA* overexpression strain tLK04 with its respective *Sac*II restriction sites. **B.** Southern Blot analysis of the *A. niger* parental strain tLK01 and five Δ*fwnA*::*lpaA* overexpression strains tLK04**.** Genomic DNA was digested with *Sac*II. A digoxigenin-labeled probe was generated with oMG504/oMG505 to hybridize with the *fwnA* downstream sequence and signals were detected with CDPstar (Roche Diagnostics). Strains used for subsequent metabolic analysis are highlighted in green.

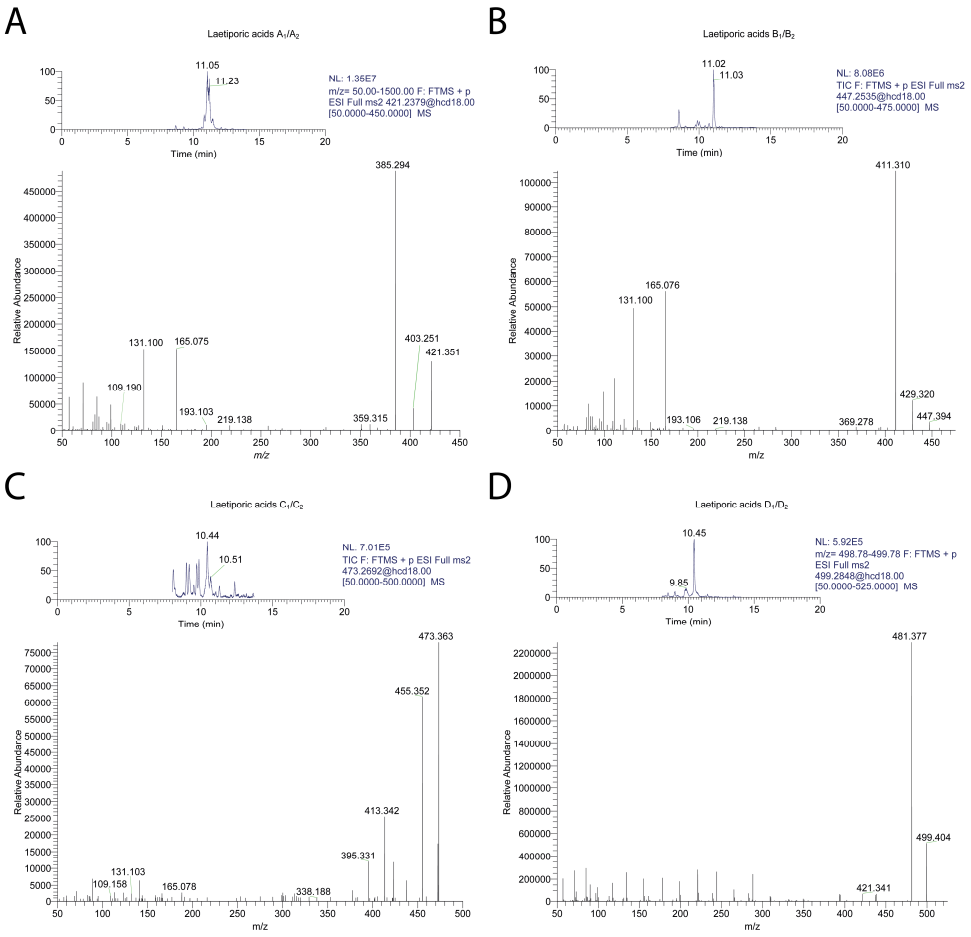

Figure S6. HR-MS and MS/MS spectra of laetiporic acids A_1-D_2 detectable in *A. niger* tLK04. High resolution MS/MS fragmentation of laetiporic acids A_1/A_2 (**A**), B_1/B_2 (**B**), C_1/C_2 (**C**) and D_1/D_2 (**D**) produced by *A. niger* tLK04. Indicated fragments are identical to the literature [1].

Reference

1. Seibold PS, Lenz C, Gressler M, Hoffmeister D: **The *Laetiporus* polyketide synthase LpaA produces a series of antifungal polyenes**. *J Antibiot (Tokyo)* 2020, **73**(10):711-720.

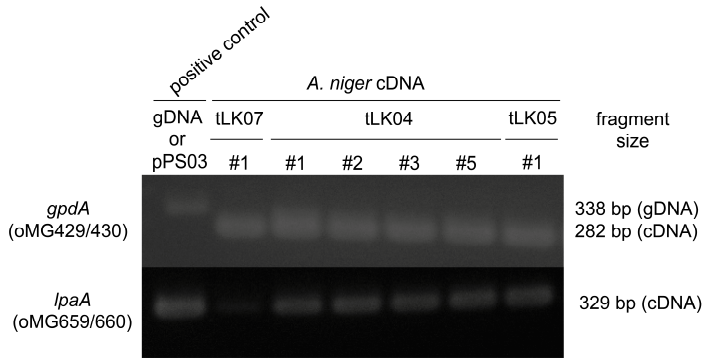

Figure S7. Expression of *lpaA* in the transgenic *A. niger* tLK07 (null mutant), tLK04 (*lpaA* expressing) and tLK05 (*lpaA*^{D1415A} expressing). Expression was profiled by semi-quantitative PCR on the laetiporic acid synthase gene (*lpaA*) and referenced to the expression of the housekeeping gene encoding the glyceraldehyde-3-phosphate dehydrogenase (*gpdA*). RNA was isolated and cDNA was synthesized after cultivation for 36 h in inducing AMM (with doxycycline) at 30°C and 180 rpm. The genomic DNA (gDNA) of tLK07 or the *lpaA*-encoding plasmid pPS03 served as positive controls for *gpdA* and *lpaA* amplification, respectively.

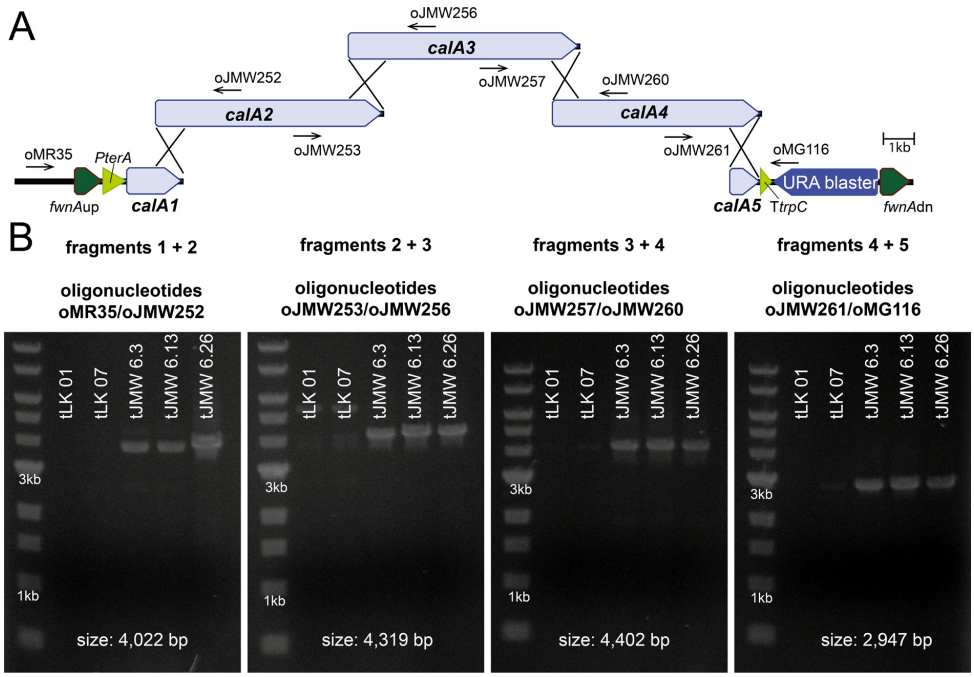

Figure S8. Integration of *calA* into the *fwnA* locus in *A.niger* tJMW06. **A.** Genomic locus of *fwnA* during recombination of the five *calA* DNA fragments in *A. niger* pJMW06. **B.** PCR amplification of four adjacent DNA fragment pairs was carried out using genomic DNA as templates. The *A. niger* parental strain tLK01 and the null mutant strain tLK07 (empty vector) served as negative controls. Three individual *calA*-expressing transformants tJMW06 #3, #13 and #26 showed the expected amplicon sizes of the recombined DNA fragments.

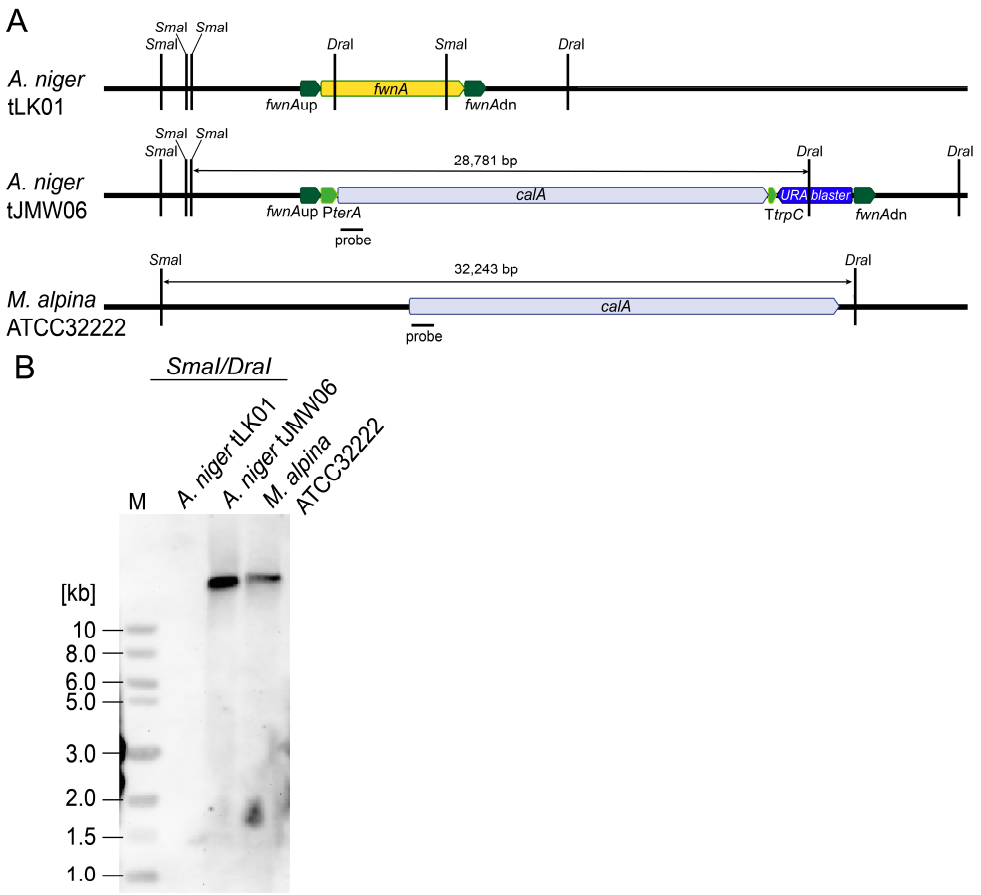

Figure S9. Southern Blot analysis for determination of the full-length *calA* integration into the genome of *A. niger* strain tJMW06. A. Schematic representation of the genomic *fwnA* locus in the strain tLK01 (ATNTΔ*akuB*), the Δ*fwnA*::*calA* overexpression locus of strain tJMW06.3 and the native *calA* locus of the *calA* gene donor strain *M. alpina* ATCC32222. **B.** Southern Blot analysis of the *A. niger* parental strain tLK01, the Δ*fwnA*::*calA* overexpression strain tJMW06 and *M. alpina* ATCC32222**.** Genomic DNA was double-digested with *Sma*I/*Dra*I. A digoxigenin-labeled probe was generated with oMG569/oMG548 to hybridize with the *fwnA* downstream sequence and signals were detected with CDPstar (Roche Diagnostics). Full-length *calA* integration was determined for *A. niger* tJMW06 and directly reflects the size of the *calA* gene fragment in the gene donor strain *M. alpina* ATCC32222.

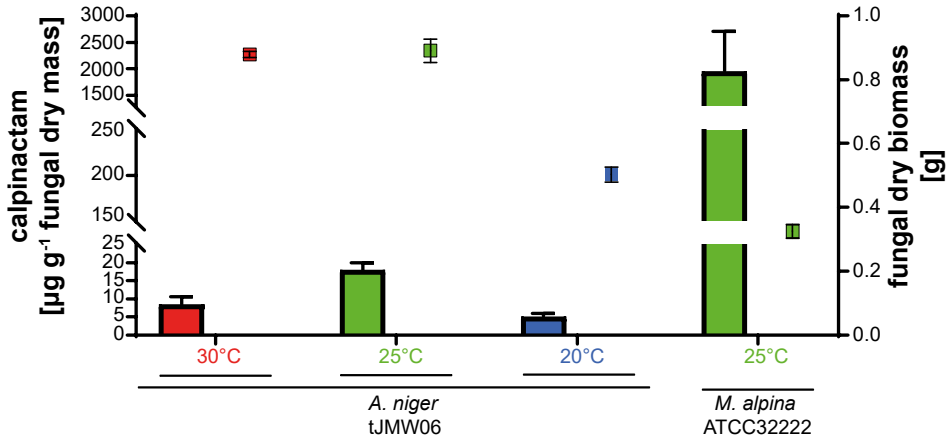

Figure S10. Temperature dependent production of calpinactam in *A. niger* tJMW06 and *M. alpina* ATCC32222. Calpinactam production (bars) and total fungal dry weight (boxes) are indicated for several cultivation conditions. The transformant *A. niger* tJMW06 was cultivated in YPD with 30 µg mL^{-1} doxycycline as inducer at 20, 25 and 30°C for 3 days. The *calA* gene donor strain *M. alpina* ATCC32222 was cultivated in MEP (25°C) for 4 days. Production rate in *A. niger* tJMW06 is optimal at 25°C, which is the growth optimum for *M. alpina.* Experiments were carried in triplicate.

4.4 Manuskript 4

Insecticidal Cyclodepsitetrapeptides from *Mortierella alpina*

Rassbach, Johannes; Merseburger, Peter; **Wurlitzer, Jacob M.**; Binnemann, Nico; Voigt, Kerstin; Rohlfs, Marko; Gressler, Markus

Manuskript zur Begutachtung eingereicht bei: *Journal of Natural Products*

Zusammenfassung:

Mortierella alpina ist innerhalb der basalen Pilze als Naturstoffproduzent etabliert. In dieser Studie werden die Cycloacetamide A-F erstmals beschrieben. Diese Threonin-enthaltenden verzweigtkettigen Cyclopeptide zeigen dabei eine hochselektive antilarvale Wirkung. Gleichzeitig konnte dabei für die Malpicycline ebenfalls eine antilarvale Wirkung nachgewiesen werden. Die Arbeit stellt einen wichtigen Schritt für das Verständnis der ökologischen Bedeutung der produzierten Naturstoffe dar.

Der Kandidat ist:

☐ Erstautor ☐ Co-Erstautor ☐ Korresp. Autor ☒ Coautor

Eigenanteil:

Autor/-in	Konzeptionell	Datenanalyse	Experimentell	Verfassen des Manuskriptes	Bereitsellung von Stämmen und Metaboliten
Raßbach, J	40%	50%	60%	25%	25%
Merseburger, P	-	20%	25%	-	-
Wurlitzer, JM	-	5%	-	-	5%
Voigt, K	-	-	-	5%	20%
Gressler, M	50%	20%	-	60%	45%
2 weitere Autoren	10%	5%	15%	10%	5%
Summe	100%	100%	100%	100%	100%

Insecticidal cyclodepsitetrapeptides from *Mortierella alpina*

Johannes Rassbach,[a] Peter Merseburger,[a] Jacob M. Wurlitzer,[a] Nico Binnemann,[b] Kerstin Voigt,[c,d] Marko Rohlfs,[b] and Markus Gressler[a,*]

[a] Friedrich-Schiller-University, Leibniz Institute for Natural Product Research and Infection Biology (Hans-Knöll-Institute), Department Pharmaceutical Microbiology, Winzerlaer Strasse 2, 07745 Jena, Germany.

[b] University of Bremen, Institute of Ecology, Chemical Ecology Group, Leobener Strasse 5, 28359 Bremen, Germany.

[c] Jena Microbial Resource Collection, Leibniz Institute for Natural Product Research and Infection Biology (Hans Knöll Institute), Adolf-Reichwein-Strasse 23, 07745 Jena, Germany.

[d] Friedrich Schiller University, Institute of Microbiology, Neugasse 25, 07743 Jena, Germany.

Supporting Information Placeholder

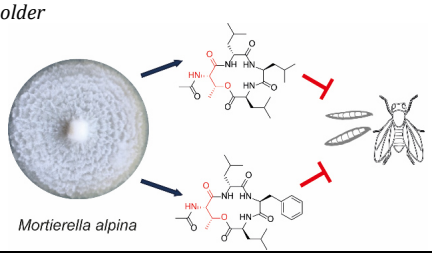

ABSTRACT: Early-diverging fungi such as *Mortierella alpina* are an emerging resource of bioactive peptides. By screening of 23 fungal isolates along with precursor-directed biosynthesis, a novel family of threonine-containing branched-chain cyclotetradepsipeptides, the cycloacetamides A-F (**1-6**), was identified. The structure elucidation was conducted using NMR and ESI-MS/MS analyses, and the absolute configuration was determined by Marfey´s analysis and total synthesis. Cycloacetamides are not cytotoxic to human cells whilst being highly selective insecticidal against fruit fly larvae.

Early-diverging fungi such as *Mortierella alpina* are commonly isolated from soil organic matter from continental or sub-arctic climate zones.[1] Food chemists drew attention to these species as they produce polyunsaturated fatty acids (PUFA), i.e. arachidonic acid and α-linolenic acid, in feasible amounts for industrial applications (up to 20 g L^{-1}).[2] Moreover, the production of pharmaceutically relevant secondary metabolites of *M. alpina* is an emerging field of research.[3,4] The genome of *M. alpina* encodes 13 genes for bacterial-like nonribosomal peptides synthetases (NRPSs), but solely three of them have been linked to specific product families: Recently, the chemical structure of the surface-active hexapeptides, malpinins A-D (**7-10**) i.e. the major peptide family in *M. alpina* was elucidated (Figure 1).[4] Three out of six adenylation domains of the corresponding NRPS MalA are highly promiscuous allowing the production of malpinin congeners depending on the amino acid supply.[5] Additionally, two series of cyclopentapeptides, malpibaldins A-C (**11-13**) and malpicyclins A-D (**14-17**), have been identified and their biosynthesis was assigned to the two NRPSs MpcA and MpbA, respectively.[6] The biosynthesis of another *Mortierella* compound, calpinactam (**18**), has not been studied yet, although this small linear peptide is a drug candidate in treatment of tuberculosis as it specifically and selectively inhibits the growth of mycobacteria among various microorganisms.[3,7]

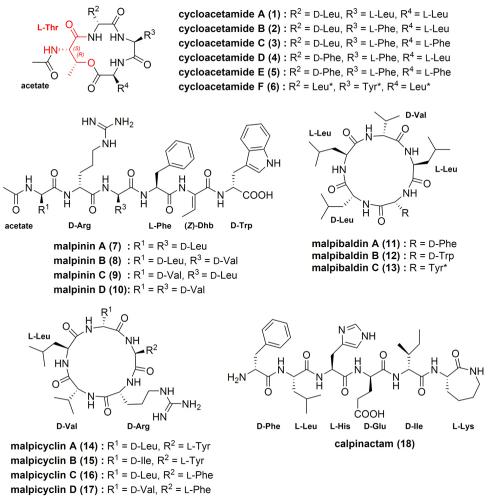

Figure 1. Oligopeptides isolated from *M. alpina*. **1-6** were isolated and described during this study. **7-18** are known compounds. * The absolute configuration of **6** and **13** was not determined. (*Z*)-Dhb, (*Z*)-dehydrobutyrine.

Whilst cyclic and linear peptides have been isolated from *M. alpina*, no branched-chain peptides (BCP) have been described yet. BCPs contain a canonical amide-linked peptide backbone and include at least one hydroxy-, carboxy-, sulfhydryl- or amine-functionalized amino acid linking an acyl or a peptidyl moiety (Figure S1).[8] Cyclic BCPs have been isolated from bacteria and higher fungi and include siderophores,[9] antibiotics,[10] phytotoxins,[11, 12] or nematotoxic compounds[13]. Threonine or hydroxycarboxylic acids are frequently observed as branching components in BCPs (Figure S1). However, BCPs have not been isolated from basal fungi yet. Since basal fungi are hardly amendable to genetic manipulation, a combination of precursor-directed feeding, MS-based chromatographic methods and total synthesis were required to identify and characterize the new BCPs.

Table 1. Analytical data of cycloacetamides A-F (1-6). Amino acid configurations in **6** were not determined.

#	Cyclo-acetamide	R^2	R^3	R^4	$[M+H]^+$	DBE	sum formula
1	A	D-Leu	L-Leu	L-Leu	482.3104	6	$C_{24}H_{42}N_4O_6$
2	B	D-Leu	L-Phe	L-Leu	516.2948	10	$C_{27}H_{40}N_4O_6$
3	C	D-Leu	L-Phe	L-Phe	550.2791	14	$C_{30}H_{38}N_4O_6$
4	D	D-Phe	L-Phe	L-Leu	550.2791	14	$C_{30}H_{38}N_4O_6$
5	E	D-Phe	L-Phe	L-Phe	584.2635	18	$C_{33}H_{36}N_4O_6$
6	F	Leu	Tyr	Leu	532.2897	10	$C_{27}H_{40}N_4O_7$

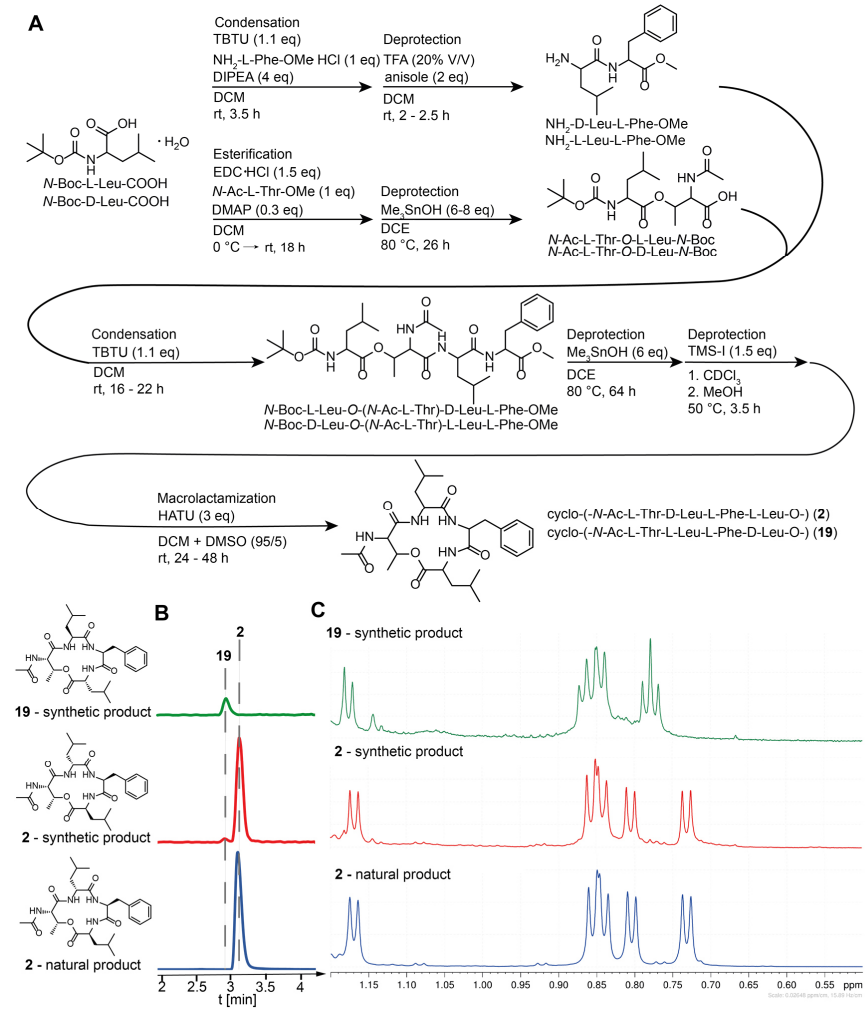

Figure 2. Total synthesis of the diastereomers 2 and 19. A. Synthesis scheme. **B.** HPLC profiles of authentic **2**, and synthetic diastereomers **2** and **19**. **C.** Magnification of the fingerprint region of ^{1}H NMR spectra of authentic **2**, and synthetic **2** and **19**.

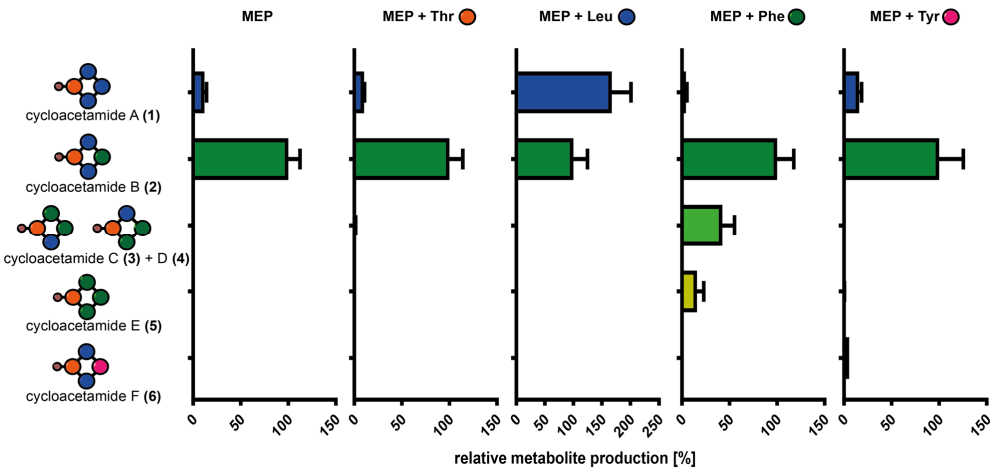

Figure 3. Metabolic diversity of the cycloacetamide family by substrate feeding. Colored circles indicate the incorporated amino acids. Feeding of L-Ile, L-Met, L-Val, or L-Trp did not alter the metabolic profile (not shown).

We screened 23 *M. alpina* isolates[14] for the production of novel natural products (Table S1). All tested isolates (100%) produced malpinins (23/23). Similarly, malpibaldins and malpicyclins were abundant in 91% (21/23) and 96% (22/23) of the strains, respectively, suggesting an evolutionary highly conserved production of these metabolite families. In contrast, calpinactam (**18**) was detectable only in 61% (14/23) of the examined fungal isolates.

Interestingly, two strains (JMRC:SF:10519 and JMRC:SF:10520) produced two novel compounds, referred to cycloacetamide A (**1**) and B (**2**), with a yield of 1.3 mg and 10.5 mg, respectively, from a 15 L culture (Figure 1, Table 1, Figure S2). High-resolution electrospray ionization mass spectrometric (HR-ESI-MS) analysis of **1** and **2** indicated the molecular formula of $C_{24}H_{42}O_6N_4$ (*m*/z 482.3104 $[M+H]^+$) and $C_{27}H_{40}O_6N_4$ (*m*/z 516.2948 $[M+H]^+$), respectively, suggesting tetrapeptides with six and ten degrees of unsaturation (Figure S3). According to HR-MS/MS fragmentation of the main compound **2**, characteristic signals for Phe moieties (*m*/z 120.08, $[M+H]^+$) and Leu moieties (*m*/z 86.60, $[M+H]^+$) were detectable. Using DMSO-d_6 as solvent, ^1H, ^{13}C and HSQC NMR analyses revealed the presence of six methyl groups, three sp^2 methylene groups, seven sp^3 methanetriyl groups, and four amide protons (Figure S4-S23, Table S2-S3). In the ^{13}C NMR spectrum, multiple carbonyl signals were detectable, but the signals are poorly resolved. Hence, the resolution was increased by using CD_3OD as solvent which led to the detection of five carbonyl functions. Subsequent analysis of COSY and HMBC correlation couplings enabled the reconstitution of the peptide backbone that is composed of the amino acid sequence Thr-Leu-Phe-Leu. However, the scalar HMBC coupling of H-5 (δ_H 5.44) of the *N*-terminal Thr to the carbonyl atom of the C-terminal Leu (C-22, δ_c 171.66), revealed that both amino acids are linked via an ester bond suggesting that **2** is a cyclodepsipeptide (Figure S19-S20). Since there were four amide protons but no amine protons detectable in the ^1H NMR spectrum, the N-terminal amine group of Thr must be acylated. Indeed, H-4 (δ_H 4.74) of Thr was connected to an unassigned carbonyl atom (C-1, δ_C 174.51) (Figure S20), which in turn showed scalar coupling to H-2 (δ_H 2.10) as part of a methyl group (Figure S19). Hence, the Thr is *N*-acetylated which was confirmed by kinetic studies of the acidic hydrolysis of **2**: Amide bonds have the characteristics of a partial dual bond and are hence thermodynamically stronger than an ester bond.[15] As expected, the ring opening of **2**, i.e. the hydrolysis of the ester bond, occurs prior to *N*-deacetylation (Figure S24). Enzymatic *N*-acetylation of a Thr residue has been shown for the BCP aspergillicin A in *Aspergillus flavus* and was assigned to the activity of a starter condensation (C_s) domain in the fungal NRPS AgiA (Figure S1).[16]

To determine the stereochemistry of **2**, acidic hydrolysates of **2** were coupled to the chiral 1-fluoro-2,4-dinitrophenyl-5-L-leucine amide (Marfey´s reagent) and detected via UHPLC-MS (Figure S25, Table S4). The analysis revealed that both Thr and Phe are L-configured. However, an equimolar ratio of L- and D-configured Leu was evident and, thus, the chirality was not assignable at this point.

We aimed at the total synthesis of the two possible isomers of **2,** i.e., cyclo-(-*N*Ac-L-Thr-D/L-Leu-L-Phe-L/D-Leu-*O*-) (Figure 2A). Main issues that were encountered were (i) to prevent the acetyl amide hydrolysis and (ii) to induce the correct cyclization, since macrolactamization is kinetically favored over -lactonization.[17] To circumvent a late-stage macrolactonization, a Steglich esterification[18] of *N*Ac-Thr and L-Leu/D-Leu was carried out as initial step that resulted in two isomeric amino acyl esters, *N*-Boc-D/L-Leu-*O*-*N*Ac-L-Thr-COOH. In parallel, two isomeric dipeptides, H_2N-L/D-Leu-L-Phe-COOMe, were synthesized by liquid phase peptide chemistry[4]. To prevent deacetylation, trimethyltin hydroxide and trimethylsilyl iodide were used for mild deprotection of the methylesters and the removal of the Boc groups.[19, 20] The corresponding educts were condensed by

classical peptide chemistry and final macrolactamization of the linear depsipeptides resulted in two isomeric cyclotetradepsipeptides. UHPLC-MS analysis revealed that cyclo(-*N*Ac-L-Thr-D-Leu-L-Phe-L-Leu-*O*-) showed the identical retention time (t_R = 3.10 min) as **2,** whilst its isomer cyclo(-*N*Ac-L-Thr-L-Leu-L-Phe-D-Leu-*O*-) (**19**) eluted earlier (r_t = 2.80 min) (Figure 2B). Comparison of the ^{1}H NMR spectra and the ESI-MS/MS fragmentation spectra confirmed cyclo(-*N*Ac-L-Thr-D-Leu-L-Phe-L-Leu-*O*-) as the sole naturally occurring **2**-isomer (Figure 2C, Figures S3, S26-S30).

It has previously been shown, that the quantity and quality of nonribosomal peptides from *M. alpina* can be modified by providing alternative, but chemically similar amino acids as substrates.[21] In order to increase the yield of **2** congeners, the culture medium was supplemented with L-Leu, L-Tyr or L-Trp (to replace the Phe moiety) or L-Val, L-Ile, L-Met or L-Phe (to replace the Leu moieties) (Figure 3). L-Leu feeding led to the enriched incorporation of Leu in place of Phe at position 3 according to its HR-MS/MS fragmentation pattern and provided sufficient amounts of **1** (*m*/z 482.3104 [*M*+H]$^+$, 3.5 mg in a 12 L scale) for subsequent extensive NMR and Marfey´s analyses (Figures S25, S31-S40, Table S4-S5). Thus, the structure of **1** was confirmed to be the *all*-Leu metabolite cyclo(-*N*Ac-L-Thr-D-Leu-L-Leu-L-Leu-*O*-) (Figure 1). Phe feeding caused the most intensive shift in the metabolite profile, resulting in three additional metabolites (**3-5**), corresponding to one additional Phe at position 2 (**3**, *m*/z 550.2791 [*M*+H]$^+$) or 4 (**4**, *m*/z 550.2791 [*M*+H]$^+$) or the triphenyl **2** congener **5** (*m*/z 584.2635 [*M*+H]$^+$) (Figures S41-S43). In addition, L-Tyr feeding resulted in minor traces of the **2** congener **6**, in which Phe is replaced by Tyr (Figure S44). Supplementation with other amino acids did not alter the metabolic profile. We isolated 1.0 mg and 4.3 mg of the two isomers **3** and **4,** respectively, and 1.0 mg of **5.** Although the amounts were insufficient for subsequent NMR analyses, the planar cyclic structure was confirmed by HR-MS/MS (Table 1, Figures S41-S44). Similar to **2**, Marfey´s analysis of **3** and **4** revealed the identical configuration of L-Thr and L-Phe at positions 1 and 3 and a D- and L-configuration of the amino acids at position 2 and 4, respectively (Figure 1, Table 1, Table S4, Figure S25).

Mortierella spec. are known to host oligopeptide synthesizing endobacteria[22] and cycloacetamides might be a bacterial rather than fungal product. The biological origin of cycloacetamides was verified by antibiotic treatment of the fungal cultures as described for basal fungi colonized by endobacteria.[23, 24] Regardless the antibiotic treatment, *M. alpina* produced equal amounts of **2**, confirming its fungal origin (Figure S45). Based on the knowledge of nonribosomal peptide synthesis in basal fungi,[6] a biosynthetic route by an NRPS can be proposed in which a C_s domain and a dual epimerization/condensation (E/C) domain are required to acetylate Thr and to introduce the D-configured Leu, respectively.

Since many BCPs are biologically active, **1** and **2** were subjected to a panel of bioactivity assays (Figure 4, Table S6). In contrast to chemically related BCPs such as the xenematides from *Xenorhabdus spec.*,[25, 26] **1** and **2** show neither antibacterial nor antifungal activities (Figure S1, Table S6). In addition, no cytotoxic, antiproliferative or immunomodulating effects on human cells and cell lines were

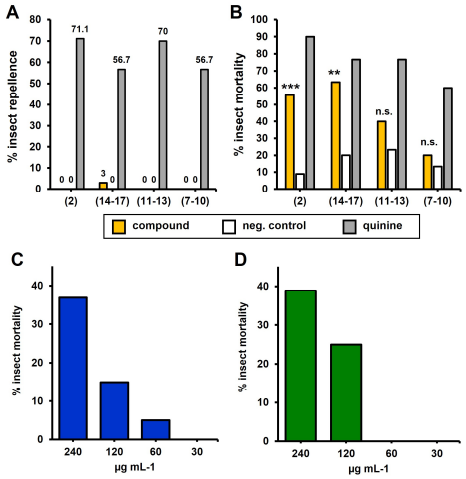

Figure 4. Insecticidal activities of *Mortierella alpina* compounds (1-17). A. Percentage of *Drosophila melanogaster* larvae repelled by saturated compound solution. Water and a quinine solution served as negative and positive control. **B.** Percentage larval mortality. Significantly higher mortality in **2** or **14-17** treatment was detected compared to the negative control at p<0.001 (***) and p<0.01 (**). Mortality for other compounds were not significant (n.s.). n ≥ 90. **C** and **D.** Percentage mortality is significantly dose-dependent for both **1** (**C**) and **2** (**D**) (p<0.001). n = 20.

observed (Table S6). In addition, **1** and **2** do not inhibit protease activity (Figure S46). Although BCPs with an *N*-acyl threonine branch such as the taxlllaids A-G[27] inhibit the growth of several protozoa, cycloacetamides do not impair the proliferation of *Trypanosoma brucei* (Table S6). In a previous report, *M. alpina* caused significant mortality of waxmoth and housefly larvae via baiting.[28] However, the toxic principle has never been determined. Hence, *Mortierella* metabolites (**1-17**) were tested for insecticidal activity on fruit fly *Drosophila melanogaster* larvae (Figure 4). Whilst mixtures of malpinins (**7-10**) and malpibaldins (**11-13**) had no or only little effect on larval vitality, malpicyclins (**14-17**) or pure **1** or **2** showed a significant toxicity which was not assigned to a food repellent activity (Figure 4A and 4B). Moreover, **1** and **2** induce mortality dose-dependently (Figure 4C and D) to a similar extent as the mycotoxins ochratoxin or tenuazonic acid.[29] Hence, cycloacetamides are highly selective insecticidal compounds. The BCPs taumycin A and B isolated from the sponge *Fascaplysinopsis* and the cyclopeptide destruxin A produced by the entomopathogen *Metarhizium aniopliae* contain a similar (iso)leucine-based peptide ring system as **1-6** and inhibit the growth of arthropods or fruit fly larvae, respectively.[30-32] The *M. alpina*-related early-diverging fungus *Podila verticillata* harbors a bacterial endosymbiont that produces anthelmintic compounds to efficiently protect the fungal host from nematodes attacks.[22] Similar to nematodes, mycophagous insects such as *Drosophila* can feed on *Mortierella* as a source of PUFAs.[28, 33] Hence, the cycloacetamides of *M. alpina* may

exert a protective role against insect predators. Moreover, cycloacetamides provide a chemical lead for a novel class of bio-pesticides that are environmentally sustainable and less toxic than conventional insecticides.

The current work describes basal fungi as a new reservoir of cyclic BCPs with biological activity. The combination of metabolic screening, precursor-directed feeding, advanced peptide synthesis and NMR-based structure elucidation not only enabled the identification of these compounds, but also provided insight into the chemically mediated interaction between basal fungi with their environment. From an applied scientific angle, cycloacetamides represent candidates for low-molecular weight insecticides with low cytotoxicity towards human cells.

ASSOCIATED CONTENT

Supporting Information

Details on strain identification, cultivation, metabolite isolation, derivatization, total synthesis, NMR and MS/MS analyses, and bioactivity assays (PDF). This material is available free of charge via the Internet at http://pubs.acs.org

AUTHOR INFORMATION

Corresponding Author

* **Markus Gressler –** Department of Pharmaceutical Microbiology at the Leibniz Institute for Natural Product Research and Infection Biology (Hans-Knöll-Institute), Friedrich-Schiller-University, Winzerlaer Strasse 2, 07745 Jena (Germany), email: markus.gressler@leibniz-hki.de

Author Contributions

The manuscript was written through contributions of all authors. All authors have given approval to the final version of the manuscript.

Ethical statement

Ethics approval was not required for this study.

ACKNOWLEDGMENT

We are grateful to Heike Heinecke, and Andrea Perner (both Hans-Knöll-Institute Jena, Germany) for their technical assistance in recording NMR and HR-MS/MS spectra, respectively. We thank Caroline Semm and Christiane Weigel (JRMC, Hans-Knöll-Institute Jena, Germany) for technical assistance in the performance of strain maintenance and antimicrobial activities, respectively. In addition, we thank Dr. Hans-Martin Dahse and Eva-Maria Neumann (both Hans-Knöll-Institute Jena, Germany) for cytotoxicity assays on mammalian cells. We acknowledge Marta Bogacz, Lukas Peltner (both Friedrich-Schiller-University Jena, Germany) and Hannah Büttner (Hans-Knöll-Institute Jena, Germany) for determination of antitrypanosomal, immunomodulating, and anthelminthic activities.

ABBREVIATIONS

BCP, branched-chain peptide; NRPS, nonribosomal peptide synthetase; NMR, nuclear magnetic resonance; MS, mass spectrometry.

REFERENCES

1. Ho, S. Y.; Chen, F. *Lett. Appl. Microbiol.* **2008,** *47*, 250-255.
2. Kikukawa, H.; Sakuradani, E.; Ando, A.; Shimizu, S.; Ogawa, J. *J. Adv. Res.* **2018,** *11*, 15-22.
3. Koyama, N.; Kojima, S.; Nonaka, K.; Masuma, R.; Matsumoto, M.; Omura, S.; Tomoda, H. *J. Antibiot. (Tokyo)* **2010,** *63*, 183-186.
4. Baldeweg, F.; Warncke, P.; Fischer, D.; Gressler, M. *Org. Lett.* **2019,** *21*, 1444-1448.
5. Wurlitzer, J. M.; Stanisic, A.; Ziethe, S.; Jordan, P. M.; Günther, K.; Werz, O.; Kries, H.; Gressler, M. *Chem. Sci.* **2022**.
6. Wurlitzer, J. M.; Stanisic, A.; Wasmuth, I.; Jungmann, S.; Fischer, D.; Kries, H.; Gressler, M. *Appl. Environ. Microbiol.* **2021,** *87*, e02051-20.
7. Nagai, K.; Koyama, N.; Sato, N.; Yanagisawa, C.; Tomoda, H. *Bioorg. Med. Chem. Lett.* **2012,** *22*, 7739-7741.
8. Futaki, S.; Nakase, I.; Suzuki, T.; Zhang, Y. J.; Sugiura, Y. *Biochemistry* **2002,** *41*, 7925-7930.
9. May, J. J.; Wendrich, T. M.; Marahiel, M. A. *J. Biol. Chem.* **2001,** *276*, 7209-7217.
10. Miao, V.; Coeffet-LeGal, M. F.; Brian, P.; Brost, R.; Penn, J.; Whiting, A.; Martin, S.; Ford, R.; Parr, I.; Bouchard, M.; Silva, C. J.; Wrigley, S. K.; Baltz, R. H. *Microbiology (Reading)* **2005,** *151*, 1507-1523.
11. Umemura, M.; Nagano, N.; Koike, H.; Kawano, J.; Ishii, T.; Miyamura, Y.; Kikuchi, M.; Tamano, K.; Yu, J.; Shin-ya, K.; Machida, M. *Fungal Genet. Biol.* **2014,** *68*, 23-30.
12. Koiso, Y.; Natori, M.; Iwasaki, S.; Sato, S.; Sonoda, R.; Fujita, Y.; Yaegashi, H.; Sato, Z. *Tetrahedron Lett.* **1992,** *33*, 4157-4160.
13. Matabaro, E.; Kaspar, H.; Dahlin, P.; Bader, D. L. V.; Murar, C. E.; Staubli, F.; Field, C. M.; Bode, J. W.; Künzler, M. *Sci. Rep.* **2021,** *11*, 3541.
14. Wagner, L.; Stielow, B.; Hoffmann, K.; Petkovits, T.; Papp, T.; Vagvolgyi, C.; de Hoog, G. S.; Verkley, G.; Voigt, K. *Persoonia* **2013,** *30*, 77-93.
15. Liebman, J. F.; Greenberg, A. *Biophys. Chem.* **1974,** *1*, 222-226.
16. Greco, C.; Pfannenstiel, B. T.; Liu, J. C.; Keller, N. P. *ACS Chem. Biol.* **2019,** *14*, 1121-1128.
17. Horton, A. E.; May, O. S.; Elsegood, M. R. J.; Kimber, M. C. *SYNLETT* **2011,** *6*, 797-800.
18. Neises, B.; Steglich, W. *Angew. Chem. Int. Ed.* **1978,** *17*, 522-524.
19. Nicolaou, K. C.; Estrada, A. A.; Zak, M.; Lee, S. H.; Safina, B. S. *Angew. Chem. Int. Ed.* **2005,** *44*, 1378-1382.
20. Jung, M. E.; Lyster, M. A. *J. Chem. Soc., Chem. Commun.* **1978**, 315-316.
21. Sonnabend, R.; Seiler, L.; Gressler, M. *J. Fungi* **2022,** *8*, 196.
22. Büttner, H.; Niehs, S. P.; Vandelannoote, K.; Cseresnyes, Z.; Dose, B.; Richter, I.; Gerst, R.; Figge, M. T.; Stinear, T. P.; Pidot, S. J.; Hertweck, C. *Proc. Natl. Acad. Sci. USA* **2021,** *118*, e2110669118.
23. Niehs, S. P.; Scherlach, K.; Hertweck, C. *Org. Biomol. Chem.* **2018,** *16*, 8345-8352.
24. Niehs, S. P.; Dose, B.; Scherlach, K.; Roth, M.; Hertweck, C. *ChemBioChem* **2018,** *19*, 2167-2172.
25. Lang, G.; Kalvelage, T.; Peters, A.; Wiese, J.; Imhoff, J. F. *J. Nat. Prod.* **2008,** *71*, 1074-1077.
26. Xi, X.; Lu, X.; Zhang, X.; Bi, Y.; Li, X.; Yu, Z. *J. Antibiot. (Tokyo)* **2019,** *72*, 736-743.
27. Kronenwerth, M.; Bozhuyuk, K. A.; Kahnt, A. S.; Steinhilber, D.; Gaudriault, S.; Kaiser, M.; Bode, H. B. *Chemistry (Easton)* **2014,** *20*, 17478-17487.
28. Edgington, S.; Thompson, E.; Moore, D.; Hughes, K. A.; Bridge, P. *Springerplus* **2014,** *3*, e289.

29. Rohlfs, M.; Obmann, B. *Mycotoxin Res* **2009,** *25*, 103-112.
30. Bishara, A.; Rudi, A.; Aknin, M.; Neumann, D.; Ben-Califa, N.; Kashman, Y. *Org. Lett.* **2008,** *10*, 4307-4309.
31. deGruyter, J. N.; Maio, W. A. *Org. Lett.* **2014,** *16*, 5196-5199.
32. Pal, S.; St Leger, R. J.; Wu, L. P. *J. Biol. Chem.* **2007,** *282*, 8969-8977.
33. Shen, L. R.; Lai, C. Q.; Feng, X.; Parnell, L. D.; Wan, J. B.; Wang, J. D.; Li, D.; Ordovas, J. M.; Kang, J. X. *J. Lipid Res.* **2010,** *51*, 2985-2992.

Insecticidal cyclodepsitetrapeptides from *Mortierella alpina*

Johannes Rassbach,[a] Peter Merseburger,[a] Jacob M. Wurlitzer,[a] Nico Binnemann,[b] Kerstin Voigt,[c,d] Marko Rohlfs,[b] and Markus Gressler[a,*]

[a] Friedrich-Schiller-University, Leibniz Institute for Natural Product Research and Infection Biology (Hans-Knöll-Institute), Department Pharmaceutical Microbiology, Winzerlaer Strasse 2, 07745 Jena, Germany.

[b] University of Bremen, Institute of Ecology, Chemical Ecology Group, Leobener Strasse 5, 28359 Bremen, Germany.

[c] Jena Microbial Resource Collection, Leibniz Institute for Natural Product Research and Infection Biology (Hans Knöll Institute), Adolf-Reichwein-Strasse 23, 07745 Jena, Germany.

[d] Friedrich Schiller University, Institute of Microbiology, Neugasse 25, 07743 Jena, Germany.

Table of content

Experimental procedures

Cultivation, extraction, metabolite quantification and purification

Organisms and cultivation. *M. alpina* strains (listed in Table S1) were retrieved from the Jena Microbial Resource Collection (JMRC), Jena, Germany (listed as public collection WDCM 919 by World Federation of Culture Collections) and were maintained on MEP agar plates (30 g L^{-1} malt extract, 3 g L^{-1} soy peptone, 18 g L^{-1} agar) at 25 °C for 7 days and were kept at 4 °C for another two weeks. For metabolite production, all strains were cultivated in 100 mL liquid MEP medium or YPD (20 g L^{-1} soy peptone, 20 g L^{-1} D-glucose, 10 g L^{-1} yeast extract) at 25°C for 11 days. If required, media were amended with 10 mM L-amino acids (L-Ile, L-Leu, L-Met, L-Phe, L-Trp, L-Tyr, L-Val).

Antibiotic treatment. Strain JMRC:SF:10519 (DSM 34346) was cultivated on MEP agar plates with and without antibiotics (ciprofloxacin 200 µg mL^{-1}, spectinomycin 200 µg mL^{-1}), known to cure hyphae infected with *Burkholderia* spec.[1] After five repetitions, the agar slants were used to inoculate 75 mL of MEP liquid medium. To keep up the antibiotic pressure, the same antibiotics were added to the liquid cultures of the treated precultures. Cultures were incubated at 25°C and 140 rpm for 10 days and the amount of **2** was determined and normalized against the fungal dry biomass. Each cultivation was carried out in duplicates.

Metabolite Detection and quantification. Metabolites were extracted from the 100 mL culture supernatants with an equal volume of ethyl acetate. Pure medium without inoculation served as control. After evaporation under reduced pressure, the residual was dissolved in 4 mL methanol by ultrasonication (1 min). Remaining particle were removed by centrifugation (20,000 × g, 10 min). Metabolites (5 µl) were routinely determined and quantified by analytical UHPLC-MS using method 1 (Table S7) using authentic standards of cycloacetamides A-E (**1-5**), malpinin A (**7**),[2] malpibaldin A (**11**),[3] and malpicyclin C (**16**)[3] and a commercially available calpinactam standard (**18**, Santa Cruz Biotechnology) as reference. Metabolites were quantified from the extracted ion chromatograms (EICs) by calculation of the area under the curve (AUC). Metabolite amounts were normalized against the fungal dry biomass.

Extraction and purification of cycloacetamides A-F (1-6). For production of **2**, *M. alpina* JMRC:SF:10519 (DSM 34346) was cultivated in 26 × 500 mL MEP medium at 25°C and 130 rpm for nine days. To produce **1** and **3-5,** the medium was additionally amended with 10 mM Leu or Phe, respectively, and a similar cultivation was performed. Mycelium was removed by filtration over Miracloth. The culture filtrate was adjusted to pH 2 by HCl and extracted three times with an equal volume of ethyl acetate. After evaporation, the residual was dissolved in 150 mL methanol, centrifuged (5000 × g) to remove cell debris, and finally subjected to purification via semipreparative HPLC. **2** was purified using method 2 and subsequently method 3 (Table S7). Compounds **3-5** were prepurified using HPLC method 4 (Table S7). Pure **5** was separated from **3** and **4** using method 5 (Table S7) and enantioselective separation of **3** and **4** were obtained using method 6 (Table S7). Compound 1 was purified using method 7 (Table S7) followed by method 3 (Table S7).

Chemical analysis

General. LC-MS experiments were performed on an Agilent 1290 Infinity II UHPLC coupled to a 6130 Single Quadrupol mass spectrometer. MS/MS measurements were conducted using a Thermo Scientific Q Exactive Plus

mass spectrometer. 1D- and 2D-NMR spectra were recorded on a Bruker Avance III 600 MHz spectrometer at 300 K. DMSO-d_6 served as both solvent and internal standard (δ_H 2.50 ppm and δ_C 39.52 ppm).

Partial acidic hydrolysis of 2. Four aliquots of **2** (1 mg mL^{-1} in methanol) in a total volume of 50 µL were hydrolyzed with 100 µL of HCl (1 M) at 90 °C for 0, 5, 15 or 25 min. Reaction was stopped by addition of 100 µL of KOH. Samples were diluted with an equal amount of methanol and applied to UHPLC-MS analysis (method 1, Table S7).

Marfey's method. Marfey's method[4] was carried out with slight modifications[5] as previously described.[2] The derivatized amino acids was analyzed by UHPLC-MS using chiral FDLA amino acid standards as reference. (method 8, Table S7). The amino acid derivatives were detected by their mass ($[M + H]^+ = M_{amino\ acid} + M_{FDLA} - M_{Fluorine}$).

Peptide synthesis.

General. Protected amino acids (L-Phe-OMe, *N*Ac-L-Thr-OMe, N-Boc-L-Leu, N-Boc-D-Leu) were purchased from Carl Roth, all other reagents were purchased from Sigma-Aldrich, Thermo Fisher Scientific or Santa Cruz Biotechnology. All reactions were performed with water-free solvent and under nitrogen atmosphere and the progress of conversion was followed by UHPLC-MS (method 1, Table S7).

Amine deprotection. The dipeptide N-Boc-L/D-Leu-L-Phe-OMe (0.125 M) was mixed with two equivalents of anisole (0.25 M) and dissolved in 15 mL dichloromethane (DCM) with 20% TFA. After 2 hours at room temperature, the reaction was stopped by neutralization with KOH and extraction with a saturated NH_4Cl solution. Due to hydrolysis sensitivity, the linear tetradepsipeptides (0.04 M) were solved in chloroform and mixed with 0.06 M trimethylsilyl iodide (TMS-I) and incubated for 1.5 hours at 50°C. The reaction was stopped by addition of methanol and the organic layer was concentrated under reduced pressure. Compounds were purified using Flash-LC method A (Table S8).

Acid deprotection. The peptide (0.1 M) was dissolved in 100 mL dichloroethane (DCE) and six equivalents of trimethyltin hydroxide (0.6 M) and incubated for 26 h (64 h for the tetrapeptide) at 80°C under argon atmosphere. The reaction was cooled to room temperature and dried *in vacuo*. The product was dissolved in 50 mL ethyl acetate and washed three times with an equal volume of 1M HCl and finally with a saturated NaCl solution. The organic phase was dried over Na_2SO_4 and evaporated under reduced pressure.

Modified Steglich Esterification. Esterification was carried out as described by Steglich.[6] As minor modification, the coupling agent 1-ethyl-3-(3-dimethylaminopropyl) carbodiimide (EDC) was used.[7] One eq. of *N*-Boc-L/D-Leu (0.2 M) was dissolved in 8 mL DCM and incubated with 1.5 eq. of EDC-HCl and 0.3 eq. of 4-dimethylaminopyridine (DMAP) for 30 min at ambient temperature. One eq. of *N*Ac-Thr-OMe dissolved in 8 mL DCM was added. The reaction was carried out for 18 h at 0°C. The final product was washed twice with 1 M HCl, twice with saturated NH_4Cl solution and finally with pure water (30 mL each). The organic phase was dried over Na_2SO_4 and concentrated *in vacuo*.

Linear peptide coupling. The deprotected acids were dissolved in DCM to give a solution of 0.2 M. Four equivalents of DIPEA (*N,N*-diisopropyl ethylamine) and 1.1 equivalents of TBTU (2-(1*H*-benzotriazole-1-yl)-1,1,3,3-tetramethylaminium tetrafluoroborate) were added and the mixture was incubated for 5 minutes. An equimolar amount of the peptide coupling solution in DCM was immediately added to give a final concentration of 0.1 M. The reaction was stopped after 3.5 hours by extraction with a saturated 15 mL NH_4Cl solution (3 times)

followed by an aqueous extraction. The organic phase was concentrated under reduced pressure. The dipeptide H_2N-D-Leu-L-Phe-OMe was dissolved in 5 mL DCM and purified using the chromatography method B (Table S8). The coupling of the dipeptide and the didepsipeptide was carried out without DIPEA for 16 h. The linear tetrapeptides were dissolved in 1 mL DCM and purified by Flash-LC method C (for N-Boc-D-Leu-*O*-*N*Ac-L-Thr-L-Leu-L-Phe-OMe) or method D (for N-Boc-L-Leu-*O*-*N*Ac-L-Thr-D-Leu-L-Phe-OMe) (Table S8).

Macrocyclization procedure. The deprotected linear tetradepsipeptides (2.5 mM) were dissolved in mixture of DCM and dimethylsulfoxide (DMSO) (95:5). The reaction was started by adding 3 eq. 1-[bis(dimethylamino)methylene]-1*H*-1,2,3-triazolo[4,5-b]pyridinium 3-oxide hexafluorophosphate (HATU) and incubated at ambient temperature for 24 or 48 h for **2** and **19**, respectively. The organic phase was removed *in vacuo*. The compounds were dissolved in DMSO and subjected to Flash chromatography using method E (Table S8). Fractions containing **2** or **19** were collected and dissolved in 1 mL of methanol and subjected to semipreparative HPLC using method 9 (Table S7).

Determination of biological activities

Antimicrobial growth inhibition assays. The following organisms were tested for their susceptibility to the compounds as described previously[8]: *Bacillus subtilis* JMRC:STI:10880, *Staphylococcus aureus* JMRC:STI:10760, *Escherichia coli* JMRC:ST:33699, *Pseudomonas aeruginosa* JMRC:ST:33772, *Pseudomonas aeruginosa* JMRC:ST:337721, *Staphylococcus aureus* JMRC:ST:33793 (MRSA), *Enterococcus faecalis* JMRC:ST:33700 (VRE), *Mycobacterium vaccae* JMRC:STI:10670, *Sporobolomyces salmonicolor* JMRC:ST:35974, *Candida albicans* JMRC:STI:25000, and *Penicillium notatum* JMRC:STI:50164. Ciprofloxacin (5 µg mL^{-1}) and amphotericin B (10 µg mL^{-1}) served as controls. In addition, a minimal inhibitory concentration of **1** was tested as previously described using rifampicin as positive control.[8, 9]

To determine growth inhibitory effects against *Streptomyces* spec., the following strains were cultivated in liquid HA medium (4 g L^{-1} glucose, 4 g L^{-1} yeast extract, 10 g L^{-1} malt extract, pH 7.2) at 30 °C overnight: *Streptomyces prunicolor* ATCC25487, *Streptomyces canus* ATCC12237, and *Streptomyces fradiae* Tü2717. An aliquot of a 100 µL of the cell suspension was plated on HA agar plates. Holes of 6 mm diameter were cut out of the agar and 50 µL of methanolic solution of **2** was added. Pure methanol and ciprofloxacin (200 µg mL^{-1}) was used as negative and positive control, respectively. The diameter of the inhibition zone was determined after incubation at 30°C for 5 days.

Antiproliferative and cytotoxicity assays. Antiproliferative and cytolytic assays were carried out for various mammalian cell lines in a microtiter scale as previously described.[2] **1** and **2** were tested with HeLa cervical cancer cells and U937 histiocytic lymphoma cells. **2** was additionally tested towards HUVEC endothelial cells and K-562 lymphoblasts. Four replicates were assayed.

Anthelmintic activity assays. Nematicide activities were determined against *Caenorhabditis elegans* by measure of the optical density (OD_{600}) of the overlaying *Escherichia coli* suspension.[10] Pure methanol and boric acid (55.6 mg mL^{-1}) served as negative and positive control, respectively.

Antitrypanosomal activity assays. Antitrypanosomal activity against *Trypanosoma brucei* was determined using the ATPlite assay system.[11] A DMSO solvent control (0.3%) and a chlorhexidine solution (1 mM) served as negative and positive control, respectively.

Antilarval activity assays. Initially, saturated solutions of the metabolites (270 µg mL^{-1} malpinins (**7-10**), 16 µg mL^{-1} malpibaldins (**10-13**), 1010 µg mL^{-1} malpicyclins (**14-17**) and 240 µg mL^{-1} of cycloacetamide B (**2**)) were prepared by dissolving the compounds in an aqueous *Drosophila* medium (15% [w/v] sucrose, 0.9% [w/v] NaCl and 1% [w/v] pectin). Pure *Drosophila* medium was used as a negative control, and *Drosophila* medium spiked with quinine (15 mM) served as a positive control. Quinine is known to repel *Drosophila*.[12] Individual freshly hatched *Drosophila melanogaster* larvae from bleached eggs were transferred to the 5 µL medium with a fine brush. At intervals of 30 minutes (for a total of 210 minutes), it was then checked whether the larvae persisted in the medium or whether they escaped. The latter is interpreted as a sign of a repelling effect of the medium. If a larva was found outside the medium within this period, it was scored as an escape behavior. After further three days, it was checked whether the larvae were still alive in order to estimate the mortality of the insects. A total set of at least n = 90 larvae was used for each compound. In a second assay, **1** and **2** were tested for dose-dependent effects by serial dilution of the saturated solutions (240 µg mL^{-1}) from undiluted to 1:8 (n=20 larvae per dilution). Statistics on repellence and mortality relative to the negative control were analyzed using binomial generalized linear models using the latest version of R (R Core Team 2022).[13]

Protease inhibition assay. An assay based on the proteolytic release of fluoresceine (FITC)-labelled amino acids from FITC-casein[14-16] was used to determine the effects of cycloacetamides A (**1**) and B (**2**) and well-investigated protease inhibitors. The following concentrations of proteases were used: 25 µg mL^{-1} proteinase K (Merck, from *Tritirachium album*, 30 mAU mg^{-1}), 125 µg mL^{-1} α-chymotrypsin (Sigma-Aldrich, from bovine pancreas, ≥40 U mg^{-1}), 50 µg mg^{-1} thermolysin (Sigma Aldrich, from *Geobacillus stearothermophilus* 30 – 175 U mg^{-1}) and 250 µg ml^{-1} papain (Sigma-Aldrich, from papaya latex, ≥10 U mg^{-1}). Assays were performed in reaction buffer A (50 mM Tris-HCl, pH 7.4) except for papain, which was carried in reaction buffer B (20 mM sodium acetate, 5.5 mM cysteine, 1.1 mM EDTA, pH 6.0). 50 µL of a 2-fold protease stock solution was added to wells of a black flat-bottomed 96-well plate. 1 µL of a 100-fold methanolic stock solution of **1** or **2** (final concentration of 100 µM) was added. Pure methanol and methanolic solutions of the commercially available protease inhibitors phenylmethylsulfonyl fluoride (PMSF; final concentration of 100 µM; against proteinase K and chymotrypsin), EDTA (100 µM; against thermolysin) or E-64 (10 µM; against papain) served as negative and positive controls, respectively. Reactions were started by addition of 50 µL of a 2-fold FITC-casein solution (Sigma-Aldrich, final concentration 50 µg mL^{-1}) and release of FITC-amino acids was monitored at 37 °C for 180 s on a CLARIOstar Plus (BMG Labtech) microplate reader using excitation wavelength of λ_{ex} = 494 nm and a detection wavelength λ_{em} = 521 nm. Experiments were carried out in triplicates. Solutions of FITC-casein in the respective reaction buffers without proteases served as blank. The maximum slope was calculated by the MARS software based on the blank corrected data with a window width of 10 s.

Quantities and physical properties of isolated metabolites and synthesized compounds

Isolated metabolites

Cycloacetamide A (**1**), 4.8 mg, white greyish amorphous powder, UV (CH_3CN) λ_{max} 210 nm, 215 nm, 220 nm; HR-ESI-MS data, see Table 1 and Figure S31; ^{1}H and ^{13}C NMR spectroscopic data, see Table S5.

Cycloacetamide B (**2**), 10.5 mg, white greyish amorphous powder, UV (CH_3CN) λ_{max} 210 nm, 215 nm, 220 nm; HR-ESI-MS data, see Table 1 and Figure S3; ^{1}H and ^{13}C NMR spectroscopic data, see Table S3.

Cycloacetamide C (**3**), 1.0 mg, white greyish amorphous powder, UV (CH_3CN) λ_{max} 210 nm, 220 nm; HR-ESI-MS data, see Table 1 and Figure S41.

Cycloacetamide D (**4**), 4.3 mg, white greyish amorphous powder, UV (CH_3CN) λ_{max} 210 nm, 220 nm; HR-ESI-MS data, see Table 1 and Figure S42.

Cycloacetamide E (**5**), 1.0 mg, white greyish amorphous powder, UV (CH_3CN) λ_{max} 210 nm, 220 nm; HR-ESI-MS data, see Table 1 and Figure S43.

Cycloacetamide F (**6**) was detected as accompanying compound by UHPLC-MS/MS (Table 1 and Figure S44) and could not be isolated in quantifiable amounts.

Synthesized compounds

Cycloacetamide B (**2**), cyclo-(-*N*Ac-L-Thr-D-Leu-L-Phe-L-Leu-*O*-), 1.0 mg, white greyish amorphous powder, UV (CH_3CN) λ_{max} 210 nm, 215 nm, 220 nm; ^{1}H NMR spectroscopic data, see Fig. S28.

Cycloacetamide B isomer (**19**), cyclo-(-*N*Ac-L-Thr-L-Leu-L-Phe-D-Leu-*O*-), 1.0 mg, white greyish amorphous powder, UV (CH_3CN) λ_{max}210 nm, 215 nm, 220 nm; ^{1}H NMR spectroscopic data, see Fig. S28.

Table S1. Strains used in this study and their corresponding metabolites. Compounds were detected by UHPLC-MS (EIC) with a threshold minimum of 2 × 10^4 mAU (AUC) per peak. Metabolite families were determined by presence of the most prominent compounds, i.e. cycloacetamide B (**2**, *m/z* 516.2948 $[M+H]^+$), malpinin A (**7,** *m/z* 859.4827 $[M+H]^+$), malpibaldin A (**11,** *m/z* 626.4062 $[M+H]^+$), malpicyclin C (**16** *m/z* 629.4343 $[M+H]^+$), and calpinactam (**18,** *m/z* 768.4330 $[M+H]^+$).

strain number	alternative strain number	cycloacetamide B (**2**)	malpinin A[a] (**7**)	malpibaldin A[a] (**11**)	malpicyclin C[a] (**16**)	calpinactam[b] (**18**)	reference[c]
JMRC:SF:010520	FSU 10520	x	x	x	x		JMRC
JMRC:SF:010519	FSU 10519; DSM 34346	x	x	x	x	x	JMRC/DSMZ
JMRC:SF:012594	ATCC32222; Peyronel 32222_TT; CBS 528.72; M136		x	x	x	x	JMRC/ATCC/CBS
JMRC:SF:010675	FSU 10675		x	x	x	x	JMRC
JMRC:SF:006524	FSU 6524		x	x	x		JMRC
JMRC:SF:000695	CBS 224.37		x	x		x	JMRC/CBS
JMRC:SF:002698	FSU 2698		x	x	x	x	JMRC
JMRC:SF:000830	CBS 331.74		x		x		JMRC/CBS
JMRC:SF:009789	CBS 210.32; SZMC 11213		x	x	x		JMRC/CBS/SZMC
JMRC:SF:008722	FSU 8722		x	x	x		JMRC
JMRC:SF:008736	FSU 8736		x		x		JMRC
JMRC:SF:008738	FSU 8738		x	x	x		JMRC
JMRC:SF:008712	FSU 8712		x	x	x		JMRC
JMRC:SF:008737	FSU 8737		x	x	x		JMRC
JMRC:SF:010551	FSU 10551		x	x	x	x	JMRC
JMRC:SF:010522	FSU 10522		x	x	x	x	JMRC
JMRC:SF:010683	FSU 10683		x	x	x	x	JMRC
JMRC:SF:010696	FSU 10696		x	x	x	x	JMRC
JMRC:SF:010716	FSU 10716		x	x	x	x	JMRC
JMRC:SF:010555	FSU 10555		x	x	x	x	JMRC
JMRC:SF:002698	FSU 2698		x	x	x	x	JMRC
JMRC:SF:010715	FSU 10715		x	x	x	x	JMRC
JMRC:SF:010706	FSU 10706		x	x	x	x	JMRC
		2/23 = 9%	23/23 = 100%	21/23 = 91%	22/23 = 96%	14/23 = 61%	

[a] Reference MS/MS spectra for **7, 11**, and **16** were obtained from previous studies.[2, 3]
[b] Reference MS/MS spectrum of **18** was obtained from a commercial standard (Santa Cruz Biotechnology).
[c] Strain reference centers are: Jena Microbial Resource Collection (JMRC), American Type Culture Collection (ATCC), Westerdijk Fungal Biodiversity Institute (CBS) and Szeged Microbiology Collection (SZMC).

Table S2. NMR data of 2 in DMSO-d_6. * overlapping signals. ** signals solely detectable in DEPT NMR spectra.

	δ ^{13}C [ppm]	type	δ ^{1}H [ppm], M (J [Hz])	COSY	HMBC
	acetate				
1	170.30	C=O			
2	22.50	CH_3	1.95, s		
	L-threonine				
3	169.80	C=O			
4	55.13	CH	4.61, dd (9.4, 4.3)	4-NH, 5	3, 5, 6
		NH	8.0, d (9.4)	4	2*, 4, 5
5	71.23	CH	5.18, dq (6.4, 4.6)	4, 6	6
6	15.15	CH_3	1.17, d (6.5)	5	4, 5
	D-leucine				
7	171.11	C=O			
8	51.40	CH	4.35, m	8-NH, 9	9
		NH	7.89, d (8.3)	8	3, 8
9	37.71	CH_2	a: 1.56, m	8, 9b	8
			b: 1.31, m	8, 9a	7, 8
10	24.20	CH	1.20, m	11, 12	8
11	21.97	CH_3	0.73*, d (6.6)	10	9, 10, 12
12	21.87	CH_3	0.81*, d (6.6)	10	9
	L-phenylalanine				
13	170.42	C=O			
14	55.66	CH	4.35, m	14-NH	13*, 15, 16
		NH	8.34, d (9.1)	14, 15	7, 14, 15
15	36.20	CH_2	a: 3.00, dd (13.6, 5.6)	14, 15b	14, 16, 17, 21
			b: 2.81, dd (13.5, 10.2)	14, 15a	14, 16, 17, 21
16	137.87	C (ar)			
17,21	128.90	CH (ar)	7.23*, m		17, 19, 21
18,20	128.02	CH (ar)	7.25*, m		16, 18, 20
19	126.25	CH (ar)	7.18, m		17 ,21
	L-leucine				
22	170.39	C=O			
23	50.19	CH	4.12, dt (7.9, 6.2)	23-NH, 24	24, 25
		NH	7.70, d (7.7)	23	13*, 23
24	39.29**	CH_2	a: 1.60, m	23, 24b	23
			b: 1.50, m	23, 24a	23, 25
25	23.99	CH	1.43, m	26, 27	23, 24, 26,27
26	22.89	CH_3	0.86, d (6.5)*	25	24, 25
27	22.67	CH_3	0.84, d (6.5)*	25	24, 26

Table S3. NMR data of 2 in CD_3OD. * overlapping signals. ** signals solely detectable in DEPT NMR spectra.

	δ ^{13}C [ppm]	type	δ ^{1}H [ppm], M (J [Hz])	COSY	HMBC
	acetate				
1	174.51	C=O			
2	22.63	CH_3	2.10, s		1
	L-threonine				
3	172.16	C=O			
4	57.43	CH	4.74, d (2.8)	5	1, 3, 5, 6
5	73.67	CH	5.44, dq (6.3, 2.9)	4, 6	4, 6, 22
6	16.03	CH_3	1.24, d (6.4)	5	4, 5
	D-leucine				
7	174.32	C=O			
8	53.15	CH	4.50, (t, 7.8 Hz)	9	7, 9
9	38.77	CH_2	a: 1.64, m	8, 9b	7, 8
			b: 1.46, m	8, 9a	7, 8
10	25.70*	CH	1.38, m	11, 12	11, 12
11	22.59*	CH_3	0.88, m*	10	
12	22.53*	CH_3	0.84, m*	10	
	L-phenylalanine				
13	172.86	C=O			
14	57.40	CH	4.57, (dd, 8.6; 7.4)		7, 13, 15, 16, 22
15	37.73	CH_2	a: 3.10, dd (13.8, 7.2)	14, 15b	13, 14, 16, 17, 21
			b: 2.87, dd (13.6, 9.0)	14, 15a	13, 14, 16, 17, 21
16	138.17	C (ar)			
17,21	130.05	CH (ar)	7.25*, m		17, 19, 21
18,20	129.51	CH (ar)	7.27*, m		16, 18, 20
19	127.86	CH (ar)	7.21, m		17 ,21
	L-leucine				
22	171.66	C=O			
23	52.63	CH	4.11, dt (t, 7.2 Hz)	24	22, 24, 25
24	40.32**	CH_2	a: 1.66, m	23, 24b	22, 23, 25, 26, 27
			b: 1.58, m	23, 24a	22, 23, 25
25	25.93*	CH	1.36*, m	26, 27	
26	23.12*	CH_3	0.86*, m	25	
27	22.67*	CH_3	0.82*, m	25	

Table S4. Determination of the absolute configuration of amino acids in 1-5 by Marfey's method. The results were compared to authentic standards. Retention times of D- and L-amino acids are highlighted in blue and red, respectively. The retention time of the L-allo-Thr standard is marked in purple.

	retention times of derivatized amino acids [min]		
sample	threonine	leucine	phenylalanine
L-allo-standard	5.56	-	-
L-standard	5.32	7.34	7.49
D-standard	6.33	8.69	8.51
cycloacetamide A (**1**)	5.32	7.34 + 8.69	-
cycloacetamide B (***2***)	5.32	7.34 + 8.69	7.49
cycloacetamide C (***3***)	5.32	7.34 + 8.70	7.49
cycloacetamide D (***4***)	5.33	7.34	7.49 + 8.51

Table S5. NMR data of 1 in DMSO-d_6. * overlapping signals. ** signals solely detectable in DEPT NMR spectra.

	δ ^{13}C [ppm]	type	δ ^{1}H [ppm], M (J [Hz])	COSY	HMBC
	acetate				
1	170.11	C=O			
2	22.22*	CH_3	1.96		1
	L-threonine				
3	169.51	C=O			
4	55.16	CH	4.62, dd (9.4, 4.4)	4-NH, 5	1, 3
		NH	8.05, d (9.3)	4	1, 4
5	71.02	CH	5.19, dq (6.4; 4.6)	4, 6	3*, 6, 19*
6	15.00	CH_3	1.18, d (6.5)	5	4, 5
	D-leucine				
7	171.44	C=O			
8	51.44	CH	4.36, m	8-NH, 9	3, 7, 9, 10
		NH	7.84, d (8.2)	8	3, 8
9	38.03	CH_2	a: 1.65, m	8, 10*	3, 8, 10*
			b: 1.45, m	8	8, 10*
10	24.33*	CH	1.46, m*	11*, 12*	
11	21.99	CH_3	0.85, d (6.5)	10*	9, 10,12
12	22.56	CH_3	0.89, d (6.6)	10*	9, 10
	L-leucine				
13	171.24	C=O			
14	49.94	CH	4.20, m	14-NH, 15	7*, 13*, 15, 16*
		NH	7.48, d (7.8)	14	7, 14
15	39.63**	CH_2	a: 1.63, m	14	13*, 14, 16*
			b: 1.42, m	14	14, 16*
16	24.43*	CH	1.51*, m	17*, 18*	
17	22.06	CH_3	0.86, d (6.6)	16*	15, 16
18	22.49	CH_3	0.87, d (6.9)	16*	15, 16
	L-leucine				
19	170.13	C=O			
20	52.61	CH	4.18, m	20-NH, 21	19*, 21, 22*
		NH	8.30, d (8.7)	20	13, 20
21	39.24**	CH_2	a: 1.56	20	20, 22, 24
			b: 1.52	20	20, 22
22	24.13	CH	1.60	23, 24	
23	22.56	CH_3	0.88, d (7.2)	22	21, 22
24	21.12	CH_3	0.81, d (6.5)	22	21, 22

Table S6. Determination of biological activities of cycloacetamide A (1) and B (2). [a]*Bacillus subtilis, Staphylococcus aureus* (MRSA, VRSA), *Escherichia coli, Pseudomonas aeruginosa;* [b]*Mycobacterium smegmatis;* [c]*Streptomyces prunicolor, Streptomyces canus, Streptomyces fradiae;* [d]*Sporidiobolus salmonicolor, Candida albicans, Penicillium notatum;*[e]cytotoxicity against HeLa, U-937, HUVEC, K-562; [f]pro/anti-inflammatory release of prostaglandines on monocyte-derived M2 macrophages; [g]*Trypanosoma brucei*; [h]*Caenorhabditis elegans.* Significant biological activities *versus* the negative control are highlighted in orange. n.d, not determined.

Cmpd.	pathogenic bacteria[a]	mycobacteria[b]	*Streptomyces spec.*[c]	fungi[d]	human cells[e]	human macrophages[f]	trypanosomes[g]	nematodes[h]
1	>1000 µg mL^{-1}	>125 µg mL^{-1}	n.d.	>1000 µg mL^{-1}	>50 µg mL^{-1}	>14.4 µg mL^{-1}	>150 µg mL^{-1}	>100 µg mL^{-1}
2	>1000 µg mL^{-1}	>125 µg mL^{-1}	> 516 µg mL^{-1}	>1000 µg mL^{-1}	>50 µg mL^{-1}	>15.5 µg mL^{-1}	>150 µg mL^{-1}	>100 µg mL^{-1}

Table S7. Analytical and semipreparative HPLC methods.

purpose	method 1	method 2	method 3	method 4	method 5
instrument	Agilent 1290 Infinity II	Agilent 1260	Agilent 1260	Agilent 1260	Agilent 1260
solvent A	water + FA 0.1%	water + 0.1 % TFA	water + 0.1 % TFA	water + 0.1 % TFA	water + 0.1 % TFA
solvent B	acetonitrile	acetonitrile	acetonitrile	acetonitrile	acetonitrile
gradient	0.0 - 4.0 min: 5 – 72 % B, 4.0 - 4.5 min: 72 – 95 % B, 4.5 - 5.0 min: 95 % B, 5.0 - 5.5 min: 95 – 5 % B, 5.5 - 6.0 min: 5 % B	0.0 - 0.5 min: 35 % B, 0.5 - 13.5 min: 35 - 80 % B, 13.5 - 17.0 min: 80 - 100 % B, 17.0 - 19.0 min: 100 % B, 19.5 - 19.5 min: 100 - 35 % B, 19.5 - 21.0 min: 35 % B	0.0 - 0.5 min: 45 % B, 0.5 - 10 min: 45 - 100 % B, 10.0 - 11.0 min: 100 % B, 11.0 - 11.5 min: 100 - 45 % B, 11.5 - 13.0 min: 45 % B	0.0 - 0.5 min: 35 % B, 0.5 - 12.5 min: 35 - 80 % B, 12.5 - 16.0 min: 80 - 100 % B, 16.0 - 17.0 min: 100 % B, 17.0 - 17.5 min: 100 - 35 % B, 17.5 - 19.0 min: 35 %	0.0 - 0.5 min: 70 % B, 0.5 - 6 min: 70 - 85 % B, 6.0 - 13.5 min: 85 - 100 % B, 13.5 - 14.5 min: 100 % B, 14.5 - 15.0 min: 100 - 70 % B, 15.0 - 16.5 min: 70 %
temperature	30 °C	12 °C	12 °C	12 °C	12 °C
flow	1 mL min^{-1}	2 mL min^{-1}	2 mL min^{-1}	2 mL min^{-1}	2 mL min^{-1}
column	Agilent Zorbax Eclipse Plus C_{18} RRHD	Agilent Zorbax Eclipse XDB-C18	Thermo Fisher Hypercarb	Agilent Zorbax Eclipse XDB-C18	Phenomenex SynergiHydro-RP
column dimension	50 × 2.1 mm, 1.8 µm	250 × 9.4 mm, 5 µm	150 × 4.6 mm, 5 µm	250 × 9.4 mm, 5 µm	250 × 10 mm, 4 µm
detection	DAD (λ = 220 nm) MS (positive ionization mode)	DAD (λ = 205 nm)	DAD (λ = 205 nm)	DAD (λ = 205 nm)	DAD (λ = 205 nm)

purpose	method 6	method 7	method 8	method 9
instrument	Agilent 1260	Agilent 1260	Agilent 1290 Infinity II	Agilent 1200
solvent A	water + 0.1 % TFA	water + 0.1 % TFA	water + FA 0.1%	water + 0.1 % FA
solvent B	acetonitrile	acetonitrile	acetonitrile	acetonitrile
gradient	0.0 - 0.5 min: 80 % B, 0.5 - 10.5 min: 80-100 % B, 10.5 - 16.0 min: 100 % B, 16.0 - 16.5 min: 100 - 80 % B, 16.5 – 21.0 min: 80%	0.0 - 0.5 min: 65 % B, 0.5 - 15.5 min: 65 - 100 % B, 15.5 - 16.5 min: 100 % B, 16.5 – 17.0 min: 100 - 65 % B, 17.0 - 18.5 min: 65 %	0.0 -10.0 min: 1 - 50% B, 10.0 – 11.0 min: 50 - 100% B, 11.0 - 11.5 min: 100-1% B	0 – 1.5 min: 30 % B, 1.5 – 16.5 min: 30-100 % B, 16.5 – 19 min: 100 % B, 19 – 19.5 min: 100 - 30 % B, 19.5 – 22 min: 30 % B
temperature	12 °C	12 °C	30 °C	12 °C
flow	3.5 mL min^{-1}	2 mL min^{-1}	1 mL min^{-1}	2 mL min^{-1}
column	Thermo Fisher Hypercarb	Agilent Zorbax Eclipse XDB-C18	Phenomenex Luna Omega Polar C_{18}	Agilent Eclipse XDB-C18-Säule
column dimension	150 × 4.6 mm, 5 µm	250 × 9.4 mm, 5 µm	50 × 2.1 mm, 1.6 µm	250 × 9.4 mm, 5 µm
detection	DAD (λ = 205 nm)	DAD (λ = 205 nm)	DAD (λ = 220 nm, 254 nm) MS (positive ionization mode)	DAD (λ = 205 nm)

Table S8. Preparative Flash-LC methods.

purpose	method A	method B	method C	method D	method E
instrument	C-810 flash chromatgraphy system (Büchi)	C-810 flash chromatgraphy system (Büchi)	C-810 flash chromatgraphy system (Büchi)	C-810 flash chromatgraphy system (Büchi)	C-810 flash chromatgraphy system (Büchi)
solvent A	water	dichloromethane	hexane	hexane	water
solvent B	acetonitrile	methanol	ethylacetate	ethylacetate	acetonitrile
gradient	0.0 – 2.5 min: 0 % B, 2.5 – 5 min: 20 % B, 5.0 – 7.5 min: 40 % B, 7.5 – 9.5 min: 60 % B, 9.5 – 11.5 min: 80 % B, 11.5 – 15.5 min: 100 % B	0.0 – 6.4 min: 0 % B, 6.4 – 9.5 min: 20 % B, 9.5 – 12.1 min: 40 % B, 12.1 – 19.6 min: 100 % B	0.0 – 1.2 min: 0 % B, 1.2 – 3.1 min: 20 % B, 3.1 – 5 min: 40 % B, 5.0 – 6.8 min: 60 % B, 6.8 – 8.7 min: 80 % B, 8.7 – 16.6 min 100 % B	0 – 2 min: 0 % B, 2 – 4 min: 20 % B, 4 – 6 min: 40 % B, 6 – 14 min: 60 – 80 % B, 14 – 23 min: 100 % B	0 - 2.5 min: 0 % B, 2.5 – 5 min: 20 % B, 5 – 7.5 min: 40 % B, 7.5 – 10 min: 60 % B, 10 – 12.5 min: 80 % B, 12.5 – 17.2 min: 100 % B
temperature	20°C	20°C	20°C	20°C	20°C
flow	30 mL min^{-1}	30 mL min^{-1}	15 mL min^{-1}	30 mL min^{-1}	30 mL min^{-1}
column	Büchi FP ID C18 12 g	Büchi FP Silica 12 g	Büchi FP Silica 4 g	Büchi FP Silica 12 g	Büchi FP ID C18 Silica 12 g
column dimension	12 g 24 mL^{-1}, particle size 35-45 µm, pore size 53-80Å	12 g 24 mL^{-1}, particle size 35-45 µm, pore size 53-80Å	4 g 5 mL^{-1}, particle size 35-45 µm, pore size 53-80Å	12 g 24 mL^{-1}, particle size 35-45 µm, pore size 53-80Å	12 g 24 mL^{-1}, particle size 35-45 µm, pore size 53-80Å
detection	DAD (λ = 220 nm)	DAD (λ = 220 nm)	DAD (λ = 220 nm)	DAD (λ = 220 nm)	DAD (λ = 220 nm)

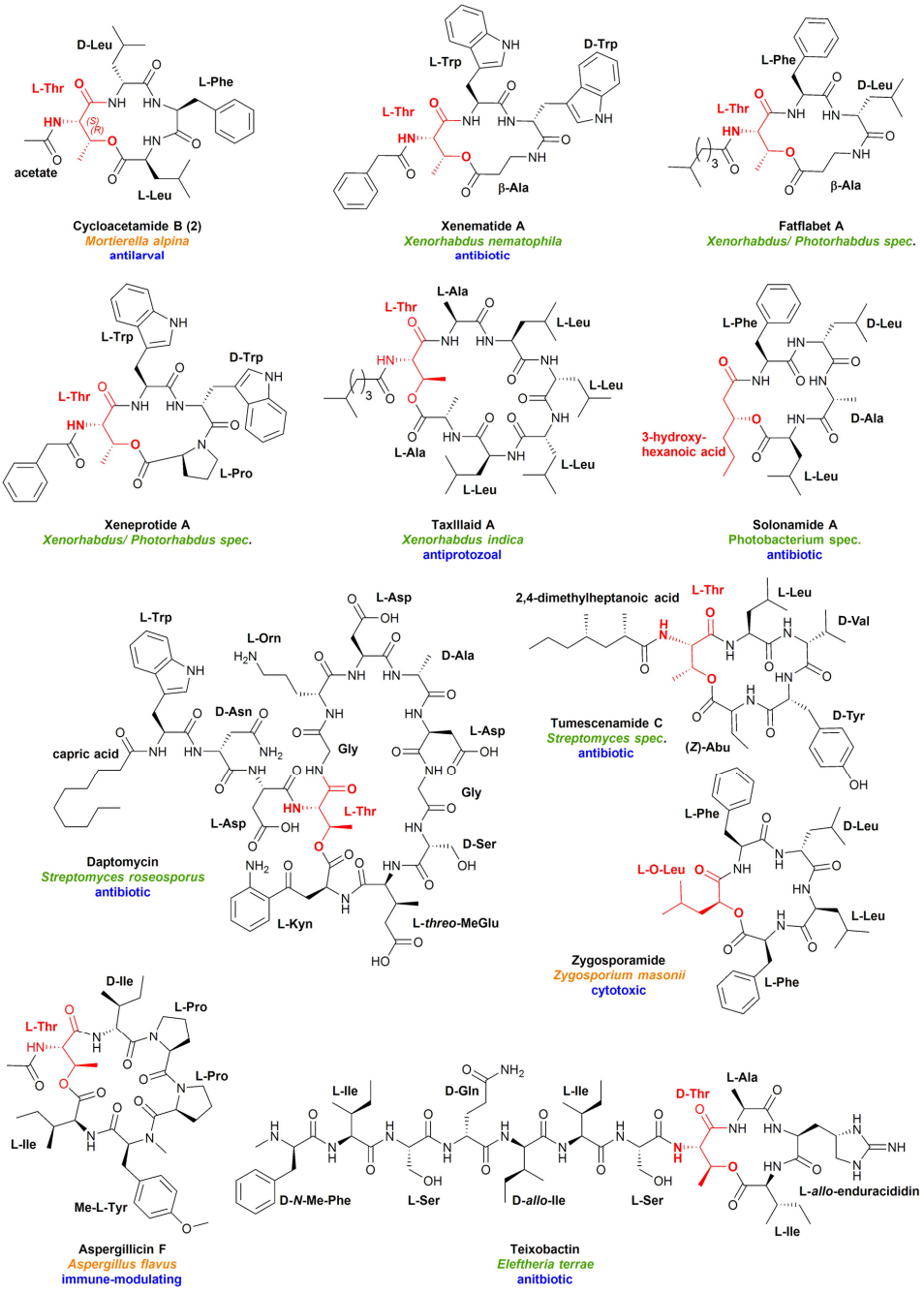

Figure S1. Branched-chain cyclopeptides (BCPs) from various species. The branching hydroxy or amino acid is highlighted in red. Fungal and bacterial species are highlighted in orange and green, respectively. Biological activities are indicated in blue. Structures, producing organisms and biological activities were extracted from the following references: Cycloactamide B (this study), xenematide A,[17] fatflabet A,[18] xeneprotide A,[18] taxlllaid A,[19] solonamide A,[20] daptomycin,[21] tumescenamide C,[22] zygosporamide,[23] aspergillicin F,[24] and teixobactin.[25] (*Z*)-Abu, (*Z*)-2-amino-2-butenoic acid; L-Kyn, L-kynurenine.

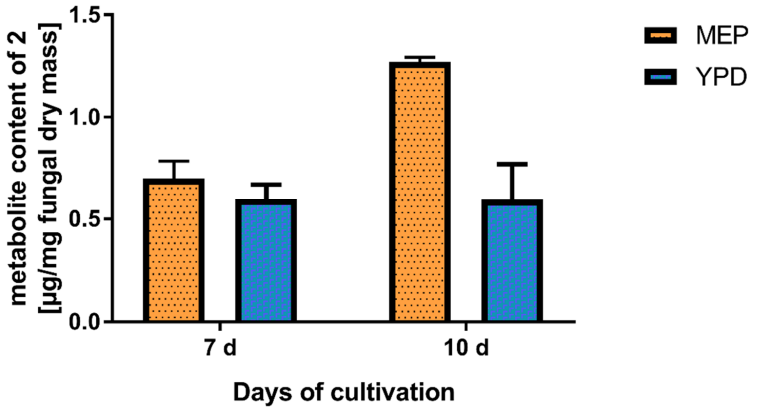

Figure S2. Time-dependent production of cycloacetamide B (2). *M. alpina* was cultured in MEP or YPD medium for 7 and 10 days and **2** production was quantified from the culture supernatant. Error bars indicate the standard error of the mean.

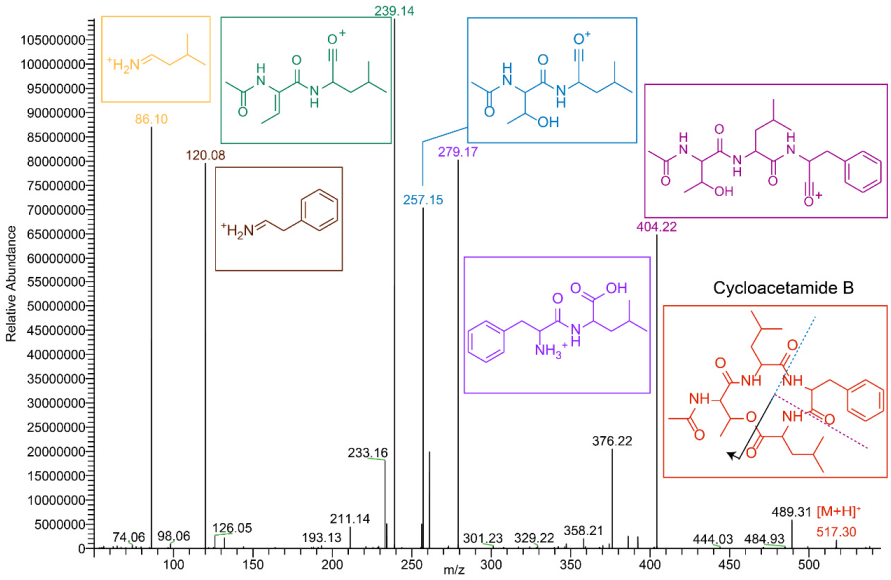

Figure S3. ESI-MS/MS spectrum of 2. Fragmentation was carried out at a higher-energy collisional dissociation (HCD) energy of 20%.

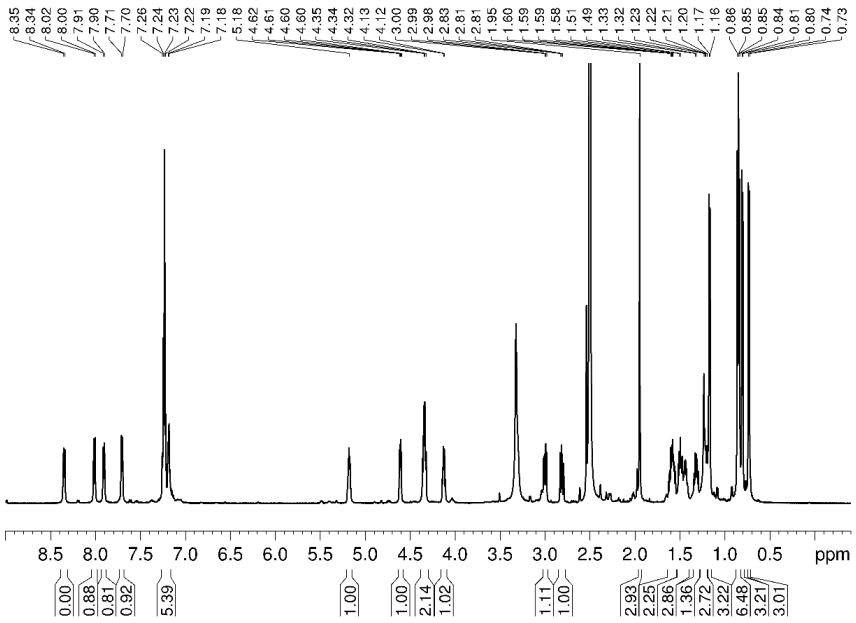

Figure S4. ^{1}H-NMR spectrum of 2 in DMSO-d_6.

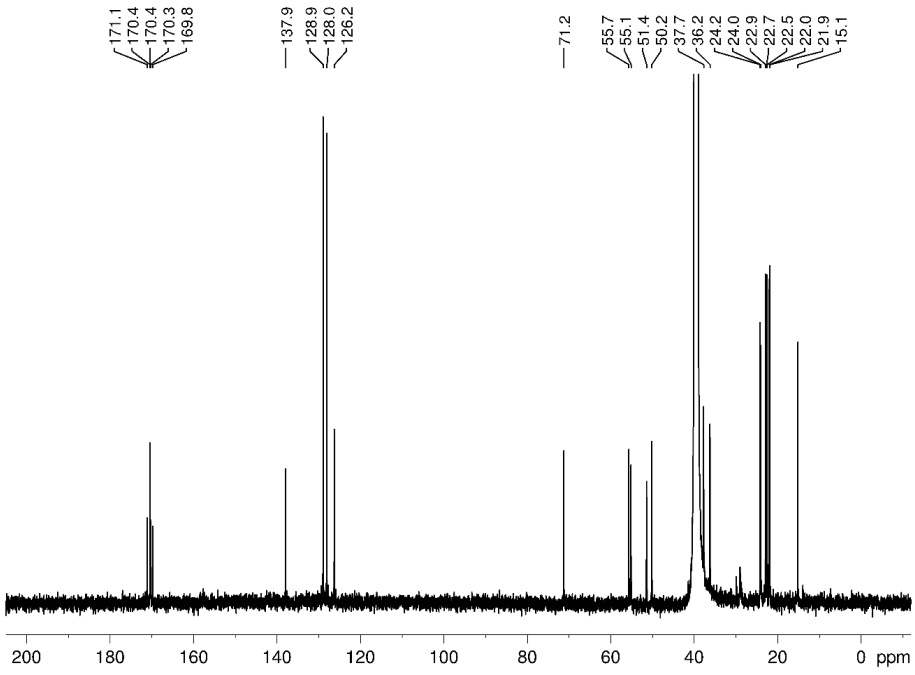

Figure S5. ^{13}C-NMR spectrum of 2 in DMSO-d_6. A magnification of the 172-169 ppm region is shown in Figure S6.

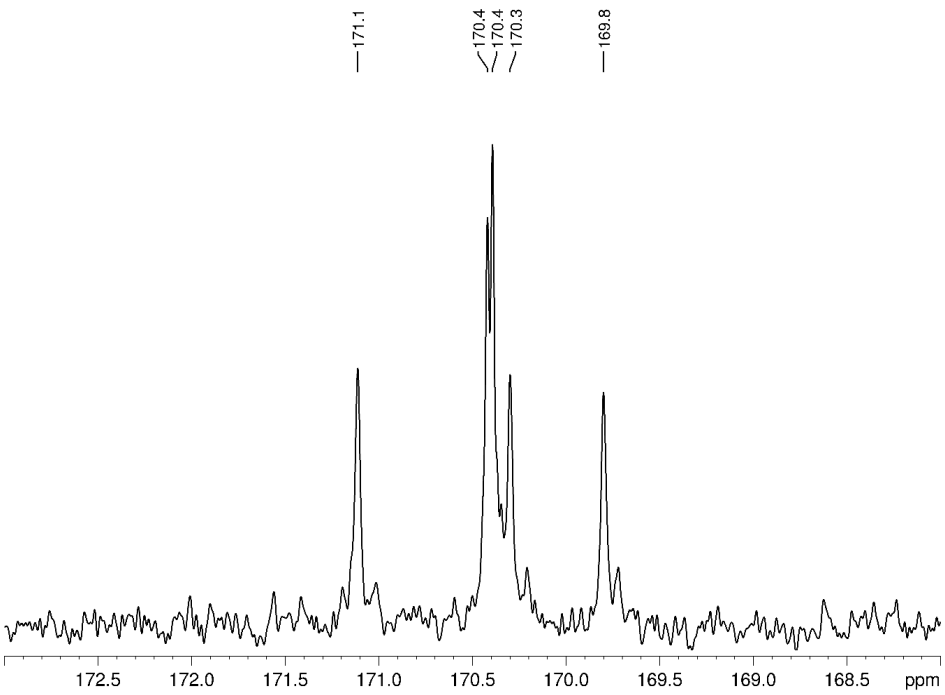

Figure S6. Detailed magnification of the ^{13}C-NMR spectrum of 2 in DMSO-d_6 at 172-169 ppm.

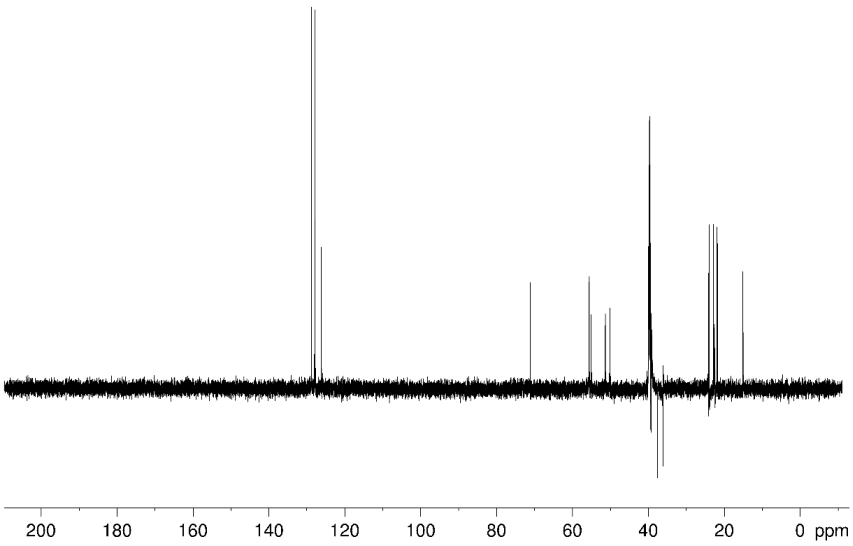

Figure S7. DEPT NMR spectrum of 2 in DMSO-d_6.

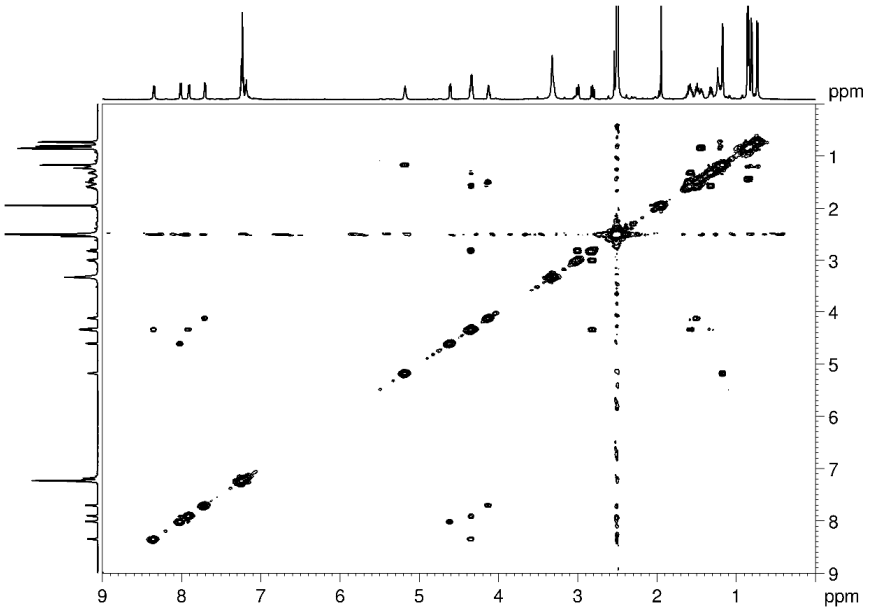

Figure S8. ^{1}H-^{1}H-COSY NMR spectrum of 2 in DMSO-d_6

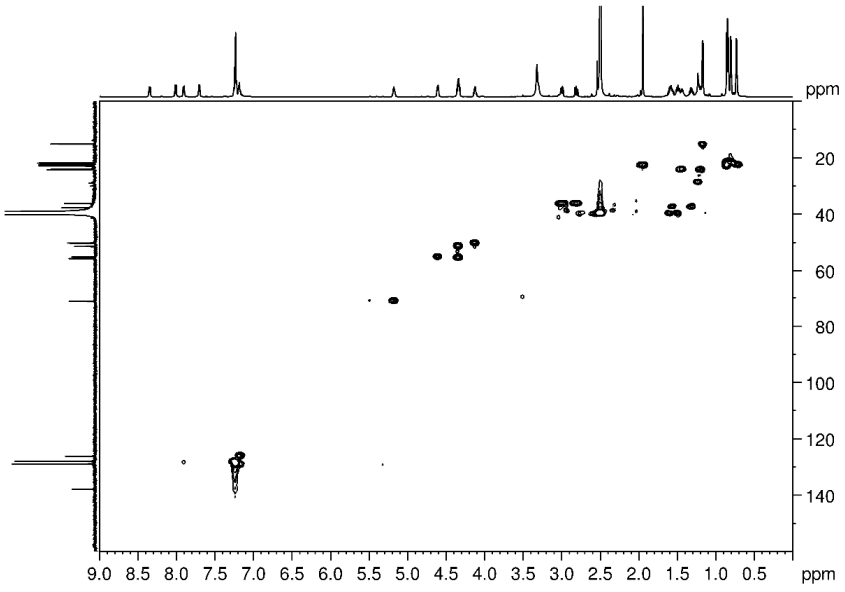

Figure S9. ^{1}H ^{13}C HSQC NMR spectrum of 2 in DMSO-d_6

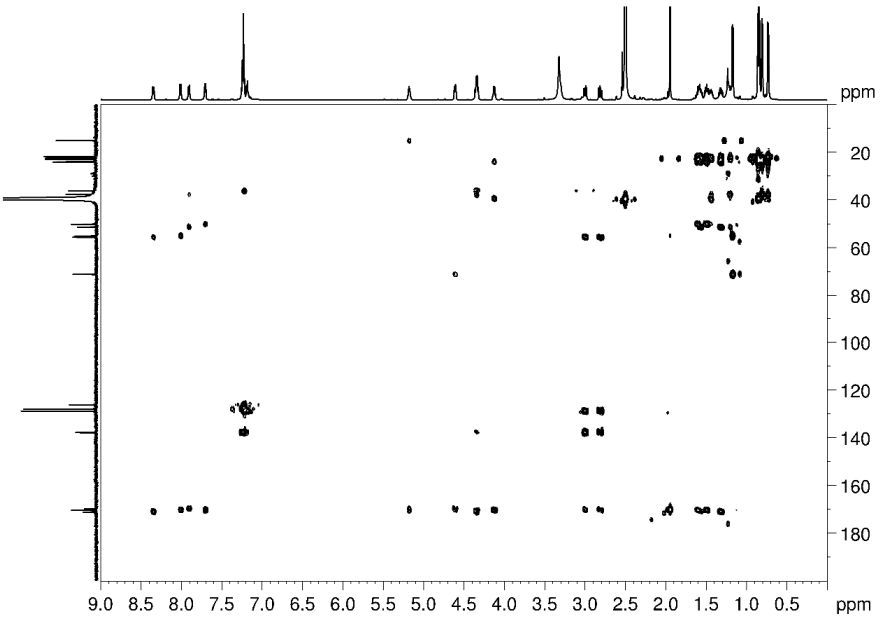

Figure S10. ^{1}H ^{13}C HMBC NMR spectrum of 2 in DMSO-*d*$_6$. A magnification of the region between δ_H 9.0- 7.2 ppm is shown in Figure S11.

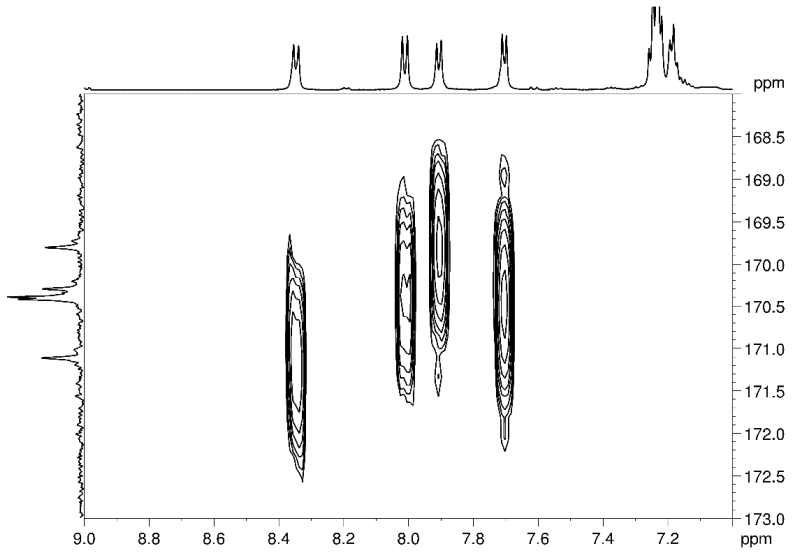

Figure S11. Magnification of the ^{1}H ^{13}C HMBC NMR spectrum of 2 in the region between δ_H 9.0- 7.2 ppm in DMSO-*d*$_6$. The four signals correspond to the four NH-C correlations in **2.**

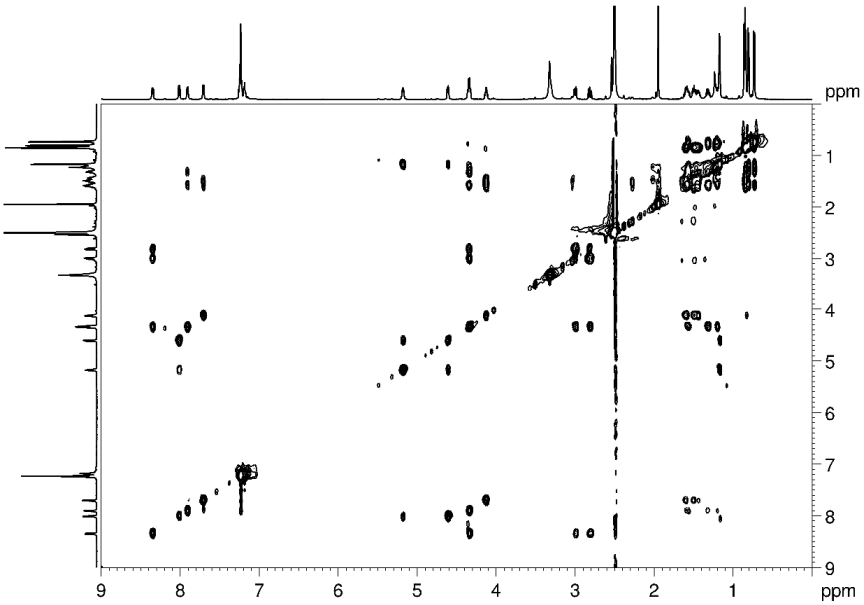

Figure S12. ^{1}H ^{1}H TOCSY NMR spectrum of 2 in DMSO-d_6.

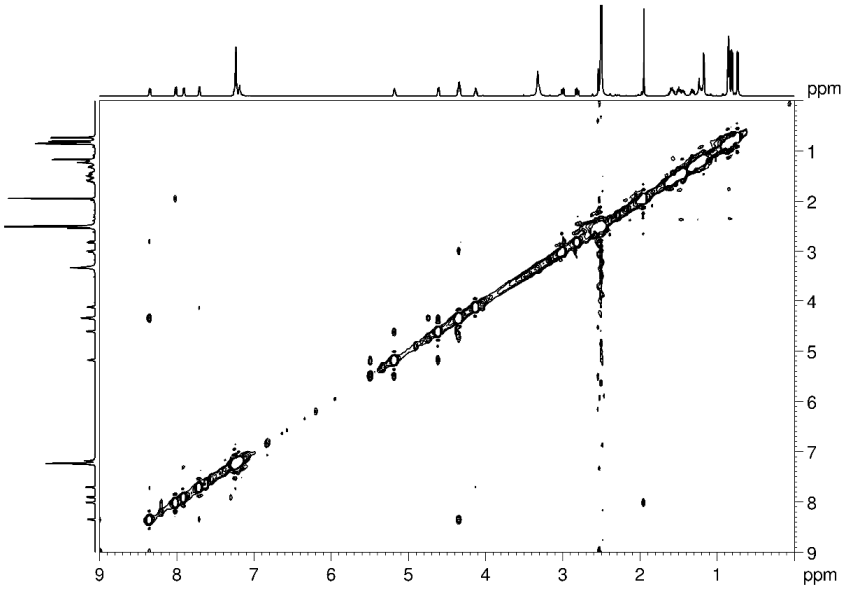

Figure S13. NOESY NMR spectrum of 2in DMSO-d_6.

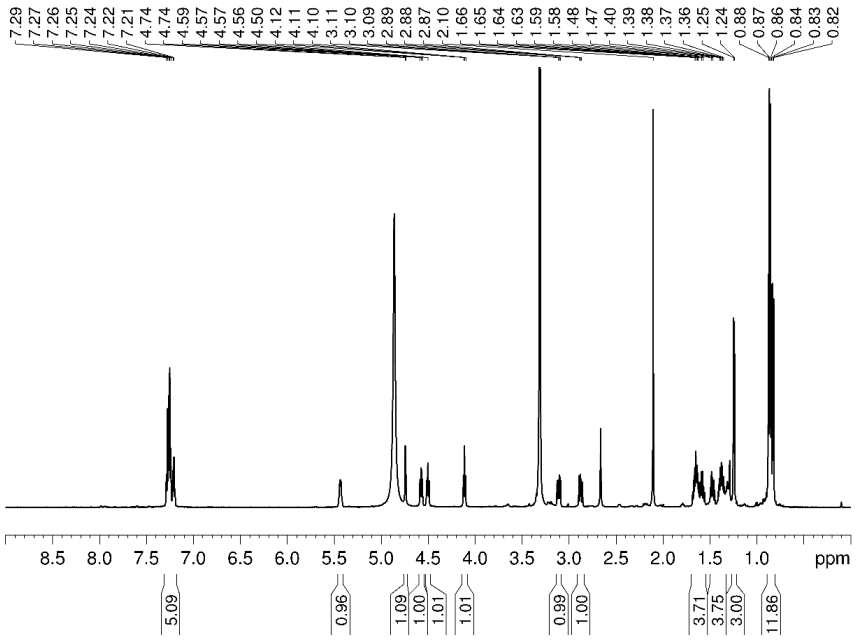

Figure S14. ^{1}H NMR spectrum of 2 in CD_3OD.

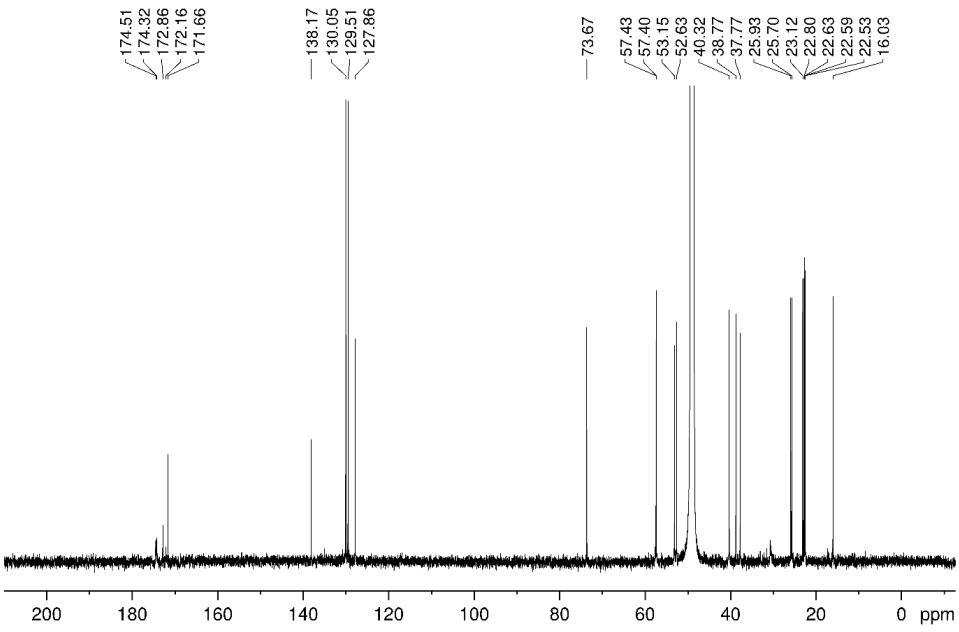

Figure S15. ^{13}C NMR spectrum of 2 in CD_3OD.

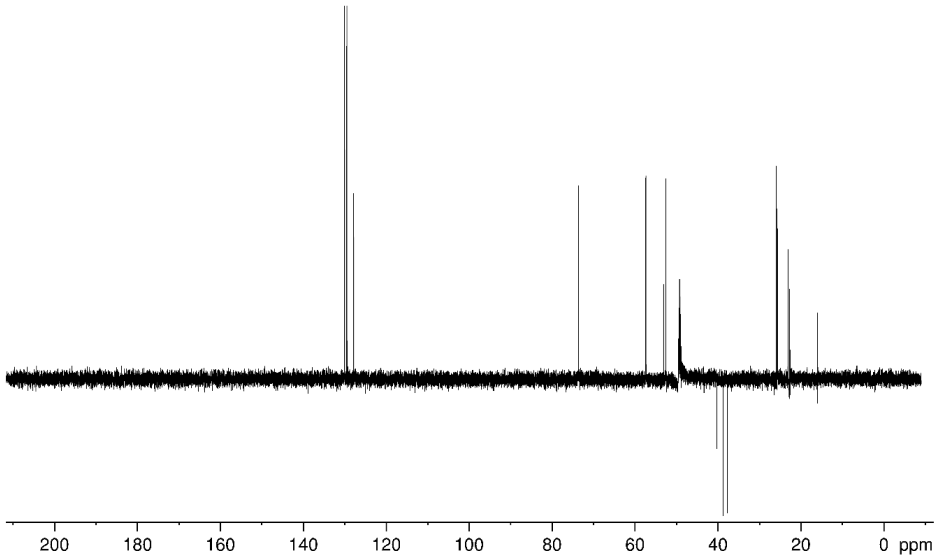

Figure S16. DEPT NMR spectrum of 2 in CD_3OD.

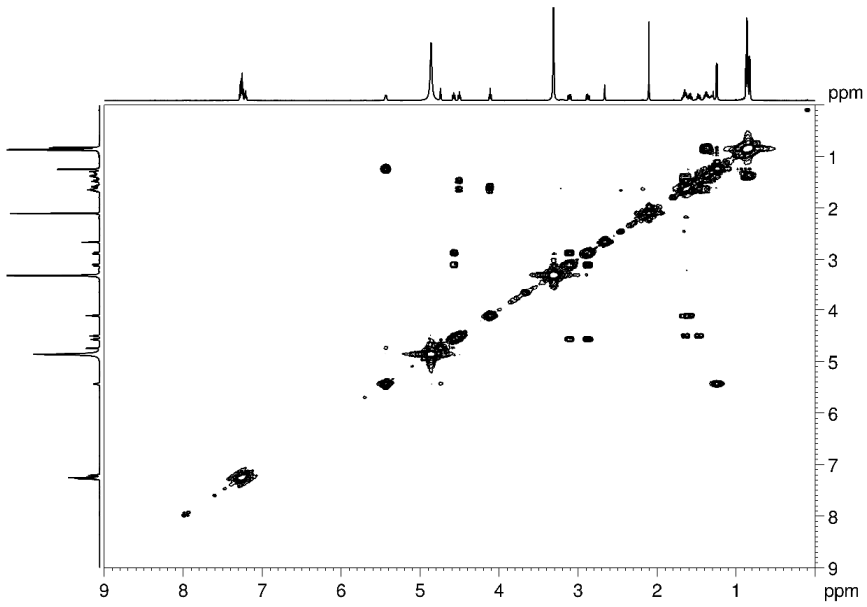

Figure S17. ^1H ^1H-COSY NMR spectrum of 2 in CD_3OD.

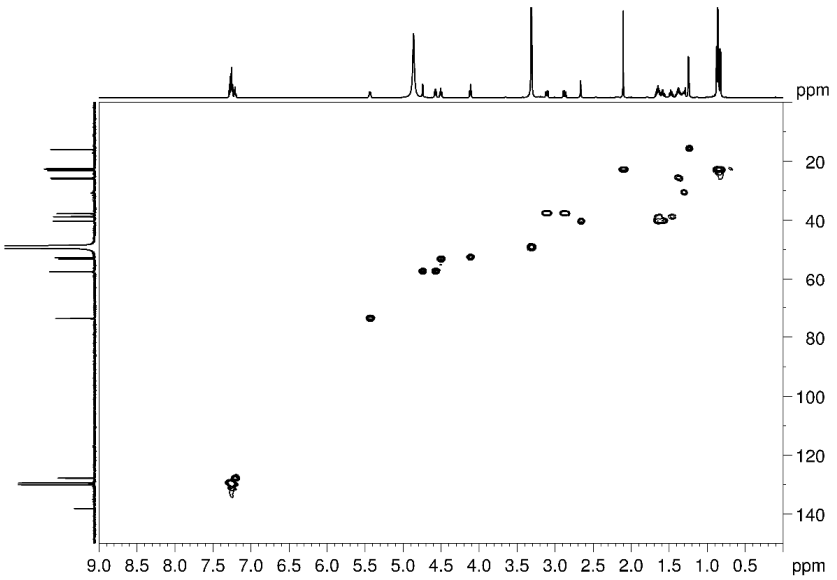

Figure S18. ^{1}H ^{13}C HSQC NMR spectrum of 2 in CD_3OD.

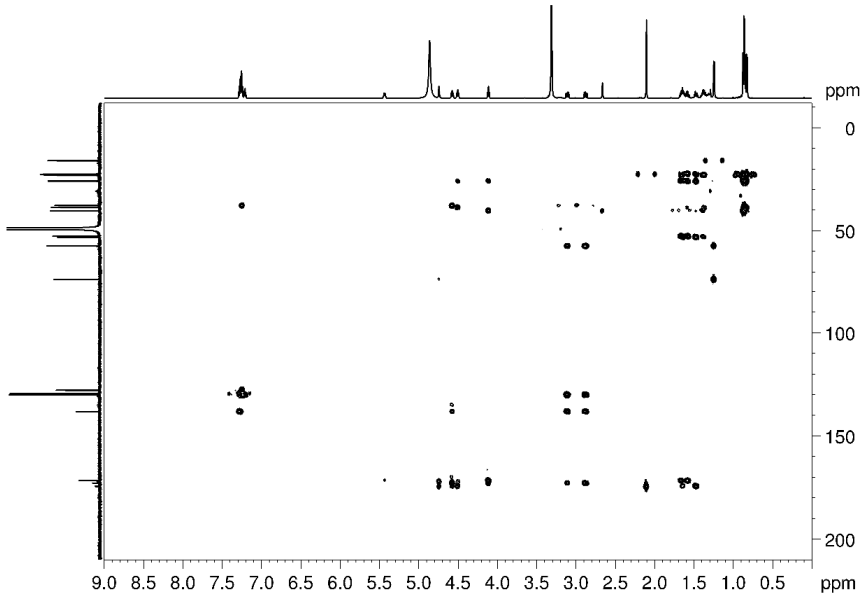

Figure S19. ^{1}H ^{13}C HMBC NMR spectrum of 2 in CD_3OD. A magnification of the region of δ_H 5.6 – 4.0 ppm is shown in Figure S20.

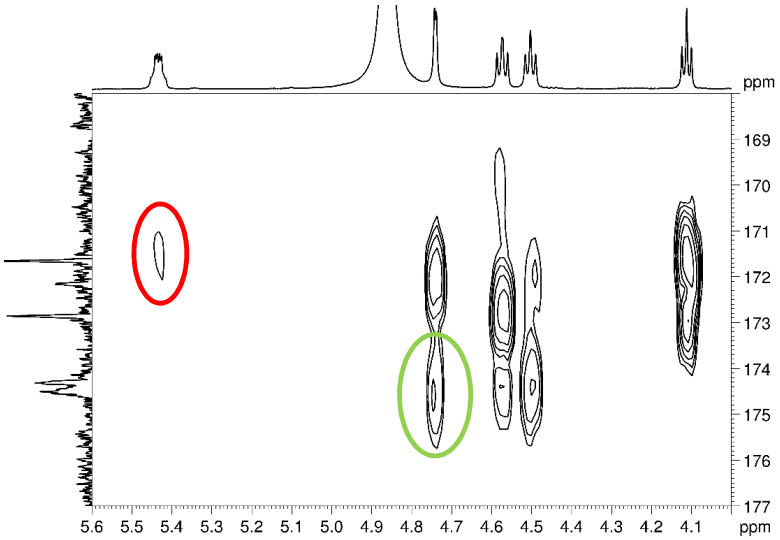

Figure S20. Magnification of the ^{1}H ^{13}C HMBC NMR spectrum of 2 in the region of δ_H 5.6 – 4.0 ppm in CD_3OD. The weak scalar coupling of the carbonyl signal of Leu2 (C-22) with the 2nd methanetriyl group of Thr (H-5) is highlighted in red and established **2** as a cyclic compound. The coupling pair of the carbonyl atom of acetate (C-1) and the proton of the 1st methanetriyl group of Thr (H-4) is marked in mint suggesting an *N*-acetylation of Thr.

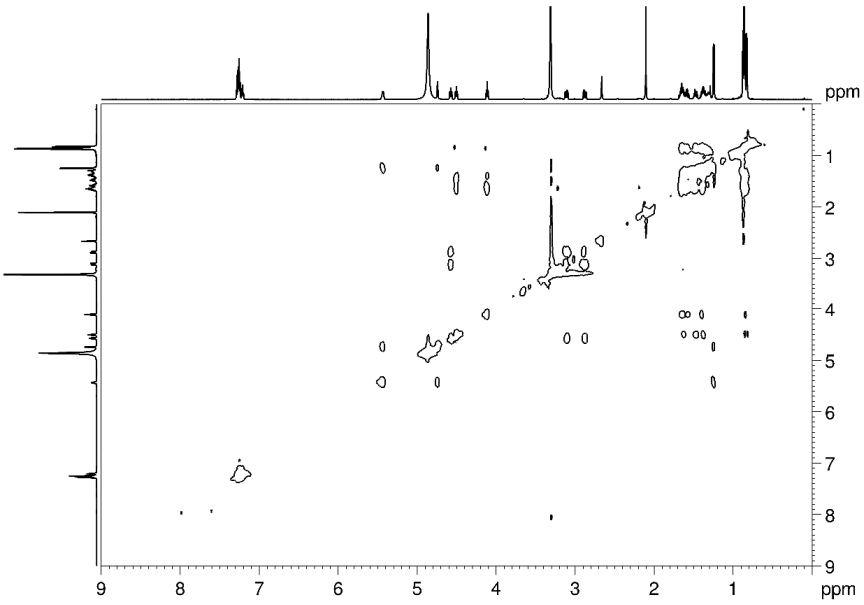

Figure S21. ^{1}H ^{1}H TOCSY NMR spectrum of 2 in CD_3OD.

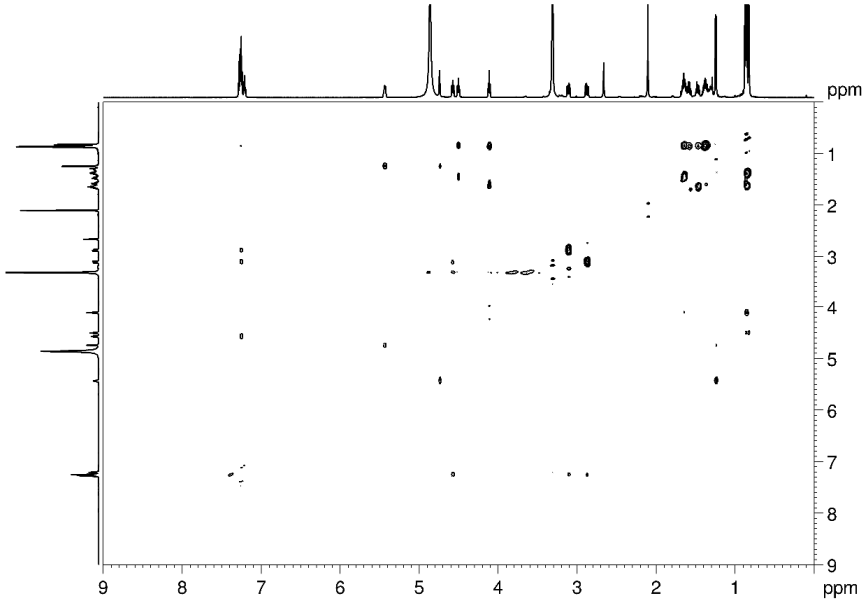

Figure S22. NOESY NMR spectrum of 2 in CD_3OD.

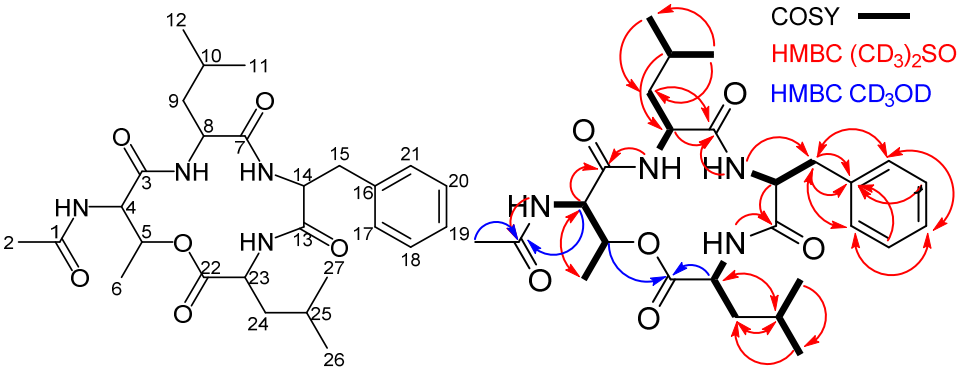

Figure S23. Atom numbering and selected COSY (bold lines) and HMBC key correlations (arrows) in 2.
HMBC correlations with different solvents were indicated in red (DMSO-d_6), and blue (CD_3OD), respectively.

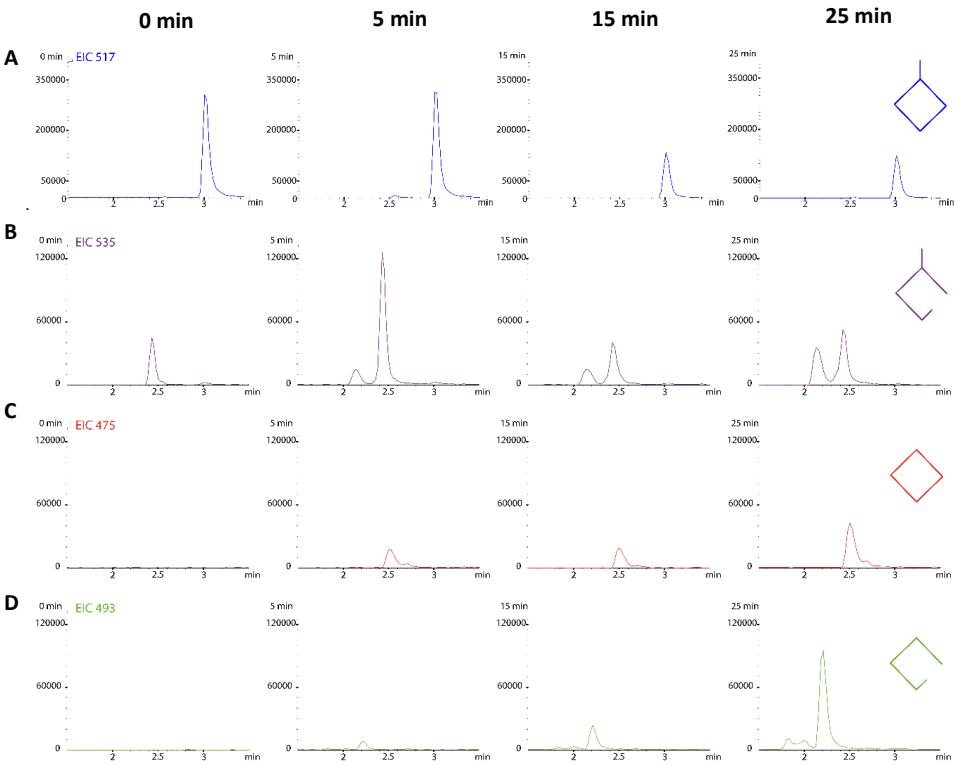

Figure S24. Time-dependent partial acidic hydrolysis of 2. The acid hydrolysis of **2** was initiated by addition of 1 M HCl and stopped after 0, 5, 15, and 25 min of incubation at 90 °C. Samples were subjected to a UHPLC-MS measurement. The extracted ion chromatograms (EIC) are shown for the native cyclic metabolite **2** at *m/z* 517 $[M + H]^+$ (**A**), the linearized (ester-hydrolyzed) **2**-peptide, *m/z* 535 $[M + H]^+$ (**B**), the cyclic, but deacetylated **2**-congener, *m/z* 475 $[M + H]^+$ (**C**) and the linearized and deacetylated **2**-congener *m/z* 493 $[M + H]^+$ (**D**). The diamonds on the right schematically represent the peptides and its hydrolytic cleavage sites. Cleavage of the ester bond (B – 5min) occurs earlier than the amid bond (D - 25min).

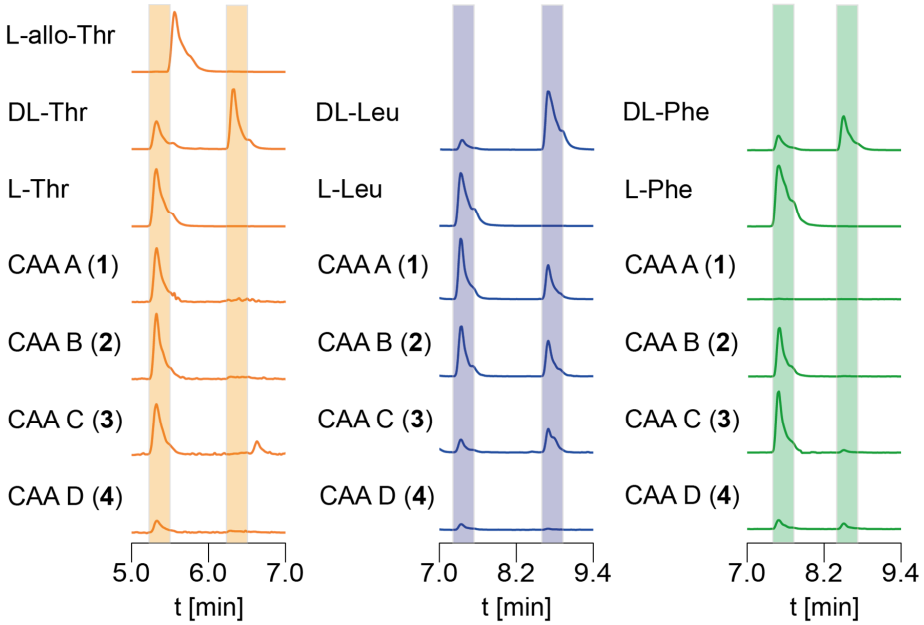

Figure S25. UHPLC-MS chromatograms of Marfey´s analysis of 1-4. Extracted ion chromatograms (EIC) are shown for the determination of the configuration of threonine (*m/z* 414 $[M+H]^+$; highlighted in orange), leucine (*m/z* 426 $[M+H]^+$; purple) and phenylalanine (*m/z* 460 $[M+H]^+$; green).

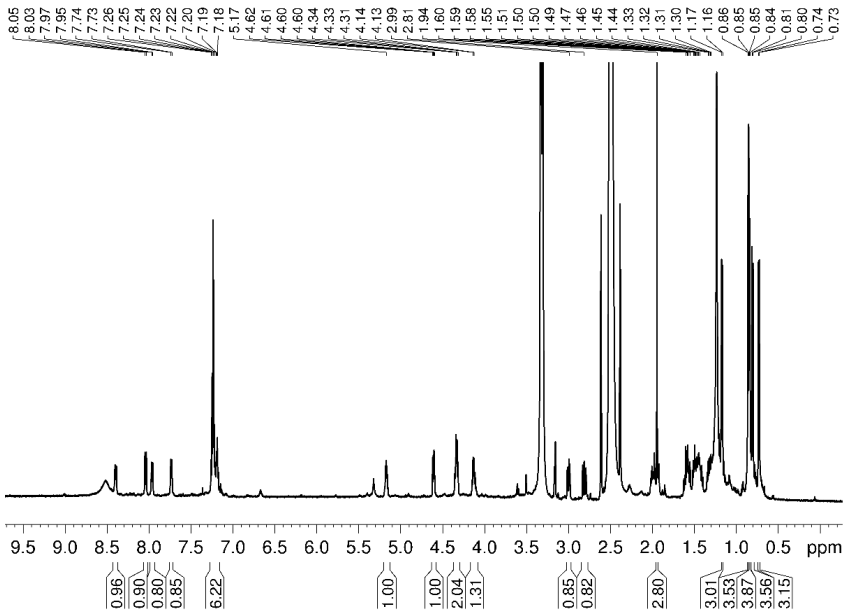

Figure S26. ^{1}H-NMR spectrum of synthetic 2 in DMSO-d_6.

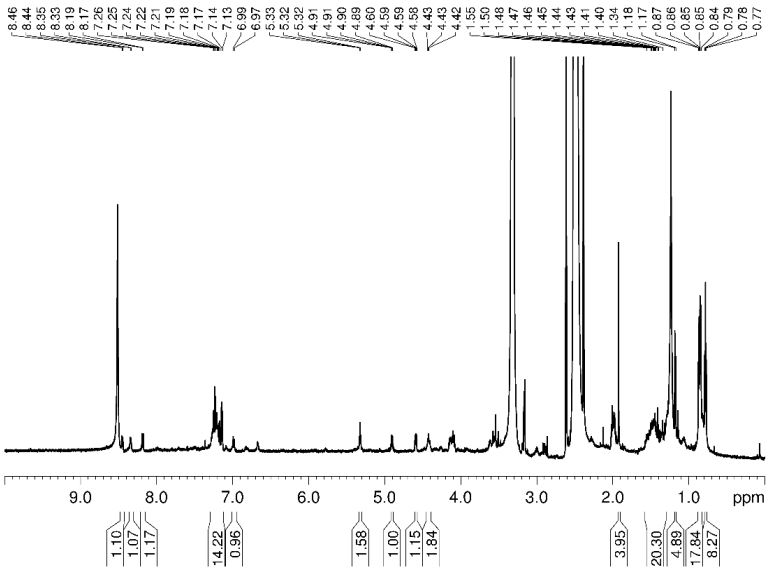

Figure S27. ^{1}H-NMR spectrum of synthetic 19 in DMSO-d_6.

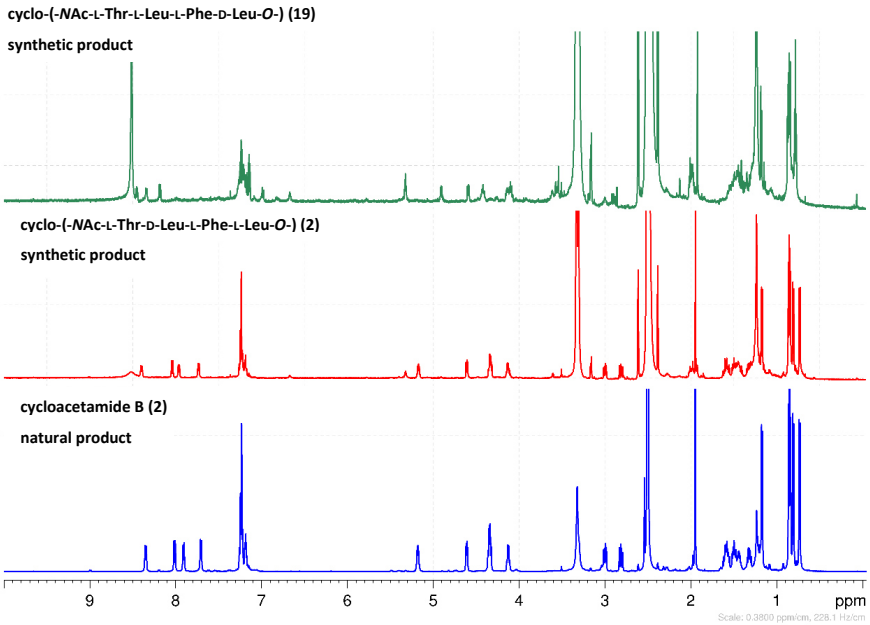

Figure S28. Comparison of ^{1}H NMR spectra of synthetic isomeric cyclopeptides 19 (green) and 2 (red), and the isolated natural product 2 (blue) in DMSO-d_6.

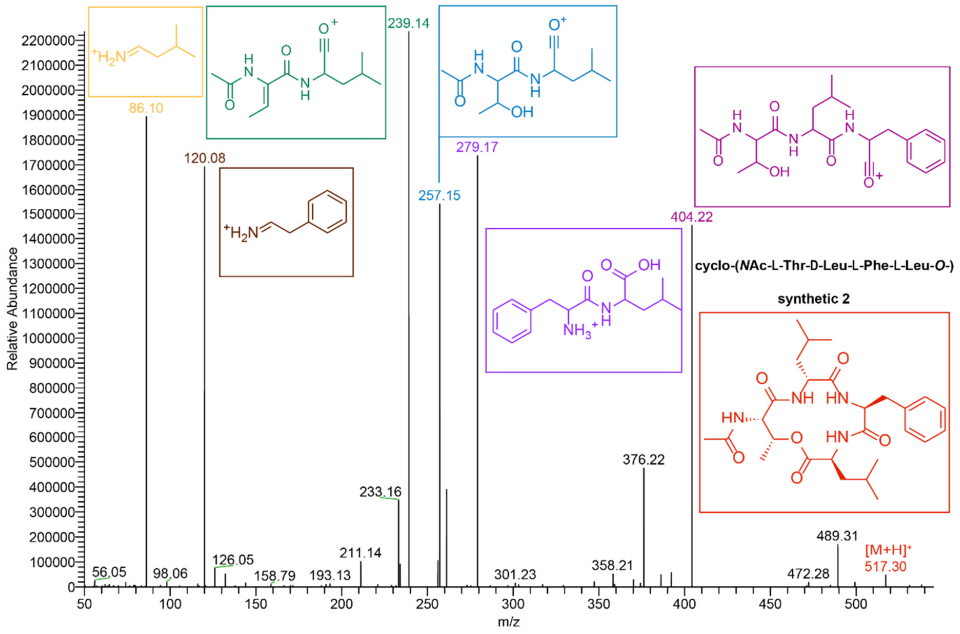

Figure S29. ESI-MS/MS spectrum of synthetic 2. Fragmentation was carried out at a higher-energy collisional dissociation (HCD) energy of 20%.

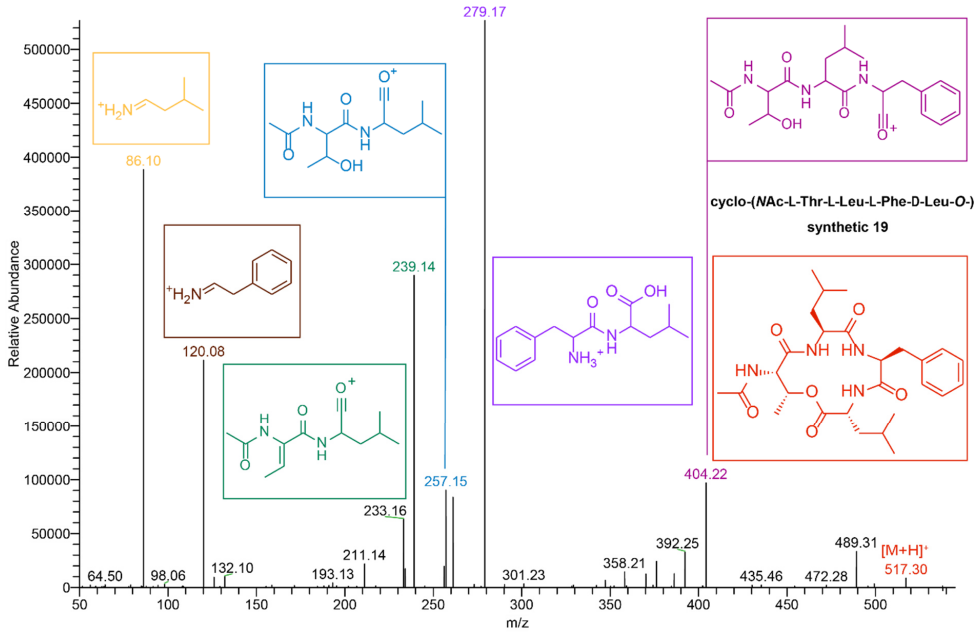

Figure S30. ESI-MS/MS spectrum of synthetic 19. Fragmentation was carried out at a higher-energy collisional dissociation (HCD) energy of 20%.

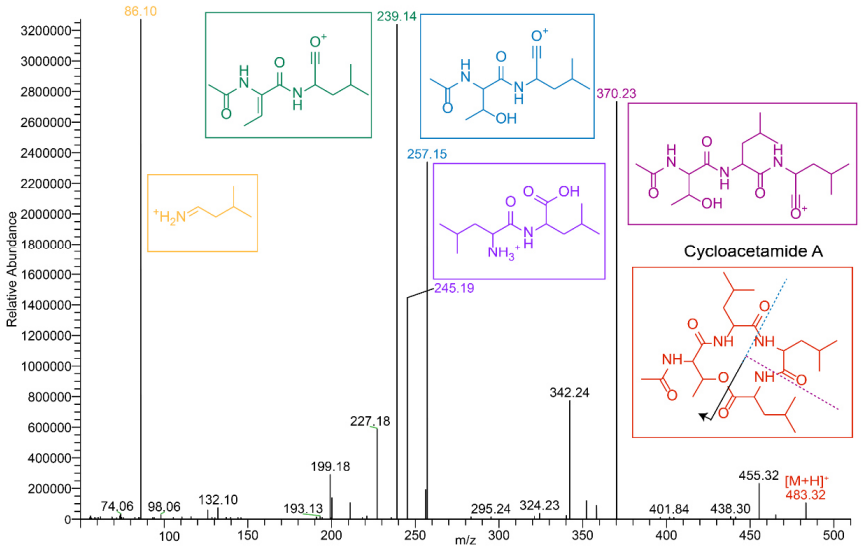

Figure S31. ESI-MS/MS spectrum of 1. Fragmentation was carried out at a higher-energy collisional dissociation (HCD) energy of 20%.

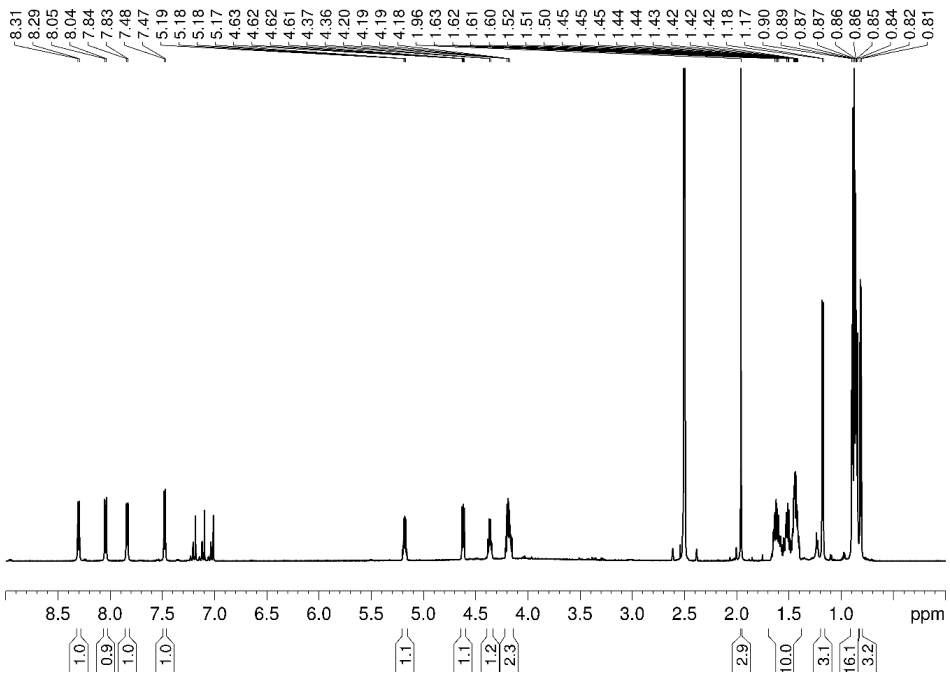

Figure S32. ^{1}H NMR spectrum of 1 in DMSO-d_6.

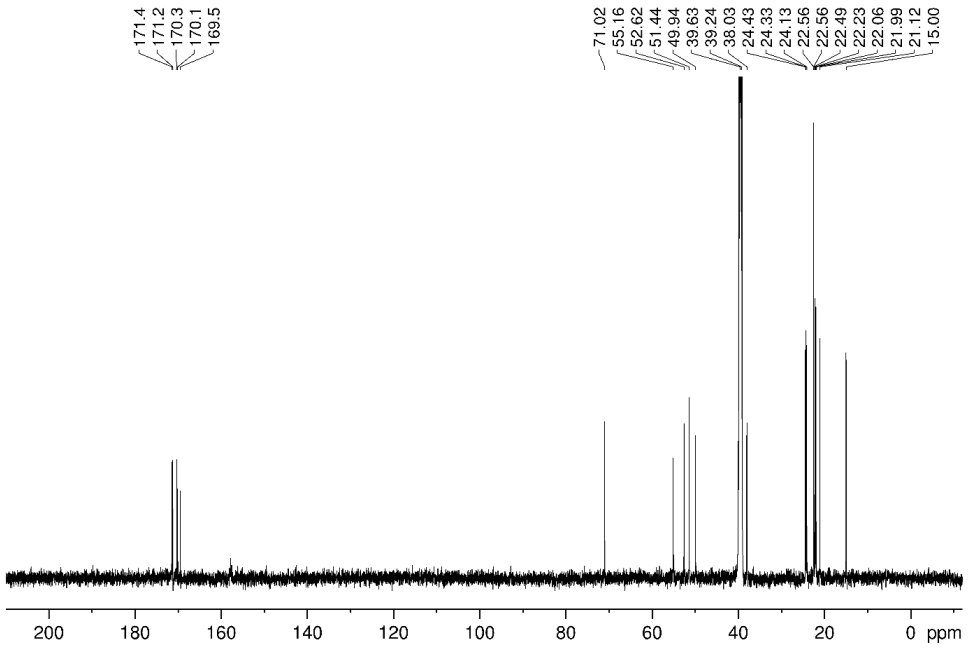

Figure S33. ^{13}C NMR spectrum of 1 in DMSO-d_6.

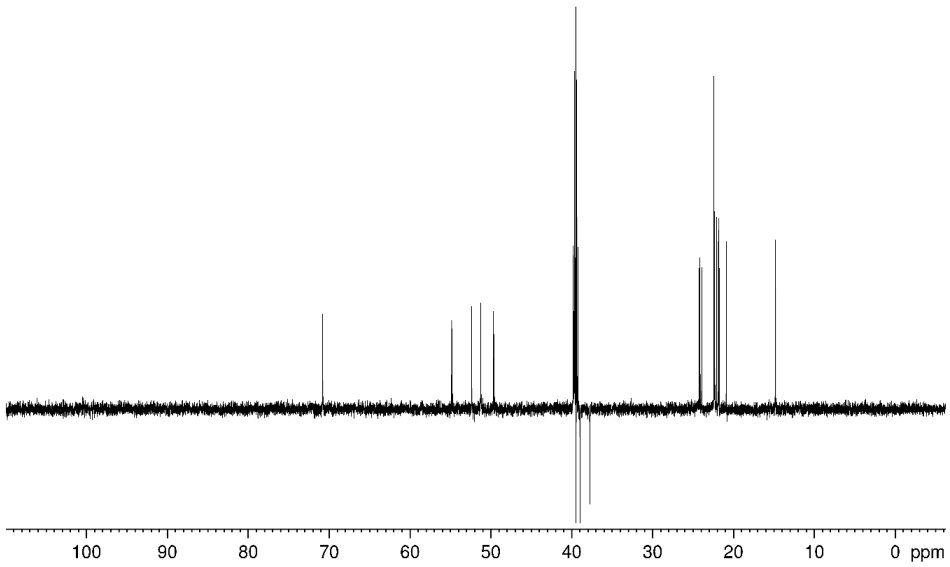

Figure S34. DEPT NMR spectrum of 1 in DMSO-d_6.

32

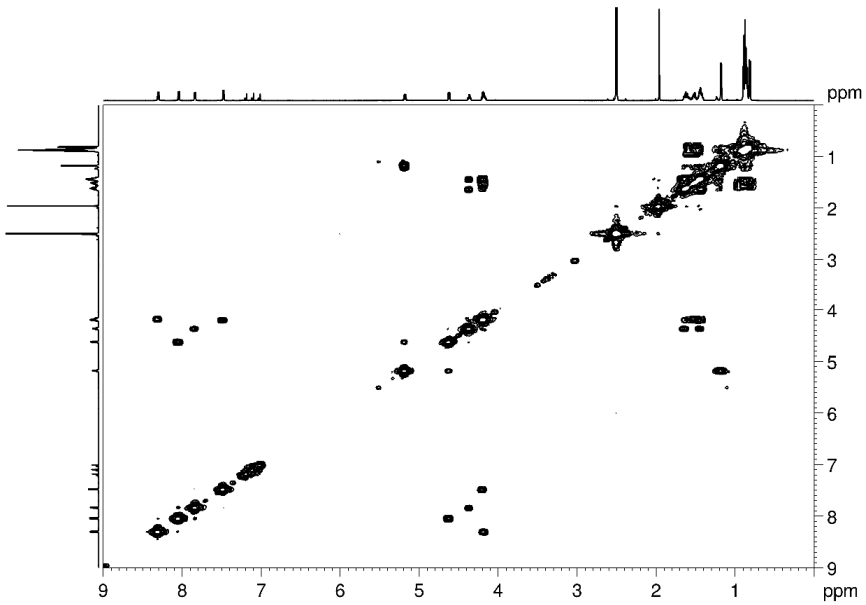

Figure S35. ^{1}H-^{1}H-COSY NMR spectrum of 1 in DMSO-d_6

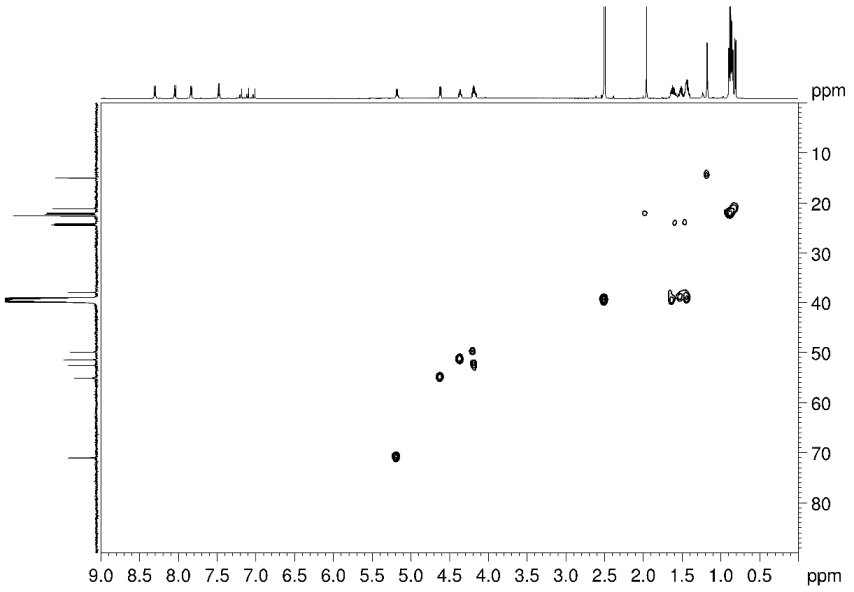

Figure S36. ^{1}H ^{13}C HSQC NMR spectrum of 1 in DMSO-d_6

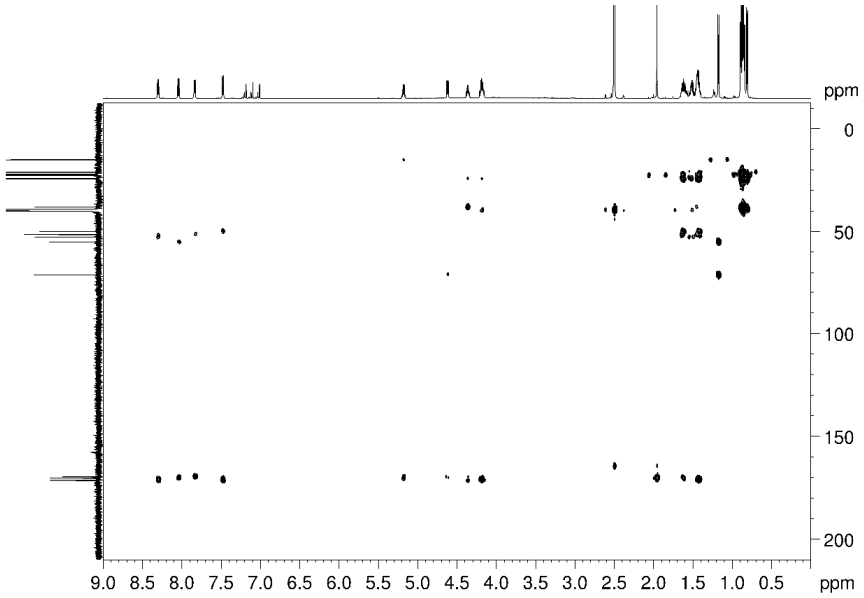

Figure S37. ^{1}H ^{13}C HMBC NMR spectrum of 1 in DMSO-d_6.

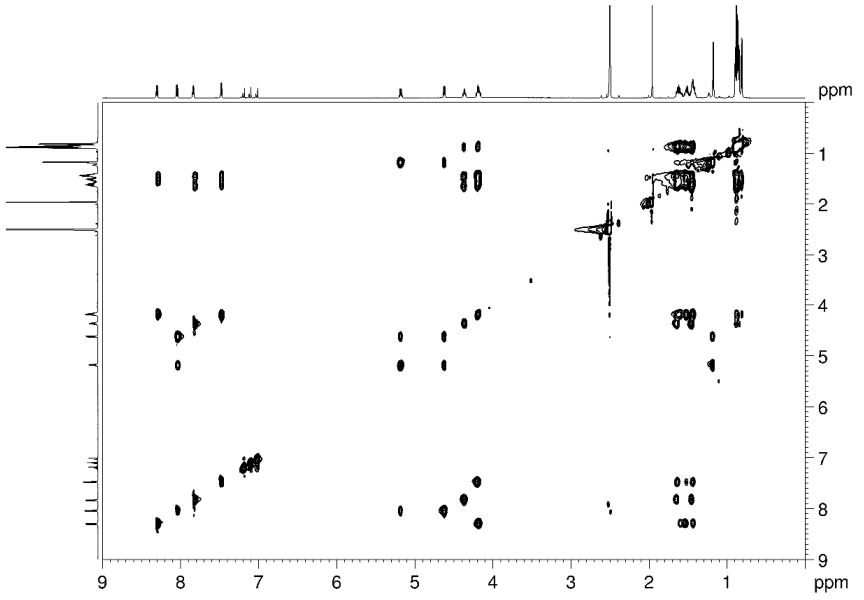

Figure S38. ^{1}H ^{1}H TOCSY NMR spectrum of 1 in DMSO-d_6.

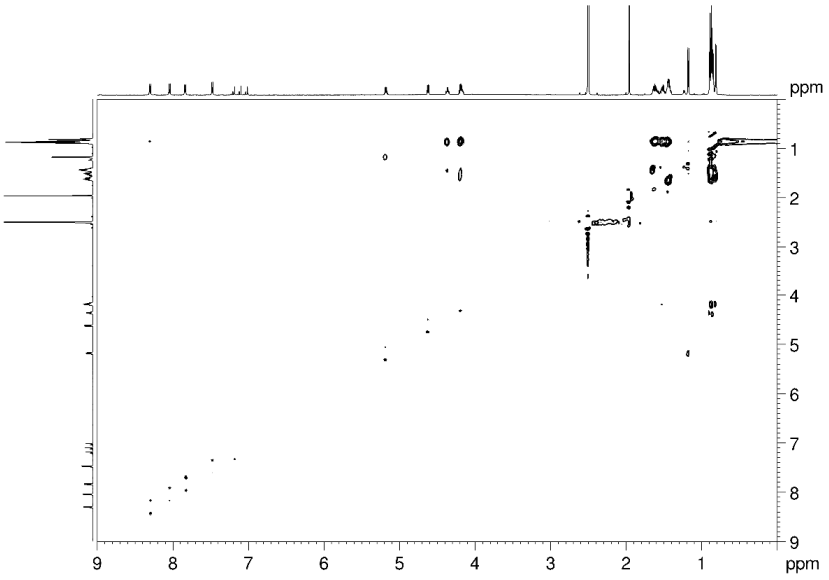

Figure S39. NOESY NMR spectrum of 1 in DMSO-d_6.

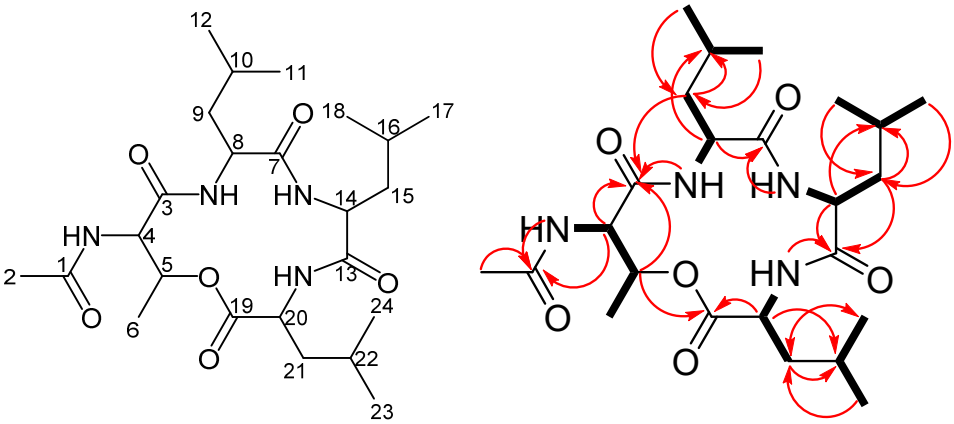

Figure S40. Atom numbering and selected COSY (bold lines) and HMBC key correlations (arrows) in 1.

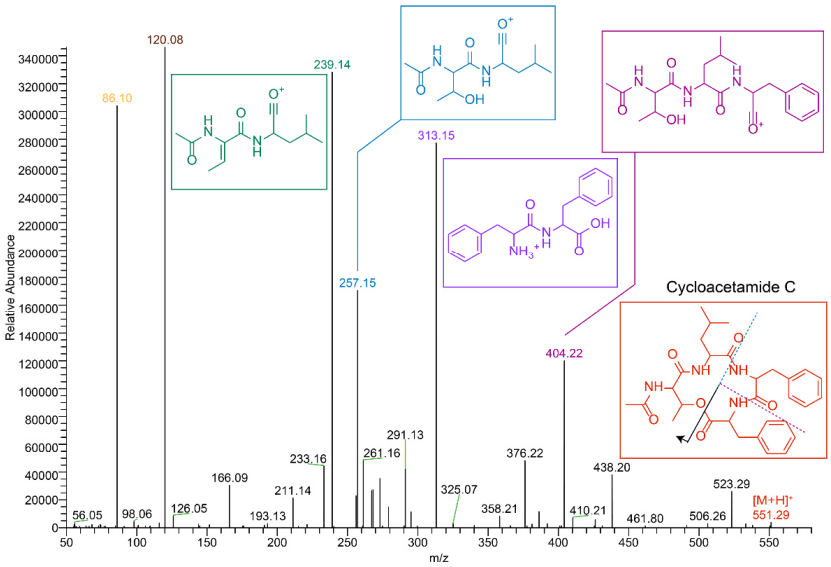

Figure S41. ESI-MS/MS spectrum of 3. Fragmentation was carried out at a higher-energy collisional dissociation (HCD) energy of 20%.

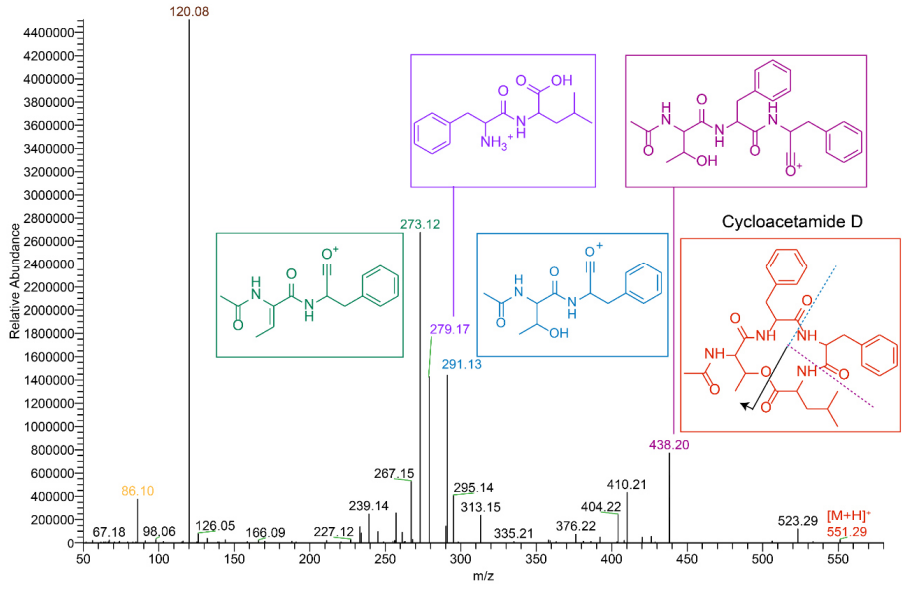

Figure S42. ESI-MS/MS spectrum of 4. Fragmentation was carried out at a higher-energy collisional dissociation (HCD) energy of 20%.

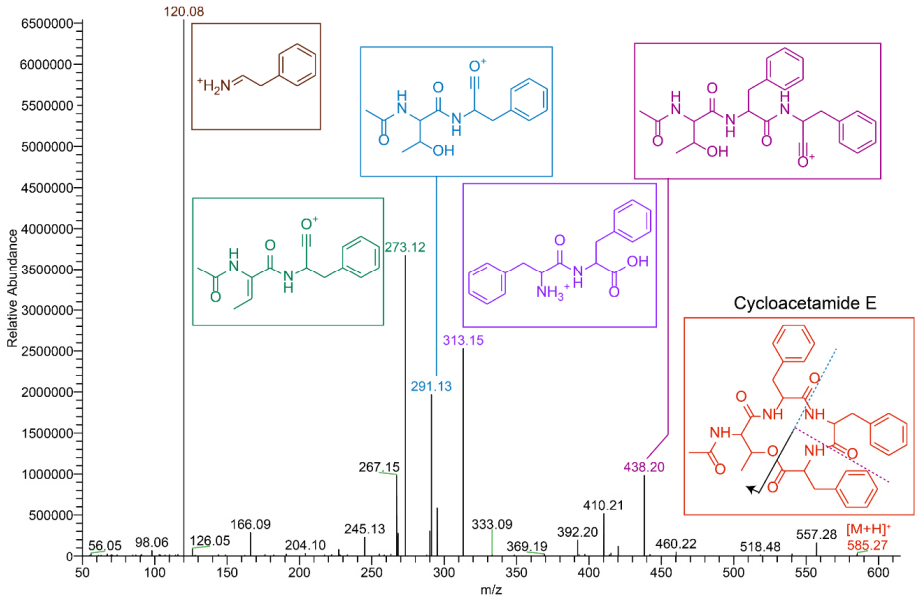

Figure S43. ESI-MS/MS spectrum of 5. Fragmentation was carried out at a higher-energy collisional dissociation (HCD) energy of 20%.

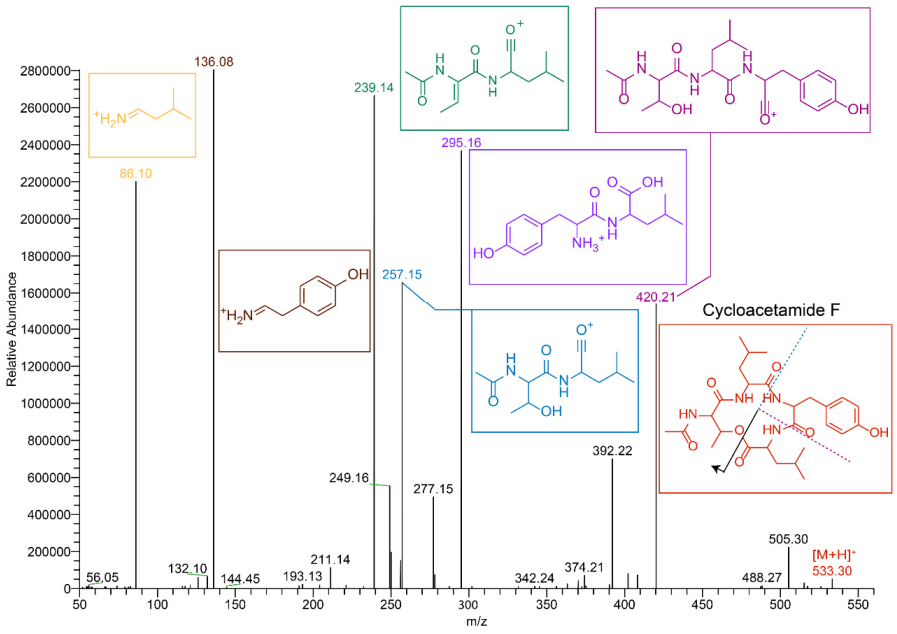

Figure S44. ESI-MS/MS spectrum of 6. Fragmentation was carried out at a higher-energy collisional dissociation (HCD) energy of 20%.

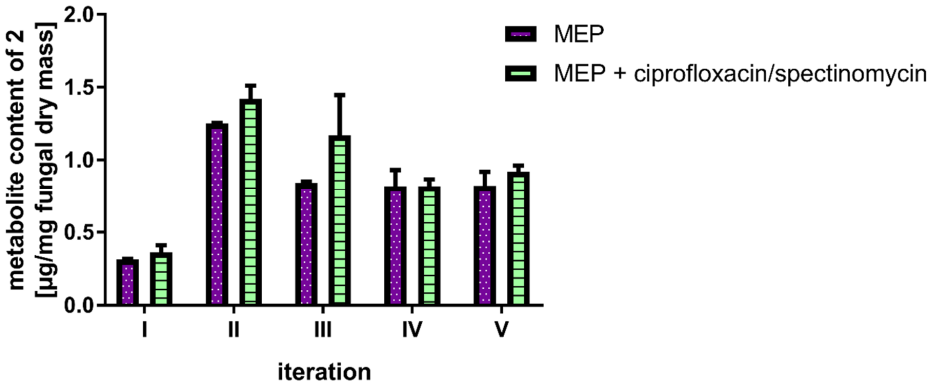

Figure S45. Production of cycloacetamide B (2) in *M. alpina* after antibiotic treatment. *M. alpina* was treated with 200 µg mL^{-1} of ciprofloxacin and 200 µg mL^{-1} of spectinomycin in five successive iterations (I-V) and metabolite amount was quantified from each fungal generation. A non-treated control (MEP) served as a control. Production of **2** is abundant regardless the antibiotic treatment suggesting a fungal and not an endobacterial origin of the compounds.

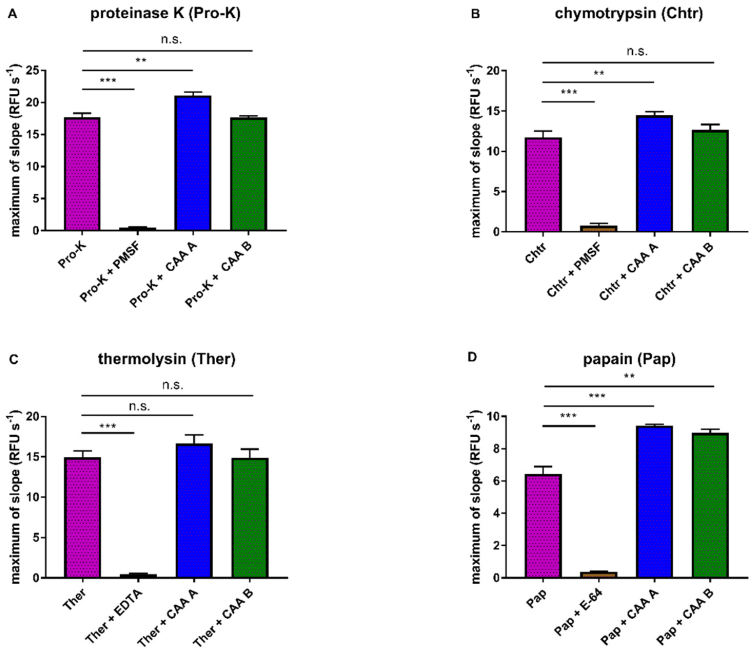

Figure S46. Protease activity assay. Fluorescein-labelled casein (FITC-casein) was used as substrate and the proteolytic release of FITC-labelled amino acids was quantified by fluorescence measurement. Activities of the serine proteases proteinase K (**A**) and chymotrypsin (**B**), the metalloprotease thermolysine (**C**) and the cysteine protease papain (**D**) were determined in absence and presence of established protease inhibitors or cycloacetamides A (**1**) and B (**2**). The well-described inhibitors phenylmethylsulfonyl fluoride (PMSF), ethylenediaminetetraacetic acid (EDTA) or E-64 served as internal control (at 100 µM).

References

1. Ibrahim, A. S.; Gebremariam, T.; Liu, M. F.; Chamilos, G.; Kontoyiannis, D. P.; Mink, R.; Kwon-Chung, K. J.; Fu, Y.; Skory, C. D.; Edwards, J. E.; Spellberg, B. *J. Infect. Dis.* **2008,** *198*, 1083-1090.
2. Baldeweg, F.; Warncke, P.; Fischer, D.; Gressler, M. *Org. Lett.* **2019,** *21*, 1444-1448.
3. Wurlitzer, J. M.; Stanišić, A.; Wasmuth, I.; Jungmann, S.; Fischer, D.; Kries, H.; Gressler, M. *Appl. Environ. Microbiol.* **2021,** *87*, e02051-20.
4. Harada, K.; Fujii, K.; Mayumi, T.; Y., H.; Suzuki, M. *Tetrahedron Lett.* **1995,** *36*, 1515-1518.
5. Fujii, K.; Ikai, Y.; Mayumi, T.; Oka, H.; Suzuki, M.; Harada, K. *Anal. Chem.* **1997,** *69*, 3346-3352.
6. Neises, B.; Steglich, W. *Angew. Chem. Int. Ed.* **1978,** *17*, 522-524.
7. Tsakos, M.; Schaffert, E. S.; Clement, L. L.; Villadsen, N. L.; Poulsen, T. B. *Nat. Prod. Rep.* **2015,** *32*, 605-632.
8. Krieg, R.; Jortzik, E.; Goetz, A. A.; Blandin, S.; Wittlin, S.; Elhabiri, M.; Rahbari, M.; Nuryyeva, S.; Voigt, K.; Dahse, H. M.; Brakhage, A.; Beckmann, S.; Quack, T.; Grevelding, C. G.; Pinkerton, A. B.; Schonecker, B.; Burrows, J.; Davioud-Charvet, E.; Rahlfs, S.; Becker, K. *Nat. Commun.* **2017,** *8*, 14478.
9. Agrawal, P.; Miryala, S.; Varshney, U. *PLoS One* **2015,** *10*, e1-e13.
10. Smith, M. P.; Laws, T. R.; Atkins, T. P.; Oyston, P. C. F.; de Pomerai, D. I.; Titball, R. W. *FEMS Microbiol. Lett.* **2002,** *210*, 181-185.
11. Wagner, A.; Le, T. A.; Brennich, M.; Klein, P.; Bader, N.; Diehl, E.; Paszek, D.; Weickhmann, A. K.; Dirdjaja, N.; Krauth-Siegel, R. L.; Engels, B.; Opatz, T.; Schindelin, H.; Hellmich, U. A. *Angew. Chem. Int. Edit.* **2019,** *58*, 3640-3644.
12. Kim, H.; Choi, M. S.; Kang, K.; Kwon, J. Y. *Chem. Senses* **2016,** *41*, 85-94.
13. R Core Team (**2020**). R: A language and environment for statistical computing. R Foundation for Statistical Computing, V., Austria. http://www.r-project.org/index.html
14. Twining, S. S. *Anal. Biochem.* **1984,** *143*, 30-34.
15. Gersch, M.; Famulla, K.; Dahmen, M.; Gobl, C.; Malik, I.; Richter, K.; Korotkov, V. S.; Sass, P.; Rubsamen-Schaeff, H.; Madl, T.; Brotz-Oesterhelt, H.; Sieber, S. A. *Nat. Commun.* **2015,** *6*, e6320.
16. Cilenti, L.; Lee, Y.; Hess, S.; Srinivasula, S.; Park, K. M.; Junqueira, D.; Davis, H.; Bonventre, J. V.; Alnemri, E. S.; Zervos, A. S. *J. Biol. Chem.* **2003,** *278*, 11489-11494.
17. Crawford, J. M.; Portmann, C.; Kontnik, R.; Walsh, C. T.; Clardy, J. *Org. Lett.* **2011,** *13*, 5144-5147.
18. Tobias, N. J.; Wolff, H.; Djahanschiri, B.; Grundmann, F.; Kronenwerth, M.; Shi, Y. M.; Simonyi, S.; Grun, P.; Shapiro-Ilan, D.; Pidot, S. J.; Stinear, T. P.; Ebersberger, I.; Bode, H. B. *Nat. Microbiol.* **2017,** *2*, 1676-1685.
19. Kronenwerth, M.; Bozhuyuk, K. A. J.; Kahnt, A. S.; Steinhilber, D.; Gaudriault, S.; Kaiser, M.; Bode, H. B. *Chem. Eur. J.* **2014,** *20*, 17478-17487.
20. Mansson, M.; Nielsen, A.; Kjaerulff, L.; Gotfredsen, C. H.; Wietz, M.; Ingmer, H.; Gram, L.; Larsen, T. O. *Mar. Drugs* **2011,** *9*, 2537-2552.
21. LaPlante, K. L.; Rybak, M. J. *Expert Opin. Pharmacother.* **2004,** *5*, 2321-2331.
22. Kishimoto, S.; Tsunematsu, Y.; Nishimura, S.; Hayashi, Y.; Hattori, A.; Kakeya, H. *Tetrahedron* **2012,** *68*, 5572-5578.
23. Wang, Y.; Zhang, F.; Zhang, Y.; Liu, J. O.; Ma, D. *Bioorg. Med. Chem. Lett.* **2008,** *18*, 4385-4387.
24. Kikuchi, H.; Hoshikawa, T.; Fujimura, S.; Sakata, N.; Kurata, S.; Katou, Y.; Oshima, Y. *J. Nat. Prod.* **2015,** *78*, 1949-1956.
25. Jin, K.; Po, K. H. L.; Kong, W. Y.; Lo, C. H.; Lo, C. W.; Lam, H. Y.; Sirinimal, A.; Reuven, J. A.; Chen, S.; Li, X. C. *Biorg. Med. Chem.* **2018,** *26*, 1062-1068.

5 Diskussion

5.1 Naturstoffbiosynthese in *Mortierella alpina*

Diese Arbeit beschäftigt sich mit den bislang weitestgehend unverstandenen Naturstoffbiosynthesen aus basalen Pilzen. Dabei wurde mit *Mortierella alpina* als Modellorganismus gearbeitet. Für Malpinine (**10**), Malpibaldine (**12**) und Calpinactam (**9**) wurden jeweils pilzliche multimodulare nichtribosomale Peptidsynthetasen (NRPSs) als biosynthetische Enzyme identifiziert. Für die neu beschriebenen Malpicycline (**20**) gelang ebenfalls der Nachweis eines Biosynthesgens (Abbildung 6). Für die Cycloacetamide (**21**) steht dieser Beweis noch aus. Die Entdeckung neuer Substanzen und deren Biosynthese trägt zum Verständnis basaler Pilze bei. Die Untersuchung von Biosynthese und Funktion von Naturstoffen aus *Mortierella alpina* ermöglicht Einblicke in eine Vielzahl ökologischer, evolutionärer, genetischer und biochemischer Besonderheiten, deren Verständnis die Grundlage weiterer Untersuchungen legt. Auf diese Aspekte soll nachfolgend im Detail eingegangen werden.

I Naturstoffe spielen eine entscheidende Rolle für die **chemische Ökologie** von Pilzen. Die Kenntnis von Substanzen, deren Biosynthese und Regulation liefert Anhaltspunkte zum Verständnis von Wechselwirkungen zwischen basalen Pilzen und ihrer Umwelt. Malpinine, Malpicycline und Calpinactam weisen u.a. oberflächenaktive, antimycobakterielle, antibakterielle und antilarvale Eigenschaften auf, die für *Mortierella* einen wichtigen ökologischen Nutzen darstellen. Unter der Annahme, dass andere basale Pilze ebenfalls Naturstoffe produzieren, kann auf Basis der Erkenntnissen aus *M. alpina* Aktivitäts-geleitet nach diesen gesucht werden.

II In *Mortierella alpina* konnten wichtige Erkenntnisse für das Verständnis der interspezifischen Übertragung von Naturstoffgenen durch **horizontalen Gentransfer (HGT)** erlangt werden. Der bakterielle Ursprung der NRPS-Gene, der wahrscheinlich auf HGT zurückzuführen ist, erlaubt Rückschlüsse auf die Bedeutung von Endosymbionten oder kommensalen Bakterien für die Evolution von *Mortierella alpina* und deren Naturstoffe. Während HGT in anderen pilzlichen Abteilungen bekannt und gut verstanden ist, konnte hier erstmals diese Thematik in EDF untersucht werden. Nicht zuletzt kann an diesem Beispiel das Auftreten von multimodularen NRPSs in Eukaryoten nachvollzogen werden.

III Die erbrachten Ergebnisse stellen einen Beitrag im Feld der **Biotechnologie** dar. Die Idee, einzelne NRPS-Domänen und Module im Baukastenprinzip zusammenzusetzen und so Peptide nach Maß herzustellen, ist dabei genauso alt wie unser Verständnis von NRPSs selbst. Die Entdeckung und Untersuchung promiskuitiver A-Domänen und deren Nutzung zur Inkorporation von nicht-proteinogenen Aminosäuren, trägt dazu bei, neue Metabolite gezielt biosynthetisch herzustellen.

IV Die Identifizierung und Charakterisierung von Naturstoffgenen und -enzymen hat Einfluss auf das Verständnis der **Genetik** basaler Pilze und der **Enzymatik** von Naturstoffbiosynthesen.

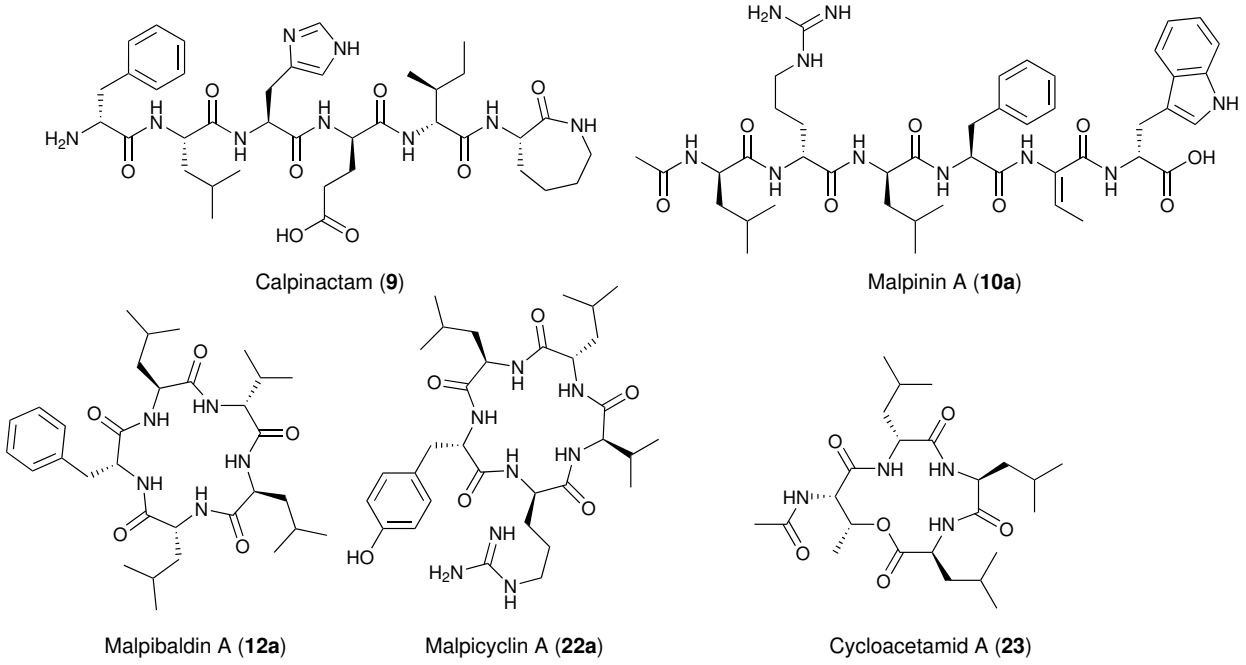

Abbildung 6: Peptidische Naturstoffe aus *Mortierella alpina*, die im Rahmen dieser Arbeit untersucht wurden; dargestellt ist jeweils nur ein Vertreter der Naturstoffklassen

5.2 Ökologische Relevanz produzierter Naturstoffe

5.2.1 Chemische Interaktionen von *Mortierella alpina*

Um die ökologische Relevanz der in basalen Pilzen produzierten Naturstoffe zu verstehen, ist die Ökologie von *M. alpina* selbst zu verstehen. Kaum eine Eigenschaft ist dabei so hervorstechend wie die Produktion und Sekretion von freien Fettsäuren [31]. Warum diese in hohen Konzentrationen gebildet werden, ist noch nicht abschließend geklärt. Ungesättigte Fettsäuren können zur Psychro-

toleranz von *Mortierella*-Arten wie *M. alpina* oder *M. antarctica* beitragen, die auch in subpolaren Klimazonen zu finden sind. Durch die Integration von PUFAs in die Zellmembran kann bei kalten Temperaturen die Membranfluidität aufrecht erhalten werden [153]. PUFAs könnten auch als Energiespeicher dienen, da diese bevorzugt bei hohen Kohlenstoff-Stickstoff-Verhältnissen gebildet werden [32]. Die Freisetzung von Fettsäuren als energiereiche Verbindungen birgt die Gefahr, von Insekten, Nematoden aber auch lipolytischen Mikroorganismen wie *Achromobacter, Burkholderia, Pseudomonas, Aspergillus* oder *Penicillium* als Kohlenstoffquelle verwendet zu werden [154–157].

Im Gegensatz zu basalen Pilzen sind in Asco- und Basidiomyceten pilzliche Naturstoffe bekannt, die als chemische Verteidigung gegen Larven und Nematoden produziert werden. So produziert z.B. der saprotrophe Basidiomycet *Omphalotus olearius* die nematiziden Omphalotine (**22**) [158]. Bei diesen handelt es sich um cyclische RIPP, bestehend aus zwölf, meist unpolaren L-konfigurierten AS mit neun N-Methylierungen des Peptidgrundgerüstes [159] (siehe Abbildung 7). Neben Pilzen, die sich im Boden gegen Nematoden und Insekten als Fraßfeinde verteidigen müssen, existieren entomopathogene und nematizide Ascomyceten, bei denen Naturstoffe Virulenzfaktoren darstellen. So produziert *Beauveria bassiana* die Cyclooctadepsipeptid Bassianolide (**23**) und das Cyclohexadepsipeptid Beauvericin (**24**) [160, 161]. Während Bassianolide (**23**) insektizid wirkten, ist für Beauvericin (**24**) eine zytotoxische Wirkung nachgewiesen worden. Beauvericin (**24**) wird dabei nicht nur durch Arten der Gattung *Beauveria*, sondern auch von verschiedenen *Fusarium*-Spezies gebildet [162]. Strukturelle Ähnlichkeit zu den bereits genannten Verbindungen zeigt das aus dem Ascomyceten *Rosellina sp.* isolierte PF1022A (**25**), welches ebenfalls stark antihelmintische Eigenschaften aufweist [163].

In Bakterien sind u.a. mit Xenobactin (**26**) ähnlich wirksame Abwehrstoffe bekannt. Das Cyclohexadepsipeptid **26** (siehe Abbildung 7) wird dabei von dem gramnegativen Bakterium *Xenorhabdus sp.*, welches endosymbiontisch mit entomopathogenen Nematoden lebt, produziert [164, 165]. Durch die antiprotozoale Aktivität von **26** trägt der Endosymbiont zur Entomopathogenität seines Wirts bei.

Neu ist der Nachweis, dass der basale Pilz *M. alpina* gezielt mit der Produktion von Naturstoffen gegen Fraßfeinde als Verteidigungsmechanismus reagiert (Manuskript 4). Bisher konnten bereits für die Malpinine starke emulgierende Eigenschaften nachgewiesen werden, wodurch eine Funktion bei dem Transport und der Sekretion von PUFAs vermutet wurde [133]. Für Calpinactam (**9**) konnte eine starke antimycobakterielle Wirkung nachgewiesen werden [130, 131]. Erst der Nachweis der

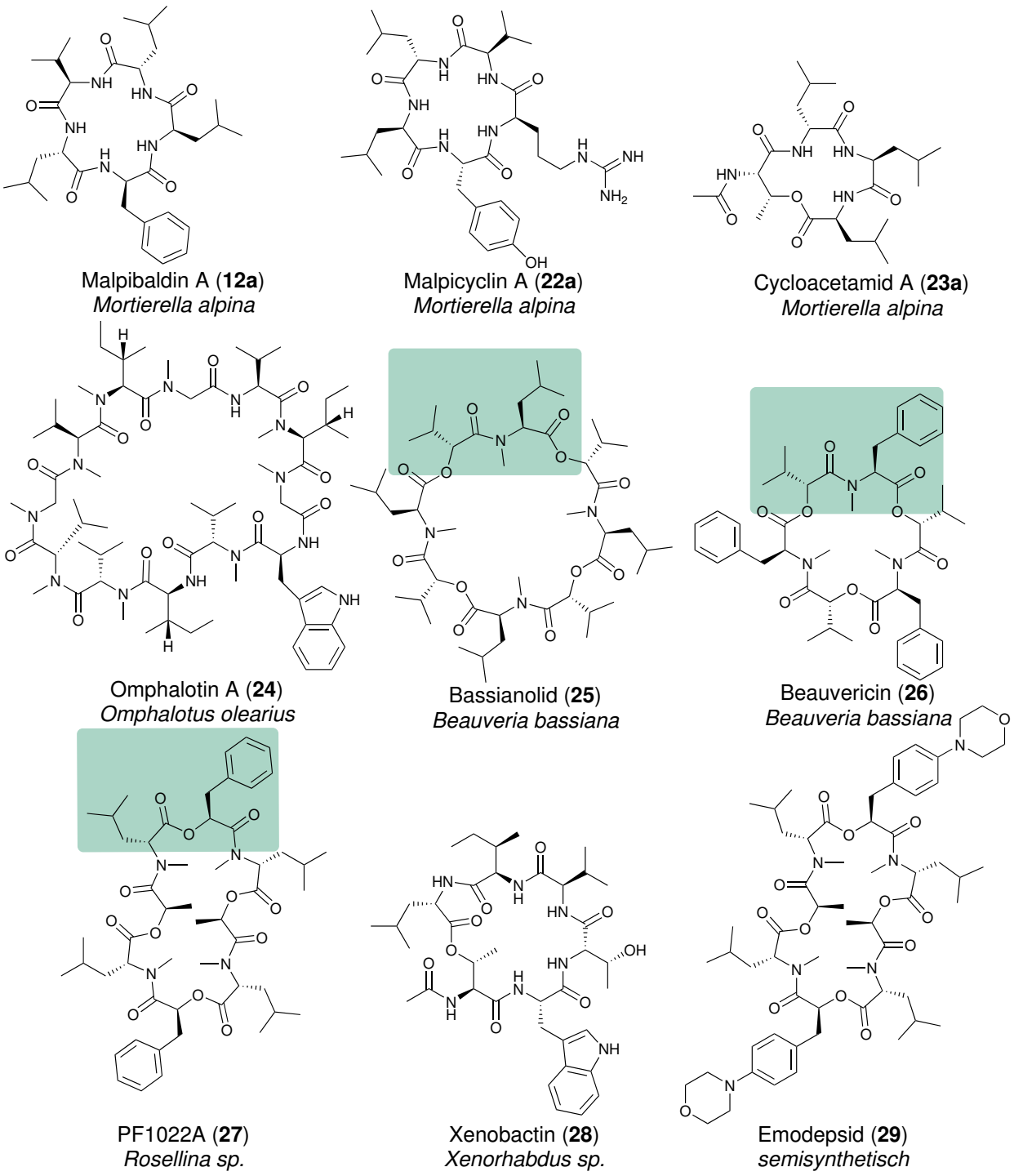

Abbildung 7: Isolierte Insektizide und Nematozide mikrobieller Herkunft mit vermutetem Pharmakophor (türkis) für Bassianolide, Beauvericin und PF1022A

antibakteriellen und antilarvalen Wirkung der Malpicycline (Manuskript 1) [166], sowie der ebenfalls antilarvalen Wirkung der Cycloacetamide (**21**) (Manuskript 4), zeigt ein umfassendes Bild chemischer Interaktion von *M. alpina* auf. Bereits in vorangegangen Studien konnte eine antilarvale Wirkung des Mycels von *M. alpina* gezeigt werden, doch ohne, dass dabei auf Naturstoffe oder Metabolite eingegangen wurde [167].

Dass in *Mortierellaceae* Naturstoffe zur Verteidigung gegen Fraßfeinde produziert werden, ist durch die Necroxime (**19**) bereits bekannt, doch erfolgt dort die Biosynthese durch einen Endosymbionten [55]. Die Necroxime zeigen nematizide Wirkung und werden in höheren Konzentrationen als ihre halbmaximalen Hemmkonzentration (IC_{50}) produziert. Obwohl die Naturstoffe nicht durch den Pilz selbst hergestellt werden, besitzen sie trotzdem eine ökologische Relevanz für den Pilz, wie bereits im Kapitel 1.4 beschrieben wurde. Gerade die Produktion hochwirksamer Substanzen wie Rhizoxin (**15**), Rhizonin (**16**) oder Holrhizin (**17**), welche wichtig für die Pathogenität des Pilzes sind, belegen dies [139, 148, 149]. Weiterhin produziert der Endosymbiont *Candidatus Mycoavidus necroximicus* in *Mortierella verticillata* das oberflächenaktive und antihelmintische Symbiosin, um seinen Wirt vor Fraßfeinden wie Nematoden zu schützen [168].

Es konnte erstmals gezeigt werden, dass niedere Pilze die intrinsische Fähigkeit zur Bildung von Naturstoffen zur gezielten Verteidigung gegen Fraßfeinde besitzen. Auf molekulare Grundlagen dieser Wirkung soll im folgenden eingegangen werden.

5.2.2 Cyclopeptide bei der Abwehr von Fraßfeinden

Während Malpinine und Calpinactam als lineare Verbindungen keine antilarvalen, insektizide oder nematizide Wirkungen zeigen, ist dies bei den zyklischen Verbindungen der Fall (Manuskript 4). Wie an den im vorangegangenen Kapitel beschriebenen Cyclopeptiden oder Cyclodepsipeptiden zu sehen, zeigen diese in der Natur häufig ausgeprägte biologische Aktivitäten [77, 169]. Ein verbindendes Element zwischen diesen Verbindungen und den zyklischen Naturstoffen aus *M. alpina* ist der hohe Anteil an unpolaren AS. Diese treten oft in wechselnden Konfigurationen auf [160], wobei in Pilzen N-Methylierungen gehäuft anzutreffen sind. Auffällig ist bei Beauvericin (**24**), den Bassianoliden (**23**) und PF1022A (**25**), dass diese rotationssymmetrische Oligomere darstellen [170]. Die formalen Monomere sind dabei Dipeptide polarer Aminosäuren wechselnder Konfiguration. Diese Substruktur, die vorsichtig als Leitstruktur bezeichnet werden kann, ist auch in fast allen anderen

hier diskutierten Naturstoffen zu finden (siehe Abbildung 7). Inwiefern diese Substruktur wirksamkeitsbestimmend ist, konnte nicht abschließend geklärt werden. Denkbar ist, dass alle Verbindungen kein gemeinsames Leitmotiv, sondern ähnliche physikochemische Eigenschaften verbindet. Nur für das Depsipeptid Emodepsid (**27**), einem semisynthetischen Produkt aus **25**, das veterinärmedizinisch Anwendung findet [163, 170, 171], konnte bisher ein Wirkziel nachgewiesen werden [172]. In *Caenorhabditis elegans* blockiert Emodepsid einen SLO1-Kaliumkanal und führt dabei zu einer Lähmung des Organismus, die final zum Tod führt. Durch die vorliegende strukturelle Ähnlichkeit kann vermutet werden, dass Malpicycline, Malpibaldine und Cycloacetamide einen ähnlichen Wirkmechanismus aufweisen und mit ähnlichen Rezeptoren interagieren.
Für Malpicycline und Malpibaldine sind die zugrundeliegenden Enzyme und die erhöhte Substratspezifität der A-Domänen bekannt. Wie anhand der Malpinine demonstriert (Manuskript 2) [173], lassen sich für diese ebenfalls Derivate produzieren, die bioorthogonal gekoppelt werden können. Isoliert und aufgereinigt könnten Malpicyclin- und Malpibaldin-Derivate anschließend als Fluorophore oder immobilisiert an Agar-Perlen zur Identifizierung molekularer Wirkziele verwendet werden [174]. Zwar wurden derartige Ansätze zur Vorläufer-dirigierte Biosynthese mit zyklischen Peptiden wie den Beauvericinen (**24**) bereits in der Vergangenheit durchgeführt [175], doch wurde dabei nicht nach möglichen Wirkzielen gesucht. Derartige Ansätze werden zurzeit sowohl für das Microcystin, als auch das Tyocidin unternommen [176, 177]. Die natürliche Substratflexibilität von *M. alpina* bietet dabei den Vorteil, dass die A-Domänen nicht gentechnisch verändert werden müssen, wie dies im Fall der Tyocidin-Biosynthese notwendig ist, um nicht-native Substrate zu akzeptieren [178] (siehe Kapitel 5.5).

5.2.3 Produktion antibakterieller Naturstoffe

Für die Malpinine, die Malpibaldine und Calpinactam sind bereits antibakterielle Aktivitäten nachgewiesen worden [130, 133]. Während Calpinactam speziell eine starke antimycobakterielle Aktivität aufweist, zeigen hingegen Malpinine und Malpibaldine nur eine schwache Wirkung gegen grampositive Bakterien. Für die Malpicycline konnte ebenfalls eine antibakterielle Aktivität nachgewiesen werden, wobei auch diese nur bei grampositiven Bakterien zu beobachten war (Manuskript 1) [166]. Allen Verbindungen haben somit eine fehlende Aktivität gegen gramnegative Bakterien gemeinsam. Da alle bisher identifizierten Endosymbioten in basalen Pilzen ebenfalls gramnegative Bakterien

darstellen [53], scheint diese fehlende Aktivität bewusst dem Schutz eventuell vorhandener Endosymbioten zu dienen. Die Luminmide, die aus dem gramnegativen γ-Proteobakterium *Photorhabdus luminescens* isoliert wurden [179], sind strukturell nahezu identisch mit Malpicyclin D [166]. Sind die Naturstoffe evolutionär aus möglichen gramnegativen Endosymbionten auf *M. alpnia* übergegangen, würde dies die fehlende Wirkung gegen diese erklären. Auf den bakteriellen Ursprung der Naturstoffgene wird in Kapitel 5.4 eingegangen.

5.2.4 Phylogenetische Einordnung anhand produzierter Naturstoffe

Malpinine werden allgegenwärtig von *M. alpina* produziert (Manuskript 4). Während diese in 23 von 23 untersuchten Stämmen gefunden wurden, konnten Malipicycline und Malpibaldine in ca. 90% und Calpinactam lediglich in 60% der Stämme nachgewiesen werden. Da eine abschließende Phylogenie der *Mortierellomycotina* immer noch stark diskutierter Gegenstand aktueller Forschungen ist [6, 38], können Naturstoffe einen Weg darstellen, Verwandschaftsverhältnisse biochemisch zu begründen.

Die Idee, Metabolom-Daten zur Systematisierung von Pilzen zu verwenden, wird seit Jahren verfolgt, insbesondere bei Vertretern der *Pezizomycota* [180]. Diese sind aufgrund ihrer umfangreichen biosynthetischen Ausstattung besonders prädestiniert für dieses Vorgehen [69]. Innerhalb der Gattung *Aspergillus* und der Sektion *Nigri* können mit einem Metabolit-basierten Ansatz einzelne Spezies voneinander unterschieden werden [180, 181]. Nachteile dieses Systems sind im Vergleich zwischen *A. flavus* und *A. oryzae* zu sehen. Während beide Arten eng verwandt und genetisch nahezu identisch sind, unterscheiden sie sich grundlegend in der Fähigkeit, Aflatoxine zu produzieren [182, 183].

M. alpina und *M. amoeboidea* zeigen eine hohe Übereinstimmung zwischen codierten NRPS-Genen (Manuskript 2) [173]. 50% der vorhergesagten Proteine zeigen hohe Sequenzidentität, und alle bisher charakterisierten Naturstoffe und Biosynthesegene aus *M. alpina* lassen sich auch in *M. amoeboidea* nachweisen. Eine kürzliche phylogenetische Umgruppierung und Umbenennung in *Linnemannia amoeboidea* lässt sich daher nicht nachvollziehen, lassen sich auf chemischer Ebene doch große Gemeinsamkeiten feststellen. Eine Überprüfungen neuer phylogenetischer Bäume auf metabolische/chemische Plausibilität kann zukünftige Hypothesen verbessern und festigen. Metabolit-basierte Ansätze besitzen allerdings den Nachteil, dass diese auf stark expressionsabhängigen phä-

notypischen Merkmalen beruhen.
Im industriellen und klinischen Umfeld ist die Proteotypisierung ein etabliertes Identifikationsverfahren [184, 185]. Dabei wird durch MALDI-TOF-Massenspektrometrie ein Massenspektrum des Proteoms des zu untersuchenden Keims erstellt und mit einer Datenbank bekannter Proteome verglichen.
Kombination aus Zellmorphologie, Molekularbiologie und Stoffwechselprodukten stellt dabei den Goldstandart zu Identifizierung von Mikroorganismen dar. Zur Differenzierung einzelner Arten und Stämme im akademischen Umfeld können produzierte Naturstoffe darüber hinaus hilfreich sein.

5.3 Synthese der Malpinine, Malpibaldine, Malpicycline und des Calpinactams

5.3.1 Biosynthese von Naturstoffen in *M. alpina*

Bei allen untersuchten Peptiden aus *M. alpina* handelt es sich um nichtribosomale Peptide. Die pentamodularen NRPSs MpbA und MpcA werden von den Genen *mpcA* und *mpbA* codiert und produzieren die Malpibaldine und Malpicycline (Manuskript 1) [166]. Die hexamodulare NRPS CalA und das Gen *calA* sind für die Synthese des Calpinactams verantwortlich, was über heterologe Expression von *calA* in *A. niger* gezeigt werden konnte (Manuskript 3) [186]. Für diese drei Peptide trifft die Kollinearitäts-Regel zu (siehe Kapitel 1.2.2) [187]. Die Malpinine als Hexapeptide werden hingegen durch die heptamodulare Synthetase MalA produziert (Manuskript 2) [173], stellen also eine Ausnahme von der Kollinearitäts-Regel dar. Die Gramicidin S-Biosynthese widerspricht ebenfalls dieser Regel, wobei dort die NRPS GrsB iterativ arbeitet und die wachsende NRPS-Kette alle Module doppelt durchläuft [188]. Im Fall von MalA wird hingegen lediglich das letzte Modul teilweise übersprungen. Es wird dabei keine neue Aminosäure übertragen, aber die vorangegangene AS durch die duale E/C-Domäne epimerisiert. Zwar gibt es Beispiele für das Überspringen einzelner oder mehrerer Module in NRPSs, PKSen und deren Hybriden, doch handelt es sich dabei jeweils um Elongationsmodule und nicht um terminale Module (Abbildung 3 in Kapitel 1.2). So werden das Hexadepsipeptid Myxochromid A und das Pentadepsipeptid Myxochromid S von denselben Enzymen MchA, MchB und MchC in *Myxococcus xanthus* und *Stigmatella aurantica* produziert [189, 190].

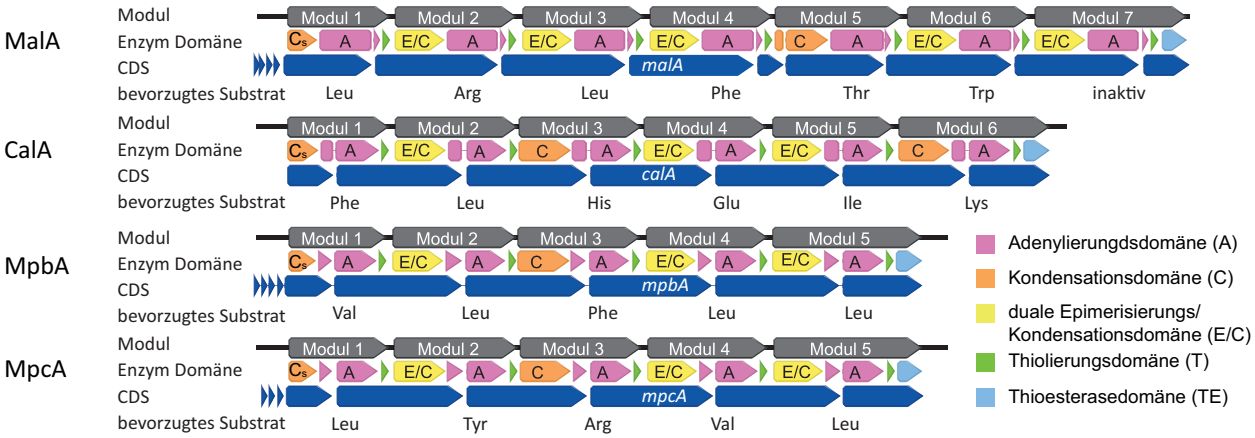

Abbildung 8: Charakterisierte NRPS aus *Mortierella alpina*

Malpinine, Malpicycline, Malpibaldine und Cycloacetamide stellen Naturstoffklassen dar, wobei sich die einzelnen Metabolite in der Zusammensetzung ihrer AS unterscheiden. Diese chemische Diversität wird durch die intrinsische Substratflexibilität der Biosyntheseenzyme generiert (siehe Kapitel 5.5) (Manuskript 1 und 2) [166, 173]. Darin unterscheidet sich *M. alpina* als basaler Pilz von höheren Pilzen wie Ascomyceten, bei denen metabolische Diversität oft durch modifizierende Enzyme (tailoring enzymes) oder iterative Enzyme erzeugt wird [68, 191].

Da es sich bei den oben genannten Naturstoffen um die ersten nachgewiesenen Biosynthesen von Naturstoffen in basalen Pilzen handelt, kommt die Frage auf, inwiefern deren Biosynthese bekannten Prinzipen aus der NRPS-Biosynthese von Bakterien, höheren Pilzen und vereinzelten höheren Eukaryoten [192] folgt. Erkenntnisse zur Biochemie und Genetik von diesen NRPS-Enzymen und -genen können den Grundstein für weitere Naturstoffforschung in basalen Pilzen, aber auch in höheren Pilzen und Bakterien, darstellen.

5.3.2 Dehydratisierung von Hydroxy-Aminosäuren

Dehydro-AS wie das Dehydrobutyrin (DHB) und Dehydroalanin sind in vielen peptidischen Naturstoffen zu finden [193–195], so auch im Malpinin [133]. Anhand enzymatischer *in vitro* Assays wurde nachgewiesen, dass DHB im Malpinin aus Threonin entsteht. Hierfür konnte jedoch kein Enzym oder NRPS-Domäne gefunden werden, die diese Reaktion katalysiert (Manuskript 2) [173]. Auch für andere NRPS-Produkte wie dem Schizotrin A [195], dem Portoamid A [194] oder dem Microcystin LR [196] ist der Einbau von Dehydro-AS ungeklärt. Für das RIPP Nisin, welches

sowohl DHB als auch Dehydroalanin enthält [193], konnte hingegen die Dehydrogenase NisB nachgewiesen werden, welche Threonin und Serin posttranslational dehydratisiert [197, 198]. Derartige Enzyme ließen sich bioinformatisch nicht in *M. alpina* finden. Erst die Aufklärung der Biosynthese des Albopeptid in *Streptomyces albofaciens* [199] gibt einen Hinweis, wie die Biosynthese in *M. alpina* ablaufen kann. Dabei soll eine spezialisierte C*-Domäne der NRPS AlbA die Dehydratisierung katalysieren. Die Autoren schlagen, basierend auf strukturellen Vorhersagen, ein Glutaminsäure (E387 in AlbB C2) vor, welche bei der Reaktion vermutlich eine zentrale Rolle zukommt [199]. Basierend auf dem für Epimerisierungsdomänen (E-Domänen) vorgeschlagenen Reaktionsmechanismus [200, 201], bei dem Glutaminsäure als Base bei der Katalyse der De- und Reprotonierung des α-C-Atoms fungiert, ist ein ähnlicher Mechanismus für dehydratisierende C*-Domänen denk-

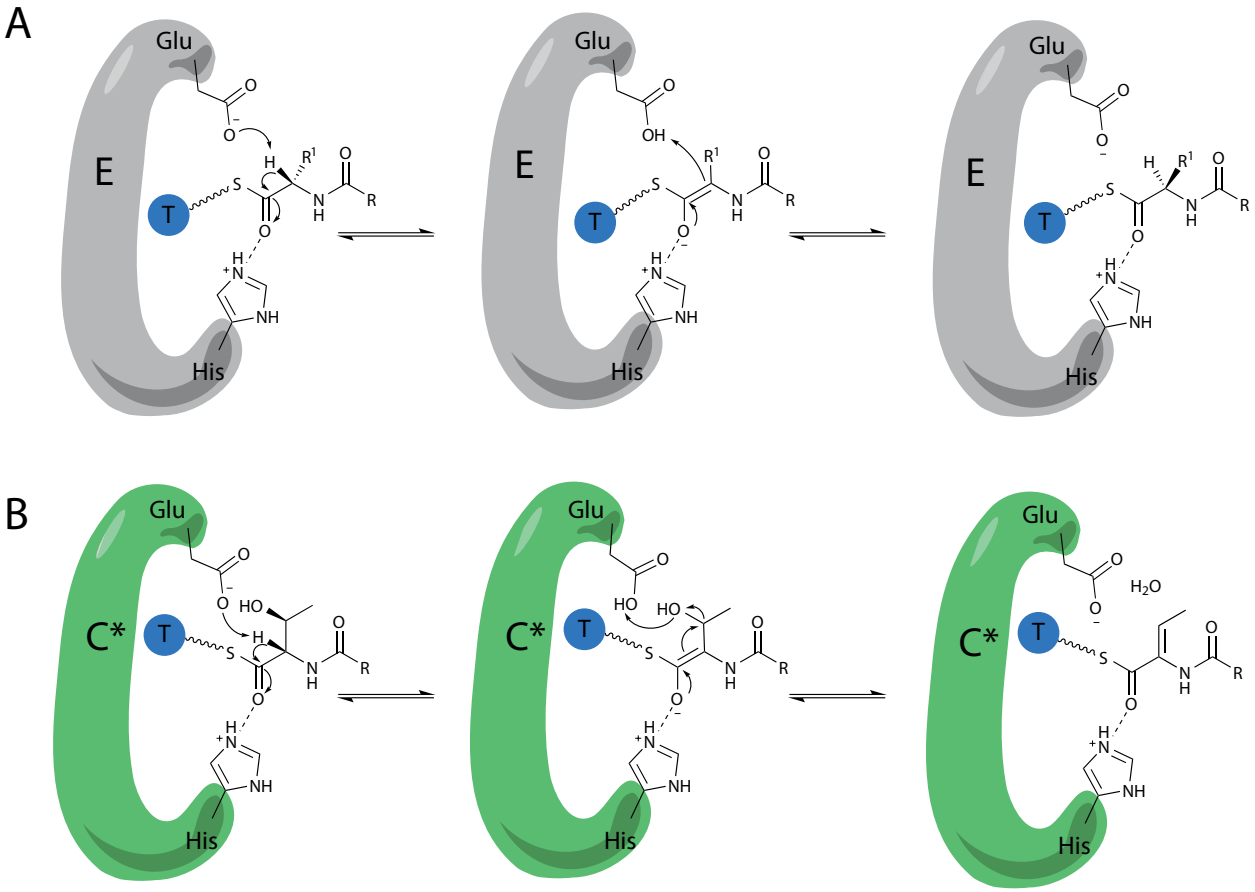

Abbildung 9: Vorgeschlagener Reaktionsmechanismus für Epimerisierungs- und Dehydratisierungsdomänen; Epimerisierungsdomänen - grau, Dehydratisierungsdomänen - grün, T-Domänen - blau; während bei der Epimerisierung die De- und Reprotonierung am selben C-Atom erfolgt (A), wird bei der Dehydratisierung das abstrahierte Proton wahrscheinlich auf die Hydroxylgruppe übertragen (B)

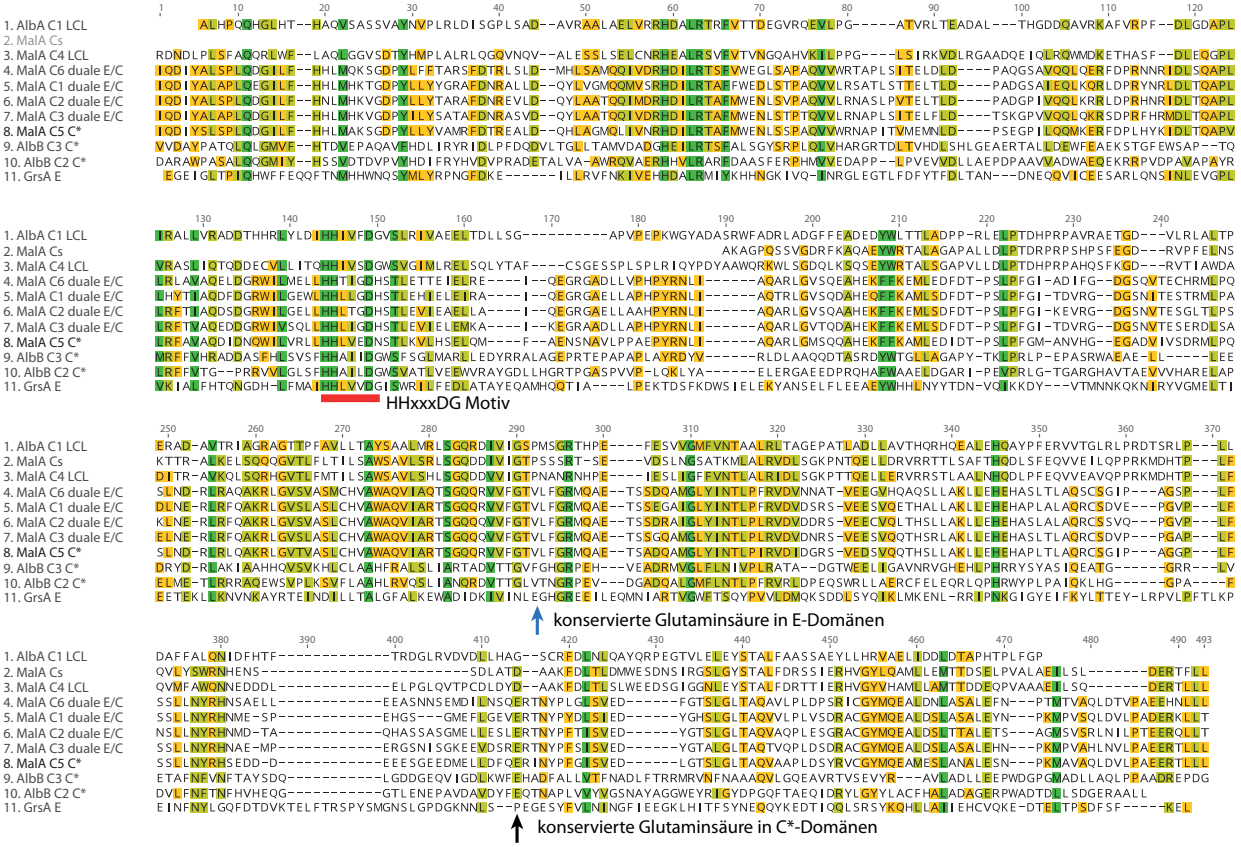

Abbildung 10: Sequenzvergleich zwischen Kondensationsdomänen der MalA und AlbA; C-Domänen-Motiv (rot), konservierte Glutaminsäure der E-Domänen (blauer Pfeil) und postulierte Glutaminsäure der Dehydratisierungsdomänen (schwarzer Pfeil)

bar (siehe Abbildung 9). Glutaminsäure kann bei der Dehydratisierung ebenfalls als Base für die Deprotonierung des α-C-Atoms beteiligt sein. Die anschließende Reprotonierung erfolgt dann hingegen in der Seitenkette, wobei Wasser abgespalten wird und eine Doppelbindung zurückbleibt.

In der C_5, die in MalA vermutlich für die Dehydratisierung zuständig ist, konnte E387 ebenfalls gefunden werden (Abbildung 10). Überraschenderweise lässt sich E387 allerdings auch in dualen E/C-Domänen aus MalA nachweisen, die keine Dehydratisierung katalysieren. Da dieser Rest konserviert unter C* und dualen E/C-Domänen ist, in C_4 aus MalA hingegen nicht vorkommt, spielt dieser vermutlich sowohl bei der Epimerisierung, als auch der Dehydratisierung der Substrate eine Rolle. Für die E-Domäne aus GrsA ist bereits nachgewiesen wurden, dass dort ebenfalls eine Glutaminsäure E892 an der enzymatischen Reaktion beteiligt ist (siehe Abbildung 10, blauer Pfeil) [108, 200]. Diese AS lässt sich aber weder in C*, noch in dualen E/C Domänen finden. Weiterführende NMR-basierte oder biochemische Experimente werden benötigt, um einen Reakti-

onsmechanismus und beteiligte AS-Reste zu identifizieren.
Anders als an den Positionen 1, 3 und 4, weisen alle Malpinine in Position 5 DHB auf (Manuskript 2) [173]. Inwiefern dieses entscheidend für die Wirksamkeit, zur Interaktion mit Zielstrukturen oder zur Ausbildung der 3D-Struktur der Malpinine ist, lässt sich nur vermuten. In *Burkholderia gladioli* kommen mit dem Haereogladin und dem Burriogladin ebenfalls Metabolite vor, die DHB enthalten [202]. Für beide dieser Metabolite konnten die Threonin-abgeleiteten DHB-Einheiten als wirksamkeitsbestimmend für die Kolonisation und Biofilmbildung auf dem Wirt identifiziert werden. Da Dehydro-AS auch in bedeutsamen Naturstoffen wie Lantibiotika oder dem Calcium-Abhängigen Antibiotikum (CDA) aus *Streptomyces coelicolor* vorkommen [203], können Untersuchungen zu der Biosynthese und Struktur-Wirkungsbeziehung der Dehydro-AS in Malpinin auch zu deren besseren Verständnis beitragen.

5.3.3 Kryptische Acetylierung der Malpinine

Lipopeptide wie Surfactin [204] oder Daptomycin [205] enthalten genau wie Malpinin N-terminale Acylreste. Diese funktionellen Gruppen sind oft entscheidend für deren Wirkung und Funktion [206] und werden bei NRPS-Produkten u.a. durch N-terminale C_S-Domänen eingeführt [77, 87]. Während die MalA zwar ebenfalls eine C_S-Domäne trägt, ist diese nicht verantwortlich für die Acetylierung des Peptides (Manuskript 2) [173]. Prinzipiell sind C_S-Domänen dazu fähig, Acetyl-Einheiten zu übertragen, obwohl häufig (mittel)lange, verzweigte Fettsäuren oder komplexe organische Säure zu Substraten dieser Domänen gehören [207]. So findet bei der Biosynthese des Cyclopeptids Heptarhizin durch HepA im Endobakterium *Mycetohabitans rhizoxinica* die N-terminale Acetylierung durch die C_S-Domäne statt [150]. Im Pilz *Aspergillus niger* ist ebenfalls die N-terminale C_S-Domäne der NRPS AgiA für die Acetylierung der ersten AS des Aspergillicin A verantwortlich [208].
Betrachtet man charakterisierte und nicht-charakterisierte NRPSs aus *Mortierella alpina*, so beginnen 13 der 16 NRPSs mit Starter-Kondensationsdomänen (C_S-Domänen) (siehe Tabelle 1), so auch MalA, CalA, MpbA und MpcA (Manuskript 1 und 2) [166, 173]. Da Malpicycline, Malpibaldine und Calpinactam keine N-terminale Acylierung aufweisen, entbehren diese Domänen dort einer offensichtlichen biosynthetischen Funktion. Die kürzlich identifizierten Cycloacetamide tragen zwar N-terminale Acetylreste, doch ist in Unkenntnis der verantwortlichen NRPS auch deren Acetylierung ungeklärt (Manuskript 4). In Sequenzvergleichen zwischen C_S-Domänen wurde offensichtlich,

dass das katalytisch aktive funktionsbestimmende HHxxxDG Motiv [87] in Domänen aus *M. alpina* fehlt und die Domänen N-terminal trunkiert sind (Manuskript 2) [173]. Neben dem fehlenden konservierten Motiv können weitere Gründe zur Inaktivität der Domänen beitragen. AmbS, aus *Xenorhabdus miraniensis*, verantwortlich für die Biosynthese von Ambactin, ist eine hexamodulare NRPS und beginnt ebenfalls mit einer trunkierten inaktiven C-Domäne [209]. Zwar ist dort das zweite Histidin des C-Domänen-Motivs gegen Prolin getauscht, doch führt gentechnische Reinsertion des zweiten Histidins nicht zur Wiederherstellung der Funktion.

Neben fehlender biosynthetischer Aktivität gibt die phylogenetische Stellung der N-terminalen C-Domänen aus *M. alpina* einen Hinweis darauf, dass es sich nicht um C_S-Domänen, sondern um Domänen einer anderen Funktion handelt. C_S-Domänen sind normalerweise phylogenetisch eng verwandt und bilden eine eigene Subgruppe [108]. Domänen aus *M. alpina* clustern hingegen mit regulären $^{L}C_L$-Domänen (Manuskript 1) [166]. Daher kann vermuten werden, dass es sich bei den Domänen aus *M. alpina* nur um trunkierte C-Domänen handelt, wie diese bei verschiedenen pilzlichen Syntheseenzymen zu finden sind. So besitzt die NRPS SimA, Biosyntheseenzym des Ciclosporins in *Tolypocladium inflatum*, ebenfalls eine N-terminale C-Domäne, die eines augenscheinlichen Zweckes entbehrt [110]. Gleichwohl sind auch bei pilzlichen und bakteriellen ACV-Synthetasen, welche für die Produktion von β-Lactamen verantwortlich sind, hoch konservierte trunkierte C-Domänen vorhanden. [210]. Die Deletion einer solchen N-terminalen Domäne führt in *Penicillium rubens* zur Inaktivät der gesamten ACVS [210]. Strukturell zeigen all diese Domänen Ähnlichkeit zu Adenylierungs-Aktivierungs-Domänen (ADA-Domänen) der α-Aminoadipat-Reduktasen [211, 212]. Auch bei diesen ADA-Domänenn handelt es sich um N-terminale Domänen, die selbst keine katalytische, sondern vermutlich nur eine strukturelle Funktion besitzen [211]. Im heterologen System führte deren vollständige oder teilweise Deletion zu einer drastischen Reduktion der enzymatischen Aktivität. Interessanterweise kann durch Zugabe einer heterolog hergestellen ADA-Domäne die Funktion des Enzyms wiederhergestellt werden [211]. Da trunkierte C-Domänen aus *M. alpina* den ADA-Domänen phylogenetisch nahe stehen (Manuskript 1) [166], ist zu vermuten, dass diese ähnlich stabilisierende Funktionen erfüllen. Dass N-terminale Strukturen/Domänen zur Stabilität eines Enzyms beitragen können, konnte in einem Mutagenesansatz zur Erhöhung der thermischen Stabilität einer industriell verwendeten Xylanase beobachtet werden. Alle neun Mutationen, die zur thermischen Stabilität des Enzyms beitrugen, sind innerhalb der ersten 80 Aminosäuren zu finden [213]. Weiterführende Untersuchungen müssen den Zweck dieser Domänen erst abschließend

zeigen.

Da die N-terminale C_S keine Acetyltransferase-Aktivität aufweist und innerhalb der NRPS keine acetylierenden Domänen vorkommen, muss die Acetylierung durch eine *cis*- oder *trans*-wirkende Acetyltransferase abgebildet werden. Weder stromaufwärts noch -abwärts des *malA*-Gens sind Acetyltransferasen oder sonstige koregulierte Gene codiert (Manuskript 2) [173]. Den Malpininen strukturell ähnliche Leucin-N-acetylcysteamin-Thioester (SNACs) wurden durch Proteinlysat aus *M. alpina*, in Anwesenheit von Acetyl-CoA, acetyliert. Dies deutet auf eine enzymatische Acetylierung hin (Manuskript 2) [173]. Bioorthogonale N-Acetylcysteamin-gekoppelte Aminosäuren werden dabei verwendet, um T-Domänen-gebundene Aminosäuren nachzuahmen. In dem γ-Proteobakterium *Xenorhabdus doucetiae* existiert die Acyltransferase *XrdE*, die bei der Biosynthese des Xenorhabdins die N-terminale Acetylierung katalysiert [214, 215]. In Analogie zur Biosynthese des Dithiolopyrrolones Holomycin in *Streptomyces clavuligerus* [216] ist die Acyltransferase Teil des biosynthetischen Genclusters (BGCs) und katalysiert die Acylierung als letzten Schritt der Synthese [214, 216]. Abschließend kann also davon ausgegangen werden, dass die N-terminale Acetat-Einheit enzymatisch durch eine *trans*-wirkende Acetyltransferase aufgeladen wird. Gewissheit können genome mining oder Expressionsanalysen mittels RNASeq bringen, da auf diese Weise ein ‚möglicherweise stark exprimiertes, Gen einer Acetyltransferase identifiziert werden kann [217].

5.3.4 Intronverteilung in Naturstoffgenen aus *M. alpina*

Introns spielen eine oft unterschätze Rolle bei der Regulation der RNA-Reifung [218]. Die Lage der Introns folgt nur selten einem festen Schema, vielmehr sind diese an scheinbar zufälligen Positionen zu finden [219]. In den Genen *malA*, *mpcA*, *mpbA* und *calA*, sowie allen anderen betrachteten NRPS-Genen in *M. alpina*, folgt die Position der Introns hingegen einem Muster (Abbildung 8). Diese liegen, bis auf wenige Ausnahmen, innerhalb der A-Domänen entweder zwischen den A-Domänen-Motiven A3 und A4 oder A8 und A9 [90]. Innerhalb eines NRPS-Gens treten die Introns immer an der selben Position der A-Domäne auf. Diese Positionen entsprechen Sequenzabschnitten, in denen Domänen wie Methyltransferasen [220], Ketoreduktasen [221], Dehydratasen [222] oder Monooxidasen [223] in das NRPS-Grundgerüst integriert sein können (Abbildung 11, Vgl. Kapitel 1.2 Abschnitt Adenylierungsdomänen) [103]. Der Grund für diese Inklusion ist bisher unbekannt. Möglich ist, dass dies für modifizierende Domänen einen strukturellen Vorteil bringt. Derart

unterbrochene A-Domänen können Pilzen und Bakterien als Plattform zur Integration fremder Domänen dienen. Dass in *M. alpina* an denselben Positionen Introns vorkommen, kann ein Relikt der Integration bakterieller Gensequenzen sein. Introns können allerdings auch der expressionellen Regulation dieser Gene dienen. Dass Introns regulierende Aufgaben bei der Naturstoffsynthese zukommen kann, wurde erst kürzlich für den Pilz *Terana caerulea* nachgewiesen [224]. Dort kommt es zu Licht-induziertem alternativen Splicen, wodurch die Expression des Naturstoffgens *corA* reguliert wird. Unklar ist, ob Erkenntnisse aus Basidiomyceten auf *M. alpina* übertragen werden können.

Biotechnologisch können unterbrochene A-Domänen für kombinatorische Ansätze in der synthetischen Mikrobiologie genutzt werden. Lässt sich verstehen welcher Logik die Verteilung und Position der Introns folgen und welche räumlichen Strukturen in A-Domänen für erfolgreiche Domänen-Integrationen notwendig sind, kann dadurch der Baukasten der nicht-ribosomalen Peptidsynthese beachtlich erweitert werden (vgl. Kapitel 5.5).

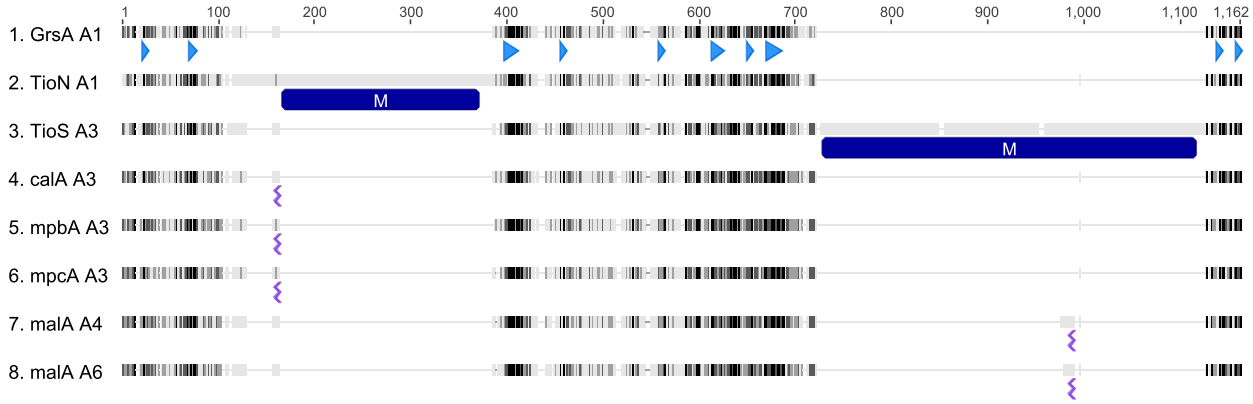

Abbildung 11: Sequenzvergleich verschiedener A-Domänen; während A-Domänen aus TioS und TioN (Thiocoralin-Synthese) Methyltransferasen (dunkelblau) enthalten, finden sich bei Domänen aus *M. alpina* Introns an dieser Position (violett), A1 aus GrsA dargestellt als Referenz mit A-Domänenmotiven (hellblau)

5.3.5 Expression stiller Gene aus *M. alpina*

Mit einem wachsenden Bedarf an neuen (antibakteriellen) Naturstoffen müssen neue Reservoirs erschlossen werden [225]. Durch Expression stiller, unexprimierter Naturstoff-Biosynthesegene können neuartige Substanzen identifiziert werden. In genetisch zugänglichen Organismen können diese Gene gezielt aktiviert und exprimiert werden, z.B. durch Insertion aktivierbarer Promotoren oder

Deletion von Repressoren [226]. Alternativ können Gene im heterologen System in anderen Modellorganismen exprimiert werden [227].

calA, welche für die hexamodulare NRPS CalA codiert, wurde heterolog in *Aspergillus niger* durch homologe Rekombination integriert und anschließend in Volllänge exprimiert (Manuskript 3) [186]. *calA* ist dabei kein stilles Gen [130], doch gestaltete sich die Amplifikation auf cDNA-Ebene schwierig. Ein rekombinatorischer Ansatz wurde gewählt, da keine Deletion in *M. alpina* möglich war und herkömmliche Vektor-basierte Expressionsverfahren nicht auf Gene > 20 kb ausgelegt sind. Durch Deletion des Gens *akuB* im Expressionswirt wurde die nichthomologe Endenreparatur (nonhomologous end joining - NHEJ) verhindert, sodass Nukleotidsequenzen bevorzugt durch homologe Rekombination ins Genom integriert wurden [228]. Die Auswahl aus heterologen Expressionssystemen fiel dabei auf das ATNT-System aus *A. niger* [227], da dieses in der Vergangenheit erfolgreich für die Expression pilzlicher Naturstoffgene von Polyketidsynthasen und NRPS-Hybriden aus Basidiomyceten verwendet wurde [224, 229, 230]. Das fünf von sechs Introns erkannt und prozessiert wurden, spricht für eine hinreichende genetische Kompatibilität zwischen *M. alpina* und *A. niger*. Für *M. alpina* existieren Protokolle zur genetischen Manipulation [231, 232], was diesen neben *Mucor circinelloides* [233, 234] damit zu einem Modellorganismus zur Untersuchung von Genen basaler Pilze macht [235]. Durch UV-Licht-induzierte zufällige Mutation des Gens der Orotat-Phosphoryl-Transferase konnte 2004 der Stamm *M. alpina* 1S-4 genetischer Veränderung zugänglich gemacht werden [236, 237]. In darauf aufbauenden Stämmen lassen sich außerdem Transformationen basierend auf homologer Rekombination realisieren [238, 239]. Dass diese Route nicht zur Untersuchung der CalA verwendet wurde, liegt u.a. an der fehlenden Verfügbarkeit dieser patentrechtlich geschützten Stämme. Gleichzeitig macht es die coenocytische Morphologie [39], sowie die Resistenz gegen viele Resistenzmarker [240] schwer, eigene Expressionssysteme zu etablieren [240]. *M. alpina* ATCC3222 lässt sich unter Laborbedingungen nicht zum Sporulieren anregen. Dadurch lassen sich auch Transformationsmethoden die auf *Rhizobium radiobacter* (ehemals *Agrobacterium tumefaciens*) basieren, nicht anwenden, da für diese Sporen des Empfängerorganismus notwendig sind. Bis eine genetische Manipulation von *M. alpina* vollends etabliert ist, steht mit der heterologen Expression in *Aspergillus niger* eine praktikable Möglichkeit zur Untersuchung unbekannter Gene zur Verfügung.

5.4 Bakterieller Ursprung der NRPS-Gene aus *M. alpina*

Während der Untersuchung von Naturstoffen in *M. alpina* stellte sich stets die Frage, warum gerade dieser basale Pilz zu einer ausgedehnten Naturstoffbiosynthese befähigt ist. Durch Resequenzierung von *M. alpina* ATCC3222 und *de novo* Sequenzierung von *Linnemania amoeboidea* CBS889.72 (Syn. *M. amoeboidea*) konnten 16 bzw. 17 NRPS-Gene gefunden werden (siehe Tabelle 1). Ältere Publikationen sehen *Mortierella* damit als Seltenheit, da in sonstigen untersuchten basalen Pilzen häufig lediglich ein bis drei entsprechende Gene identifiziert werden konnten [13]. Basierend auf bioinformatischen Voraussagen lassen sich in vielen basalen Pilzen wie *Blakeslea*, *Mucor* oder *Rhizopus* eine zweistellige Zahl von Naturstoffgenen annotieren [71]. Ein biochemischer oder RNA Seq-basierter Beweis steht für diese noch aus. Unter diesen Genen dominieren in den meisten Gattungen Terpencyclasen-codierende Gene, während lediglich bei den *Mortierellomycotina* NRPS-Gene überwiegen [70]. Somit stellt sich eher die Frage, warum in *M. alpina* die NRPS-Biosynthese dominiert.

Bei der *in silico* Untersuchung der gefundenen Gene konnten mehrere Indizien gefunden werden, die einzeln betrachtet bereits auf einen bakteriellen Ursprung der Gene hindeuten, zusammengenommen aber für horizontalen Gentransfer (HGT) von einem unbekannten Bakterium auf *M. alpina* sprechen.

So können in elf der 16 NRPSs aus *Mortierella alpina* duale E/C-Domänen vorhergesagt werden (siehe Tabelle 1). Diese Unterart der Kondensationsdomänen sind normalerweise fast ausschließlich in gramnegativen Bakterien wie *Pseudomonas*, *Burkholedria* oder *Xanthomonas* [87], z.B. bei der Biosynthese des unpolaren cyclischen Lipopeptides Arthrofactin [241], zu finden. In *M. alpina* enden außerdem 13 von 16 der codierten NRPSs mit TE-Domänen. Während in Pilzen TE-Domänen nur in jeder fünften NRPSs zu finden, enden bakterielle NRPSs in drei von vier Fällen auf TE-Domänen (siehe Tabelle 1) [69]. Am signifikantesten ist die phylogenetische Verwandtschaft der Adenylierungsdomänen (A-Domänen) mit denen von gramnegativen Bakterien zu sehen. Normalerweise zeigen pilzliche A-Domänen höhere Sequenzhomologien zu pilzlichen Domänen der gleichen Enzymklasse [242], während die Phylogenie bakterieller A-Domänen weitestgehend dem phylogenetischen Baum der Bakterien entspricht. Insbesondere die Nähe von A-Domänen aus *M. alpina* zu denen aus bekannten bakteriellen Endosymbionten wie *Paraburkholderia* oder *Mycoavidus*, die ebenfalls in *Mortierellaceae* vorkommen können (Siehe Kapitel 1.1.3), ist der entscheidende Hinweis auf

Tabelle 1: In *M. alpina* identifizierte NRPSs; modifiziert nach Manuskript 2 [173]; TD- terminale Reduktase-Domäne; C_S-Domänen - grau, duale E/C-Domänen - blau, TE-Domänen - rosa

Bezeichnung	**Domänenarchitektur**
Nps1	C_S-A-T-C-A-T-E/C-A-T-E/C-A-T-C-A-T-C-A-T-E/C-A-T-C-A-T-E/C A-T-TE
Nps2	A-T-E/C-A-T-C-A-T-E/C-A-T-C-A-T-C-A-T-C-A-T-C-A-T-TE
MalA	C_S-A-T-E/C-A-T-E/C-A-T-E/C-A-T-C-A-T-E/C-A-T-E/C-A-T-TE
Nps4	C_S-A-T-C-A-T-C-A-T-E/C-A-T-E/C-A-T-E/C-A-T-C-A-T-TE
CalA	C_S-A-T-E/C-A-T-C-A-T-E/C-A-T-E/C-A-T-C-A-T-TE
Nps6	C_S-A-T-C-A-T-C-A-T-C-A-T-C-A-T-E/C-A-T-TE
Nps7	C_S-A-T-E/C-A-T-C-A-T-C-A-T-C-A-T-C-A-T-TE
MpcA	C_S-A-T-E/C-A-T-C-A-T-E/C-A-T-E/C-A-T-TE
MpbA	C_S-A-T-E/C-A-T-C-A-T-E/C-A-T-E/C-A-T-TE
Nps10	C_S-A-T-E/C-A-T-C-A-T-C-A-T-TD
Nps11	C_S-A-T-C-A-T-E/C-A-T-E/C-A-T-TE
Nps12	C_S-A-T-C-A-T-C-A-T-C-A-T-TE
Nps13	C_S-A-T-C-A-T-TE
Nps14	A-T-C-A-T-C-A-TD
Nps15	C_S-A-T-TE
Lys2	A-T-TD

einen horizontalen Gentransfer (HGT). Mit der steigenden Verfügbarkeit genomischer Daten lassen sich Genübertragungen einfacher finden und nachweisen. Als ein Beispiel für HGT zwischen Bakterium und Pilz werden derzeit die ACV-Synthetasen, welche für die Produktion von β-Lactamen wie Penicillin verantwortlich sind, diskutiert. Gene, die für diese codieren, wurden wahrscheinlich von *Actinobacteria* auf die *Hypocreales* übertragen [98, 243–245]. Wie im Fall von *M. alpina* zeigen auch hier bakterielle und pilzliche A-Domänen eine hohe Sequenzübereinstimmung [246]. Phylogenetische Untersuchungen anhand von Enzym-Domänen führte auch zur Entdeckung von HGT zwischen *Burkholderia* und *Ascomycota* [247]. Dort konnten nah verwandte Adenylierungs- und Ketosynthase-Domänen in NRPS/PKS-Hybriden entdeckt werden.

Da die A-Domänen aus *M. alpina* eine hohe Ähnlichkeit zu endobakteriellen Domänen aufweisen,

handelt es sich wahrscheinlich um den Sonderfall des endosymbiontischen Gentransfers (EGT). EGT hat dabei den Vorteil, dass Nukleinsäuren nicht mehr die Zellwand bzw. Zellmembran des Wirts überwinden müssen, da diese bereits intrazellulär vorkommen. Gerade bei Pilzen stellt Transformation oft den limitierenden Schritt genetischer Manipulation dar [248]. Beispielhaft für EGT ist die Übertragung von Genen aus frühen Plastiden auf ihre Wirte [249]. Einhergehend mit dem Verlust dieser Gene wurden frühe Cyanobakterien derart von der Genexpression und Proteinbiosynthese ihrer Symbiosepartner abhängig, dass diese nicht mehr als eigenständig angesehen werden konnten. Somit beruht die Endosymbiontentheorie ebenfalls auf EGT als wichtige Triebfeder [250]. Da *Mortierellaceae* dafür bekannt sind Endosymbionten zu beherbergen [53], erscheint die Übertragung von NRPS-Genen aus einem einstigen Endosymbionten auf *M. alpina* als plausibel. Nicht zuletzt wurde in einer nicht unabhängig überprüften Studie gezeigt, dass *Mortierellomycota* NOD-like Rezeptoren (**N**ukleotid-bindende **O**ligomerisations**d**omäne-ähnliche Rezeptoren) durch horizontalen Gentransfer aus *Mycoavidus cysteinexigens* erhalten haben [251].

Die Hypothese eines HGT-Ereignisse, durch welche die Grundlage zur Naturstoff-Biosynthese in *M. alpina* gelegt wurde, wird durch den bakteriellen Charakter der Naturstoffgene, sowie dem Vorkommen von Endosymbionten in *Mortierella* gestützt. Daraus lassen sich wiederum Hypothesen für die Entstehung der Naturstoff-Biosynthese in Pilzen ableiten. Bei Eukaryonten kommen, bis auf wenige Ausnahmen, NRPS-Gene lediglich in Pilzen vor [192, 252, 253], wobei deren Ursprung nicht abschließend geklärt ist. In anderen Eukaryoten sind zwar Didomänen aus A-Domänen und T-Domänen gefunden wurden, z.B. Aminoadipat-Dehydrogenasen (AASDHs) im Lysin-Katabolismus, die ähnliche Reaktionen katalysieren [254], doch sind keine multimodularen Multienzymkomplexe zu finden. Daher existiert die Hypothese, dass alle Multidomänen-NRPSs in Pilzen ursprünglich das Resultat horizontalen Gentransfers waren [192]. Chemische Diversität der peptidischen Naturstoffsynthese entstand anschließend durch Weiterentwicklung und Modifikation übertragener Gene. Herkunft und Entwicklung von NRPSs ist immer noch teilweise unbekanntes Terrain; mono- und bimodulare-NRPS/NRPS-ähnliche Enzyme scheinen dabei aber eine zentrale Rolle einzunehmen [246]. In diesen Gruppen von Naturstoffgenen zeigen bakterielle und pilzliche Gene die höchste Übereinstimmung, sodass die Vermutung nahe liegt, dass diese vor der Teilung von Pro- und Eukaryoten entstanden sind. Zusätzlich zeigen diese hohe Übereinstimmungen mit α-Aminoadipat-Reduktasen, welche im pilzlichen Primärstoffwechsel zur Lysin-Biosynthese zu finden sind [255]. Ausgehend von diesen sind multimodulare NRPSs dann wahrscheinlich durch Duplikation, Rekombination, Mutation und

Integration neuer Enzyme später in der Entwicklung der Pilze und Bakterien entstanden [256]. HGT ist ein Phänomen, welches in allen pilzlichen Linien nachgewiesen werden konnte [257]. Gerade Prozesse wie Duplikationen, Insertionen, Rekombinationen, Mutationen und Umorganisation machen es beinahe unmöglich nachzuvollziehen, ob es sich ursprünglich um horizontalen oder vertikalen Gentransfer gehandelt hat [258]. *Mortierella alpina* kann hierbei für weitere Untersuchungen als Modellorganismus fungieren (Manuskript 1 und 2) [166, 173].
Anhand von bekannten Genen, die durch HGT von Endosymbionten auf basale Pilze übergegangen sind, lässt sich außerdem durch Sequenzvergleiche eine Zeitachse des Übertragungsereignisses erstellen [259], wodurch Rückschlüsse auf die zeitliche Entwicklung der Endosymbiose gezogen werden können. In ähnlicher Weise ließ sich bereits eine zeitliche Eingrenzung für die Entstehung der Methanogenese durch Mikroorganismen durchführen [260]. Dieses Vorgehen, dass eine gleichbleibende Substitutionsrate von Basen annimmt, ist bereits aus der Phylogenie bekannt [261]. Auf diese Weise werden „Zeitbäume“ zur Visualisierung von evolutionären Entwicklungen dargestellt. Mit Kenntnis der horizontal übertragenen Gene in *Mortierella* kann daher geklärt werden, wann es zu einer Übertragung der Gene gekommen ist, wobei dies ein Thema für zukünftige Arbeiten darstellt.

5.5 NRPSs aus *M. alpina* in der biotechnologischen Anwendung

Peptidische Naturstoffe nach Maß biotechnologisch zu produzieren ist seit der Entdeckung des nicht-ribosomalen Codes Ziel vieler Forschungsbestrebungen; früher durch Subsitutionsfütterungen und heute v.a. im Rahmen der synthetischen Mikrobiologie [262–264]. Austausch einzelner Domänen, Rekombination ganzer Module oder Fütterung von Vorläufermolekülen sind dabei etablierte Ansätze [77].
A-Domänen aus MalA, MpbA und MpcA besitzen eine hohe Substratflexibilität (Manuskript 1 und 2) [166, 173]. Werden derartige Domänen für Domänentausch-Ansätze oder Modul-Kombination verwendet, lassen sich anschließend die produzierten Metabolite durch Vorläufer-dirigierte Biosynthese (precursor-directed biosynthesis, PDB) einfach verändern. Durch PDB ließ sich so z.B. die Gruppe der cyclischen Microcystine auf über 250 Verbindungen erweitern [176, 265]. Abseits peptidischer Naturstoffe lässt sich ebenfalls Substratflexibilität beobachten. Für die Tryptophansynthetase TrpB aus *Psilocybe cubensis* konnte ebenfalls gezeigt werden, dass diese verschiedene Indole als Substrat akzeptiert [266]. Auffällig ist dabei, dass in *Psilocybe* auch die nachfolgenden

Enzyme der Psilocybin-Biosynthese PsiD und PsiK [79] die selbe Substratflexibilität teilen [266]. Neben A-Domänen stehen C-Domänen ebenfalls in der Diskussion an der Substratauswahl beteiligt zu sein [267]. So konnten bei der Pyoverdin-Synthetase PvdD nur C-Domänen getauscht werden, deren vorangegangene A-Domänen dasselbe Substratspezifität aufwiesen [268]. In aktuellen Publikationen konnten hingegen derartige Einschränkungen widerlegt werden [269]. Genauso existieren C-Domänen, welche andere Substratspezifitäten aufweisen können als die korrespondierenden A-Domänen [267, 270]. Übereinstimmend dazu konnte bei der Biosynthese des Glykopeptid-Antibiotikums Teicoplanin ein engeres Substatspektrum der C-Domäne nachgewiesen werden als bei der A-Domäne [270]. C-Domänen aus *M. alpina* zeigen dieselbe Substratflexibilität wie die betrachteten A-Domänen. So wird L-Methionin als nicht-natives Substrat anstatt L-Leucin sowohl von der A-Domäne, als auch von der dualen E/C Domäne erkannt und ebenfalls epimerisiert, ohne dass dadurch eine Einbuße der Naturstofftiter zu beobachten ist (Manuskript 2) [173]. Die Regulation der Biosynthese kann in *M. alpina* durch Verfügbarkeit und Fluss von Substraten gesteuert werden. Derartige C-Domänen, die für beide Domänenfunktionen eine hohe Substratflexibilität aufweisen, können biotechnologisch einen hohen Wert haben.

Neben der Inkorporation von biogenen Aminosäuren liegt der größte biochemische Nutzen promiskuitiver Domänen in der Integration funktionalisierbarer Monomere (siehe Abbildung 12). So ließen sich durch einfache Fütterung von 4-Bromo-L-Phenylalanin Derivate des Malpinins herstellen, die anschließend für bioorthogonale Kopplung [271] zur Verfügung standen. Aufgrund des geringeren Preises, der höheren Stabilität und der unkomplizierten Synthese zu 4-Azido-L-Phenylalanin besitzt 4-Br-L-Phe praktische und ökonomische Vorteile gegenüber entsprechenden Azid- oder Alkin-Derivaten [272]. 4-Br-L-Phe wurde außerdem von A-Domänen der MpcA und MpbA akzeptiert und in Malpicycline und Malpibaldine inkoorporiert (nicht publiziert). Ähnliche Ansätze sind bereits weit verbreitet in der Naturstoffforschung. So sind für Pseudoxylallemycine [273], Microcystine [176, 265] und Tyocidin [177] ebenfalls über PDB „clickbare“ Derivate erzeugt wurden, die anschließend mit Fluorophoren über Kupfer-katalysierten „Click“ -Reaktionen [274] gekoppelt wurden. PDB-Ansätze finden häufig Anwendung, da diese auch in Unkenntnis der Naturstoffgene durchgeführt werden können (Manuskript 4) [77]. Während die Malpinin-Synthetase MalA im Wildtyp bereits clickbare Aminosäuren mit hoher Spezifität akzeptiert, mussten die Bindetaschen der A-Domänen in der Tyocidin-Synthetase TycA und der Gramicidin S-Synthetase GrsA angepasst werden, um nicht-proteinogene AS zu akzeptieren. In den Bindetaschen wurde jeweils ein Tryptophan (W239

bei der GrsA) gegen Serin getauscht. Dadurch wurde eine größere Zahl an Substraten, einschließlich bioorthogonal-zugänglicher Substrate, akzeptiert [177, 178].

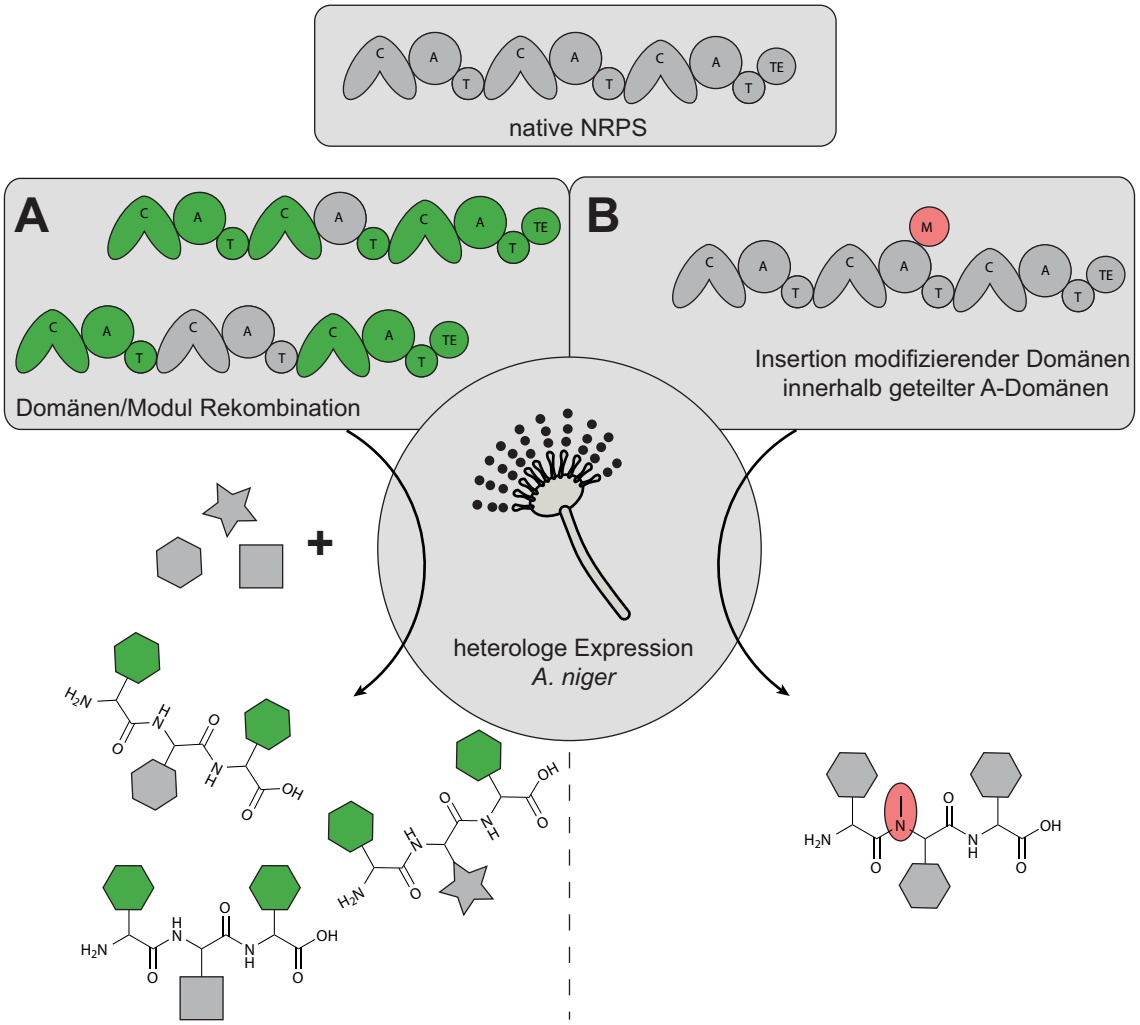

Abbildung 12: Mögliche biotechnologische Anwendungen untersuchter Enzyme; A) promiskuitive Domänen und Module nativer NRPSs (grau) aus *M. alpina* können gentechnisch in andere NRPSs (grün) eingebracht werden, um, z.B. im heterologen System, durch Vorläufer-dirigierte Biosynthese neue Derivate zu generieren; B) unterbrochene A-Domänen können möglicherweise als Integrationspositionen modifizierender Domänen, z.B. M-Domänen (rot), verwendet werden, um ebenfalls neue Strukturen zu generieren

Kombinatorische Ansätze, bei denen Domänen oder Module entfernt, getauscht oder hinzugefügt werden, können, anders als reine Mutationsansätze, zur Bildung gänzlich neuer Peptide führen. Erste Ansätze dieser kombinatorischen Genetik kamen zu Beginn des 21. Jahrhunderts auf [275, 276]. Dabei wurden die Sequenzen gut untersuchter NRPS-Produkte Surfactin und Daptomycin verändert, um u.a. mögliche neue Antibiotika zu generieren. In fortgeschritteneren Ansätzen werden

„Austauscheinheiten“ (exchange units) bereits frei kombiniert, wodurch neue synthetische Metaboliten *in vitro* zuverlässig hergestellt werden können [277]. Die Grenzen dieser exchange units sind dabei im Vergleich zu regulären CAT-Modulen C-terminal verschoben und starten/enden jeweils mit C-A-Linker-Regionen [107]. Anstatt NRPS-Untereinheiten auf genetischer Ebene zu rekombinieren, können diese durch „synthetic zipper“, designte kurze Peptide die mit hoher Affinität miteinander interagieren [278, 279], auf Protein-Ebene kombiniert werden. Dadurch können auch größere NRPSs, die anderweitig zu groß für vektorbasierte heterologe Expressionsansätze in *E. coli* wären, in zwei getrennten Vektoren transformiert und produziert werden. Dadurch lässt sich sowohl die Erfolgswahrscheinlichkeit der Kombination, als auch die Produktivität des neuen Enzyms steigern [264, 280].

Viele der bereits beschriebenen Ansätze der synthetischen Mikrobiologie sind auf ein heterologes Expressionssystem angewiesen. Einschränkungen die viele heterologe Systeme besitzen, ist die fehlende Kompatibilität mit Genen > 12-15 kb [281, 282] oder dass Gene auf cDNA-Ebene transformiert werden müssen, weil Introns nicht kompatibel sind bzw. prokaryotische Expressionsstämme verwendet werden. Das in Manuskript 4 beschriebene Expressionssystem birgt dabei viele Vorteile für synthetische Ansätze: Wie am Gen *lpaA* demonstriert wurde, lassen sich basierend auf diesem System Punktmutationen einfach einbringen und deren Auswirkung auf die Funktion des produzierten Enzyms untersuchen. Genauso können Genfragmente verschiedener Biosynthesegene erst *in vivo* im *Expressionsstamm* kombiniert werden, wodurch die Anzahl notwendiger Zwischenklonierungen reduziert werden kann. *Aspergillus niger* ist zusätzlich seit Dekaden als biotechnologischer Modellorganismus etabliert [283]. Durch die genetischen Kompatibilität zu *M. alpina* bietet sich das Potential, sowohl bei der biotechnologischen Produktion nativer Naturstoffe aus *M. alpina* Anwendung zu finden, als auch bei der Expression synthetischer Naturstoffgene, die Gensequenzen basaler Pilze enthalten.

Biotechnologische Herstellung neuer Metabolite kann nur Anwendung finden, wenn diese der chemischen Route überlegen ist. Lineare Peptide mit simplen Aminosäuren sind chemisch mit einfachen Methoden zugänglich, weswegen biosynthetische Ansätze keinen ökonomischen Vorteil besitzen. Für cyclische Peptide, deren Synthese in geringeren Ausbeuten resultiert [133] oder Peptide, deren AS instabil oder anfällig für Racemisierung sind, kann eine Produktion im biologischen System von Vorteil sein. Zunehmend wichtig zur Beurteilung verschiedener Syntheserouten sind ökologische Aspekte. Für biosynthetische Ansätze, die oft auf toxische Katalysatoren verzichten können,

besteht darin ein weiterer Vorteil.

5.6 Ausblick

Während basale Pilze für viele Jahrzehnte im Schatten der Asco- und Basidiomyceten als pilzliche Naturstoffproduzenten standen, eröffnen sich auf der Grundlage der vorliegenden Arbeit neue Möglichkeiten, auch deren biosynthetisches Potential auszuschöpfen. Da basale Pilze in allen biologischen Nischen und auf allen Kontinenten zu finden sind, ist es wahrscheinlich, dass unzählige Wechselwirkungen existieren, bei denen Naturstoffe eine Rolle spielen. Da bisher kaum Metabolite aus basalen Pilzen bekannt sind, ist das Risiko von Reidentifizierungen wesentlich geringer als bei Dikarya.
Gleichzeitig ist das Maß an chemischer Diversität beachtlich, welches durch Rekombination von Naturstoffgenen erzeugt werden kann, die durch horizontalen Gentransfer (HGT) aufgenommen wurden, wie man am Beispiel der Malpicycline, Malpibaldine, Malpinine und Calpinactam sieht. Anhand dieser und weiteren peptidischen Naturstoffen können Rückschlüsse auf die Entstehung von NRPSs in Pilzen und den Einfluss von HGT bei diesem Prozess untersucht werden
Zwar beschränkte sich diese Arbeit lediglich auf NRPSs, doch besitzen basale Pilze das Potential zu einer diversen Naturstoffproduktion [70, 71]. Vorhergesagte Terpenzyklasen, PKSs oder NRPSs können mit den hier etablierten Methoden untersucht und z.B. heterolog in *Aspergillus* produziert werden. Nicht zuletzt können in basalen Pilzen Enzyme mit bisher unbekannten Eigenschaften oder Substratspezifitäten gefunden werden. Da basale Pilze eine diverse paraphyletische Gruppe darstellen, lässt sich vermuten, dass auch produzierte Enzyme eine hohe Diversität aufweisen. Im Leucin-Metabolismus von *M. alpina* ließen sich bereits Enzyme identifizieren, deren Funktion sich von denen höherer Pilze unterscheidet [284]. Gerade im Bereich des biosynthetischen Designs von Naturstoffen und der Biotechnologie im allgemeinen, können Enzyme mit einer hhohen Substratflexibilität von außergewöhnlichem Nutzen sein. So lassen sich neue Derivate einfach biokatalytisch produzieren, ohne diese vollsynthetisch herstellen zu müssen. Gleichzeitig können „clickbare“ oder bioorthogonal-gekoppelte Metabolite Einsatz in Forschung, Diagnostik oder Pharmazie finden. In *M. alpina* sind bisher weniger als ein Drittel der Naturstoffgene mit Naturstoffen verknüpft, doch bereits jetzt stellt *M. alpina* ein reiches Reservoir neuer Naturstoffe dar. Zygomyceten, wie die bereits sequenzierte Gattungen *Mortierella*, *Basidiobolus* oder *Gigaspora*, können dabei lohnens-

werte Kandidaten für folgende Untersuchungen darstellen, um den weiter steigenden Bedarf an Antiinfektiva u.v.m zu decken.

6 Zusammenfassung

Während Asco- und Basidiomyceten als herausragende Produzenten von Naturstoffen etabliert sind, wurden basale Pilze, traditionell als Zygomyceten bezeichnet, als unfähig zur Produktion von sekundären Metaboliten abgetan. Basierend auf analytisch-chemischen Methoden wurden zwar vereinzelt Naturstoffe in diesen nachgewiesen, doch blieben die genetischen Grundlagen dafür enigmatisch. In dieser Arbeit wurde anhand des Modellorganismus *Mortierella alpina* gezeigt, dass basale Pilze wohl zu ausgedehnter Naturstoffbiosyntese befähigt sind.

Neben den bereits bekannten Malpininen, Malpibaldinen und Calpinactam, konnten die Malpicycline, als pentapeptidische Cyclopeptide, identifiziert und strukturell aufgeklärt werden.
Für diese vier Naturstoffe/Naturstoffklassen konnten NRPSs als deren Biosyntheseenzyme identifiziert werden. Die Calpinactamsynthetase CalA wurde dabei heterolog in Vollänge in *Aspergillus niger* mithilfe eines neu etablierten Expressionssystems produziert. Die chemische Diversität der einzelnen Derivate der Malpinine, Malpicycline und Malpibaldine konnte dabei auf eine hohe Substratflexibilität der A-Domänen zurückgeführt werden. Bei den Biosynthesegenen *malA*, *mpbA*, *calA* und *mpcA* handelt es sich um pilzliche Gene, die jedoch bakteriellen Ursprungs sind und durch horizontalen Gentransfer auf *M. alpina* übertragen worden sind.

Der Nachweis einer antibakteriellen und antilarvalen Aktivität für die Malpicycline und eine insektizide Wirkung der ebenfalls neu beschriebenen Cycloacetamide, lässt ein vollständigeres Bild der chemischen Ökologie von *M. alpina* entstehen, bei dem Naturstoffe zur Verteidigung gegen Fraßfeinde produziert werden.

Durch die biochemische Charakterisierung der Biosyntheseenzyme und deren Domänen ließen sich promiskuitive A- und duale E/C-Domänen identifizieren, die einen Mehrwert bei der *de novo* Synthese von Naturstoffen darstellen können. Die Substratflexibilität der A-Domänen erlaubt außerdem die Inkorporation nichtproteinogener AS, die anschließend für bioorthogonale Kopplung zur Verfügung stehen. Derart fluorophor-gekoppelte Malpinin-Derivate wurden als potentielle Trägerpeptide zum gerichteten Wirkstofftransport in humane Immunzellen identifiziert.

Mit der Identifikation von vier Naturstoffbiosynthesen in *Mortierella alpina* konnte ein basaler Pilz als herrausragender Produzent bioaktiver Naturstoffe identifiziert werden. Auf der Grundlage der Ergebnisse dieser Arbeit können weitere Untersuchungen angestellt werden, um ein bisher noch nicht erforschtes Reservoir für sekundäre Naturstoffe zu erforschen.

7 Abstract

The Asco- and Basidiomycetes have been recognized as prolific producers of secondary metabolites. Early diverging fungi, traditionally refered to as zygomycetes, have been dismissed as poor producers of bioactive natural products. Solely based on analytical chemical methods, new metabolites have rarely been identified, but their genetic basics remain enigmatic.
In this work the early diverging fungus *Mortierella alpina*, a commercially relevant producer of polyunsaturated fatty acids, was used as a model organism.

In addition to the already known malpinins, malpibaldins and calpinactam, a new class of peptides, the cyclic pentapeptide malpicyclins, was identified and their structure elucidated.
For these four natural products, NRPSs could be identified as their biosynthetic enzymes. The full-length calpinactam synthetase CalA was produced heterologously in *Aspergillus niger* using a newly established expression system. The chemical diversity of the individual derivatives of malpinine, malpicycline and malpibaldine could be attributed to the high substrate flexibility of the A-domains. All biosynthetic genes *malA*, *mpbA*, *calA* and *mpcA* are genuine fungal genes, but of bacterial origin.
The detection of antibacterial and antilarval activities of the malpicyclins and insecticidal activity for the newly described cycloacetamides, allow for a more complete picture of the chemical ecology of *M. alpina*, in which natural products are produced as defence against predators.

Through the biochemical characterization of the biosynthetic enzymes and their domains, promiscuous A- and dual E/C-domains could be identified, which can represent added value for the *de novo*

synthesis of natural products. The substrate flexibility of the A domains also allows the incorporation of non-proteinogenic AA, which are then available for bioorthogonal coupling. Fluorophore-coupled malpinin derivatives were synthesized and have been identified as potential carrier peptides for the targeted transport of active substances into human immune cells.

The identification of four natural product biosyntheses illustrates the basal fungi *Mortierella alpina* as a promising producer of bioactive secondary metabolites. Based on the results of this work, further investigations can be undertaken to explore a previously unexplored reservoir for secondary natural products.

8 Thesen

I *Mortierella alpina* ist zu umfangreicher Naturstoffproduktion befähigt und ist dabei nicht auf die Syntheseleistung eines Endosymbionten angewiesen.

II Die nichtribosomale Peptidsynthetase MalA codiert für die oberflächenaktiven Malpinine.

III Die Adenylierungsdomänen der MalA zeigen ausgedehnte Substratflexibilität, die zu einer nährmediumsabhängigen Diversifizierung der gebildeten Malpinine führt.

IV Malpinine werden selektiv in phagozytierende Humanzellen aufgenommen und können für gerichteten Wirkstofftransport in diese angewendet werden.

V Die NRPSen MpbA und MpcA, codiert durch die zwei Gene *mpbA* und *mpcA*, sind für die Produktion der zyklischen Pentapeptidklassen der Malpibaldine und Malpicycline verwantwortlich.

VI *calA* ist das codierende Gen für die Synthese von Calpinactam, einem potenten antimycobakteriellen Wirkstoff.

VII Gene, die für modulare Multienzymkomplexe wie NRPSen codieren, und Abschnitte von mehr als 20 kb DNA überspannen, lassen sich durch homologe Rekombination in *Aspergillus niger* heterolog exprimieren. Dadurch können stille Gene und Gencluster untersucht werden.

VIII NRPS-Gene sind durch horizontalen Gentransfer von einem Endosymbionten auf *Mortierella alpina* übergegangen.

IX Cycloacetamide und Malpicycline zeigen antilarvale Eigenschaften und stellen so eine Möglichkeit für *M. alpina* dar, sich gezielt vor Fraßfeinden zu schützen

9 Quellen

(1) www.speciesfungorum.org, 17.01.2023.

(2) Blackwell, M. *American Journal of Botany* **2011**, *98*, 426–438.

(3) Hawksworth, D. L.; Lücking, R. *Microbiology Spectrum* **2017**, *5*, 1–17.

(4) Barr, D. J. S. *Mycologia* **1992**, *84*, 1–11.

(5) Shelest, E.; Voigt, K. in *Fungal Genomics*, Nowrousian, M., Hrsg.; The Mycota Ser; Springer: Berlin, Heidelberg, **2014**, S. 31–60.

(6) Wagner, L.; Stielow, B.; Hoffmann, K.; Petkovits, T.; Papp, T.; Vágvölgyi, C.; de Hoog, G. S.; Verkley, G.; Voigt, K. *Persoonia* **2013**, *30*, 77–93.

(7) James, T. Y.; Kauff, F.; Schoch, C. L.; Matheny, P. B.; Hofstetter, V.; Cox, C. J.; Celio, G.; Gueidan, C.; Fraker, E. u. a. *Nature* **2006**, *443*, 818–822.

(8) Hibbett, D. S.; Binder, M.; Bischoff, J. F.; Blackwell, M.; Cannon, P. F.; Eriksson, O. E.; Huhndorf, S.; James, T. Y.; Kirk, P. M. u. a. *Mycological Research* **2007**, *111*, 509–547.

(9) Voigt, K.; James, T. Y.; Kirk, P. M.; Santiago, A. L. C. M. d. A.; Waldman, B.; Griffith, G. W.; Fu, M.; Radek, R.; Strassert, J. F. H. u. a. *Fungal Diversity* **2021**, 1–40.

(10) Spatafora, J. W.; Chang, Y.; Benny, G. L.; Lazarus, K.; Smith, M. E.; Berbee, M. L.; Bonito, G.; Corradi, N.; Grigoriev, I. V. u. a. *Mycologia* **2016**, *108*, 1028–1046.

(11) Bautista-Baños, S.; Bosquez-Molina, E.; Barrera-Necha, L. L. in *Postharvest Decay*; Elsevier: **2014**; Bd. 18, S. 1–44.

(12) Beekman, A. M.; Barrow, R. A. *Australian Journal of Chemistry* **2014**, *67*, 827.

(13) Voigt, K.; Wolf, T.; Ochsenreiter, K.; Nagy, G.; Kaerger, K.; Shelest, E.; Papp, T. in *Biochemistry and Molecular Biology*, Hoffmeister, D., Hrsg.; Springer International Publishing: Cham, **2016**; Bd. 99, S. 361–385.

(14) Schueffler, A.; Anke, T. *Natural Product Reports* **2014**, *31*, 1425–1448.

(15) Ribes, J. A.; Vanover-Sams, C. L.; Baker, D. J. *Clinical Microbiology Reviews* **2000**, *13*, 236–301.

(16) Choudhary, N. K.; Jain, A. K.; Soni, R.; Gahlot, N. *Clinical Epidemiology and Global Health* **2021**, *12*, 100900.

(17) Hesseltine, C. W. *Annual Review of Microbiology* **1983**, *37*, 575–601.

(18) Hesseltine, C. W. *Mycologist* **1991**, *5*, 162–169.

(19) Chang, C.-T.; Hsu, C.-K.; Chou, S.-T.; Chen, Y.-C.; Huang, F.-S.; Chung, Y.-C. *International Journal of Food Science & Technology* **2009**, *44*, 799–806.

(20) Trusdell, D. D.; Green, N. R.; Acosta, P. B. *Journal of Food Science* **1987**, *52*, 493–494.

(21) Tamang, J. P.; Sarkar, P. K.; Hesseltine, C. W. *Journal of the Science of Food and Agriculture* **1988**, *44*, 375–385.

(22) Tamang, J. P.; Sarkar, P. K. *Microbios* **1995**, *81*, 115–122.

(23) Zhang, Z. Y.; Jin, B.; Kelly, J. M. *Biochemical Engineering Journal* **2007**, *35*, 251–263.

(24) Yin, P.; Nishina, N.; Kosakai, Y.; Yahiro, K.; Pakr, Y.; Okabe, M. *Journal of Fermentation and Bioengineering* **1997**, *84*, 249–253.

(25) Ehrlich, F. *Berichte der deutschen chemischen Gesellschaft* **1911**, *44*, 3737–3742.

(26) Mehta, B. J.; Salgado, L. M.; Bejarano, E. R.; Cerdá-Olmedo, E. *Applied and Environmental Microbiology* **1997**, *63*, 3657–3661.

(27) Choudhari, S. M.; Ananthanarayan, L.; Singhal, R. S. *Bioresource Technology* **2008**, *99*, 3166–3173.

(28) Mohapatra, B.; Banerjee, U.; Bapuji, M. *Journal of Biotechnology* **1998**, *60*, 113–117.

(29) Lee, S.; Jang, Y.; Lee, Y. M.; Lee, J.; Lee, H.; Kim, G.-H.; Kim, J.-J. *Journal of Microbiology and Biotechnology* **2011**, *21*, 1322–1329.

(30) Petrič, S.; Hakki, T.; Bernhardt, R.; Zigon, D.; Crešnar, B. *Journal of Biotechnology* **2010**, *150*, 428–437.

(31) Totani, N.; Oba, K. *Lipids* **1987**, *22*, 1060–1062.

(32) Mamani, L. D. G.; Magalhães, A. I.; Ruan, Z.; de Carvalho, J. C.; Soccol, C. R. *Biotechnology Research and Innovation* **2019**, *3*, 103–119.

(33) Yamada, H.; Shimizu, S.; Shinmen, Y. *Agricultural and Biological Chemistry* **1987**, *51*, 785–790.

(34) Aki, T.; Nagahata, Y.; Ishihara, K.; Tanaka, Y.; Morinaga, T.; Higashiyama, K.; Akimoto, K.; Fujikawa, S.; Kawamoto, S. u. a. *Journal of the American Oil Chemists' Society* **2001**, *78*, 599–604.

(35) Ruan, Z.; Zanotti, M.; Wang, X.; Ducey, C.; Liu, Y. *Bioresource Technology* **2012**, *110*, 198–205.

(36) Bresson, J.-L.; Flynn, A.; Heinonen, M.; Hulshof, K.; Korhonen, H.; Lagiou, P.; Løvik, M.; Marchelli, R.; Martin, A. u. a. *EFSA Journal* **2008**, *6*, 1–15.

(37) Vadivelan, G.; Venkateswaran, G. *BioMed Research International* **2014**, *2014*, 657414.

(38) Vandepol, N.; Liber, J.; Desirò, A.; Na, H.; Kennedy, M.; Barry, K.; Grigoriev, I. V.; Miller, A. N.; O'Donnell, K. u. a. *Fungal Diversity* **2020**, *104*, 267–289.

(39) Yadav, D. R.; Kim, S. W.; Babu, A. G.; Adhikari, M.; Kim, C.; Lee, H. B.; Lee, Y. S. *Mycobiology* **2014**, *42*, 401–404.

(40) www.gbif.org Global Biodiversity Information Facility, 17.01.2023.

(41) Gams, W. *Persoonia* **1977**, *9*, 381–391.

(42) Del Frate, G.; Caretta, G. *Polar Biology* **1990**, *11*, 1–7.

(43) Tedersoo, L.; Bahram, M.; Põlme, S.; Kõljalg, U.; Yorou, N. S.; Wijesundera, R.; Villarreal Ruiz, L.; Vasco-Palacios, A. M.; Thu, P. Q. u. a. *Science* **2014**, *346*, 1256688.

(44) Bonfante, P.; Venice, F. *Fungal Biology Reviews* **2020**, *34*, 100–113.

(45) Yu, N. H.; Park, S.-Y.; Kim, J. A.; Park, C.-H.; Jeong, M.-H.; Oh, S.-O.; Hong, S. G.; Talavera, M.; Divakar, P. K. u. a. *Fungal Systematics and Evolution* **2018**, *2*, 263–272.

(46) Salt, G. A. *Forestry* **1977**, *50*, 113–115.

(47) Johnson, J. M.; Ludwig, A.; Furch, A. C. U.; Mithöfer, A.; Scholz, S.; Reichelt, M.; Oelmüller, R. *Molecular Plant-Microbe Interactions* **2019**, *32*, 351–363.

(48) Zhang, K.; Bonito, G.; Hsu, C.-M.; Hameed, K.; Vilgalys, R.; Liao, H.-L. *Agronomy* **2020**, *10*, 754.

(49) Li, F.; Zhang, S.; Wang, Y.; Li, Y.; Li, P.; Chen, L.; Jie, X.; Hu, D.; Feng, B. u. a. *Soil Biology and Biochemistry* **2020**, *151*, 108017.

(50) Ozimek, E.; Hanaka, A. *Agriculture* **2021**, *11*, 7.

(51) Eroshin, V. K.; Dedyukhina, E. G. *World Journal of Microbiology and Biotechnology* **2002**, *18*, 165–167.

(52) Uehling, J.; Gryganskyi, A.; Hameed, K.; Tschaplinski, T.; Misztal, P. K.; Wu, S.; Desirò, A.; Vandepol, N.; Du, Z. u. a. *Environmental Microbiology* **2017**, *19*, 2964–2983.

(53) Desirò, A.; Hao, Z.; Liber, J. A.; Benucci, G. M. N.; Lowry, D.; Roberson, R. W.; Bonito, G. *The ISME Journal* **2018**, *12*, 1743–1757.

(54) Herlambang, A.; Guo, Y.; Takashima, Y.; Narisawa, K.; Ohta, H.; Nishizawa, T. *Microbiology Resource Announcements* **2022**, *11*, e0110121.

(55) Büttner, H.; Niehs, S. P.; Vandelannoote, K.; Cseresnyés, Z.; Dose, B.; Richter, I.; Gerst, R.; Figge, M. T.; Stinear, T. P. u. a. *Proceedings of the National Academy of Sciences of the United States of America* **2021**, *118*, e2110669118.

(56) Editorial *Nature Chemical Biology* **2007**, *3*, 351.

(57) Liermann, J. C.; Opatz, T.; Kolshorn, H.; Antelo, L.; Hof, C.; Anke, H. *European Journal of Organic Chemistry* **2009**, *12*, 1256–1262.

(58) Das, A.; Prasad, R.; Srivastava, A.; Giang, P. H.; Bhatnagar, K.; Varma, A. in *Microbial Siderophores*, Varma, A., Chincholkar, S. B., Hrsg.; Soil Biology, Bd. 12; Springer: Berlin, **2007**, S. 1–42.

(59) Lysøe, E.; Seong, K.-Y.; Kistler, H. C. *Molecular Plant-Microbe Interactions* **2011**, *24*, 995–1000.

(60) Lind, A. L.; Lim, F. Y.; Soukup, A. A.; Keller, N. P.; Rokas, A. *mSphere* **2018**, *3*, e00050–18.

(61) Ng, W.-L.; Bassler, B. L. *Annual review of genetics* **2009**, *43*, 197–222.

(62) Karwehl, S.; Stadler, M. *Current Topics in Microbiology and Immunology* **2016**, *398*, 303–338.

(63) Keller, N. P. *Nature Reviews Microbiology* **2019**, *17*, 167–180.

(64) Singh, A. K.; Rana, H. K.; Pandey, A. K. in *Recent Advancement in White Biotechnology Through Fungi*, Yadav, A. N., Singh, S., Mishra, S., Gupta, A., Hrsg.; Fungal Biology, Bd. 8; Springer International Publishing: Cham, **2019**, S. 229–248.

(65) Gressler, M.; Löhr, N. A.; Schäfer, T.; Lawrinowitz, S.; Seibold, P. S.; Hoffmeister, D. *Natural Product Reports* **2021**, *38*, 702–722.

(66) Korpi, A.; Järnberg, J.; Pasanen, A.-L. *Critical reviews in toxicology* **2009**, *39*, 139–193.

(67) Rokas, A.; Wisecaver, J. H.; Lind, A. L. *Nature reviews. Microbiology* **2018**, *16*, 731–744.

(68) Slot, J. C. *Advances in Genetics* **2017**, *100*, 141–178.

(69) Robey, M. T.; Caesar, L. K.; Drott, M. T.; Keller, N. P.; Kelleher, N. L. *Proceedings of the National Academy of Sciences of the United States of America* **2021**, *118*, e2020230118.

(70) Koczyk, G.; Pawłowska, J.; Muszewska, A. *Journal of Fungi* **2021**, *7*, 285.

(71) Tabima, J. F.; Trautman, I. A.; Chang, Y.; Wang, Y.; Mondo, S.; Kuo, A.; Salamov, A.; Grigoriev, I. V.; Stajich, J. E. u. a. *G3* **2020**, *10*, 3417–3433.

(72) Karunanithi, P. S.; Zerbe, P. *Frontiers in Plant Science* **2019**, *10*, 1166.

(73) Oldfield, E.; Lin, F.-Y. *Angewandte Chemie* **2012**, *124*, 1150–1163.

(74) Hertweck, C. *Angewandte Chemie International Edition* **2009**, *48*, 4688–4716.

(75) Herbst, D. A.; Townsend, C. A.; Maier, T. *Natural Product Reports* **2018**, *35*, 1046–1069.

(76) Arnison, P. G.; Bibb, M. J.; Bierbaum, G.; Bowers, A. A.; Bugni, T. S.; Bulaj, G.; Camarero, J. A.; Campopiano, D. J.; Challis, G. L. u. a. *Natural Product Reports* **2013**, *30*, 108–160.

(77) Süssmuth, R. D.; Mainz, A. *Angewandte Chemie International Edition* **2017**, *56*, 3770–3821.

(78) Obermaier, S.; Müller, M. *Angewandte Chemie International Edition* **2020**, *59*, 12432–12435.

(79) Fricke, J.; Blei, F.; Hoffmeister, D. *Angewandte Chemie International Edition* **2017**, *56*, 12352–12355.

(80) Dell, M.; Dunbar, K. L.; Hertweck, C. *Natural Product Reports* **2022**, *39*, 453–459.

(81) Finking, R.; Marahiel, M. A. *Annual Review of Microbiology* **2004**, *58*, 453–488.

(82) Bloudoff, K.; Schmeing, T. M. *Biochimica et Biophysica Acta - Proteins and Proteomics* **2017**, *1865*, 1587–1604.

(83) Lambalot, R. H.; Gehring, A. M.; Flugel, R. S.; Zuber, P.; LaCelle, M.; Marahiel, M. A.; Reid, R.; Khosla, C.; Walsh, C. T. *Chemistry & Biology* **1996**, *3*, 923–936.

(84) Conti, E.; Stachelhaus, T.; Marahiel, M. A.; Brick, P. *The EMBO journal* **1997**, *16*, 4174–4183.

(85) Kittilä, T.; Mollo, A.; Charkoudian, L. K.; Cryle, M. J. *Angewandte Chemie International Edition* **2016**, *55*, 9834–9840.

(86) Shaw-Reid, C. A.; Kelleher, N. L.; Losey, H. C.; Gehring, A. M.; Berg, C.; Walsh, C. T. *Chemistry & Biology* **1999**, *6*, 385–400.

(87) Dekimpe, S.; Masschelein, J. *Natural Product Reports* **2021**, *38*, 1910–1937.

(88) Mullowney, M. W.; McClure, R. A.; Robey, M. T.; Kelleher, N. L.; Thomson, R. J. *Natural Product Reports* **2018**, *35*, 847–878.

(89) Schoenafinger, G.; Schracke, N.; Linne, U.; Marahiel, M. A. *Journal of the American Chemical Society* **2006**, *128*, 7406–7407.

(90) Marahiel, M. A.; Stachelhaus, T.; Mootz, H. D. *Chemical Reviews* **1997**, *97*, 2651–2674.

(91) Mootz, H. D.; Schwarzer, D.; Marahiel, M. A. *Chemical Biology & Biological Chemistry* **2002**, *3*, 490.

(92) Gulick, A. M. *ACS Chemical Biology* **2009**, *4*, 811–827.

(93) Kalb, D.; Heinekamp, T.; Lackner, G.; Scharf, D. H.; Dahse, H.-M.; Brakhage, A. A.; Hoffmeister, D. *Applied and Environmental Microbiology* **2015**, *81*, 1594–1600.

(94) Schneider, P.; Bouhired, S.; Hoffmeister, D. *Fungal Genetics and Biology* **2008**, *45*, 1487–1496.

(95) Braesel, J.; Götze, S.; Shah, F.; Heine, D.; Tauber, J.; Hertweck, C.; Tunlid, A.; Stallforth, P.; Hoffmeister, D. *Chemistry & Biology* **2015**, *22*, 1325–1334.

(96) Stachelhaus, T.; Mootz, H. D.; Marahiel, M. A. *Chemistry & Biology* **1999**, *6*, 493–505.

(97) Von Döhren, H. *Fungal Genetics and Biology* **2009**, *46*, 45–52.

(98) Martín, J. F.; Liras, P. in *Horizontal Gene Transfer*, Villa, T. G., Viñas, M., Hrsg.; Springer International Publishing: Cham, **2019**; Bd. 46, S. 337–359.

(99) Kalb, D.; Lackner, G.; Hoffmeister, D. *Fungal Biology Reviews* **2013**, *27*, 43–50.

(100) Lombó, F.; Velasco, A.; Castro, A.; de La Calle, F.; Braña, A. F.; Sánchez-Puelles, J. M.; Méndez, C.; Salas, J. A. *Chemical Biology & Biological Chemistry* **2006**, *7*, 366–376.

(101) Fujimori, D. G.; Hrvatin, S.; Neumann, C. S.; Strieker, M.; Marahiel, M. A.; Walsh, C. T. *Proceedings of the National Academy of Sciences of the United States of America* **2007**, *104*, 16498–16503.

(102) Tillett, D.; Dittmann, E.; Erhard, M.; von Döhren, H.; Börner, T.; Neilan, B. A. *Chemistry & Biology* **2000**, *7*, 753–764.

(103) Labby, K. J.; Watsula, S. G.; Garneau-Tsodikova, S. *Natural Product Reports* **2015**, *32*, 641–653.

(104) Crécy-Lagard, V. d.; Marlière, P.; Saurin, W. *Comptes rendus de l'Academie des sciences. Serie III, Sciences de la vie* **1995**, *318*, 927–936.

(105) Reimer, J. M.; Eivaskhani, M.; Harb, I.; Guarné, A.; Weigt, M.; Schmeing, T. M. *Science* **2019**, *366*, eaaw4388.

(106) Belshaw, P. J.; Walsh, C. T.; Stachelhaus, T. *Science* **1999**, *284*, 486–489.

(107) Samel, S. A.; Schoenafinger, G.; Knappe, T. A.; Marahiel, M. A.; Essen, L.-O. *Structure* **2007**, *15*, 781–792.

(108) Rausch, C.; Hoof, I.; Weber, T.; Wohlleben, W.; Huson, D. H. *BMC Evolutionary Biology* **2007**, *7*, 78.

(109) Kraas, F. I.; Helmetag, V.; Wittmann, M.; Strieker, M.; Marahiel, M. A. *Chemistry & Biology* **2010**, *17*, 872–880.

(110) Yang, X.; Feng, P.; Yin, Y.; Bushley, K.; Spatafora, J. W.; Wang, C. *mBio* **2018**, *9*, e01211–18.

(111) Thörner, W. *Berichte der deutschen chemischen Gesellschaft* **1878**, *11*, 533–535.

(112) Edwards, R. L.; Kale, N. *Tetrahedron* **1965**, *21*, 2095–2107.

(113) Dias, D. A.; Urban, S.; Roessner, U. *Metabolites* **2012**, *2*, 303–336.

(114) Bentley, S. D.; Chater, K. F.; Cerdeño-Tárraga, A.-M.; Challis, G. L.; Thomson, N. R.; James, K. D.; Harris, D. E.; Quail, M. A.; Kieser, H. u. a. *Nature* **2002**, *417*, 141–147.

(115) Gross, H. *Applied Microbiology and Biotechnology* **2007**, *75*, 267–277.

(116) Bode, H. B.; Bethe, B.; Höfs, R.; Zeeck, A. *Chemical Biology & Biological Chemistry* **2002**, *3*, 619.

(117) Hewage, R. T.; Aree, T.; Mahidol, C.; Ruchirawat, S.; Kittakoop, P. *Phytochemistry* **2014**, *108*, 87–94.

(118) Seyedsayamdost, M. R. *Journal of Industrial Microbiology & Biotechnology* **2019**, *46*, 301–311.

(119) Ziemert, N.; Alanjary, M.; Weber, T. *Natural Product Reports* **2016**, *33*, 988–1005.

(120) Medema, M. H.; Blin, K.; Cimermancic, P.; de Jager, V.; Zakrzewski, P.; Fischbach, M. A.; Weber, T.; Takano, E.; Breitling, R. *Nucleic Acids Research* **2011**, *39*, W339–46.

(121) Blin, K.; Shaw, S.; Kloosterman, A. M.; Charlop-Powers, Z.; van Wezel, G. P.; Medema, M. H.; Weber, T. *Nucleic Acids Research* **2021**, *49*, W29–W35.

(122) Grigoriev, I. V.; Cullen, D.; Goodwin, S. B.; Hibbett, D. S.; Jeffries, T. W.; Kubicek, C. P.; Kuske, C.; Magnuson, J. K.; Martin, F. u. a. *Mycology* **2011**, *2*, 192–09.

(123) Grigoriev, I. V. in *The Ecological Genomics of Fungi*, Martin, F., Hrsg.; John Wiley & Sons, Inc: Hoboken, NJ, **2013**; Bd. 467, S. 1–20.

(124) Grigoriev, I. V.; Nikitin, R.; Haridas, S.; Kuo, A.; Ohm, R. A.; Otillar, R.; Riley, R.; Salamov, A.; Zhao, X. u. a. *Nucleic Acids Research* **2014**, *42*, D699–704.

(125) Gooday, G. W.; Carlile, M. J. *Mycologist* **1997**, *11*, 126–130.

(126) Wöstemeyer, J.; Schimek, C. in *Sex in fungi*, Heitman, J., Kronstad, J. W., Hrsg.; ASM Press: Washington, D.C, **2007**, S. 431–443.

(127) Schachtschabel, D.; David, A.; Menzel, K.-D.; Schimek, C.; Wöstemeyer, J.; Boland, W. *Chemical Biology & Biological Chemistry* **2008**, *9*, 3004–3012.

(128) Dekker, K. A.; Aiello, R. J.; Hirai, H.; Inagaki, T.; Sakakibara, T.; Suzuki, Y.; Thompson, J. F.; Yamauchi, Y.; Kojima, N. *The Journal of Antibiotics* **1998**, *51*, 14–20.

(129) Kamiyama, T.; Umino, T.; Nakayama, N.; Itezono, Y.; Satoh, T.; Yamashita, Y.; Yamaguchi, A.; Yokose, K. *The Journal of Antibiotics* **1992**, *45*, 424–427.

(130) Koyama, N.; Kojima, S.; Nonaka, K.; Masuma, R.; Matsumoto, M.; Omura, S.; Tomoda, H. *The Journal of Antibiotics* **2010**, *63*, 183–186.

(131) Koyama, N.; Kojima, S.; Fukuda, T.; Nagamitsu, T.; Yasuhara, T.; Omura, S.; Tomoda, H. *Organic Letters* **2010**, *12*, 432–435.

(132) Kawahara, T.; Itoh, M.; Izumikawa, M.; Sakata, N.; Tsuchida, T.; Shin-Ya, K. *The Journal of Antibiotics* **2017**, *70*, 226–229.

(133) Baldeweg, F.; Warncke, P.; Fischer, D.; Gressler, M. *Organic Letters* **2019**, *21*, 1444–1448.

(134) Grunwald, A. L.; Berrue, F.; Robertson, A. W.; Overy, D. P.; Kerr, R. G. *Journal of Natural Products* **2017**, *80*, 2677–2683.

(135) Soman, A. G.; Gloer, J. B.; Wicklow, D. T. *Journal of Natural Products* **1999**, *62*, 386–388.

(136) Iwasaki, S.; Kobayashi, H.; Furukawa, J.; Namikoshi, M.; Okuda, S.; Sato, Z.; Matsuda, I.; Noda, T. *The Journal of Antibiotics* **1984**, *37*, 354–362.

(137) Tsuruo, T.; Oh-hara, T.; Iida, H.; Tsukagoshi, S.; Sato, Z.; Matsuda, I.; Iwasaki, S.; Okuda, S.; Shimizu, F. u. a. *Cancer Research* **1986**, *46*, 381–385.

(138) Takahashi, M.; Iwasaki, S.; Kobayashi, H.; Okuda, S.; Murai, T.; Sato, Y. *Biochimica et Biophysica Acta - General Subjects* **1987**, *926*, 215–223.

(139) Partida-Martinez, L. P.; Hertweck, C. *Nature* **2005**, *437*, 884–888.

(140) Scherlach, K.; Partida-Martinez, L. P.; Dahse, H.-M.; Hertweck, C. *Journal of the American Chemical Society* **2006**, *128*, 11529–11536.

(141) Partida-Martinez, L. P.; Groth, I.; Schmitt, I.; Richter, W.; Roth, M.; Hertweck, C. *International Journal of Systematic and Evolutionary Microbiology* **2007**, *57*, 2583–2590.

(142) Scherlach, K.; Graupner, K.; Hertweck, C. *Annual Review of Microbiology* **2013**, *67*, 375–397.

(143) Kluge, M.; Mollenhauer, D.; Wolf, E.; Schüßler, A. in *Cyanobacteria in Symbiosis*, Rai, A. N., Bergman, B., Rasmussen, U., Hrsg.; Kluwer Academic Publishers: Dordrecht, **2003**; Bd. 30, S. 19–30.

(144) Bianciotto, V.; Lumini, E.; Bonfante, P.; Vandamme, P. *International Journal of Systematic and Evolutionary Microbiology* **2003**, *53*, 121–124.

(145) Sato, Y.; Narisawa, K.; Tsuruta, K.; Umezu, M.; Nishizawa, T.; Tanaka, K.; Yamaguchi, K.; Komatsuzaki, M.; Ohta, H. *Microbes and Environments* **2010**, *25*, 321–324.

(146) Ohshima, S.; Sato, Y.; Fujimura, R.; Takashima, Y.; Hamada, M.; Nishizawa, T.; Narisawa, K.; Ohta, H. *International Journal of Systematic and Evolutionary Microbiology* **2016**, *66*, 2052–2057.

(147) Lackner, G.; Moebius, N.; Partida-Martinez, L. P.; Boland, S.; Hertweck, C. *BMC Genomics* **2011**, *12*, 210.

(148) Partida-Martinez, L. P.; de Looss, C. F.; Ishida, K.; Ishida, M.; Roth, M.; Buder, K.; Hertweck, C. *Applied and Environmental Microbiology* **2007**, *73*, 793–797.

(149) Niehs, S. P.; Scherlach, K.; Hertweck, C. *Organic & Biomolecular Chemistry* **2018**, *16*, 8345–8352.

(150) Niehs, S. P.; Dose, B.; Scherlach, K.; Roth, M.; Hertweck, C. *Chemical Biology & Biological Chemistry* **2018**, *19*, 2167–2172.

(151) Niehs, S. P.; Dose, B.; Richter, S.; Pidot, S. J.; Dahse, H.-M.; Stinear, T. P.; Hertweck, C. *Angewandte Chemie International Edition* **2020**, *59*, 7766–7771.

(152) Partida-Martinez, L. P.; Monajembashi, S.; Greulich, K.-O.; Hertweck, C. *Current Biology* **2007**, *17*, 773–777.

(153) Hassan, N.; Anesio, A. M.; Rafiq, M.; Holtvoeth, J.; Bull, I.; Williamson, C. J.; Hasan, F. *Extremophiles* **2020**, *24*, 135–145.

(154) Kaul, T. K.; Reis Rodrigues, P.; Ogungbe, I. V.; Kapahi, P.; Gill, M. S. *PLoS one* **2014**, *9*, e86979.

(155) Bringaud, F.; Rivière, L.; Coustou, V. *Molecular and Biochemical Parasitology* **2006**, *149*, 1–9.

(156) Haba, E.; Bresco, O.; Ferrer, C.; Marqués, A.; Busquets, M.; Manresa, A. *Enzyme and Microbial Technology* **2000**, *26*, 40–44.

(157) Furini, G.; Berger, J. S.; Campos, J. A. M.; van der Sand, S. T.; Germani, J. C. *Anais da Academia Brasileira de Ciencias* **2018**, *90*, 2955–2965.

(158) Büchel, E.; Mayer, A.; Martini, U.; Anke, H.; Sterner, O. *Pesticide Science* **1998**, *54*, 309–311.

(159) Büchel, E.; Martini, U.; Mayer, A.; Anke, H.; Sterner, O. *Tetrahedron* **1998**, *54*, 5345–5352.

(160) Xu, Y.; Orozco, R.; Kithsiri Wijeratne, E. M.; Espinosa-Artiles, P.; Leslie Gunatilaka, A. A.; Patricia Stock, S.; Molnár, I. *Fungal Genetics and Biology* **2009**, *46*, 353–364.

(161) Hamill, R. L.; Higgens, C. E.; Boaz, H. E.; Gorman, M. *Tetrahedron Letters* **1969**, *10*, 4255–4258.

(162) Logrieco, A.; Moretti, A.; Castella, G.; Kostecki, M.; Golinski, P.; Ritieni, A.; Chelkowski, J. *Applied and Environmental Microbiology* **1998**, *64*, 3084–3088.

(163) Sasaki, T.; Takagi, M.; Yaguchi, T.; Miyadoh, S.; Okada, T.; Koyama, M. *The Journal of Antibiotics* **1992**, *45*, 692–697.

(164) Grundmann, F.; Kaiser, M.; Kurz, M.; Schiell, M.; Batzer, A.; Bode, H. B. *RSC Advances* **2013**, *3*, 22072.

(165) Chaston, J. M.; Suen, G.; Tucker, S. L.; Andersen, A. W.; Bhasin, A.; Bode, E.; Bode, H. B.; Brachmann, A. O.; Cowles, C. E. u. a. *PLoS one* **2011**, *6*, e27909.

(166) Wurlitzer, J. M.; Stanišić, A.; Wasmuth, I.; Jungmann, S.; Fischer, D.; Kries, H.; Gressler, M. *Applied and Environmental Microbiology* **2021**, *87*, e02051–20.

(167) Edgington, S.; Thompson, E.; Moore, D.; Hughes, K. A.; Bridge, P. *SpringerPlus* **2014**, *3*, 289.

(168) Büttner, H.; Pidot, S. J.; Scherlach, K.; Hertweck, C. *Chemical Science* **2022**, *14*, 103–112.

(169) Wang, X.; Gong, X.; Li, P.; Lai, D.; Zhou, L. *Molecules* **2018**, *23*, 169.

(170) Süssmuth, R. D.; Müller, J.; von Döhren, H.; Molnár, I. *Natural Product Reports* **2011**, *28*, 99–124.

(171) Harder, A. *International Journal of Antimicrobial Agents* **2003**, *22*, 318–331.

(172) Welz, C.; Krüger, N.; Schniederjans, M.; Miltsch, S. M.; Krücken, J.; Guest, M.; Holden-Dye, L.; Harder, A.; von Samson-Himmelstjerna, G. *PLOS Pathogens* **2011**, *7*, e1001330.

(173) Wurlitzer, J. M.; Stanišić, A.; Ziethe, S.; Jordan, P. M.; Günther, K.; Werz, O.; Kries, H.; Gressler, M. *Chemical Science* **2022**, *13*, 9091–9101.

(174) Rognan, D. *Molecular Informatics* **2010**, *29*, 176–187.

(175) Xu, Y.; Zhan, J.; Wijeratne, E. M. K.; Burns, A. M.; Gunatilaka, A. A. L.; Molnár, I. *Journal of Natural Products* **2007**, *70*, 1467–1471.

(176) Moschny, J.; Lorenzen, W.; Hilfer, A.; Eckenstaler, R.; Jahns, S.; Enke, H.; Enke, D.; Schneider, P.; Benndorf, R. A. u. a. *Journal of Natural Products* **2020**, *83*, 1960–1970.

(177) Niquille, D. L.; Folger, I. B.; Basler, S.; Hilvert, D. *Journal of the American Chemical Society* **2021**, *143*, 2736–2740.

(178) Kries, H.; Wachtel, R.; Pabst, A.; Wanner, B.; Niquille, D. L.; Hilvert, D. *Angewandte Chemie* **2014**, *126*, 10269–10272.

(179) Fu, J.; Bian, X.; Hu, S.; Wang, H.; Huang, F.; Seibert, P. M.; Plaza, A.; Xia, L.; Müller, R. u. a. *Nature Biotechnology* **2012**, *30*, 440–446.

(180) Frisvad, J. C.; Larsen, T. O.; de Vries, R.; Meijer, M.; Houbraken, J.; Cabañes, F. J.; Ehrlich, K.; Samson, R. A. *Studies in Mycology* **2007**, *59*, 31–37.

(181) Frisvad, J. C.; Hubka, V.; Ezekiel, C. N.; Hong, S.-B.; Nováková, A.; Chen, A. J.; Arzanlou, M.; Larsen, T. O.; Sklenář, F. u. a. *Studies in Mycology* **2019**, *93*, 1–63.

(182) Nikkuni, S.; Nakajima, H.; Hoshina, S.-I.; Ohno, M.; Suzuki, C.; Kashiwagi, Y.; Mori, K. *The Journal of General and Applied Microbiology* **1998**, *44*, 225–230.

(183) Chang, P.-K.; Ehrlich, K. C. *International Journal of Food Microbiology* **2010**, *138*, 189–199.

(184) Grenga, L.; Pible, O.; Armengaud, J. *Clinical mass spectrometry* **2019**, *14 Pt A*, 9–17.

(185) Karlsson, R.; Gonzales-Siles, L.; Boulund, F.; Svensson-Stadler, L.; Skovbjerg, S.; Karlsson, A.; Davidson, M.; Hulth, S.; Kristiansson, E. u. a. *Systematic and applied microbiology* **2015**, *38*, 246–257.

(186) Kirchgaessner, L.; Wurlitzer, J. M.; Seibold, P. S.; Rakhmanov, M.; Gressler, M. *Fungal Biology and Biotechnology* **2023**, *10*, 4.

(187) Strieker, M.; Tanović, A.; Marahiel, M. A. *Current Opinion in Structural Biology* **2010**, *20*, 234–240.

(188) Hoyer, K. M.; Mahlert, C.; Marahiel, M. A. *Chemistry & Biology* **2007**, *14*, 13–22.

(189) Wenzel, S. C.; Müller, R. *Current Opinion in Chemical Biology* **2005**, *9*, 447–458.

(190) Wenzel, S. C.; Meiser, P.; Binz, T. M.; Mahmud, T.; Müller, R. *Angewandte Chemie International Edition* **2006**, *45*, 2296–2301.

(191) Löhr, N. A.; Urban, M. C.; Eisen, F.; Platz, L.; Hüttel, W.; Gressler, M.; Müller, M.; Hoffmeister, D. *Chembiochem* **2022**, e202200649.

(192) Tiburzi, F.; Visca, P.; Imperi, F. *IUBMB life* **2007**, *59*, 730–733.

(193) Buchman, G. W.; Banerjee, S.; Hansen, J. N. *The Journal of Biological Chemistry* **1988**, *263*, 16260–16266.

(194) Leão, P. N.; Pereira, A. R.; Liu, W.-T.; Ng, J.; Pevzner, P. A.; Dorrestein, P. C.; König, G. M.; Vasconcelos, V. M.; Gerwick, W. H. *Proceedings of the National Academy of Sciences of the United States of America* **2010**, *107*, 11183–11188.

(195) Pergament, I.; Carmeli, S. *Tetrahedron Letters* **1994**, *35*, 8473–8476.

(196) Honkanen, R. E.; Zwiller, J.; Moore, R. E.; Daily, S. L.; Khatra, B. S.; Dukelow, M.; Boynton, A. L. *Journal of Biological Chemistry* **1990**, *265*, 19401–19404.

(197) Koponen, O.; Tolonen, M.; Qiao, M.; Wahlström, G.; Helin, J.; Saris, P. E. J. *Microbiology* **2002**, *148*, 3561–3568.

(198) Garg, N.; Salazar-Ocampo, L. M. A.; van der Donk, W. A. *Proceedings of the National Academy of Sciences of the United States of America* **2013**, *110*, 7258–7263.

(199) Wang, S.; Fang, Q.; Lu, Z.; Gao, Y.; Trembleau, L.; Ebel, R.; Andersen, J. H.; Philips, C.; Law, S. u. a. *Angewandte Chemie International Edition* **2021**, *60*, 3229–3237.

(200) Kim, W. E.; Patel, A.; Hur, G. H.; Tufar, P.; Wuo, M. G.; McCammon, J. A.; Burkart, M. D. *Chembiochem* **2019**, *20*, 147–152.

(201) Stachelhaus, T.; Walsh, C. T. *Biochemistry* **2000**, *39*, 5775–5787.

(202) Thongkongkaew, T.; Ding, W.; Bratovanov, E.; Oueis, E.; Garcı A-Altares, M. A.; Zaburannyi, N.; Harmrolfs, K.; Zhang, Y.; Scherlach, K. u. a. *ACS Chemical Biology* **2018**, *13*, 1370–1379.

(203) Hojati, Z.; Milne, C.; Harvey, B.; Gordon, L.; Borg, M.; Flett, F.; Wilkinson, B.; Sidebottom, P. J.; Rudd, B. A. u. a. *Chemistry & Biology* **2002**, *9*, 1175–1187.

(204) Kakinuma, A.; Sugino, H.; Isono, M.; Tamura, G.; Arima, K. *Agricultural and Biological Chemistry* **1969**, *33*, 973–976.

(205) Baltz, R. H.; Miao, V.; Wrigley, S. K. *Natural Product Reports* **2005**, *22*, 717–741.

(206) Götze, S.; Stallforth, P. *Natural Product Reports* **2020**, *37*, 29–54.

(207) Hamley, I. W. *Chemical communications* **2015**, *51*, 8574–8583.

(208) Greco, C.; Pfannenstiel, B. T.; Liu, J. C.; Keller, N. P. *ACS Chemical Biology* **2019**, *14*, 1121–1128.

(209) Schimming, O.; Fleischhacker, F.; Nollmann, F. I.; Bode, H. B. *Chemical Biology & Biological Chemistry* **2014**, *15*, 1290–1294.

(210) Iacovelli, R.; Mózsik, L.; Bovenberg, R. A. L.; Driessen, A. J. M. *MicrobiologyOpen* **2021**, *10*, e1145.

(211) Kalb, D.; Lackner, G.; Rappe, M.; Hoffmeister, D. *Chemical Biology & Biological Chemistry* **2015**, *16*, 1426–1430.

(212) Hijarrubia, M. J.; Aparicio, J. F.; Martín, J. F. *The Journal of Biological Chemistry* **2003**, *278*, 8250–8256.

(213) Palackal, N.; Brennan, Y.; Callen, W. N.; Dupree, P.; Frey, G.; Goubet, F.; Hazlewood, G. P.; Healey, S.; Kang, Y. E. u. a. *Protein Science* **2004**, *13*, 494–503.

(214) Bode, E.; Brachmann, A. O.; Kegler, C.; Simsek, R.; Dauth, C.; Zhou, Q.; Kaiser, M.; Klemmt, P.; Bode, H. B. *Chemical Biology & Biological Chemistry* **2015**, *16*, 1115–1119.

(215) Bode, E.; He, Y.; Vo, T. D.; Schultz, R.; Kaiser, M.; Bode, H. B. *Environmental Microbiology* **2017**, *19*, 4564–4575.

(216) Li, B.; Walsh, C. T. *Biochemistry* **2011**, *50*, 4615–4622.

(217) Morin, R.; Bainbridge, M.; Fejes, A.; Hirst, M.; Krzywinski, M.; Pugh, T.; McDonald, H.; Varhol, R.; Jones, S. u. a. *BioTechniques* **2008**, *45*, 81–94.

(218) Chorev, M.; Carmel, L. *Frontiers in Genetics* **2012**, *3*, 55.

(219) Cho, G.; Doolittle, R. F. *Journal of Molecular Evolution* **1997**, *44*, 573–584.

(220) Zolova, O. E.; Garneau-Tsodikova, S. *The Journal of Antibiotics* **2014**, *67*, 59–64.

(221) Magarvey, N. A.; Ehling-Schulz, M.; Walsh, C. T. *Journal of the American Chemical Society* **2006**, *128*, 10698–10699.

(222) Cociancich, S.; Pesic, A.; Petras, D.; Uhlmann, S.; Kretz, J.; Schubert, V.; Vieweg, L.; Duplan, S.; Marguerettaz, M. u. a. *Nature Chemical Biology* **2015**, *11*, 195–197.

(223) Weinig, S.; Hecht, H.-J.; Mahmud, T.; Müller, R. *Chemistry & Biology* **2003**, *10*, 939–952.

(224) Lawrinowitz, S.; Wurlitzer, J. M.; Weiss, D.; Arndt, H.-D.; Kothe, E.; Gressler, M.; Hoffmeister, D. *Microbiology Spectrum* **2022**, *10*, e0106522.

(225) Ventola, C. L. *Pharmacy and Therapeutics* **2015**, *40*, 277–283.

(226) Covington, B. C.; Xu, F.; Seyedsayamdost, M. R. *Annual Review of Biochemistry* **2021**, *90*, 763–788.

(227) Geib, E.; Brock, M. *Fungal Biology and Biotechnology* **2017**, *4*, 13.

(228) da Silva Ferreira, M. E.; Kress, M. R. V. Z.; Savoldi, M.; Goldman, M. H. S.; Härtl, A.; Heinekamp, T.; Brakhage, A. A.; Goldman, G. H. *Eukaryotic Cell* **2006**, *5*, 207–211.

(229) Seibold, P. S.; Lenz, C.; Gressler, M.; Hoffmeister, D. *The Journal of Antibiotics* **2020**, *73*, 711–720.

(230) Löhr, N. A.; Eisen, F.; Thiele, W.; Platz, L.; Motter, J.; Hüttel, W.; Gressler, M.; Müller, M.; Hoffmeister, D. *Angewandte Chemie International Edition* **2022**, *61*, e202116142.

(231) Ando, A.; Sumida, Y.; Negoro, H.; Suroto, D. A.; Ogawa, J.; Sakuradani, E.; Shimizu, S. *Applied and Environmental Microbiology* **2009**, *75*, 5529–5535.

(232) Hao, G.; Chen, H.; Wang, L.; Gu, Z.; Song, Y.; Zhang, H.; Chen, W.; Chen, Y. Q. *Applied and Environmental Microbiology* **2014**, *80*, 2672–2678.

(233) van Heeswijck, R.; Roncero, M. I. G. *Carlsberg Research Communications* **1984**, *49*, 691–702.

(234) Garre, V.; Barredo, J. L.; Iturriaga, E. A. in *Genetic Transformation Systems in Fungi, Volume 1*, van den Berg, M. A., Maruthachalam, K., Hrsg.; Fungal Biology, Bd. 230; Springer International Publishing: Cham, **2015**, S. 49–59.

(235) Mohamed, H.; Naz, T.; Yang, J.; Shah, A. M.; Nazir, Y.; Song, Y. *Journal of Fungi* **2021**, *7*, 1061.

(236) Takeno, S.; Sakuradani, E.; Murata, S.; Inohara-Ochiai, M.; Kawashima, H.; Ashikari, T.; Shimizu, S. *Applied Microbiology and Biotechnology* **2004**, *65*, 419–425.

(237) Ando, A.; Sakuradani, E.; Horinaka, K.; Ogawa, J.; Shimizu, S. *Current Genetics* **2009**, *55*, 349–356.

(238) Kikukawa, H.; Sakuradani, E.; Ando, A.; Okuda, T.; Ochiai, M.; Shimizu, S.; Ogawa, J. *Journal of Biotechnology* **2015**, *208*, 63–69.

(239) Zhang, H.; Cui, Q.; Song, X. *World Journal of Microbiology and Biotechnology* **2021**, *37*, 4.

(240) Sachse, S., *Untersuchungen zur genetischen Transformation des Naturstoffproduzenten Mortierella alpina: Diplomarbeit*, Friedrich-Schiller-Universität Jena, **2021**.

(241) Balibar, C. J.; Vaillancourt, F. H.; Walsh, C. T. *Chemistry & Biology* **2005**, *12*, 1189–1200.

(242) Kalb, D.; Lackner, G.; Hoffmeister, D. *Applied and Environmental Microbiology* **2014**, *80*, 6175–6183.

(243) Brakhage, A. A.; Al-Abdallah, Q.; Tüncher, A.; Spröte, P. *Phytochemistry* **2005**, *66*, 1200–1210.

(244) Buades, C.; Moya, A. *Journal of Molecular Evolution* **1996**, *42*, 537–542.

(245) Weigel, B. J.; Burgett, S. G.; Chen, V. J.; Skatrud, P. L.; Frolik, C. A.; Queener, S. W.; Ingolia, T. D. *Journal of Bacteriology* **1988**, *170*, 3817–3826.

(246) Bushley, K. E.; Turgeon, B. G. *BMC Evolutionary Biology* **2010**, *10*, 26.

(247) Lawrence, D. P.; Kroken, S.; Pryor, B. M.; Arnold, A. E. *PLoS one* **2011**, *6*, e28231.

(248) Rivera, A. L.; Magaña-Ortíz, D.; Gómez-Lim, M.; Fernández, F.; Loske, A. M. *Physics of Life Reviews* **2014**, *11*, 184–203.

(249) Ponce-Toledo, R. I.; López-García, P.; Moreira, D. *The New Phytologist* **2019**, *224*, 618–624.

(250) Gray, M. W. *Molecular Biology of the Cell* **2017**, *28*, 1285–1287.

(251) Ciach, M.; Pawłowska, J.; Muszewska, A. *BioRxiv/Preprint* **2021**, DOI: 10.1101/2021.12.02.471044.

(252) Shou, Q.; Feng, L.; Long, Y.; Han, J.; Nunnery, J. K.; Powell, D. H.; Butcher, R. A. *Nature Chemical Biology* **2016**, *12*, 770–772.

(253) Richardt, A.; Kemme, T.; Wagner, S.; Schwarzer, D.; Marahiel, M. A.; Hovemann, B. T. *The Journal of Biological Chemistry* **2003**, *278*, 41160–41166.

(254) Kasahara, T.; Kato, T. *Nature* **2003**, *422*, 832.

(255) Dairi, T.; Kuzuyama, T.; Nishiyama, M.; Fujii, I. *Natural Product Reports* **2011**, *28*, 1054–1086.

(256) Baunach, M.; Chowdhury, S.; Stallforth, P.; Dittmann, E. *Molecular Biology and Evolution* **2021**, *38*, 2116–2130.

(257) Marcet-Houben, M.; Gabaldón, T. *Trends in Genetics* **2010**, *26*, 5–8.

(258) Wang, H.; Sivonen, K.; Fewer, D. P. *Current Opinion in Genetics & Development* **2015**, *35*, 79–85.

(259) Davín, A. A.; Tannier, E.; Williams, T. A.; Boussau, B.; Daubin, V.; Szöllősi, G. J. *Nature Ecology & Evolution* **2018**, *2*, 904–909.

(260) Wolfe, J. M.; Fournier, G. P. *Nature Ecology & Evolution* **2018**, *2*, 897–903.

(261) Berbee, M. L.; Taylor, J. W. in *Systematics and Evolution*, McLaughlin, D. J., McLaughlin, E. G., Lemke, P. A., Hrsg.; Springer Berlin Heidelberg: Berlin, Heidelberg, **2001**; Bd. 90, S. 229–245.

(262) Cane, D. E.; Walsh, C. T.; Khosla, C. *Science* **1998**, *282*, 63–68.

(263) Brown, A. S.; Calcott, M. J.; Owen, J. G.; Ackerley, D. F. *Natural Product Reports* **2018**, *35*, 1210–1228.

(264) Bozhüyük, K. A. J.; Fleischhacker, F.; Linck, A.; Wesche, F.; Tietze, A.; Niesert, C.-P.; Bode, H. B. *Nature Chemistry* **2018**, *10*, 275–281.

(265) Meyer, S.; Kehr, J.-C.; Mainz, A.; Dehm, D.; Petras, D.; Süssmuth, R. D.; Dittmann, E. *Cell Chemical Biology* **2016**, *23*, 462–471.

(266) Blei, F.; Baldeweg, F.; Fricke, J.; Hoffmeister, D. *Chemistry* **2018**, *24*, 10028.

(267) Stanišić, A.; Hüsken, A.; Stephan, P.; Niquille, D. L.; Reinstein, J.; Kries, H. *ACS Catalysis* **2021**, *11*, 8692–8700.

(268) Ackerley, D. F.; Lamont, I. L. *Chemistry & Biology* **2004**, *11*, 971–980.

(269) Calcott, M. J.; Owen, J. G.; Ackerley, D. F. *Nature Communications* **2020**, *11*, 4554.

(270) Kaniusaite, M.; Tailhades, J.; Marschall, E. A.; Goode, R. J. A.; Schittenhelm, R. B.; Cryle, M. J. *Chemical Science* **2019**, *10*, 9466–9482.

(271) Bertozzi, C. R. *Accounts of Chemical Research* **2011**, *44*, 651–653.

(272) Andersen, J.; Madsen, U.; Björkling, F.; Liang, X. *Synlett* **2005**, 2209–2213.

(273) Guo, H.; Schmidt, A.; Stephan, P.; Raguž, L.; Braga, D.; Kaiser, M.; Dahse, H.-M.; Weigel, C.; Lackner, G. u. a. *Chemical Biology & Biological Chemistry* **2018**, *19*, 2307–2311.

(274) Rostovtsev, V. V.; Green, L. G.; Fokin, V. V.; Sharpless, K. B. *Angewandte Chemie International Edition* **2002**, *41*, 2596–2599.

(275) Mootz, H. D.; Kessler, N.; Linne, U.; Eppelmann, K.; Schwarzer, D.; Marahiel, M. A. *Journal of the American Chemical Society* **2002**, *124*, 10980–10981.

(276) Nguyen, K. T.; Ritz, D.; Gu, J.-Q.; Alexander, D.; Chu, M.; Miao, V.; Brian, P.; Baltz, R. H. *Proceedings of the National Academy of Sciences of the United States of America* **2006**, *103*, 17462–17467.

(277) Bozhueyuek, K. A. J.; Watzel, J.; Abbood, N.; Bode, H. B. *Angewandte Chemie International Edition* **2021**, *60*, 17531–17538.

(278) Thompson, K. E.; Bashor, C. J.; Lim, W. A.; Keating, A. E. *ACS Synthetic Biology* **2012**, *1*, 118–129.

(279) Hahn, M.; Stachelhaus, T. *Proceedings of the National Academy of Sciences of the United States of America* **2006**, *103*, 275–280.

(280) Bozhüyük, K. A. J.; Linck, A.; Tietze, A.; Kranz, J.; Wesche, F.; Nowak, S.; Fleischhacker, F.; Shi, Y.-N.; Grün, P. u. a. *Nature Chemistry* **2019**, *11*, 653–661.

(281) Smith, M. A.; Bidochka, M. J. *Canadian Journal of Microbiology* **1998**, *44*, 351–355.

(282) Casali, N.; Preston, A., *E. coli Plasmid Vectors*; Humana Press: New Jersey, **2003**; Bd. 235.

(283) Cairns, T. C.; Nai, C.; Meyer, V. *Fungal Biology and Biotechnology* **2018**, *5*, 13.

(284) Sonnabend, R.; Seiler, L.; Gressler, M. *Journal of Fungi* **2022**, *8*, 196.

10 Anhang

Eigenanteil an Originalartikeln

Manuskript 1

veröffentlich unter: Wurlitzer, J. M. et al. *Applied and Environmental Microbiology* **2021**, 87, e0521-20

Beitrag des Doktoranden zu Abbildungen, die experimentelle Daten wiedergeben:

Abbildung 2-4, 6	☒	100%
Abbildung 5	☒	20% (Produktion der untersuchten Proteine)
Abbildung S1-S27, S29, S31-S36	☒	100%
Abbildung S28, S30	☒	20% (Aufreinigung der untersuchten Metabolite)

Manuskript 2

veröffentlich unter: Wurlitzer, J. M. et al. *Chemical Science* **2022**, 13, 9091-9101

Beitrag des Doktoranden zu Abbildungen, die experimentelle Daten wiedergeben:

Abbildung 1,3 und 4	☒	100%
Abbildung 2	☒	20% (Produktion der untersuchten Proteine)
Abbildung 5	☒	50% (Abbildungsteil A)
Abbildung S1-S5, S7, S9-S34, S37-S60, S62	☒	100%
Abbildung S6	☒	20%
Abbildung S35 und S36, S61	☒	20% (Aufreinigung der untersuchten Metabolite)

Manuskript 3

veröffentlich unter: Kirchgaessner, L. et al. *Fungal biology and biotechnology* **2023**, 10, 4

Beitrag des Doktoranden zu Abbildungen, die experimentelle Daten wiedergeben:

Abbildung 1-3	☐	0%
Abbildung 4 und 5	☒	100%
Abbildung S8 und S10	☒	100%

Manuskript 4

Manuskript zur Begutachtung eingereicht bei: *Journal of Natural Products*

Beitrag des Doktoranden zu Abbildungen, die experimentelle Daten wiedergeben:

Abbildung 1-3	☐	0%
Abbildung 4	☒	5% (Aufreinigung der untersuchten Metabolite)
Abbildung S1-S46	☐	0%

Ehrenwörtliche Erklärung

Hiermit erkläre ich, dass diese hier vorliegende Arbeit

Biosynthese und Funktion von Naturstoffen aus *Mortierella alpina*

selbstständig angefertigt wurde und keine Textabschnitte eines Dritten Seite ohne Kennzeichnung übernommen wurden. Die Promotionsordnung der Fakultät für Biowissenschaften an der FSU Jena ist mit bekannt. Es wurde keine Hilfe eines kommerziellen Promotionsvermittlers in Anspruch genommen und es wurden keine geldwerte Leistungen, die inhaltlich im Bezug zu dieser Dissertation stehen, an Dritte getätigt. Weiterhin ist diese Dissertation nirgendwo als Prüfungsarbeit für eine staatliche oder wissenschaftliche Prüfung eingereicht worden.

Jena, den

Jacob Martin Wurlitzer

Danksagung

Eine Doktorarbeit stellt eine große Herausforderung dar. Ihr Gelingen ist nicht nur abhängig von der eigenen Anstrengung, sondern auch von der Hilfe und Unterstützung anderer. Daher möchte ich mich bei all denen Bedanken, die im Laufe dieser Arbeit geholfen haben.

Zuerst möchte ich mich bei Prof. Dr. Dirk Hoffmeister bedanken, für die Chance diese Arbeit an seinem Lehrstuhl durchzuführen. Danke für das wecken meiner Begeisterung für Mikrobiologie, die immer offene Tür und das entgegengebrachte Vertrauen.
Genauso gilt mein besonderer Dank Dr. Markus Greßler, durch dessen Betreuung ich die spannende Welt der Zygomyceten erforschen konnte. Danke für deinen unermüdlichen Einsatz, deine Ideen, für deine Hilfe, deinen Rat und deine Unterstützung.

Ich bedanke mich auch bei allen Koorperationspartnern:innen aus der Pharmazeutischen Technologie, der Pharmazeutischen Chemie und der Arbeitsgruppe Biosynthetisches Design von Naturstoffen am HKI Jena, die mich mit Ihrer Expertise unterstützt haben. Besonderer Dank gilt dabei Aleksa und Hajo, die mir mit Ihrem HAMA-Assay unzählige Stunden im Isotopenlabor erspart haben.
Des weiteren bin ich Dr. Florian Baldeweg für die hervorragende Einarbeitung in den ersten Monaten zu großem Dank verpflichtet. Sowohl der fachliche als auch der persönliche Austausch in dieser Zeit hat einen wichtigen Grundstein für den Erfolg dieser Arbeit gelegt.
Ich danke allen Kolleginnen und Kollegen des Lehrstuhls für Pharmazeutische Mikrobiologie. Danke für alle wundervollen Gespräche, fachlich und nicht-fachlich. Danke an Tine, Julia, Max, Johannes und alle anderen.

Genauso gilt mein Dank meiner Familie, die mich in allen Phasen meines Lebens unterstützt hat.

Zuletzt gilt mein tiefster Dank meiner Frau Susanne Löffler. Als Laborpartner konnten wir die Last unserer Promotion teilen. Du bereicherst jeden Tag meines Lebens.

Publikationsliste und Poster

Publikationen

2021 **Wurlitzer, J. M.**; Stanišić, A.; Wasmuth, I.; Jungmann, S.; Fischer, D.; Kries, H.; Gressler, M.; Bacterial-Like Nonribosomal Peptide Synthetases Produce Cyclopeptides in the Zygomycetous Fungus *Mortierella alpina Applied and Environmental Microbiology* **2021**, 87, e02051–20.

2022 **Wurlitzer, J. M.**; Stanišić, A.; Ziethe, S.; Jordan, P. M.; Günther, K.; Werz, O.; Kries, H.; Gressler, M.; Macrophage-targeting Oligopeptides from *Mortierella alpina Chemical Science* **2022**, 13, 9091–9101.

2022 Dörner, S.;Rogge, K.; Fricke, J.; Schäfer, T.; **Wurlitzer, J. M.**; Gressler, M.; Pham, D. N. K.; Manke, D. R.; Chadeayne, A. R.; Hoffmeister, D.; Genetic Survey of *Psilocybe* Natural Products *Chembiochem* **2022**, 23, e202200249

2022 Lawrinowitz, S.; **Wurlitzer, J. M.**; Weiss, D.; Arndt, H.-D.; Kothe, E.; Gressler, M.; Hoffmeister, D.; Blue Light-Dependent Pre-mRNA Splicing Controls Pigment Biosynthesis in the Mushroom *Terana caerulea Microbiology Spectrum* **2022**, 10, e0106522.

2023 Kirchgässner, L.; **Wurlitzer, J. M.**; Seibold, P. S.; Rakhmanov, M.; Gressler, M.; A Genetic Tool to Express Long Fungal Biosynthetic Genes *Fungal biology and biotechnology* **2023**, 10, 4

Poster

2019 **International VAAM Workshop 2019 - Biology of Microorganims Producing Natural products**

Malpicyclins - novel nonribosomal peptides from *Mortierella alpina*

2022 **31st Fungal Genectics Conference**

The Genetic Basis of Oligopeptide Biosynthesis in early diverging Fungus *Mortierella alpina*